

**ORGANOCATALYTIC HALOFUNCTIONALIZATION
OF OLEFINS**

TAY WEILIANG DANIEL

NATIONAL UNIVERSITY OF SINGAPORE

2014

**ORGANOCATALYTIC HALOFUNCTIONALIZATION
OF OLEFINS**

TAY WEILIANG DANIEL
(B.A.Sc. (Hons.)), NUS

A THESIS SUBMITTED

FOR THE DEGREE OF DOCTOR OF PHILOSOPHY

**NUS GRADUATE SCHOOL FOR INTEGRATIVE
SCIENCES AND ENGINEERING**

NATIONAL UNIVERSITY OF SINGAPORE

2014

Thesis Declaration

I hereby declare that the thesis is my original work and it has been written by me in its entirety. I have duly acknowledged all the sources of information which have been used in the thesis.

This thesis has also not been submitted for any degree in any university previously.



Tay Weiliang Daniel

10th January 2014

Acknowledgements

I would like to take this opportunity to express my heartfelt gratitude and deepest appreciation to everyone who have helped, encouraged and supported me during these four years. This thesis would not have been possible without them.

Foremost, I would like to thank my PhD advisors. Dr Keith Carpenter, for all the support that I am given throughout my time as his student. I have been extremely fortunate to work in a fully-equipped world-class laboratory in his institute. Next, A/P Dr Yeung Ying-Yeung, a supervisor who is so dedicated to research and cared so much about my work. Not only have I grown as an experimentalist under his guidance but the space and freedom he gave me in developing projects has allowed me to improve myself to be an all-rounded scientist. There is no doubt that I have been inspired by his attitude towards research, so much so that I want to be a member of the academic family. Next, Dr Leung Yiu Chung, for his patience as my laboratory mentor. His immense knowledge and vast experimental skills have of tremendous help to me all the time.

I would also like to thank friends and colleagues from Organic Chemistry at Helios (A*STAR) for their continuous support throughout these years. In particular, Dr Charles Johannes for his kind and helpful advices, Mr Jahangir, Ms Alexia Loh and Mr Sim Hui Tat for all the logistic support that they have

provided, Mr Cheong Choon Boon for proof-reading this thesis and not forgetting, Dr Howard Jong and Mr Chew Xinying, for the multiple BPL sessions that we had during the weekends. I am also grateful to the other members of the Yeung's group for their timely advices and help during my research.

Next, I am extremely grateful to my parents who have nurtured me throughout my life and I appreciate the patience that they always had for me.

None of this would have been possible without my wife, Xuefen. I would like to thank her for always being there for me throughout these 4 years. She is always willing to listen to my problems, be it chemistry or non-chemistry related, always offering me support, encouragement, advices and never failing to make me smile during the tough times. Her patience in taking care of our baby boy, Lucas, also allowed me to fully concentrate on my research without having much to worry about.

Last but not least, I would like to thank A*STAR Graduate Academy (A*GA) for providing me with a research scholarship.

Table of Contents

Thesis Declaration	i
Acknowledgements	iii
Table of Contents	iv
Summary	ix
List of Tables	xi
List of Schemes	xiii
List of Figures	xvii
List Abbreviations	xviii
List of Publications & Presentations	xxi
 Chapter 1 Halocyclization Reactions	 1
1.1 Introduction	2
1.2 Nomenclature of Halogen Cations	4
1.3 General Strategies for Catalysis of Halocyclization	5
1.4 Engineering Enantioselectivity in Halocyclization	7
1.5 Halolactonization Reactions	11
1.5.1 Racemic Halolactonizations	11
1.5.2 Asymmetric Halolactonization	19
1.6 Haloetherification Reactions	30
1.6.1 Racemic Haloetherifications	31
1.6.2 Asymmetric Haloetherifications	33

1.7 Halolactamization and Haloamination Reactions	41
1.7.1 Racemic Halolactamization and Haloamination Reactions	42
1.7.2 Asymmetric Halolactamization and Haloamination Reactions	46
1.8 Other Halocyclization Reactions	48
1.9 Aims & Approach	52
1.10 References	54
 Chapter 2 Enantioselective Synthesis of 2-Substituted and 3- Substituted Piperidines through a Bromoaminocyclization Process	 61
2.1 Introduction	62
2.2 Results and Discussion	63
2.2.1 Catalyst Screening	63
2.2.2 Reaction Conditions Optimization	67
2.2.3 Substrate Scope	69
2.2.4 Scale-up Synthesis and Synthesis of Enantiomer of 2-7	71
2.2.5 Silver Salt Promoted Rearrangement	72
2.2.6 Applications – Syntheses of Chiral Pharmaceutical Building Blocks	77
2.2.7 Applications – Synthesis of Preclamol	78
2.3 Summary	82
2.4 Experimental	82
2.5 References	126

Chapter 3 Enantioselective Desymmetrizing Bromoetherification of Diolefinic Diols – Application to the Synthesis of Novel Chiral Spirocycles	131
3.1 Introduction	132
3.2 Results and Discussion	134
3.2.1 Catalyst Screening	134
3.2.2 Reaction Conditions Optimization	137
3.2.3 Substrate Scope	139
3.2.4 Investigation on Catalyst Loading	143
3.2.5 Synthesis of Spirocycles	143
3.2.6 Mechanistic Studies	147
3.2.7 Desymmetrizing Halocyclization of Other Substrates	150
3.3 Summary	152
3.4 Experimental	152
3.5 References	204
 Chapter 4 Lewis Basic Selenium Catalyzed Chloroamidation of Olefins Using Nitriles as Amide Source	 209
4.1 Introduction	210
4.2 Results and Discussion	212
4.2.1 Catalyst Screening	212
4.2.2 Reaction Conditions Optimization	214
4.2.3 Effect of Halogen Source	215
4.2.4 Substrate Scope	217

4.2.5 Haloamidation of Acid Labile Substrates	222
4.2.6 Haloamidation Using Different Nitriles	224
4.2.7 Mechanistic Studies	224
4.3 Summary	227
4.4 Experimental	227
4.5 References	243
 Chapter 5 Towards the Development of a New Catalyst for Asymmetric Halocyclization	 247
5.1 Introduction	248
5.2 Results and Discussion	249
5.2.1 Synthesis of Catalysts and Preliminary Testing	249
5.2.2 Reaction Conditions Optimization	257
5.2.3 Effect of Halogen Source	258
5.2.4 Catalyst Screening	259
5.3 Summary	261
5.4 Experimental	262
5.5 References	268
 Appendices – NMR Spectra of Synthetic Intermediates and Products	
Appendix A (Chapter 2)	269
Appendix B (Chapter 3)	307
Appendix C (Chapter 4)	361

Summary

Halogenated heterocyclic compounds are one of the most important synthetic intermediates for synthetic chemist as they form the fundamental units of many pharmaceuticals and biologically relevant molecules. Significant effort has been devoted to the development of efficient enantioselective halocyclization processes to synthesize such compounds. While, asymmetric halolactonization reactions have already been thoroughly researched, there are significantly less reports on asymmetric haloetherification and haloamination reactions, primarily attributed to the difficulty of developing an efficient synthetic method.

To explore the scope of haloamination reactions, a catalytic enantioselective bromocyclization of olefinic amides using amino-thiocarbamates as the catalysts has been developed. The resulting enantioenriched 2-substituted 3-bromopiperidines can readily be transformed to 3-substituted piperidines through a silver salt-mediated rearrangement. This process has been applied to the synthesis of a dopaminergic drug, Preclamol.

Next, catalytic enantioselective synthesis of hetero spirocycles through a double-halocyclization strategy is reported. The first of the double cyclization involves a desymmetrization-asymmetric bromoetherification process which gives rise to two quaternary stereogenic carbons in the cyclic ether products. Subsequently, a variety of diastereoselective halocyclizations can be performed to

yield a series of chiral hetero spiro systems. This protocol enabled access to a class of chiral novel spirocycles that is distinctly absent in the literature.

In a separate study, the intramolecular chloroamidation of olefinic substrates using diphenyl selenide as the catalyst is developed—the first example reported using a Lewis base promoter. The reaction conditions were found to be mild and suitable for a wide range of substrates including those which are acid labile. The methodology is also complementary to existing strategies that utilize Lewis acid catalysts.

Lastly, preliminary results for the development of a new class of catalyst for halocyclization reactions are reported. Novel proline-based amino-selenocarbamate catalysts were prepared for but it was found that this class of catalyst was unstable and decomposed to form the diselenide products. The diselenide was derivatized to form different amino-selenium compounds and their catalytic ability for halocyclization reactions was investigated. The amino-selenoether catalyst produced excellent yields and encouraging enantioselectivity. These results are an excellent starting point for further investigations which is beyond the scope of this thesis.

List of Tables

Table 1.1	Catalyst survey for Lewis base catalyzed iodolactonization.	16
Table 1.2	Recent efforts in racemic bromolactonization.	17
Table 2.1	Catalyst screening for bromoaminocyclization of 2-5a .	66
Table 2.2	Reaction conditions optimization.	68
Table 2.3	Enantioselective bromoaminocyclization.	70
Table 2.4	Survey of silver salts on rearrangement of 2-7a .	75
Table 2.5	Silver-salt promoted rearrangement of 2-7a .	76
Table 3.1	Catalyst screening for bromoetherification of 3-10a .	136
Table 3.2	Solvent and temperature optimization of bromoetherification of 3-10a .	138
Table 3.3	Effect of halogen source and additives on bromoetherification of 3-10a .	139
Table 3.4	Bromoetherification of diolefinic diol 3-10 .	140
Table 3.5	Bromoetherification of diols with unsymmetrical unsaturated systems.	142
Table 3.6	Investigation on the catalyst loading on reaction.	143
Table 3.7	Synthesis of spirocycles.	145
Table 3.8	Cyclization of 3-26 using different catalysts.	149
Table 4.1	Reaction conditions optimization.	215
Table 4.2	Effect of halogenating reagents on reaction yields.	216
Table 4.3	Haloamidation of olefins.	218
Table 4.4	Haloamidation of acid labile substrates.	223
Table 4.5	Chloroamidation of 4-9a with different nitrile partners.	224
Table 5.1	Bromolactonization using different amino-selenium catalysts.	255

Table 5.2	Solvent optimization for the bromolactonization of 5-20 .	257
Table 5.3	Halogen source screening for the bromolactonization of 5-20 .	258
Table 5.4	Catalyst screening for the bromolactonization of 5-20 .	260
Table 5.5	Importance of the Lewis basic selenium atom in the catalyst.	261

List of Schemes

Scheme 1.1	Electrophilic halogen addition to alkenes.	2
Scheme 1.2	Halocyclization of olefinic substrates.	3
Scheme 1.3	Macro-iodolactonization using bis(collidine)-iodonium hexafluorophosphate.	13
Scheme 1.4	Iodolactonization using Pb(OAc) ₄ and NaI system.	13
Scheme 1.5	Diastereoselective iodocyclization using stoichmetric Lewis acidic catalyst.	14
Scheme 1.6	Triphenylphosphine sulfide catalyzed bromo- and iodolactonization.	14
Scheme 1.7	Chloramin-T as an effective electrophilic chlorine source.	18
Scheme 1.8	Iodolactonization using chiral primary amine and ICl.	19
Scheme 1.9	Quarternary ammonium salt catalyzed enantioselective iodolactonization.	20
Scheme 1.10	Borhan's (DHQD) ₂ PHAL 1-28 catalyzed enantioselective chlorolactonization.	21
Scheme 1.11	Amino-urea catalyzed bromolactonization of enye 1-30 to yield allene 1-32 .	22
Scheme 1.12	Aminourea catalyzed iodolactonization.	23
Scheme 1.13	C ₃ -Symmetric trisimidazoline catalyzed bromolactonization.	25
Scheme 1.14	Amino-thiocarbamate catalyzed enantioselective bromolactonization.	26
Scheme 1.15	Enantioselectivity of selected analogues of amino-thiocarbamates.	27
Scheme 1.16	Iodolactonization catalyzed by 1-52 -HNTf ₂ .	30
Scheme 1.17	(dppf)PdCl ₂ catalyzed iodoetherification.	31
Scheme 1.18	Selected example of Lewis base catalyzed iodoetherification.	32
Scheme 1.19	Example of non-alcohol substrate undergoing iodoetherification.	32
Scheme 1.20	Asymmetric desymmetrizing haloetherification catalyzed by Ti(OiPr) ₄ .	34
Scheme 1.21	Co(II) and Cr (III) salen complexes catalyzed iodoetherifications.	35

Scheme 1.22	Enantioselective fluorocyclization catalyzed by (DHQ) ₂ PHAL.	36
Scheme 1.23	Enantioselective desymmetrizing haloetherification using chiral phosphates.	37
Scheme 1.24	Shi's bromoetherification catalyzed by chiral phosphoric acid.	38
Scheme 1.25	Denmark's bromoetherification using chiral phosphoric acid.	40
Scheme 1.26	Competing halo- <i>N</i> -cyclization and halo- <i>O</i> -cyclization for olefinic amides.	42
Scheme 1.27	Halolactamization performed on a highly constrained olefinic lactam.	43
Scheme 1.28	<i>N</i> -tosylated amide bromolactamization.	43
Scheme 1.29	Synthesis of bicyclic ureas and isoureas using double cyclization strategy.	44
Scheme 1.30	Selected bromo- and chloro- <i>N</i> -cyclizations using palladium catalysis.	45
Scheme 1.31	Chiral auxiliary induced enantioselective iodolactamization.	46
Scheme 1.32	Amino-thiocarbamate catalyzed bromoaminoocyclization.	48
Scheme 1.33	Enantioselective polyenecyclization catalyzed by chiral phosphoramidites.	49
Scheme 1.34	Chiral titanium complex catalyzed iodocarbocyclization.	51
Scheme 2.1	Bromocyclization of olefinic amides.	63
Scheme 2.2	Asymmetric bromoaminocyclization of 2-9 .	64
Scheme 2.3	Synthesis of ent-2-5a using catalyst 2-11n .	72
Scheme 2.4	Attempted synthesis of 2-13 results in the formation of ent-2-8a .	72
Scheme 2.5	1,2-Aryl shift for the synthesis of unsaturated piperidine 2-15 .	74
Scheme 2.6	Possible explanation for the observed stereoselectivity.	77
Scheme 2.7	Synthesis of pharmaceutical intermediates.	78
Scheme 2.8	Synthesis of Preclamol using kinetic resolution.	79
Scheme 2.9	Synthesis of intermediate of Preclamol using dynamic kinetic resolution.	80

Scheme 2.10	Synthesis of Preclamol.	81
Scheme 2.11	Synthesis of 2-35 .	81
Scheme 3.1	Synthesis of hetero spirocycles through the asymmetric bromination and desymmetrization of diolefinic diol.	134
Scheme 3.2	Mechanistic studies of bromoetherification using thiocarbamate catalysts.	148
Scheme 3.3	Synthesis of diazaspirocycles via desymmetrizing halocyclization.	150
Scheme 3.4	Attempted synthesis of intermediate 3-30 .	150
Scheme 3.5	Attempted synthesis of intermediate 3-31 .	151
Scheme 3.6	Attempted synthesis of intermediate 3-34 .	151
Scheme 4.1	General scheme for haloamidation of olefins.	210
Scheme 4.2	Lewis acid catalyzed haloamidation in the synthesis of Tamiflu®.	211
Scheme 4.3	InBr ₃ catalyzed bromoamidation.	211
Scheme 4.4	Lewis base catalyst screening for bromoamidation.	213
Scheme 4.5	Hydrolytic decomposition of <i>sp</i> ² -type catalysts.	213
Scheme 4.6	Possible transition state of chloroamidation.	217
Scheme 4.7	Synthesis of 4-14 using NCS.	225
Scheme 4.8	Examination of 4-14 as the catalyst in the chloroamidation.	226
Scheme 4.9	Proposed mechanism of the Lewis basic selenium catalyzed chloroamidation.	226
Scheme 5.1	Synthesis of prolinol 5-6 .	250
Scheme 5.2	Synthesis of amino-selenocarbamate catalyst 5-9 .	251
Scheme 5.3	Proposed mechanism for the rearrangement of 5-8 to 5-9 .	251
Scheme 5.4	Decomposition of 5-9 to form 5-10 .	252
Scheme 5.5	Derivatization of diselenide 5-16 .	254

Scheme 5.6	Bromocyclizations of olefinic substrates 5-22 and 5-24 using 5-19a .	255
-------------------	---	-----

List of Figures

Figure 1.1	Nomenclature of halogen cations.	4
Figure 1.2	Strategies for catalyzed halofunctionalization.	6
Figure 1.3	Chiral catalyst maintains association with haliranium ion.	7
Figure 1.4	Strategies for catalyzed halocyclization.	8
Figure 1.5	Plausible mechanisms for the activation of DCDPH 1-29 .	21
Figure 1.6	Proposed mechanism of the aminothiobicarbamate catalyzed bromolactonization.	28
Figure 1.7	Proposed transition state for Shi's bromoetherification.	39
Figure 1.8	Proposed transition state for Denmark's bromoetherification.	40
Figure 1.9	Ishihara's stereochemical model for the observed enantioselectivity.	50
Figure 2.1	Examples of bioactive substituted piperidines.	62
Figure 2.2	X-ray crystal structure of 2-7a .	71
Figure 2.3	X-ray crystal structure of <i>ent</i> - 2-8a .	73
Figure 3.1	Examples of chiral ligands with spirocyclic backbone.	132
Figure 3.2	Examples of bioactive natural products with spirocyclic scaffolds.	132
Figure 3.3	X-ray crystallographic study of compound 3-16 .	147
Figure 4.1	¹ H-NMR spectrum of 4-11i .	220
Figure 4.2	Proton decoupling experiments for anti-markovnikov product 4-11i .	221
Figure 5.1	Other selenocarbamate catalysts synthesized to probe stability.	253

List of Abbreviations

Ac	Acetyl
Å	Angstrom
Ar	Aromatic
Bn	Benzyl
Boc	<i>tert</i> -Butyloxycarbonyl
Bz	Benzoyl
Bu	Butyl
Conc.	Concentration
DBH	1,3-dibromo-5,5-dimethylhydantoin
DCDPH	1,3-dichloro-2,2-diphenylhydantoin
DMAP	4-Dimethylaminopyridine
DMF	Dimethylformamide
DMSO	Dimethyl sulfoxide
d	Doublet
dr	Diastereomeric ratio
ee	Enantiomeric excess
er	Enantiomeric ratio
eq	Equivalent
Et	Ethyl
HPLC	High performance liquid chromatography
IPA	<i>iso</i> -Propanol

m	Multiplet
m/z	Mass-to-charge ratio
Me	Methyl
Ms	Methane sulfonyl
NBP	<i>N</i> -bromophthalimide
NBS	<i>N</i> -bromosuccinimide
NCS	<i>N</i> -chlorosuccinimide
NIS	<i>N</i> -iodosuccinimide
NR	No reaction
Nu	Nucleophile
Pr	Propyl
ppm	Parts per million
q	Quartet
s	Singlet
TABCO	2,4,4,6-tetrabromo-2,5-cyclohexadienone
TBS	<i>tert</i> -butyldimethylsilyl
TEA	Triethylamine
TFA	Trifluoromethylacetic acid
THF	Tetrahydrofuran
t	Triplet

List of Publications & Presentations

Publications:

1. L. Zhou, D.W. Tay, J. Chen, Y.C. Leung, Y.Y. Yeung, Enantioselective synthesis of 2-substituted and 3-substituted piperidines through a bromoaminocyclization process. *Chem. Commun.*, **2013**, 49, 4412-4414. (Accepted on 2nd October 2012)
2. D.W. Tay, I.T. Tan, Y.C. Leung, Y.Y. Yeung Lewis Basic Selenium Catalyzed Chloroamidation of Olefins Using Nitriles as the Nucleophiles. *Org. Lett.*, **2013**, 15, 1310–1313. (Accepted on 5th March 2013)
3. D.W. Tay, Y.C. Leung, Y.Y. Yeung mino-thiocarbamate Catalyzed Enantioselective Desymmetrizing Bromoetherification of Diolefinic Diols—Application to the Synthesis of Novel Chiral Spirocycles. *Angew. Chem.* (Submitted 15th November 2013)

Presentations:

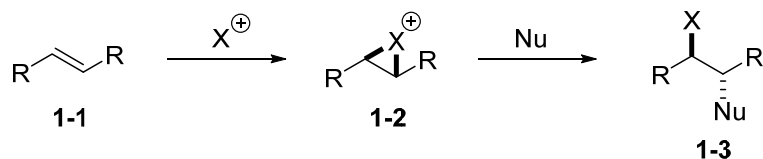
1. “Enantioselective Synthesis of 2-Substituted and 3-Substituted Piperidines through a Bromoaminocyclization Process” *Presented at* 13th Tetrahedron Symposium, Taipei, Taiwan 2012. (Poster)
2. “Lewis Basic Selenium Catalyzed Chloroamidation of Olefins Using Nitriles as the Nucleophiles” *Presented at* 14th Tetrahedron Symposium, Vienna, Austria 2013. (Poster)

Chapter 1

Halocyclization Reactions

1.1 Introduction

The addition of electrophilic reagents to olefins is perhaps one of the most fundamental transformations for the rapid construction of complex organic molecules. In fact, electrophilic functionalization of olefins was already a classic textbook transformation in the early 1930s.¹ Amongst all these examples, halogen electrophiles are most commonly utilized in these addition reactions. Typically, these reactions proceed via the formation of cyclic halonium (haliranium, see later) ions **1-2** which is followed by an S_N2 ring-opening by a nucleophile, yielding *anti* products **1-3** (Scheme 1.1).

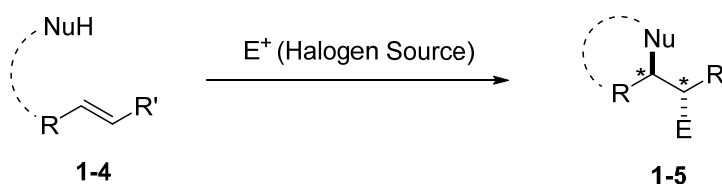


Scheme 1.1 Electrophilic halogen addition to alkenes.

The incorporation of a halogen atom in a molecule can alter both the physical and biological activity of the molecule. This is typically due to the effected changes in steric and electronic properties.² For example, halogenated amino acids analogues and active pharmaceuticals have demonstrated to have enhanced cytotoxicity when they are evaluated against their non-halogenated counterparts.³ Currently, over 4500 halogen-containing natural products have been documented, of which, most of the carbon-halogen bonds are constructed enzymatically.^{2a, 4} Another distinct advantage of having a halogen atom in a molecule is the

versatility that comes with it as alkyl halides can function as precursors or modification points for the construction of carbon–carbon bonds, amines, ethers, sulfides and epoxides.⁵ Chiral carbons that have a halogen attached to it may also undergo stereospecific S_N2 reactions with the inversion of chirality.

Even though halogenation of olefins is a reaction that has been known for some time, enantioselective versions of this class of reaction have only been recently developed. This is especially so for halocyclization reactions, a sub-class of halofunctionalization reactions, whereby heterocyclic rings are the resultant products. For example, lactones can be synthesized through the halocyclization of olefinic acids; cyclic lactams can be synthesized through the halocyclization of olefinic amides; and cyclic ethers can be synthesized via the halocyclization of olefinic alcohols. These reactions typically occur through the intramolecular addition of a heteronucleophile to a carbon–carbon double bond in the presence of an electrophilic halogen source (Scheme 1.2).



Scheme 1.2 Halocyclization of olefinic substrates.

Despite being regarded as an important breakthrough in organic chemistry, these reports only flagged the beginning of an emerging topic in this field. This chapter of the thesis will give a detailed analysis of the development of

enantioselective halocyclization reactions and highlight the critical challenges faced in developing useful methodologies for this class of reactions.

1.2 Nomenclature of Halogen Cations

To begin, the nomenclature of halogen cations needs to be first introduced. By correlating the terms drawn up for electron-deficient species in Group V and VI on the periodic table where hypercoordinate species are called ammonium and oxonium ion respectively, the corresponding Group VII cation is termed as a halonium ion (Figure 1.1). In unique cases whereby the cation occurs within a cyclic structure, it is termed differently, depending on the ring size.

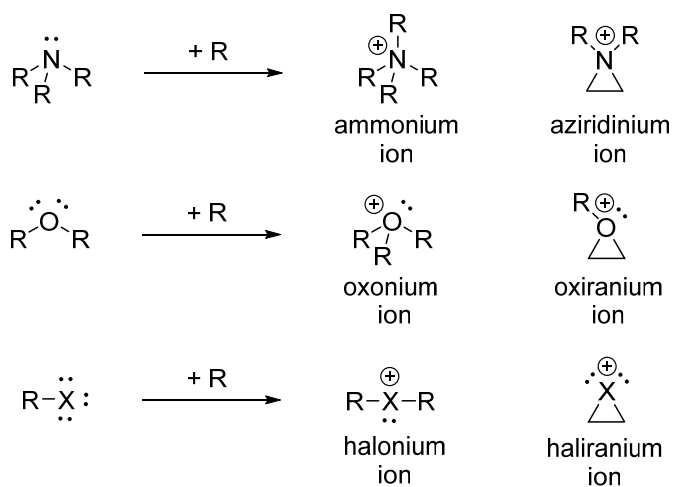


Figure 1.1 Nomenclature of halogen cations.

For example, iranium is used for the 3-membered ring, etidium and olidinium for the 4-membered and 5-membered rings respectively.⁶ To put these into

context, electrophilic addition reactions precede by the formation of a 3-membered cyclic intermediate termed either as “haliranium” or as the commonly known “cyclic halonium”. Both terms would be used interchangeably throughout this thesis.

1.3 General Strategies for Catalysis of Halocyclization

After an extensive survey for enantioselective halocyclization reactions that were reported in the past decade, it is observed that a trend can be drawn out for the general strategies that were employed. Generally, halocyclization reactions can be catalyzed by Lewis acids, Brønsted acids, Lewis bases and phase transfer catalysts (Figure 1.2).

Lewis acids and Brønsted acids increase the electrophilicity and hence the reactivity of halogen sources by binding to the halogenating reagent intermolecularly, reducing electron density, and thus increasing electrophilicity. Brønsted acids, in addition, can generate the reactive electrophile by protonating the *N*-halosuccinimide. This can result in the transfer of the halogen to the conjugate base of the Brønsted acid.⁷

Lewis bases can activate halogen reagents by donating its lone pair of electrons to the electrophilic halogen. Likewise, this will generate a more reactive electrophilic halogen atom. Mechanistically, this is an example of the concept on

Lewis base activation of Lewis acids.⁸ This strategy requires the halogenating reagent to be adequately unreactive such that the substrate will not undergo uncatalyzed, consequently unselective halofunctionalization.

Phase transfer catalysts work differently from the above catalysts and usually do not depend on the reactivity of the halogen sources. This is because the substrates and halogen sources are separated into different phases such that they will only react when they are being brought together by the phase transfer catalyst.

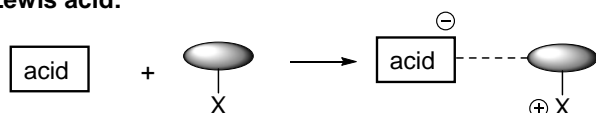
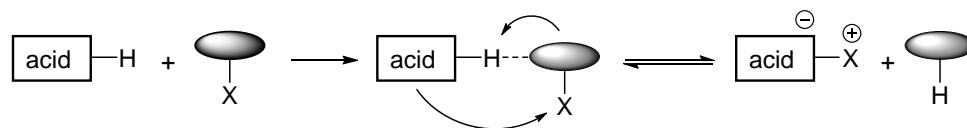
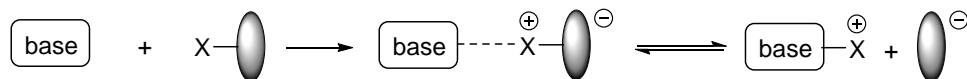
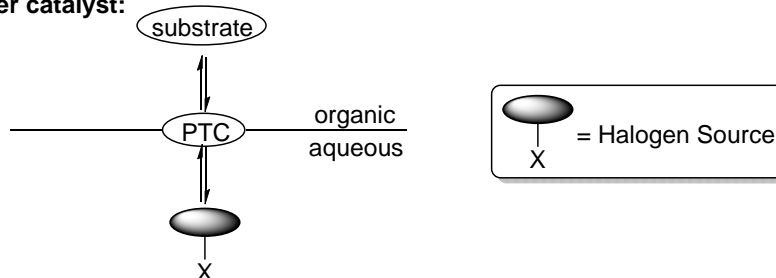
Lewis acid:**Brønsted acid:****Lewis base:****Phase transfer catalyst:**

Figure 1.2 Strategies for catalyzed halofunctionalization.⁹

1.4 Engineering Enantioselectivity in Halocyclization

One of the key difficulties encountered in asymmetric halocyclization is the engineering of enantioselectivity, which is a far more challenging issue when compared to catalyzing the racemic reaction. In devising a successful strategy, it is important to note that the chiral catalyst and the cyclic halonium intermediate must maintain association throughout, until nucleophilic capture is completed (Figure 1.3). Failure to do so will ultimately result in the racemization of the haliranium ion. This is observed to be especially so for bromo- and iodocyclization reactions.⁹

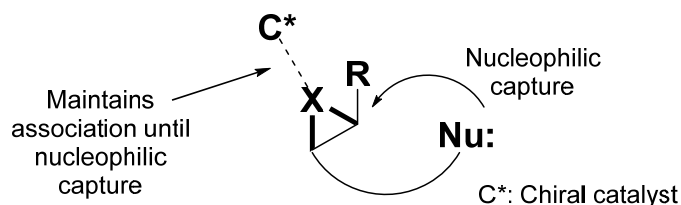


Figure 1.3 Chiral catalyst maintains association with haliranium ion.

The tactics used to engineer enantioselectivity for fluoro- and chlorocyclization is similar to those that are used for bromo- and iodofunctionalization in that the initial delivery of the halonium ion employs the same type of strategies compared to the bromo- and iodo counterparts. However, it is observed that the fluoro- and chlorocyclization do not suffer from significant racemization compared to the bromo- and iodocyclization due to olefin–olefin transfer and therefore the association of the catalyst and cyclic halonium ion is not as vital.^{8b}

In recent years, many catalysts for enantioselective halocyclization have been developed. Although it seems like each utilizes different means for engineering enantioselectivity, the strategies used can be generally classified into four main categories (Figure 1.4). The differentiation into these categories can be attributed to the type of catalyst used and, more importantly, the strategy applied to maintain the association between the catalyst and the cyclic halonium ion. Generally, the main types of strategies are as follow:

Type A: Chiral Lewis base

Type B: Chiral counterion and anion binding

Type C: Hydrogen bonding

Type D: Chiral Lewis acid

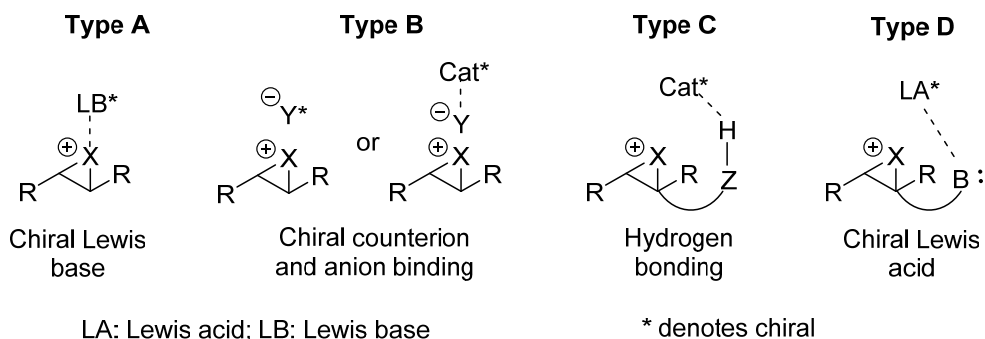


Figure 1.4 Strategies for catalyzed halocyclization.⁹

One of the most important tactics used in creating the chiral environment for asymmetric halofunctionalization is *via* the use of a chiral Lewis base (**Type A**). As mentioned earlier, it is important that the Lewis base–haliranium complex

maintain association before nucleophilic capture is completed to ensure that the chirality can be effectively transferred. The Lewis base complex tactic is also known to be most effective when employed with the other control strategies.

Brønsted acids can also form comparable interaction with the haliranium ion with the exception that the coordination between the Brønsted acid and the haliranium ion is ionic instead of being dative (**Type B**). The advantage of this chiral counterion strategy lies in the intensity of the coordination that can be derived from such ionic interactions such that the association between the catalyst and haliranium ion can be maintained till nucleophilic capture. This is especially so in non-polar organic media when both the cations and anions are being forced to be in close proximity. The formation of chiral ion pairs is by far the most prominent strategies for enantioselective halocyclizations.

A large fraction of the reported enantioselective halocyclization requires the use of hydrogen bonding interactions to maintain close proximity of the catalyst to the substrate (**Type C**). Unlike the first two strategies discussed above, the hydrogen bonding strategy is different due to the site where the chiral catalyst transfers the chirality. In this case, the catalyst is associated to a secondary site on the substrate instead of being directly associated to the haliranium ion. This strategy is most useful when the catalyst contains hydrogen bond donors such as hydroxy groups, carboxylic acids, sulfonamides, ureas, and thiocarbamates, or hydrogen bond acceptors such as phosphoryl groups and tertiary or heteroaromatic amines.

The last type of asymmetric induction for halocyclization involves the use of Lewis acids which can activate either the electrophile or the nucleophile (**Type D**). The Lewis acid–nucleophile activation type of asymmetric induction has been performed predominantly with the use of titanium complexes and this method has been very well-established over the years.¹⁰ The chiral information is imparted from the chiral ligands used to form these titanium complexes.¹¹ The Lewis acid–electrophile (halogen) activation type of enantioselective halocyclization has been mainly performed using cobalt (II)/Salen or chromium (III) chloride/salen complexes.¹²

Although these four strategies have been identified and differentiated, it must be noted that the methods commonly employed in the successful examples so far, are a combination of these tactics. In many of the cases described in the later part of the chapter, the available data suggests the action of multiple mechanisms per transformation. Despite this fact, this classification still serves as an important and valuable framework for analyzing what has is known so far, as well as what is rapidly emerging in this field. The following sections in this chapter will continue to showcase how these tactics are employed in various types of asymmetric halocyclization reactions.

1.5 Halolactonization Reactions

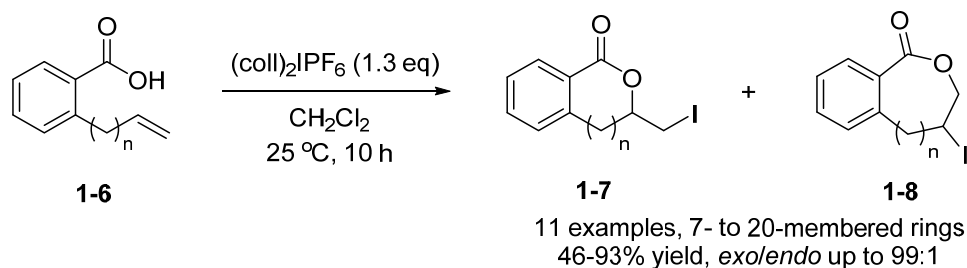
Halolactonization is one the most common and well-studied type of electrophilic halocyclization. The first example of such a reaction is a bromolactonization reaction discovered by Fittig and Stobbe in the late 19th century.¹³ This was soon followed by the discovery of the iodine variant, which quickly became a useful reaction owing to the enhanced reactivity of the carbon–iodine bond that allows easy functionalization.¹⁴ The chlorine variant was however only discovered 20 years after and (just like the other halocyclization reactions) was the least preferred choice and therefore infrequently utilized.¹⁵ Fluorolactonization is, in principle, missing in the field of electrophilic halocyclization and thus will have no mention here. This section begins with the discussion of some examples of racemic halolactonization, the catalysts used and new methods used to carry out these reactions. This will be followed by a detailed discussion on the developments in enantioselective halolactonization, particularly in the last 5 years.

1.5.1 Racemic Halolactonizations

Although iodolactonization was discovered in the early 20th century, the mechanism of the reaction was not fully understood and investigated until Linstead and May suggested that the activation of the olefin by iodine proceeded

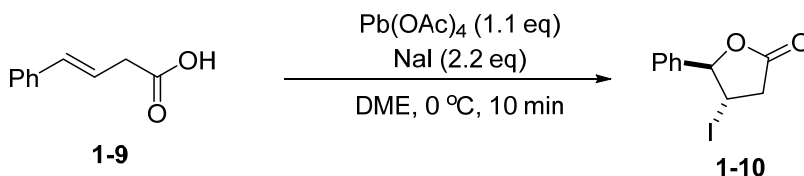
before nucleophilic attack by the carboxylate nucleophile.¹⁶ This was widely regarded as the mechanism until van Tamelen and Shamma proposed the formation of the cyclic iodonium ion as the intermediate in an attempt to reason the difference in rates of 5-*exo* and 6-*endo* cyclization.¹⁷ Klein further refined their explanation by suggesting that the lactone formed had the iodine atom and carboxylate nucleophile in an *anti*-configuration.¹⁸

Iodolactonization was later carried out widely by using Bougault conditions¹⁴, using iodine and potassium iodide in aqueous sodium bicarbonate, until it was observed that ICN in chloroform can also perform such a reaction.¹⁹ However, the reaction inevitably produced one equivalent of HCN as the by-product and its toxicity prompted the need for further improvements to be made to the reagents. Shortly after, Cook and co-workers utilized *N*-iodosuccinimide as a highly effective electrophilic iodine reagent for iodolactonization.²⁰ Rousseau also showed the feasibility of using bis(collidine)-iodonium hexafluorophosphate ((coll)₂IPF₆) as a effective iodine source for the macro-iodolactonization (Scheme 1.3).²¹



Scheme 1.3 Macro-iodolactonization using bis(collidine)-iodonium hexafluorophosphate.

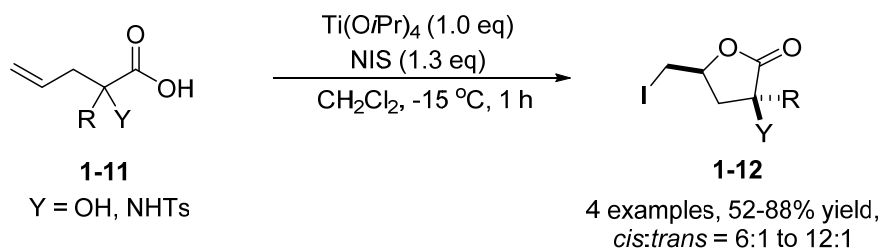
Fujimoto followed by reporting an unconventional reaction system using a combination of $\text{Pb}(\text{OAc})_4$ and NaI (Scheme 1.4).²² Although this methodology generally gives poor *exo* and *endo* selectivity, it is worth a mention due to its unique iodine source. The iodide salt is believed to undergo an *in situ* oxidation to form the iodonium electrophile for the iodolactonization.



Scheme 1.4 Iodolactonization using $\text{Pb}(\text{OAc})_4$ and NaI system.

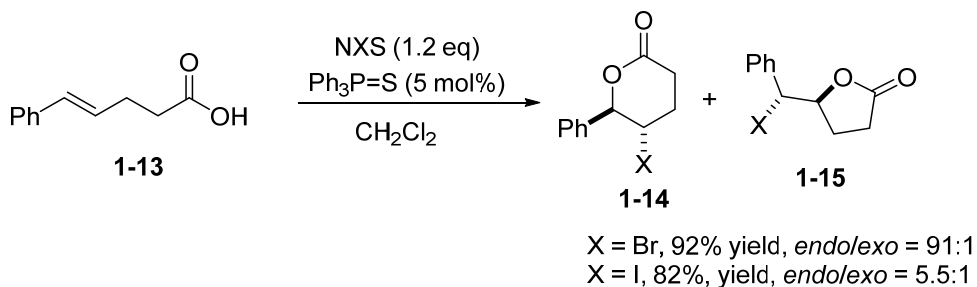
Soon after, a diastereoselective iodolactonization for substrates with a hydroxyl (OH) or sulfonamide (NHTs) moiety on the α -carbon of the carboxylic acid was reported by Taguchi and co-workers (Scheme 1.5).²³ In this case, a Lewis acid, $\text{Ti}(\text{Oi-Pr})_4$ was used in stoichiometric quantities while the iodine source employed was NIS. It was postulated that the catalyst coordinates to the substrate

prior to cyclization such that a high *cis* to *trans* ratio of products was obtained after NIS was added.



Scheme 1.5 Diastereoselective iodocyclization using stoichiometric Lewis acidic catalyst.

More recently, Denmark and co-workers carried out an extensive investigations on the catalytic ability of Lewis base catalysts in an attempt to improve selectivity and yields of bromo- and iodolactonization (Scheme 1.6).²⁴ A good range of Lewis base catalysts were surveyed for this purpose and NIS was used as the electrophilic iodine source.



Scheme 1.6 Triphenylphosphine sulfide catalyzed bromo- and iodolactonization.

Denmark used the concept of Lewis base activation of Lewis acid and showed how Lewis basic catalysts can activate electrophilic iodine (Lewis acids)

resulting in the formation of the more reactive iodonium ion. As expected, the selectivity and reactivity can be tuned by varying the steric and electronic properties of the catalysts.

First and foremost, the most obvious trend that can be observed is that the rates of catalyzed iodolactonization are affected most significantly by the Lewis base donor (Table 1.1). Catalyst containings sulfur ($R_2C=S$ and $R_3P=S$) and selenium ($R_3P=Se$) increased the rate of the reaction by the most while catalysts containing oxygen ($R_3P=O$ and $R_2C=O$) have little effect. Denmark and co-workers observed that the rate varies according to the “softness” of the donor atom, with the softer donor atoms (such as S and Se) being the more efficient catalysts.

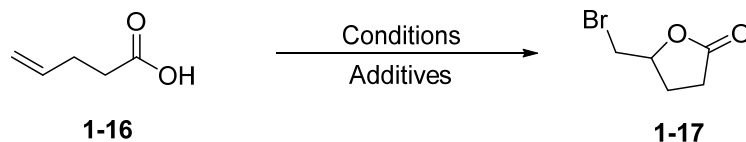
Bromolactonization is also an important sub-class of halolactonization reactions and has gained importance over the years. The reaction, like the iodolactonization, was initially carried out using molecular halogen, in this case using bromine, as the halogen source. One distinct difference is that halogenated organic solvents were initially used as the reaction medium instead of the aqueous conditions which were adopted for the first iodolactonization reactions.

Table 1.1 Catalyst survey for Lewis base catalyzed iodolactonization.²⁴

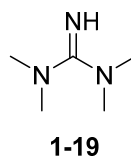
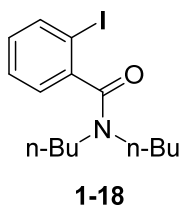
Reaction scheme: 1-13 $\xrightarrow[\text{CH}_2\text{Cl}_2, -45\text{ }^\circ\text{C}]{\text{NIS (1.2 eq), Catalyst (5 mol\%)}}$ 1-14 + 1-15

Entry	Catalyst	Reaction Time (h)	Yield (%)	1-14:1-15
1	No Catalyst	2	4	9.5:1
2	(Me ₂ N) ₂ C=O	3	10	20:1
3	n-Bu ₃ P=O	3	14	16:1
4	(Me ₂ N) ₃ P=O	3	33	20:1
5	Me ₂ SO	3	4	NA
6	(Me ₂ N) ₂ C=S	1	91	4.7:1
7	Ph ₃ P=S	1	92	5.5:1
8	n-Bu ₃ P=S	1	72	6.1:1
9	Cy ₃ P=S	1	93	1.7:1
10	(Me ₂ N) ₃ P=S	1	97	2.5:1
11	(CH ₂) ₄ S	1	97	5.8:1
12	Me ₂ S	3	45	5.8:1
13	(PhS) ₂	3	2	NA
14	n-Bu ₃ P=Se	1	77	8.5:1
15	(Me ₂ N) ₃ P=Se	1	95	4.6:1
16	(PhSe) ₂	1	82	10:1
17	n-Bu ₃ P	2	94	5.1:1
18	(Me ₂ N) ₃ P	2	53	1.4:1
19	I ₂	3	10	24:1
20	TFA	3	0	NA

It is observed that most of the classic bromolactonization reactions are variants of iodolactonization reactions and therefore will not be discussed here. Instead, recent developments in expanding the scope of racemic halolactonization are summarized in Table 1.2.

Table 1.2 Recent efforts in racemic bromolactonization.²⁵

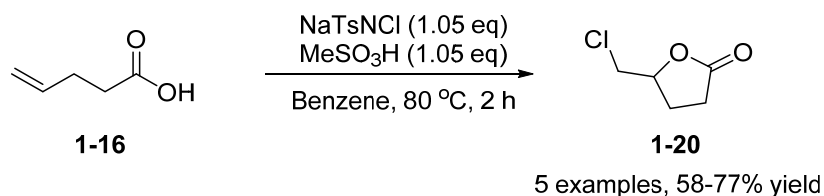
Entry	Conditions	Additives	Time (h)	Yield (%)
1	Br ₂ , Et ₂ O	aq NaHCO ₃ (excess)	24	32
2	Br ₂ , CH ₂ Cl ₂	Tl ₂ CO ₃ (80 mol%)	24	54
3	NBS, THF	-	24	46
4	NBS, DMF	-	24	34
5	NBS, CDCl ₃	-	15	15
6	NBS, CH ₂ Cl ₂	-	24	57
7	NBS, CH ₂ Cl ₂	-	54	99
8	NBS, CH ₃ CN	(PhSe) ₂ (5 mol%)	2	55
9	NBS, CDCl ₃	1-18	0.3	100
10	NBS, CDCl ₃	DMF (100 mol%)	0.5	100
11	NBS, CDCl ₃	DMA (10 mol%)	0.5	89
12	NBS, CDCl ₃	1-19 (1 mol%)	0.25	92
13	NBS, CH ₂ Cl ₂	3 Å MS	4.5	98



In the past two decades, most efforts were focused on increasing the rate and efficiency of bromolactonization. The use of NBS as the electrophilic halogen source has also gained popularity over the years due to the ease of handling the reagent, as well as the relative unreactivity of the reagent such that uncatalyzed and consequently unselective bromolactonization can be minimized. A number of useful additives that can efficiently activate NBS for bromolactonization reactions

have been identified and they consist of diselenides, 2-iodobenzylamides, Lewis bases as well as simple molecular sieves (Table 1.2, entries 9-12).

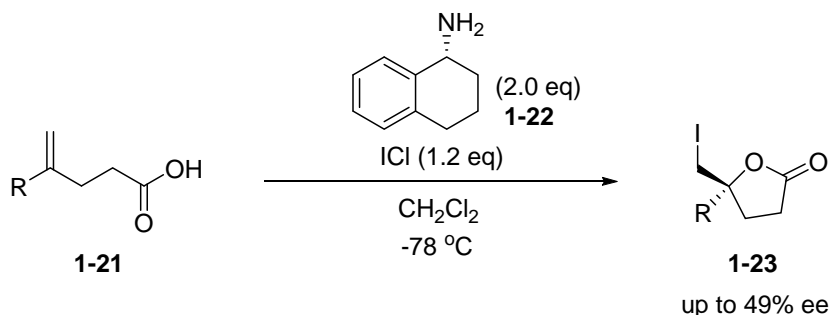
Chlorolactonization was the latest to be discovered amongst the halolactonization reactions and it is also the least developed variant as well. The first reported chlorolactonization was carried out with an aqueous mixture of CaCl_2 and HOCl .¹⁵ The relatively less reactive alkyl chloride obtained through the reaction was probably one of the reasons why bromo- and iodolactonization reactions are more developed. Another reason was perhaps the need to work with the hazardous chlorine gas, the most obvious and abundant chlorine source. This however did not prevent Woodward and Singh from utilizing chlorine gas to achieve a chlorolactonization as a key step in the total synthesis of allo-patulins.²⁶ Later on, chloramin-T was identified as an effective substitute for chlorine gas (Scheme 1.7).²⁷



Scheme 1.7 Chloramin-T as an effective electrophilic chlorine source.

1.5.2 Asymmetric Halolactonization

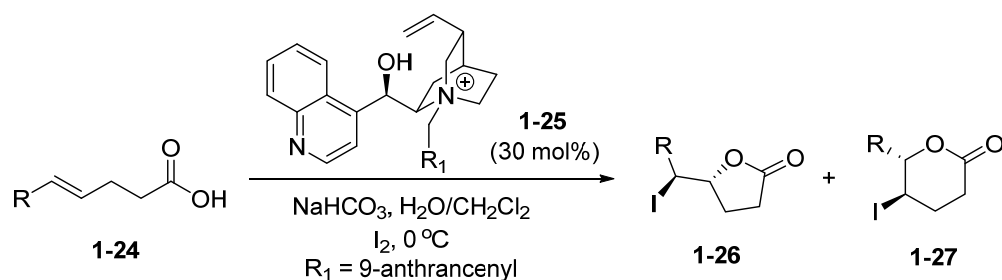
One of the earliest work on enantioselective halolactonization was carried out by Wirth and co-workers (Scheme 1.8).²⁸ Two equivalents of commercially available chiral primary amine **1-22** together with ICl were used to form halogen-amine complexes that effect the cyclization reaction. The enantioselectivity observed for these transformations were moderate and at that point in time, these results served as good starting point for further development of this class of reaction.



Scheme 1.8 Iodolactonization using chiral primary amine and ICl.

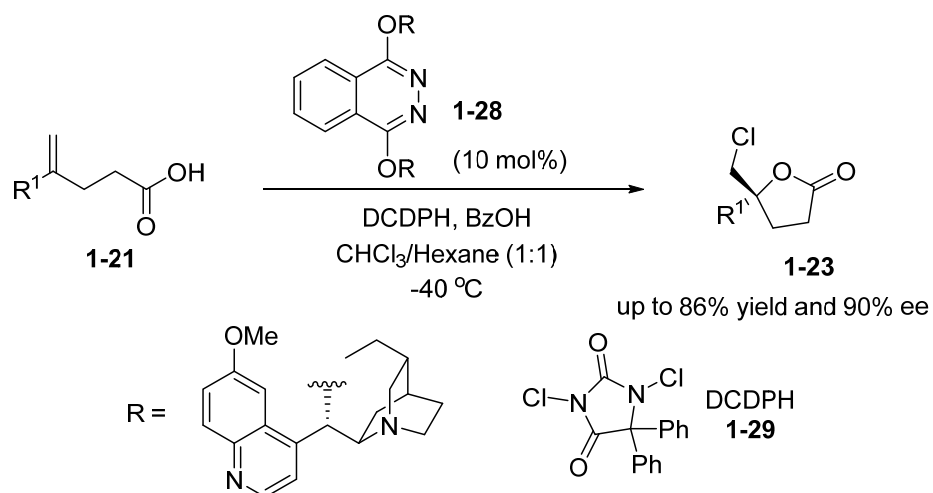
Gao and co-workers then reported the asymmetric iodolactonization of *trans*-1,2-disubstituted olefin **1-24** (Scheme 1.9).²⁹ In the report, a quaternary ammonium salt **1-25** derived from cinchonidine was employed as an effective phase-transfer catalyst for the iodolactonization reaction to give a mixture of the 5-membered ring lactone **1-26** and 6-membered ring lactone **1-27**. The authors suggested that NaHCO_3 first deprotonates the carboxylic acid such that the carboxylate forms an ionic interaction with the chiral quaternary ammonium salt

1-25. The bulky chiral cation **1-25** maintains association during the nucleophilic capture, inducing chirality of the lactones **1-26** and **1-27** formed in the process. The enantioselectivity obtained from the reaction were moderate, with 42% ee obtained for the 5-membered ring lactone **1-26** and 31% ee obtained for the 6-membered ring lactone **1-27**. However, these moderate enantioselectivities obtained were sufficient as a proof of concept of asymmetric halolactonization at that point in time.



Scheme 1.9 Quarternary ammonium salt catalyzed enantioselective iodolactonization.

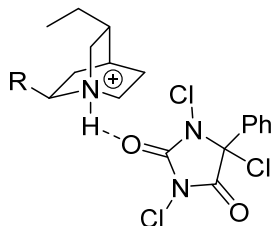
Next, Borhan and co-workers developed a protocol for the enantioselective chlorolactonization of 1,1-diolefinic acids **1-21**, giving the 5-membered chlorolactone **1-23** as the sole product in the reaction (Scheme 1.10).^{21d} (DHQD)₂PHAL **1-28** was utilized as the catalyst while 1,3-dichloro-2,2-diphenylhydantoin (DCDPH) **1-29** was used as the electrophilic chlorine source in the reaction.



Scheme 1.10 Borhan's (DHQD)₂PHAL **1-28** catalyzed enantioselective chlorolactonization.

The authors suggested two possible mechanisms for the reaction. The first involved the protonation of the quinidine nitrogen with BzOH followed by the formation of the ammonium–DCDPH complex before the transfer of the chloronium to the olefin. The second mechanism proposed was via the activation of DCDPH by the formation of a tertiary amine–chloronium species. After this ionic interaction has been formed, the second equivalent of chlorine can then be delivered to the olefin (Figure 1.5).

Proposed Mechanism A:



Proposed Mechanism B:

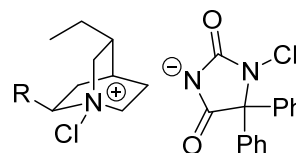
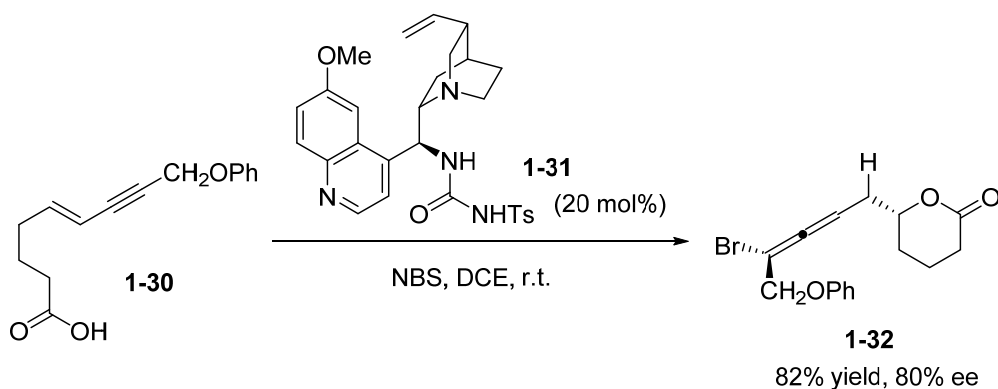


Figure 1.5 Plausible mechanisms for the activation of DCDPH **1-29**.

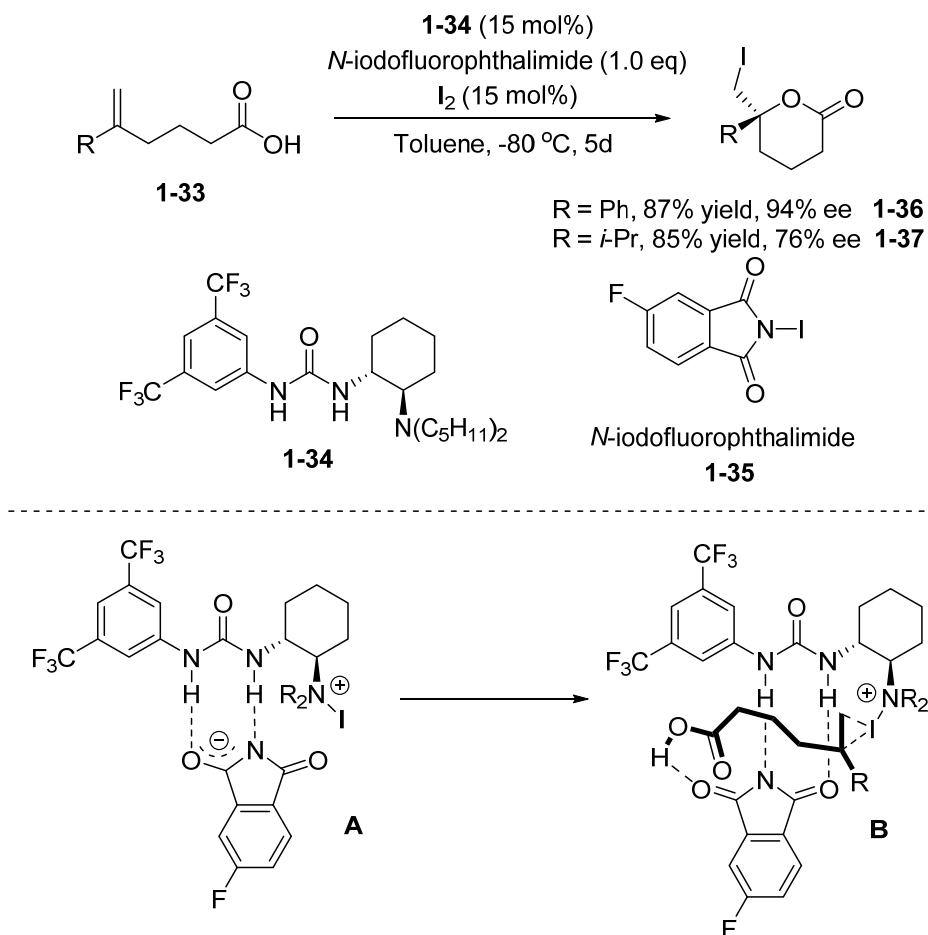
Concurrently, Tang and co-workers developed a cinchonidine-derived amino-urea bifunctional catalyst **1-31** for the bromolactonization of enynes (Scheme 1.11).³⁰ The elegant reaction produced stereospecific allenes as products.



Scheme 1.11 Amino-urea catalyzed bromolactonization of enyne **1-30** to yield allene **1-32**.

The authors suggested that bifunctionality of the catalyst allows it to effect the bromolactonization by deprotonating of the carboxylic acid while forming hydrogen bonds with NBS.

In another example involving chiral ion pair catalysis, Jacobsen and co-workers utilized an anion binding strategy for the iodolactonization of 1,1-disubstituted olefin acids **1-33** with a urea type catalyst **1-34** while using *N*-iodofluorophthalimide **1-35** as the iodine source (Scheme 1.12).³¹ It was observed that both alkyl-type and arene-type substrates were able to cyclize with high enantioselectivity.

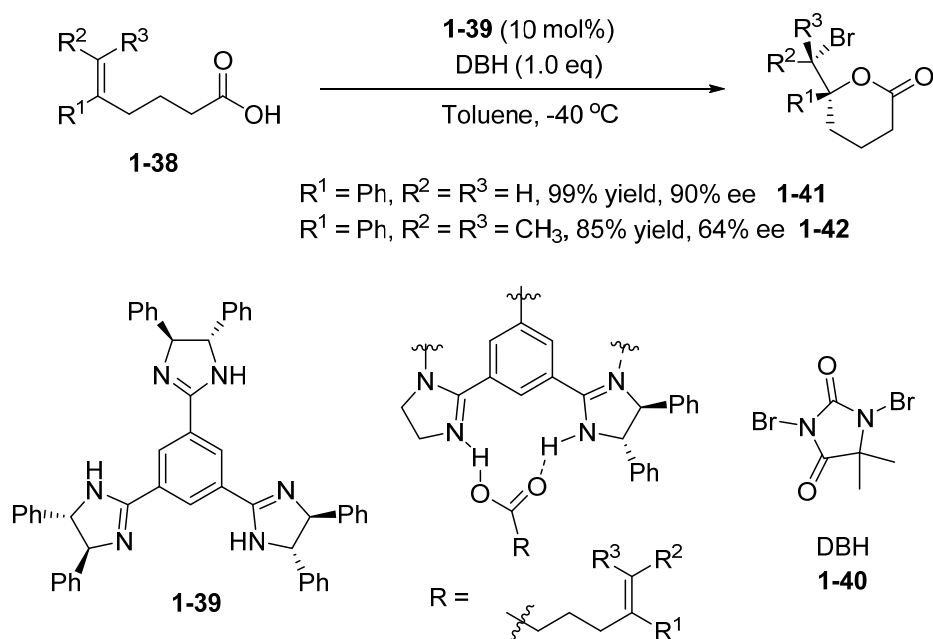


Scheme 1.12 Aminourea catalyzed iodolactonization.

Iodine was added as an additive and it was proposed that its main function is to form an activated complex with *N*-fluorophthalimide **1-35**. The mechanism of the reaction is believed to be the binding of the urea moiety to *N*-fluorophthalimide, with the amine acting as a Lewis base for the formation of complex **A**. The resulting iodo-ammonium ion delivers the iodonium ion to the olefin **1-33** while the *N*-fluorophthalimide **1-35**, which is still hydrogen bonded to the urea, assists in the deprotonation of the carboxylic acid. It was postulated that the highly

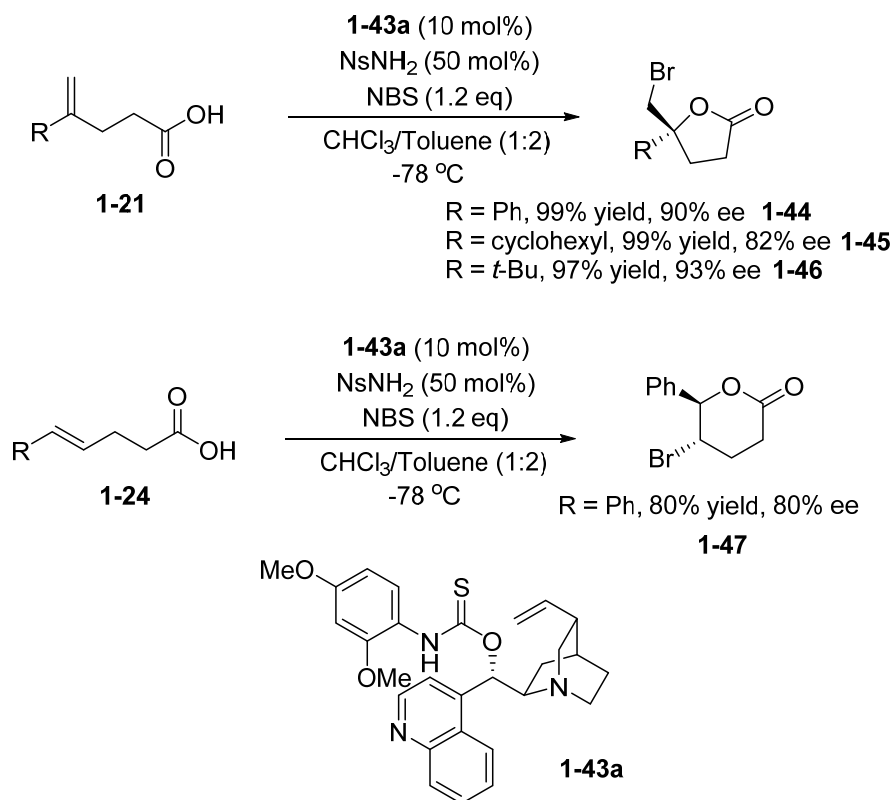
electron-withdrawing fluorine atom on the phthalimide helps in the formation of the iodonium ion by weakening the N–I bond of the phthalimide and enhances the rate of reaction. The enantioselectivity was observed to be poor when other halogen sources were used instead.

In the same year, Fujioka reported another attractive C_3 -symmetric trisimidazoline catalyst **1-39** which was used to catalyze the bromolactonization of 1,1-disubstituted, tri- and tetra-substituted olefins **1-38**.³² Stoichiometric amounts of 1,3-dibromo-5,5-dimethylhydantoin (DBH) **1-40** was employed as the electrophilic bromine reagent. Although all the substrates reported were 5-aryl-5-hexenoic acids, it was shown that various aromatic and aliphatic groups can be accommodated in the R^2 and R^3 position of the tri- or tetra-substituted olefin **1-38**. Fujioka further explained the origin of the catalysis by proposing the deprotonation of the carboxylic acid forming the imidazolinium–carboxylate ion pair. The chiral imidazolinium then directs the carboxylate for the enantioselective nucleophilic capture of the bromiranium ion which was formed on the olefin.



Scheme 1.13 C_3 -Symmetric trisimidazoline catalyzed bromolactonization.

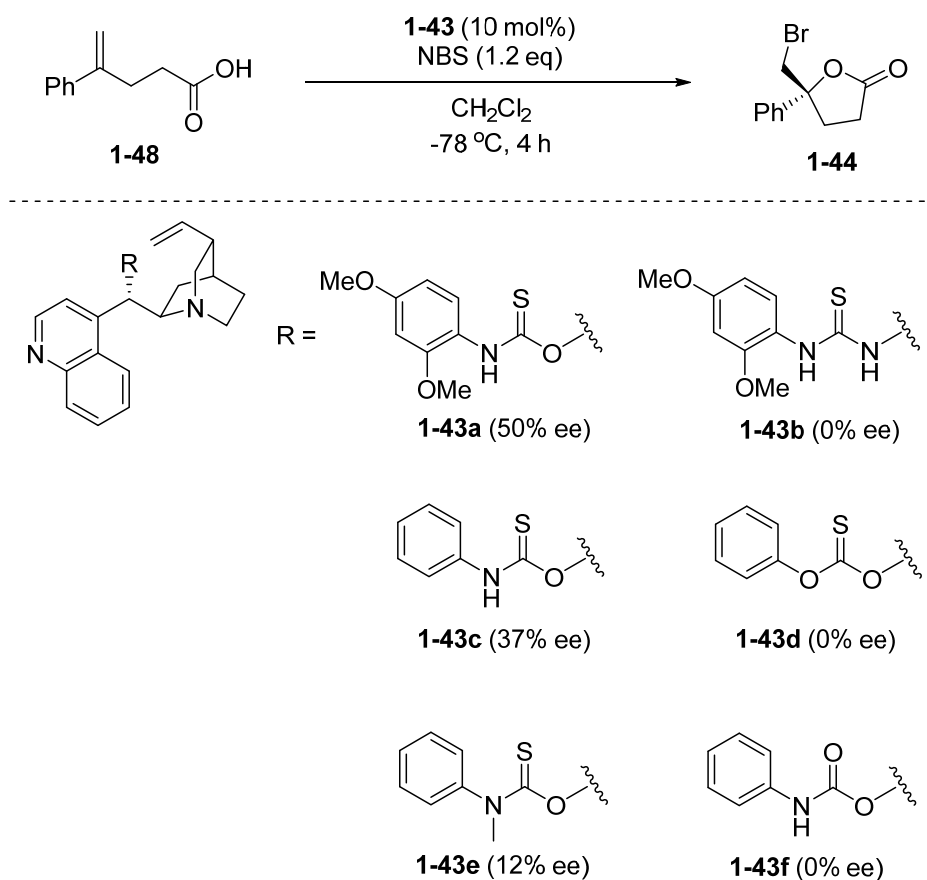
More recently, our group demonstrated that asymmetric bromolactonization can be carried out with the use of a novel bifunctional catalyst (Scheme 1.14).³³ The bifunctional catalyst **1-43a** consist of a Brønsted base (amino group) and a Lewis base (thiocarbamate) on the cinchona alkaloid scaffold. Both 1,1-disubstituted **1-21** and trans-1,2-disubstituted **1-24** olefinic acid were able to undergo the cyclization to excellent yields and ee.



Scheme 1.14 Amino-thiocarbamate catalyzed enantioselective bromolactonization.

Some mechanistic insights were obtained through the synthesis of various analogues of the catalyst. When the Lewis basic sulfur atom was replaced with an oxygen atom (catalyst **1-43f**), the reaction produced products with no ee. Similarly, when the N–H of the thiocarbamate was replaced with an oxygen atom, the resulting thiocarbonate **1-43d** offered no enantioselectivity. When the oxygen atom of the thiocarbamate was replaced with the N–H group, the thiourea catalyst **1-43b** furnished no enantioselectivity as well. The enantioselectivity of the catalyst dropped significantly when the nitrogen of the thiocarbamate was

methyated (catalyst **1-43e**). The series of experiments concluded the importance of the Lewis basic sulfur atom as well as N-H moiety in achieving high enantioselectivity in the bromolactonization reaction.



Scheme 1.15 Enantioselectivity of selected analogues of amino-thiocarbamates.

Further experiments also found that aryl substituents on the nitrogen of the thiocarbamate were necessary to furnish any enantioselectivity. For example, the phenyl substituent gives lower enantioselectivity as opposed to 2,4-

dimethoxyphenyl substituent. These results suggested that the catalyst reactivity might be tunable by modifications to the *N*-aryl substituents.

The results from these studies, together with the known reactivity of sulfur containing catalyst (from Denmark's work), were then used as a follow-up in suggesting the mode of action of the catalyst. It was proposed that the N–H moiety forms a hydrogen bond with NBS such that the Lewis basic sulfur atom of the thiocarbamate is in proximity to the bromine atom and can activate it (through the Lewis base activation of Lewis acid concept described earlier) (Figure 1.6). The catalyst then delivers the bromonium ion to the olefin while the nitrogen atom of quinuclidine deprotonates the carboxylic acid and directs the carboxylate nucleophile towards the bromiranium enantioselectively.

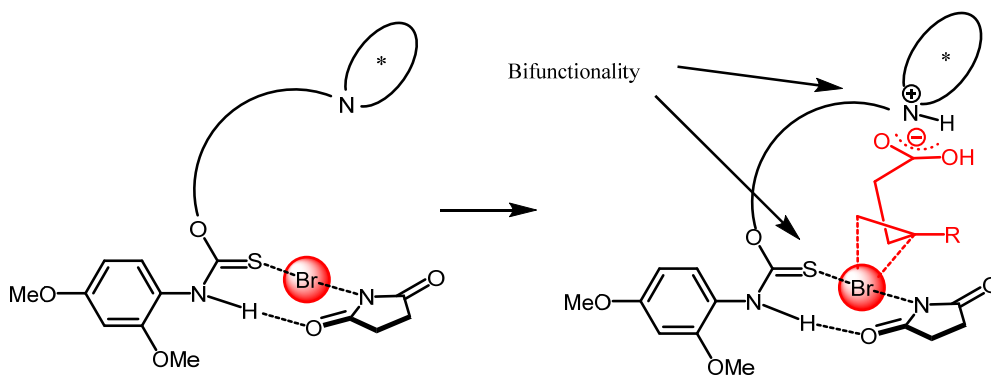
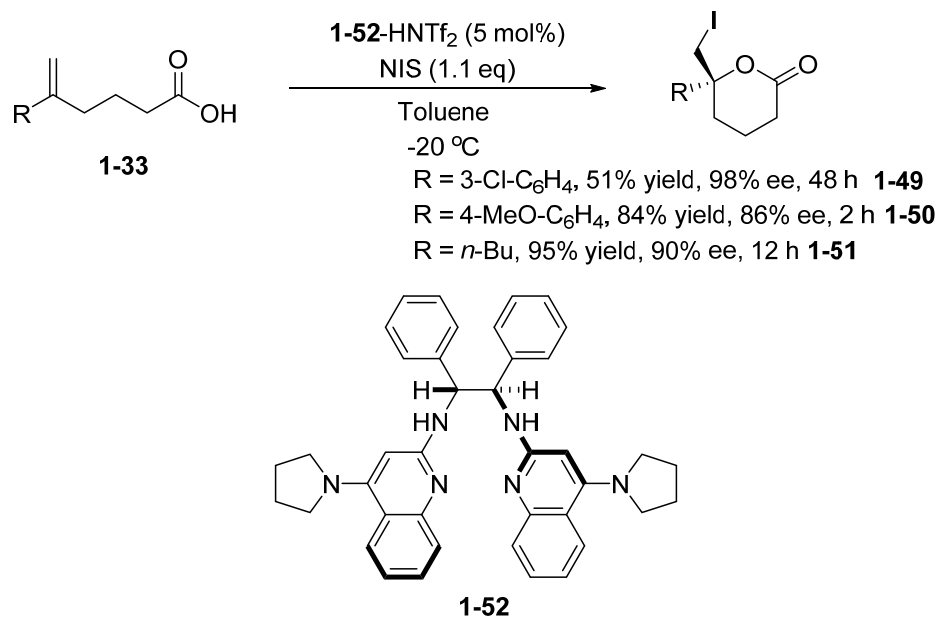


Figure 1.6 Proposed mechanism of the aminothiobicarbamate catalyzed bromolactonization.

Lastly, an asymmetric iodolactonization of 1,1-disubstituted hexenoic acid **1-33** was reported by Johnston and co-workers (Scheme 1.16).³⁴ The reaction which

was catalyzed by stilbene bis(4-pyrrolidinylquinoliny)l) bisamidine hydrogen triflimide **1-52**-NHTf₂, furnished products in high enantioselectivity and good yields. Although the reaction was very selective to 1,1-disubstituted alkenes, it appears that the enantioselectivity of the catalyst is not significantly affected by the electronic properties of the substrates. Interestingly, the reaction rates for electron-rich aryl substituents were much higher than electron-deficient aryl substituents. The authors suggested that the substrate is activated by a Brønsted base through the deprotonation of the carboxylic acid to generate the carboxylate, whereas NIS is activated by a Brønsted acid. However, since there are several Brønsted basic sites on the catalyst, it was difficult for the authors to pin-point the exact origin of the stereoselectivity.



Scheme 1.16 Iodolactonization catalyzed by **1-52**-HNTf₂.

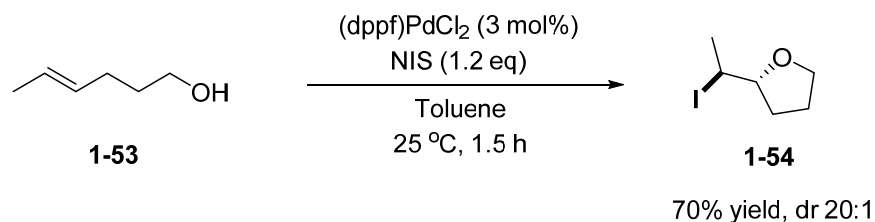
1.6 Haloetherification Reactions

Haloetherification is an extremely important synthetic transformation that can produce substituted cyclic ethers such as oxetanes, tetrahydrofurans, tetrahydropyrans and larger ring systems. Although it is a reaction that was discovered later in compared halolactonization, its development has been similar to that of halolactonization. Effective racemic reactions using stoichiometric reagents are well-known and thus less effort is spent on improving them. Instead, most of the current efforts are devoted to achieving the more challenging task of carrying out asymmetric haloetherification.

1.6.1 Racemic Haloetherifications

The first example of haloetherification was reported by Williams and co-workers in which 4-pentenyl alcohol was treated with iodine in aqueous potassium iodide to furnish the substituted tetrahydrofuran as the sole product.^{21d} It was nearly 20 years later that Yoshida and co-workers did a thorough investigation of iodoetherification reactions.³⁵ A range of simple olefinic alcohols were subjected to several cyclization conditions and it was observed that the iodine–NaHCO₃ system was the preferred protocol.

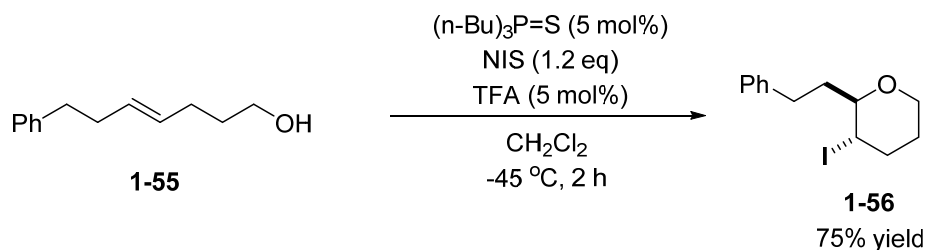
More recent efforts in development of racemic iodoetherification focus on using catalysts to activate milder iodination reagent such as NIS. One elegant piece of work by Morgan and co-workers uses a low loading of (dppf)PdCl₂ as catalyst (Scheme 1.17).³⁶ The reaction conditions allowed the iodoetherification to be completed rapidly with good yields obtained.



Scheme 1.17 (dppf)PdCl₂ catalyzed iodoetherification.

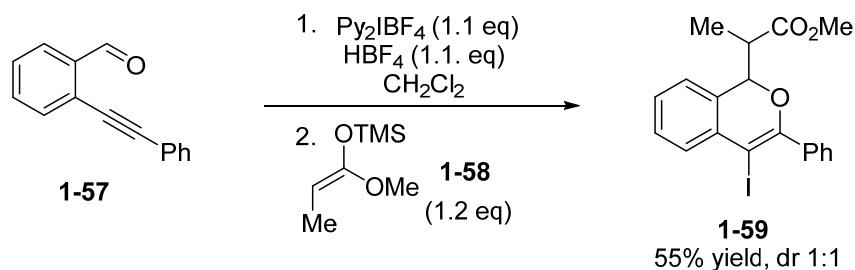
Iodoetherification reactions also proceeded well with Denmark's Lewis base activation protocols (Scheme 1.18).^{8b, 24} Both reaction rate and selectivity for

iodoetherification was markedly improved by using Lewis base to activate NIS for the reaction.



Scheme 1.18 Selected example of Lewis base catalyzed iodoetherification.

Apart from the standard olefinic alcohols, it has also been shown that iodoetherification can also be carried out on non-alcohol substrates. For example, Barluenga demonstrated that the oxygen atom of an aldehyde may behave like a nucleophile and attack an iodonium ion formed on an alkyne (Scheme 1.19).³⁷ Silyl ketene acetal **1-58** was then added as an external secondary nucleophile to quench the oxonium intermediate to furnish the interesting heterocyclic product **1-59**.



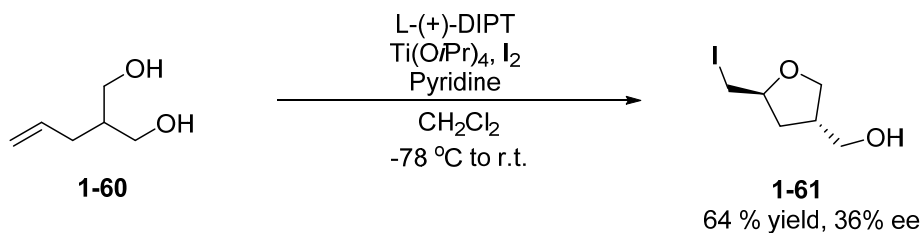
Scheme 1.19 Example of non-alcohol substrate undergoing iodoetherification.

In contrast to iodoetherification, there are fewer reports on bromoetherification, and thus the bromine variant has been utilized to a much lesser extent. The earliest report on such a transformation utilized bromine and a base in organic solvent.³⁸ More bromoetherification reagents were subsequently shown to be able to effect bromoetherification then after. In particular, 2,4,4,6-tetrabromo-2,5-cyclohexadienone (TABCO) has been used as an effective halogen source and was used in two natural product total syntheses in the late 1980s and early 1990s.³⁹

1.6.2 Asymmetric Haloetherifications

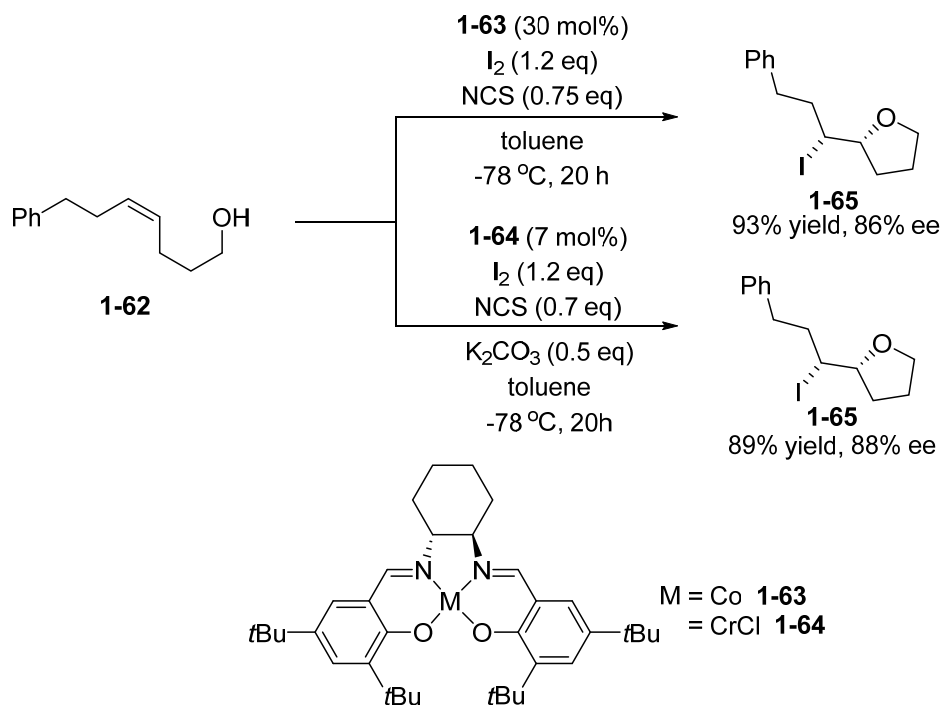
In contrast to asymmetric halolactonization, there are significantly less reports on asymmetric haloetherification. The development of such transformations is particularly challenging as an efficient method for asymmetric haloetherification lies in improving the rate of nucleophilic capture as opposed to the olefin-olefin halogen exchange which causes racemization.⁴⁰

One of the first reports of an enantioselective haloetherification was the desymmetrization of a diol via a haloetherification process reported by Taguchi and co-workers (Scheme 1.20).⁴¹ The symmetrical olefinic diol **1-60** was treated with Lewis acidic $\text{Ti}(\text{OiPr})_4$, iodine, pyridine and L-(+)-diisopropyl tartrate results in the desymmetrization of the diol and the formation of an iodoether product **1-61** with some appreciable enantioselectivity.



Scheme 1.20 Asymmetric desymmetrizing haloetherification catalyzed by Ti(OiPr)₄.

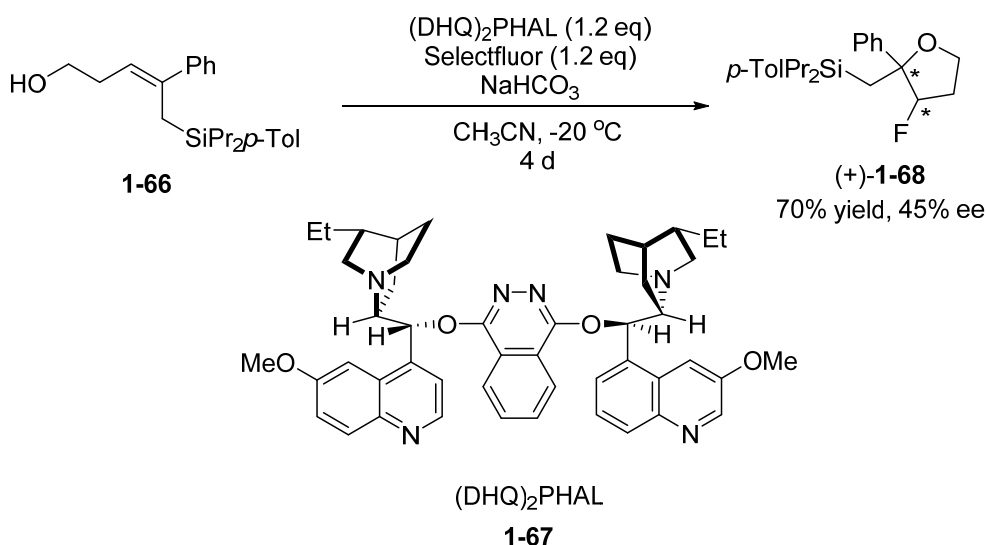
Kang and co-workers then reported a Lewis acid catalyzed iodoetherification of (*Z*)-5-substituted-5-pentenols giving 2-substituted tetrahydrofurans with good yields and enantioselectivity.¹² Salen complexes of cobalt (II) **1-63** and chromium (III) **1-64** were used as the Lewis acid catalyst, and it was observed that both metal complexes gave similar yields and enantioselectivity.



Scheme 1.21 Co(II) and Cr (III) salen complexes catalyzed iodoetherifications.

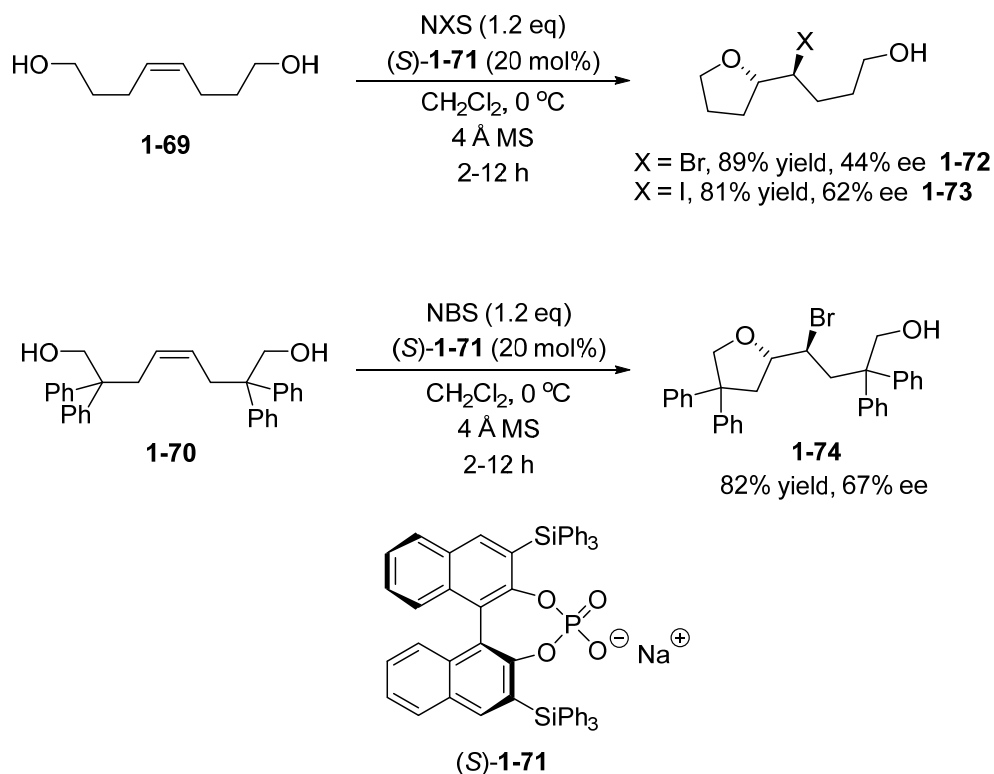
The atypical reaction conditions, in which two electrophilic halogen sources, iodine and NCS, were utilized, resulted in the proposal of two plausible mechanisms for the reaction. The first postulates that the NCS reacts with iodine to form ICl which can be further activated by the Lewis acid catalyst. In this proposal, it is important that ICl is formed and released slowly into the system as opposed to the use of ICl reagent itself. This is to minimize the uncatalyzed reaction when high concentration of ICl is present in the reaction mixture. In the second proposal, NCS is thought to oxidize Cr (III) to a chromium species with higher oxidation state and this helps to enhance the Lewis acidity. The iodoetherification proceeds after this newly formed chormiun species activates the iodine in the system.

Enantioselective fluorocyclization of alkenes are rare; in fact, the only example that gave appreciable enantioselectivity was reported by Gouvernuer in 2009 (Scheme 1.22).⁴² (DHQ)₂PHAL **1-67** was employed to induce the chirality while Selectfluor was used as the electrophilic fluorine source. Mechanistically, the fluorocyclization pathway differs from typical bromo or iodocyclization reactions. The reaction, as postulated by the author, does not form the 3-membered cyclic fluoronium species, but instead, proceeds via the formation of a carbocation intermediate that is stabilized by the silane moiety.



Scheme 1.22 Enantioselective fluorocyclization catalyzed by (DHQ)₂PHAL.

Several reports of enantioselective haloetherification surfaced in 2010. Hennecke was the first to introduce chiral phosphate counter anions in halocyclization reactions by utilizing chiral sodium phosphates **1-71** in the desymmetrizing haloetherification of olefinic diols (Scheme 1.23).⁴³

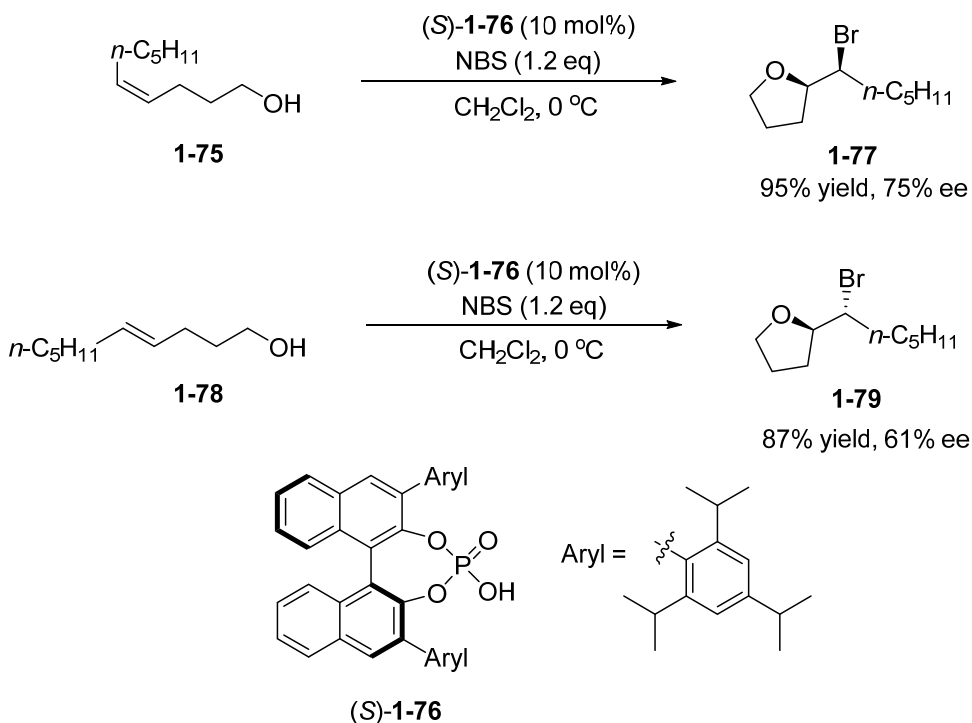


Scheme 1.23 Enantioselective desymmetrizing haloetherification using chiral phosphates.

Despite the lack of substrate scope and moderate enantioselectivities that were obtained, this report was an elegant proof of concept. Since the haliranium ion formed is meso, the observed enantioselectivity confirms the existence of an association of the chiral phosphate anion with the haliranium intermediate until nucleophilic capture is accomplished. The author suggested that the phosphate anion acts like a Lewis base which could have potentially formed the phosphate hypoiodite intermediate.

Two other enantioselective haloetherification protocols were developed by both Denmark and Shi at the same time. Both groups employed the same chiral phosphoric acid catalyst (*S*)-**1-76** in their reactions, but there were key differences in terms of their reaction conditions, and this also led to possible mechanistic differences in the reactions.

In the Shi system, (*S*)-**1-76** was utilized as the only catalyst in the system (Scheme 1.24).⁴⁴ Generally, it was observed that both the (*Z*)-olefins **1-75** and (*E*)-olefins **1-78** can undergo cyclization to give exocyclic bromofurans with moderate to good enantioselectivity.



Scheme 1.24 Shi's bromoetherification catalyzed by chiral phosphoric acid.

The author postulated that the observed enantioselectivity is based on a transition state whereby the substrate functions as a hydrogen bond donor while NBS acts as a hydrogen bond acceptor and coordinates to the catalyst (Figure 1.7). The chiral phosphoric acid, possessing both acidic and basic sites, acts as a bifunctional catalyst to activate both NBS and the hydroxy group of the substrate prior to nucleophilic capture.

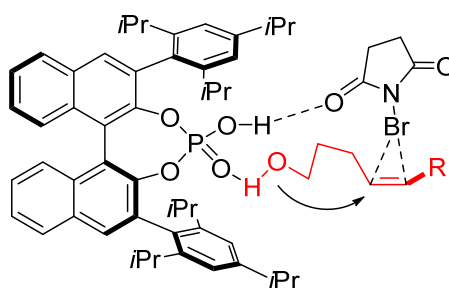
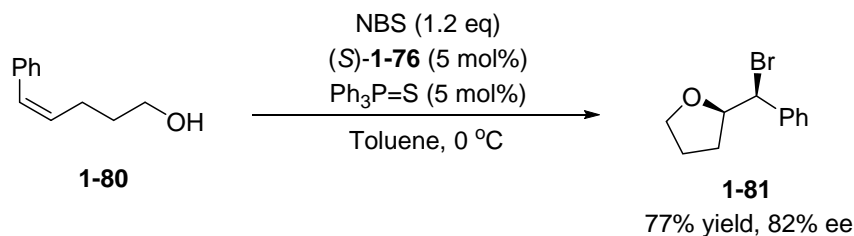


Figure 1.7 Proposed transition state for Shi's bromoetherification.

In comparison, in Denmark's system, triphenylphosphine sulfide was used as a co-catalyst that may have invoked in a different reaction pathway. Similar to Shi's case, both (*Z*)- and (*E*)-olefins gave the product of exocyclization with good to excellent enantioselectivity using the Denmark protocol.⁴⁵ The efficiency of the catalytic system was demonstrated using aryl substituted olefinic substrates as opposed to Shi's report where he worked predominantly alkyl substituted olefins.



Scheme 1.25 Denmark's bromoetherification using chiral phosphoric acid.

Denmark proposed a cooperative activation of NBS by both the chiral phosphoric acid and the Lewis basic triphenylphosphine sulfide (Figure 1.8). He postulated that a phosphate hypobromite species which is initially formed transfers bromine to the substrate while using hydrogen bonding to maintain association with the substrate.

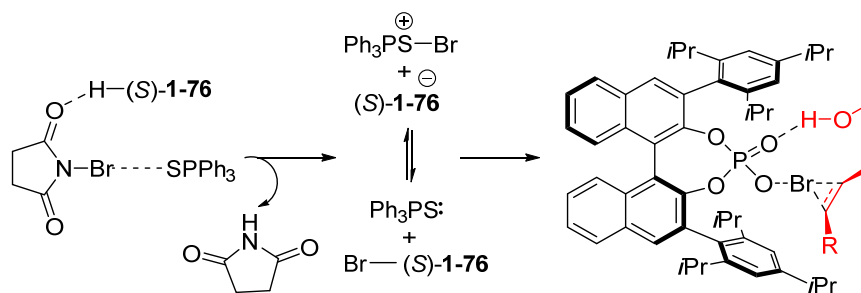


Figure 1.8 Proposed transition state for Denmark's bromoetherification.

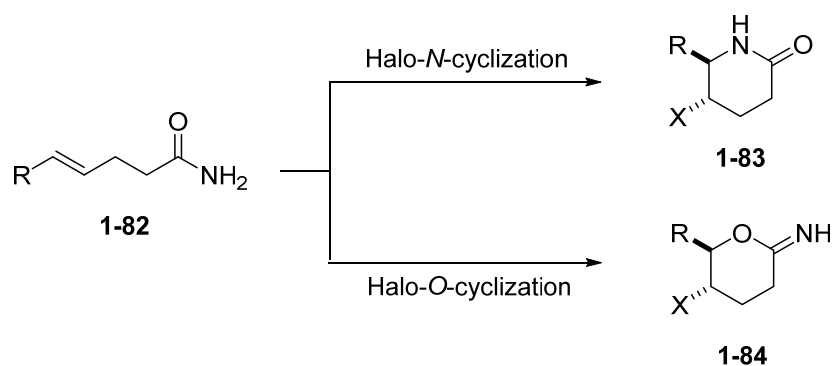
The distinct lack of asymmetric haloetherification methods shown in this discussion above (five examples with only three that gives any useful enantioselectivity) can be attributed to the slow rate of nucleophilic capture as opposed to the rate of catalyst-bromonium ion dissociation. As such, this triggers the need for more asymmetric haloetherification to be developed and it is foreseen

that there will be continued interest in developing enantioselective haloetherification strategies in the near future.

1.7 Halolactamization and Haloamination Reactions

The two halocyclization reactions introduced thus far in this discussion belong to the class of halo-*O*-cyclization. It is also important to emphasize the importance of halo-*N*-cyclization as it allows the addition of a halogen together with a nitrogen functionality across a carbon-carbon double bond. This is viewed as an extremely important transformation to synthetic chemists as it provides access to important pharmaceutical intermediates as well as biologically active natural products.⁴⁶

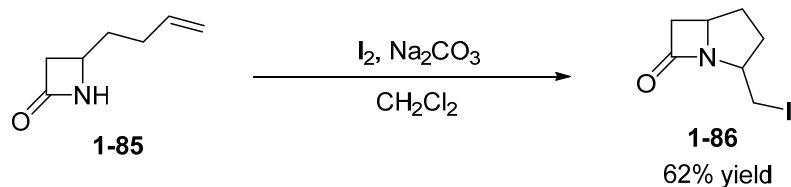
Such transformations, however, are usually far more challenging to execute than it may appear to be. This is due to the inherent nature of the relatively more electronegative amide oxygen atom that causes the *O*-cyclization to be more favourable as compared to the *N*-cyclization (Scheme 1.26). As such, most attempts in the development of halolactamization have focused on enhancing the electronegativity of the nitrogen atom such that its nucleophilicity is higher than that of the oxygen atom.



Scheme 1.26 Competing halo-*N*-cyclization and halo-*O*-cyclization for olefinic amides.

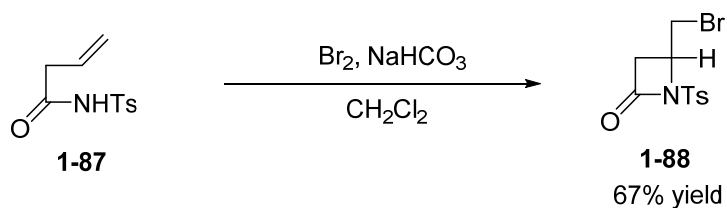
1.7.1 Racemic Halolactamization and Haloamination Reactions

The earliest halolactamization was demonstrated by Durst and co-workers who avoided the fundamental reactivity issue by choosing a highly constrained olefinic lactam **1-85** as the substrate (Scheme 1.27).⁴⁷ The reaction was conducted in CH_2Cl_2 with iodine used as the electrophilic halogen source and Na_2CO_3 a proton scavenger. For this geometrically constrained system, the oxygen atom is positioned far from the cyclic iodonium ion such the *O*-cyclization will not precede, thus forming the *N*-cyclized product **1-86**.



Scheme 1.27 Halolactamization performed on a highly constrained olefinic lactam.

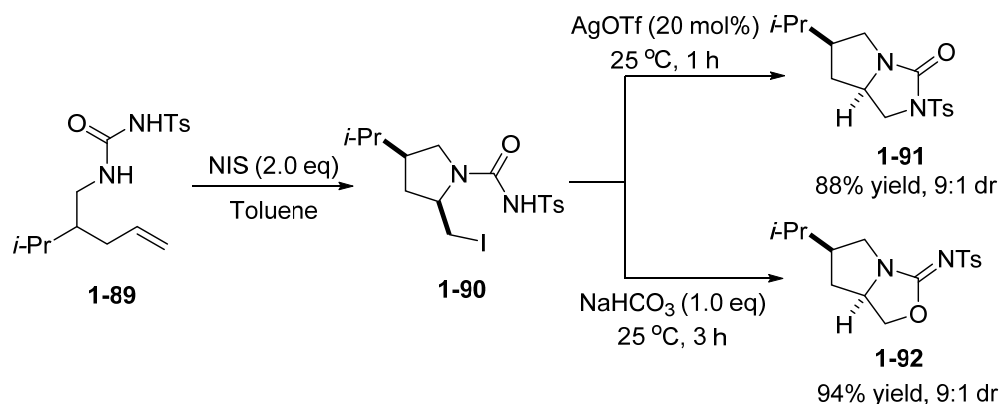
The genuine solution was however presented by Ganem and co-workers when *N*-tosylated amide **1-87** was used instead of the unfunctionalized amide (Scheme 1.28).⁴⁸ The tosylation of the amide increased the electronegativity on the nitrogen atom which resulted in the nitrogen becoming more nucleophilic as compared to the oxygen atom. Thus, the resulting product **1-88** formed was predominantly *N*-cyclized.



Scheme 1.28 *N*-tosylated amide bromolactamization.

With this report setting a precedent, soon after, more *N*-haloamination reactions were discovered, many of which were by simple modifications of the functional group attached on the nitrogen atom as well as the type of halogen used. The typical starting materials include ureas⁴⁹, thioimides⁵⁰, and oxazolines⁵¹ and *O*-acyl hydroxamates.⁵²

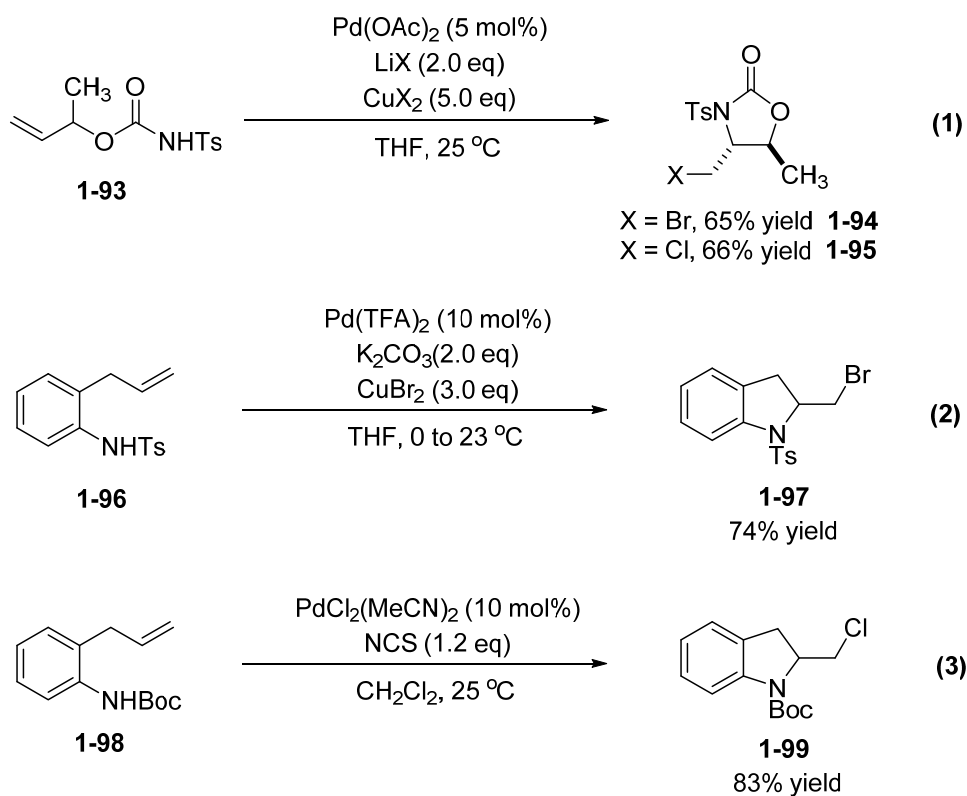
More recently, Widenhoefer and Li used *N*-tosylated ureas with NIS to produce bicyclic ureas **1-91** and isoureas **1-92** (Scheme 1.29).⁴⁹ The first step involves an *N*-iodocyclization to form the *N*-protected pyrrolidine **1-90**. The use of AgOTf in the subsequent step enabled the bicyclic urea **1-91** to be formed, while switching to the use of NaHCO₃ produced the isourea derivative **1-92**.



Scheme 1.29 Synthesis of bicyclic ureas and isoureas using double cyclization strategy.

Lastly, several groups also utilized palladium catalysis to effect the *N*-halocyclization reaction. For example, Lu and co-workers demonstrated the use of CuBr₂ and LiBr in the presence of catalytic amounts of Pd(OAc)₂ for the bromolactamization of isoureas **1-93** (Scheme 1.30, equation 1).⁵³ The procedure was also readily adapted for chlorolactamization by using CuCl₂ and LiCl instead. Concurrently, Chemler and co-workers worked on the intramolecular bromoamination of *N*-tosylated allyl anilines **1-96** (Scheme 1.30, equation 2).⁵⁴

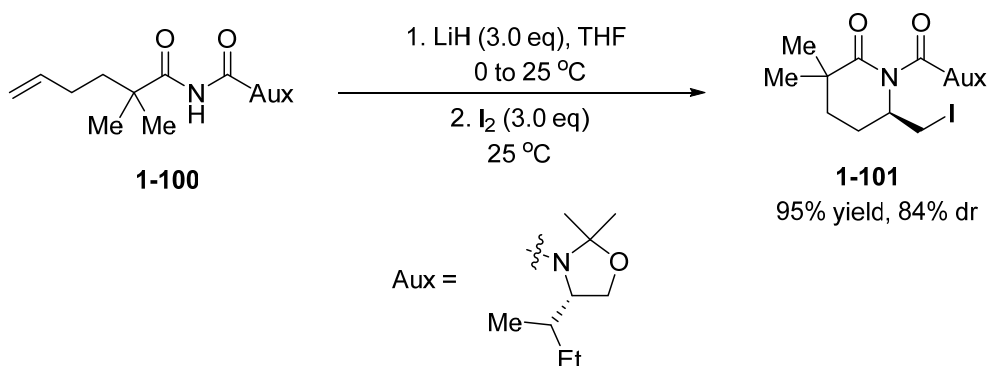
Indolines **1-97** were obtained as the products in the reaction which utilized catalytic amount of $\text{Pd}(\text{TFA})_2$ and stoichiometric amount of CuBr_2 in the reaction system. More recently, Michael and co-workers showed the feasibility of using catalytic $\text{PdCl}_2(\text{MeCN})_2$ with NCS as the halogen source for the 5-*exo*-chloroamination of *N*-Boc-*ortho*-allyl anilines **1-98** (Scheme 1.30, equation 3).⁵⁵



Scheme 1.30 Selected bromo- and chloro- *N*-cyclizations using palladium catalysis.

1.7.2 Asymmetric Halolactamization and Haloamination Reactions

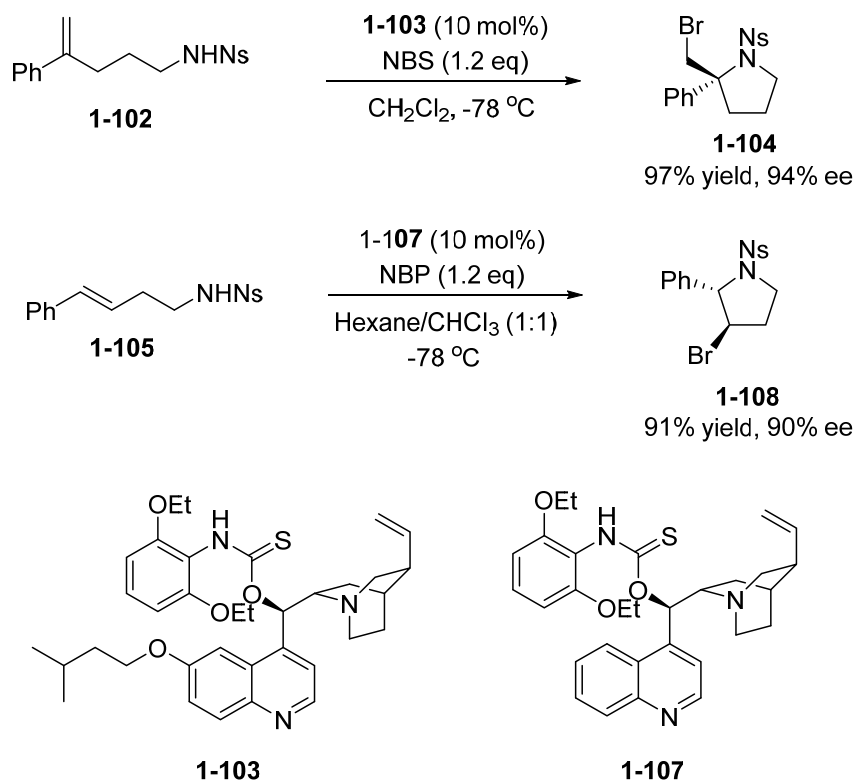
To the best of my knowledge, it was not until the 2004 that the first enantioselective halolactamization reaction was reported (Scheme 1.31).⁵⁶ In the account, an acyclic imide, attached with a chiral oxazolidine auxiliary was used for the induction of enantioselectivity, was utilized as the starting material. The cyclization was carried out firstly by the deprotonation of the imide **1-100** using LiH. Addition of iodine subsequently yielded the cyclic iodo-imides **1-101** in good yields and diastereoselectivity. The highly effective and stereoselective nature of the reaction was postulated to be due to the coordination of the lithium counterion to the oxygen atoms of the imide, creating a rigid intermediate.



Scheme 1.31 Chiral auxiliary induced enantioselective iodolactamization.

There was no follow-up of any enantioselective haloamination work until 2010 when Yeung and co-workers developed highly enantioselective bromoaminocyclization protocols using the amino-thiocarbamate catalysts

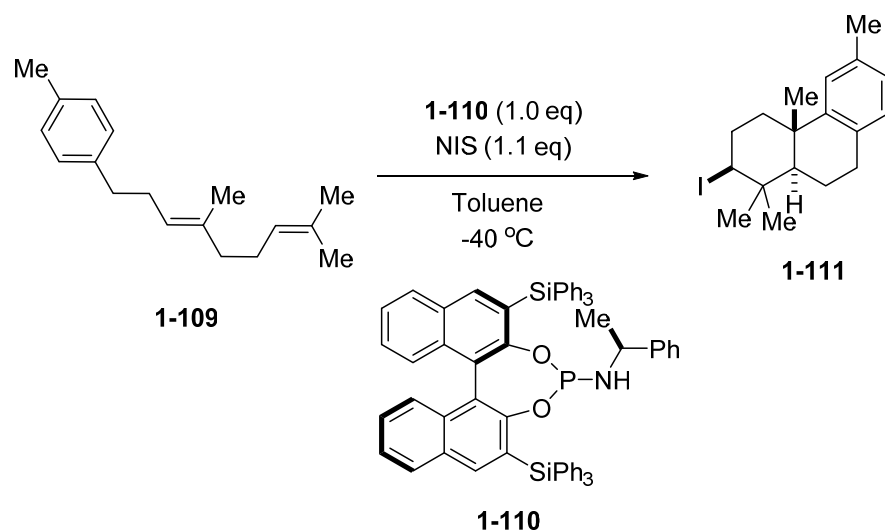
(Scheme 1.32).⁵⁷ This class of organocatalysts was previously reported as efficient catalyst for asymmetric bromolactonization reactions (Scheme 1.14). The aminocyclization reactions were somewhat analogous to the lactonization reactions, with the carboxylic acid functionality now exchanged for the sulfonamide moiety. To achieve high enantioselectivity, modified catalysts **1-103**, **1-107** were used, but the general structure of the catalysts remained the same. Both 1,1-disubstituted **1-102** and 1,2-trans-disubstituted **1-105** olefinic sulfonamides were subjected to the cyclization conditions yielding the 2,2-disubstituted pyrrolidine **1-104** and 2,3-disubstituted pyrrolidine **1-108** respectively.



Scheme 1.32 Amino-thiocarbamate catalyzed bromoaminoocyclization.

1.8 Other Halocyclization Reactions

Besides the three main classes of halocyclization reactions discussed above, there are two other types of reactions that are worth a discussion here. In 2007, Ishihara and co-workers showcased the catalytic ability of chiral phosphoramidite **1-110** in a highly enantioselective halopolyene cyclization reaction (Scheme 1.33).⁵⁸ Polyprenoids were utilized as the starting materials in the reaction with NIS as the halogen source.



Scheme 1.33 Enantioselective polyenecyclization catalyzed by chiral phosphoramidites.

The authors suggested that the chiral nucleophilic phosphoramidite **1-110**, used in stoichiometric quantities, activates the NIS such that it is held in place in a chiral environment. In dichloromethane, it was observed that only the racemic products were obtained. In toluene, however, the authors suggested that a stronger ion pair is formed such that hydrogen bonding between the succinimide counterion and the phosphoramidite N–H further restricted the rotation around the P–N bond, resulting to the better enantioselectivity observed.

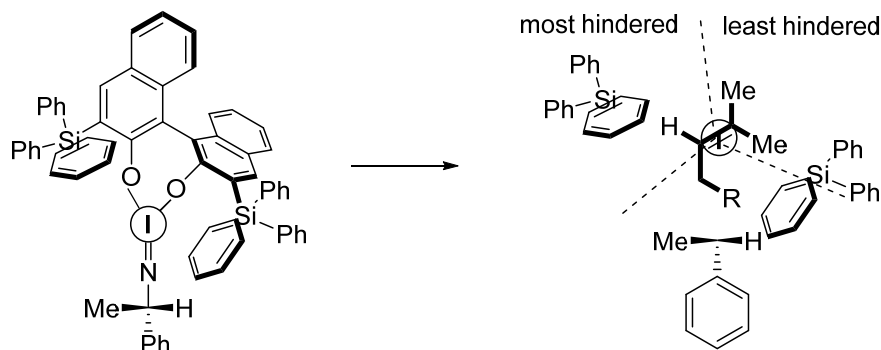
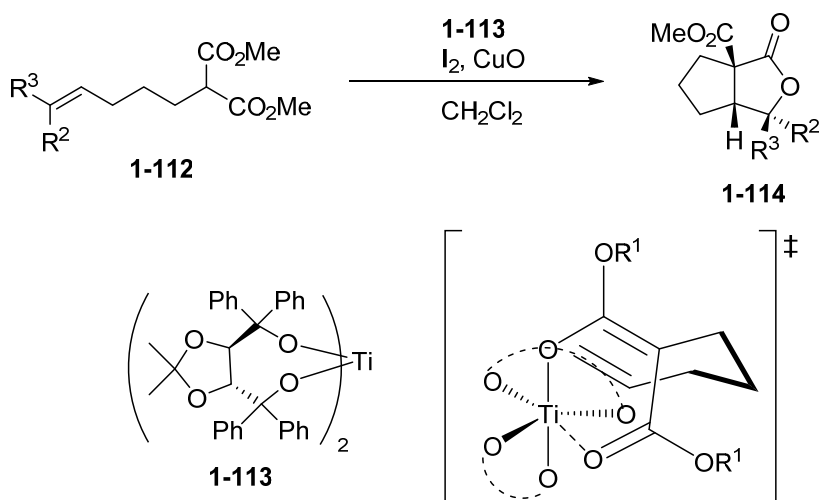


Figure 1.9 Ishihara's stereochemical model for the observed enantioselectivity.

Ishihara built a stereochemical model to explain the enantioselectivity obtained in the reaction (Figure 1.9). The reactive site is divided into three sectors as shown above with the most favourable conformation putting the sterically-demanding gem-dimethyl group in the least hindered position and the hydrogen atom in the most hindered position. This model was developed based on the assumption that any enantioselectivity obtained is kinetically controlled and the capture of the iodonium ion by the weak nucleophile is highly unlikely. In addition, the formation of a tricyclic product also suggests that the cyclic iodonium ion formation is reversible. The strategy was applied in the enantioselective syntheses of several halogenated cyclic terpenoids which are bioactive natural products isolated from marine organisms.

Such halocyclization reactions involving the intramolecular addition of a carbon nucleophile on an olefin that is activated by a halogenating reagent are rare. In fact, the only other report which may be worth mentioning is the

enantioselective iodocarbocyclization of 4-alkenylmalonate derivatives **1-112** reported by Taguchi and co-workers using a chiral titanium complex **1-113**.⁵⁹



Scheme 1.34 Chiral titanium complex catalyzed iodocarbocyclization.

It was postulated that the chiral spiro-titanate catalyst **1-113** most likely functions as a base instead of a Lewis acid, producing the chiral $Ti(IV)$ enolate by deprotonation of the malonate substrate. The transition state is postulated to be chair-like with one side of the enolate moiety shielded by the chiral ligand such that during iodocarbocyclization, the olefinic moiety of the carbon chain faces the opposite face. The iodine and the enolate can then approach and add to the equatorial position in a *trans*-addition fashion, resulting in the formation of the stereoselective product **1-114**.

1.9 Aims & Approach

From the examples of halocyclization reactions mentioned above, it can be observed that asymmetric halolactonization reactions have already been very well-reported. In contrast, there are significantly less reports on asymmetric haloetherification and haloamination reactions, owing to the extremely challenging task of developing an efficient method. A successful haloetherification strategy lies in improving the rate of the nucleophilic capture relative to the rate of catalyst-halonium ion dissociation which forms racemic products. In contrast, an efficient haloamination methodology needs to circumvent the inherent possibility of *O*-cyclization rather than *N*-cyclization of an amide substrate. Both of these reactions are viewed as extremely important synthetic transformations to organic chemists as it enables entry to valuable pharmaceutical intermediates and bioactive natural products. As such, the aim of this project is to develop and explore new enantioselective halocyclization strategies, in particular, haloetherification and haloamination that can lead to access to important intermediates or functional molecules.

Our approach is to carry out a systematic search for new or existing organocatalysts that can efficiently carry out these reactions enantioselectively. Upon identifying suitable catalysts, the reactions will be optimized to furnish chiral products with high ee.

While it is our primary objective to develop and explore new halocyclization reactions, it is also our aim to showcase the value of these synthetic transformations by applying these protocols in useful applications. As such, we also aim to apply these developed protocols to the synthesis of important pharmaceuticals and functional molecules.

1.10 References

1. Gilman, H., *Organic Chemistry: An Advanced Treatise*. Wiley, New York: 1938; Vol. 1, p 36.
2. (a) Vaillancourt, F. H.; Yeh, E.; Vosburg, D. A.; Garneau-Tsodikova, S.; Walsh, C. T., *Chem. Rev.* **2006**, *106*, 3364; (b) Butler, A.; Sandy, M., *Nature* **2009**, *460*, 848.
3. (a) Kukhar, V. S., V.A., *Fluorine-Containing Amino Acids, Synthesis and Properties*. John Wiley & Sons, Chichester: 1995; (b) Filler, R. K., Y., *Biomedical Aspects of Fluorine Chemistry*. Kodansha/Elsevier Biomedical Press, New York: 1982; (c) Banks, R. E., *J. Fluorine Chem.* **1998**, *87*, 1.
4. (a) Takahashi, Y.; Daitoh, M.; Suzuki, M.; Abe, T.; Masuda, M., *J. Nat. Prod.* **2002**, *65*, 395; (b) Brito, I.; Cueto, M.; Diaz-Marrero, A. R.; Darias, J.; San, M. A., *J. Nat. Prod.* **2002**, *65*, 946.
5. (a) House, H., *Modern Synthetic Reactions*. 2nd ed.; W.A. Benjamin, New York: 1972; (b) De Kimpe, N. V., R., *The Chemistry of α -Haloketones, α -Haloaldehydes, and α -Haloimines*. John Wiley & Sons, New York: 1988.
6. Perkins, C. W.; Martin, J. C.; Arduengo, A. J.; Lau, W.; Alegria, A.; Kochi, J. K., *J. Am. Chem. Soc.* **1980**, *102*, 7753.
7. (a) Olah, G. A.; Wang, Q.; Sandford, G.; Surya, P. G. K., *J. Org. Chem.* **1993**, *58*, 3194; (b) Prakash, G. K. S.; Mathew, T.; Hoole, D.; Esteves, P. M.; Wang, Q.; Rasul, G.; Olah, G. A., *J. Am. Chem. Soc.* **2004**, *126*, 15770.

8. (a) Gutmann, V., *Coord. Chem. Rev.* **1975**, *15*, 207; (b) Denmark, S. E.; Beutner, G. L., *Angew. Chem., Int. Ed.* **2008**, *47*, 1560.
9. Denmark, S. E.; Williams, E. K.; Matthew, T. B., *Angew. Chem., Int. Ed.* **2012**, *51*, 10938.
10. Urabe, H.; Sato, F. In *Titanium(IV) Lewis acids*, Wiley-VCH Verlag GmbH: 2000; pp 653.
11. Mikami, K.; Terada, M. In *Chiral Titanium(IV) Lewis acids*, Wiley-VCH Verlag GmbH: 2000; pp 799.
12. Kang, S. H.; Lee, S. B.; Park, C. M., *J. Am. Chem. Soc.* **2003**, *125*, 15748.
13. (a) Fittig, R., *Ann. Physik* **1898**, 165; (b) Stobbe, H., *Ann. Physik* **1899**, 89.
14. Bougault, M. J., *Ann. Chim. Phys.* **1911**, *22*, 125.
15. Bloomfield, G. F.; Farmer, E. H., *J. Chem. Soc.* **1932**, 2062.
16. Linstead, R. P.; May, C. J., *J. Chem. Soc.* **1927**, 2565.
17. van Tamelen, E. E.; Shamma, M., *J. Am. Chem. Soc.* **1954**, *76*, 2315.
18. Klein, J., *J. Am. Chem. Soc.* **1959**, *81*, 3611.
19. Arnold, R. T.; Lindsay, K. L., *J. Am. Chem. Soc.* **1953**, *75*, 1048.
20. Cook, C. H.; Cho, Y. S.; Jew, S. S.; Suh, Y. G.; Kang, E. K., *Arch. Pharm. Res.* **1983**, *6*, 45.
21. (a) Simonot, B.; Rousseau, G., *J. Org. Chem.* **1994**, *59*, 5912; (b) Simonot, G., *Tetrahedron Lett.* **1993**, *34*, 4527; (c) Rousseau, G.; Strzalko, T.; Roux, M.-C., *Tetrahedron Letters* **2004**, *45*, 4503; (d) Roux, M.-C.; Paugam, R.; Rousseau, G., *The Journal of Organic Chemistry* **2001**, *66*, 4304.

-
22. Motohashi, S.; Satomi, M.; Fujimoto, Y.; Tatsuno, T., *Heterocycles* **1985**, 23, 2035.
23. Kitagawa, O.; Sato, T.; Taguchi, T., *Chem. Lett.* **1991**, 177.
24. Denmark, S. E.; Burk, M. T., *Proc. Natl. Acad. Sci. U. S. A.* **2010**, 107, 20655.
25. Snyder, S. A.; Treitler, D. S.; Brucks, A. P., *Aldrichimica Acta* **2011**, 44, 27.
26. Woodward, R. B.; Singh, G., *J. Am. Chem. Soc.* **1950**, 72, 5351.
27. Damin, B.; Forestiere, A.; Garapon, J.; Sillion, B., *J. Org. Chem.* **1981**, 46, 3552.
28. Wirth, T., *Angew. Chem., Int. Ed.* **1995**, 34, 1726.
29. Wang, M.; Gao, L. X.; Mai, W. P.; Xia, A. X.; Wang, F.; Zhang, S. B., *J. Org. Chem.* **2004**, 69, 2874.
30. Zhang, W.; Zheng, S.; Liu, N.; Werness, J. B.; Guzei, I. A.; Tang, W., *J. Am. Chem. Soc.* **2010**, 132, 3664.
31. Veitch, G. E.; Jacobsen, E. N., *Angew. Chem., Int. Ed.* **2010**, 49, 7332.
32. (a) Murai, K.; Matsushita, T.; Nakamura, A.; Fukushima, S.; Shimura, M.; Fujioka, H., *Angew. Chem., Int. Ed.* **2010**, 49, 9174; (b) Murai, K.; Nakamura, A.; Matsushita, T.; Shimura, M.; Fujioka, H., *Chem. - Eur. J.* **2012**, 18, 8448.
33. (a) Zhou, L.; Tan, C. K.; Jiang, X.; Chen, F.; Yeung, Y.-Y., *J. Am. Chem. Soc.* **2010**, 132, 15474; (b) Tan, C. K.; Zhou, L.; Yeung, Y.-Y., *Org. Lett.* **2011**, 13, 2738; (c) Tan, C. K.; Le, C.; Yeung, Y.-Y., *Chem. Commun.*
-

- 2012**, 48, 5793; (d) Tan, C. K.; Zhou, L.; Yeung, Y.-Y., *Synlett* **2011**, 1335.
34. Dobish, M. C.; Johnston, J. N., *J. Am. Chem. Soc.* **2012**, 134, 6068.
35. Tamaru, Y.; Kawamura, S.; Yoshida, Z., *tetrahedron Lett.* **1985**, 26, 2885.
36. Doroski, T. A.; Cox, M. R.; Morgan, J. B., *Tetrahedron Letters* **2009**, 50, 5162.
37. Barluenga, J.; Vázquez-Villa, H.; Ballesteros, A.; González, J. M., *Journal of the American Chemical Society* **2003**, 125, 9028.
38. Pariselle, H., *Ann. Chim.* **1911**, 24, 315.
39. (a) Tonn, C. E.; Palazón, J. M.; Ruiz-Pérez, C.; Rodríguez, M. L.; Martín, V. S., *Tetrahedron Letters* **1988**, 29, 3149; (b) Jung, M. E.; D'Amico, D. C.; Lew, W., *Tetrahedron Letters* **1993**, 34, 923.
40. (a) Brown, R. S., *Acc. Chem. Res.* **1997**, 30, 131; (b) Denmark, S. E.; Burk, M. T.; Hoover, A. J., *Journal of the American Chemical Society* **2010**, 132, 1232.
41. Kitagawa, O.; Hanano, T.; Tanabe, K.; Shiro, M.; Taguchi, T., *J. Chem. Soc., Chem. Commun.* **1992**, 1005.
42. Wilkinson, S. C.; Lozano, O.; Schuler, M.; Pacheco, M. C.; Salmon, R.; Gouverneur, V., *Angew. Chem., Int. Ed.* **2009**, 48, 7083.
43. Hennecke, U.; Muller, C. H.; Frohlich, R., *Org. Lett.* **2011**, 13, 860.
44. Huang, D.; Wang, H.; Xue, F.; Guan, H.; Li, L.; Peng, X.; Shi, Y., *Org. Lett.* **2011**, 13, 6350.
45. Denmark, S. E.; Burk, M. T., *Org. Lett.* **2012**, 14, 256.

-
46. (a) O'Hagan, D., *Nat. Prod. Rep.* **2000**, *17*, 435; (b) Asano, N.; Nash, R. J.; Molyneux, R. J.; Fleet, G. W. J., *Tetrahedron: Asymmetry* **2000**, *11*, 1645; (c) Lillelund, V. H.; Jensen, H. H.; Liang, X.; Bols, M., *Chem. Rev.* **2002**, *102*, 515.
47. Aida, T.; Legault, R.; Dugat, D.; Durst, T., *Tetrahedron Lett.* **1979**, *20*, 4993.
48. Biloski, A. J.; Wood, R. D.; Ganem, B., *J. Am. Chem. Soc.* **1982**, *104*, 3233.
49. Li, H.; Widenhoefer, R. A., *Tetrahedron* **2010**, *66*, 4827.
50. (a) Takahata, H.; Takamatsu, T.; Mozumi, M.; Chen, Y.-S.; Yamazaki, T.; Aoe, K., *J. Chem. Soc. Chem. Commun.* **1987**, 1627; (b) Kano, S.; Yokomatsu, T.; Iwasawa, H.; Shibuya, S., *Heterocycles* **1987**, *26*, 359.
51. kurth, M. J.; Bloom, S. H., *J. Org. Chem.* **1989**, *54*, 411.
52. Rajendra, G.; Miller, M. J., *J. Org. Chem.* **1987**, *52*, 4471.
53. Lei, A.; Lu, X.; Liu, G., *Tetrahedron Lett.* **2004**, *45*, 1785.
54. Manzoni, M. R.; Zabawa, T. P.; Kasi, D.; Chemler, S. R., *Organometallics* **2004**, *23*, 5618.
55. Michael, F. E.; Sibbald, P. A.; Cochran, B. M., *Org. Lett.* **2008**, *10*, 793.
56. Shen, M.; Li, C., *J. Org. Chem.* **2004**, *69*, 7906.
57. (a) Zhou, L.; Chen, J.; Tan, C. K.; Yeung, Y.-Y., *J. Am. Chem. Soc.* **2011**, *133*, 9164; (b) Chen, J.; Zhou, L.; Yeung, Y.-Y., *Org. Biomol. Chem.* **2012**, *10*, 3808.
58. Sakakura, A.; Ukai, A.; Ishihara, K., *Nature* **2007**, *445*, 900.
-

59. Inoue, T.; Kitagawa, O.; Kurumizawa, S.; Ochiai, O.; Taguchi, T.,
Tetrahedron Lett. **1995**, 36, 1479.

Chapter 2

Enantioselective Synthesis of 2-Substituted and 3-Substituted Piperidines through a Bromoaminocyclization Process

2.1 Introduction

Piperidine is an important cyclic amine motif that is present in various areas. For instance, 2- and 3-substituted piperidines are the fundamental units of many pharmaceuticals and biologically relevant molecules.¹ Some examples of these bioactive compounds are shown in Figure 2.1.

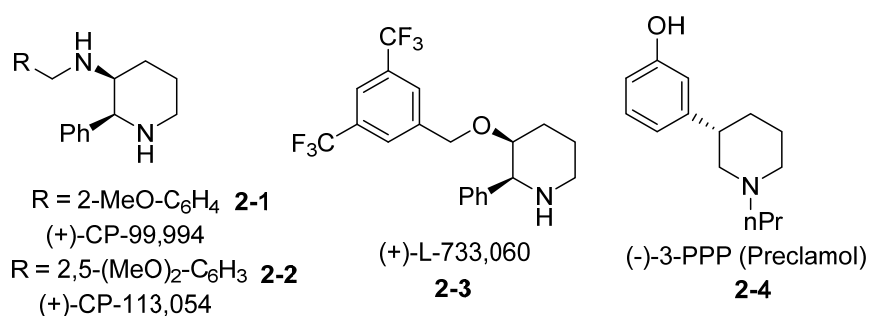
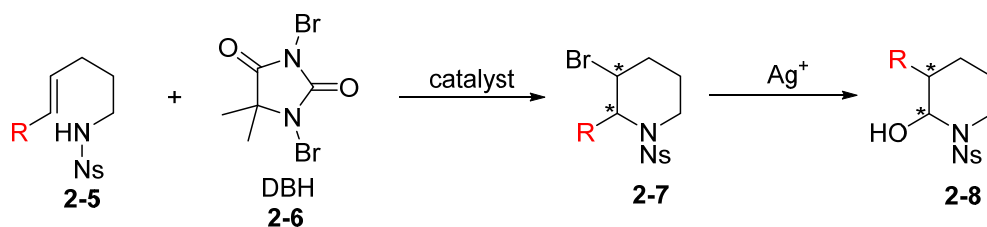


Figure 2.1 Examples of bioactive substituted piperidines.

Significant efforts have been devoted to the synthesis of non-racemic piperidine derivatives over the past few decades.² Reagent-controlled methods for the enantioselective piperidine synthesis, such as dynamic kinetic resolution using phenylglycinol³, sugar chiral auxiliary⁴, and *N*-sulfinyl imidate synthons⁵, are well documented. Nonetheless, catalytic enantioselective synthesis of piperidine derivatives, in particular 3-substituted piperidines, is still a challenging task.⁶

Halocyclization of olefinic amine/amide provides a direct access to piperidine and the halogen on the piperidine ring can offer a handle for subsequent manipulation.⁷ However, a catalytic enantioselective entry towards halocyclization of olefinic amides resulting in the formation of chiral piperidines

remains nontrivial.^{8,9} Herein we disclose a facile and efficient asymmetric cyclization of olefinic amide **2-5** using 1,3-dibromo-5,5-dimethylhydantoin (DBH) as the stoichiometric halogen source and amino-thiocarbamates as the catalyst, yielding 2-substituted-3-bromopiperidines **2-7** in good yields and ees. In addition, it was found that **2-7** can readily undergo rearrangement to give 3-substituted piperidines **2-8** in the presence of a silver salt (Scheme 2.1). This approach was applied to the synthesis of a dopaminergic drug, Preclamol.

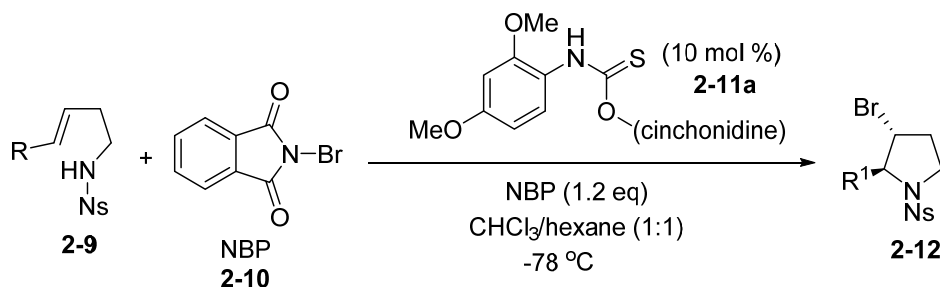


Scheme 2.1 Bromocyclization of olefinic amides.

2.2 Results and Discussion

2.2.1 Catalyst Screening

Recently, we reported a thiocarbamate-catalyzed asymmetric bromoaminocyclization of **2-9** resulting in the formation of enantioenriched 2-substituted-3-bromopyrrolidine **2-12** (Scheme 2.2).



Scheme 2.2 Asymmetric bromoaminocyclization of **2-9**.

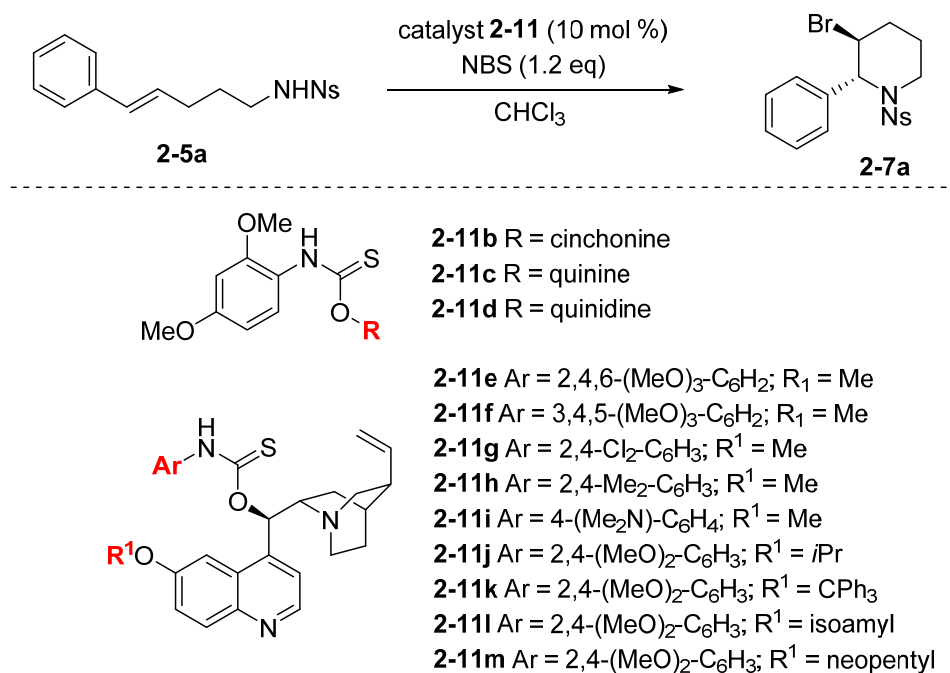
However, when the same conditions were applied to the homolog substrate **2-5**, the reaction was sluggish and neglectable enantioselectivity was observed (Table 2.1, entry 1). As such, we revisited our catalyst library in an attempt to search for a suitable catalyst. We first looked at the cinchonine catalyst analogue **2-11b** and found that it behaves like the cinchonidine catalyst **2-11a** giving poor yields and enantioselectivity (Table 2.1, entry 2). Instead, the quinine version **2-11c** gave products with moderate enantioselectivity (Table 2.1, entry 3). When the pseudo-enantiomeric quinidine thiocarbamate catalyst **2-11d** was used instead, it was observed that the ee was low (Table 2.1, entry 4).

It was interesting to observe that the olefinic amide homologs **2-5** and **2-9** gave opposite enantiomeric products **2-12** and **2-7a** when using the catalysts with the same configuration. This was unexpected as they did not follow the same trend in the catalysis. The reasons for this unusual phenomenon, however, remain unclear and are subject to further investigation.¹⁰

Next, we proceeded to examine the handles on catalyst **2-11c**. It was surprising to find that 2,4,6-trimethoxyphenyl (catalyst **2-11e**), 3,4,5-

trimethoxyphenyl (catalyst **2-11f**), 2,4-dichlorophenyl (catalyst **2-11g**), 2,4-dimethylphenyl (catalyst **2-11h**) and 4-dimethylaminophenyl (catalyst **2-11i**) substituents on the thiocarbamate caused the reaction to produce no products (Table 2.1, entries 5-9). Instead, substrate **2-5a** was recovered quantitatively from these reactions. It was deduced that the 2,4-dimethoxyphenyl substituent remained the superior choice for the thiocarbamate aryl-substituent.

We then turned our attention to the 6-alkoxy group of the quinoline system. When the isopropyl group (catalyst **2-11j**) was installed to replace the methyl substituent, the reaction yield increased drastically to 81% and the resulting product was observed to have 63% ee (Table 2.1, entry 10). The encouraging results prompted us to further investigate how different substituents at this position can influence the yield and enantioselectivity of the reaction. We increased the steric bulk of the alkoxy substituent using the triphenyl group (catalyst **2-11k**) and noticed that yield dropped slightly to 67% but the ee increased to 68% (Table 2.1, entry 11). When the isoamyl (catalyst **2-11l**) and the neopentyl groups (catalyst **2-11m**) were installed, the products had 55% ee and 73% ee respectively (Table 2.1, entries 12-13). Catalyst **2-11m** due to its high enantioselectivity observed was then identified as a potential catalyst for further optimization to be carried out.

Table 2.1 Catalyst screening for bromaminocyclization of **2-5a**.

Entry ^a	Catalyst	Temp (°C)	Time (d)	Yield (%) ^b	ee (%)
1	2-11a	-50	3	17	2
2	2-11b	-50	3	21	0
3	2-11c	-50	3	15	46
4	2-11d	-50	3	10	-9
5	2-11e	-50	5	NR	-
6	2-11f	-50	4	NR	-
7	2-11g	-50	3	NR	-
8	2-11h	-50	3	NR	-
9	2-11i	-50	3	NR	-
10	2-11j	-62	3	81	63
11	2-11k	-62	3	67	68
12	2-11l	-50	3	63	55
13	2-11m	-50	4	50	73

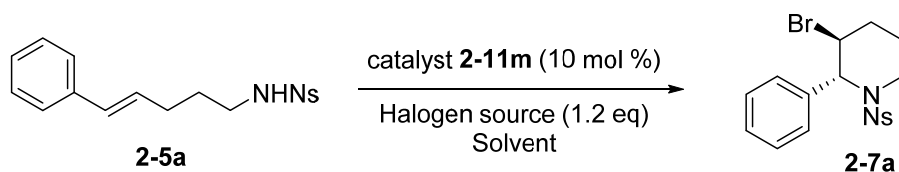
^a Reactions were carried out with **2-5a** (0.1 mmol), NBS (0.12 mmol), catalyst **2-11** (0.01 mmol) in CHCl₃ (5 mL). ^b Isolated yield.

2.2.2 Reaction Conditions Optimization

Once we had identified catalyst **2-11m** as the most promising catalyst, different brominating reagents, solvent systems and reaction temperatures were investigated. The efficiency of three brominating reagents in the form of NBS, NBP and DBH were first investigated, using chloroform as the reaction solvent. Of the three bromine sources, DBH gave the highest yield of 97%, while NBP was the most promising in terms of enantioselectivity, giving products with 86% ee (Table 2.2, entries 1-3). Next, a series of solvents and solvent blends were looked into and it was observed that the reaction did not proceed in toluene at -60 °C (Table 2.2, entries 4 and 5). When the reactions were carried out with NBS in chloroform/toluene (1:1) and chloroform/hexane (1:1) blends, it was observed that the yield and ee were distinctively higher for the latter (Table 2.2, entries 6 and 7). With NBP, the ee of product remained the same when temperature was decreased from -60 to -78 °C (Table 2.2, entries 8-9). Further optimizations looked into varying the ratio of chloroform to hexane to find the ideal composition. When the ratio of chloroform is increased, the ee increased to 88% (Table 2.2, entry 11), and when the ratio of hexane is increased, 92% ee was obtained for the products when the reaction was ran at -78 °C (Table 2.2, entry 12). Although the ee values obtained were encouraging, the yields obtained were poor. When we attempted using DBH as the brominating source, similar trends were observed (Table 2.2, entries 15-18). After extensive consideration, we took a balance between reactivity and enantioselectivity, and selected chloroform/DBH and

chloroform/hexane (1:1)/DBH systems to be the optimum conditions for the asymmetric cyclization of **2-5a**.

Table 2.2 Reaction conditions optimization.



Entry ^a	Halogen source	Solvent	Temp (°C)	Yield (%) ^b	ee (%)
1	NBS	CHCl ₃	-60	39	75
2	NBP	CHCl ₃	-60	78	86
3	DBH	CHCl₃	-60	97	83
4	NBS	Toluene	-60	trace	-
5	NBP	Toluene	-60	trace	-
6	NBS	CHCl ₃ /Toluene (1:1)	-60	71	80
7	NBS	CHCl ₃ /Hexane (1:1)	-60	89	86
8	NBP	CHCl ₃ /Hexane (1:1)	-60	86	86
9	NBP	CHCl ₃ /Hexane (1:1)	-78	56	87
10	NBP	CHCl ₃ /Hexane (1:2)	-78	24	92
11	NBP	CHCl ₃ /Hexane (2:1)	-78	18	88
12	NBP	CHCl ₃ /Hexane (2:3)	-78	55	92
13	NBP	CHCl ₃ /Hexane (1:2)	-60	24	76
14	NBP	CHCl ₃ /Hexane (2:3)	-60	55	90
15	DBH	CHCl ₃ /Hexane (1:2)	-78	24	80
16	DBH	CHCl₃/Hexane (1:1)	-78	85	90
17	DBH	CHCl ₃ /Hexane (2:1)	-78	74	90
18	DBH	CHCl ₃ /Hexane (2:3)	-60	69	67

^a Reactions were carried out with **2-5a** (0.1 mmol), halogen source (0.12 mmol), catalyst **2-11m** (0.01 mmol) in solvent (5 mL). ^b Isolated yield.

2.2.3 Substrate Scope

Next, aryl substrates with different electronic properties were examined and the results are shown in Table 2.3. Substrates with electron-deficient phenyl substituents such as 4-fluorophenyl, 4-chlorophenyl, 4-bromophenyl produced products of good yields and ees (Table 2.3, entries 1-3). In contrast, the electron-rich 4-methoxyphenyl substituent produced product with low ee (Table 2.3, entry 4). This was consistent with the results obtained for electron-rich substrate **2-5i** where relatively low ee was observed (Table 2.3, entry 8).

When the 3-substituted aryl substrates were subject to the reaction conditions, both electron-rich and electron-poor aryl substituents gave products with good yields and ees (Table 2.3, entries 5-7).

Heterocyclic aromatic substituents were next investigated. 3-Thienyl substrate **2-5j** returned with good ee while the 2-thienyl substrate **2-5k** gave lower enantioselectivity (Table 2.3, entries 9 and 10).

The absolute configuration of piperidines **2-7** was confirmed by an X-ray study on the piperidine product **2-7a** (Figure 2.2).

Table 2.3 Enantioselective bromoaminocyclization.

Reaction scheme: **2-5** (R-CH=CH-CH₂-CH₂-NHNs) $\xrightarrow[\text{DBH (1.2 eq), 5 d, -60 }^{\circ}\text{C}]{\text{catalyst } \mathbf{2-11m} \text{ (10 mol \%)}} \mathbf{2-7}$ (Brominated piperidine derivative)

Entry ^a	Substrate	R	Solvent	Yield (%) ^c	ee (%)
1	2-5b	4-F-C ₆ H ₄	CHCl ₃	89	83
			CHCl ₃ / <i>n</i> -hexane (1:1)	78	80
2	2-5c	4-Cl-C ₆ H ₄	CHCl ₃	92	73
			CHCl ₃ / <i>n</i> -hexane (1:1)	23	52
3	2-5d	4-Br-C ₆ H ₄	CHCl ₃	56	70
			CHCl ₃ / <i>n</i> -hexane (1:1) ^b	63	72
4	2-5e	4-MeO-C ₆ H ₄	CHCl ₃	93	14
			CHCl ₃ / <i>n</i> -hexane (1:1)	60	34
5	2-5f	3-Cl-C ₆ H ₄	CHCl ₃	84	87
			CHCl ₃ / <i>n</i> -hexane (1:1) ^b	98	90
6	2-5g	3-Me-C ₆ H ₄	CHCl ₃	98	86
			CHCl ₃ / <i>n</i> -hexane (1:1)	95	88
7	2-5h	3-MeO-C ₆ H ₄	CHCl ₃	97	86
			CHCl ₃ / <i>n</i> -hexane (1:1)	90	83
8	2-5i	2-Naphthyl	CHCl ₃	47	68
			CHCl ₃ / <i>n</i> -hexane (1:1)	36	73
9	2-5j	3-Thienyl	CHCl ₃	87	82
			CHCl ₃ / <i>n</i> -hexane (1:1)	76	77
10	2-5k	2-Thienyl	CHCl ₃	98	54
			CHCl ₃ / <i>n</i> -hexane (1:1)	92	56

^a Reactions were carried out with **2-5** (0.1 mmol), DBH (0.12 mmol) in solvent (5 mL) at -60 °C. ^b The reaction was conducted at -50 °C. ^c Isolated yield.

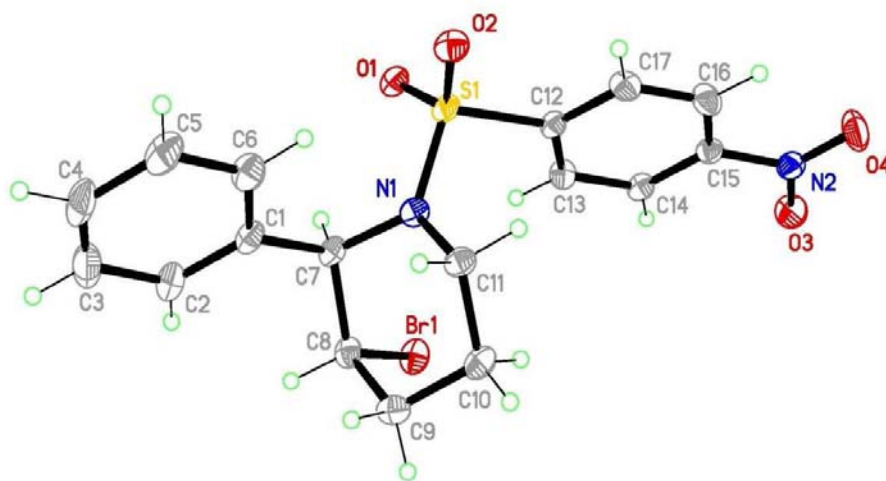
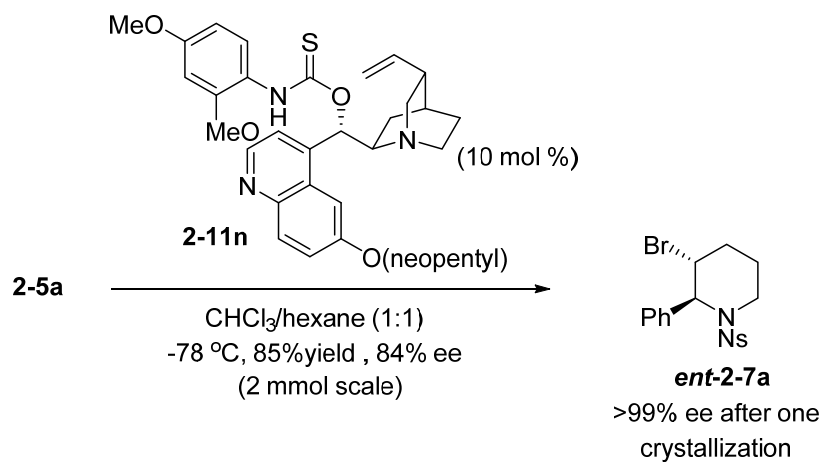


Figure 2.2 X-ray crystal structure of **2-7a**.

2.2.4 Scale-up Synthesis and Synthesis of Enantiomer of **2-7**

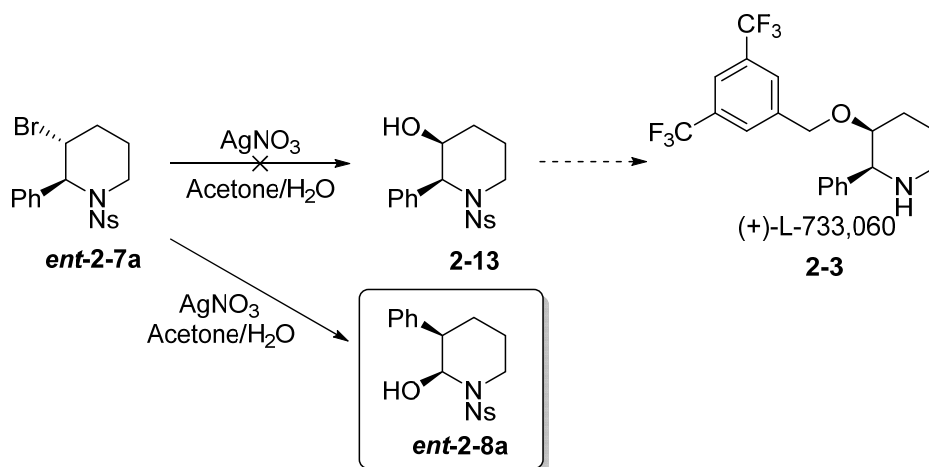
Enantiomer of **2-7a** (*ent*-**2-7a**) could be prepared (84% ee) by using the pseudo-enantiomer quinidine catalyst **2-11n**. This reaction was also readily scalable and a single recrystallization gave enantiopure *ent*-**2-7a** (>99% ee) (Scheme 2.3).



Scheme 2.3 Synthesis of **ent-2-5a** using catalyst **2-11n**.

2.2.5 Silver Salt Promoted Rearrangement

In an attempt to synthesize (+)-L-733,060 **2-3**, we treated **ent-2-7a** with silver nitrate under acetone/water (3:1) conditions and obtained a product that matches the ^1H and ^{13}C NMR spectra of compound **2-13**.



Scheme 2.4 Attempted synthesis of **2-13** results in the formation of **ent-2-8a**.

However, on further examination, we realized that the product obtained was not compound **2-13**, but a product that had undergone a 1,2-aryl shift. The structure and absolute configuration of **ent-2-8a** was established by an X-ray crystallography study (Figure 2.3)

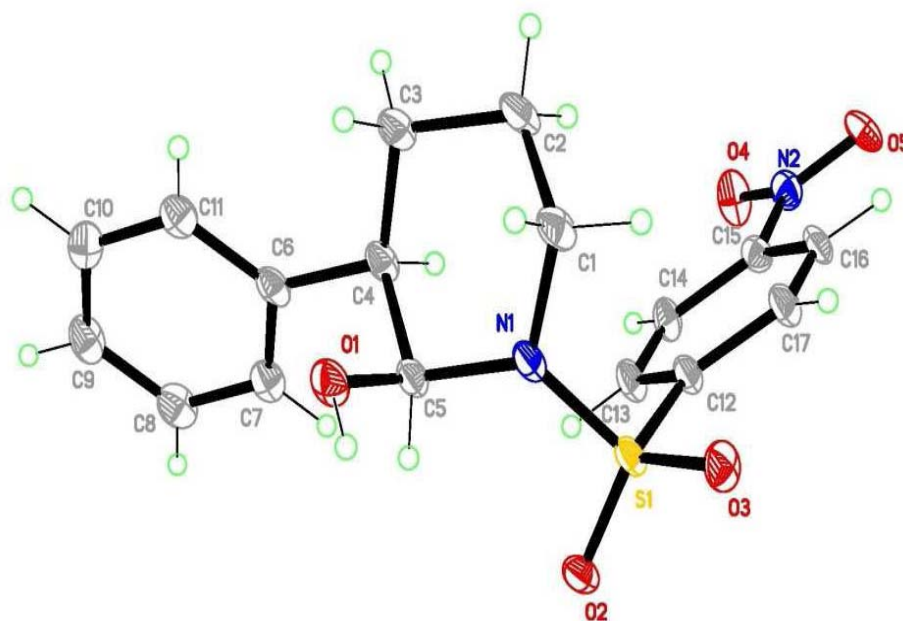
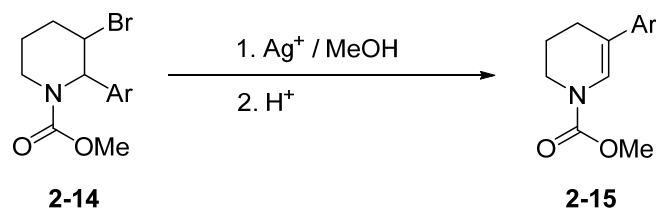


Figure 2.3 X-ray crystal structure of **ent-2-8a**.

In fact, similar reactions were documented and they involved the use of silver nitrate in MeOH. Thereafter, an acidic work-up resulted in the formation of the eliminated product (Scheme 2.5).¹¹

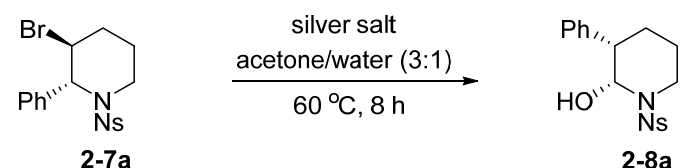


Scheme 2.5 1,2-Aryl shift for the synthesis of unsaturated piperidine **2-15**.

However, by modifying the work-up conditions to use a basic work-up, we were able to obtain the 2-hydroxy-3-aryl product *ent*-**2-8a** exclusively. When we proceeded to check the ee of the resulting product, we were pleased to observe that the product formed with the retention of the chirality.

A survey on various silver salts was performed and it was observed that silver acetate (AgOAc), silver carbonate (Ag_2CO_3), silver phosphate (Ag_3PO_4) and silver sulfate (Ag_2SO_4) resulted in no product being formed when they were utilized (Table 2.4, entries 1, 2, 4 and 5). When silver triflate (AgOTf) and silver tosylate (AgOTs) were used, moderate yields of 43% and 37% were obtained (Table 2.4, entries 6 and 7). Of all, silver nitrate (AgNO_3) and silver trifluoroacetate ($\text{Ag}(\text{O}_2\text{CCF}_3)$) were found to be optimal, with the latter giving slightly higher yields of 86% (Table 2.4, entries 3 and 8).

Table 2.4 Survey of silver salts on rearrangement of **2-7a**.



2-7a **2-8a**

Entry ^a	Silver salt	Substrate	Yield ^b
1	AgOAc	2-7a	0
2	Ag ₂ CO ₃	2-7a	0
3	AgNO ₃	2-7a	83
4	Ag ₃ PO ₄	2-7a	0
5	Ag ₂ SO ₄	2-7a	0
6	AgOTf	2-7a	43
7	AgOTs	2-7a	37
8	Ag(O ₂ CCF ₃)	2-7a	86

^a Reactions were carried out with **2-7a** (0.1 mmol), silver salt (0.1 mmol) in acetone/water (3:1 v/v, 5 mL) at 60 °C. ^b Isolated yield.

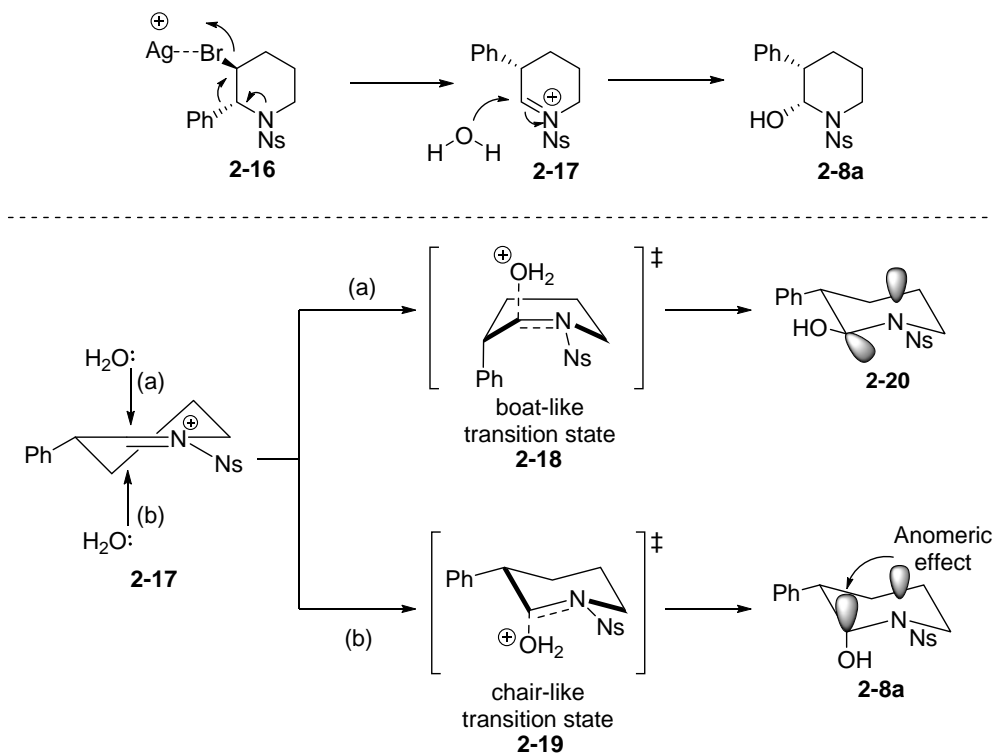
Some substrates **2-7** were subject to investigation, and the results are presented in Table 2.5 (entries 1–5). Generally, good yields were achieved and the enantioselectivities were preserved in this rearrangement.

Table 2.5 Silver-salt promoted rearrangement of **2-7**.

Entry ^a	Silver Salt	Substrate	R	yield ^b	ee (%)
1 ^c	Ag(O ₂ CCF ₃)	ent-2-7a , 99% ee	Ph	86	99
2	Ag(O ₂ CCF ₃)	2-7b , 83% ee	4-F-C ₆ H ₄	83	83
3	Ag(O ₂ CCF ₃)	2-7d , 72% ee	4-Br-C ₆ H ₄	76	72
4	Ag(O ₂ CCF ₃)	2-7g , 86% ee	3-Me-C ₆ H ₄	89	86
5	Ag(O ₂ CCF ₃)	2-7h , 83% ee	3-MeO-C ₆ H ₄	80	83

^a Reactions were carried out with **2** (0.1 mmol), Ag(O₂CCF₃) (0.1 mmol) in acetone–water (3:1 v/v, 5 mL) at 60 °C. ^b Isolated yield. ^c **ent-2-7a** was used and the corresponding **ent-2-8a** was isolated as the product.

We proposed that the rearrangement was initiated by the coordination of the silver ion with the bromide, resulting in concerted 1,2-aryl shift, in the process eliminating silver bromide and forming the iminium ion **2-17**. Subsequently, a molecule of water quenches the iminium ion **2-17** by attacking the adjacent carbon atom. The attack may lead to the formation of two possible products, one via a boat-like transition state **2-18**, while the other through a chair-like transition state **2-19**. The chair-like transition state is more favoured and hence the product **2-8a** is formed. In addition, product **2-8a** also exhibits anomeric effect which adds extra stability to the product formed. This may be another contributing reason to why only **2-8a** was observed as the only product formed (Scheme 2.6).

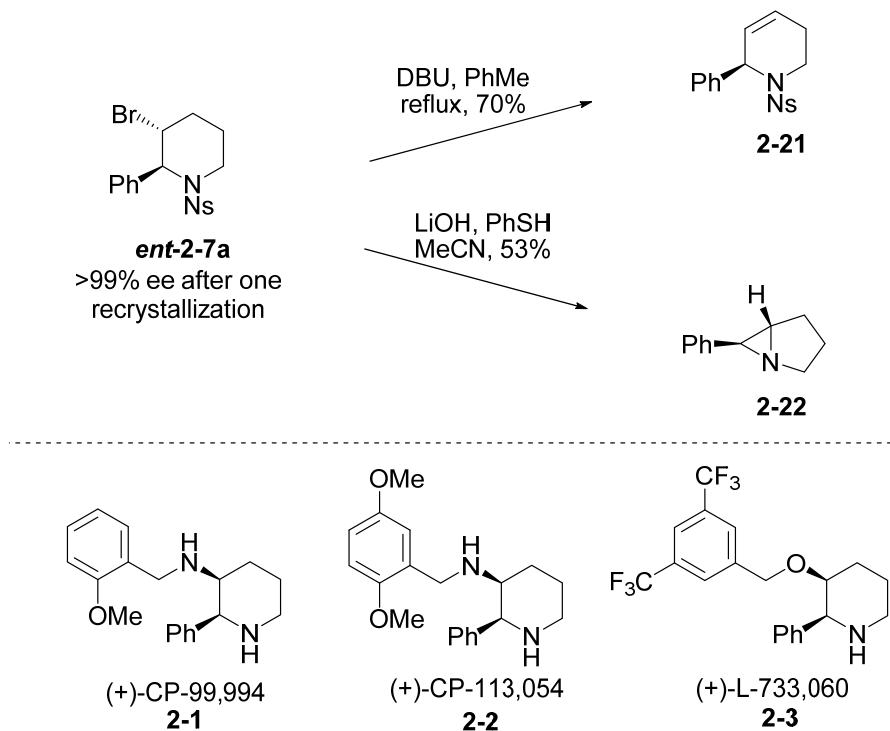


Scheme 2.6 Possible explanation for the observed stereoselectivity.

2.2.6 Applications – Syntheses of Chiral Pharmaceutical Building Blocks

2-Phenyl 3-bromopiperidine *ent*-**2-7a** could be transformed to other useful building blocks. Treatment of *ent*-**2-7a** with DBU in refluxing toluene offered unsaturated piperidine **2-21**. On the other hand, when *ent*-**2-7a** was treated with LiOH and PhSH in acetonitrile, the Ns group was removed and further intramolecular displacement occurred to yield bicycle **2-22**.¹² These molecules resemble some drug candidates that were introduced earlier in the chapter, such as

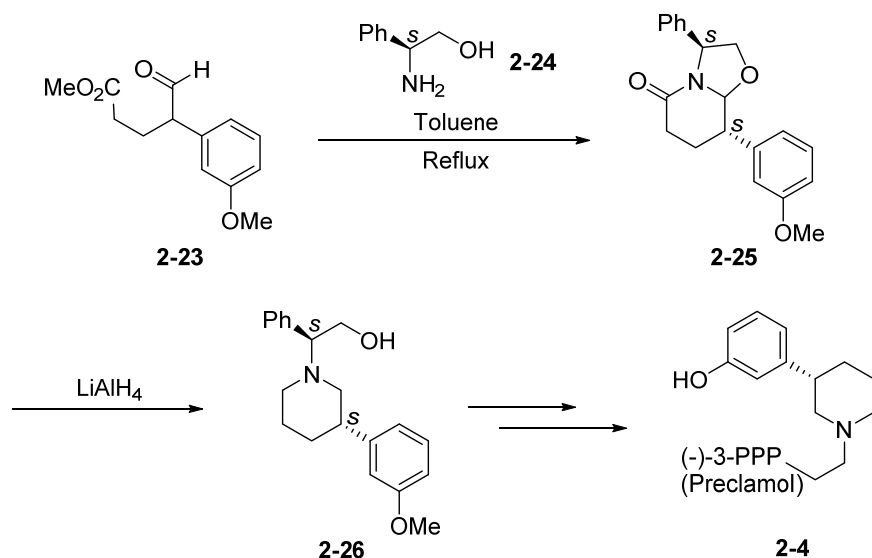
(+)-CP-99,994, (+)-CP-113,054, and (+)-L-733,060 (Scheme 2.7).¹³



Scheme 2.7 Synthesis of pharmaceutical intermediates.

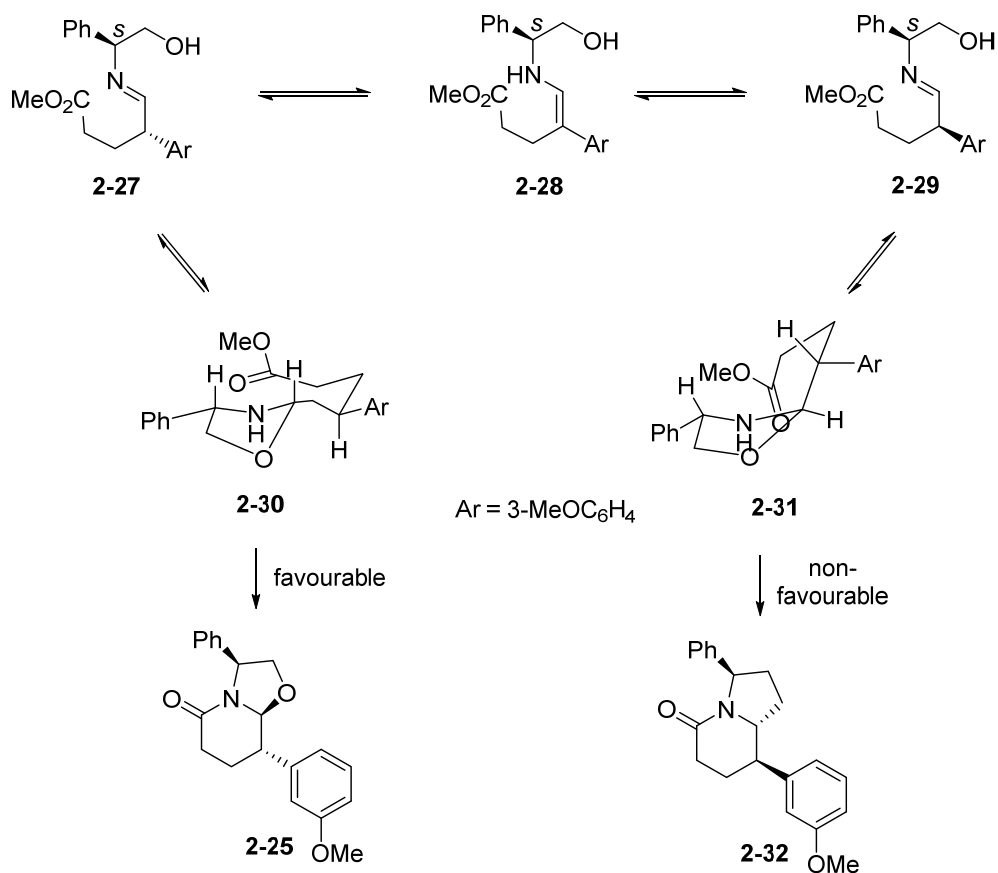
2.2.7 Applications – Synthesis of Preclamol

Preclamol is a dopaminergic drug currently undergoing preclinical trials for schizophrenic treatment.¹⁴ This drug was previously synthesized using dynamic kinetic resolution via the stereoselective cyclodehydration of racemic γ -aryl- δ -oxoesters with (*S*)-phenylglycinol (Scheme 2.8).^{14a} Chiral bicyclic δ -lactams were obtained in the process and subsequent reduction of the lactams resulted in enantioenriched 3-aryl piperidines.



Scheme 2.8 Synthesis of Preclamol using kinetic resolution.

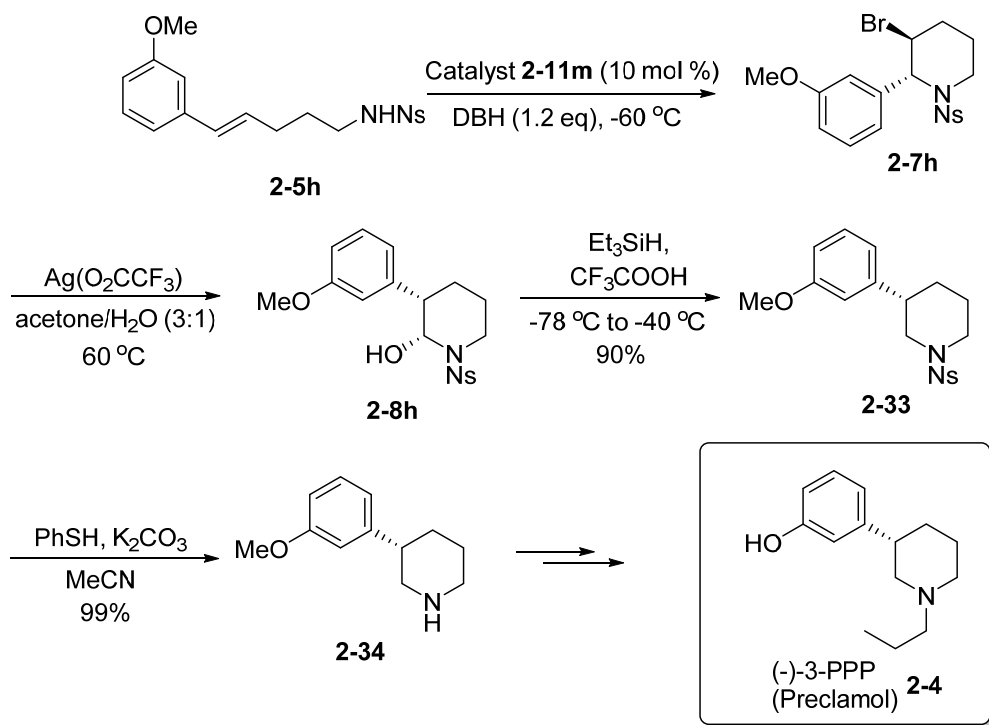
Initially, diastereomeric imines **2-27** and **2-29** were formed after racemic oxoester **2-23** was subject to condensation with (*S*)-phenylglycinol **2-24** (Scheme 2.9). The two imines are in equilibrium via the enamine **2-28**. Lactamization occurs through a transition state, in which the aryl substituent lies in the equatorial position of a chair-like six-membered transition state, leading to the formation of isomers **2-25** (major) and **2-32** (minor). The preferential formation of **2-25** is a consequence of a faster lactamization from the diastereomeric oxazolidine **2-30** as it allows a less hindered approach of the nitrogen atom to the ester moiety. The major product **2-25** was easily converted to (*S*)-3-aryl piperidine **2-26** by LiAlH_4 reduction. Subsequent debenzylation by hydrogenolysis, demethylation and *N*-propylation resulted in formation of Preclamol **2-4**.



Scheme 2.9 Synthesis of intermediate of Preclamol using dynamic kinetic resolution.

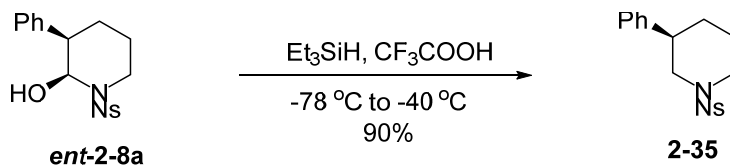
The poor atom economy of this procedure prompted the need for an efficient alternative way of synthesizing Preclamol. One elegant strategy to synthesize Preclamol is via utilizing the combination of both the bromoaminocyclization and silver salt rearrangement protocols developed. As discussed above, **2-8h** can be synthesized in two steps starting from **2-5h** with good yield and ee (Scheme 2.10). Removal of the hydroxyl group in **2-8h** using a triethylsilane/trifluoroacetic acid

protocol gave piperidine **2-33** in good yield. Subsequent deprotection gave **2-34**, a key intermediate in the synthesis of the dopaminergic drug Preclamol.



Scheme 2.10 Synthesis of Preclamol.

Under similar conditions, *ent*-**2-8a** could also be converted to **2-35** which is a demethoxy antipode of **2-33** (Scheme 2.11).



Scheme 2.11 Synthesis of **2-35**.

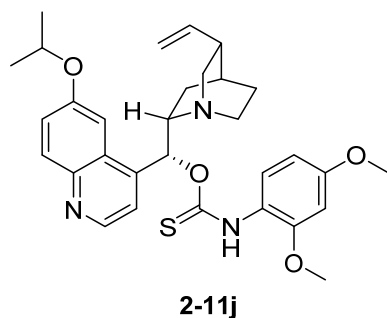
2.3 Summary

In summary, we have developed an efficient and enantioselective bromocyclization of olefinic amides **2-5** resulting in the formation of enantioenriched 2-substituted-3-bromopiperidines **2-7**. In the presence of silver trifluoroacetate, **2-7** undergoes a 1,2-aryl shift to give the corresponding valuable 3-substituted piperidines **2-8**. The importance of these methodologies were showcased in the synthesis of the dopaminergic drug Preclamol **2-4**.

2.4 Experimental

(A) Catalysts **6a-6i** were synthesized according to the report procedure.⁹ⁱ

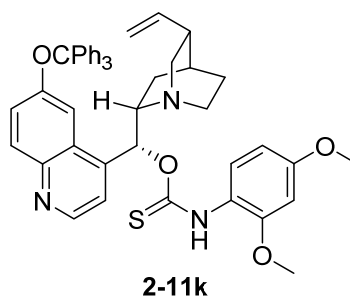
Amino-thiocabamate (**2-11j**):



Yield: 72%; light yellow solid, $[\alpha]_D^{28} +155.9$ (c 1.0, CH_2Cl_2); IR (KBr): 2939, 1618, 1524, 1307, 1209, 1161 cm^{-1} ; ^1H NMR (the compound existed as a mixture of rotamers and the major rotamer was assigned) (300 MHz, CDCl_3): δ 8.70 (d, J

= 4.1 Hz, 1H), 8.50-8.45 (m, 1H), 7.98 (d, $J = 9.1$ Hz, 1H), 7.50-7.29 (m, 5H), 6.45 (s, 2H), 5.85-5.77 (m, 1H), 4.97-4.94 (m, 2H), 4.78-4.63 (m, 1H), 3.80 (s, 6H), 3.46-3.42 (m, 1H), 3.20-3.01 (m, 2H), 2.69-2.49 (m, 2H), 2.18-2.04 (m, 1H), 1.90-1.52 (m, 5H), 1.39 (d, $J = 3.5$ Hz, 6H); ^{13}C NMR (75 MHz, CDCl_3): δ 188.0, 158.6, 155.9, 151.9, 147.1, 144.5, 141.7, 131.5, 127.1, 124.6, 123.1, 122.9, 119.4, 118.9, 114.3, 103.9, 103.5, 98.7, 81.7, 70.0, 59.8, 56.6, 55.4, 42.5, 39.6, 27.5, 24.1, 21.8; HRMS (ESI) calcd for $\text{C}_{31}\text{H}_{38}\text{N}_3\text{O}_4\text{S}$ m/z $[\text{M} + \text{H}]^+$: 548.2578; found: 548.2597.

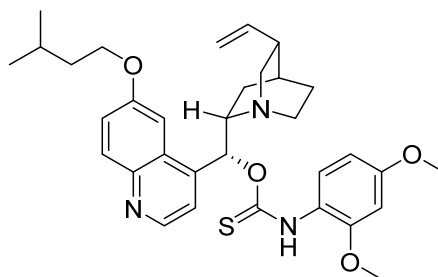
Amino-thiocabamate (2-11k):



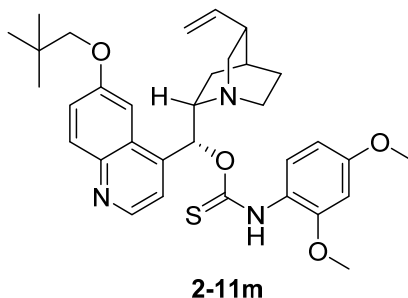
Yield: 69%; light yellow solid, $[\alpha]_D^{28} +72.6$ (c 1.0, CH_2Cl_2); IR (KBr): 2941, 1639, 1526, 1209, 1159, 1034 cm^{-1} ; ^1H NMR (the compound existed as a mixture of rotamers and the major rotamer was assigned) (400 MHz, CDCl_3): δ 8.90 (brs, 1H), 8.71 (d, $J = 4.5$ Hz, 1H), 7.99 (d, $J = 9.2$ Hz, 1H), 7.48-7.28 (m, 5H), 6.43 (s, 2H), 5.79-5.72 (m, 1H), 4.97-4.94 (m, 2H), 3.77-3.62 (m, 8H), 3.41-3.39 (m, 1H), 3.13-3.01 (m, 2H), 2.67-2.57 (m, 2H), 2.28-2.15 (m, 1H), 1.84-1.42 (m, 5H), 1.07 (s, 9H); ^{13}C NMR (100 MHz, CDCl_3): δ 186.2, 158.2, 154.6, 152.3, 147.8, 143.8,

141.9, 129.0, 127.9, 127.3, 126.3, 126.0, 114.2, 113.0, 103.9, 98.8, 91.2, 81.7, 60.0, 59.1, 55.5, 42.5, 42.2, 39.8, 27.7, 27.6, 24.1; HRMS (ESI) calcd for $C_{47}H_{46}N_3O_4S$ m/z $[M + H]^+$: 748.3204; found: 748.3231.

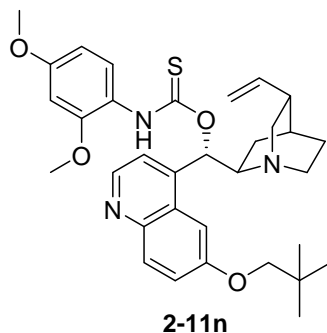
Amino-thiocabamate (2-11i):



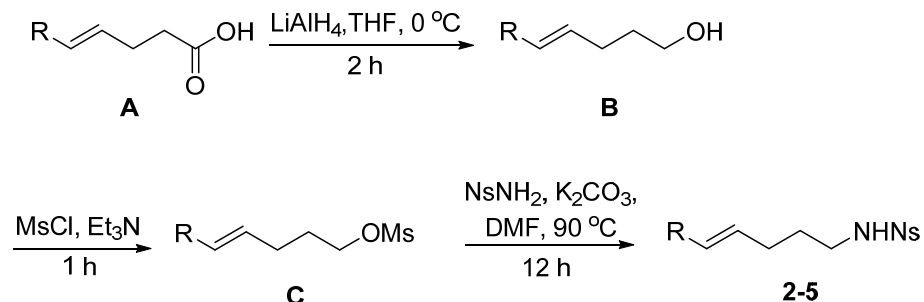
Yield: 73%; light yellow solid, $[\alpha]_D^{28} +149.4$ (c 1.6, CH_2Cl_2); IR (KBr): 2951, 1619, 1513, 462, 1209, 1160, 1034 cm^{-1} ; 1H NMR (the compound existed as a mixture of rotamers and the major rotamer was assigned) (400 MHz, $CDCl_3$): δ 8.71 (d, $J = 4.3$ Hz, 1H), 8.44 (br, 1H), 7.98 (d, $J = 9.2$ Hz, 1H), 7.64-7.31 (m, 5H), 6.47-6.44 (m, 2H), 5.83-5.77 (m, 1H), 5.00-4.95 (m, 2H), 4.16-4.01 (m, 2H), 3.86-3.68 (m, 6H), 3.45-3.42 (m, 1H), 3.14-2.99 (m, 2H), 2.62-2.56 (m, 2H), 2.24-2.15 (m, 1H), 1.92-1.43 (m, 8H), 0.99 (d, $J = 6.5$ Hz, 6H); ^{13}C NMR (100 MHz, $CDCl_3$): δ 188.1, 158.6, 157.3, 151.9, 147.2, 144.7, 143.0, 141.8, 131.5, 127.2, 124.6, 122.3, 119.4, 119.3, 114.3, 103.9, 103.4, 102.6, 98.7, 81.7, 66.8, 59.7, 56.5, 55.5, 42.5, 39.7, 37.8, 27.5, 25.1, 24.1, 22.6; HRMS (ESI) calcd for $C_{33}H_{42}N_3O_4S$ m/z $[M + H]^+$: 576.2891; found: 576.2935.

Amino-thiocabamate (2-11m):

Yield: 78%; light yellow solid, $[\alpha]_D^{28} +149.4$ (c 1.6, CH_2Cl_2); IR (KBr): 2957, 1620, 1525, 1466, 1215, 1037 cm^{-1} ; ^1H NMR (the compound existed as a mixture of rotamers and the major rotamer was assigned) (400 MHz, CDCl_3): δ 8.90 (brs, 1H), 8.71 (d, $J = 4.5$ Hz, 1H), 7.99 (d, $J = 9.2$ Hz, 1H), 7.48-7.28 (m, 5H), 6.43 (s, 1H), 5.79-5.72 (m, 1H), 4.97-4.94 (m, 2H), 3.77-3.62 (m, 8H), 3.41-3.39 (m, 1H), 3.13-3.01 (m, 2H), 2.67-2.57 (m, 2H), 2.28-2.15 (m, 1H), 1.84-1.42 (m, 5H), 1.07 (s, 9H); ^{13}C NMR (100 MHz, CDCl_3): δ 188.0, 170.8, 158.6, 157.6, 152.3, 146.9, 144.4, 143.0, 141.5, 131.1, 126.8, 125.1, 122.1, 119.1, 114.1, 103.8, 102.4, 98.6, 81.2, 78.0, 60.1, 59.2, 56.3, 55.2, 42.4, 39.4, 31.7, 27.3, 26.4, 23.6; HRMS (ESI) calcd for $\text{C}_{33}\text{H}_{42}\text{N}_3\text{O}_4\text{S}$ m/z $[\text{M} + \text{H}]^+$: 576.2891; found: 576.2913.

Amino-thiocabamate (2-11n):

Yield: 75%; light yellow solid, $[\alpha]_D^{28} -150.2$ (c 0.9, CH_2Cl_2); IR (KBr): 2953, 1620, 1525, 1463, 1209, 1036 cm^{-1} ; ^1H NMR (the compound existed as a mixture of rotamers and the major rotamer was assigned) (300 MHz, CDCl_3): δ 8.76-8.72 (m, 2H), 8.00 (d, $J = 9.2$ Hz, 1H), 7.62-7.56 (m, 1H), 7.41-7.30 (m, 4H), 6.54-6.44 (m, 2H), 6.13-5.92 (m, 1H), 5.25-5.06 (m, 2H), 3.81-3.67 (m, 8H), 3.42-3.39 (m, 1H), 2.92-2.76 (m, 4H), 2.26-2.00 (m, 2H), 1.81-1.77 (m, 1H), 1.56-1.52 (m, 3H), 1.10 (s, 9H); ^{13}C NMR (75 MHz, CDCl_3): δ 187.9, 157.6, 151.6, 147.0, 144.4, 143.4, 140.2, 131.1, 127.3, 124.3, 123.4, 122.2, 119.3, 118.4, 114.5, 103.8, 102.5, 98.6, 80.4, 78.0, 60.1, 59.7, 55.3, 49.1, 40.0, 31.7, 27.8, 26.5, 26.2, 24.0; HRMS (ESI) calcd for $\text{C}_{33}\text{H}_{42}\text{N}_3\text{O}_4\text{S}$ m/z $[\text{M} + \text{H}]^+$: 576.2891; found: 576.2903.

(B) General procedure for the preparation of olefinic amide 2-5.

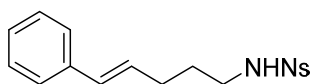
To a solution of acid **A** (1.0 mmol, 1.0 eq) (synthesized according to the literature procedure³) in THF (10 mL) was added LiAlH₄ (76 mg, 2.0 mmol, 2.0 eq) at 0 °C under N₂. The resulting mixture was stirred at 0 °C for 10 min and then was warmed to 25 °C and stirred for another 3 h. After TLC revealed the absence of the starting material, the reaction was quenched with crushed ice. The mixture was filtered through a thin pad of silica gel and eluted with EtOAc (20 mL). The filtrate was concentrated *in vacuo*, which was used directly without further purification, or purified by a short column (hexane/EtOAc 3:1) to give alcohol **B**.

To a solution of alcohol **B** (1.0 mmol, 1.0 eq) and triethylamine (418 μL, 3.0 mmol, 3.0 eq) in CH₂Cl₂ (5 mL) was added MsCl (116 μL, 1.5 mmol, 1.5 eq) at 0 °C. The resulting mixture was stirred at 0 °C for 10 min and then was warmed to 25 °C and stirred for another 2 h. After TLC revealed the absence of the starting material, the reaction was quenched with water (4 mL) and extracted with CH₂Cl₂ (3 × 5 mL). The combined organic extracts were dried over Na₂SO₄, filtered and

concentrated. The residue was purified by flash column chromatography (hexane/EtOAc 3:1) to give the compound **C**.

A modified literature² procedure was used for the direct conversion of Ms-activated alcohols to the corresponding 4-nitrobenzenesulfonamides. A solution of compound **C** (1.0 mmol, 1.0 eq), NsNH_2 (404 mg, 2.0 mmol, 2.0 eq) and K_2CO_3 (276 mg, 2.0 mmol, 2.0 eq) in DMF (5 mL) was stirred at 90 °C for 12 h. The reaction mixture was diluted with water (10 mL) and extracted with Et_2O (3×15 mL). The combined organic extracts were washed with water (3×10 mL) and brine, dried over Na_2SO_4 , filtered and concentrated. The residue was purified by flash column chromatography (CH_2Cl_2 /hexane 2:1 to pure CH_2Cl_2) to give the product **2-5**.

(E)-4-Nitro-N-(5-phenylpent-4-enyl)benzenesulfonamide (**2-5a**):

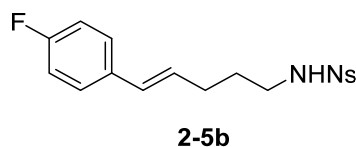


2-5a

Yellow solid, IR (KBr): 3259, 3103, 1546, 1350, 1160, 1061 cm^{-1} ; ^1H NMR (300 MHz, CDCl_3): δ 8.30 (d, $J = 8.8$ Hz, 2H), 8.05 (d, $J = 9.0$ Hz, 2H), 7.29-7.19 (m, 5H), 6.34 (d, $J = 15.8$ Hz, 1H), 6.08 (dt, $J = 15.8, 6.9$ Hz, 1H), 5.18 (t, $J = 5.8$ Hz, 1H), 3.06 (dt, $J = 6.7$ Hz, 2H), 2.23 (dt, $J = 6.9$ Hz, 2H), 1.74-1.65 (m, 2H); ^{13}C NMR (75 MHz, CDCl_3): δ 149.9, 145.7, 137.0, 131.1, 128.5, 128.4, 128.2, 127.2,

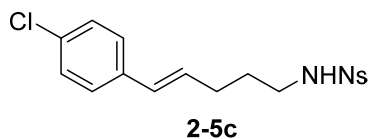
125.8, 124.3, 42.6, 29.6, 29.0; HRMS (ESI) calcd for $C_{17}H_{17}N_2O_4S$ m/z $[M - H]^-$: 345.0915; found: 345.0920.

(E)-N-[5-(4-Fluorophenyl)pent-4-enyl]-4-nitrobenzenesulfonamide (**2-5b**):



Yellow solid, IR (KBr): 3258, 1531, 1351, 1307, 1162, 1091 cm^{-1} ; 1H NMR (500 MHz, $CDCl_3$): δ 8.32 (d, J = 8.2 Hz, 2H), 8.05 (d, J = 8.5 Hz, 2H), 7.23 (dd, J = 8.2, 5.7 Hz, 2H), 6.96 (dd, J = 8.5 Hz, 2H), 6.29 (d, J = 15.8 Hz, 1H), 5.98 (dt, J = 15.1, 6.9 Hz, 1H), 5.06 (t, J = 5.8 Hz, 1H), 3.06 (dt, J = 6.3 Hz, 2H), 2.21 (dt, J = 7.0 Hz, 2H), 1.71-1.65 (m, 2H); ^{13}C NMR (125 MHz, $CDCl_3$): δ 162.0 (d, J = 245.0 Hz), 150.0, 145.8, 133.3 (d, J = 3.6 Hz), 130.0, 128.2, 128.2 (d, J = 1.8 Hz), 127.3 (d, J = 7.3 Hz), 124.4, 115.4 (d, J = 21.9 Hz), 42.7, 29.6, 29.1; HRMS (ESI) calcd for $C_{17}H_{16}FN_2O_4S$ m/z $[M - H]^-$: 363.0820; found: 363.0813.

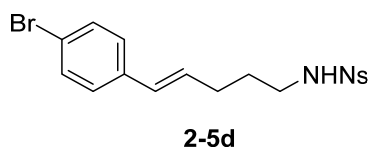
(E)-N-[5-(4-Chlorophenyl)pent-4-enyl]-4-nitrobenzenesulfonamide (**2-5c**):



Yellow solid, IR (KBr): 3278, 1530, 1350, 1314, 1164, 1088 cm^{-1} ; 1H NMR (500 MHz, $CDCl_3$): δ 8.34 (d, J = 8.8 Hz, 2H), 8.04 (d, J = 8.8 Hz, 2H), 7.25 (d, J = 8.6 Hz, 2H), 7.21 (d, J = 8.6 Hz, 2H), 6.30 (d, J = 15.8 Hz, 1H), 6.07 (dt, J = 15.8,

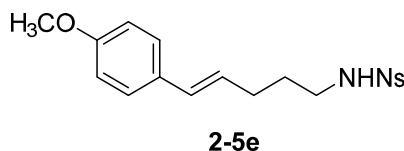
6.9 Hz, 1H), 4.69 (t, $J = 6.0$ Hz, 1H), 3.08 (dt, $J = 6.9$ Hz, 2H), 2.23 (dt, $J = 6.4$ Hz, 2H), 1.73-1.58 (m, 2H); ^{13}C NMR (125 MHz, CDCl_3): δ 150.1, 145.9, 135.6, 132.9, 130.2, 129.1, 128.7, 128.3, 127.2, 124.4, 42.8, 29.7, 29.2; HRMS (ESI) calcd for $\text{C}_{17}\text{H}_{16}\text{ClN}_2\text{O}_4\text{S}$ m/z $[\text{M} - \text{H}]^-$: 379.0525; found: 379.0516.

(E)-N-[5-(4-Bromophenyl)pent-4-enyl]-4-nitrobenzenesulfonamide (**2-5d**):



Yellow solid, IR (KBr): 3279, 1529, 1412, 1349, 1163, 1050 cm^{-1} ; ^1H NMR (300 MHz, Acetone- d_6): δ 8.42 (dd, $J = 9.0$ Hz, 2H), 8.13 (d, $J = 9.0$ Hz, 2H), 7.45 (d, $J = 8.5$ Hz, 2H), 7.30 (d, $J = 8.5$ Hz, 2H), 6.90 (brs, 1H), 6.37 (d, $J = 16.1$ Hz, 1H), 6.26 (dt, $J = 15.8, 6.3$ Hz, 1H), 3.06 (dt, $J = 6.8$ Hz, 2H), 2.24 (dt, $J = 7.1$ Hz, 2H), 1.74-1.65 (m, 2H); ^{13}C NMR (125 MHz, Acetone- d_6): δ 149.8, 146.6, 136.7, 131.2, 130.3, 129.1, 128.1, 127.5, 124.1, 119.8, 42.2, 29.5, 29.0; HRMS (ESI) calcd for $\text{C}_{17}\text{H}_{16}\text{BrN}_2\text{O}_4\text{S}$ m/z $[\text{M} - \text{H}]^-$: 423.0020; found: 423.0016.

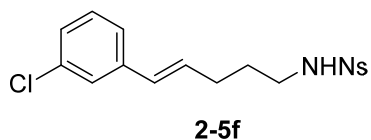
(E)-N-[5-(4-methoxyphenyl)pent-4-enyl]-4-nitrobenzenesulfonamide (**2-5e**):



Yellow solid, IR (KBr): 3282, 1529, 1349, 1240, 1165, 1041 cm^{-1} ; ^1H NMR (300 MHz, CDCl_3): δ 8.31 (d, $J = 9.0$ Hz, 2H), 7.83 (d, $J = 9.0$ Hz, 2H), 7.22-7.17 (m,

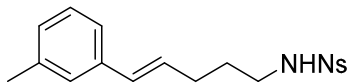
2H), 6.82 (dd, $J = 6.8, 2.0$ Hz, 2H), 6.26 (d, $J = 15.8$ Hz, 1H), 5.91 (dt, $J = 15.6, 6.9$ Hz, 1H), 4.91 (t, $J = 6.0$ Hz, 1H), 3.80 (s, 3H), 3.05 (dt, $J = 6.9$ Hz, 2H), 2.20 (dt, $J = 7.0$ Hz, 2H), 1.72-1.62 (m, 2H); ^{13}C NMR (75 MHz, CDCl_3): δ 158.9, 150.0, 145.8, 130.6, 128.2, 127.0, 126.1, 126.0, 124.3, 113.9, 55.3, 42.6, 29.7, 29.2; HRMS (ESI) calcd for $\text{C}_{18}\text{H}_{19}\text{N}_2\text{O}_5\text{S}$ m/z $[\text{M} - \text{H}]^-$: 375.1020; found: 375.1018.

(E)-N-[5-(3-Chlorophenyl)pent-4-enyl]-4-nitrobenzenesulfonamide (**2-5f**):



Yellow solid, IR (KBr): 32608, 1534, 1351, 1310, 1160, 1091 cm^{-1} ; ^1H NMR (400 MHz, CDCl_3): δ 8.29 (d, $J = 8.9$ Hz, 2H), 8.01 (d, $J = 9.0$ Hz, 2H), 7.23-7.08 (m, 4H), 6.24 (d, $J = 15.9$ Hz, 1H), 6.05 (dt, $J = 15.8, 6.9$ Hz, 1H), 4.97 (t, $J = 6.1$ Hz, 1H), 3.02 (dt, $J = 6.9$ Hz, 2H), 2.19 (dt, $J = 7.3, 1.2$ Hz, 2H), 1.69-1.61 (m, 2H); ^{13}C NMR (100 MHz, CDCl_3): δ 150.0, 145.8, 139.0, 134.4, 130.0, 129.9, 129.7, 128.2, 127.1, 125.8, 124.4, 124.2, 42.6, 29.6, 29.0; HRMS (ESI) calcd for $\text{C}_{17}\text{H}_{16}\text{ClN}_2\text{O}_4\text{S}$ m/z $[\text{M} - \text{H}]^-$: 379.0525; found: 379.0529.

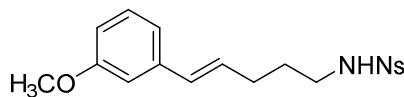
(E)-4-Nitro-N-(5-m-tolylpent-4-enyl)benzenesulfonamide (2-5g):



2-5g

Yellow solid, IR (KBr): 3280, 1530, 1413, 1351, 1162, 1049 cm^{-1} ; ^1H NMR (400 MHz, CDCl_3): δ 8.30 (d, $J = 9.0$ Hz, 2H), 8.04 (d, $J = 9.0$ Hz, 2H), 7.17 (d, $J = 7.5$ Hz, 1H), 7.09-7.02 (m, 3H), 6.29 (d, $J = 15.8$ Hz, 1H), 6.06 (dt, $J = 15.8, 6.9$ Hz, 1H), 5.17 (t, $J = 6.0$ Hz, 1H), 3.06 (dt, $J = 6.9$ Hz, 2H), 2.33 (s, 3H), 2.22 (dt, $J = 6.4, 1.1$ Hz, 2H), 1.70-1.67 (m, 2H); ^{13}C NMR (100 MHz, CDCl_3): δ 149.9, 145.7, 138.0, 137.0, 131.2, 128.4, 128.2, 128.1, 128.0, 126.6, 124.3, 123.0, 42.6, 29.6, 29.0, 21.3; HRMS (ESI) calcd for $\text{C}_{18}\text{H}_{19}\text{N}_2\text{O}_4\text{S}$ m/z $[\text{M} - \text{H}]^-$: 359.1071; found: 359.1076.

(E)-N-[5-(4-methoxyphenyl)pent-4-enyl]-4-nitrobenzenesulfonamide (2-5h):

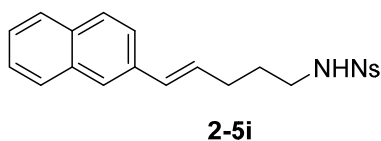


2-5h

Yellow solid, IR (KBr): 3264, 1533, 1349, 1162, 1090 cm^{-1} ; ^1H NMR (300 MHz, CDCl_3): δ 8.31 (d, $J = 8.9$ Hz, 2H), 8.03 (d, $J = 9.0$ Hz, 2H), 7.20 (dd, $J = 7.7$ Hz, 1H), 6.88-6.74 (m, 3H), 6.30 (d, $J = 15.9$ Hz, 1H), 6.06 (dt, $J = 15.7, 6.9$ Hz, 1H), 4.97 (t, $J = 6.1$ Hz, 1H), 3.80 (s, 3H), 3.05 (dt, $J = 6.9$ Hz, 2H), 2.22 (dt, $J = 6.9$ Hz, 2H), 1.73-1.63 (m, 2H); ^{13}C NMR (75 MHz, CDCl_3): δ 159.7, 150.0, 145.8,

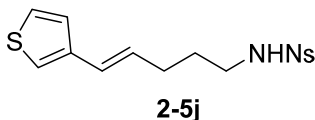
138.5, 131.1, 129.5, 128.7, 128.2, 124.4, 118.6, 112.6, 111.5, 55.2, 42.6, 29.6, 29.0; HRMS (ESI) calcd for $C_{18}H_{19}N_2O_5S$ m/z $[M - H]^-$: 375.1020; found: 375.1012.

(E)-N-[5-(naphthalen-2-yl)-pent-4-enyl]-4-nitrobenzenesulfonamide (**2-5i**):



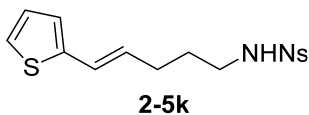
Yellow solid, IR (KBr): 3255, 1532, 1349, 1309, 1159, 1061 cm^{-1} ; δ ^1H NMR (300 MHz, Acetone- d_6): δ 8.42 (d, $J = 8.9$ Hz, 2H), 8.15 (d, $J = 8.9$ Hz, 2H), 7.84-7.79 (m, 3H), 7.72 (s, 1H), 7.61 (dd, $J = 8.6, 1.7$ Hz, 1H), 7.50-7.40 (m, 2H), 6.92 (t, $J = 5.6$ Hz, 1H), 6.56 (d, $J = 15.8$ Hz, 1H), 6.37 (dt, $J = 15.8, 6.9$ Hz, 1H), 3.10 (dt, $J = 6.8$ Hz, 2H), 2.30 (dt, $J = 6.9$ Hz, 2H), 1.78-1.68 (m, 2H); ^{13}C NMR (75 MHz, Acetone- d_6): δ 149.8, 146.6, 135.0, 133.6, 132.6, 130.5, 129.7, 128.1, 127.8, 127.6, 127.4, 126.0, 125.4, 125.2, 124.2, 123.2, 42.3, 29.5, 29.0; HRMS (ESI) calcd for $C_{21}H_{19}N_2O_4S$ m/z $[M - H]^-$: 395.1071; found: 395.1078.

(E)-4-nitro-N-[5-(thiophen-3-yl)pent-4-enyl]benzenesulfonamide (2-5j):



Yellow solid, IR (KBr): 3254, 1546, 1349, 1159, 1063, 967 cm^{-1} ; ^1H NMR (300 MHz, CDCl_3): δ 8.28 (d, $J = 8.9$ Hz, 2H), 8.00 (d, $J = 9.0$ Hz, 2H), 7.22-7.19 (m, 1H), 7.07 (dd, $J = 4.9, 1.0$ Hz, 1H), 6.99 (dd, $J = 3.0, 1.1$ Hz, 1H), 6.30 (d, $J = 15.8$ Hz, 1H), 5.88 (dt, $J = 15.8, 6.9$ Hz, 1H), 4.98 (t, $J = 6.1$ Hz, 1H), 3.01 (dt, $J = 6.9$ Hz, 2H), 2.15 (ddd, $J = 8.4, 7.2, 1.3$ Hz, 2H), 1.69-1.58 (m, 2H); ^{13}C NMR (75 MHz, CDCl_3): δ 150.0, 145.8, 139.7, 128.3, 128.2, 126.0, 125.5, 124.7, 124.4, 121.0, 42.6, 29.5, 29.1; HRMS (ESI) calcd for $\text{C}_{15}\text{H}_{16}\text{N}_2\text{O}_4\text{S}_2$ m/z $[\text{M} - \text{H}]^-$: 351.0479; found: 351.0461.

(E)-4-nitro-N-[5-(thiophen-2-yl)pent-4-enyl]benzenesulfonamide (2-5k):



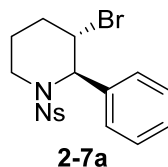
Yellow solid, IR (KBr): 3249, 1531, 1348, 1310, 1159, 1065 cm^{-1} ; ^1H NMR (300 MHz, CDCl_3): δ 8.33 (d, $J = 9.0$ Hz, 2H), 8.04 (d, $J = 9.1$ Hz, 2H), 7.10 (d, $J = 5.1$ Hz, 1H), 6.92 (dd, $J = 5.1, 3.5$ Hz, 1H), 6.83 (d, $J = 3.3$ Hz, 1H), 6.45 (d, $J = 15.6$ Hz, 1H), 5.89 (dt, $J = 15.6, 7.1$ Hz, 1H), 4.86 (t, $J = 5.8$ Hz, 1H), 3.05 (dt, $J = 6.7$ Hz, 2H), 2.19 (ddd, $J = 8.4, 7.1, 1.1$ Hz, 2H), 1.72-1.62 (m, 2H); ^{13}C NMR (125 MHz, CDCl_3): δ 150.0, 145.8, 142.2, 128.3, 128.2, 127.3, 124.8, 124.5, 124.4,

123.6, 42.6, 29.5, 29.0; HRMS (ESI) calcd for $C_{15}H_{15}N_2O_4S_2$ m/z $[M - H]^-$: 351.0479; found: 351.0461.

(C) General Procedure for the Bromoamidation.

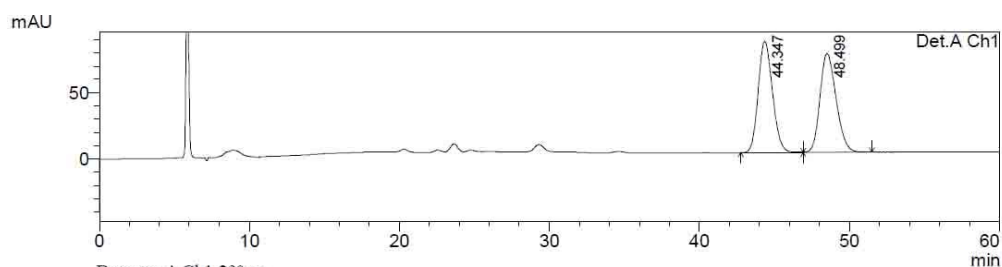
To a solution of olefinic amide **2-5** (0.1 mmol, 1.0 equiv), catalyst **2-11m** (0.01 mmol, 0.1 equiv) in the corresponding solvent (0.02 M) at corresponding temperature in dark under N_2 was added brominating source (0.12 mmol, 1.2 equiv). The resulting mixture was stirred at that temperature and monitored by TLC. The reaction was quenched with saturated Na_2SO_3 (2.0 mL) and then was warmed to 25 °C. The solution was diluted with water (3.0 mL) and extracted with CH_2Cl_2 (3×5 mL). The combined extracts were washed with brine (5.0 mL), dried ($MgSO_4$), filtered and concentrated *in vacuo*. The residue was purified by flash column chromatography on silica gel (CH_2Cl_2 /hexane 2:1) to yield the corresponding piperidine **2-7**.

(2S,3R)-3-Bromo-1-(4-nitrophenylsulfonyl)-2-phenylpiperidine (**2-7a**):



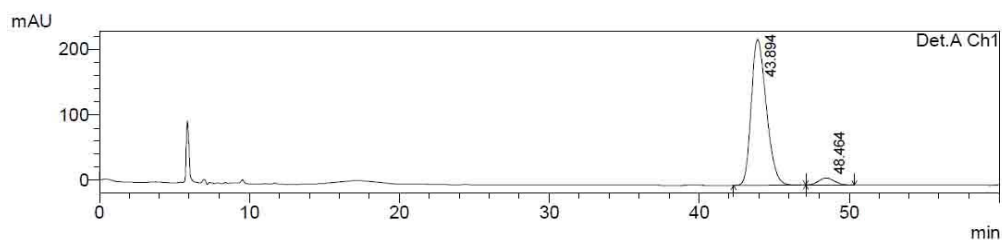
White solid, $[\alpha]_D^{26} -17.6$ (c 1.4, CH_2Cl_2 , 90% ee); IR (KBr): 2939, 1526, 1349, 1312, 1160, 1108 cm^{-1} ; 1H NMR (300 MHz, $CDCl_3$): δ 8.31 (d, $J = 8.8$ Hz, 2H),

8.06 (d, $J = 9.0$ Hz, 2H), 7.39-7.29 (m, 5H), 5.51 (s, 1H), 4.97 (d, $J = 2.6$ Hz, 1H), 3.90 (d, $J = 15.7$ Hz, 1H), 3.33 (ddd, $J = 15.2, 12.2, 2.9$ Hz, 1H), 2.04-1.81 (m, 3H), 1.52-1.48 (m, 1H); ^{13}C NMR (75 MHz, CDCl_3): δ 149.9, 146.2, 136.9, 129.1, 128.8, 128.0, 126.7, 123.9, 63.8, 51.5, 42.2, 27.2, 19.5; HRMS (EI) calcd for $\text{C}_{17}\text{H}_{17}\text{BrN}_2\text{O}_4\text{S}$ m/z $[\text{M}]^+$: 424.0087; found: 424.0080. HPLC (Daicel Chiralpak IC, i -PrOH/hexane = 45/55, 0.6 mL/min, 230 nm) $t_1 = 43.9$ min (major), $t_2 = 48.5$ min (minor).



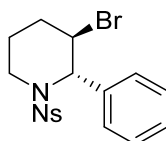
Detector A Ch1 230nm

Peak#	Ret. Time	Area	Height	Area %	Height %
1	44.347	5572945	83852	49.970	52.951
2	48.499	5579747	74507	50.030	47.049
Total		11152693	158358	100.000	100.000

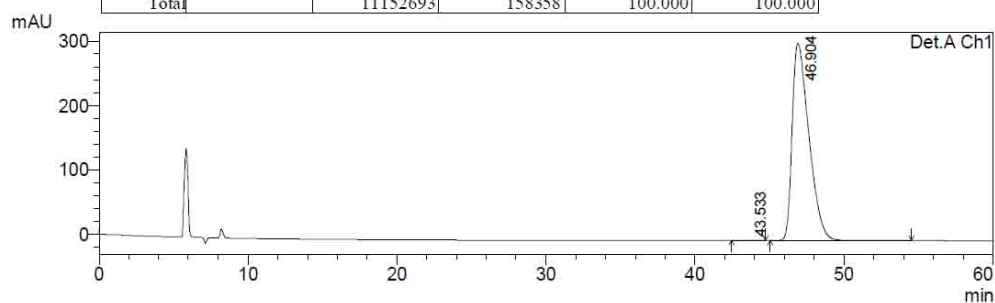
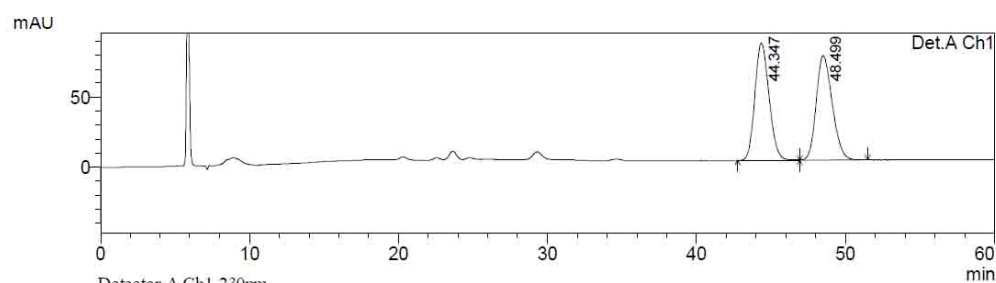


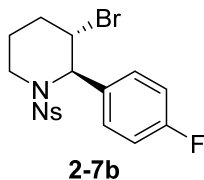
Detector A Ch1 230nm

Peak#	Ret. Time	Area	Height	Area %	Height %
1	43.894	15566957	222857	94.968	95.368
2	48.464	824771	10825	5.032	4.632
Total		16391728	233682	100.000	100.000

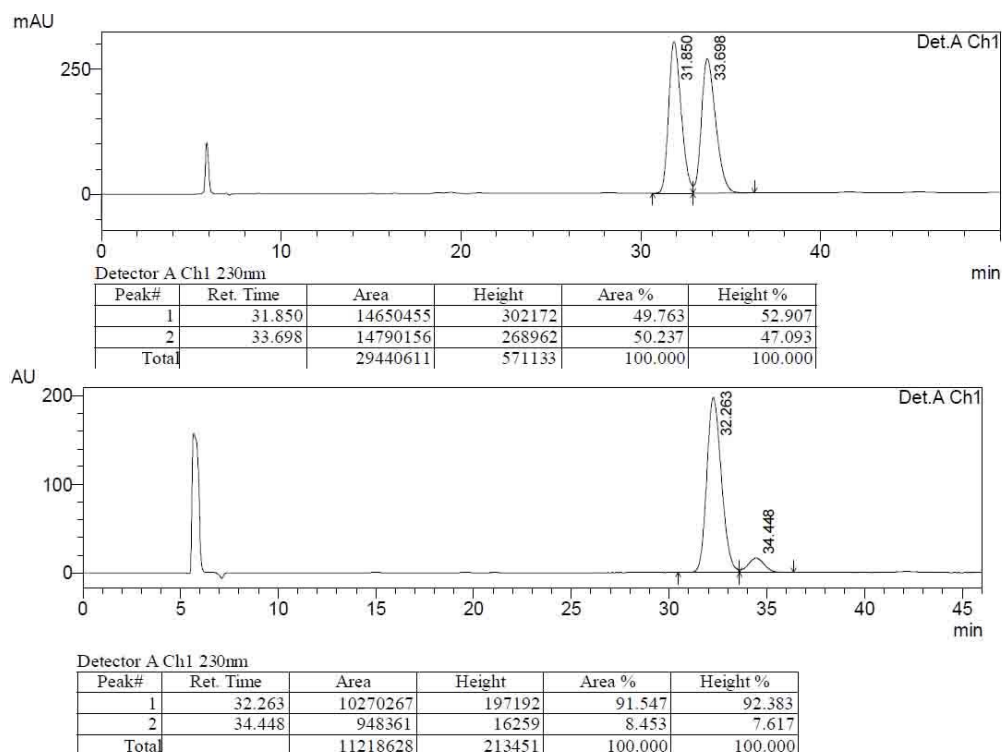
(2*R*,3*S*)-3-Bromo-1-(4-nitrophenylsulfonyl)-2-phenylpiperidine (*ent*-2-7a):**ent-2-7a**

$[\alpha]_D^{26} +22.4$ (*c* 1.0, CH₂Cl₂, 99% ee);

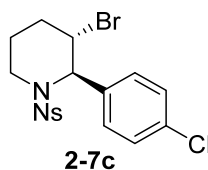


(2*S*,3*R*)-3-Bromo-2-(4-fluorophenyl)-1-(4-nitrophenylsulfonyl)piperidine (2-7b):

White solid, $[\alpha]_D^{26} -12.6$ (*c* 1.0, CH₂Cl₂, 83% ee); IR (KBr): 2962, 1605, 1531, 1347, 1164, 1010 cm⁻¹; ¹H NMR (300 MHz, CDCl₃): δ 8.34 (d, *J* = 9.0 Hz, 2H), 8.04 (d, *J* = 9.1 Hz, 2H), 7.34-7.29 (m, 2H), 7.07 (dd, *J* = 8.5 Hz, 2H), 5.47 (s, 1H), 4.93 (dd, *J* = 5.4, 2.3 Hz, 1H), 3.86 (dd, *J* = 14.3, 2.9 Hz, 1H), 3.30 (ddd, *J* = 14.2, 12.2, 3.0 Hz, 1H), 1.95-1.83 (m, 3H), 1.54-1.48 (m, 1H); ¹³C NMR (75 MHz, CDCl₃): δ 162.2 (d, *J* = 247.1), 150.0, 146.0, 132.6, 128.8, 128.5 (d, *J* = 7.6 Hz), 124.0, 116.1 (d, *J* = 21.8), 63.3, 51.2, 42.1, 27.2, 19.4; HRMS (EI) calcd for C₁₇H₁₆FBrN₂O₄S *m/z* [M]⁺: 441.9993; found: 441.9992. HPLC (Daicel Chiralpak IC, *i*-PrOH/hexane = 45/55, 0.6 mL/min, 230 nm) *t*₁ = 32.3 min (major), *t*₂ = 34.4 min (minor).

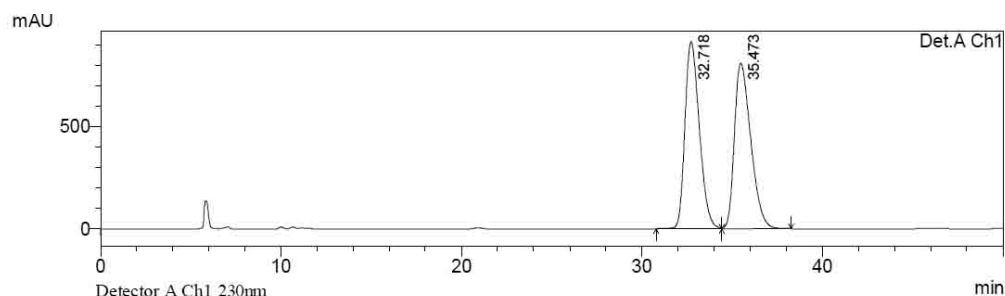


(2*S*,3*R*)-3-Bromo-2-(4-chlorophenyl)-1-(4-nitrophenylsulfonyl)piperidine (**2-7c**):



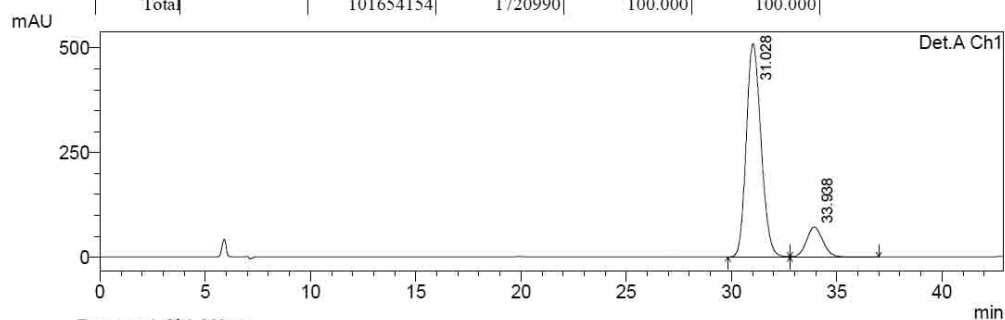
White solid, $[\alpha]_D^{26} -15.4$ (c 0.57, CH_2Cl_2 , 73% ee); IR (KBr): 2958, 1607, 1530, 1346, 1162, 1108 cm^{-1} ; ^1H NMR (500 MHz, CDCl_3): δ 8.34 (d, $J = 8.8$ Hz, 2H), 8.10 (d, $J = 8.2$ Hz, 2H), 7.36 (d, $J = 8.2$ Hz, 2H), 7.28 (d, $J = 8.2$ Hz, 2H), 5.46 (s, 1H), 4.92 (d, $J = 3.2$ Hz, 1H), 3.86 (d, $J = 12.6$ Hz, 1H), 3.29 (ddd, $J = 14.5$, 12.0, 3.2 Hz, 1H), 1.92-1.82 (m, 3H), 1.55-1.48 (m, 1H); ^{13}C NMR (100 MHz,

CDCl_3): δ 150.0, 146.0, 135.4, 134.1, 129.3, 128.8, 128.2, 124.0, 63.3, 51.0, 42.2, 27.3, 19.4; HRMS (EI) calcd for $\text{C}_{17}\text{H}_{16}\text{ClBrN}_2\text{O}_4\text{S}$ m/z $[\text{M}]^+$: 457.9697; found: 457.9693. HPLC (Daicel Chiralpak IC, *i*-PrOH/hexane = 45/55, 0.6 mL/min, 230 nm) t_1 = 31.0 min (major), t_2 = 33.9 min (minor).



Detector A Ch1 230nm

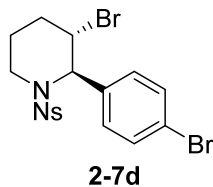
Peak#	Ret. Time	Area	Height	Area %	Height %
1	32.718	50657898	912900	49.834	53.045
2	35.473	50996256	808090	50.166	46.955
Total		101654154	1720990	100.000	100.000



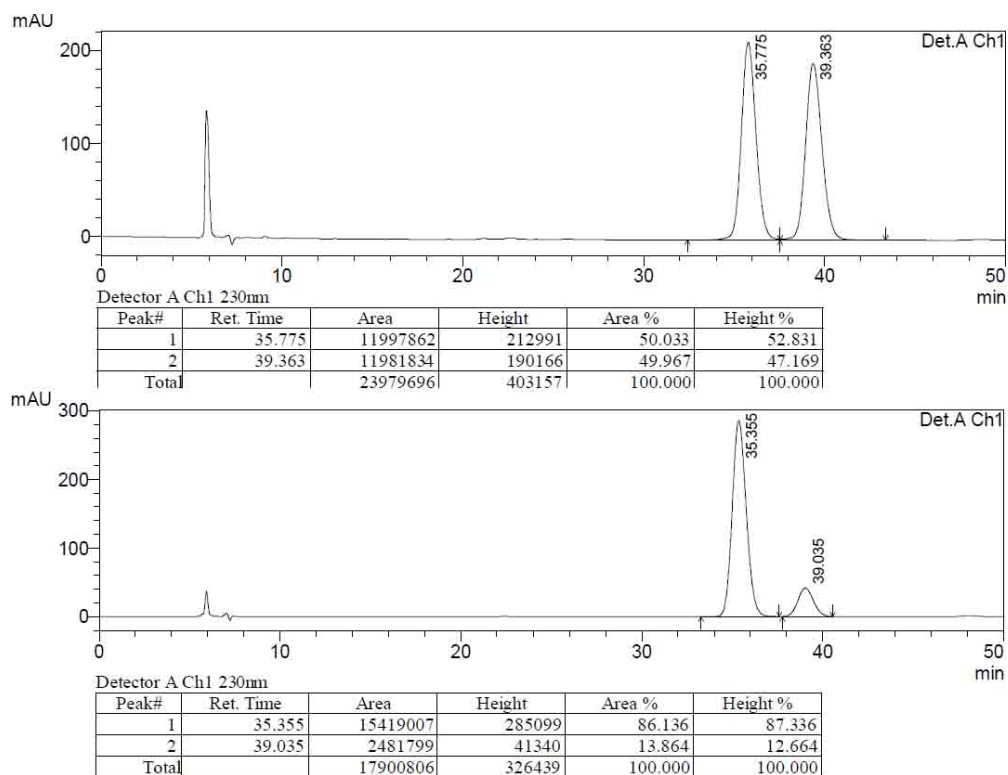
Detector A Ch1 230nm

Peak#	Ret. Time	Area	Height	Area %	Height %
1	31.028	24922230	510135	86.539	87.720
2	33.938	3876500	71417	13.461	12.280
Total		28798730	581552	100.000	100.000

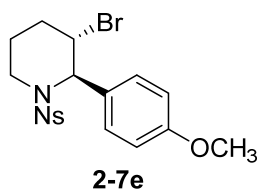
(2*S*,3*R*)-3-Bromo-2-(4-bromophenyl)-1-(4-nitrophenylsulfonyl)piperidine (2-7d):



White solid, $[\alpha]_D^{25} -17.4$ (c 1.0, CH_2Cl_2 , 72% ee); IR (KBr): 2927, 1523, 1489, 1350, 1160, 1109 cm^{-1} ; ^1H NMR (500 MHz, CDCl_3): δ 8.34 (d, $J = 8.7$ Hz, 2H), 8.10 (d, $J = 8.7$ Hz, 2H), 7.51 (d, $J = 8.5$ Hz, 2H), 7.22 (d, $J = 8.5$ Hz, 2H), 5.43 (s, 1H), 4.92 (d, $J = 2.5$ Hz, 1H), 3.86 (d, $J = 13.3$ Hz, 1H), 3.29 (ddd, $J = 14.9$, 12.2, 2.8 Hz, 1H), 1.93-1.79 (m, 3H), 1.51-1.25 (m, 1H); ^{13}C NMR (100 MHz, CDCl_3): δ 150.1, 146.0, 136.0, 132.3, 128.9, 128.5, 124.0, 122.2, 63.4, 50.9, 42.2, 27.4, 19.5; HRMS (EI) calcd for $\text{C}_{17}\text{H}_{16}\text{Br}_2\text{N}_2\text{O}_4\text{S}$ m/z $[\text{M}]^+$: 501.9192; found: 501.9200. HPLC (Daicel Chiralpak IC, i -PrOH/hexane = 40/60, 0.6 mL/min, 230 nm) $t_1 = 35.4$ min (major), $t_2 = 39.0$ min (minor).

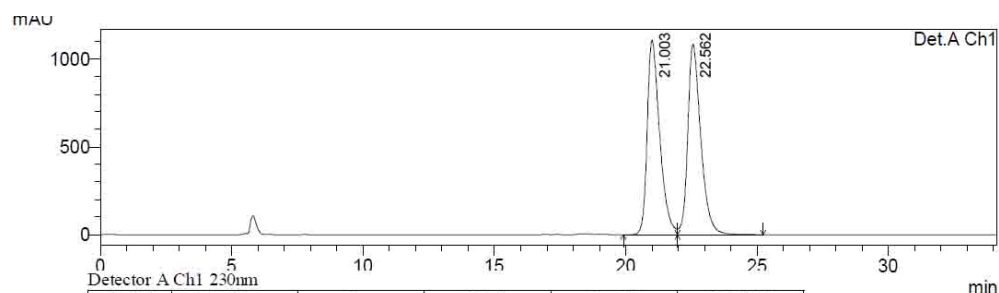


(2*S*,3*R*)-3-Bromo-2-(4-methoxyphenyl)-1-(4-nitrophenylsulfonyl)piperidine (2-7e):

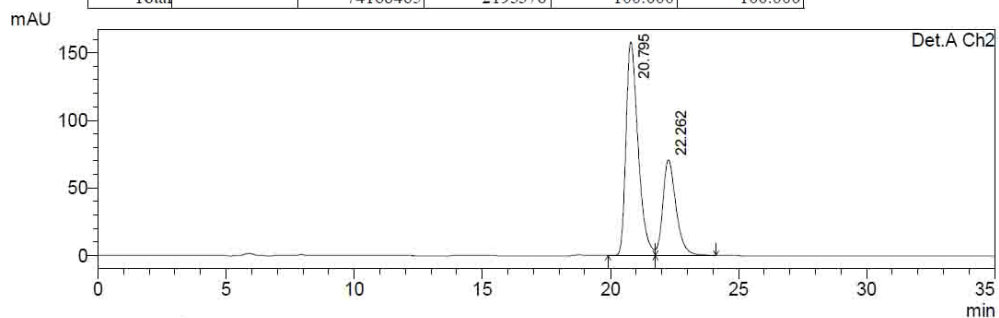


White solid, $[\alpha]_D^{25} -4.0$ (c 0.5, CH_2Cl_2 , 34% ee); IR (KBr): 2954, 1607, 1525, 1351, 1162, 1107 cm^{-1} ; ^1H NMR (500 MHz, CDCl_3): δ 8.32 (d, $J = 8.8$ Hz, 2H), 8.04 (d, $J = 8.9$ Hz, 2H), 7.34 (d, $J = 1.9$ Hz, 1H), 7.26-7.24 (m, 2H), 6.87 (d, $J = 8.8$ Hz, 2H), 7.04 (s, 1H), 5.40 (s, 1H), 4.85 (dd, $J = 5.6, 2.9$ Hz, 1H), 3.89 (s, 3H), 3.89-3.86 (m, 1H), 3.30 (ddd, $J = 14.4, 11.4, 2.6$ Hz, 1H), 1.97-1.87 (m, 3H),

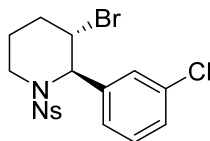
1.55-1.42 (m, 1H); ^{13}C NMR (125 MHz, CDCl_3): δ 155.5, 150.0, 146.0, 131.6, 130.2, 128.7, 127.3, 124.0, 112.2, 112.1, 62.9, 56.3, 51.0, 42.3, 27.3, 19.6; HRMS (EI) calcd for $\text{C}_{18}\text{H}_{19}\text{BrN}_2\text{O}_5\text{S}$ m/z $[\text{M}]^+$: 454.0193; found: 454.0190. HPLC (Daicel Chiralpak IB, *i*-PrOH/hexane = 45/55, 0.6 mL/min, 230 nm) t_1 = 20.8 min (major), t_2 = 22.3 min (minor).



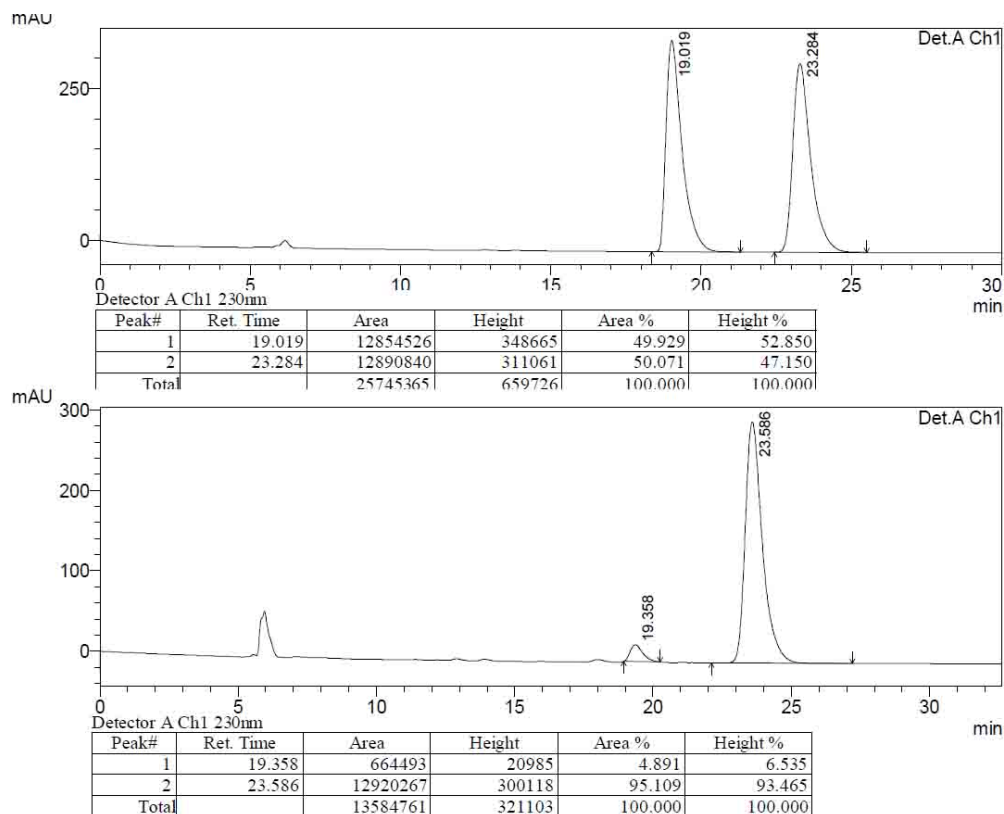
Peak#	Ret. Time	Area	Height	Area %	Height %
1	21.003	36729598	1108802	49.522	50.552
2	22.562	37438867	1084574	50.478	49.448
Total		74168465	2193376	100.000	100.000



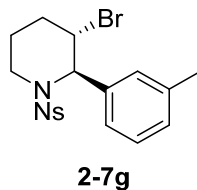
Peak#	Ret. Time	Area	Height	Area %	Height %
1	20.793	13298165	405460	67.044	69.066
2	22.260	6536819	181599	32.956	30.934
Total		19834984	587059	100.000	100.000

(2*S*,3*R*)-3-Bromo-2-(3-chlorophenyl)-1-(4-nitrophenylsulfonyl)piperidine (2-7f):**2-7f**

White solid, $[\alpha]_D^{25} -24.2$ (*c* 1.0, CH₂Cl₂, 90% ee); IR (KBr): 2928, 1526, 1346, 1160, 1108, 951 cm⁻¹; ¹H NMR (400 MHz, CDCl₃): δ 8.33 (d, *J* = 8.9 Hz, 2H), 8.07 (d, *J* = 8.9 Hz, 2H), 7.34-7.28 (m, 2H), 7.26-7.21 (m, 2H), 5.46 (s, 1H), 4.90 (dd, *J* = 5.6, 2.8 Hz, 1H), 3.90 (dd, *J* = 13.8, 2.8 Hz, 1H), 3.31 (ddd, *J* = 13.9, 12.0, 2.9 Hz, 1H), 2.04-1.82 (m, 3H), 1.55-1.50 (m, 1H); ¹³C NMR (100 MHz, CDCl₃): δ 150.0, 145.9, 139.0, 135.2, 130.5, 128.8, 128.3, 127, 125.0, 124.1, 63.3, 50.8, 42.3, 27.3, 19.4; HRMS (EI) calcd for C₁₇H₁₆ClBrN₂O₄S *m/z* [M]⁺: 457.9697; found: 457.9693. HPLC (Daicel Chiralpak AD, *i*-PrOH/hexane = 40/60, 0.6 mL/min, 230 nm) *t*₁ = 19.4 min (minor), *t*₂ = 23.6 min (major).

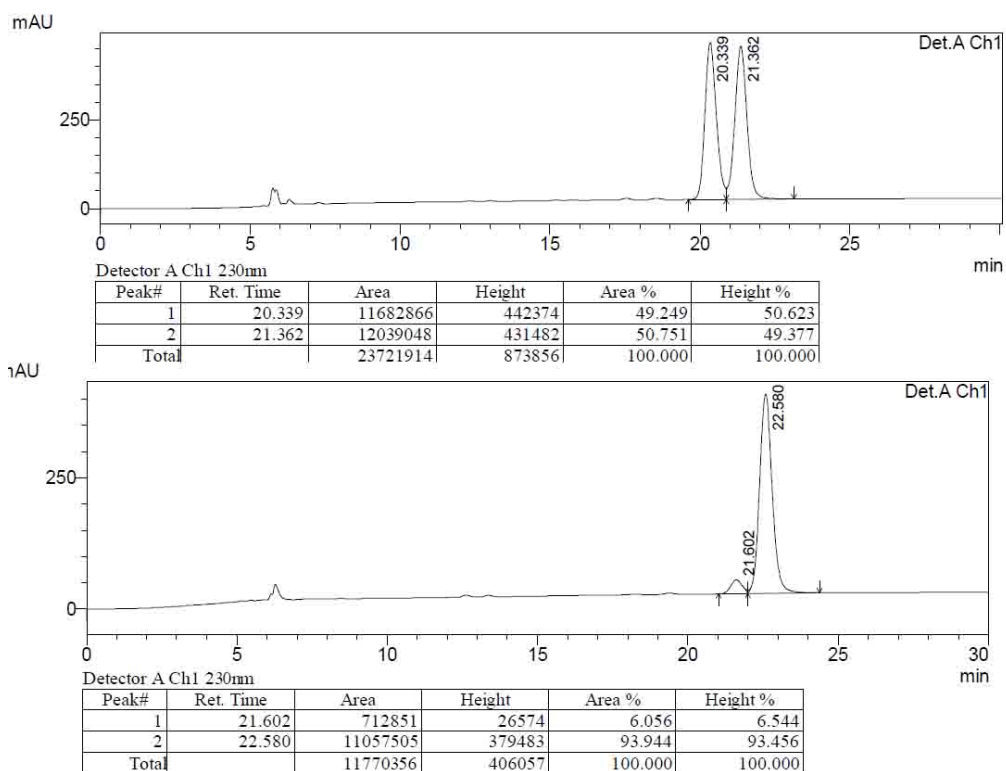


(2*S*,3*R*)-3-Bromo-1-(4-nitrophenylsulfonyl)-2-*p*-tolylpiperidine (**2-7g**):

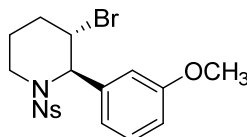


White solid, $[\alpha]_D^{25} -17.5$ (*c* 1.0, CH₂Cl₂, 88% ee); IR (KBr): 2927, 1526, 1346, 1160, 1108 cm⁻¹; ¹H NMR (500 MHz, CDCl₃): δ 8.30 (d, *J* = 8.8 Hz, 2H), 8.05 (d, *J* = 8.8 Hz, 2H), 7.23 (dd, *J* = 7.7 Hz, 1H), 7.09 (d, *J* = 8.5 Hz, 2H), 7.04 (s, 1H), 5.47 (s, 1H), 4.95 (dd, *J* = 5.6, 2.9 Hz, 1H), 3.90 (dd, *J* = 14.0, 2.9 Hz, 1H), 3.35 (ddd, *J* = 14.8, 12.0, 3.1 Hz, 1H), 2.32 (s, 3H), 1.98-1.83 (m, 3H), 1.53-1.49 (m,

^1H); ^{13}C NMR (125 MHz, CDCl_3): δ 149.8, 146.2, 138.9, 136.8, 129.0, 128.8, 128.7, 127.4, 123.9, 123.8, 63.8, 51.7, 42.3, 27.2, 21.6, 19.5; HRMS (EI) calcd for $\text{C}_{18}\text{H}_{19}\text{BrN}_2\text{O}_4\text{S}$ m/z $[\text{M}]^+$: 438.0243; found: 438.0233. HPLC (Daicel Chiralpak IA, i -PrOH/hexane = 15/85, 0.6 mL/min, 230 nm) t_1 = 21.6 min (minor), t_2 = 22.6 min (major).

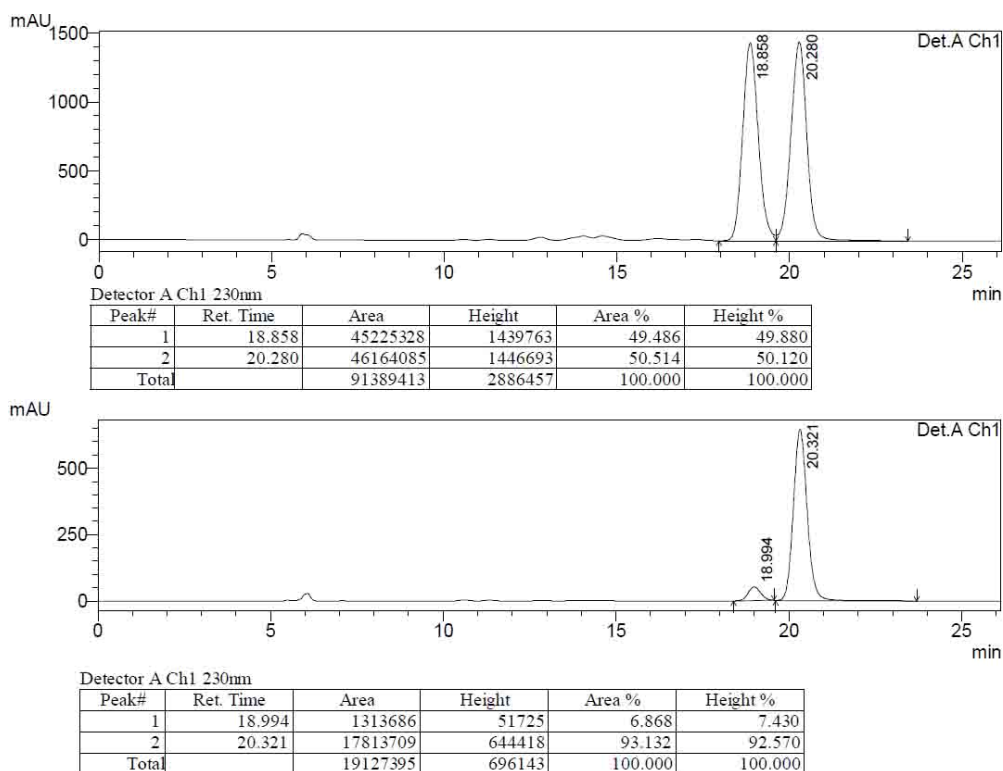


(2*S*,3*R*)-3-Bromo-2-(3-methoxyphenyl)-1-(4-nitrophenylsulfonyl)piperidine(2-7h):

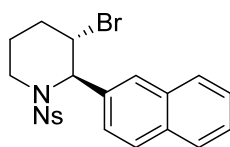


2-7h

White solid, $[\alpha]_D^{25} -11.8$ (c 1.0, CH_2Cl_2 , 86% ee); IR (KBr): 3021, 1531, 1349, 1216, 1164 cm^{-1} ; ^1H NMR (400 MHz, CDCl_3): δ 8.30 (d, $J = 9.0$ Hz, 2H), 8.02 (d, $J = 9.0$ Hz, 2H), 7.29-7.25 (m, 1H), 6.88-6.80 (m, 3H), 5.48 (s, 1H), 4.95 (dd, $J = 5.5, 2.9$ Hz, 1H), 3.88 (dd, $J = 13.8, 2.8$ Hz, 1H), 3.78 (s, 3H), 3.33 (ddd, $J = 13.9, 12.0, 2.9$ Hz, 1H), 1.99-1.86 (m, 3H), 1.53-1.49 (m, 1H); ^{13}C NMR (100 MHz, CDCl_3): δ 160.2, 149.9, 146.1, 138.5, 130.2, 128.8, 123.9, 118.9, 113.2, 112.8, 63.7, 55.3, 51.5, 42.3, 27.2, 19.4; HRMS (EI) calcd for $\text{C}_{18}\text{H}_{19}\text{BrN}_2\text{O}_5\text{S}$ m/z $[\text{M}]^+$: 454.0193; found: 454.0190. HPLC (Daicel Chiralpak IA, i -PrOH/hexane = 40/60, 0.6 mL/min, 230 nm) $t_1 = 19.0$ min (minor), $t_2 = 20.3$ min (major).



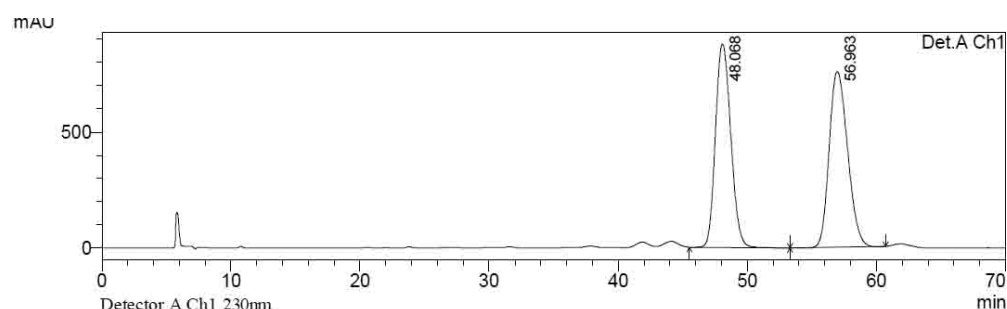
(2*S*,3*R*)-3-Bromo-2-(naphthalen-2-yl)-1-(4-nitrophenylsulfonyl)piperidine (2-7i):



2-7i

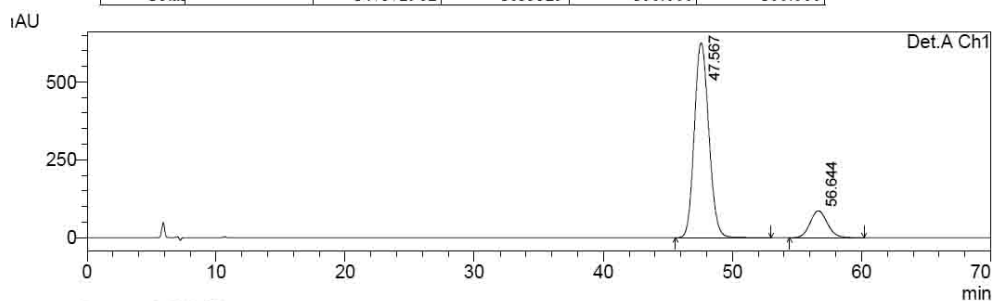
White solid, $[\alpha]_D^{25} -19.6$ (c 1.0, CH₂Cl₂, 72% ee); IR (KBr): 2943, 1532, 1351, 1310, 1161, 1107 cm⁻¹; ¹H NMR (400 MHz, CDCl₃): δ 8.25 (d, *J* = 8.8 Hz, 2H), 8.06 (d, *J* = 8.8 Hz, 2H), 7.85-7.82 (m, 2H), 7.73 (d, *J* = 5.8 Hz, 1H), 7.67 (s, 1H), 7.53-7.48 (m, 2H), 7.41 (dd, *J* = 8.6, 1.8 Hz, 1H), 5.64 (s, 1H), 5.90 (dd, *J* = 5.8, 2.8 Hz, 1H), 3.96 (d, *J* = 13.7 Hz, 1H), 3.47 (ddd, *J* = 13.8, 11.0, 3.0 Hz, 1H),

2.04-1.91 (m, 3H), 1.57-1.53 (m, 1H); ^{13}C NMR (100 MHz, CDCl_3): δ 149.9, 146.2, 134.2, 133.1, 132.6, 129.1, 128.8, 128.0, 127.6, 126.78, 126.76, 126.2, 124.3, 123.9, 64.1, 51.4, 52.6, 27.5, 19.7; HRMS (EI) calcd for $\text{C}_{21}\text{H}_{19}\text{BrN}_2\text{O}_4\text{S}$ m/z $[\text{M}]^+$: 474.0243; found: 474.0233. HPLC (Daicel Chiralpak IC, *i*-PrOH/hexane = 40/60, 0.6 mL/min, 230 nm) t_1 = 47.6 min (major), t_2 = 56.6 min (minor).



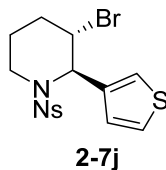
Detector A Ch1 230nm

Peak#	Ret. Time	Area	Height	Area %	Height %
1	48.068	72469901	878289	49.174	53.707
2	56.963	74903061	757040	50.826	46.293
Total		147372962	1635329	100.000	100.000

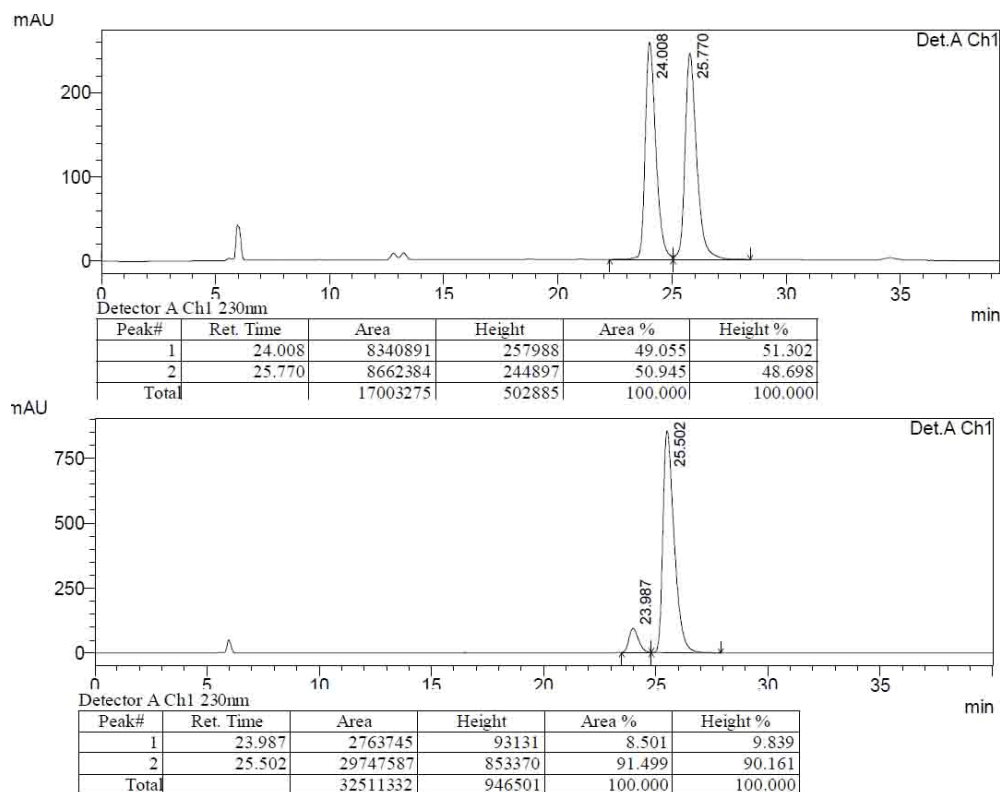


Detector A Ch1 230nm

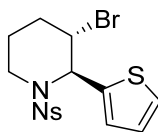
Peak#	Ret. Time	Area	Height	Area %	Height %
1	47.567	48674211	624806	86.004	87.912
2	56.644	7921048	85909	13.996	12.088
Total		56595259	710715	100.000	100.000

(2*S*,3*R*)-3-Bromo-1-(4-nitrophenylsulfonyl)-2-(thiophen-3-yl)piperidine (2-7j):

White solid, $[\alpha]_D^{25} -17.8$ (*c* 0.5, CH₂Cl₂, 83% ee); IR (KBr): 2960, 1525, 1344, 1168, 1093 cm⁻¹; ¹H NMR (400 MHz, CDCl₃): δ 8.32 (d, *J* = 8.8 Hz, 2H), 8.08 (d, *J* = 8.9 Hz, 2H), 7.34 (dd, *J* = 5.0, 2.9 Hz, 1H), 7.17-7.16 (m, 1H), 7.02 (d, *J* = 5.0 Hz, 1H), 5.51 (s, 1H), 4.87 (brs, 1H), 3.78 (d, *J* = 13.0 Hz, 1H), 3.24 (ddd, *J* = 13.9, 12.0, 2.7 Hz, 1H), 1.99-1.88 (m, 3H), 1.54-1.48 (m, 1H); ¹³C NMR (100 MHz, CDCl₃): δ 149.9, 146.0, 138.1, 128.8, 127.1, 126.4, 124.0, 123.0, 61.0, 50.8, 41.7, 27.4, 19.5; HRMS (EI) calcd for C₁₅H₁₅BrN₂O₄S₂ *m/z* [M]⁺: 429.9651; found: 429.9654. HPLC (Daicel Chiralpak IB, *i*-PrOH/hexane = 30/70, 0.6 mL/min, 230 nm) *t*₁ = 24.0 min (minor), *t*₂ = 25.5 min (major).



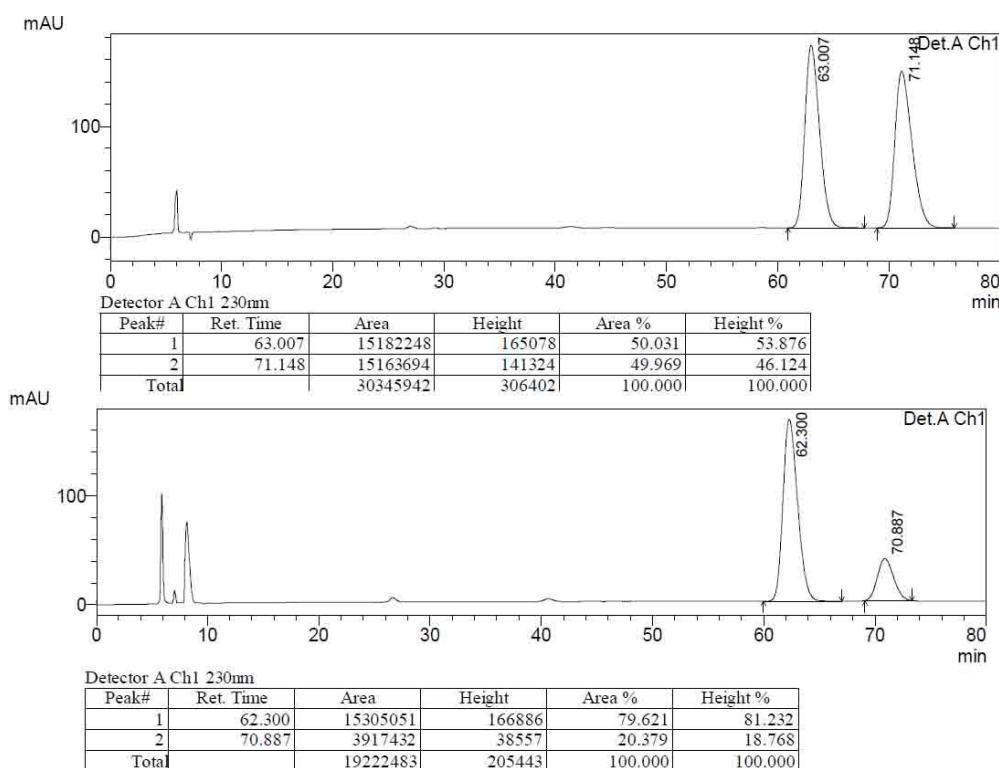
(2*S*,3*R*)-3-Bromo-1-(4-nitrophenylsulfonyl)-2-(thiophen-2-yl)piperidine (**2-7k**):



2-7k

White solid, $[\alpha]_D^{25} -20.2$ (c 1.0, CH_2Cl_2 , 59% ee); IR (KBr): 2944, 1532, 1350, 1162, 1092 cm^{-1} ; ^1H NMR (500 MHz, CDCl_3): δ 8.26 (d, J = 8.9 Hz, 2H), 7.97 (d, J = 8.7 Hz, 2H), 7.23 (dd, J = 5.1, 1.2 Hz, 1H), 7.02 (dd, J = 2.5, 1.2 Hz, 1H), 6.98 (dd, J = 5.1, 3.7 Hz, 1H), 5.73 (s, 1H), 4.72 (d, J = 2.3 Hz, 1H), 3.83 (dd, J = 13.3, 3.7 Hz, 1H), 3.24 (ddd, J = 13.3, 10.3, 3.0 Hz, 1H), 2.19-2.00 (m, 3H), 1.98-1.58

(m, 1H); ^{13}C NMR (125 MHz, CDCl_3): δ 149.9, 145.7, 139.6, 128.7, 127.1, 127.0, 125.9, 123.9, 60.5, 50.8, 41.6, 27.2, 19.4; HRMS (EI) calcd for $\text{C}_{15}\text{H}_{15}\text{BrN}_2\text{O}_4\text{S}_2$ m/z $[\text{M}]^+$: 429.9651; found: 429.9666. HPLC (Daicel Chiralpak IC, *i*-PrOH/hexane = 40/60, 0.6 mL/min, 230 nm) t_1 = 62.3 min (major), t_2 = 70.9 min (minor).

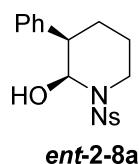


(D) Representative procedure for the silver salt mediated rearrangement.

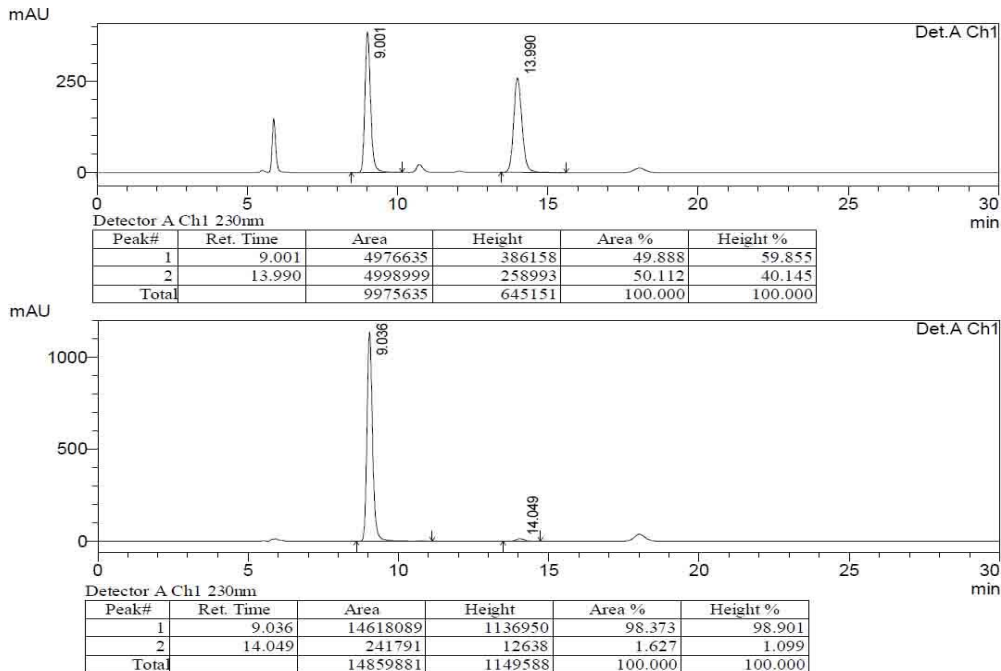
A solution of **ent-2-7a** (85 mg, 0.2 mmol, 1.0 eq) and silver trifluoroacetate (133 mg, 0.6 mmol, 3.0 eq) in acetone (3.0 mL) and water (1.0 mL) was stirred at 60 °C for 8 h in dark. After the mixture was cooled to room temperature, to the solution was added sat. NaCl (2.0 mL) and stirred for 5 min. The mixture was

filtered by celite and washed with EtOAc. The filtrate was separated and the aqueous phase was extracted with EtOAc (3×5 mL). The combined extracts were washed with brine, dried and concentrated in *vacuo*. The residue was purified by column chromatography to give the desired product **ent-2-8a** as a yellow solid (50 mg, 68%).

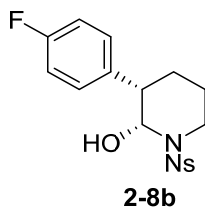
(2*S*,3*S*)-1-(4-nitrophenylsulfonyl)-2-phenylpiperidin-3-ol (**ent-2-8a**):



$[\alpha]_D^{25}$ -110.9 (c 1.0, CH_2Cl_2 , 99% ee); IR (KBr): 3491, 2946, 1527, 1348, 1165, 1089 cm^{-1} ; ^1H NMR (400 MHz, CDCl_3): δ 8.31 (d, $J = 8.9$ Hz, 2H), 8.04 (d, $J = 8.9$ Hz, 2H), 7.37-7.34 (m, 2H), 7.28-7.25 (m, 3H), 5.64 (t, $J = 2.9$ Hz, 1H), 3.69 (dt, $J = 12.7, 2.9$ Hz, 1H), 3.05-2.97 (m, 2H), 2.16-2.05 (m, 1H), 1.98-1.93 (m, 1H), 1.86-1.75 (m, 3H); ^{13}C NMR (100 MHz, CDCl_3): δ 150.0, 145.3, 140.2, 129.1, 128.9, 128.0, 127.6, 124.0, 79.9, 47.5, 40.2, 25.1, 21.8; HRMS (ESI) calcd for $\text{C}_{17}\text{H}_{17}\text{N}_2\text{O}_5\text{S}$ m/z $[\text{M} - \text{H}]^-$: 361.0864; found: 361.0864. HPLC (Daicel Chiralpak IA, *i*-PrOH/hexane = 40/60, 0.6 mL/min, 230 nm) $t_1 = 9.0$ min (major), $t_2 = 14.0$ min (minor).

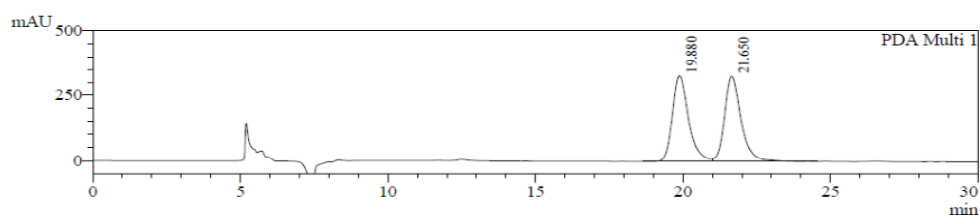


(2R,3R)-3-(4-fluorophenyl)-1-(4-nitrophenylsulfonyl)piperidin-2-ol (**2-8b**):



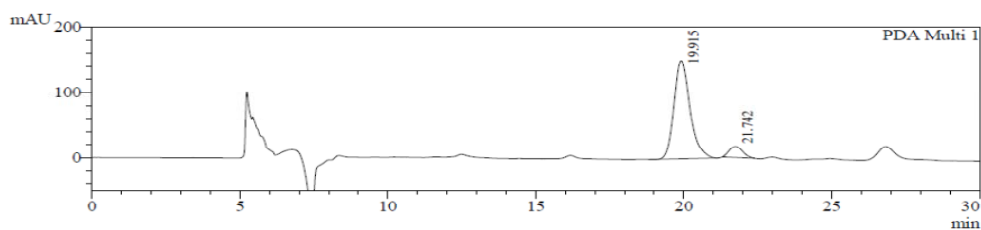
Yellow oil. $[\alpha]_D^{25} +18$ (c 1.0, CHCl_3 , 83% ee); IR (film): 3498, 2929, 1530, 1349, 1164, 1091 cm^{-1} ; ^1H NMR (600 MHz, CDCl_3) δ 8.33 (d, $J = 8.8$ Hz, 2H), 8.05 (d, $J = 8.8$ Hz, 2H), 7.25 – 7.21 (m, 2H), 7.05 (d, $J = 8.6$ Hz, 2H), 5.61 (s, 1H), 3.70 (d, $J = 11.3$ Hz, 1H), 3.04 – 2.98 (m, 2H), 2.07 (dd, $J = 13.0, 3.6$ Hz, 1H), 1.95 (d, $J = 13.6$ Hz, 1H), 1.81 – 1.73 (m, 3H); ^{13}C NMR (150 MHz, CDCl_3) δ 162.9, 161.3, 150.1, 145.3, 136.0, 129.6, 129.5, 129.0, 124.1, 115.8, 115.7, 79.6, 46.8, 40.1, 29.7, 25.1, 22.2; HRMS (ESI) calcd for $\text{C}_{17}\text{H}_{17}\text{FN}_2\text{O}_5\text{SNa}$ m/z $[\text{M} + \text{Na}]^+$:

403.0734; found: 403.0740. HPLC (Daicel Chiralpak IC, *i*-PrOH/hexane = 15/85, 0.6 mL/min, 230 nm) t_1 = 19.9 min (major), t_2 = 21.7 min (minor).



PDA Ch1 230nm 4nm

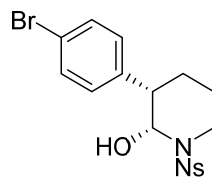
Peak#	Ret. Time	Area	Height	Area %	Height %
1	19.880	12584568	329695	49.660	50.152
2	21.650	12757075	327699	50.340	49.848
Total		25341643	657393	100.000	100.000



PDA Ch1 230nm 4nm

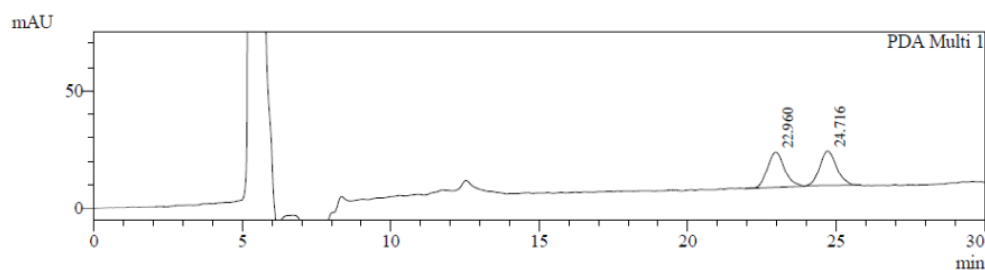
Peak#	Ret. Time	Area	Height	Area %	Height %
1	19.915	5674005	150756	91.292	89.801
2	21.742	541226	17122	8.708	10.199
Total		6215231	167878	100.000	100.000

(2R,3R)-3-(4-bromophenyl)-1-(4-nitrophenylsulfonyl)piperidin-2-ol (**2-8d**):



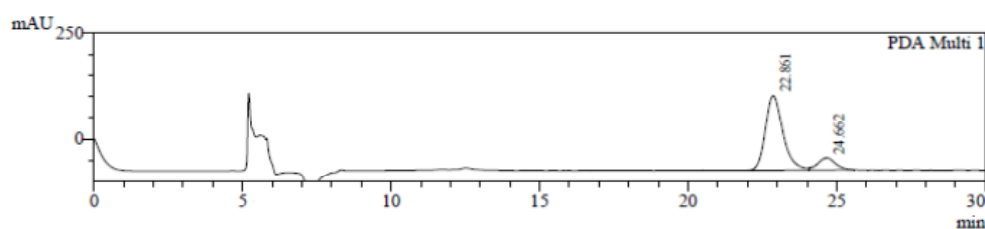
2-8d

Yellow oil. $[\alpha]_D^{25} +27$ (c 1.0, CHCl_3 , 72% ee); IR (film): 3369, 2923, 1532, 1349, 1162, 1009 cm^{-1} ; ^1H NMR (600 MHz, CDCl_3) δ 8.33 (d, $J = 8.8$ Hz, 2H), 8.04 (d, $J = 8.8$ Hz, 2H), 7.48 (d, $J = 8.4$ Hz, 2H), 7.14 (d, $J = 8.4$ Hz, 2H), 5.63 – 5.59 (m, 1H), 3.69 (d, $J = 11.8$ Hz, 1H), 3.02 (dd, $J = 16.9, 7.5$ Hz, 1H), 2.98 – 2.93 (m, 1H), 2.05 (dd, $J = 12.0, 4.6$ Hz, 1H), 1.95 (d, $J = 13.7$ Hz, 1H), 1.82 – 1.73 (m, 3H); ^{13}C NMR (151 MHz, CDCl_3) δ 150.1, 145.3, 139.3, 132.0, 129.8, 129.0, 124.1, 121.6, 79.5, 47.1, 40.1, 24.98, 22.0; HRMS (ESI) calcd for $\text{C}_{17}\text{H}_{17}\text{BrN}_2\text{O}_5\text{SNa}$ m/z $[\text{M} + \text{Na}]^+$: 462.9934; found: 462.9924. HPLC (Daicel Chiralpak IC, i -PrOH/hexane = 15/85, 0.6 mL/min, 230 nm) $t_1 = 22.9$ min (major), $t_2 = 24.7$ min (minor).



PDA Ch1 230nm 4nm

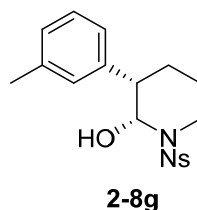
Peak#	Ret. Time	Area	Height	Area %	Height %
1	22.960	593506	14751	50.943	50.513
2	24.716	571529	14451	49.057	49.487
Total		1165035	29203	100.000	100.000



PDA Ch1 230nm 4nm

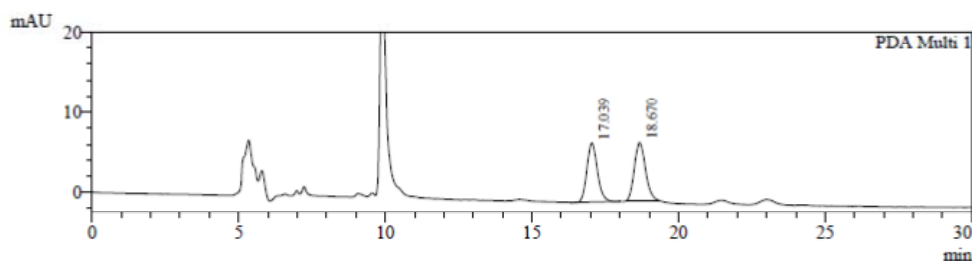
Peak#	Ret. Time	Area	Height	Area %	Height %
1	22.861	7196694	174560	86.248	86.058
2	24.662	1147452	28280	13.752	13.942
Total		8344145	202840	100.000	100.000

(2R,3R)- 1-(4-nitrophenylsulfonyl)-3-(m-tolyl)piperidin-2-ol (2-8g):



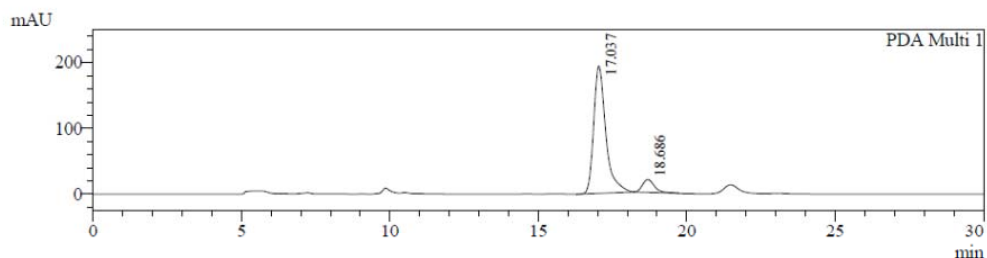
Yellow oil. $[\alpha]_D^{25} +77$ (*c* 1.0, CHCl₃, 82% ee); IR (film): 3494, 2935, 1529, 1349, 1162, 1091 cm⁻¹; ¹H NMR (600 MHz, CDCl₃) δ 8.31 (d, *J* = 8.8 Hz, 2H), 8.05 (d, *J* = 8.8 Hz, 2H), 7.24 (d, *J* = 7.6 Hz, 1H), 7.12 – 7.03 (m, 3H), 5.64 (s, 1H), 3.70 (d, *J* = 10.9 Hz, 1H), 2.99 (dd, *J* = 16.9, 13.1 Hz, 2H), 2.35 (s, 3H), 2.09 (dd, *J* = 13.0, 3.2 Hz, 1H), 1.95 (d, *J* = 13.7 Hz, 1H), 1.83 – 1.74 (m, 3H); ¹³C NMR (150

MHz, CDCl₃) δ 150.0, 145.3, 140.1, 138.8, 129.2, 128.9, 128.8, 128.4, 124.8, 123.98, 79.9, 47.3, 40.2, 25.0, 21.7, 21.4; HRMS (ESI) calcd for C₁₈H₂₀N₂O₅SNa m/z [M + Na]⁺: 399.0985; found: 399.0977. HPLC (Daicel Chiralpak IC, *i*-PrOH/hexane = 20/80, 0.6 mL/min, 230 nm) t_1 = 17.0 min (major), t_2 = 18.7 min (minor).



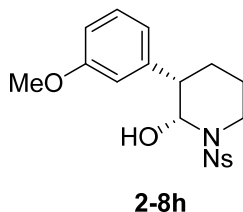
PDA Ch1 230nm 4nm

Peak#	Ret. Time	Area	Height	Area %	Height %
1	17.039	180878	7355	49.007	50.450
2	18.670	188208	7223	50.993	49.550
Total		369086	14578	100.000	100.000

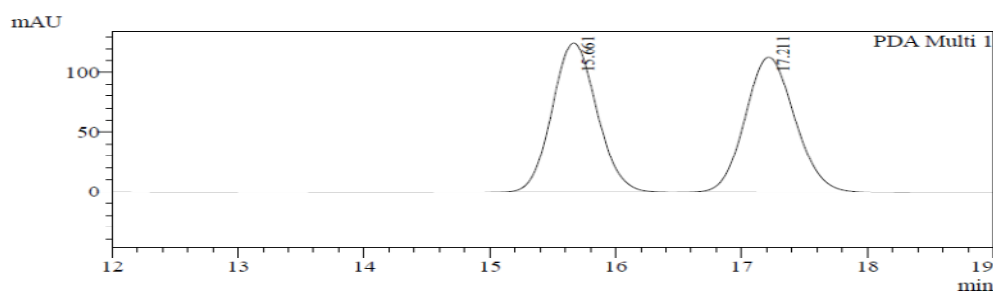


PDA Ch1 230nm 4nm

Peak#	Ret. Time	Area	Height	Area %	Height %
1	17.037	5493506	193906	90.924	90.832
2	18.686	548371	19571	9.076	9.168
Total		6041877	213477	100.000	100.000

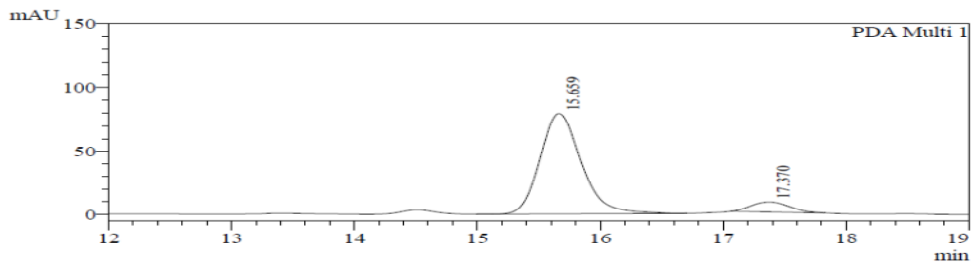
(2R,3R)- 1-(4-nitrophenylsulfonyl)-3-methoxypiperidin-2-ol (2-8h):

Yellow oil. $[\alpha]_D^{25} +92$ (*c* 0.2, CHCl₃, 83% ee); IR (film): 3513, 2931, 1529, 1349, 1161, 1090 cm⁻¹; ¹H NMR (600 MHz, CDCl₃) δ 8.32 (d, *J* = 8.8 Hz, 2H), 8.05 (d, *J* = 8.8 Hz, 2H), 7.28 (d, *J* = 7.9 Hz, 1H), 6.86 – 6.79 (m, 3H), 5.65 (s, 1H), 3.81 (s, 3H), 3.69 (d, *J* = 9.7 Hz, 1H), 3.03 – 2.96 (m, 2H), 2.09 – 2.04 (m, 1H), 1.98 – 1.91 (m, 1H), 1.83 – 1.75 (m, 3H); ¹³C NMR (151 MHz, CDCl₃) δ 160.0, 150.0, 145.2, 141.8, 130.0, 129.1, 124.0, 120.1, 114.0, 112.7, 79.8, 55.3, 47.5, 40.2, 25.0, 21.8; HRMS (ESI) calcd for C₁₈H₂₀N₂O₆SNa *m/z* [M + Na]⁺: 415.0934; found: 416.0946. HPLC (Daicel Chiralpak IC, *i*-PrOH/hexane = 40/60, 0.6 mL/min, 230 nm) *t*₁ = 15.6 min (major), *t*₂ = 17.3 min (minor).



PDA Ch1 230nm 4nm

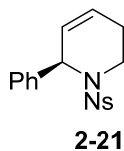
Peak#	Ret. Time	Area	Height	Area %	Height %
1	15.661	3077324	124814	49.888	52.561
2	17.211	3091088	112652	50.112	47.439
Total		6168412	237466	100.000	100.000



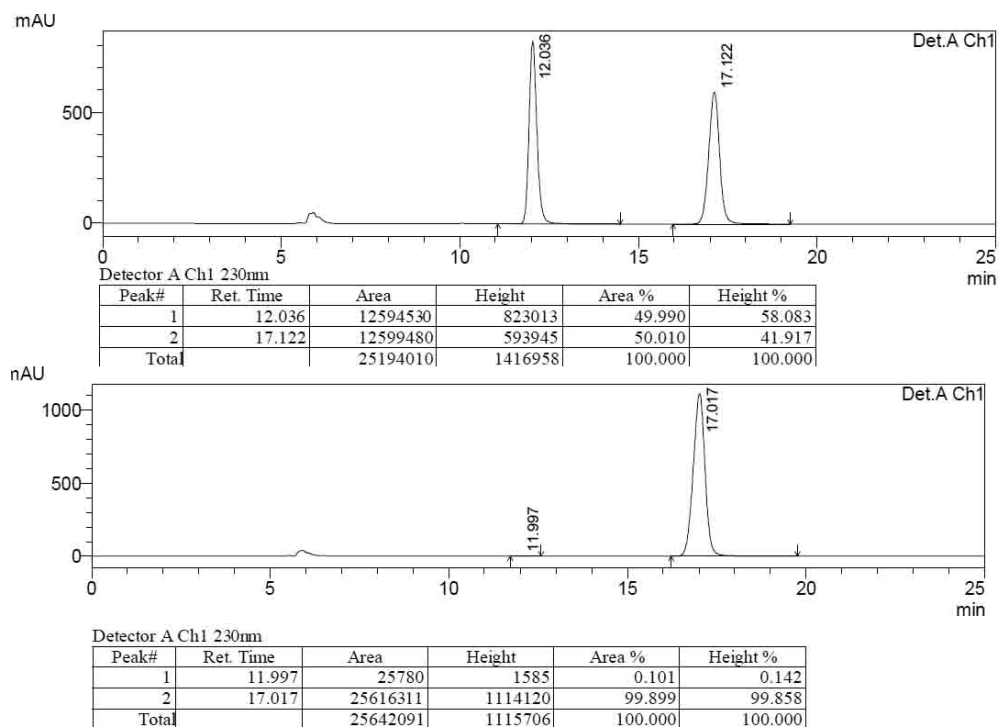
PDA Ch1 230nm 4nm

Peak#	Ret. Time	Area	Height	Area %	Height %
1	15.659	1850243	79128	91.628	90.942
2	17.370	169053	7881	8.372	9.058
Total		2019296	87009	100.000	100.000

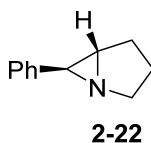
(R)-1-(4-Nitrophenylsulfonyl)-6-phenyl-1,2,3,6-tetrahydropyridine (2-21):



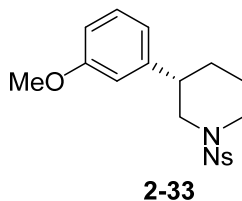
White solid, $[\alpha]_D^{25} +264.6$ (c 1.0, CH_2Cl_2 , 99% ee); IR (KBr): 2932, 1532, 1346, 1163, 1097, 940 cm^{-1} ; ^1H NMR (400 MHz, CDCl_3): δ 8.21 (d, J = 8.9 Hz, 2H), 7.85 (d, J = 8.9 Hz, 2H), 7.37-7.35 (m, 2H), 7.31-7.28 (m, 3H), 5.93-5.89 (m, 1H), 5.85-5.80 (m, 1H), 5.53 (s, 1H), 3.85 (ddd, J = 13.8, 6.2, 1.0 Hz, 1H), 3.15 (ddd, J = 16.2, 11.3, 5.0 Hz, 1H), 2.14-1.97 (m, 2H); ^{13}C NMR (100 MHz, CDCl_3): δ 149.7, 146.9, 138.7, 128.5, 128.3 (2 carbons), 128.2, 128.1, 126.0, 124.0, 56.6, 38.7, 23.8; HRMS (EI) calcd for $\text{C}_{17}\text{H}_{16}\text{N}_2\text{O}_4\text{S}$ m/z $[\text{M}]^+$: 344.0825; found: 344.0834. HPLC (Daicel Chiralpak IA, i -PrOH/hexane = 40/60, 0.6 mL/min, 230 nm) t_1 = 12.0 min (minor), t_2 = 17.0 min (major).



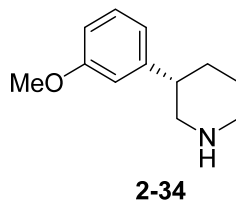
(6*S*)-6-Phenyl-1-azabicyclo[3.1.0]hexane (2-22):



^1H NMR (400 MHz, CDCl_3): δ 7.29-7.18 (m, 5H), 3.20 (ddd, $J = 12.2, 8.4, 1.3$ Hz, 1H), 3.05 (dt, $J = 11.5, 7.6$ Hz, 1H), 2.44 (d, $J = 4.8, 2.8$ Hz, 1H), 2.35 (d, $J = 2.6$ Hz, 1H), 2.23 (d, $J = 13.3, 8.1$ Hz, 1H), 2.03-1.93 (m, 1H), 1.78-1.70 (m, 1H), 1.65-1.56 (m, 1H); ^{13}C NMR (100 MHz, CDCl_3): δ 140.2, 128.2, 126.7, 126.0, 53.1, 50.6, 39.7, 26.6, 20.7; HRMS (ESI) calcd for $\text{C}_{11}\text{H}_{14}\text{N}$ m/z $[\text{M} + \text{H}]^+$: 160.1121; found: 160.1114.

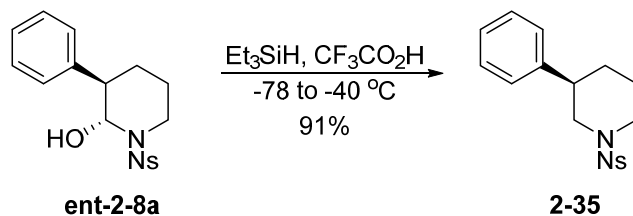
(R)-1-(4-nitrophenylsulfonyl)-3-phenylpiperidine (2-33):

$[\alpha]_D^{25} +215$ (*c* 1.0, CHCl_3 , 83% ee); IR (film): 2936, 1529, 1349, 1170, 1089, 1047, 960 cm^{-1} ; ^1H NMR (600 MHz, CDCl_3): ^1H NMR (600 MHz, CDCl_3) δ 8.37 (d, $J = 8.9$ Hz, 2H), 7.93 (d, $J = 8.9$ Hz, 2H), 7.25 – 7.21 (m, 1H), 6.79 (ddd, $J = 8.3, 2.6, 0.6$ Hz, 1H), 6.75 (d, $J = 7.6$ Hz, 1H), 6.73 – 6.69 (m, 1H), 3.94 – 3.89 (m, 2H), 3.79 (s, 3H), 2.86 (tt, $J = 11.7, 3.7$ Hz, 1H), 2.35 (td, $J = 12.0, 2.9$ Hz, 1H), 2.28 (t, $J = 11.4$ Hz, 1H), 2.03 – 1.95 (m, 1H), 1.88 (ddd, $J = 12.9, 6.4, 3.2$ Hz, 1H), 1.83 – 1.74 (m, 1H), 1.45 (ddd, $J = 25.6, 12.6, 3.9$ Hz, 1H). ^{13}C NMR (151 MHz, CDCl_3) δ 159.8, 150.1, 143.6, 142.5, 129.7, 128.7, 124.3, 119.4, 113.3, 112.0, 55.2, 52.5, 46.4, 42.2, 30.3, 25.0; HRMS (ESI) calcd for $\text{C}_{18}\text{H}_{20}\text{N}_2\text{O}_5\text{SNa}$ m/z $[\text{M} + \text{Na}]^+$: 399.0985; found: 399.0988.

(S)-3-(3-methoxyphenyl)piperidine (2-34):

To a stirred solution of **9** (18 mg, 0.05 mmol, 1.0 eq) in 0.5 mL of MeCN was added thiophenol (16 μ L, 0.25 mmol, 5.0 eq) followed by K_2CO_3 (35 mg, 0.25 mmol, 5.0 eq). After the reaction was stirred for 12 hours, the reaction was quenched with saturated $NaHCO_3$ (2 mL) and extracted with EtOAc (3 x 5 mL). The combined organic layer was dried using $MgSO_4$, filtered, and concentrated under reduced pressure.

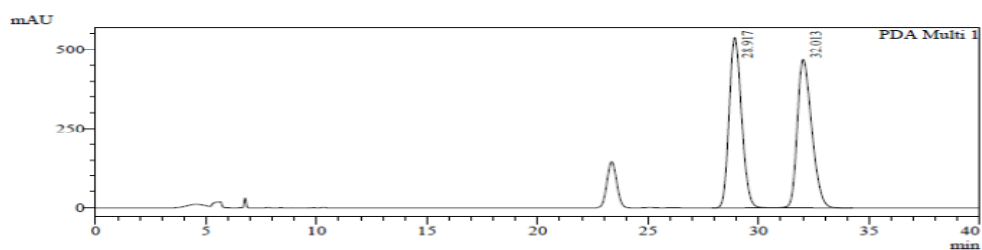
$[\alpha]_D^{25} +8.0$ (c 1.0, MeOH, 83% ee); IR (film): 2931, 1601, 1436, 1160, 1089, 1046, 750 cm^{-1} ; 1H NMR (600 MHz, $CDCl_3$) δ 7.25 – 7.19 (m, 1H), 6.80 (d, J = 7.5 Hz, 1H), 6.78 – 6.71 (m, 2H), 3.80 (s, 3H), 3.25 (dd, J = 25.6, 11.8 Hz, 3H), 2.81 (ddd, J = 15.1, 11.6, 8.2 Hz, 1H), 2.77 – 2.66 (m, 2H), 2.07 – 1.99 (m, 1H), 1.92 – 1.81 (m, 1H), 1.80 – 1.70 (m, 1H), 1.62 (ddd, J = 16.2, 12.9, 3.9 Hz, 1H). ^{13}C NMR (151 MHz, $CDCl_3$) δ 159.71, 145.27, 129.50, 119.37, 113.06, 111.69, 77.21, 77.00, 76.79, 55.17, 52.43, 45.73, 42.90, 31.50, 25.68. HRMS (ESI) calcd for $C_{12}H_{18}NO$ m/z $[M + H]^+$: 191.1383; found: 191.1367.

(R)-1-(4-nitrophenylsulfonyl)-3-phenylpiperidine (2-35):

To a stirred solution of **ent-2-8a** (36 mg, 0.1 mmol, 1.0 eq) in 4 mL of CH_2Cl_2 was added triethylsilane (80 μL , 0.5 mmol, 5.0 eq) at -78°C . The mixture was added trifluoroacetic acid (38 μL , 0.5 mmol, 5.0 eq), stirred and allowed to warm up to room temperature overnight. The reaction was quenched with NaHCO_3 and extracted with CH_2Cl_2 . The organic phase was dried with MgSO_4 , filtered and removed under reduced pressure. The residue was purified by column chromatography to yield the desired product **11** as a yellow solid (31 mg, 91%).

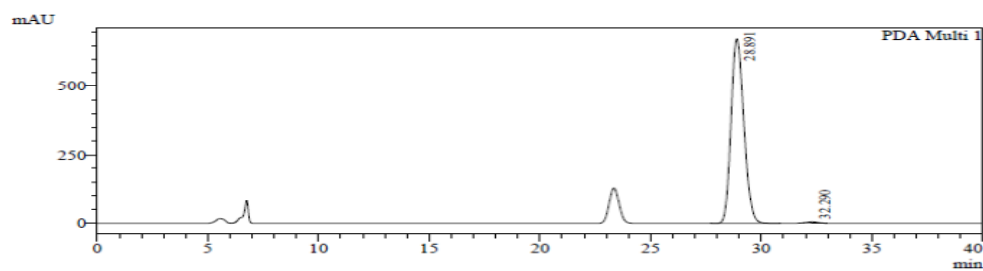
$[\alpha]_D^{25}$ -18.0 (c 1.0, CHCl_3 , 99% ee); IR (film): 2935, 1529, 1350, 1168, 1089 cm^{-1} ; ^1H NMR (600 MHz, CDCl_3): ^1H NMR (600 MHz, CDCl_3) δ 8.37 (d, J = 8.7 Hz, 2H), 7.93 (d, J = 8.7 Hz, 2H), 7.31 (t, J = 7.4 Hz, 2H), 7.25 (d, J = 7.4 Hz, 1H), 7.17 (d, J = 7.2 Hz, 2H), 3.92 (d, J = 11.5 Hz, 2H), 2.92 – 2.85 (m, 1H), 2.35 (td, J = 12.0, 2.5 Hz, 1H), 2.29 (t, J = 11.4 Hz, 1H), 1.99 (d, J = 13.3 Hz, 1H), 1.92 – 1.86 (m, 1H), 1.86 – 1.75 (m, 1H), 1.47 (ddd, J = 25.6, 12.7, 3.8 Hz, 1H); ^{13}C NMR (150 MHz, CDCl_3) δ 150.13, 142.51, 141.97, 128.72, 127.19, 127.10, 124.33, 52.59, 46.40, 42.17, 30.31, 25.04; HRMS (ESI) calcd for $\text{C}_{18}\text{H}_{20}\text{N}_2\text{O}_3\text{S}$ m/z $[\text{M} + \text{Na}]^+$: 367.1087; found: 367.1094. HPLC (Daicel Chiralpak IC, i -

PrOH/hexane = 40/60, 0.6 mL/min, 230 nm) t_1 = 28.9 min (major), t_2 = 32.3 min (minor).



PDA Ch1 230nm 4nm

Peak#	Ret. Time	Area	Height	Area %	Height %
1	28.917	21092373	538388	49.934	53.501
2	32.013	21148372	467920	50.066	46.499
Total		42240744	1006308	100.000	100.000



PDA Ch1 230nm 4nm

Peak#	Ret. Time	Area	Height	Area %	Height %
1	28.891	27190421	675997	99.502	99.420
2	32.290	136141	3941	0.498	0.580
Total		27326562	679938	100.000	100.000

2.5 References

1. (a) O'Hagan, D., *Nat Prod Rep* **2000**, *17*, 435; (b) Asano, N.; Nash, R. J.; Molyneux, R. J.; Fleet, G. W. J., *Tetrahedron: Asymmetry* **2000**, *11*, 1645; (c) Lillielund, V. H.; Jensen, H. H.; Liang, X.; Bols, M., *Chem. Rev.* **2002**, *102*, 515.
2. (a) Baran, P. S.; Corey, E. J., *J. Am. Chem. Soc.* **2002**, *124*, 7904; (b) Bowie, A. L., Jr.; Trauner, D., *J. Org. Chem.* **2009**, *74*, 1581; (c) Julian, L. D.; Hartwig, J. F., *J. Am. Chem. Soc.* **2010**, *132*, 13813; (d) Hoover, J. M.; Di, P. A.; Mayer, J. M.; Michael, F. E., *J. Am. Chem. Soc.* **2010**, *132*, 5043.
3. (a) Amat, M.; Bassas, O.; Llor, N.; Canto, M.; Perez, M.; Molins, E.; Bosch, J., *Chem. - Eur. J.* **2006**, *12*, 7872; (b) Amat, M.; Perez, M.; Bosch, J., *Chem. - Eur. J.* **2011**, *17*, 7724.
4. (a) Pfrengle, W.; Kunz, H., *J. Org. Chem.* **1989**, *54*, 4261; (b) Randolph, J. T.; McClure, K. F.; Danishefsky, S. J., *J. Am. Chem. Soc.* **1995**, *117*, 5712; (c) Roberge, J. Y.; Beebe, X.; Danishefsky, S. J., *Science* **1995**, *269*, 202; (d) Weymann, M.; Pfrengle, W.; Schollmeyer, D.; Kunz, H., *Synthesis* **1997**, 1151; (e) Dragoli, D. R.; Thompson, L. A.; O'Brien, J.; Ellman, J. A., *J. Comb. Chem.* **1999**, *1*, 534; (f) Paterson, I.; Donghi, M.; Gerlach, K., *Angew. Chem., Int. Ed.* **2000**, *39*, 3315; (g) Zech, G.; Kunz, H., *Chem. - Eur. J.* **2004**, *10*, 4136.

5. Liu, R.-H.; Fang, K.; Wang, B.; Xu, M.-H.; Lin, G.-Q., *J. Org. Chem.* **2008**, *73*, 3307.
6. (a) Law, H.; Leclerc, G. A.; Neumeyer, J. L., *Tetrahedron: Asymmetry* **1991**, *2*, 989; (b) Sonesson, C.; Lindborg, J., *Tetrahedron Lett.* **1994**, *35*, 9063; (c) Wong, Y.-S.; Marazano, C.; Gnecco, D.; Genisson, Y.; Chiaroni, A.; Das, B. C., *J. Org. Chem.* **1997**, *62*, 729; (d) Johnson, T. A.; Curtis, M. D.; Beak, P., *J. Am. Chem. Soc.* **2001**, *123*, 1004; (e) Weihofen, R.; Dahnz, A.; Tverskoy, O.; Helmchen, G., *Chem. Commun.* **2005**, 3541; (f) Esquivias, J.; Arrayas, R. G.; Carretero, J. C., *Angew. Chem., Int. Ed.* **2007**, *46*, 9257; (g) Girling, P. R.; Kiyoi, T.; Whiting, A., *Org. Biomol. Chem.* **2011**, *9*, 3105; (h) Cui, Z.; Yu, H.-J.; Yang, R.-F.; Gao, W.-Y.; Feng, C.-G.; Lin, G.-Q., *J. Am. Chem. Soc.* **2011**, *133*, 12394; (i) Ye, M.; Gao, G.-L.; Edmunds, A. J. F.; Worthington, P. A.; Morris, J. A.; Yu, J.-Q., *J. Am. Chem. Soc.* **2011**, *133*, 19090.
7. (a) Hobson, J. D.; Riddell, W. D., *Chem. Commun.* **1968**, 1178; (b) Tamaru, Y.; Kawamura, S.; Bando, T.; Tanaka, K.; Hojo, M.; Yoshida, Z., *J. Org. Chem.* **1988**, *53*, 5491; (c) Edstrom, E. D., *Tetrahedron Lett.* **1991**, *32*, 5709; (d) Corey, E. J.; Loh, T. P.; AchyuthaRao, S.; Daley, D. C.; Sarshar, S., *J. Org. Chem.* **1993**, *58*, 5600; (e) Helaja, J.; Goettlich, R., *Chem. Commun.* **2002**, 720; (f) Sasaki, M.; Yudin, A. K., *J. Am. Chem. Soc.* **2003**, *125*, 14242; (g) Chen, G.; Sasaki, M.; Li, X.; Yudin, A. K., *J. Org. Chem.* **2006**, *71*, 6067.

8. (a) Chen, G.; Ma, S., *Angew. Chem., Int. Ed.* **2010**, *49*, 8306; (b) Castellanos, A.; Fletcher, S. P., *Chem. - Eur. J.* **2011**, *17*, 5766; (c) Hennecke, U., *Chem. - Asian J.* **2012**, *7*, 456; (d) Zhang, W.; Liu, N.; Schienebeck, C. M.; Decloux, K.; Zheng, S.; Werness, J. B.; Tang, W., *Chem. - Eur. J.* **2012**, *18*, 7296; (e) Dobish, M. C.; Johnston, J. N., *J. Am. Chem. Soc.* **2012**, *134*, 6068; (f) Murai, K.; Nakamura, A.; Matsushita, T.; Shimura, M.; Fujioka, H., *Chem. - Eur. J.* **2012**, *18*, 8448.
9. (a) Jiang, X.; Tan, C. K.; Zhou, L.; Yeung, Y.-Y., *Angew. Chem., Int. Ed.* **2012**, *51*, 7771; (b) Chen, J.; Zhou, L.; Tan, C. K.; Yeung, Y.-Y., *J. Org. Chem.* **2012**, *77*, 999; (c) Chen, J.; Zhou, L.; Yeung, Y.-Y., *Org. Biomol. Chem.* **2012**, *10*, 3808; (d) Tan, C. K.; Le, C.; Yeung, Y.-Y., *Chem. Commun.* **2012**, *48*, 5793; (e) Tan, C. K.; Zhou, L.; Yeung, Y.-Y., *Org. Lett.* **2011**, *13*, 2738; (f) Tan, C. K.; Chen, F.; Yeung, Y.-Y., *Tetrahedron Lett.* **2011**, *52*, 4892; (g) Tan, C. K.; Zhou, L.; Yeung, Y.-Y., *Synlett* **2011**, 1335; (h) Zhou, L.; Chen, J.; Tan, C. K.; Yeung, Y.-Y., *J. Am. Chem. Soc.* **2011**, *133*, 9164; (i) Zhou, L.; Tan, C. K.; Jiang, X.; Chen, F.; Yeung, Y.-Y., *J. Am. Chem. Soc.* **2010**, *132*, 15474.
10. Veitch, G. E.; Jacobsen, E. N., *Angew. Chem., Int. Ed.* **2010**, *49*, 7332.
11. (a) Matsumura, Y.; Terauchi, J.; Yamamoto, T.; Konno, T.; Shono, T., *Tetrahedron* **1993**, *49*, 8503; (b) Thaler, F.; Varasi, M.; Colombo, A.; Boggio, R.; Munari, D.; Regalia, N.; Rozio, M. G.; Reali, V.; Resconi, A. E.; Mai, A.; Gagliardi, S.; Dondio, G.; Minucci, S.; Mercurio, C., *ChemMedChem* **2010**, *5*, 1359.

12. (a) Takayama, H.; Kitajima, M.; Ogata, K.; Sakai, S., *J. Org. Chem.* **1992**, 57, 4583; (b) Ori, M.; Toda, N.; Takami, K.; Tago, K.; Kogen, H., *Tetrahedron* **2005**, 61, 2075.
13. (a) Desai, M. C.; Lefkowitz, S. L.; Thadeio, P. F.; Longo, K. P.; Snider, R. M., *J. Med. Chem.* **1992**, 35, 4911; (b) Rosen, T.; Seeger, T. F.; McLean, S.; Desai, M. C.; Guarino, K. J.; Bryce, D.; Pratt, K.; Heym, J.; Chalabi, P. M.; et, a., *J. Med. Chem.* **1993**, 36, 3197; (c) Harrison, T.; Williams, B. J.; Swain, C. J.; Ball, R. G., *Bioorg. Med. Chem. Lett.* **1994**, 4, 2545; (d) Kamel, A.; Davis, J.; Potchoiba, M. J.; Prakash, C., *Xenobiotica* **2006**, 36, 235.
14. (a) Amat, M.; Canto, M.; Llor, N.; Escolano, C.; Molins, E.; Espinosa, E.; Bosch, J., *J. Org. Chem.* **2002**, 67, 5343; (b) Macchia, M.; Cervetto, L.; Demontis, G. C.; Longoni, B.; Minutolo, F.; Orlandini, E.; Ortore, G.; Papi, C.; Sbrana, A.; Macchia, B., *J. Med. Chem.* **2003**, 46, 161; (c) Chang, M.-Y.; Hsu, R.-T.; Chen, H.-P.; Lin, P.-J., *Heterocycles* **2006**, 68, 1173; (d) Hacksell, U.; Arvidsson, L. E.; Svensson, U.; Nilsson, J. L. G.; Sanchez, D.; Wikstroem, H.; Lindberg, P.; Hjorth, S.; Carlsson, A., *J. Med. Chem.* **1981**, 24, 1475; (e) Thorberg, S. O.; Gawell, L.; Csoeregh, I.; Nilsson, J. L. G., *Tetrahedron* **1985**, 41, 129; (f) Grayson, N. A.; Bowen, W. D.; Rice, K. C., *Heterocycles* **1992**, 34, 2281.

Chapter 3

*Enantioselective Desymmetrizing
Bromoetherification of Diolefinic
Diols—Application to the Synthesis of
Novel Chiral Spirocycles*

3.1 Introduction

Chiral spirocycles are a special class of compounds that have attracted much attention over the past decades. Due to the inherent rigidity and well-defined three-dimensional molecular structure, chiral non-racemic spiro molecules have been applied in various areas including catalysis, metal complexation, and molecular architecture.¹

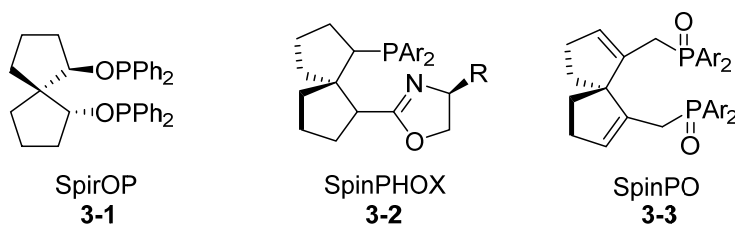


Figure 3.1 Examples of chiral ligands with spirocyclic backbone.

The unique structural features of spirocycles also open a new avenue for exploring new pharmacological space. In fact, many bioactive natural products have been identified to possess the spirocyclic scaffold.²

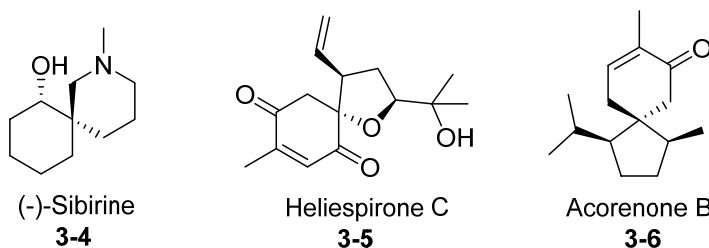


Figure 3.2 Examples of bioactive natural products with spirocyclic scaffolds.

Recently, multifunctional chiral hetero spirocycles with readily modifiable handles gained significant interest as they are particularly useful in modern drug

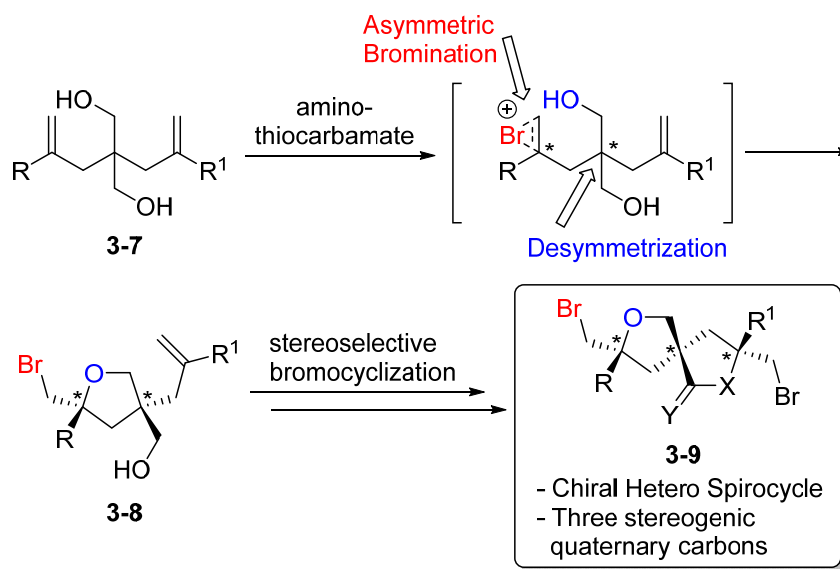
discovery.³ However, facile and efficient asymmetric pathways towards enantioenriched spirocycles remain sporadic. The tremendous difficulty encountered in controlling the regio- and stereochemistry of quaternary carbon centres has caused the synthesis of these privileged scaffolds to remain as a huge challenge for synthetic chemists.¹

Halocyclization of olefinic compounds, an important synthetic transformation that was discovered more than a century ago,⁴ is a powerful method for the construction of heterocycles. However, it was not until recently that significant efforts were devoted to the development of catalytic enantioselective halolactonization, haloetherification, and haloaminocyclization.⁵ The resulting heterocyclic intermediates with modifiable halogen handles are important building blocks to synthetic chemists as it typically resembles the fundamental core of many valuable pharmaceutical intermediates as well as biologically active natural products.⁶

The challenge in developing an efficient method for halocyclization lies in improving the rate of nucleophilic capture as opposed to the olefin-olefin halogen exchange racemization.⁷ Recently, we reported the asymmetric bromolactonization and bromo-aminocyclization reactions using amino-thiocarbamate catalysts.⁸

Herein we are pleased to disclose the catalytic enantioselective synthesis of hetero spirocycles through a double-halocyclization strategy. The first cyclization involves a desymmetrization-asymmetric halogenation process which gives rise to

two quaternary stereogenic carbons in the cyclic ether products **3-8**. Subsequently, a diastereoselective bromoetherification can be performed to yield a series of chiral hetero spiro systems **3-9** (Scheme 3.1). This protocol allow us to access a class of chiral novel spirocycles that is distinctively missing in the literature.¹



Scheme 3.1 Synthesis of hetero spirocycles through the asymmetric bromination and desymmetrization of diolefinic diol.

3.2 Results and Discussion

3.2.1 Catalyst Screening

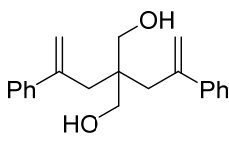
At the initial stage of this project, we screened our library of amino-thiocarbamate catalysts to look for a suitable catalyst that can carry out the

desymmetrization of the diolefinic diol **3-10a** with good enantioselectivity and diastereoselectivity. We first screened for a suitable catalyst core and observed that quinine (catalyst **3-12c**) and quinidine (catalyst **3-12d**) gave better dr and er as compared to cinchonine (catalyst **3-12a**) and cinchonidine (catalyst **3-12b**) (Table 3.1, entries 1–4). It was also worthy to note that quinine (catalyst **3-12c**) and quinidine (catalyst **3-12d**) gave opposite enantioselectivities (entries 3 and 4).

We proceeded to examine the aryl handles on catalyst **3-12d**. Electron-rich aryl substituents were observed to increase the enantioselectivity of the catalysts, with the 4-ethoxyphenyl substituent (catalyst **3-12h**) on the thiocarbamate proving the most selective (Table 3.1 entry 8).

We also investigated the 6-alkoxy substituent of the quinoline through the use of longer straight chain alkyl groups (Table 3.1, entries 10–12) as well as branched alkyl group (Table 3.1, entry 13). The *n*-butyl catalyst **3-12k** was identified to be superior compared to the rest of the catalysts. (Table 3.1 entry 11).

Table 3.1 Catalyst screening for bromoetherification of **3-10a**.



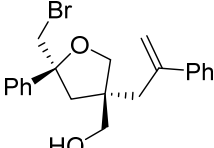
3-10a

Catalyst **3-12** (10 mol %)

NBS (1.2 eq)

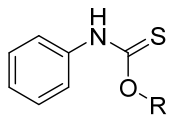
CHCl₃/Hexane (1:1)

-50 °C



3-11a

Catalysts:

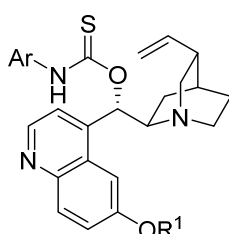


3-12a R = cinchonine

3-12b R = cinchonidine

3-12c R = quinine

3-12d R = quinidine



3-12e Ar = 4-MeO-C₆H₄; R¹ = Me

3-12f Ar = 2,4-(MeO)₂-C₆H₃; R¹ = Me

3-12g Ar = 2,4,6-(MeO)₃-C₆H₂; R¹ = Me

3-12h Ar = 4-EtO-C₆H₄; R¹ = Me

3-12i Ar = 4-BuO-C₆H₄; R¹ = Me

3-12j Ar = 4-EtO-C₆H₄; R¹ = Et

3-12k Ar = 4-EtO-C₆H₄; R¹ = *n*-Bu

3-12l Ar = 4-EtO-C₆H₄; R¹ = *n*-Hex

3-12m Ar = 4-EtOPrO-C₆H₄; R¹ = *i*-Pr

Entry ^a	Catalyst	Yield (%) ^b	dr	er
1	3-12a	87	69:31	35:65
2	3-12b	90	67:33	65:35
3	3-12c	93	74:26	30:70
4	3-12d	95	75:25	70:30
5	3-12e	93	78:22	73:27
6	3-12f	94	70:30	65:35
7	3-12g	95	64:36	62:38
8	3-12h	90	78:22	77:23
9	3-12i	97	76:24	75:25
10	3-12j	95	75:25	78:22
11	3-12k	96	77:23	83:17
12	3-12l	93	74:26	81:19
13	3-12m	94	75:25	78:22

^aReactions were carried out with **3-10a** (0.05 mmol), catalyst (0.005 mmol), and NBS (0.06 mmol) in CHCl₃/hexane (1:1) (5.0 mL) at -50 °C for 12 h in the absence of light. ^b Isolated yields.

3.2.2 Reaction Conditions Optimization

Once the most effective catalyst was identified, a series of temperature and solvent optimization experiments were conducted. The solvent blends chloroform/*n*-hexane (1:1) and chloroform/toluene (1:1) was compared and it was observed that *n*-hexane was more suitable as a co-solvent as compared to toluene, yielding products with higher er (Table 3.2, entries 1–2). When the temperature was decreased to -60 °C, the er improved slightly but on further reduction of the temperature to -65 °C, the reaction yielded virtually no products (Table 3.2, entries 3–4). This was not a surprising result as it was observed that the reaction mixture had solidified at this temperature.

We proceeded to examine the ratio of chloroform to *n*-hexane. When the proportion of chloroform was increased, the er was observed to decrease. On the contrary, when the proportion of *n*-hexane was increased, the er appears increase with increasing proportion of *n*-hexane and reaches the highest with CHCl₃/*n*-hexane (4:7) before decreasing with further increase in proportion of *n*-hexane (Table 3.2, entries 6–8 and 10). Under these conditions, the diastereomeric ratio was determined to be 84:16 and enantioselectivity as 90:10 (Table 3.2, entry 10).

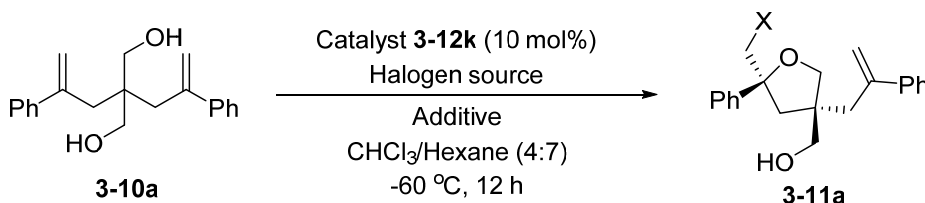
Table 3.2 Solvent and temperature optimization of bromoetherification of **3-10a**.

Entry ^a	Solvent	Temp (°C)	Yield (%) ^b	dr	er
1	CHCl ₃ / <i>n</i> -hexane (1:1)	-50	96	77:23	83:17
2	CHCl ₃ /Toluene (1:1)	-50	97	75:25	69:31
3	CHCl ₃ / <i>n</i> -hexane (1:1)	-60	94	77:23	85:15
4	CHCl ₃ / <i>n</i> -hexane (1:1)	-65	trace	-	-
5	CHCl ₃ / <i>n</i> -hexane (2:1)	-60	92	73:27	75:25
6	CHCl ₃ / <i>n</i> -hexane (2:3)	-60	95	80:20	87:13
7	CHCl ₃ / <i>n</i> -hexane (3:7)	-60	61	77:23	83:17
8	CHCl ₃ / <i>n</i> -hexane (1:4)	-60	33	55:45	66:34
9 ^c	CHCl ₃ / <i>n</i> -hexane (2:3)	-60	94	80:20	87:13
10^c	CHCl₃/<i>n</i>-hexane (4:7)	-60	94	84:16	90:10

^a Reactions were carried out with **3-10a** (0.05 mmol), catalyst (0.005 mmol), and NBS (0.06 mmol) in solvent (5.0 mL) at the indicated temperature for 12 h in the absence of light. ^b Isolated yields. ^c Total reaction volume is 5.5 mL.

To further improve the enantioselectivity of the reaction further, we turned our attention towards alternative halogen sources. After screening, recrystallized *N*-bromophthalimide (NBP) was found to be better and returned with 93:7 er, while other halogen sources gave much lower enantioselectivity or even no reaction (Table 3.3, entries 1–6). Interestingly, it was observed that the addition of 4Å molecular sieves can improve the er up to 96:4 (Table 3.3, entries 7–9). The reaction was found to be readily scalable without diminishing the yield, dr, and er (Table 3.3, entry 10).

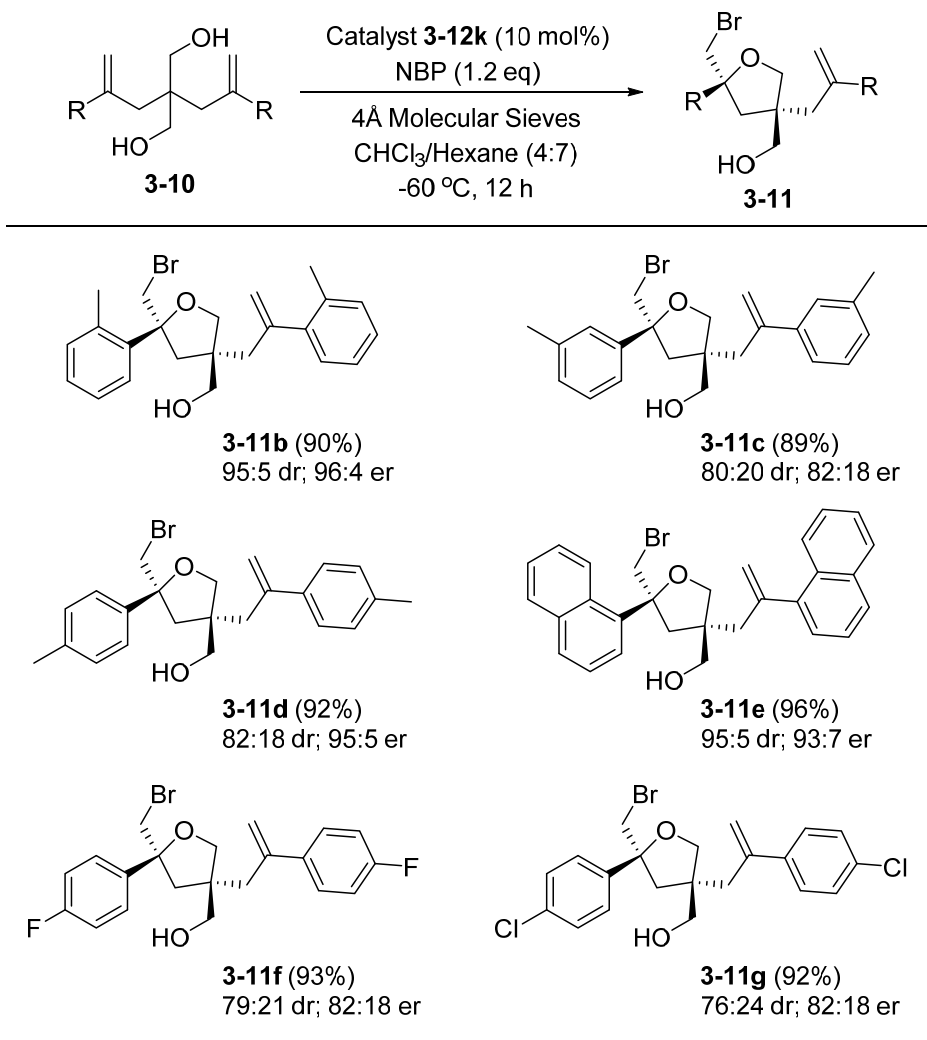
Table 3.3 Effect of halogen source and additives on bromoetherification of **3-10a**.

					
Entry ^a	Halogen Source	Additive	Yield (%) ^b	dr	er
1	NBP	-	90	85:15	92:8
2	DBH	-	93	70:30	67:33
3	TABCO	-	trace	-	-
4	NCS	-	NR	-	-
5	NIS	-	NR	-	-
6	NBP ^c	-	95	85:15	93:7
7	NBP ^c	3Å MS	91	83:17	92:8
8	NBP ^c	4Å MS	93	84:16	96:4
9	NBP ^c	5Å MS	92	86:14	93:7
10^d	NBP^c	4Å MS	91	83:17	95:5

^a Reactions were carried out with **3-10a** (0.05 mmol), catalyst (0.005 mmol), and NBS (0.06 mmol) in CHCl₃/Hexane (4:7) (5.5 mL) at -60 °C for 12 h in the absence of light. ^b Isolated yields. ^c Recrystallized NBP was used. ^d Reaction was carried out using 1 mmol of **3-10a**.

3.2.3 Substrate Scope

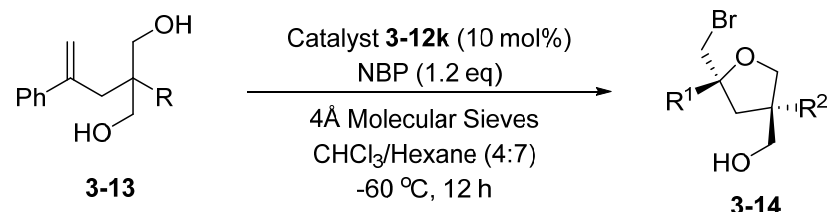
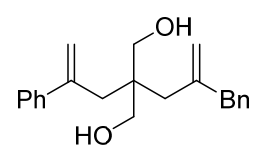
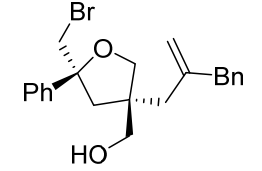
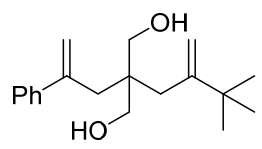
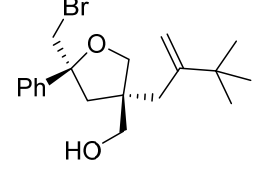
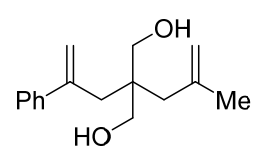
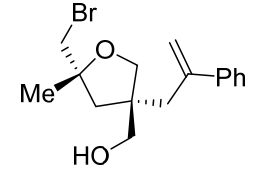
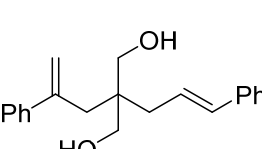
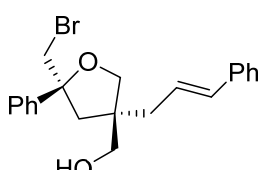
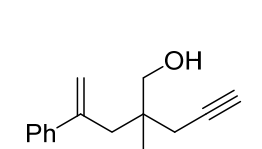
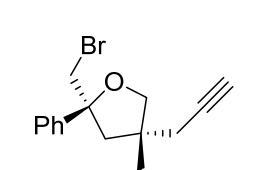
Using the optimized conditions, we examined substrates that possess a symmetrical diol system. In general, the reactions with different diolefinic diols **3-10** proceeded smoothly to give the corresponding bromoethers **3-11** with good to excellent dr and er, in particular, for those that have electron-rich substituents (Table 3.4).

Table 3.4 Bromoetherification of diolefinic diol **3-10**.

Reactions were carried out with **3-10** (0.05 mmol), catalyst (0.005 mmol), and NBS (0.06 mmol) in CHCl₃/Hexane (4:7) (5.5 mL) at -60 °C for 12 h in the absence of light. The yields indicated in the parentheses are the isolated yields.

Diols with unsymmetrical unsaturated systems were also investigated and the results are shown in Table 3.5. Again, good to excellent dr were obtained. For the relatively bulkier alkyl-substituted olefinic substrates **3-13a** and **3-13b**, the cyclization favoured the phenyl olefin with good er (Table 3.5, entries 1–2). On the other hand, the methyl substituted mixed olefin **3-13c** gave rise to **3-14c**, a result of cyclization at the less sterically hindered methyl olefin (Table 3.5, entry 3). Substrate **3-13d**, which contains a 1,1- and a 1,2-disubstituted olefins, returned with product **3-14d** (94%) in good er of 92:8 (Table 3.5, entry 4). An alkene-alkyne mixed system **3-13e** was also examined, which gave **3-14e** exclusively with excellent enantioselectivity (99:1 er) (Table 3.5, entry 5).

Table 3.5 Bromoetherification of diols with unsymmetrical unsaturated systems.

<div style="display: flex; align-items: center; justify-content: center;"> <div style="text-align: center;">  </div> </div>		
Entry ^a	Substrate	Product
1	 3-13a	 3-14a (90%) 88:12 dr 93:7 er
2	 3-13b	 3-14b (91%) 94:6 dr 90:10 er
3	 3-13c	 3-14c (90%) 86:14 dr 70:30 er
4	 3-13d	 3-14d (94%) 79:21 dr 92:8 er
5	 3-13e	 3-14e (91%) 84:16 dr 99:1 er

^a Reactions were carried out with **3-13** (0.05 mmol), catalyst **3-12k** (0.005 mmol), and NBS (0.06 mmol) in CHCl₃/hexane (4:7) (5.5 mL) at -60 °C for 12 h in the absence of light. The yields indicated in the parentheses are the isolated yields.

3.2.4 Investigation on Catalyst Loading

We also examined the catalyst loading that was required to maintain the high *dr* and *er* of the reaction and we observed that under a low catalyst loading of 2%, the *dr* and *er* of the reaction remain almost unchanged (Table 3.6).

Table 3.6 Investigation on the catalyst loading on reaction.

Reaction scheme: **3-10a** $\xrightarrow[\text{CHCl}_3/\text{Hexane (4:7), -60 } ^\circ\text{C, 12 h}]{\text{Catalyst 3-12k (X mol\%), NBP (1.2 eq), 4\text{\AA} MS}}$ **3-11a**

Entry ^a	3-12k (mol %)	Yield (%) ^b	<i>dr</i>	<i>er</i>
1	5	90	81:19	96:4
2	2	93	83:17	94:6

^aReactions were carried out with **3-10a** (0.05 mmol), catalyst (0.005 mmol), and NBS (0.06 mmol) in CHCl₃/Hexane (4:7) (5.5 mL) at -60 °C for 12 h in the absence of light. ^bIsolated yields.

3.2.5 Synthesis of Spirocycles

Substituted tetrahydrofurans **3-11** and **3-14**, which contain two stereogenic quaternary carbons, were further cyclized to yield the corresponding hetero spirocycles. Treatment of **3-11b** with NBS and catalytic amounts of triphenylphosphine sulfide in dichloromethane furnished **3-15** with excellent *dr* (94:6). **3-11b-COOH**, which was obtained by oxidizing **3-11b** using PCC followed by NaClO, could also be cyclized stereoselectively to yield the mixed

cyclic ether-lactone spirocycle **3-16** in 98% yield and 93:7 dr. NIS could also be used in place of NBS to give mixed spirocycle **3-17** that contains both bromo and iodo handles. The reactivity between Br and I can readily be differentiated which is beneficial for subsequent manipulation. Under similar conditions, carboxylic acid derivative **3-14e-COOH** (obtained by oxidizing **3-14e**) could be cyclized to yield spirocycle **3-18** which contains a vinyl bromide substituent. A lower diastereoselectivity was obtained when cyclizing **3-14b** and **3-14d**. Next, the hydroxyl group in **3-11b** was replaced with a *N*-benzyl group to give **3-11b-NHBn**. Unexpectedly, iodocyclization of **3-11b-NHBn** gave rise to the tetrahydrofuran-piperidine mixed spirocycle **3-21** exclusively.

Table 3.7 Synthesis of spirocycles.

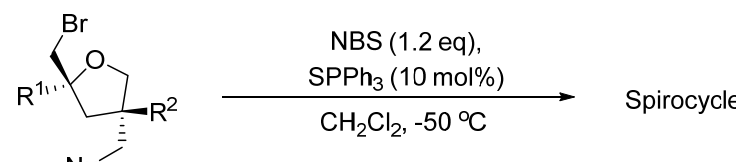
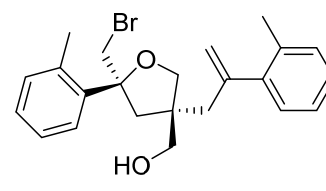
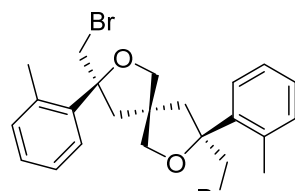
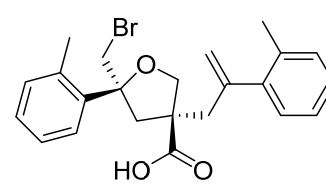
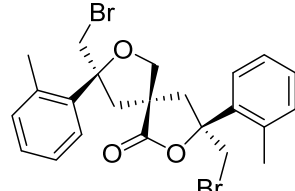
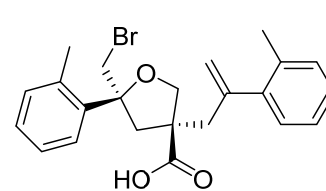
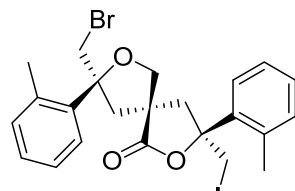
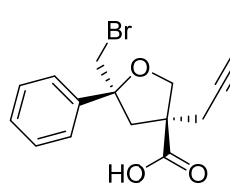
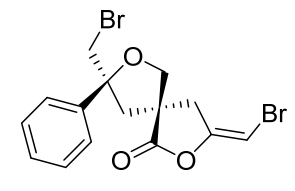
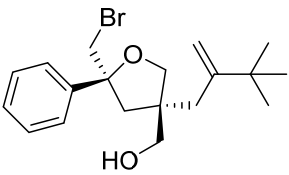
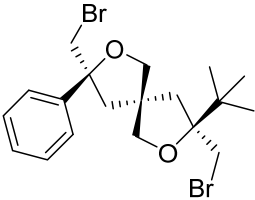
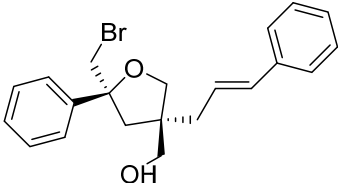
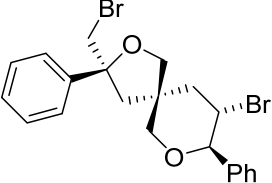
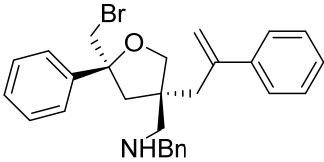
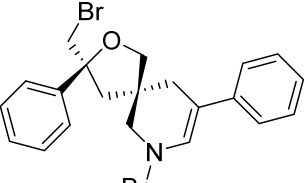
		
Entry	Substrate	Spirocycle
1	 3-11b	 3-15 (96%); 94:6 dr
2	 3-11b-COOH	 3-16 (98%); 93:7 dr
3 ^c	 3-11b-COOH	 3-17 (93%); 93:7 dr
4 ^d	 3-14e-COOH	 3-18 (98%); >99:1 dr

Table 3.7 Synthesis of spirocycles. (cont'd)

Entry	Substrate	Spirocycle
5	 3-14b	 3-19 (91%); 60:40 dr
6	 3-14d	 3-20 (92%); 50:50 dr
7 ^c	 3-11a-NHBn	 3-21 (78%); >99:1 dr

^a Reactions were carried out with substrate (0.05 mmol), catalyst (0.005 mmol), and NBS (0.06 mmol) in CH₂Cl₂ (5.0 mL) at -50 °C for 12 h in the absence of light. ^b The yields indicated in the parentheses are the isolated yields. ^c NIS was used instead of NBS. ^d NaHCO₃ (1.1 eq) was used instead of SPhPh₃

The absolute configurations of the bromoethers as well as the corresponding spirocycles were established based on the X-ray crystallographic study of compound **3-16** (Figure 3.3).

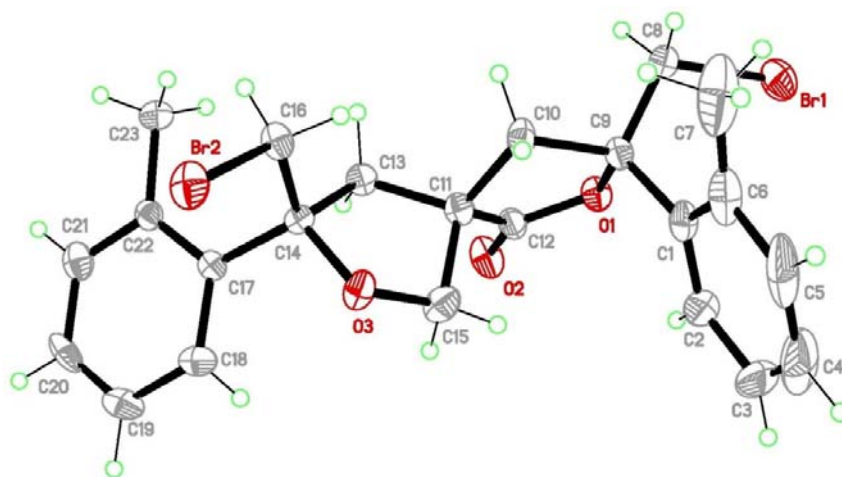
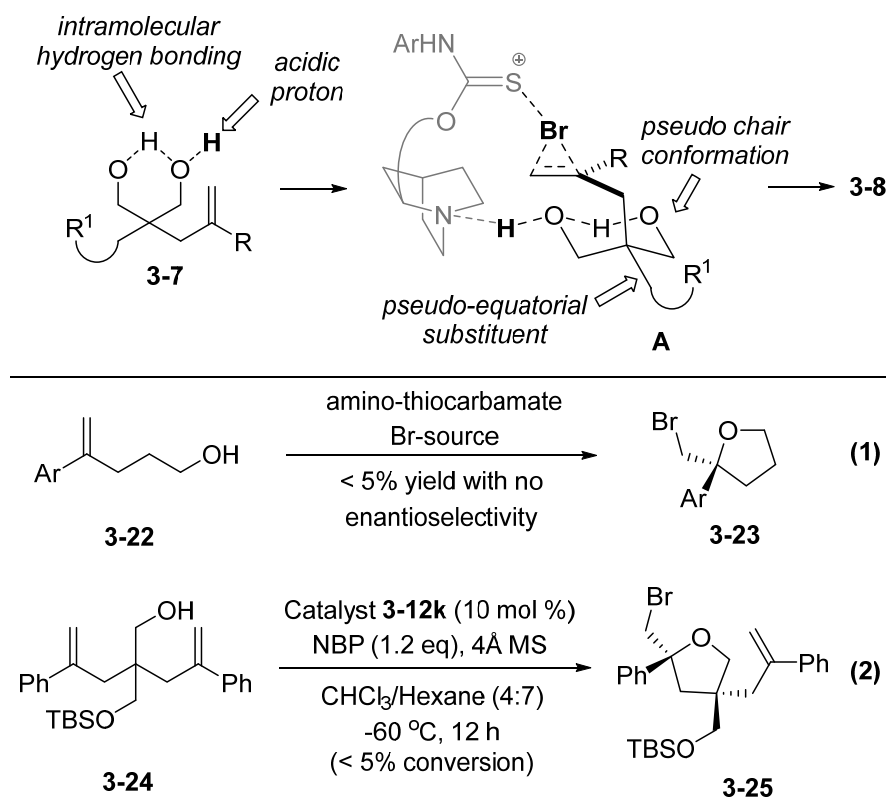


Figure 3.3 X-ray crystallographic study of compound **3-16**.

3.2.6 Mechanistic Studies

With regards to the reactivity of the substrate, we realized the diol system is critical as no reaction occurred when cyclizing olefinic alcohol **3-22** under the optimized conditions (Scheme 3.2, eq. 1). In our previous studies on amino-thiocarbamate catalysis, the nucleophiles (e.g. carboxylic acid) in the olefinic substrates have relatively lower pK_a that allowed deprotonation by the quinucilidine and in turn helps to increase the rate of nucleophilic capture.⁸ In comparison, we believe that the deprotonation of the alcohol is not favourable due to its higher pK_a , thus disfavour the stereoselective etherification. For diol systems, it has been reported that the hydroxyl proton's acidity is enhanced due to the intramolecular hydrogen bonding.⁹ As such, we believe that the acidic proton in the 1,3-diol may interact with the quinucilidine nitrogen of the amino-

thiocarbamate catalyst. A plausible mechanistic picture was constructed as indicated in Scheme 3.2. We speculate that the transition state **A** may consist of several important components: (1) an intramolecular hydrogen bonding which helps to lock the 1,3-diol in a pseudo six-membered ring chair conformation; (2) the bulkier substituent sits at the pseudo-equatorial position; and (3) the amino-thiocarbamate bi-functional pocket helps to restrict the geometry of the intermediate.



Scheme 3.2 Mechanistic studies of bromoetherification using thiocarbamate catalysts.

To gain further information on the mechanism, we prepared substrate **3-24** with one of the hydroxyl groups being protected as a TBSO-ether. Subjecting **3-24** under the optimized bromocyclization conditions returned with sluggish reaction, which further supports the importance of the hydrogen bonding (Scheme 3.2, eq. 2). In fact, we have also examined benzyl substituted substrate **3-26** which also returned with good dr and er. Poor diastereo- and enantioselectivity were observed when using triphenylphosphine sulfide or potassium carbonate to mediate the reaction. This result reinforces the importance of the bi-functionality in which the catalyst is controlling the diastereo- and enantioselectivity (Table 3.8).

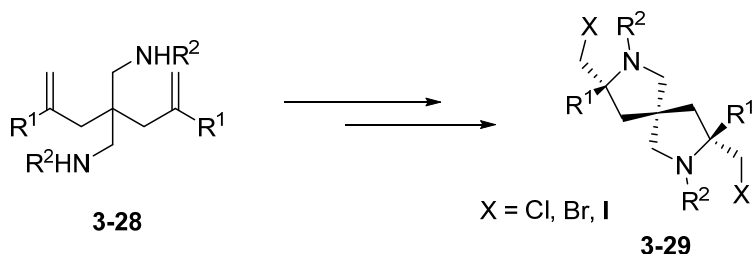
Table 3.8 Cyclization of **3-26** using different catalysts.

Entry ^a	Catalyst	Yield (%) ^b	<i>cis</i> - 3-27 : <i>trans</i> - 3-12	er of <i>cis</i> - 3-27
1	3-12k (10 mol%)	91	84:16	89:11
2	K ₂ CO ₃ (100 mol%)	92	45:55	-
3	Ph ₃ PS (10 mol%)	95	59:41	-

^a Reactions were carried out with **3-26** (0.05 mmol), catalyst, and NBS (0.06 mmol) in CHCl₃/Hexane (4:7) (5.5 mL) at -60 °C for 12 h in the absence of light. ^b Isolated yields.

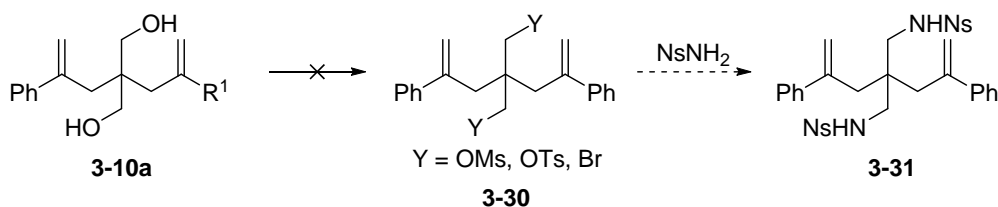
3.2.7 Desymmetrizing Halocyclization of Other Substrates

Next, we attempted to use the same strategy for the synthesis of diazaspirocycles **3-29**, another class of spirocycles that is absent in the literature.¹



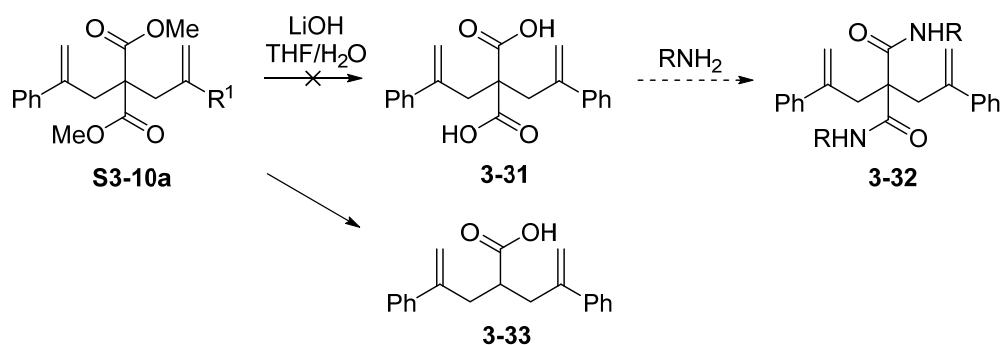
Scheme 3.3 Synthesis of diazaspirocycles via desymmetrizing halocyclization.

We tried to synthesize the diamino diolefin **3-31** from the diol **3-10a** via the intermediate **3-30**, in which the two hydroxyl groups are converted into leaving groups. (Scheme 3.4) The diamino diolefin **3-31** can subsequently be obtained by displacing the leaving groups using 4-nitrobenzenesulfonamide. However, various attempts to convert the hydroxyl groups into the mesylate, tosylate or bromide were unsuccessful, giving complex mixtures in each of the reactions.



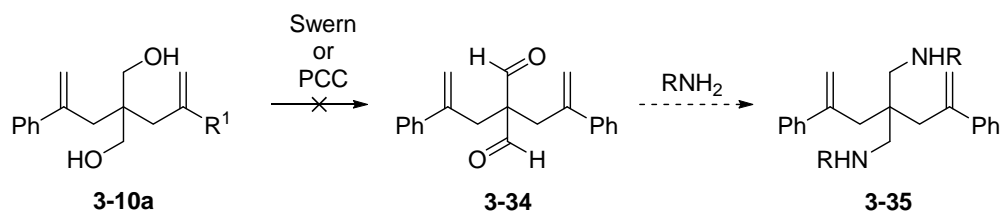
Scheme 3.4 Attempted synthesis of intermediate **3-30**.

Next, we changed our strategy and tried to install the nitrogen atoms using via the formation of the amide from the dicarboxylic acid **3-31** (Scheme 3.5). Attempts to make the dicarboxylic acid **3-31** from the disubstituted malonate **S3-10a** resulted in decarboxylation, furnishing the monocarboxylic acid **3-33** as the sole product.



Scheme 3.5 Attempted synthesis of intermediate **3-31**.

Lastly, we attempted to synthesize the dialdehyde **3-34** which can be manipulated to form the diamino compound **3-35** during reduction amination protocols (Scheme 3.6). Neither the swern nor pyridinium chlorochromate oxidation yielded the di-aldehyde. Both reactions gave complex mixtures instead.



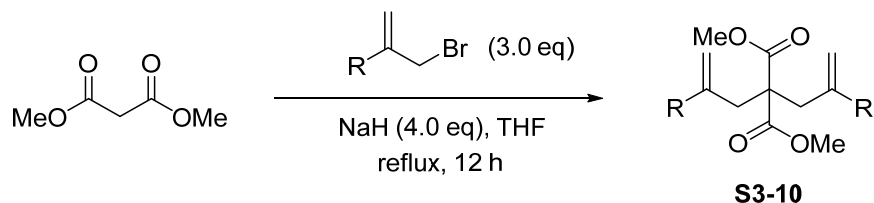
Scheme 3.6 Attempted synthesis of intermediate **3-34**.

3.3 Summary

In summary, a facile and highly enantioselective bromoetherification of diolefinic diols has been developed using amino-thiocarbamate as the catalyst. Further manipulations of the bromoether products enabled entry into a new class of spirocycles that are distinctively lacking in the literature. The importance of the diol functionality also substantiated mode of action of the catalyst that was proposed in earlier studies.

3.4 Experimental

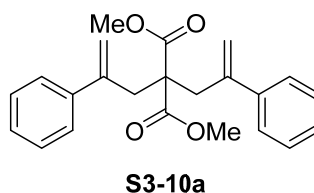
(A) General procedure for the preparation of diolefinic malonates (S3-10a–g).



To a stirred solution of dimethyl malonate (5.0 mmol, 1.0 eq) in THF (15 mL) was added NaH (20.0 mmol, 4.0 eq) at 0 °C under argon. The resulting mixture was allowed to warm to 25 °C and stirred for another 1 h before the 2-substituted allyl bromide (15.0 mmol, 3.0 eq) was added into the solution. The mixture was stirred and refluxed for 12 h. The reaction was quenched with water (10 mL) and extracted with EtOAc (3 x 10 mL). The combined organic extracts were washed

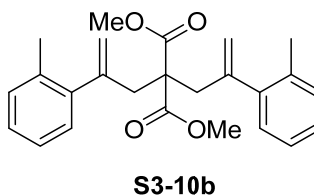
with brine (10 mL), dried over MgSO_4 , filtered and concentrated under reduced pressure. The residue was purified using flash column chromatography (hexane/EtOAc 10:1) to give the malonate (**S3-10**).

dimethyl 2,2-bis(2-phenylallyl)malonate (**S3-10a**)



Colourless oil; IR (film): 2951, 1733, 1626, 1438, 1211, 1092, 907 cm^{-1} ; ^1H NMR (600 MHz, CDCl_3) δ 7.31 – 7.26 (m, 8H), 7.23 (d, J = 6.2 Hz, 2H), 5.23 (d, J = 1.5 Hz, 2H), 5.09 (d, J = 1.1 Hz, 2H), 3.16 (d, J = 1.1 Hz, 4H), 3.13 (s, 6H); ^{13}C NMR (151 MHz, CDCl_3) δ 170.95, 144.46, 141.86, 127.97, 127.37, 126.95, 118.72, 56.64, 51.81, 36.96; HRMS (ESI) calcd for $\text{C}_{23}\text{H}_{24}\text{O}_4\text{Na}$ m/z $[\text{M} + \text{Na}]^+$: 387.1567; found: 387.1584.

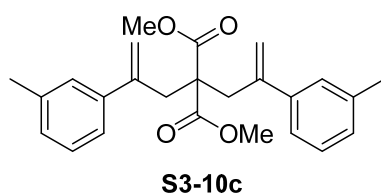
dimethyl 2,2-bis(2-(*o*-tolyl)allyl)malonate (**S3-10b**)



Colourless oil; IR (film): 2951, 1735, 1627, 1435, 1211, 1093, 913 cm^{-1} ; ^1H NMR (600 MHz, CDCl_3) δ 7.15 – 7.08 (m, 6H), 7.07 – 7.03 (m, 2H), 5.00 – 4.97 (m,

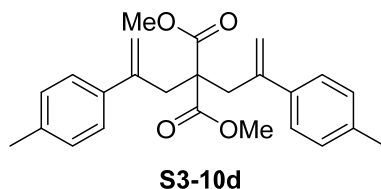
2H), 4.96 (d, $J = 2.1$ Hz, 2H), 3.16 (s, 6H), 3.09 (d, $J = 1.0$ Hz, 4H), 2.28 (s, 6H); ^{13}C NMR (151 MHz, CDCl_3) δ 170.72, 144.86, 141.68, 135.30, 130.06, 129.13, 127.06, 125.29, 120.37, 57.20, 51.81, 38.73, 19.97; HRMS (ESI) calcd for $\text{C}_{25}\text{H}_{28}\text{O}_4\text{Na}$ m/z $[\text{M} + \text{Na}]^+$: 415.1880; found: 415.1894.

dimethyl 2,2-bis(2-(*m*-tolyl)allyl)malonate (S3-10c)



Colourless oil; IR (film): 2950, 1735, 1627, 1436, 1217, 1063, 912 cm^{-1} ; ^1H NMR (600 MHz, CDCl_3) δ 7.25 – 6.88 (m, 8H), 5.22 (d, $J = 2.6$ Hz, 2H), 5.05 (d, $J = 3.4$ Hz, 2H), 3.19 (s, 6H), 3.15 (s, 4H), 2.33 (d, $J = 3.6$ Hz, 6H); ^{13}C NMR (151 MHz, CDCl_3) δ 171.03, 144.61, 141.89, 137.39, 128.08, 127.88, 127.59, 124.08, 118.19, 56.78, 51.76, 36.92, 21.39; HRMS (ESI) calcd for $\text{C}_{25}\text{H}_{28}\text{O}_4\text{Na}$ m/z $[\text{M} + \text{Na}]^+$: 415.1880; found: 415.1889.

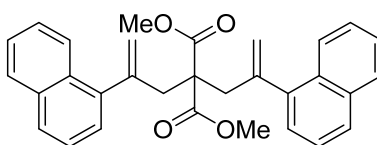
dimethyl 2,2-bis(2-(*p*-tolyl)allyl)malonate (S3-10d)



Colourless oil; IR (film): 2950, 1734, 1625, 1437, 1207, 1112, 905 cm^{-1} ; ^1H NMR (600 MHz, CDCl_3) δ 7.16 (dd, $J = 8.4, 2.0$ Hz, 4H), 7.14 – 7.02 (m, 4H), 5.20 (d,

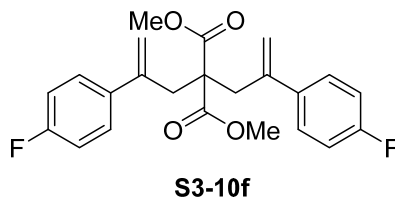
$J = 1.7$ Hz, 2H), 5.10 – 5.02 (m, 2H), 3.18 (s, 6H), 3.13 (s, 6H), 2.31 (s, 6H); ^{13}C NMR (151 MHz, CDCl_3) δ 171.05, 144.36, 139.02, 137.03, 128.63, 128.61, 126.78, 117.76, 56.82, 51.82, 37.04, 21.06; HRMS (ESI) calcd for $\text{C}_{25}\text{H}_{28}\text{O}_4\text{Na}$ m/z $[\text{M} + \text{Na}]^+$: 415.1880; found: 415.1900.

dimethyl 2,2-bis(2-(naphthalen-1-yl)allyl)malonate (S3-10e)

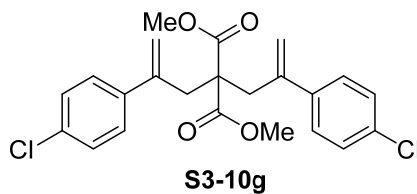


S3-10e

Colourless oil; IR (film): 2950, 1735, 1627, 1436, 1218, 1070, 912 cm^{-1} ; ^1H NMR (600 MHz, CDCl_3) δ 7.94 – 7.88 (m, 2H), 7.84 – 7.78 (m, 2H), 7.72 (d, $J = 8.0$ Hz, 2H), 7.50 – 7.41 (m, 4H), 7.38 (d, $J = 1.3$ Hz, 2H), 7.21 (d, $J = 6.9$ Hz, 2H), 5.07 (d, $J = 2.0$ Hz, 2H), 5.00 (s, 2H), 3.31 (s, 4H), 2.93 (s, 6H); ^{13}C NMR (151 MHz, CDCl_3) δ 170.60, 143.78, 140.02, 133.50, 131.07, 128.22, 127.58, 125.99, 125.84, 125.69, 125.62, 125.06, 121.49, 57.75, 51.56, 39.45; HRMS (ESI) calcd for $\text{C}_{31}\text{H}_{28}\text{O}_4\text{Na}$ m/z $[\text{M} + \text{Na}]^+$: 487.1880; found: 488.1870

dimethyl 2,2-bis(2-(4-fluorophenyl)allyl)malonate (S3-10f)

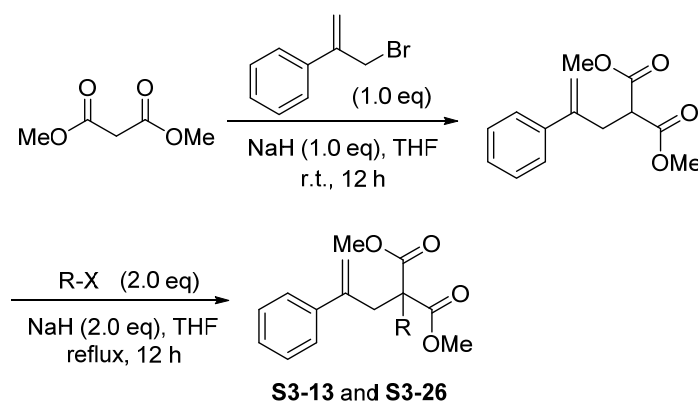
Colourless oil; IR (film): 2951, 1735, 1602, 1508, 1438, 1251, 1093, 908 cm^{-1} ; ^1H NMR (600 MHz, CDCl_3) δ 7.23 (dd, $J = 8.8, 5.3$ Hz, 4H), 6.96 (t, $J = 8.7$ Hz, 4H), 5.20 (d, $J = 1.4$ Hz, 2H), 5.07 (d, $J = 1.2$ Hz, 2H), 3.22 (s, 6H), 3.11 (d, $J = 1.1$ Hz, 4H); ^{13}C NMR (151 MHz, CDCl_3) δ 170.82, 162.22 (d, $J = 246.7$ Hz), 143.45, 137.85 (d, $J = 3.2$ Hz), 128.52 (d, $J = 8.0$ Hz), 118.66, 114.82 (d, $J = 21.4$ Hz), 56.70, 51.94, 37.21; HRMS (ESI) calcd for $\text{C}_{23}\text{H}_{22}\text{O}_4\text{F}_2\text{Na}$ m/z $[\text{M} + \text{Na}]^+$: 401.1559; found: 401.1547.

dimethyl 2,2-bis(2-(4-chlorophenyl)allyl)malonate (S3-10g)

Colourless oil; IR (film): 2951, 1731, 1626, 1435, 1211, 1093, 910 cm^{-1} ; ^1H NMR (600 MHz, Chloroform- d) δ 7.25 (d, $J = 8.6$ Hz, 4H), 7.18 (d, $J = 8.5$ Hz, 4H), 5.23 (d, $J = 1.3$ Hz, 2H), 5.12 – 5.03 (m, 2H), 3.23 (s, 6H), 3.10 (d, $J = 1.1$ Hz, 4H); ^{13}C NMR (151 MHz, CDCl_3) δ 170.75, 143.35, 140.22, 133.31, 128.19,

128.13, 119.01, 77.21, 51.98, 37.03; HRMS (ESI) calcd for $C_{23}H_{22}O_4Cl_2Na$ m/z $[M + Na]^+$: 455.0787; found: 455.0796.

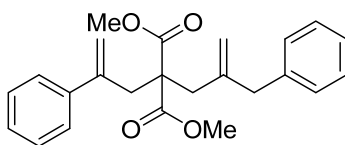
(B) General procedure for the preparation of di-substituted malonates (S3-13 and S3-26)



To a stirred solution of dimethyl malonate (5.0 mmol, 1.0 eq) in THF (15 mL) was added NaH (5.0 mmol, 1.0 eq) at 0 °C under argon. The resulting mixture was allowed to warm to 25 °C and stirred for another 1 h before the 2-phenyl allyl bromide (5.0 mmol, 1.0 eq) was added into the solution. The mixture was stirred at room temperature for 12 h. The reaction was quenched with water (10 mL) and extracted with EtOAc (3 x 10 mL). The combined organic extracts was washed with brine (10 mL), dried over $MgSO_4$, filtered and concentrated under reduced pressure. The residue was purified using flash column chromatography (hexane/EtOAc 10:1) to give the mono-substituted malonate.

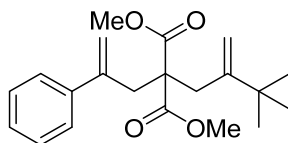
The purified mono-substituted malonate (5.0 mmol, 1.0 eq) was dissolved in THF (15 mL) and NaH (10.0 mmol, 2.0 eq) at 0 °C under argon. The resulting mixture was allowed to warm to 25 °C and stirred for another 1 h before the corresponding alkylating agent (10.0 mmol, 2.0 eq) was added into the solution. The mixture was stirred and refluxed for 12 h. The reaction was quenched with water (10 mL) and extracted with EtOAc (3 x 10 mL). The combined organic extracts were washed with brine (10 mL), dried over MgSO₄, filtered and concentrated under reduced pressure. The residue was purified using flash column chromatography (hexane/EtOAc 10:1) to give the di-substituted malonate (**S3-13**).

dimethyl 2-(2-benzylallyl)-2-(2-phenylallyl)malonate (**S3-13a**)

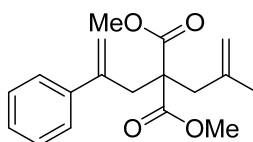


S3-13a

Colourless oil; IR (film): 2951, 1731, 1626, 1434, 1198, 1177, 904 cm⁻¹; ¹H NMR (600 MHz, CDCl₃) δ 7.37 – 7.17 (m, 8H), 7.16 – 7.07 (m, 2H), 5.18 (d, *J* = 1.6 Hz, 1H), 5.05 (d, *J* = 1.3 Hz, 1H), 4.84 – 4.81 (m, 1H), 4.77 (d, *J* = 1.5 Hz, 1H), 3.42 (s, 6H), 3.29 (d, *J* = 1.0 Hz, 2H), 3.17 (s, 2H), 2.66 – 2.60 (m, 2H); ¹³C NMR (151 MHz, CDCl₃) δ 171.35, 144.39, 144.35, 141.61, 139.13, 129.15, 128.25, 128.01, 127.40, 126.88, 126.14, 118.50, 114.73, 56.83, 52.13, 43.90, 37.90, 37.36; HRMS (ESI) calcd for C₂₄H₂₆O₄Na *m/z* [M + Na]⁺: 401.1723; found: 401.1733.

dimethyl 2-(3,3-dimethyl-2-methylenebutyl)-2-(2-phenylallyl)malonate (S3-13b)**S3-13b**

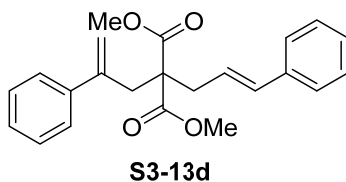
Colourless oil; IR (film): 2956, 1729, 1626, 1435, 1215, 1100, 911 cm^{-1} ; ^1H NMR (600 MHz, CDCl_3) δ 7.34 – 7.26 (m, 4H), 7.23 (d, $J = 7.0$ Hz, 1H), 5.23 (d, $J = 1.7$ Hz, 1H), 5.09 – 5.07 (m, 1H), 4.91 (t, $J = 1.4$ Hz, 1H), 4.67 (d, $J = 1.9$ Hz, 1H), 3.42 (s, 6H), 3.40 (d, $J = 0.9$ Hz, 2H), 2.66 (s, 2H), 0.99 (s, 9H); ^{13}C NMR (151 MHz, CDCl_3) δ 171.62, 152.72, 144.55, 141.37, 128.02, 127.43, 126.80, 118.49, 106.25, 56.38, 52.22, 37.43, 36.56, 32.32, 29.28; HRMS (ESI) calcd for $\text{C}_{21}\text{H}_{28}\text{O}_4\text{Na}$ m/z $[\text{M} + \text{Na}]^+$: 367.1880; found: 367.1870.

dimethyl 2-(2-methylallyl)-2-(2-phenylallyl)malonate (S3-13c)**S3-13c**

Colourless oil; IR (film): 2952, 1732, 1626, 1435, 1207, 1178, 1071, 901 cm^{-1} ; ^1H NMR (600 MHz, CDCl_3) δ 7.30 – 7.27 (m, 4H), 7.25 – 7.21 (m, 1H), 5.25 (d, $J = 1.6$ Hz, 1H), 5.17 – 5.14 (m, 1H), 4.85 – 4.83 (m, 1H), 4.67 (dd, $J = 1.8, 1.0$ Hz, 1H), 3.42 (s, 6H), 3.24 (d, $J = 1.0$ Hz, 2H), 2.66 – 2.63 (m, 2H), 1.61 (s, 3H); ^{13}C NMR (151 MHz, CDCl_3) δ 171.40, 144.58, 141.69, 140.92, 127.98, 127.38,

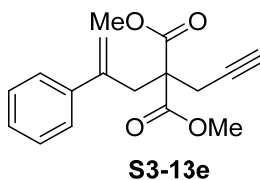
126.94, 118.64, 114.62, 56.74, 52.07, 39.62, 37.70, 23.61; HRMS (ESI) calcd for $C_{18}H_{22}O_4Na$ m/z $[M + Na]^+$: 325.1410; found: 325.1413.

dimethyl 2-cinnamyl-2-(2-phenylallyl)malonate (S3-13d)



Colourless oil; IR (film): 2951, 1731, 1626, 1435, 1202, 1176, 967, 908 cm^{-1} ; 1H NMR (600 MHz, $CDCl_3$) δ 7.41 – 7.17 (m, 10H), 6.25 (dt, $J = 15.7, 1.5$ Hz, 1H), 5.94 (dt, $J = 15.7, 7.5$ Hz, 1H), 5.29 (d, $J = 1.6$ Hz, 1H), 5.20 – 5.16 (m, 1H), 3.47 (s, 6H), 3.21 (d, $J = 1.0$ Hz, 2H), 2.71 (dd, $J = 7.5, 1.4$ Hz, 2H); ^{13}C NMR (151 MHz, $CDCl_3$) δ 171.02, 144.53, 141.63, 137.11, 134.02, 128.46, 128.08, 127.52, 127.36, 127.01, 126.17, 123.95, 118.73, 57.92, 52.16, 37.77, 35.71; HRMS (ESI) calcd for $C_{23}H_{24}O_4Na$ m/z $[M + Na]^+$: 387.1567; found: 387.1574.

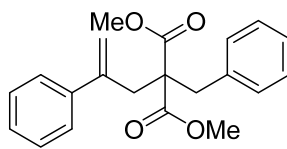
dimethyl 2-(2-phenylallyl)-2-(prop-2-yn-1-yl)malonate (S3-13e)



Colourless oil; IR (film): 3288, 2952, 1736, 1626, 1436, 1211, 1067, 911 cm^{-1} ; 1H NMR (600 MHz, $CDCl_3$) δ 7.32 – 7.27 (m, 4H), 7.25 – 7.22 (m, 1H), 5.31 (d, $J = 1.7$ Hz, 1H), 5.29 (s, 1H), 3.42 (s, 6H), 3.33 (d, $J = 0.9$ Hz, 2H), 2.77 (d, $J = 2.7$

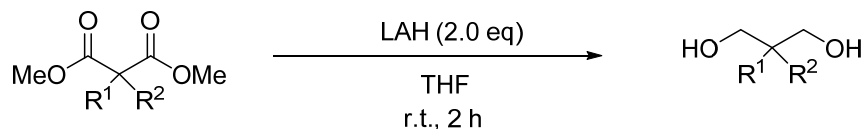
Hz, 2H), 2.07 – 2.02 (m, 1H); ^{13}C NMR (151 MHz, CDCl_3) δ 169.94, 143.81, 140.87, 128.04, 127.60, 126.91, 119.01, 79.19, 71.72, 56.40, 52.45, 36.88, 22.32; HRMS (ESI) calcd for $\text{C}_{17}\text{H}_{18}\text{O}_4\text{Na}$ m/z $[\text{M} + \text{Na}]^+$: 309.1097; found: 309.1096.

dimethyl 2-benzyl-2-(2-phenylallyl)malonate (S3-26)

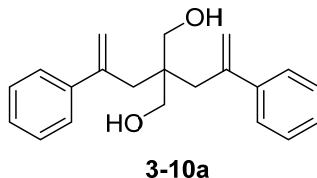


S3-26

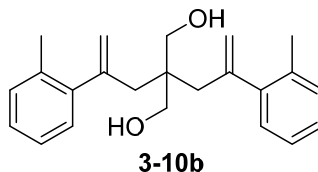
Colourless oil; IR (film): 2951, 1734, 1628, 1436, 1208, 1083, 910 cm^{-1} ; ^1H NMR (600 MHz, CDCl_3) δ 7.33 – 7.29 (m, 4H), 7.24 – 7.18 (m, 4H), 7.06 (s, 2H), 5.32 (d, J = 1.4 Hz, 1H), 5.22 (d, J = 1.3 Hz, 1H), 3.41 (s, 6H), 3.22 (s, 2H), 3.14 (d, J = 1.1 Hz, 2H); ^{13}C NMR (151 MHz, CDCl_3) δ 171.10, 144.56, 141.89, 136.25, 129.99, 128.15, 128.06, 127.46, 126.99, 126.86, 118.68, 58.72, 52.01, 38.37, 38.04; HRMS (ESI) calcd for $\text{C}_{21}\text{H}_{22}\text{O}_4\text{Na}$ m/z $[\text{M} + \text{Na}]^+$: 361.1410; found: 361.1401.

(C) General procedure for the reduction of malonates to diols.

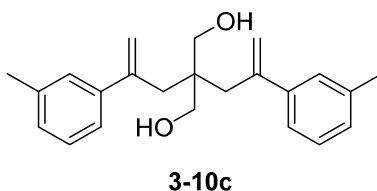
To a stirred solution of malonate (5.0 mmol, 1.0 eq) in THF (15 mL) was added LAH (10.0 mmol, 2.0 eq) at 0 °C under argon. The resulting mixture was allowed to warm to 25 °C and stirred for another 2 h it was quenched with water (2 mL) and NaOH (2.0M, 2mL). The mixture was filtered over celite to remove the white precipitate and the filtrate was concentrated under reduced pressure. The residue was purified using flash column chromatography (hexane/EtOAc 4:1) to give the diol (**3-10**).

2,2-bis(2-phenylallyl)propane-1,3-diol (3-10a**)**

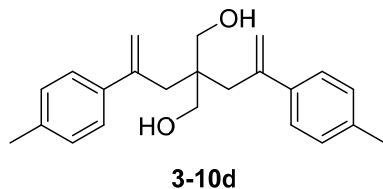
Colourless oil; IR (film): 3429, 2930, 1623, 1444, 1027, 904 cm⁻¹; ¹H NMR (600 MHz, CDCl₃) δ 7.36 (dd, *J* = 8.2, 1.3 Hz, 4H), 7.32 (td, *J* = 6.8, 6.3, 1.8 Hz, 4H), 7.29 – 7.26 (m, 2H), 5.28 (d, *J* = 1.8 Hz, 2H), 5.15 – 5.10 (m, 2H), 3.26 (s, 4H), 2.63 (d, *J* = 0.9 Hz, 4H); ¹³C NMR (151 MHz, CDCl₃) δ 146.09, 143.06, 128.57, 127.63, 126.23, 117.92, 67.25, 44.22, 38.69; HRMS (ESI) calcd for C₂₁H₂₄O₂Na *m/z* [M + Na]⁺: 331.1669; found: 331.1659.

2,2-bis(2-(*o*-tolyl)allyl)propane-1,3-diol (3-10b)

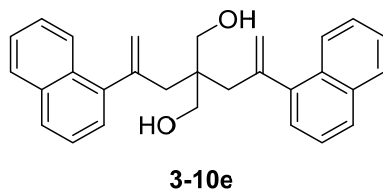
Colourless oil; IR (film): 3404, 2931, 1625, 1443, 1029, 910 cm^{-1} ; ^1H NMR (600 MHz, CDCl_3) δ 7.24 – 7.14 (m, 8H), 5.23 – 5.14 (m, 2H), 5.08 – 4.99 (m, 2H), 3.30 (s, 4H), 2.55 (s, 4H), 2.34 (s, 6H), 1.42 (m, 2H); ^{13}C NMR (151 MHz, CDCl_3) δ 145.91, 143.15, 134.56, 130.90, 128.07, 127.20, 125.82, 119.88, 67.68, 44.73, 40.20, 20.32; HRMS (ESI) calcd for $\text{C}_{23}\text{H}_{28}\text{O}_2\text{Na}$ m/z $[\text{M} + \text{Na}]^+$: 359.1982; found: 359.1973.

2,2-bis(2-(*m*-tolyl)allyl)propane-1,3-diol (3-10c)

Colourless oil; IR (film): 3378, 2921, 1600, 1446, 1024, 900 cm^{-1} ; ^1H NMR (600 MHz, CDCl_3) δ 7.20 (d, $J = 7.5$ Hz, 2H), 7.19 – 7.14 (m, 4H), 7.10 – 7.06 (m, 2H), 5.26 (d, $J = 1.9$ Hz, 2H), 5.13 – 5.10 (m, 2H), 3.26 (d, $J = 6.3$ Hz, 4H), 2.61 (d, $J = 0.9$ Hz, 4H), 2.35 (s, 6H); ^{13}C NMR (151 MHz, CDCl_3) δ 146.25, 143.12, 138.21, 128.45, 128.40, 127.00, 123.30, 117.64, 67.26, 44.31, 38.77, 21.49; HRMS (ESI) calcd for $\text{C}_{23}\text{H}_{29}\text{O}_2$ m/z $[\text{M} + \text{H}]^+$: 337.2162; found: 337.2166.

2,2-bis(2-(*p*-tolyl)allyl)propane-1,3-diol (**3-10d**)

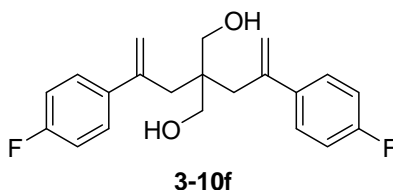
Colourless oil; IR (film): 3392, 2937, 1620, 1449, 1027, 913 cm^{-1} ; ^1H NMR (600 MHz, CDCl_3) δ 7.26 (m, 4H), 7.13 (d, $J = 7.9$ Hz, 4H), 5.25 (d, $J = 1.9$ Hz, 2H), 5.08 (d, $J = 1.9$ Hz, 2H), 3.26 (d, $J = 6.3$ Hz, 4H), 2.60 (s, 4H), 2.33 (s, 6H), 1.51 (s, 2H); ^{13}C NMR (151 MHz, CDCl_3) δ 146.00, 140.17, 137.42, 129.28, 126.12, 117.14, 67.18, 44.30, 38.80, 21.08; HRMS (ESI) calcd for $\text{C}_{23}\text{H}_{28}\text{O}_2\text{Na}$ m/z $[\text{M} + \text{Na}]^+$: 359.1982; found: 359.1995.

2,2-bis(2-(naphthalen-1-yl)allyl)propane-1,3-diol (**3-10e**)

Colourless oil; IR (film): 3360, 2941, 1626, 1440, 1029, 911 cm^{-1} ; ^1H NMR (600 MHz, CDCl_3) δ 8.10 – 8.01 (m, 2H), 7.84 (dd, $J = 7.9, 1.7$ Hz, 2H), 7.78 – 7.69 (m, 2H), 7.53 – 7.41 (m, 4H), 7.38 (dd, $J = 8.2, 7.0$ Hz, 2H), 7.32 (dd, $J = 7.0, 1.3$ Hz, 2H), 5.34 (d, $J = 2.4$ Hz, 2H), 5.22 (d, $J = 2.2$ Hz, 2H), 3.29 (d, $J = 6.0$ Hz, 4H), 2.78 (s, 4H), 1.37 (t, $J = 6.1$ Hz, 2H); ^{13}C NMR (151 MHz, CDCl_3) δ 144.35, 141.50, 134.01, 130.56, 128.62, 127.71, 126.11, 125.84, 125.58, 125.10, 124.83,

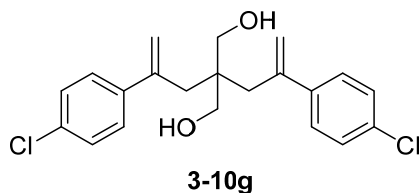
121.14, 67.65, 44.97, 41.02; HRMS (ESI) calcd for $C_{31}H_{28}O_4Na$ m/z $[M + Na]^+$: 431.1982; found: 431.1996.

2,2-bis(2-(4-fluorophenyl)allyl)propane-1,3-diol (3-10f)



Colourless oil; IR (film): 3372, 2938, 1623, 1440, 1024, 904 cm^{-1} ; 1H NMR (600 MHz, $CDCl_3$) δ 7.33 (dd, $J = 8.7, 5.3$ Hz, 4H), 7.01 (t, $J = 8.6$ Hz, 4H), 5.24 (d, $J = 1.7$ Hz, 2H), 5.13 – 5.09 (m, 2H), 3.26 (s, 4H), 2.58 (d, $J = 0.9$ Hz, 4H); ^{13}C NMR (151 MHz, $CDCl_3$) δ 162.29 (d, $J = 247.6$ Hz), 145.08, 139.03 (d, $J = 4.5$ Hz), 127.86 (d, $J = 7.6$ Hz), 117.89, 115.35 (d, $J = 21.1$ Hz), 67.19, 44.18, 38.80; HRMS (ESI) calcd for $C_{21}H_{22}O_2F_2Na$ m/z $[M + H]^+$: 345.1661; found: 345.1659.

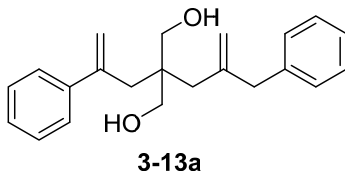
2,2-bis(2-(4-chlorophenyl)allyl)propane-1,3-diol (3-10g)



Colourless oil; IR (film): 3378, 2927, 1621, 1490, 1025, 907 cm^{-1} ; 1H NMR (600 MHz, $CDCl_3$) δ 7.33 – 7.26 (m, 8H), 5.27 (d, $J = 1.7$ Hz, 2H), 5.18 – 5.06 (m, 2H), 3.26 (d, $J = 5.6$ Hz, 4H), 2.58 (s, 4H), 1.61 – 1.55 (m, 2H); ^{13}C NMR (151 MHz, $CDCl_3$) δ 144.96, 141.42, 133.44, 128.62, 127.58, 118.40, 67.15, 44.16,

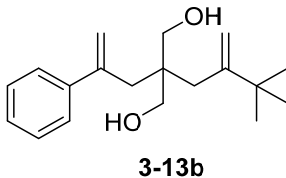
38.55; HRMS (ESI) calcd for $C_{21}H_{22}O_2Cl_2Na$ m/z $[M + Na]^+$: 399.0889; found: 399.0901.

2-(2-benzylallyl)-2-(2-phenylallyl)propane-1,3-diol (**3-13a**)



Colourless oil; IR (film): 3367, 2924, 1626, 1451, 1028, 900 cm^{-1} ; 1H NMR (600 MHz, $CDCl_3$) δ 7.38 – 7.35 (m, 2H), 7.35 – 7.31 (m, 2H), 7.31 – 7.26 (m, 3H), 7.23 – 7.20 (m, 1H), 7.19 – 7.15 (m, 2H), 5.26 (d, J = 1.8 Hz, 1H), 5.16 – 5.12 (m, 1H), 4.92 (d, J = 4.0 Hz, 2H), 3.51 (d, J = 11.2 Hz, 2H), 3.46 (d, J = 11.1 Hz, 2H), 3.38 (s, 2H), 2.68 (d, J = 0.9 Hz, 2H), 2.07 (d, J = 0.9 Hz, 2H); ^{13}C NMR (151 MHz, $CDCl_3$) δ 146.18, 146.09, 143.10, 139.58, 129.11, 128.60, 128.34, 127.65, 126.26, 126.17, 117.92, 116.45, 67.54, 44.91, 44.14, 38.91, 38.25 ; HRMS (ESI) calcd for $C_{22}H_{26}O_2Na$ m/z $[M + Na]^+$: 345.1825; found: 345.1828.

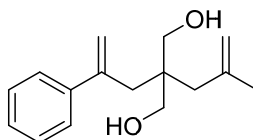
2-(3,3-dimethyl-2-methylenebutyl)-2-(2-phenylallyl)propane-1,3-diol (**3-13b**)



Colourless oil; IR (film): 3399, 2956, 1624, 1466, 1029, 901 cm^{-1} ; 1H NMR (600 MHz, $CDCl_3$) δ 7.42 – 7.38 (m, 2H), 7.33 (ddd, J = 7.7, 6.8, 1.2 Hz, 2H), 7.29 –

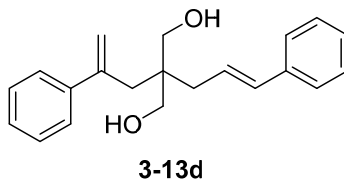
7.26 (m, 1H), 5.29 (d, $J = 1.9$ Hz, 1H), 5.19 – 5.16 (m, 1H), 5.07 (s, 1H), 4.92 (d, $J = 0.9$ Hz, 1H), 3.60 (d, $J = 11.2$ Hz, 2H), 3.52 (d, $J = 11.2$ Hz, 2H), 2.76 (d, $J = 0.9$ Hz, 2H), 2.08 (d, $J = 1.3$ Hz, 2H), 1.00 (s, 9H); ^{13}C NMR (151 MHz, CDCl_3) δ 154.22, 146.32, 143.20, 128.54, 127.58, 126.29, 117.82, 109.36, 68.35, 43.82, 38.34, 37.14, 32.45, 29.32; HRMS (ESI) calcd for $\text{C}_{19}\text{H}_{28}\text{O}_2\text{Na}$ m/z $[\text{M} + \text{Na}]^+$: 311.1982; found: 311.1982.

2-(2-methylallyl)-2-(2-phenylallyl)propane-1,3-diol (3-13c)

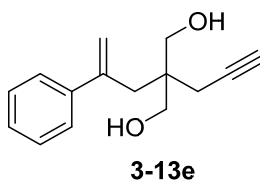


3-13c

Colourless oil; IR (film): 3345, 2935, 1638, 1444, 1028, 896 cm^{-1} ; ^1H NMR (600 MHz, CDCl_3) δ 7.44 – 7.37 (m, 2H), 7.36 – 7.32 (m, 2H), 7.30 – 7.26 (m, 1H), 5.29 (d, $J = 1.8$ Hz, 1H), 5.20 – 5.15 (m, 1H), 4.90 (dd, $J = 2.5, 1.4$ Hz, 1H), 4.75 (dd, $J = 2.3, 1.1$ Hz, 1H), 3.50 (d, $J = 11.2$ Hz, 2H), 3.44 (d, $J = 11.2$ Hz, 2H), 2.68 (d, $J = 0.9$ Hz, 2H), 2.09 (d, $J = 0.9$ Hz, 2H), 1.80 (m, 5H); ^{13}C NMR (151 MHz, CDCl_3) δ 146.23, 143.17, 143.16, 128.60, 127.64, 126.28, 117.92, 115.17, 67.75, 43.91, 41.17, 38.81, 25.30; HRMS (ESI) calcd for $\text{C}_{16}\text{H}_{22}\text{O}_2\text{Na}$ m/z $[\text{M} + \text{Na}]^+$: 269.1512; found: 269.1519.

2-cinnamyl-2-(2-phenylallyl)propane-1,3-diol (3-13d)

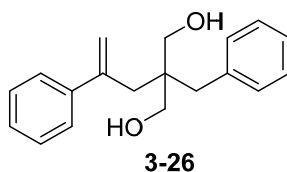
Colourless oil; IR (film): 3338, 2931, 1625, 1439, 1028, 905 cm^{-1} ; ^1H NMR (600 MHz, CDCl_3) δ 7.44 – 7.40 (m, 2H), 7.37 – 7.33 (m, 2H), 7.33 – 7.28 (m, 5H), 7.22 (d, J = 6.5 Hz, 1H), 6.37 – 6.32 (m, 1H), 6.19 (dt, J = 15.5, 7.6 Hz, 1H), 5.31 (d, J = 1.8 Hz, 1H), 5.23 – 5.19 (m, 1H), 3.50 (s, 4H), 2.65 (d, J = 0.9 Hz, 2H), 2.20 (dd, J = 7.6, 1.3 Hz, 2H); ^{13}C NMR (151 MHz, CDCl_3) δ 146.03, 143.17, 137.36, 133.12, 128.59, 128.52, 127.67, 127.16, 126.38, 126.04, 125.74, 117.94, 68.15, 43.79, 37.43, 35.81; HRMS (ESI) calcd for $\text{C}_{21}\text{H}_{24}\text{O}_2\text{Na}$ m/z $[\text{M} + \text{Na}]^+$: 311.1669; found: 311.1672.

2-(2-phenylallyl)-2-(prop-2-yn-1-yl)propane-1,3-diol (3-13e)

Colourless oil; IR (film): 3275, 2943, 1625, 1444, 1022, 899 cm^{-1} ; ^1H NMR (600 MHz, CDCl_3) δ 7.44 – 7.39 (m, 2H), 7.34 (ddd, J = 7.7, 6.8, 1.3 Hz, 2H), 7.31 – 7.27 (m, 1H), 5.32 (d, J = 1.8 Hz, 1H), 5.27 – 5.24 (m, 1H), 3.51 (q, J = 11.1 Hz, 4H), 2.69 (d, J = 0.9 Hz, 2H), 2.19 (d, J = 2.7 Hz, 2H), 2.05 (t, J = 2.7 Hz, 1H);

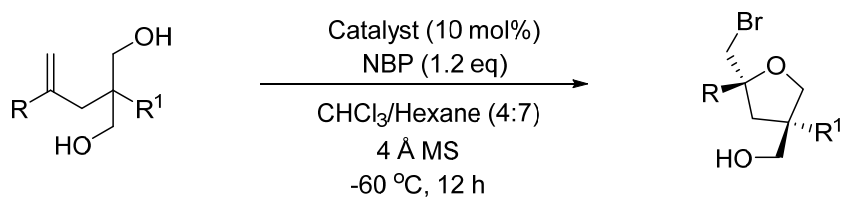
^{13}C NMR (151 MHz, CDCl_3) δ 145.17, 142.63, 128.60, 127.75, 126.25, 118.08, 81.10, 71.20, 67.27, 43.13, 36.61, 21.86; HRMS (ESI) calcd for $\text{C}_{15}\text{H}_{18}\text{O}_2\text{Na}$ m/z $[\text{M} + \text{Na}]^+$: 253.1199; found: 253.1207.

2-benzyl-2-(2-phenylallyl)propane-1,3-diol (3-26)



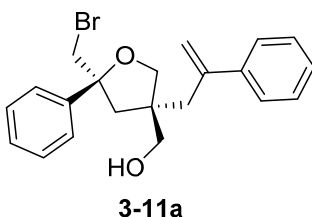
Colourless oil; IR (film): 3399, 2928, 1622, 1445, 1027, 906 cm^{-1} ; ^1H NMR (600 MHz, CDCl_3) δ 7.40 – 7.37 (m, 2H), 7.33 (ddd, $J = 7.8, 6.9, 0.8$ Hz, 2H), 7.29 – 7.26 (m, 3H), 7.23 – 7.19 (m, 3H), 5.31 (d, $J = 1.8$ Hz, 1H), 5.19 – 5.17 (m, 1H), 3.44 – 3.36 (m, 4H), 2.70 (s, 2H), 2.66 (d, $J = 0.9$ Hz, 2H); ^{13}C NMR (151 MHz, CDCl_3) δ 146.21, 143.07, 137.70, 130.56, 128.61, 128.11, 127.67, 126.25, 126.24, 117.86, 66.89, 44.02, 39.40, 38.68; HRMS (ESI) calcd for $\text{C}_{19}\text{H}_{22}\text{O}_2\text{Na}$ m/z $[\text{M} + \text{Na}]^+$: 305.1512; found: 305.1510.

(D) General procedure for enantioselective bromoetherification of the diolefinic diols.



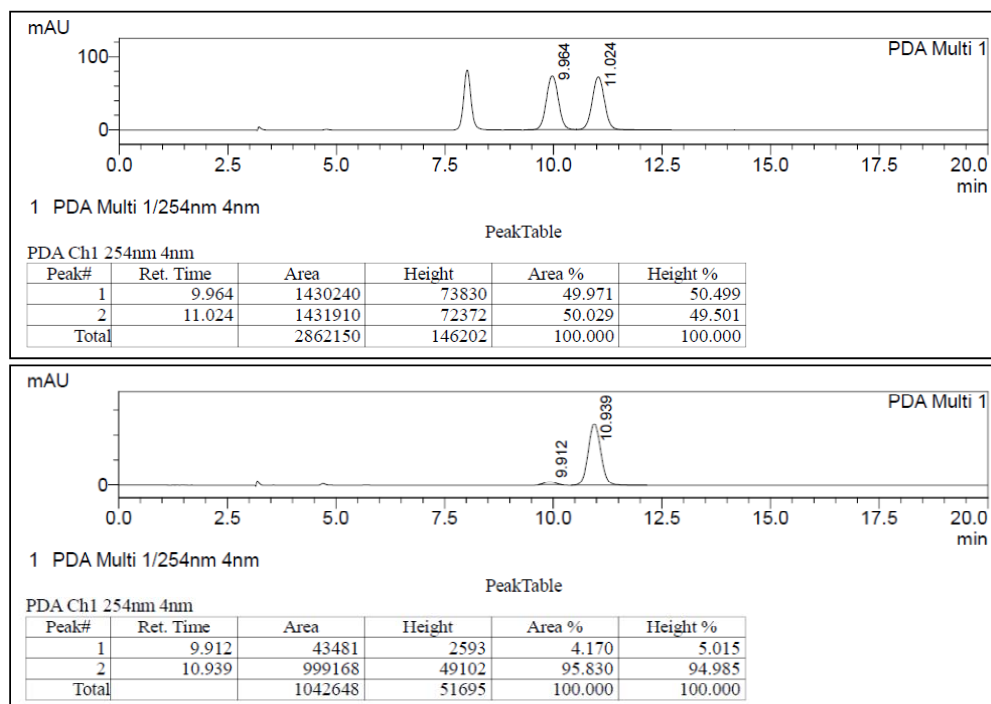
To a stirred solution of the diol (0.05 mmol, 1.0 eq) in CHCl_3 /Hexane (2: 3.5 mL) was added catalyst (0.005 mmol, 0.1 eq) and 275mg of 4 Å molecular sieves under argon. The mixture was cooled to -60°C before N-bromophthalimide (0.06 mmol, 1.2 eq) was added. The reaction was stirred at -60°C for 12 h before it was quenched with Na_2SO_3 (3.0 mL) and extracted with CHCl_3 (3 x 5 mL). The combined organic extracts was dried over MgSO_4 , filtered and concentrated under reduced pressure. The residue was purified using flash column chromatography (hexane/ Et_2O 1:1) to give the product.

((3R,5R)-5-(bromomethyl)-5-phenyl-3-(2-phenylallyl)tetrahydrofuran-3-yl)methanol (3-11a)

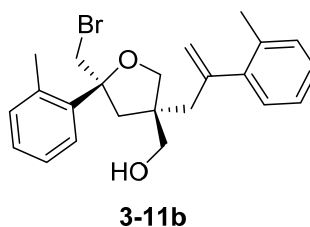


Colourless oil; $[\alpha]_D^{26} +4$ (c 1.0, CHCl_3 , 96:4 v/v); IR (film): 3462, 2944, 1724, 1623, 1446, 1303, 1029, 906 cm^{-1} ; ^1H NMR (600 MHz, CDCl_3) δ 7.42 – 7.38 (m, 2H), 7.36 – 7.33 (m, 4H), 7.31 – 7.28 (m, 3H), 7.23 (m, 1H), 5.30 (d, $J = 1.7$ Hz, 1H), 5.24 – 5.20 (m, 1H), 3.81 (d, $J = 9.1$ Hz, 1H), 3.68 (d, $J = 9.1$ Hz, 1H), 3.54 (d, $J = 2.1$ Hz, 2H), 3.10 (d, $J = 10.9$ Hz, 1H), 3.03 (d, $J = 10.9$ Hz, 1H), 2.90 – 2.86 (m, 1H), 2.81 (d, $J = 13.8$ Hz, 1H), 2.32 (d, $J = 13.4$ Hz, 1H), 2.14 (d, $J = 13.4$ Hz, 1H); ^{13}C NMR (151 MHz, CDCl_3) δ 146.51, 143.94, 142.38, 128.58, 128.27, 127.77, 127.38, 126.40, 125.37, 117.33, 85.24, 77.21, 65.03, 50.11, 43.89,

43.12, 39.73 ; HRMS (ESI) calcd for $C_{21}H_{23}BrO_2Na$ m/z $[M + Na]^+$: 409.0774; found: 409.0770; HPLC (Daicel Chiralpak IA, *i*-PrOH/hexane = 5/95, 1.0 mL/min, 254 nm) t_1 = 9.9 min (minor), t_2 = 10.9 min (major).

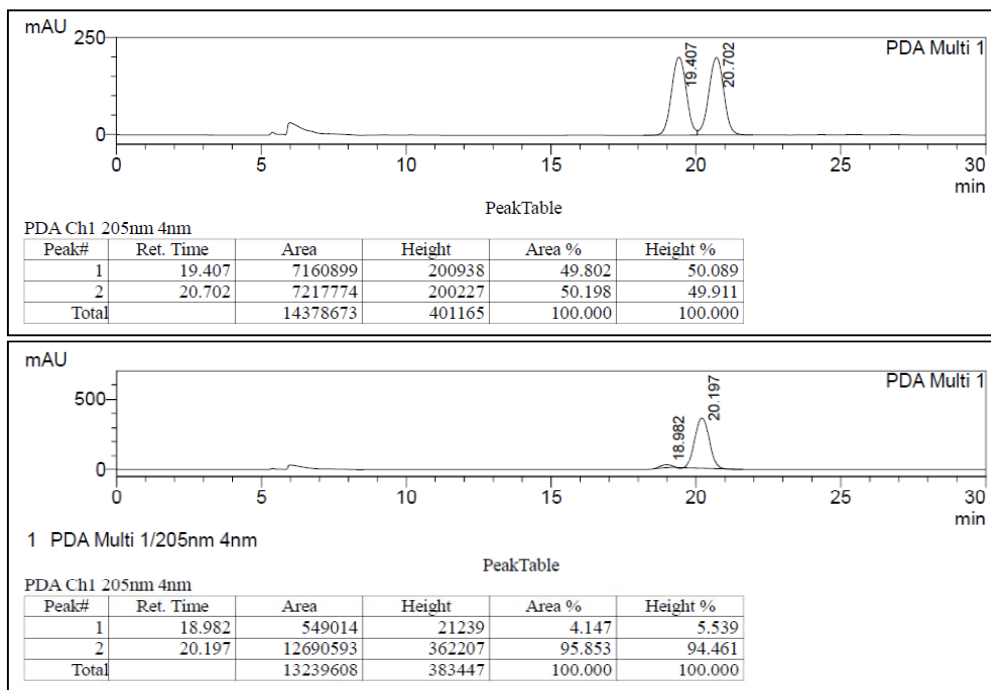


((3*R*,5*R*)-5-(bromomethyl)-5-(*o*-tolyl)-3-(2-(*o*-tolyl)allyl)tetrahydrofuran-3-yl)methanol (3-11b)

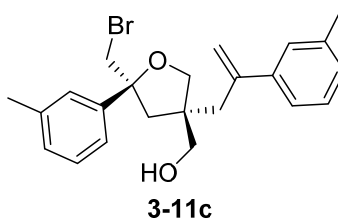


Colourless oil; $[\alpha]_D^{26}$ -17 (c 1.0, $CHCl_3$, 96:4 *er*); IR (film): 3433, 2926, 1627, 1446, 1303, 1029, 906 cm^{-1} ; 1H NMR (600 MHz, $CDCl_3$) δ 7.60 – 7.55 (m, 1H),

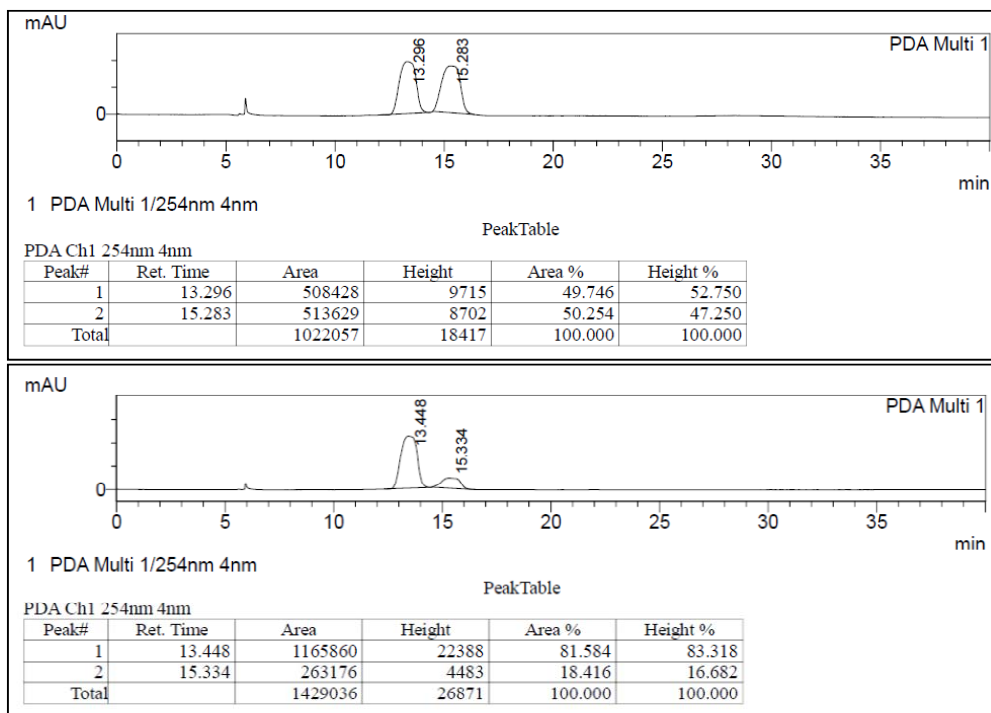
7.22 – 7.16 (m, 2H), 7.18 – 7.12 (m, 4H), 7.10 (d, $J = 3.8$ Hz, 1H), 5.40 – 5.34 (m, 1H), 5.07 (d, $J = 2.1$ Hz, 1H), 3.78 – 3.70 (m, 2H), 3.70 – 3.61 (m, 2H), 3.19 – 3.07 (m, 2H), 2.85 (dd, $J = 13.8, 1.0$ Hz, 1H), 2.76 (dd, $J = 13.8, 0.9$ Hz, 1H), 2.37 (s, 3H), 2.23 (d, $J = 17.1$ Hz, 4H), 2.09 (d, $J = 13.4$ Hz, 1H), 1.06 (t, $J = 5.9$ Hz, 1H); ^{13}C NMR (151 MHz, CDCl_3) δ 146.93, 142.46, 141.74, 134.63, 133.37, 132.06, 130.74, 128.34, 127.52, 127.38, 126.29, 125.85, 125.79, 118.93, 85.61, 74.78, 65.46, 50.09, 44.24, 41.64, 41.52, 21.26, 20.25; HRMS (ESI) calcd for $\text{C}_{23}\text{H}_{28}\text{BrO}_2 m/z$ $[\text{M} + \text{H}]^+$: 415.1267; found: 415.1266; HPLC (Daicel Chiralpak IA, *i*-PrOH/hexane = 2.5/97.5, 0.6 mL/min, 205 nm) $t_1 = 19.0$ min (minor), $t_2 = 20.2$ min (major).



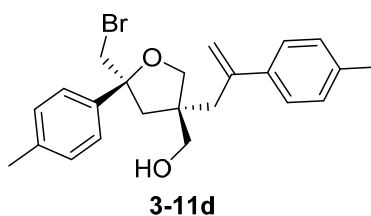
((3*R*,5*R*)-5-(bromomethyl)-5-(*m*-tolyl)-3-(2-(*m*-tolyl)allyl)tetrahydrofuran-3-yl)methanol (3-11c)



Colourless oil; $[\alpha]_D^{26} +3$ (c 1.0, CHCl_3 , 82:18); IR (film): 3453, 2922, 1603, 1447, 1235, 1043, 899 cm^{-1} ; ^1H NMR (600 MHz, CDCl_3) δ 7.23 – 7.16 (m, 5H), 7.13 – 7.10 (m, 2H), 7.06 – 7.02 (m, 1H), 5.28 (d, $J = 1.8$ Hz, 1H), 5.22 – 5.19 (m, 1H), 3.82 (d, $J = 9.1$ Hz, 1H), 3.68 (d, $J = 9.1$ Hz, 1H), 3.54 (d, $J = 1.4$ Hz, 2H), 3.11 (d, $J = 11.0$ Hz, 1H), 3.04 (d, $J = 11.0$ Hz, 1H), 2.87 (dd, $J = 13.7, 0.9$ Hz, 1H), 2.82 – 2.78 (m, 1H), 2.36 (s, 3H), 2.34 – 2.31 (m, 4H), 2.13 (d, $J = 13.3$ Hz, 1H), 1.21 (t, $J = 7.0$ Hz, 1H); ^{13}C NMR (151 MHz, CDCl_3) δ 146.62, 143.90, 142.39, 138.21, 137.90, 128.53, 128.46, 128.13, 128.12, 127.12, 126.00, 123.42, 122.47, 117.04, 85.25, 75.09, 65.17, 50.17, 43.88, 43.21, 39.80, 21.58, 21.49; HRMS (ESI) calcd for $\text{C}_{23}\text{H}_{27}\text{BrO}_2\text{Na}$ m/z $[\text{M} + \text{Na}]^+$: 437.1087; found: 437.1088; HPLC (Daicel Chiralpak IA, *i*-PrOH/hexane = 5/95, 0.6 mL/min, 254 nm) $t_1 = 13.4$ min (major), $t_2 = 15.3$ min (minor).

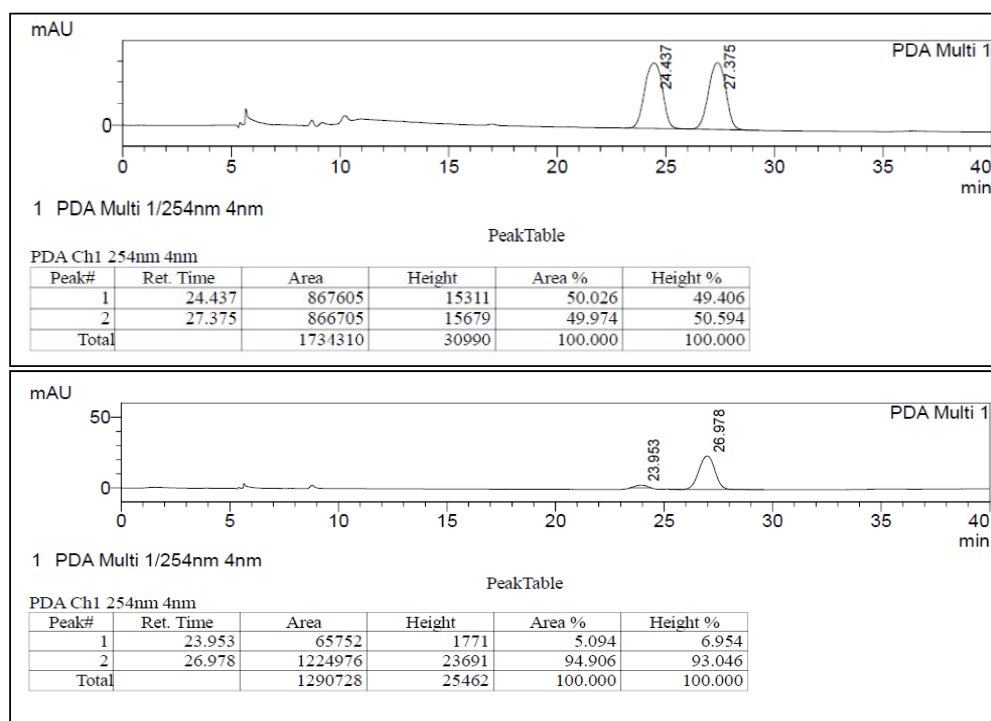


((3R,5R)-5-(bromomethyl)-5-(p-tolyl)-3-(2-(p-tolyl)allyl)tetrahydrofuran-3-yl)methanol (3-11d)

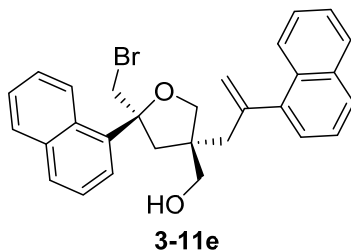


Colourless oil; $[\alpha]_D^{26} +8$ (c 1.0, CHCl_3 , 95:5 er); IR (film): 3448, 2922, 1726, 1619, 1451, 1303, 1038, 901 cm^{-1} ; ^1H NMR (600 MHz, CDCl_3) δ 7.29 (d, $J = 8.1$ Hz, 2H), 7.23 (d, $J = 8.2$ Hz, 2H), 7.16 – 7.13 (m, 2H), 7.11 (dd, $J = 8.2, 0.9$ Hz, 2H), 5.26 (d, $J = 1.8$ Hz, 1H), 5.19 – 5.15 (m, 1H), 3.80 (d, $J = 9.0$ Hz, 1H), 3.65 (d, $J = 9.0$ Hz, 1H), 3.53 (d, $J = 2.3$ Hz, 2H), 3.10 (dd, $J = 11.0, 6.1$ Hz, 1H), 3.02

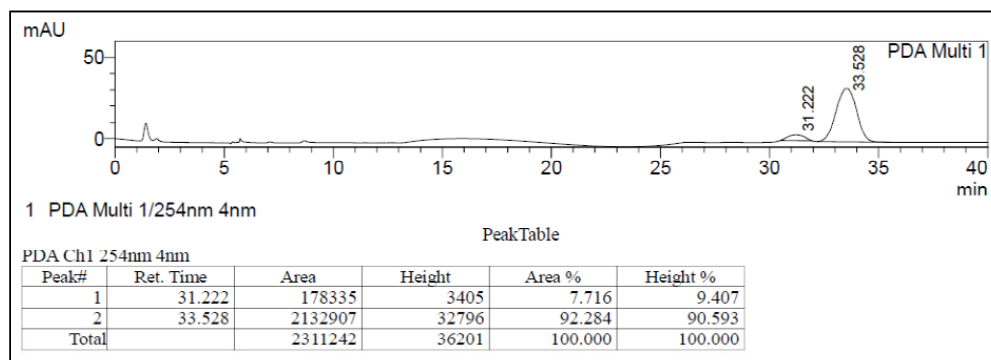
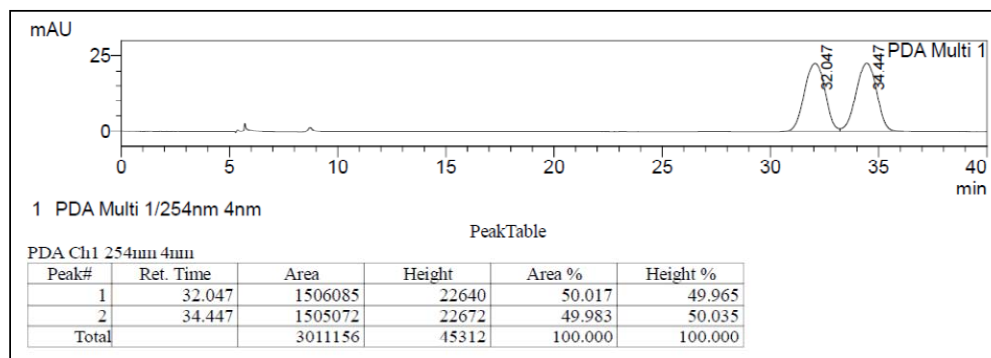
(dd, $J = 11.0, 5.7$ Hz, 1H), 2.85 (dd, $J = 13.8, 1.0$ Hz, 1H), 2.78 (dd, $J = 13.8, 0.9$ Hz, 1H), 2.35 (s, 3H), 2.33 – 2.29 (m, 4H), 2.13 (d, $J = 13.3$ Hz, 1H), 1.08 (t, $J = 6.0$ Hz, 1H); ^{13}C NMR (151 MHz, CDCl_3) δ 146.35, 140.96, 139.44, 137.56, 137.01, 129.27, 128.97, 126.22, 125.29, 116.57, 85.17, 75.01, 65.14, 50.16, 43.87, 43.26, 39.78, 21.10, 21.00; HRMS (ESI) calcd for $\text{C}_{23}\text{H}_{28}\text{BrO}_2\text{Na}$ m/z $[\text{M} + \text{Na}]^+$: 437.1087; found: 437.1097; HPLC (Daicel Chiralpak IA, *i*-PrOH/hexane = 2.5/97.5, 0.6 mL/min, 254 nm) $t_1 = 24.0$ min (minor), $t_2 = 27.0$ min (major).



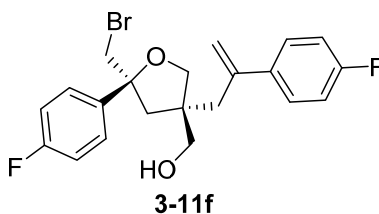
((3*R*,5*R*)-5-(bromomethyl)-5-(naphthalen-1-yl)-3-(2-(naphthalen-1-yl)allyl)tetrahydrofuran-3-yl)methanol (3-11e)



Colourless oil; $[\alpha]_D^{26} -19$ (*c* 1.0, CHCl₃, 93:7 *er*); IR (film): 3217, 2925, 1725, 1606, 1448, 1378, 1305, 1053, 908 cm⁻¹; ¹H NMR (600 MHz, CDCl₃) δ 8.13 – 8.08 (m, 1H), 7.88 (dd, *J* = 5.4, 3.1 Hz, 4H), 7.77 (dd, *J* = 5.5, 3.0 Hz, 3H), 7.50 (s, 2H), 7.45 – 7.40 (m, 3H), 7.37 (dd, *J* = 7.0, 1.3 Hz, 1H), 5.65 – 5.60 (m, 1H), 5.34 (d, *J* = 2.1 Hz, 1H), 3.91 (d, *J* = 11.3 Hz, 1H), 3.82 (s, 2H), 3.76 (d, *J* = 11.1 Hz, 1H), 3.14 – 3.03 (m, 4H), 2.47 (d, *J* = 13.3 Hz, 1H), 2.38 (d, *J* = 14.2 Hz, 1H), 0.93 (t, *J* = 5.9 Hz, 1H); ¹³C NMR (151 MHz, CDCl₃) δ 167.70, 145.43, 140.94, 134.58, 134.33, 133.95, 132.61, 130.72, 129.54, 128.76, 128.64, 127.89, 126.22, 125.94, 125.75, 125.50, 125.23, 125.19, 125.16, 125.05, 123.61, 120.29, 74.66, 65.36, 44.71, 42.64, 42.41, 29.70; HRMS (ESI) calcd for C₂₉H₂₈BrO₂ *m/z* [M + H]⁺: 487.1267; found: 487.1273; HPLC (Daicel Chiralpak IA, *i*-PrOH/hexane = 2.5/97.5, 0.6 mL/min, 254 nm) *t*₁ = 31.2 min (minor), *t*₂ = 33.5 min (major).

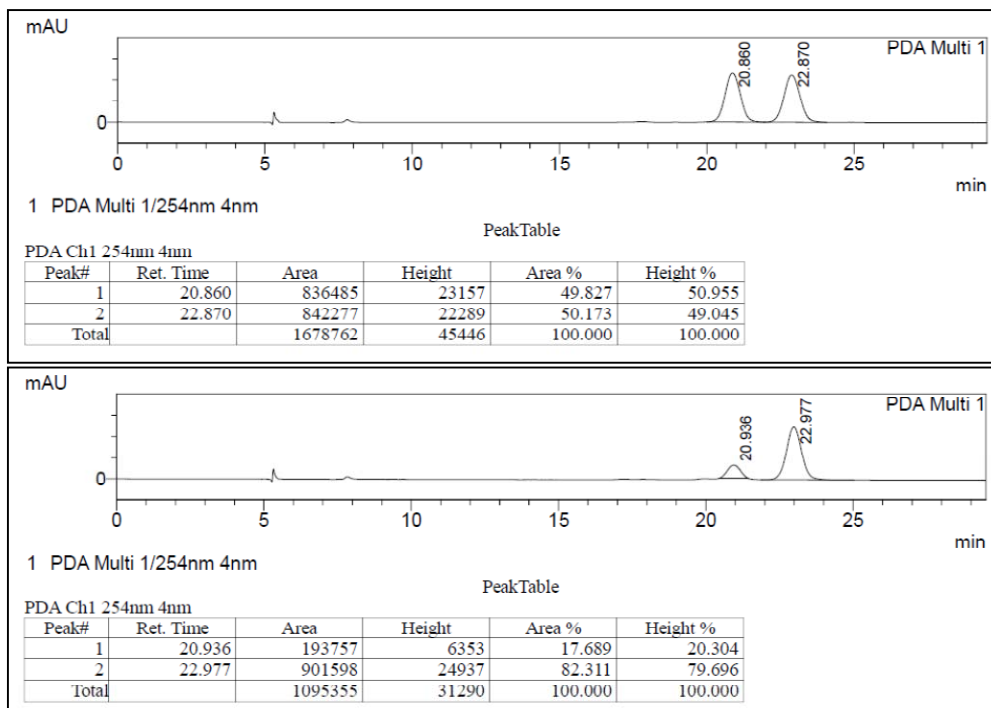


((3R,5R)-5-(bromomethyl)-5-(4-fluorophenyl)-3-(2-(4-fluorophenyl)allyl)tetrahydrofuran-3-yl)methanol (3-11f)

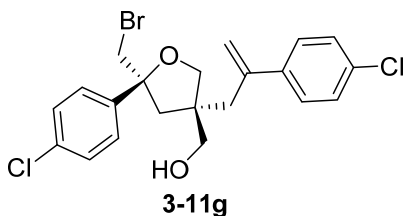


Colourless oil; $[\alpha]_D^{26} +4$ (c 0.5, CHCl_3 , 82:18 er); IR (film): 2924, 1726, 1602, 1462, 1299, 1053, 910 cm^{-1} ; ^1H NMR (600 MHz, CDCl_3) δ 7.37 (dd, $J = 8.7, 5.3$ Hz, 2H), 7.31 (dd, $J = 8.8, 5.3$ Hz, 2H), 7.03 (t, $J = 8.6$ Hz, 2H), 6.99 (t, $J = 8.7$ Hz, 2H), 5.27 (d, $J = 1.6$ Hz, 1H), 5.20 (d, $J = 1.5$ Hz, 1H), 3.78 (d, $J = 9.1$ Hz,

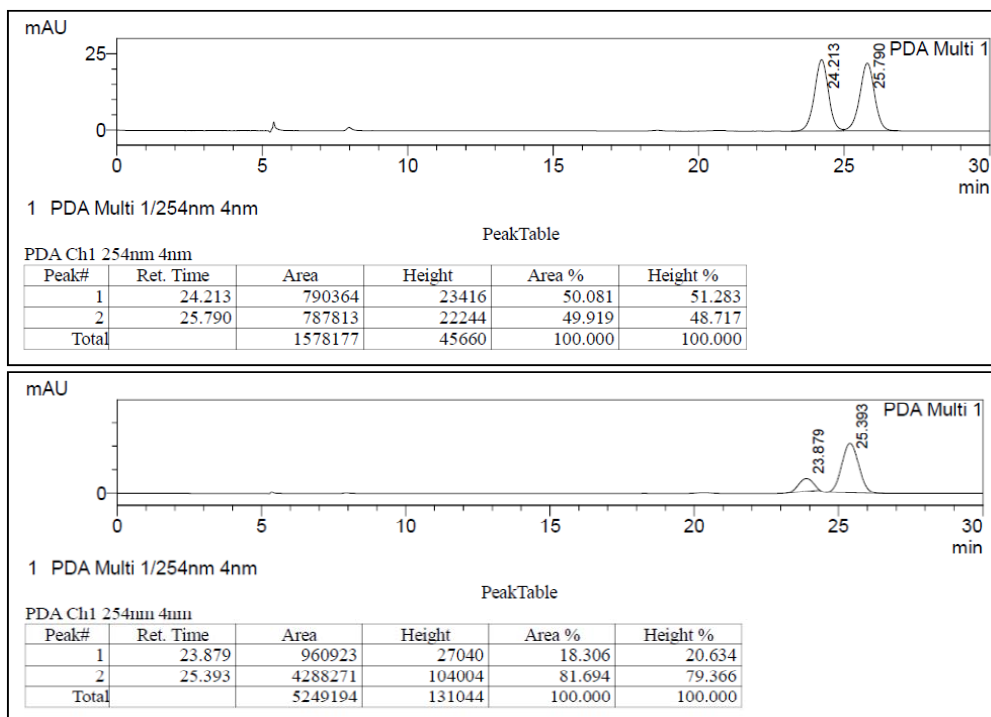
1H), 3.65 (d, $J = 9.1$ Hz, 1H), 3.54 – 3.45 (m, 2H), 3.12 (d, $J = 10.7$ Hz, 1H), 3.04 (d, $J = 10.7$ Hz, 1H), 2.84 (dd, $J = 13.8, 0.9$ Hz, 1H), 2.78 (dd, $J = 13.7, 0.9$ Hz, 1H), 2.28 (d, $J = 13.4$ Hz, 1H), 2.11 (d, $J = 13.4$ Hz, 1H); ^{13}C NMR (151 MHz, CDCl_3) δ 162.39 (d, $J = 247.2$ Hz), 162.00 (d, $J = 246.3$ Hz), 145.33, 139.67 (d, $J = 3.2$ Hz), 138.28 (d, $J = 3.3$ Hz), 128.02 (d, $J = 7.9$ Hz), 127.15 (d, $J = 8.2$ Hz), 117.42, 115.41 (d, $J = 21.4$ Hz), 115.11 (d, $J = 21.4$ Hz), 84.92, 74.92, 64.88, 50.03, 43.86, 42.96, 39.71; HRMS (ESI) calcd for $\text{C}_{21}\text{H}_{21}\text{BrF}_2\text{O}_2\text{Na}$ m/z [$\text{M} + \text{Na}$] $^+$: 445.0585; found: 445.0575; HPLC (Daicel Chiralpak IA, *i*-PrOH/hexane = 5/95, 0.6 mL/min, 254 nm) $t_1 = 20.9$ min (minor), $t_2 = 23.0$ min (major).



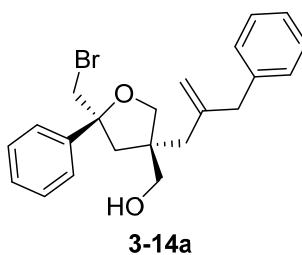
((3*R*,5*R*)-5-(bromomethyl)-5-(4-chlorophenyl)-3-(2-(4-chlorophenyl)allyl)tetrahydrofuran-3-yl)methanol (3-11g)



Colourless oil; $[\alpha]_D^{26} +5$ (*c* 0.5, CHCl_3 , 82:18 *er*); IR (film): 3455, 2927, 1625, 1490, 1378, 1294, 1041, 908 cm^{-1} ; ^1H NMR (600 MHz, CDCl_3) δ 7.34 – 7.30 (m, 4H), 7.28 (m, 4H), 5.30 (d, $J = 1.5$ Hz, 1H), 5.22 (d, $J = 1.5$ Hz, 1H), 3.77 (d, $J = 9.1$ Hz, 1H), 3.65 (d, $J = 9.1$ Hz, 1H), 3.53 – 3.45 (m, 2H), 3.11 (d, $J = 10.7$ Hz, 1H), 3.03 (d, $J = 10.7$ Hz, 1H), 2.84 (dd, $J = 13.9, 1.0$ Hz, 1H), 2.77 (dd, $J = 13.8, 0.8$ Hz, 1H), 2.27 (d, $J = 13.4$ Hz, 1H), 2.10 (d, $J = 13.4$ Hz, 1H); ^{13}C NMR (151 MHz, CDCl_3) δ 145.17, 142.48, 140.67, 133.61, 133.32, 128.68, 128.45, 127.71, 126.89, 117.96, 84.92, 74.89, 64.81, 50.00, 43.79, 42.69, 39.37; HRMS (ESI) calcd for $\text{C}_{21}\text{H}_{21}\text{BrCl}_2\text{O}_2\text{Na}$ m/z $[\text{M} + \text{Na}]^+$: 476.9994; found: 476.9989; HPLC (Daicel Chiralpak IA, *i*-PrOH/hexane = 5/95, 0.6 mL/min, 254 nm) $t_1 = 23.9$ min (minor), $t_2 = 25.4$ min (major).

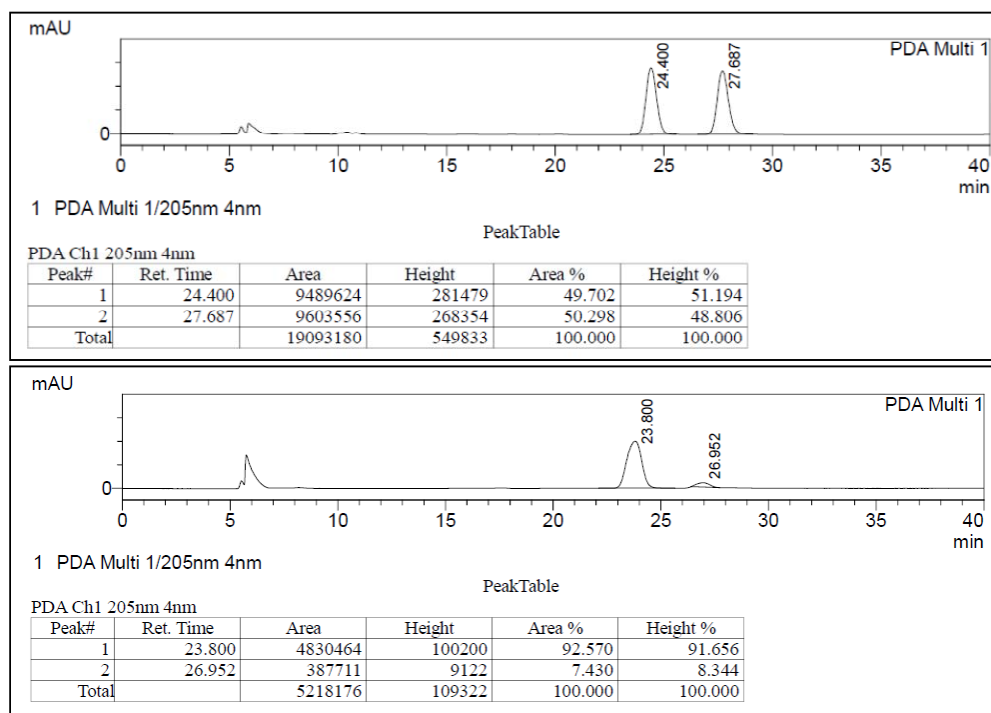


((3*R*,5*R*)-3-(2-benzylallyl)-5-(bromomethyl)-5-phenyltetrahydrofuran-3-yl)methanol (3-14a)

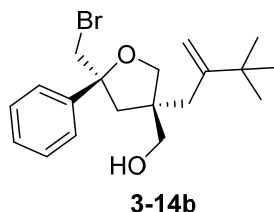


Colourless oil; $[\alpha]_D^{26} -7$ (c 0.5, CHCl_3 , 93:7); IR (film): 3458, 2920, 1638, 1448, 1234, 1046, 905 cm^{-1} ; ^1H NMR (600 MHz, CDCl_3) δ 7.42 (dd, $J = 8.3, 1.3$ Hz, 2H), 7.33 (ddd, $J = 21.2, 8.2, 6.7$ Hz, 4H), 7.28 (d, $J = 7.3$ Hz, 1H), 7.25 – 7.19 (m, 3H), 5.00 – 4.95 (m, 1H), 4.91 (d, $J = 1.6$ Hz, 1H), 3.96 (d, $J = 8.9$ Hz, 1H),

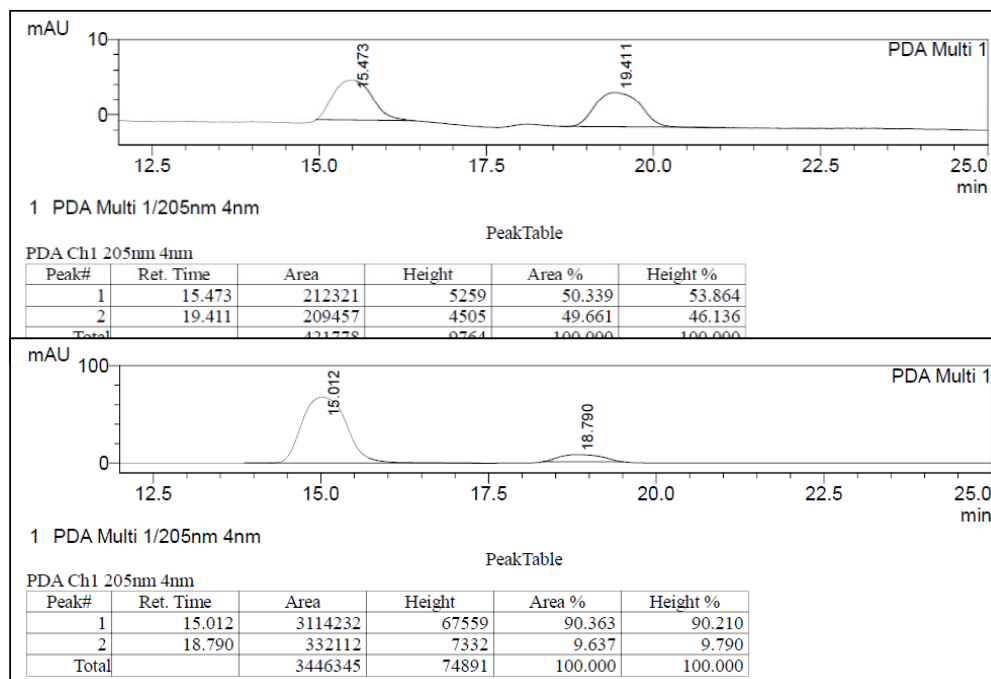
3.90 (d, $J = 8.9$ Hz, 1H), 3.62 – 3.55 (m, 2H), 3.39 (d, $J = 3.5$ Hz, 2H), 3.29 (d, $J = 10.9$ Hz, 1H), 3.25 (d, $J = 10.9$ Hz, 1H), 2.40 (d, $J = 0.8$ Hz, 2H), 2.30 (dd, $J = 2.2, 1.0$ Hz, 2H); ^{13}C NMR (151 MHz, CDCl_3) δ 146.39, 144.00, 139.11, 129.07, 128.48, 128.33, 127.45, 126.37, 125.38, 115.78, 85.35, 75.62, 65.15, 49.77, 44.60, 44.07, 43.17, 39.98; HRMS (ESI) calcd for $\text{C}_{22}\text{H}_{25}\text{BrO}_2\text{Na}$ m/z $[\text{M} + \text{Na}]^+$: 423.0930; found: 423.0940; HPLC (Daicel Chiralpak IC, *i*-PrOH/hexane = 2.5/97.5, 0.6 mL/min, 205 nm) $t_1 = 23.8$ min (major), $t_2 = 27.0$ min (minor).



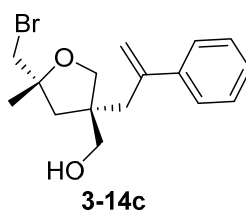
((3*R*,5*R*)-5-(bromomethyl)-3-(3,3-dimethyl-2-methylenebutyl)-5-phenyltetrahydrofuran-3-yl)methanol (3-14b)



Colourless oil; $[\alpha]_D^{26} -3$ (*c* 2.0, CHCl₃, 90:10 *er*); IR (film): 3466, 2957, 1635, 1448, 1362, 1226, 1054, 895 cm⁻¹; ¹H NMR (600 MHz, CDCl₃) δ 7.48 – 7.38 (m, 2H), 7.35 (dd, *J* = 8.5, 6.9 Hz, 2H), 7.29 – 7.26 (m, 1H), 5.03 (s, 1H), 4.70 (t, *J* = 1.5 Hz, 1H), 4.03 (d, *J* = 8.9 Hz, 1H), 3.97 (d, *J* = 8.9 Hz, 1H), 3.62 (s, 2H), 3.41 – 3.30 (m, 2H), 2.48 (q, *J* = 13.2 Hz, 2H), 2.44 – 2.36 (m, 2H), 1.08 (s, 9H); ¹³C NMR (151 MHz, CDCl₃) δ 154.19, 143.96, 128.34, 127.44, 125.40, 108.21, 85.28, 77.21, 77.00, 76.79, 76.37, 64.87, 49.36, 45.36, 43.01, 36.78, 35.33, 29.19; HRMS (ESI) calcd for C₁₉H₂₇BrO₂Na *m/z* [M + Na]⁺: 389.1087; found: 389.1081; HPLC (Daicel Chiralpak IA, *i*-PrOH/hexane = 2.5/97.5, 0.6 mL/min, 205 nm) *t*₁ = 15.0 min (major), *t*₂ = 18.8 min (minor).

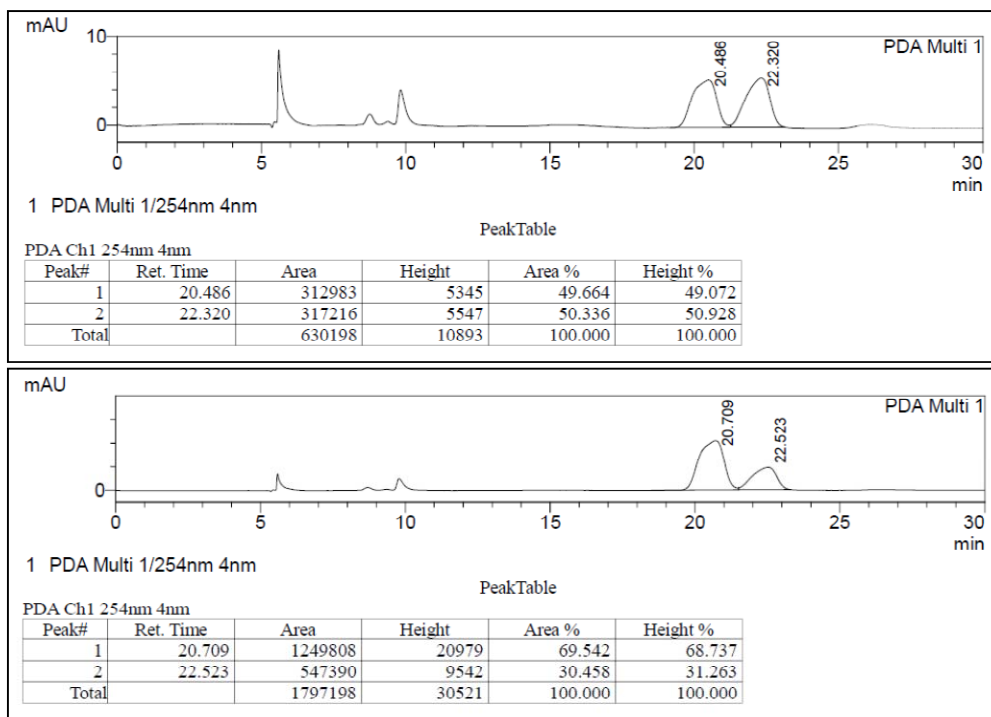


((3R,5R)-5-(bromomethyl)-3-(2-methylallyl)-5-phenyltetrahydrofuran-3-yl)methanol (3-14c)



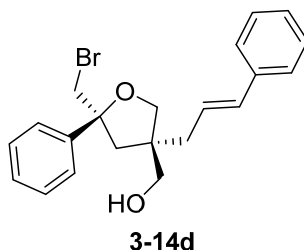
Colourless oil; $[\alpha]_D^{26} -3$ (c 0.5, CHCl_3 , 70:30 er); IR (film): 3446, 2974, 2876, 1623, 1446, 1375, 1033, 907 cm^{-1} ; ^1H NMR (600 MHz, CDCl_3) δ 7.39 – 7.35 (m, 2H), 7.33 (ddd, $J = 7.7, 6.7, 1.3$ Hz, 2H), 7.31 – 7.27 (m, 1H), 5.29 (d, $J = 1.7$ Hz, 1H), 5.18 – 5.13 (m, 1H), 3.66 – 3.57 (m, 2H), 3.41 – 3.34 (m, 3H), 3.32 (d, $J = 10.8$ Hz, 1H), 2.80 (d, $J = 1.0$ Hz, 1H), 2.75 – 2.71 (m, 1H), 1.82 (d, $J = 13.6$ Hz,

1H), 1.66 (d, $J = 13.6$ Hz, 1H), 1.37 (s, 3H); ^{13}C NMR (151 MHz, CDCl_3) δ 146.45, 142.51, 128.58, 127.75, 126.34, 117.50, 82.00, 73.87, 66.15, 50.10, 43.32, 41.41, 40.31, 25.46; HRMS (ESI) calcd for $\text{C}_{16}\text{H}_{21}\text{BrO}_2\text{Na}$ m/z $[\text{M} + \text{Na}]^+$: 347.0617; found: 347.0615; HPLC (Daicel Chiralpak IB, *i*-PrOH/hexane = 2.5/97.5, 0.6 mL/min, 254 nm) $t_1 = 20.7$ min (major), $t_2 = 22.5$ min (minor).

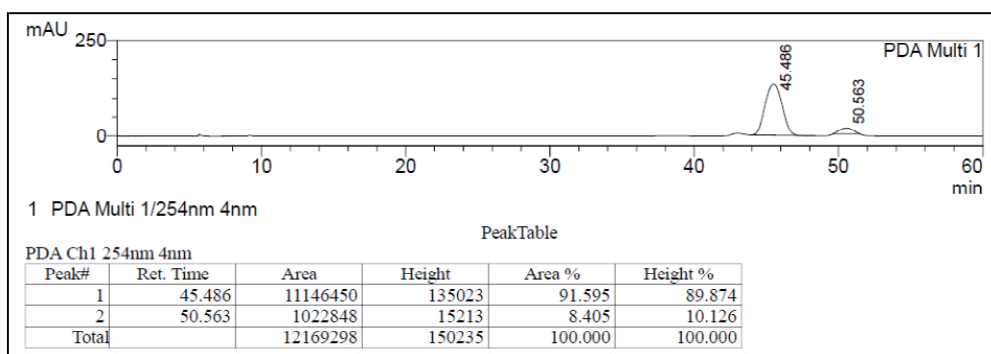
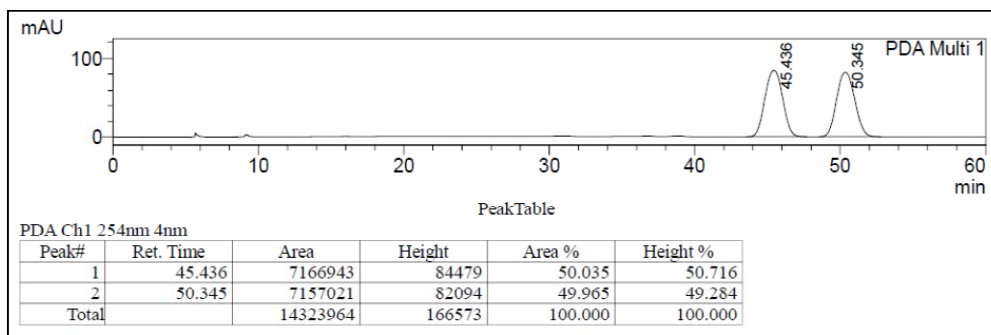


((3*R*,5*R*)-5-(bromomethyl)-3-cinnamyl-5-phenyltetrahydrofuran-3-yl)

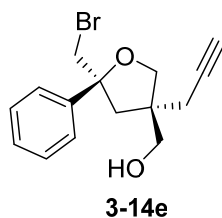
methanol (3-14d)



Colourless oil; $[\alpha]_D^{26} +7$ (c 1.0, CHCl_3 , 92:8 er); IR (film): 3418, 2930, 1648, 1494, 1447, 1288, 1224, 1055, 967, 913 cm^{-1} ; ^1H NMR (600 MHz, CDCl_3) δ 7.44 – 7.41 (m, 2H), 7.38 – 7.27 (m, 7H), 7.24 (d, $J = 7.3$ Hz, 1H), 6.53 (dt, $J = 15.8$, 1.4 Hz, 1H), 6.25 (dt, $J = 15.4$, 7.6 Hz, 1H), 3.97 (d, $J = 9.0$ Hz, 1H), 3.88 (d, $J = 9.0$ Hz, 1H), 3.65 – 3.58 (m, 2H), 3.30 (d, $J = 2.2$ Hz, 2H), 2.60 – 2.49 (m, 2H), 2.44 (d, $J = 13.2$ Hz, 1H), 2.33 (d, $J = 13.2$ Hz, 1H); ^{13}C NMR (151 MHz, CDCl_3) δ 143.75, 137.16, 133.30, 128.57, 128.39, 127.51, 127.34, 126.12, 126.02, 125.46, 85.65, 74.87, 66.01, 49.91, 43.66, 42.90, 38.42; HRMS (ESI) calcd for $\text{C}_{21}\text{H}_{23}\text{BrO}_2\text{Na}$ m/z $[\text{M} + \text{Na}]^+$: 409.0774; found: 409.0782; HPLC (Daicel Chiralpak IA, *i*-PrOH/hexane = 2.5/97.5, 0.6 mL/min, 254 nm) $t_1 = 45.5$ min (major), $t_2 = 50.6$ min (minor).

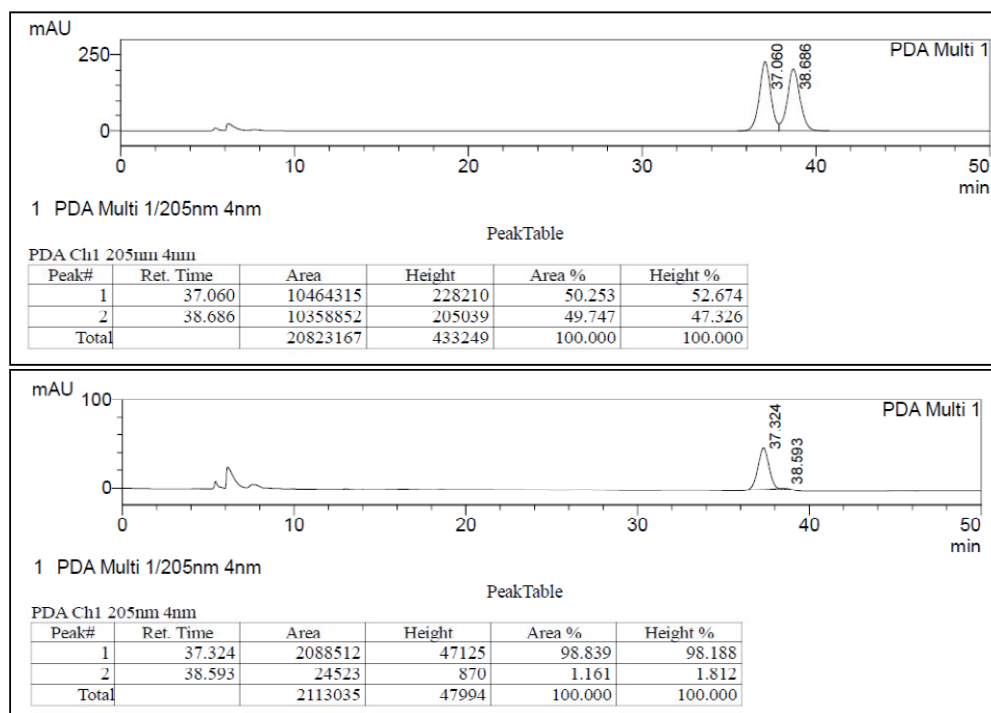


((3R,5R)-5-(bromomethyl)-5-phenyl-3-(prop-2-yn-1-yl)tetrahydrofuran-3-yl)methanol (3-14e)



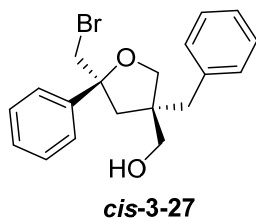
Colourless oil; $[\alpha]_D^{26} +21$ (c 0.25, CHCl_3 , 95:5 er); IR (film): 3404, 2936, 1603, 1447, 1296, 1043, 916 cm^{-1} ; ^1H NMR (600 MHz, CDCl_3) δ 7.41 (dd, $J = 8.3, 1.3$ Hz, 2H), 7.35 (dd, $J = 8.5, 6.9$ Hz, 2H), 7.30 – 7.26 (m, 1H), 3.94 (d, $J = 9.2$ Hz, 1H), 3.83 (d, $J = 9.2$ Hz, 1H), 3.62 (s, 2H), 3.40 (d, $J = 2.2$ Hz, 2H), 2.62 – 2.51

(m, 2H), 2.46 (d, $J = 13.4$ Hz, 1H), 2.35 (d, $J = 13.4$ Hz, 1H), 2.03 (t, $J = 2.7$ Hz, 1H); ^{13}C NMR (151 MHz, CDCl_3) δ 143.52, 128.41, 127.57, 125.43, 85.73, 81.33, 74.11, 70.32, 65.74, 49.10, 43.60, 42.49, 24.42; HRMS (ESI) calcd for $\text{C}_{15}\text{H}_{17}\text{BrO}_2\text{Na}$ m/z $[\text{M} + \text{Na}]^+$: 331.0304; found: 331.0316; HPLC (Daicel Chiralpak IA, *i*-PrOH/hexane = 2.5/97.5, 0.6 mL/min, 205 nm) $t_1 = 37.3$ min (major), $t_2 = 38.6$ min (minor).

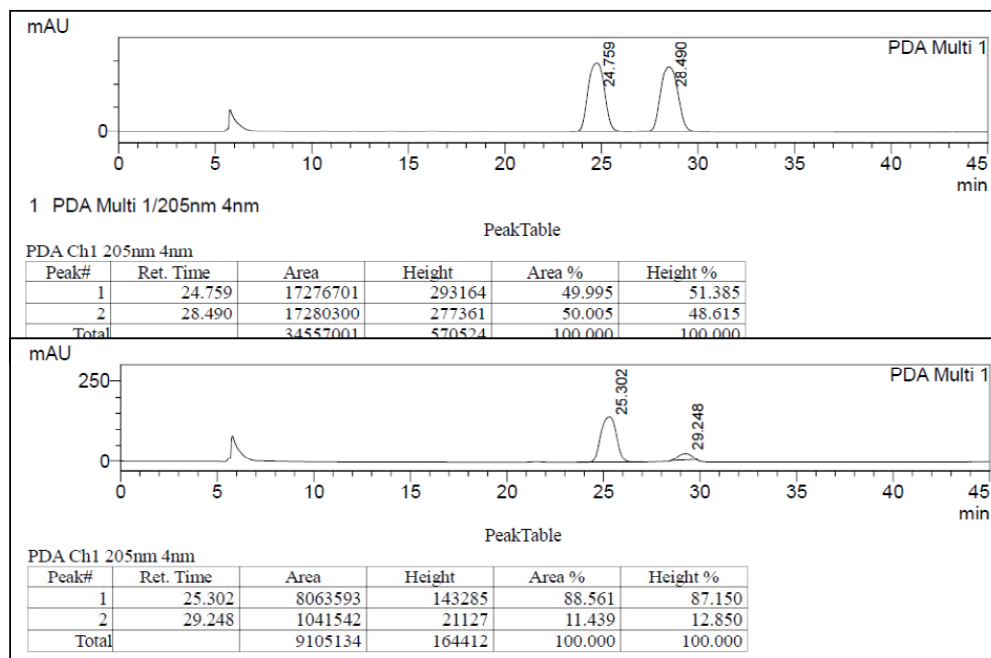


((3R,5R)-3-benzyl-5-(bromomethyl)-5-phenyltetrahydrofuran-3-yl)

methanol (*cis*-3-27)



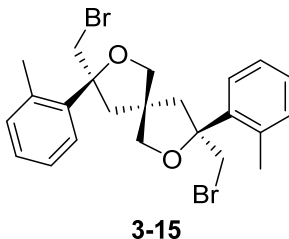
Colourless oil; $[\alpha]_D^{26} +21$ (c 0.5, CHCl₃, 89:11 er); IR (film): 3441, 2929, 1603, 1495, 1447, 1291, 1227, 1029, 917 cm⁻¹; ¹H NMR (600 MHz, CDCl₃) δ 7.41 – 7.36 (m, 2H), 7.35 – 7.29 (m, 4H), 7.27 – 7.23 (m, 4H), 4.02 (d, *J* = 8.9 Hz, 1H), 3.88 (d, *J* = 8.9 Hz, 1H), 3.58 (q, *J* = 10.8 Hz, 2H), 3.20 – 3.12 (m, 2H), 2.97 (d, *J* = 13.3 Hz, 1H), 2.87 (d, *J* = 13.3 Hz, 1H), 2.50 (d, *J* = 13.3 Hz, 1H), 2.20 (d, *J* = 13.3 Hz, 1H); ¹³C NMR (151 MHz, CDCl₃) δ 143.95, 138.01, 130.06, 128.37, 128.32, 127.44, 126.50, 125.39, 85.51, 75.03, 64.64, 50.37, 43.66, 43.10, 39.98; HRMS (ESI) calcd for C₁₉H₂₁BrO₂Na *m/z* [M + Na]⁺: 383.0617; found: 383.0623; HPLC (Daicel Chiralpak IB, *i*-PrOH/hexane = 2.5/97.5, 0.6 mL/min, 205 nm) t₁ = 25.3 min (major), t₂ = 29.2 min (minor).



(D) General procedure for the 2nd Cyclization to Spirocycles

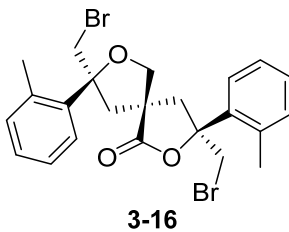
To a stirred solution of the bromoether (0.05 mmol, 1.0 eq) in CH₂Cl₂ (2.0 mL) was added triphenylphosphine sulfide (0.005 mmol, 0.1 eq). The mixture was cooled to -50 °C before N-bromosuccinimide (0.06 mmol, 1.2 eq) was added. The reaction was stirred at -50°C for 12 h before it was quenched with Na₂SO₃ (2.0 mL) and extracted with CH₂Cl₂ (3 x 2 mL). The combined organic extracts was dried over MgSO₄, filtered and concentrated under reduced pressure. The residue was purified using flash column chromatography (hexane/Et₂O 4:1) to give the product.

(3*R*,5*S*,8*S*)-3,8-bis(bromomethyl)-3,8-di-*o*-tolyl-2,7-dioxaspiro[4.4]nonane (3-15)



Colourless oil; $[\alpha]_D^{26}$ -16 (*c* 2.0, CHCl₃, 95:5 *er*); IR (film): 2967, 2867, 1482, 1445, 1203, 1044 cm⁻¹; ¹H NMR (600 MHz, CDCl₃) δ 7.56 (dd, *J* = 7.4, 1.9 Hz, 2H), 7.23 – 7.09 (m, 6H), 3.79 (d, *J* = 11.2 Hz, 2H), 3.70 (d, *J* = 11.2 Hz, 2H), 3.65 (d, *J* = 8.8 Hz, 2H), 3.56 (d, *J* = 8.8 Hz, 2H), 2.71 (d, *J* = 13.1 Hz, 2H), 2.63 (d, *J* = 13.1 Hz, 2H), 2.38 (s, 6H); ¹³C NMR (151 MHz, CDCl₃) δ 141.07, 133.67, 132.31, 127.83, 126.15, 126.02, 85.45, 76.16, 52.82, 46.68, 41.09, 21.39; HRMS (ESI) calcd for C₂₃H₂₇Br₂O₂ *m/z* [M + H]⁺: 493.0372; found: 493.0358.

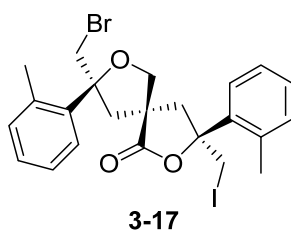
(3*S*,5*S*,8*R*)-3,8-bis(bromomethyl)-3,8-di-*o*-tolyl-2,7-dioxaspiro[4.4]nonan-1-one (3-16)



Colourless oil; $[\alpha]_D^{26}$ -14.2 (*c* 5.0, CHCl₃, 95:5 *er*); IR (film): 2926, 2865, 1773, 1623, 1483, 1446, 1384, 1293, 1247, 1186, 1078, 1015, 953 cm⁻¹; ¹H NMR (600

MHz, CDCl_3) δ 7.47 (d, $J = 7.7$ Hz, 2H), 7.27 (s, 1H), 7.25 – 7.13 (m, 5H), 3.91 (d, $J = 11.6$ Hz, 1H), 3.83 (d, $J = 11.6$ Hz, 1H), 3.73 (d, $J = 11.5$ Hz, 1H), 3.62 (d, $J = 11.5$ Hz, 1H), 3.55 (dd, $J = 8.7, 1.4$ Hz, 1H), 3.42 (dd, $J = 8.8, 1.3$ Hz, 1H), 3.16 (d, $J = 13.7$ Hz, 1H), 3.09 – 3.02 (m, 2H), 2.82 (dd, $J = 13.5, 1.3$ Hz, 1H), 2.46 (s, 3H), 2.35 (s, 3H); ^{13}C NMR (151 MHz, CDCl_3) δ 176.41, 140.31, 138.28, 134.05, 133.51, 132.98, 132.57, 128.92, 128.18, 126.60, 126.24, 125.55, 125.11, 86.63, 85.11, 75.73, 53.13, 48.58, 46.14, 40.16, 39.89, 21.49, 21.18; HRMS (ESI) calcd for $\text{C}_{23}\text{H}_{24}\text{Br}_2\text{O}_3\text{Na}$ m/z $[\text{M} + \text{Na}]^+$: 530.9966; found: 530.9949.

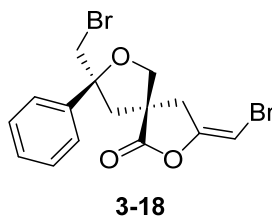
(3*S*,5*S*,8*R*)-8-(bromomethyl)-3-(iodomethyl)-3,8-di-*o*-tolyl-2,7-dioxaspiro[4.4]nonan-1-one (3-17)



Colourless oil; $[\alpha]_D^{26}$ -13.6 (c 1.0, CHCl_3 , 95:5 er); IR (film): 2968, 1773, 1448, 1248, 1188, 1079, 1056, 1015, 953, 910 cm^{-1} ; ^1H NMR (600 MHz, CDCl_3) δ 7.44 (ddd, $J = 18.3, 7.9, 1.4$ Hz, 2H), 7.31 – 7.13 (m, 7H), 3.85 (d, $J = 11.4$ Hz, 1H), 3.77 (d, $J = 11.4$ Hz, 1H), 3.73 (d, $J = 11.5$ Hz, 1H), 3.61 (d, $J = 11.5$ Hz, 1H), 3.50 (dd, $J = 8.7, 1.5$ Hz, 1H), 3.36 (dd, $J = 8.7, 1.3$ Hz, 1H), 3.27 (d, $J = 13.6$ Hz, 1H), 3.05 (d, $J = 13.4$ Hz, 1H), 2.91 (dd, $J = 13.8, 1.5$ Hz, 1H), 2.81 (dd, $J = 13.4, 1.3$ Hz, 1H), 2.46 (s, 3H), 2.35 (s, 3H); ^{13}C NMR (151 MHz, CDCl_3) δ 176.25,

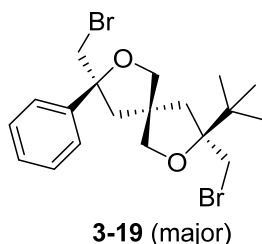
140.27, 138.14, 134.04, 133.02, 132.56, 128.80, 128.17, 126.53, 126.23, 125.46, 125.09, 86.59, 84.50, 75.20, 53.30, 48.46, 47.81, 40.16, 21.47, 21.17, 16.14; HRMS (ESI) calcd for $C_{23}H_{24}BrIO_3Na$ m/z $[M + Na]^+$: 576.9846; found: 576.9832.

(5*S*,8*R*,*E*)-8-(bromomethyl)-3-(bromomethylene)-8-phenyl-2,7-dioxaspiro[4.4]nonan-1-one (3-18)



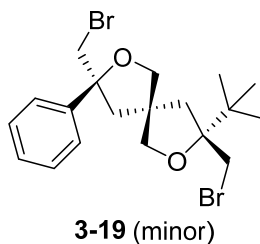
Colourless oil; $[\alpha]_D^{26} +22$ (c 2.0, $CHCl_3$, 95:5 v/v); IR (film): 2997, 1808, 1672, 1447, 1165, 1124, 1033, 955, 905 cm^{-1} ; 1H NMR (600 MHz, $CDCl_3$) δ 7.42 – 7.37 (m, 4H), 7.35 – 7.31 (m, 1H), 6.05 (t, $J = 2.3$ Hz, 1H), 4.04 (dd, $J = 8.8, 1.1$ Hz, 1H), 3.89 (dd, $J = 8.7, 1.1$ Hz, 1H), 3.65 (d, $J = 11.3$ Hz, 1H), 3.58 (d, $J = 11.3$ Hz, 1H), 3.35 (dd, $J = 17.7, 2.0$ Hz, 1H), 3.09 (ddd, $J = 17.7, 2.7, 1.0$ Hz, 1H), 3.04 (d, $J = 13.4$ Hz, 1H), 2.71 (dd, $J = 13.4, 1.2$ Hz, 1H); ^{13}C NMR (151 MHz, $CDCl_3$) δ 175.59, 149.93, 142.29, 128.79, 128.21, 125.40, 87.03, 86.58, 76.51, 51.89, 47.85, 41.30, 40.07; HRMS (ESI) calcd for $C_{15}H_{14}Br_2O_3Na$ m/z $[M + Na]^+$: 422.9202; found: 422.9287.

(3*S*,5*S*,8*R*)-3,8-bis(bromomethyl)-3-(*tert*-butyl)-8-phenyl-2,7-dioxaspiro[4.4]nonane (3-19)



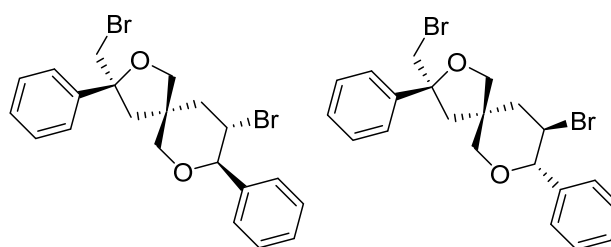
Colourless oil; $[\alpha]_D^{26} +10$ (c 1.0, CHCl_3 , 90:10 er); IR (film): 2917, 1722, 1597, 1492, 1447, 1260, 1219, 1126, 1045, 961 cm^{-1} ; ^1H NMR (600 MHz, CDCl_3) δ 7.43 – 7.37 (m, 2H), 7.33 (dd, $J = 8.4, 6.8$ Hz, 2H), 7.29 – 7.26 (m, 1H), 4.07 – 3.98 (m, 2H), 3.72 (d, $J = 10.9$ Hz, 1H), 3.65 (d, $J = 1.1$ Hz, 2H), 3.60 (d, $J = 10.8$ Hz, 1H), 3.57 (dd, $J = 9.1, 1.4$ Hz, 1H), 3.48 (d, $J = 9.0$ Hz, 1H), 2.78 (d, $J = 12.8$ Hz, 1H), 2.61 (dd, $J = 12.9, 0.9$ Hz, 1H), 2.36 (d, $J = 14.2$ Hz, 1H), 2.21 (d, $J = 14.1$ Hz, 1H), 0.96 (s, 9H); ^{13}C NMR (151 MHz, CDCl_3) δ 143.28, 128.25, 127.58, 125.44, 88.55, 85.21, 80.17, 79.95, 52.19, 47.67, 42.70, 40.74, 40.42, 38.76, 26.21; HRMS (ESI) calcd for $\text{C}_{19}\text{H}_{26}\text{Br}_2\text{O}_2\text{Na}$ m/z $[\text{M} + \text{Na}]^+$: 469.0173; found: 469.0173.

(3*R*,5*S*,8*R*)-3,8-bis(bromomethyl)-3-(*tert*-butyl)-8-phenyl-2,7-
dioxaspiro[4.4]nonane (**3-19**)



^1H NMR (600 MHz, CDCl_3) δ 7.41 – 7.37 (m, 2H), 7.35 – 7.30 (m, 2H), 7.28 – 7.26 (m, 1H), 4.24 (dd, $J = 8.5, 0.9$ Hz, 1H), 4.16 (dd, $J = 8.5, 1.1$ Hz, 1H), 3.72 (d, $J = 9.0$ Hz, 1H), 3.64 (s, 2H), 3.62 (d, $J = 10.9$ Hz, 1H), 3.55 (d, $J = 11.0$ Hz, 1H), 3.21 (dd, $J = 9.0, 1.1$ Hz, 1H), 2.68 (d, $J = 12.6$ Hz, 1H), 2.46 (dd, $J = 12.7, 0.9$ Hz, 1H), 2.29 (d, $J = 1.8$ Hz, 2H), 0.98 (s, 9H); ^{13}C NMR (151 MHz, CDCl_3) δ 143.21, 128.30, 127.61, 125.43, 88.56, 85.06, 80.84, 79.38, 52.21, 48.92, 42.57, 40.75, 40.07, 39.24, 26.31.

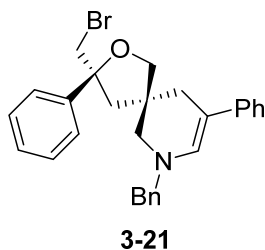
(3R,5R,8R,9S)-9-bromo-3-(bromomethyl)-3,8-diphenyl-2,7-dioxaspiro[4.5]decane
and (3R,5R,8S,9R)-9-bromo-3-(bromomethyl)-3,8-diphenyl-2,7-
dioxaspiro[4.5]decane (1:1) (3-20)



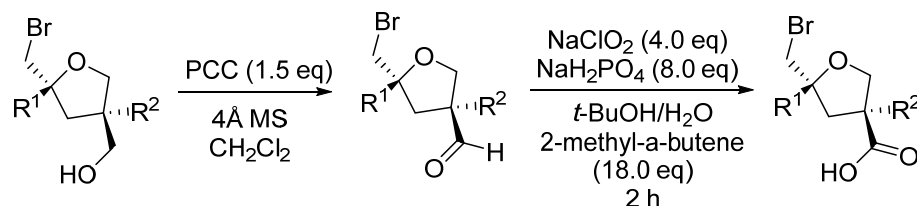
3-20 (1:1)

Colourless oil; IR (film): 3061, 3030, 2957, 2923, 2853, 1494, 1447, 1301, 1221, 1176, 1075, 1048, 902 cm^{-1} ; ^1H NMR (600 MHz, CDCl_3) δ 7.46 – 7.39 (m, 4H), 7.37 – 7.31 (m, 13H), 7.26 (s, 4H), 4.37 (d, J = 8.6 Hz, 1H), 4.21 (t, J = 10.0 Hz, 2H), 4.14 – 4.07 (m, 2H), 3.95 – 3.86 (m, 2H), 3.71 (d, J = 9.1 Hz, 1H), 3.68 – 3.58 (m, 4H), 3.55 (dd, J = 11.4, 2.5 Hz, 1H), 3.44 (dd, J = 11.3, 2.5 Hz, 1H), 3.32 (dd, J = 11.4, 1.8 Hz, 1H), 3.25 (dd, J = 11.5, 1.8 Hz, 1H), 2.97 (d, J = 12.8 Hz, 1H), 2.67 (s, 2H), 2.48 (dd, J = 12.9, 1.8 Hz, 1H), 2.41 (d, J = 13.2 Hz, 1H), 2.29 (t, J = 12.7 Hz, 1H), 2.21 – 2.13 (m, 2H); ^{13}C NMR (151 MHz, CDCl_3) δ 143.28, 142.78, 138.58, 138.57, 128.75, 128.69, 128.62, 128.49, 128.32, 128.26, 127.76, 127.72, 127.43, 127.34, 125.33, 125.29, 86.30, 85.20, 85.06, 84.59, 75.09, 75.00, 74.38, 74.15, 49.90, 49.65, 48.10, 48.07, 45.65, 45.51, 45.20, 43.76, 42.66, 42.54; HRMS (ESI) calcd for $\text{C}_{21}\text{H}_{22}\text{Br}_2\text{O}_2\text{Na}$ m/z $[\text{M} + \text{Na}]^+$: 488.9860; found: 488.9847.

(3*R*,5*S*)-7-benzyl-3-(bromomethyl)-3,9-diphenyl-2-oxa-7-azaspiro[4.5]dec-8-ene (3-21)



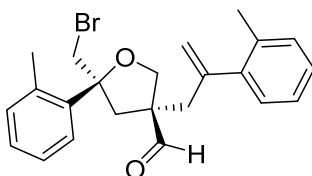
Colourless oil; $[\alpha]_D^{26} +13$ (*c* 0.4, CHCl_3 , 95:5 *er*); IR (film): 3060, 3027, 2924, 2852, 1956, 1722, 1675, 1631, 1595, 1494, 1447, 1364, 1210, 1048, 973, 911 cm^{-1} ; ^1H NMR (600 MHz, $\text{Chloroform-}d$) δ 7.37 – 7.32 (m, 2H), 7.32 – 7.26 (m, 5H), 7.26 – 7.23 (m, 5H), 7.12 – 7.02 (m, 3H), 6.67 (s, 1H), 4.03 (d, $J = 14.8$ Hz, 1H), 3.94 – 3.84 (m, 2H), 3.82 (s, 1H), 3.62 (s, 2H), 2.58 – 2.44 (m, 4H), 2.43 – 2.35 (m, 2H); ^{13}C NMR (151 MHz, CDCl_3) δ 144.06, 141.11, 137.80, 133.17, 128.50, 128.38, 128.29, 127.82, 127.35, 125.40, 123.97, 122.46, 104.66, 99.98, 85.53, 77.37, 77.21, 77.00, 76.79, 59.35, 53.32, 47.16, 42.89, 42.85, 34.64; HRMS (ESI) calcd for $\text{C}_{28}\text{H}_{29}^{81}\text{BrNO}$ m/z $[\text{M}+\text{H}]^+$: 476.1407; found: 476.1394.

(E) General two-step procedure for the oxidation of alcohol to acid

To a stirred solution of the alcohol (0.5 mmol, 1.0 eq) in CH₂Cl₂ (4.0 mL) was added 100mg of 4Å molecular sieves, followed by PCC (0.75 mmol, 1.5 eq). The reaction was traced using TLC. After the disappearance of the starting material, the reaction was filtered over a plug of silica. The filtrate was concentrated under reduced pressure to give the aldehyde.

The aldehyde was dissolved in *t*-BuOH (3.0 mL). This was followed by the addition of 2-methyl-2-butene (9.0 mmol, 18.0 eq), water (3.0 mL), NaH₂PO₄ (4.0 mmol, 8.0 eq) and NaClO₂ (2.0 mmol, 2.0 eq). The mixture was allowed to stir for 2 hours before it is quenched with brine and extracted with CHCl₃. (3 x 5mL) The combined organic extracts was dried over MgSO₄, filtered and concentrated under reduced pressure. The residue was purified using flash column chromatography (hexane/EtOAc 1:1) to give the acid.

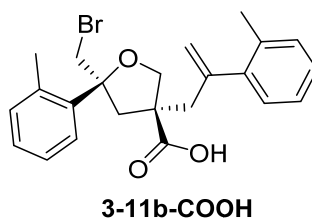
(3*R*,5*R*)-5-(bromomethyl)-5-(*o*-tolyl)-3-(2-(*o*-tolyl)allyl)tetrahydrofuran-3-carbaldehyde (3-11b-CHO)



3-11b-CHO

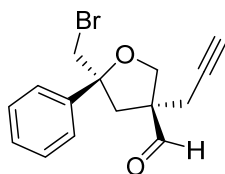
Colourless oil; $[\alpha]_D^{26} -8.0$ (*c* 10.0, CHCl₃, 95:5 *er*); IR (film): 2926, 1728, 1636, 1488, 1218, 1063, 910 cm⁻¹; ¹H NMR (600 MHz, CDCl₃) δ 9.07 (s, 1H), 7.45 (dd, *J* = 7.6, 1.8 Hz, 1H), 7.19 – 7.10 (m, 6H), 7.02 (dd, *J* = 7.5, 1.4 Hz, 1H), 5.21 (d, *J* = 1.3 Hz, 1H), 5.00 (d, *J* = 1.5 Hz, 1H), 4.11 (d, *J* = 9.3 Hz, 1H), 3.89 (d, *J* = 9.2 Hz, 1H), 3.73 (d, *J* = 11.3 Hz, 1H), 3.66 (d, *J* = 11.3 Hz, 1H), 2.99 (dd, *J* = 4.4, 1.2 Hz, 2H), 2.77 (d, *J* = 13.3 Hz, 1H), 2.46 (d, *J* = 13.3 Hz, 1H), 2.32 (s, 3H), 2.29 (s, 3H); ¹³C NMR (151 MHz, CDCl₃) δ 201.97, 145.34, 141.32, 139.88, 134.87, 133.58, 132.27, 130.52, 128.57, 127.94, 127.64, 126.45, 125.98, 125.78, 118.68, 86.14, 72.42, 59.27, 42.93, 42.46, 40.88, 21.37, 19.88; HRMS (ESI) calcd for C₂₃H₂₅BrO₂Na *m/z* [M + Na]⁺: 435.0930; found: 435.0938.

(3*R*,5*R*)-5-(bromomethyl)-5-(*o*-tolyl)-3-(2-(*o*-tolyl)allyl)tetrahydrofuran-3-carboxylic acid (3-11b-COOH)



Colourless oil; $[\alpha]_D^{26} +7.1$ (*c* 10.0, CHCl₃, 95:5 *er*); IR (film): 2927, 1704, 1635, 1454, 1276, 1260, 1054, 918 cm⁻¹; ¹H NMR (600 MHz, CDCl₃) δ 7.54 – 7.49 (m, 1H), 7.12 (d, *J* = 2.9 Hz, 3H), 7.04 – 6.96 (m, 4H), 5.24 (d, *J* = 1.4 Hz, 1H), 4.98 (d, *J* = 1.7 Hz, 1H), 4.01 (d, *J* = 9.2 Hz, 1H), 3.81 (d, *J* = 9.2 Hz, 1H), 3.69 – 3.63 (m, 2H), 3.05 – 2.95 (m, 2H), 2.91 (d, *J* = 13.5 Hz, 1H), 2.45 (d, *J* = 13.5 Hz, 1H), 2.33 (s, 3H), 2.27 (s, 3H); ¹³C NMR (151 MHz, CDCl₃) δ 178.45, 145.65, 141.35, 140.05, 134.95, 133.92, 132.25, 130.11, 128.90, 127.85, 127.27, 126.30, 125.88, 125.32, 118.33, 86.14, 73.73, 55.06, 44.62, 43.22, 40.72, 21.35, 19.87; HRMS (ESI) calcd for C₂₃H₂₅BrO₃Na *m/z* [M + Na]⁺: 451.0879; found: 451.0863.

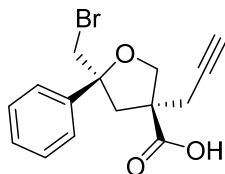
(3R,5R)-5-(bromomethyl)-5-phenyl-3-(prop-2-yn-1-yl)tetrahydrofuran-3-carbaldehyde (3-14e-CHO)



3-14e-CHO

Colourless oil; $[\alpha]_D^{26} +19$ (*c* 3.0, CHCl₃, 95:5 *er*); IR (film): 3289, 3006, 2990, 1727, 1447, 1275, 1260, 1054 cm⁻¹; ¹H NMR (600 MHz, CDCl₃) δ 9.32 (s, 1H), 7.40 – 7.35 (m, 4H), 7.30 (d, *J* = 7.1 Hz, 1H), 4.21 (d, *J* = 9.5 Hz, 1H), 4.10 (d, *J* = 9.5 Hz, 1H), 3.67 (s, 2H), 2.80 (d, *J* = 13.6 Hz, 1H), 2.71 – 2.66 (m, 2H), 2.62 (dd, *J* = 16.9, 2.7 Hz, 1H); ¹³C NMR (151 MHz, CDCl₃) δ 200.57, 141.93, 128.63, 128.06, 125.52, 86.45, 79.43, 71.80, 71.16, 58.09, 42.76, 41.46, 22.65; HRMS (ESI) calcd for C₁₅H₁₆BrO₂ *m/z* [M + H]⁺: 307.0328; found: 307.0328.

(3R,5R)-5-(bromomethyl)-5-phenyl-3-(prop-2-yn-1-yl)tetrahydrofuran-3-carboxylic acid (3-14e-COOH)



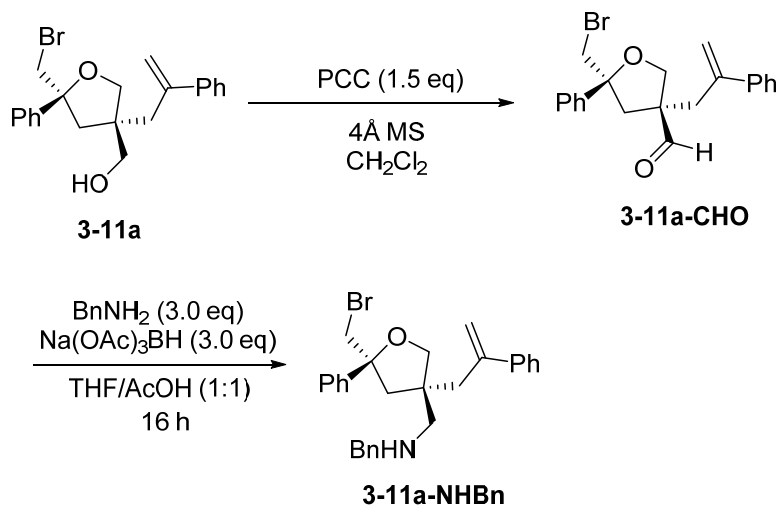
3-14e-COOH

Colourless oil; $[\alpha]_D^{26} +22$ (*c* 3.0, CHCl₃, 95:5 *er*); IR (film): 3293, 3006, 2989, 1709, 1623, 1448, 1276, 1261, 1051 cm⁻¹; ¹H NMR (600 MHz, CDCl₃) δ 7.38

(dd, $J = 8.4, 1.3$ Hz, 2H), 7.31 (dd, $J = 8.5, 7.0$ Hz, 2H), 7.25 – 7.20 (m, 1H), 4.14 (d, $J = 9.3$ Hz, 1H), 4.00 (d, $J = 9.3$ Hz, 1H), 3.65 – 3.56 (m, 2H), 2.95 (d, $J = 13.5$ Hz, 1H), 2.77 (dd, $J = 2.7, 1.7$ Hz, 2H), 2.64 (d, $J = 13.6$ Hz, 1H), 2.06 (t, $J = 2.6$ Hz, 1H); ^{13}C NMR (151 MHz, CDCl_3) δ 178.47, 142.10, 128.40, 127.83, 125.57, 86.20, 79.55, 73.36, 71.06, 54.40, 43.54, 41.60, 26.29; HRMS (ESI) calcd for $\text{C}_{15}\text{H}_{15}\text{BrO}_3\text{Na}$ m/z $[\text{M} + \text{Na}]^+$: 345.0097; found: 345.0090.

(F) Synthesis of Compound 3-11a-NHBn and Compound 3-24

N-benzyl-1-((3*S*,5*R*)-5-(bromomethyl)-5-phenyl-3-(2-phenylallyl)tetrahydrofuran-3-yl)methanamine (**3-11a-NHBn**)

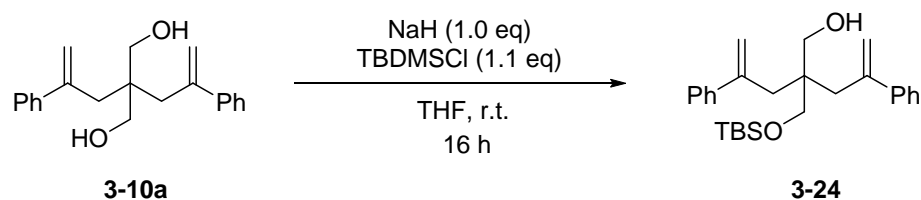


Using the general procedure in (E), **3-11a** (0.5 mmol, 1.0 eq) was first oxidized to the aldehyde **3-11a-CHO**. The aldehyde was dissolved in THF/AcOH (1:1) (4.0 mL) followed by the addition of benzylamine (1.5 mmol, 3.0 eq) and sodium

triacetoxyborohydride (1.5 mmol, 3.0 eq). The reaction was allowed to stir overnight. The reaction mixture was quenched, made alkaline with aqueous NaOH and extracted with CH₂Cl₂. (3 x 5mL) The combined organic extracts was dried over MgSO₄, filtered and concentrated under reduced pressure. The residue was purified using flash column chromatography (hexane/EtOAc 1:1) to give the amine **3-11a-NHBn**.

Colourless oil; $[\alpha]_D^{26} -6$ (*c* 1.0, CHCl₃, 95:5 *er*); IR (film): 3025, 2925, 1600, 1493, 1447, 1226, 1109, 1050, 1028, 905 cm⁻¹; ¹H NMR (600 MHz, CDCl₃) δ 7.35 – 7.27 (m, 9H), 7.25 – 7.18 (m, 4H), 6.98 – 6.90 (m, 2H), 5.23 (d, *J* = 1.7 Hz, 1H), 5.16 (s, 1H), 3.81 (d, *J* = 8.8 Hz, 1H), 3.58 (d, *J* = 8.8 Hz, 1H), 3.54 (s, 2H), 3.16 (s, 2H), 2.81 (s, 2H), 2.36 (d, *J* = 13.1 Hz, 1H), 2.29 (d, *J* = 13.1 Hz, 1H), 2.16 (d, *J* = 12.2 Hz, 1H), 2.05 (d, *J* = 12.2 Hz, 1H); ¹³C NMR (151 MHz, CDCl₃) δ 146.77, 144.25, 142.67, 128.41, 128.17, 128.16, 127.86, 127.54, 127.22, 126.71, 126.49, 125.46, 117.11, 85.00, 76.55, 54.11, 52.92, 49.21, 45.09, 43.34, 40.66; HRMS (ESI) calcd for C₂₈H₃₁BrNO *m/z* [M + H]⁺: 478.1567; found: 478.1549.

2-(((tert-butyldimethylsilyl)oxy)methyl)-4-phenyl-2- (2-phenylallyl) pent-4-en-1-ol (**3-24**)



To a stirred solution of diol **3-10a** (1.0 mmol, 1.0 eq) in THF (5.0 mL) was added NaH (1.0 mmol, 1.0 eq) under argon conditions. After stirring for 30 minutes, *tert*-butyldimethylsilyl chloride (TBDMSCl) (1.0 mmol, 1.0 eq) was added. The reaction was allowed to stir for 16 h before it was quenched with saturated NH_4Cl and extracted with CH_2Cl_2 . (3 x 5mL) The combined organic extracts was dried over MgSO_4 , filtered and concentrated under reduced pressure. The residue was purified using flash column chromatography (hexane/EtOAc 4:1) to give the **3-24**.

Colourless oil; IR (film): 3448, 2953, 2857, 1623, 1471, 1251, 1090, 1032, 902 cm^{-1} ; ^1H NMR (600 MHz, CDCl_3) δ 7.34 – 7.28 (m, 8H), 7.26 – 7.22 (m, 2H), 5.24 (d, $J = 2.0$ Hz, 2H), 5.09 – 5.06 (m, 2H), 3.25 (d, $J = 6.6$ Hz, 4H), 0.84 (s, 9H), -0.13 (s, 6H); ^{13}C NMR (151 MHz, CDCl_3) δ 146.20, 143.40, 128.31, 127.32, 126.37, 117.56, 68.01, 67.86, 43.88, 38.24, 25.88, 18.11, -5.86; HRMS (ESI) calcd for $\text{C}_{27}\text{H}_{38}\text{O}_2\text{SiNa}$ m/z $[\text{M} + \text{Na}]^+$: 445.2533; found: 445.2533.

3.5 References

1. (a) Rios, R. *Chem. Soc. Rev.* **2012**, *41*, 1060; (b) Ding, K., Han, Z., Wang, Z., *Chem. Asian J.* **2009**, *4*, 32; (c) Franz, A. K., Hanhan, N. V., Ball-Jones, N.R., *ACS Catal.* **2013**, *3*, 540; (d) Yang, Z., Hao, L., Yin, B., She, M., Obst, M., Kappler, A., Li, J., *Org. Lett.* **2013**, *15*, 4334; (e) Chen, X. Q., Pradhan, T., Wang, F., Kim, J. S., Yoon, J., *Chem. Rev.* **2012**, *112*, 1910; (f) Yang, Y. M., Zhao, Q., Feng, W., Li, F. Y., *Chem. Rev.* **2013**, *113*, 192; (g) Ko, S., Yang, Y., Tae, J., Shin, I., *J. Am. Chem. Soc.* **2006**, *128*, 14150; (h) Yang, K., Zhou, Z. G., Huang, K. W., Yu, M. X., Li, F. Y., Yi, T., Huang, C. H., *Org. Lett.* **2007**, *9*, 4729; (i) Du, J. J., Fan, J. L., Peng, X. J., Sun, P. P., Wang, J. Y., Li, H. L., Sun, S. G., *Org. Lett.* **2010**, *12*, 476.
2. (a) Galloway, W. R. J. D., Isidro-Llobet, A., Spring, D. R., *Nat. Commun.* **2010**, *1*, 80; (b) Singh, G. S., Desta, Z. Y., *Chem. Rev.* **2012**, *112*, 6104; (c) Jenkins, I. D., Lacrampe, F., Ripper, J., Alcaraz, L., Le, P. V., Nikolakopoulos, G., de Almeida Leone, P., White, R. H., Quinn, R. J., *J. Org. Chem.* **2009**, *74*, 1304; (d) Painter, T. O., Bunn, J. R., Schoenen, F. J., Douglas, J. T., Day, V. W., Santini, C., *J. Org. Chem.* **2013**, *78*, 3720.
3. (a) Burkhard, J. A., Wuitschik, G., Rogers-Evans, M., Müller, K., Carreira, E. M., *Angew. Chem. Int. Ed.* **2010**, *49*, 9052; (b) Burkhard, J. A., Guérot, C., Knust, H., Carreira, E. M., *Org. Lett.* **2012**, *14*, 66; (c) Li, D. B., Rogers-Evans, M., Carreira, E. M., *Org. Lett.* **2011**, *13*, 6134; (d) Guérot,

- C., Tchitchanov, B. H., Knust, H., Carreira, E. M., *Org. Lett.* **2011**, *13*, 780; (e) Burkhard, J. A., Wagner, B., Fischer, H., Schuler, F., Müller, K., Carreira, E. M., *Angew. Chem. Int. Ed.* **2010**, *49*, 3524; (f) Burkhard, J. A., Guérot, C., Knust, H., Rogers-Evans, M., Carreira, E. M., *Org. Lett.* **2010**, *12*, 1944; (g) Burkhard, J. A., Carreira, E. M., *Org. Lett.* **2008**, *10*, 3525; (h) Wuitschik, G., Rogers-Evans, M., Buckl, A., Bernasconi, M., Märki, M., Godel, T., Fischer, H., Wagner, B., Parrilla, I., Schuler, F., Schneider, J., Alker, A., Schweizer, W. B., Müller, K., Carreira, E. M., *Angew. Chem. Int. Ed.* **2008**, *47*, 4512.
4. (a) Ranganathan, S., Muraleedharan, K. M., Vaish, N. K., Jayaraman, N., *Tetrahedron* **2004**, *60*, 5273; (b) French, A. N., Bissmire, S., Wirth, T., *Chem. Soc. Rev.* **2004**, *33*, 354; (c) Rodríguez, F., Fañanás, F. J., In *Handbook of Cyclization Reactions*; S. Ma Ed; Wiley-VCH: New York, **2010**; Vol. 4, pp. 951–990; (d) Gilman, H., *Organic Chemistry: An Advanced Treatise*, Wiley, New York, **1938**, Vol. 1, pp. 36–43.
5. For reviews, see: (a) Chen, G. F., Ma, S., *Angew. Chem. Int. Ed.* **2010**, *49*, 8306; (b) Castellanos, A., Fletcher, S. P., *Chem. Eur. J.* **2011**, *17*, 5766; (c) Tan, C. K., Zhou, L., Yeung, Y.-Y., *Synlett* **2011**, 1335; (d) Snyder, S. A., Treitler, D. S., Brucks, A. P., *Aldrichimica Acta* **2011**, *44*, 27; (e) Hennecke, U., *Chem. Asian. J.* **2012**, *7*, 456; (f) Denmark, S. E., Kuester, W. E., Burk, M. T., *Angew. Chem. Int. Ed.* **2012**, *51*, 10938; (g) Murai, K., Fujioka, H., *Heterocycles* **2013**, *87*, 763; (h) Tan, C. K., Yeung, Y.-Y., *Chem. Commun.* **2013**, *49*, 7985.

6. (a) Gordon, G. W., *J. Nat. Prod.* **1992**, *55*, 1353; (b) Gordon, G. W., *Chem. Soc. Rev.* **1999**, *28*, 335; (c) Gordon, G. W., *Acc. Chem. Res.* **1999**, *31*, 141; (d) Gordon, G. W., *J. Chem. Edu.* **2004**, *81*, 1441; (e) Wang, B.-G., Gloer, J. B., Ji, N.-Y., Zhao, J.-C., *Chem. Rev.* **2013**, *113*, 3632.
7. (a) Brown, R. S., Nagorski, R. W., Bennet, A. J., McClung, R. E. D., Aarts, G. H. M., Klobukowski, M., McDonald, R., Santarsiero, B. D., *J. Am. Chem. Soc.* **1994**, *116*, 2448; (b) Neverov, A. A., Brown, R. S., *J. Org. Chem.* **1996**, *61*, 962; (c) Brown, R. S., *Acc. Chem. Res.* **1997**, *30*, 131; (d) Denmark, S. E., Burk, M. T., Hoover, A. J., *J. Am. Chem. Soc.* **2010**, *132*, 1232.
8. (a) Zhou, L., Tan, C. K., Jiang, X., Chen, F., Yeung, Y.-Y., *J. Am. Chem. Soc.* **2010**, *132*, 15474; (b) Tan, C. K., Zhou, L., Yeung, Y.-Y., *Org. Lett.* **2011**, *13*, 2738; (c) Zhou, L., Chen, J., Tan, C. K., Yeung, Y.-Y., *J. Am. Chem. Soc.* **2011**, *133*, 9164; (d) Tan, C. K., Chen, F., Yeung, Y.-Y., *Tetrahedron Lett.* **2011**, *52*, 4892; (e) Chen, J., Zhou, L., Tan, C. K., Yeung, Y.-Y., *J. Org. Chem.* **2012**, *77*, 999; (f) Chen, J., Zhou, L., Yeung, Y.-Y., *Org. Biomol. Chem.* **2012**, *10*, 3808; (g) Tan, C. K., Le, C., Yeung, Y.-Y., *Chem. Commun.* **2012**, *48*, 5793; (h) Jiang, X., Tan, C. K., Zhou, L., Yeung, Y.-Y., *Angew. Chem. Int. Ed.* **2012**, *51*, 7771; (i) Cheng, Y. A., Chen, T., Tan, C. K., Heng, J. J., Yeung, Y.-Y., *J. Am. Chem. Soc.* **2012**, *134*, 16492; (j) Zhou, L., Tay, D. W., Chen, J., Leung, G. Y. C., Yeung, Y.-Y., *Chem Commun.* **2013**, *49*, 4412; (k) Zhao, Y., Jiang, X., Yeung, Y.-

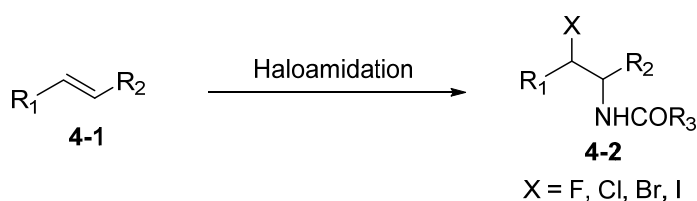
- Y., *Angew. Chem. Int. Ed.* **2013**, 52, 8597; (l) Tay, D. W., Tsoi, I. T., Er, J. C., Leung, G. Y. C., Yeung, Y.-Y., *Org. Lett.* **2013**, 15, 1310.
9. (a) Berkessel, A., Vormittag, S. S., Schlörer, N. E., Neudörfl, J.-M., *J. Org. Chem.* **2012**, 77, 10145; (b) Seebach, D., Beck, A. K., Heckel, A., *Angew. Chem., Int. Ed.* **2001**, 40, 92; (c) Beck, A. K., Bastani, B., Plattner, D. A., Petter, W., Seebach, D., Braunschweiler, H., Gysi, P., La Vecchia, L., *Chimia* **1991**, 45, 238; (d) Berkessel, A., Etzenbach-Effers, K., In *Hydrogen Bonding in Organic Synthesis*; Pihko, P., Ed.; Wiley-VCH: Weinheim, Germany, **2009**; pp 15–42; (e) Berkessel, A., Etzenbach-Effers, K., *Top. Curr. Chem.* **2010**, 291, 1; (f) Christ, P., Lindsay, A. G., Vormittag, S. S., Neudörfl, J.-M., Berkessel, A., O'Donoghue, A. C., *Chem. Eur. J.* **2011**, 17, 8524.

Chapter 4

*Lewis Basic Selenium Catalyzed
Chloroamidation of Olefins Using
Nitriles as Amide Source*

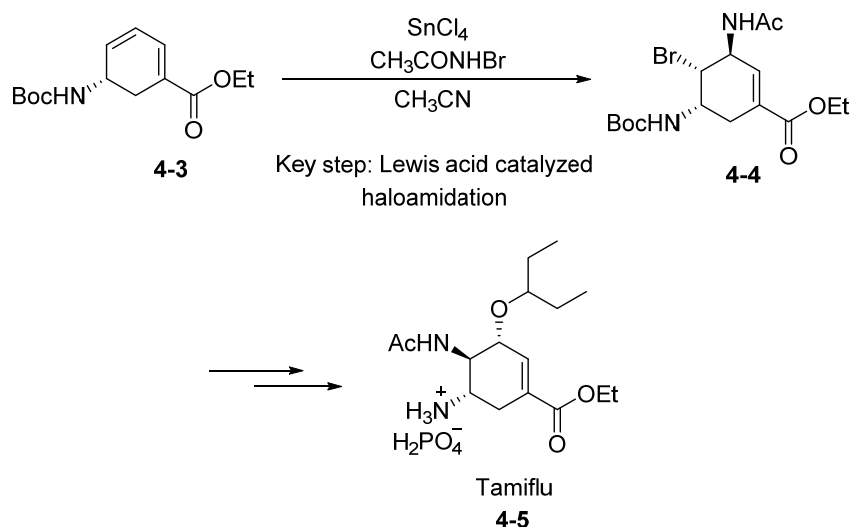
4.1 Introduction

Haloamidation of an olefin is a practical and useful synthetic transformation for synthetic chemists. The resulting product, a vicinal haloamide, is an important synthetic intermediate, with the halogen offering a handle for subsequent manipulation (Scheme 4.1).¹



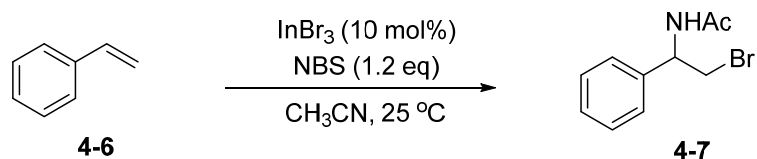
Scheme 4.1 General scheme for haloamidation of olefins.

In the literature, there are several methods to install a *trans*-1,2-haloamide/amine functionality directly from an olefin.² A common approach involves the use of a nitrogen nucleophile to open a cyclic halonium ion intermediate derived from an olefin. In order to achieve the desired products with reasonable reaction efficiency, Lewis acids are usually employed to activate the stoichiometric halogen source in the olefin halogenation process. For example, Corey and co-workers reported the use of strongly Lewis acidic catalysts, such as SnCl_4 and $\text{BF}_3\cdot\text{OEt}_2$, in the bromoamidation of olefins.³ The transformation was an important step towards the synthesis of the anti-fluenza medicine, Oseltamivir (Tamiflu®) **4-5**, in which NBS was used as the halogen source and acetonitrile as the nitrogen source for the process (Scheme 4.2).



Scheme 4.2 Lewis acid catalyzed haloamidation in the synthesis of Tamiflu®).

Subsequently, the Yadav group reported a similar procedure using InBr_3 as the catalyst in the haloamidation (Scheme 4.3).⁴ The substrate scope, however, is limited to vinyl arenes only.



Scheme 4.3 InBr_3 catalyzed bromoamidation.

The harsh Lewis acidic conditions, lack of generality and limited substrate scope prompted us to initiate a search for new catalysts to achieve this synthetic transformation. Since the Lewis acids utilized were for the purpose of activating the halogen source, we reckoned that the search for new catalysts may begin from halogen activators. In our recent publications, we reported the use of Lewis basic sulfur for the activation of halogenating reagents in various bromocyclization

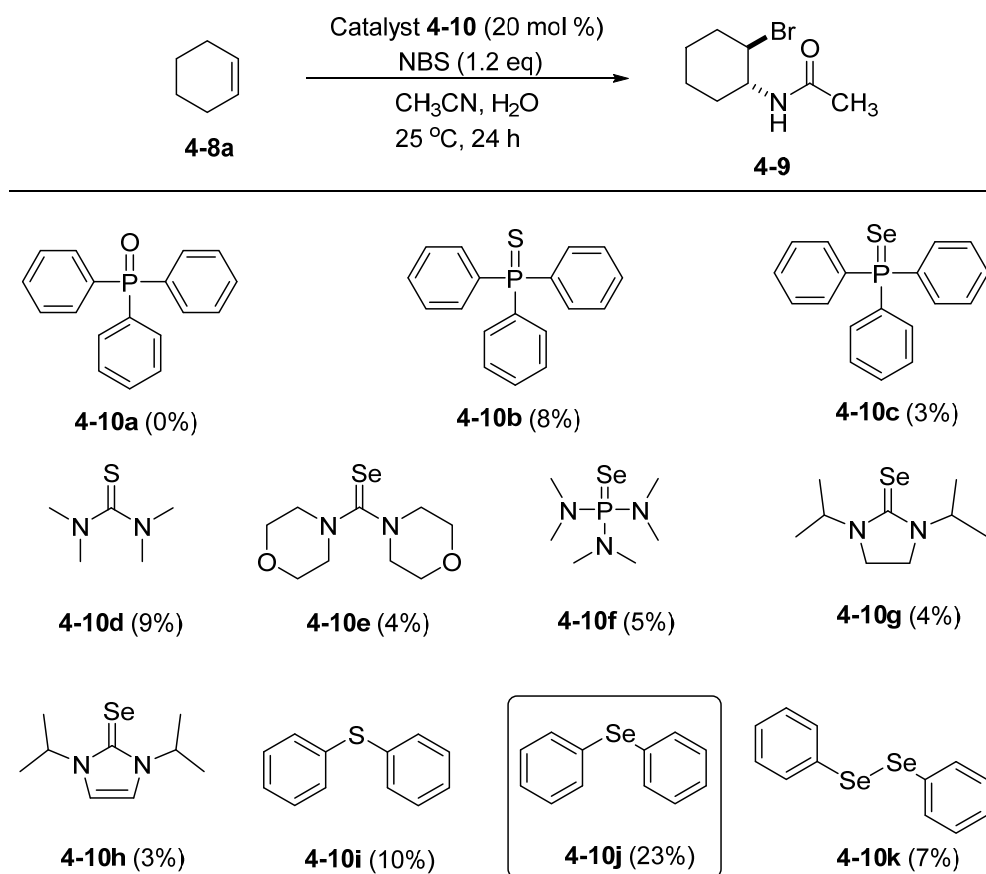
processes.⁵ We rationalized that a similar Lewis basic system may be used to catalyze the haloamidation process, which can offer milder reaction conditions.

Herein, we disclose a facile, mild, and efficient chloroamidation of olefins using the commercially available and Lewis basic diphenylselenide as the catalyst and *N*-chlorosuccinimide (NCS) and acetonitrile as the halogen and nitrogen source, respectively. This method was found to be applicable to a wide range of substrates, which makes it a good complement to the existing strategies, especially for the haloamidation of acid-sensitive compounds.

4.2 Results and Discussion

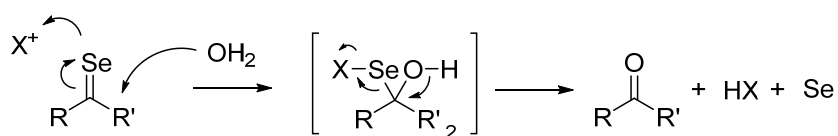
4.2.1 Catalyst Screening

Cyclohexene **4-8a** was used in our initial study and various Lewis basic chalcogen-containing catalysts **4-10** were examined (Scheme 4.4). Triphenylphosphine oxide **4-10a** was found to be inactive in catalyzing the haloamidation reaction. For the catalysts **4-10b–h** which contain either a C=X or a P=X (X = S, Se) system, very low reaction efficiency was observed. In fact, these catalysts were unstable in the reaction system; elemental sulfur or selenium evolved gradually during the reaction, which could be attributed to the hydrolytic decomposition of the catalysts in the presence of water and a halogen source (Scheme 4.5).^{5k}



^a Reactions were carried out with cyclohexene **4-8a** (0.25 mmol), catalyst **4-10** (0.05 mmol), NBS (0.25 mmol), and water (0.25 mmol) in MeCN (2.5 mL) at 25 °C. The yields indicated in the parentheses were the isolated yields of **4-9a**.

Scheme 4.4 Lewis base catalyst screening for bromoamidation.



Scheme 4.5 Hydrolytic decomposition of sp^2 -type catalysts.

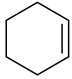
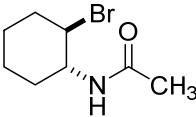
This result prompted further screening on the diaryl sulfur and selenium catalysts, which led to the discovery that diphenyl selenide (**4-10j**) was exceptionally active in catalyzing this type of reaction.

4.2.2 Reaction Conditions Optimization

After identifying a suitable catalyst, other parameters were optimized. It was observed that water is an essential component in the reaction as a controlled reaction carried out in moisture-free conditions resulted in almost no product formed (Table 4.1, entry 1). The amount of water did not significantly affect the reaction and the yield was unchanged upon the addition of up to 10 equivalents of water (Table 4.1, entries 2–5). In addition, no formation of halohydrins was observed despite the drastic increase in the concentration of water.

The concentration of the reaction, however, did appreciably affect the reaction yield and an optimum concentration was found to be at 0.4 M (Table 4.1, entries 6–12).

Table 4.1 Reaction conditions optimization.

<div style="display: flex; align-items: center; justify-content: center;"> <div style="text-align: center; margin-right: 20px;">  <p>4-8a</p> </div> <div style="text-align: center; margin-right: 20px;"> $\xrightarrow[\text{CH}_3\text{CN, H}_2\text{O}]{\text{4-10j (20 mol \%), NBS}}$ 25 °C, 24 h </div> <div style="text-align: center; margin-left: 20px;">  <p>4-9a</p> </div> </div>			
Entry	H ₂ O (equiv)	Concentration (M)	Isolated yield (%)
1	0	0.10	2
2	1.2	0.10	23
3	3.0	0.10	23
4	5	0.10	22
5	10	0.10	24
6	1.2	0.65	30
7	1.2	0.60	28
8	1.2	0.50	35
9	1.2	0.40	36
10	1.2	0.30	35
11	1.2	0.20	28
12	1.2	0.15	26

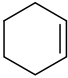
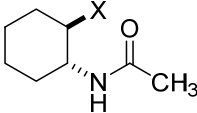
^a Reactions were carried out with cyclohexene (**4-11a**) (0.25 mmol), NBS (0.25 mmol), **4-10j** (0.05 mmol), and water at 25 °C. ^b Yields were calculated based on the ¹H NMR analysis of the crude reaction mixture using hexamethylbenzene as the internal standard.

4.2.3 Effect of Halogen Source

While investigating various halogenating sources, it was found that brominating reagents including NBP, *N*-bromoacetamide (NBA), 2,4,4,6-tetrabromo-2,5-hexadienone (TABCO), and DBH gave similar yields to that of NBS (Table 4.2, entries 1–5). Interestingly, a 52% yield of the chlorinated product was obtained when NCS was used (Table 4.2, entry 7), but *N*-iodosuccinimide

(NIS) did not result in any desired product (Table 4.2, entry 8). Finally, it was found that the yields could be further enhanced by increasing the amount of halogenating reagents (Table 4.2, entries 9–10).

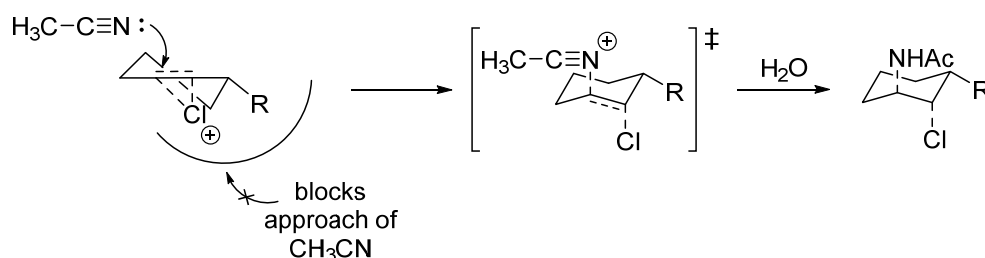
Table 4.2 Effect of halogenating reagents on reaction yields.

<div style="display: flex; align-items: center; justify-content: space-around;"> <div style="text-align: center;">  <p>4-8a</p> </div> <div style="text-align: center;"> <p>4-10j (20 mol %), Halogen source</p> <p>CH₃CN, H₂O 25 °C, 24 h</p> </div> <div style="text-align: center;">  <div style="display: flex; flex-direction: column; align-items: center;"> <p>X = Br 4-9</p> <p>Cl 4-11a</p> <p>I 4-12</p> </div> </div> </div>			
Entry ^a	Halogen Source (equiv)	Product	Yield (%) ^b
1	NBS (1.0)	4-9	36
2	NBP (1.0)	4-9	35
3	NBA (1.0)	4-9	30
4	TABCO (1.0)	4-9	31
5	DBH (1.0)	4-9	31
6	DCH (1.0)	4-11a	34
7	NCS (1.0)	4-11a	52
8	NIS (1.0)	4-12	0
9	NBS (2.0)	4-9	56
10	NCS (2.0)	4-11a	85
11	NBS (3.0)	4-9	59
12	NCS (3.0)	4-11a	84

^a Reactions were carried out with cyclohexene (**4-8a**) (0.25 mmol), **4-10j** (0.05 mmol) in MeCN (0.65 mL) at 25 °C. ^b Yields were calculated based on the ¹H NMR analysis of the crude reaction mixture using hexamethylbenzene as the internal standard.

4.2.4 Substrate Scope

Upon identifying a suitable reaction system, we continued to examine the substrate scope and the results are tabulated in Table 4.3. The reactions were found to proceed efficiently giving good yields with both alkyl olefins and vinyl arenes. For the substituted cyclohexenes **4-8b-e**, excellent diastereo- and regioselectivity were observed (Table 4.3, entries 1–4). The high diastereoselectivity could be explained by the proposed mechanism depicted in Scheme 4.6, which shows that the nucleophilic nitrile may be approaching from the less sterically hindered face of the halonium intermediate.



Scheme 4.6 Possible transition state of chloroamidation.

Markovnikov-type products were obtained for aryl olefins **4-8f-h** (Table 4.3, entries 5–7). However, anti-Markovnikov product **4-11i** was achieved (86 % yield) when using **4-8i** as the substrate (Table 4.3, entry 8). The selectivity can be rationalized by the stabilization effect of the carbocation at the terminal carbon by the Si–C σ -bond.⁶

Table 4.3 Haloamidation of olefins.

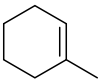
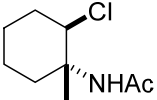
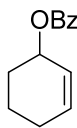
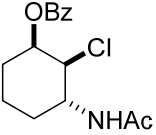
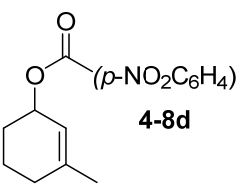
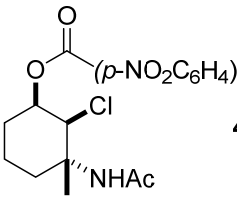
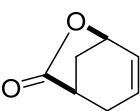
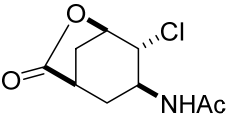
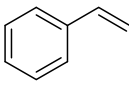
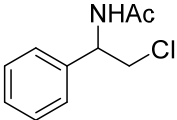
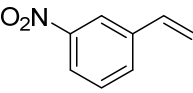
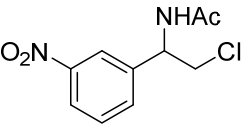
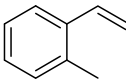
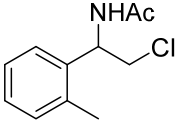

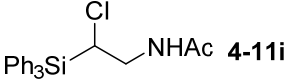
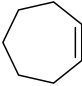
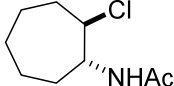
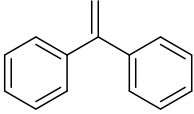
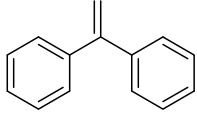
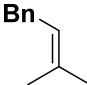
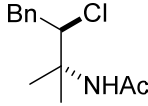
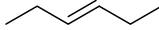
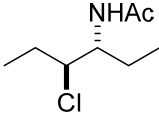
$ \begin{array}{c} \text{R}^1 \\ \diagup \\ \text{C} = \text{C} \\ \diagdown \quad \diagup \\ \text{R}^2 \quad \text{R}^3 \\ \textbf{4-8} \end{array} \xrightarrow[\text{H}_2\text{O, MeCN}]{\text{NCS, 4-10j (20 mol \%)}} \begin{array}{c} \text{R}^1 \text{---} \text{C} \text{---} \text{Cl} \\ \\ \text{R}^2 \text{---} \text{C} \text{---} \text{NHAc} \\ \\ \text{R}^3 \\ \textbf{4-11} \end{array} $ 25 °C, 18 h			
Entry ^a	Substrate	Product	Yield (%) ^b
1	 4-8b	 4-11b	65
2	 4-8c	 4-11c	76
3	 4-8d	 4-11d	55
4	 4-8e	 4-11e	79
5	 4-8f	 4-11f	65
6	 4-8g	 4-11g	89

Table 4.3 Haloamidation of olefins. (cont'd)

Entry ^a	Substrate	Product	Yield (%) ^b
7	 4-8h	 4-11h	50
8	 4-8i	 4-11i	86
9	 4-8j	 4-11j	7
10	 4-8k	 4-11k	0
11	 4-8l	 4-11l	0
12	 4-8m	 4-11m	16

^a Reactions were carried out with olefin **4-8** (0.25 mmol), NCS (0.50 mmol), and **4-10j** (0.05 mmol) in MeCN (0.65 mL) at 25 °C for 18 h.

^b Isolated yield.

220

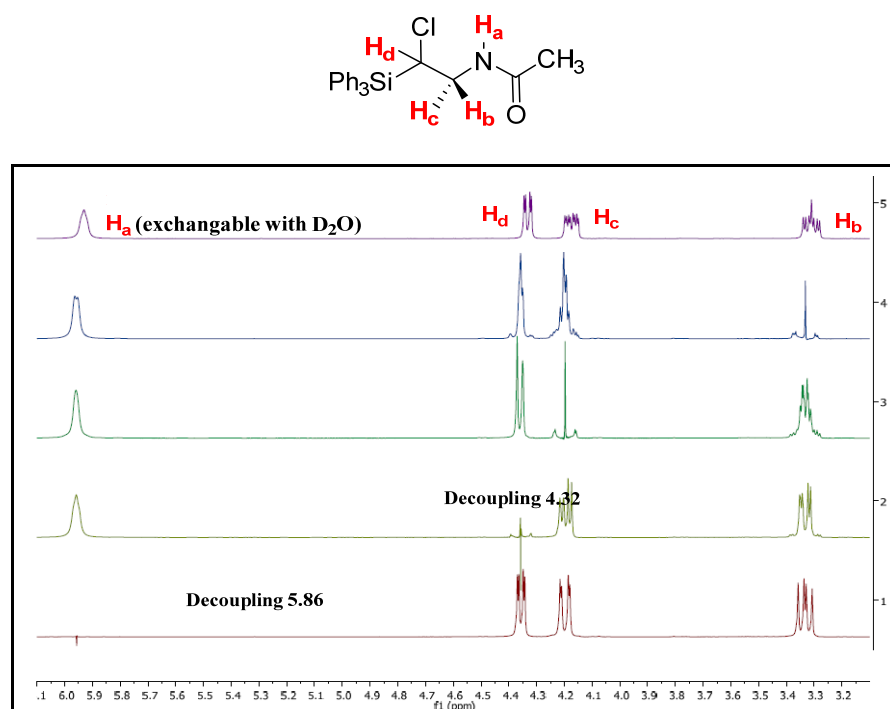


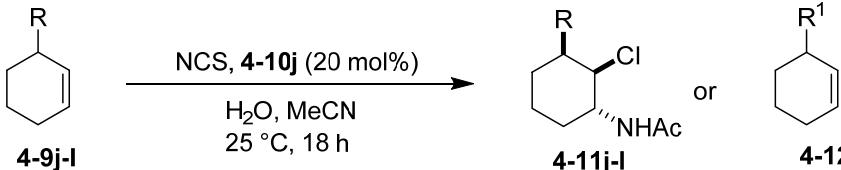
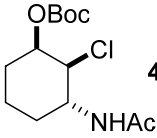
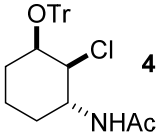
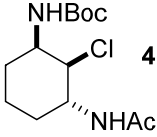
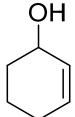
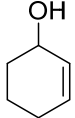
Figure 4.2 Proton decoupling experiments for anti-markovnikov product **4-11i**.

Low yield (7% yield) was observed for cycloheptene **4-8j** with most of the starting material recovered. No products were observed for both 1,1-diphenylethylene **4-8k** as well as the tri-substituted olefin **4-8l**. Similarly, the starting materials were observed to be unreacted from the crude ^1H NMR. We postulate that this is due to the relatively bulkier substituents on the alkenes which hindered the nucleophilic attack of the nitrile. Next, (*E*)-hex-3-ene **4-8m** also resulted in poor yield (16% yield) when subjected to the same reaction condition. This is probably due to the volatile starting materials which caused the concentration of it in the reaction mixture to be lower than expected.

4.2.5 Haloamidation of Acid Labile Substrates

Besides the wide substrate scope, it is also important to note that the reaction can accommodate acid sensitive functional groups. Thus, this Lewis base catalyzed haloamidation can be considered as a complementary method to the corresponding Lewis acid protocols.³⁻⁴ Some examples are shown in Table 4.4. Substrates **4-9j**–**4-9l** gave the desired products smoothly using catalyst **4-10j** (Table 4.4, entries 1–3), this was in comparison to the deprotected precursors (Table 4.4, entries 4 and 6) and the complex mixture obtained (Table 5.4, entry 5) when the respective Lewis acids were employed as catalysts.

Table 4.4 Haloamidation of acid labile substrates

				
Entry ^a	R	Catalyst	Product	Yield (%) ^b
1	OBoc	4-10j	 4-11j	76
2 ^c	OTr	4-10j	 4-11k	70
3	NHBoc	4-10j	 4-11l	40
4	OBoc	InBr ₃ or InCl ₃	 4-12a	90
5	OBoc	BF ₃ ·Et ₂ O or SnCl ₄	complex mixture	-
6	OTr	BF ₃ ·Et ₂ O or SnCl ₄	 4-12a	90
7	NHBoc	SnCl ₄	no reaction	-

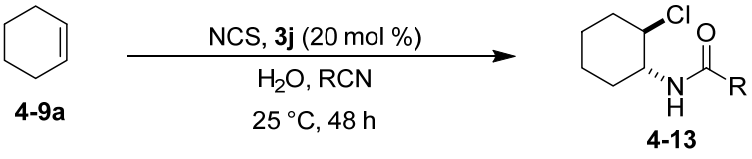
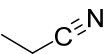
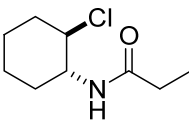
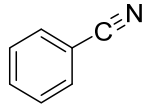
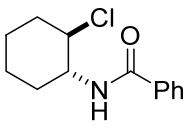
^a Reactions were carried out with olefin **4-9** (0.25 mmol), NCS (0.50 mmol), and **4-10j** (0.05 mmol) in MeCN (0.65 mL) at 25 °C for 18 h. ^b Isolated yield.

^c The reaction time was 3 days.

4.2.6 Haloamidation Using Different Nitriles

To further illustrate the scope of the reaction, we proceeded to examine a variety of nitriles. As shown in Table 4.5, both propionitrile and benzonitrile were able to produce good yields of the corresponding products **4-13a** and **4-13b**, respectively.

Table 4.5 Chloroamidation of **4-9a** with different nitrile partners.

				
Entry ^a	RCN	Product		Yield (%) ^b
1			4-13a	70
2			4-13b	83

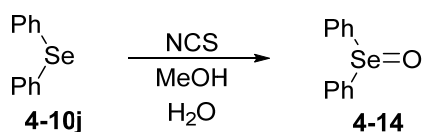
^a Reactions were carried out with cyclohexene (**4-9a**) (0.25 mmol) and **4-10j** (0.05 mmol) in RCN (0.65 mL) at 25 °C. ^b Isolated yield.

4.2.7 Mechanistic Studies

During our examination of the crude spectra, especially of the non-aromatic products, it was observed that ¹H NMR signals in the aromatic region corresponding to the proton signals of the catalyst was shifted downfield. This

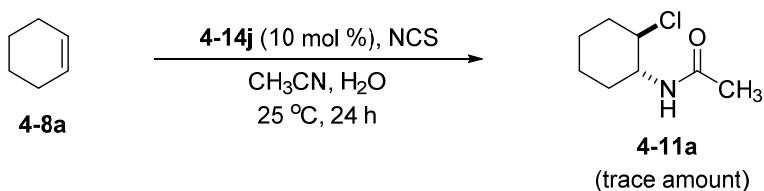
prompted us to probe the mechanism more closely through a series of ^1H NMR experiments carried out in deuterated acetonitrile.

We initially suspected that the active catalytic species might have been diphenyl selenium oxide (**4-14**), which can be synthesized by treating diphenyl selenide (**4-10j**) with NCS in MeOH/H₂O (Scheme 4.7).⁷



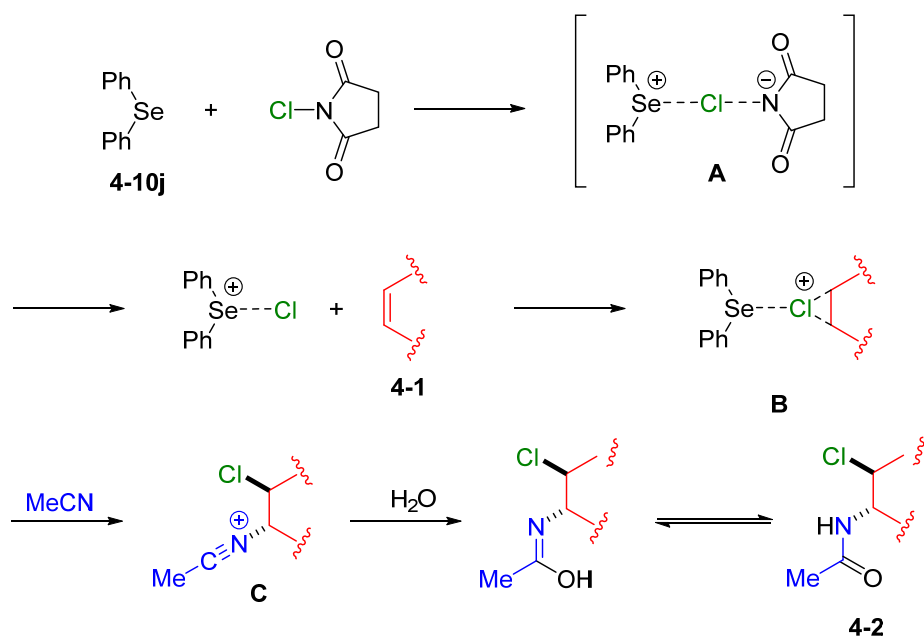
Scheme 4.7 Synthesis of **4-14** using NCS.

As such, catalyst **4-10j** and NCS were dissolved in deuterated chloroform and ^1H NMR spectra were obtained at various time intervals. We observed a gradual, as opposed to rapid, consumption of **4-10j** to form a new compound over the course of 6 hours. The product was isolated and identified to be diphenyl selenium oxide, Ph₂SeO (**4-14**). Nonetheless, when **4-14**, prepared using the oxidation of **4-10j** using NCS in MeOH, was employed as the catalyst instead of **4-10j** as the catalyst, the reaction was very sluggish. This leads us to suggest that the reaction was indeed catalyzed by diphenyl selenide **4-10j** instead of diphenyl selenium oxide **4-14**.



Scheme 4.8 Examination of **4-14** as the catalyst in the chloroamidation.

A plausible mechanism for the reaction is described in Scheme 4.8. The first step is likely to involve the activation of the chlorine atom on NCS via the Lewis basic diphenyl selenide to form intermediate **A**. The electrophilic Cl might then be delivered to olefin **4-8** to form the halonium intermediate **B**. At this point, acetonitrile could attack intermediate **B** (i.e. **B**→**C**) which would subsequently be quenched by a molecule of water to form the haloamide product **4-11**.



Scheme 4.9 Proposed mechanism of the Lewis basic selenium catalyzed chloroamidation.

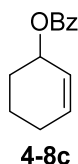
4.3 Summary

In summary, we have developed a highly efficient Lewis base catalyzed chloroamidation which can be applied to a wide range of substrates including those that are acid labile. Further application of this methodology to other areas is currently being investigated.

4.4 Experimental

(A) Synthesis of olefins 4-8.

Cyclohex-2-en-1-yl benzoate (4-8c):

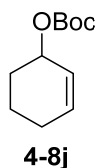


To a solution of 2-cyclohex-2-en-1-ol (0.320 g, 3.26 mmol, 1 eq) in 20 mL of methylene chloride was added triethylamine (1.3 mL, 9.32 mmol, 2.85 eq). Benzoyl chloride (1.04 mL, 8.95 mmol, 2.75 eq) was then added dropwise via syringe and the reaction allowed to stir overnight. The resulting yellow solution was quenched with 30 mL of deionized water and extracted with Et₂O (4 x 50 mL) and concentrated *in vacuo*. The residue was then purified by flash column chromatography (9:1 hexane/ethyl acetate) to afford the benzoyl-protected alcohol as a colourless liquid. ¹H NMR (600 MHz, CDCl₃) δ 8.07 – 8.04 (m, 2H), 7.54 (ddd, *J* = 8.7, 2.6, 1.2 Hz, 1H), 7.45 – 7.41 (m, 2H), 6.03 – 5.99 (m, 1H), 5.84

(ddt, $J = 10.0, 4.0, 2.2$ Hz, 1H), 5.51 (dtd, $J = 6.8, 3.6, 1.7$ Hz, 1H), 2.18 – 2.11 (m, 1H), 2.05 (dtdd, $J = 11.0, 7.4, 3.5, 1.7$ Hz, 1H), 1.98 (dddd, $J = 13.3, 9.9, 4.8, 3.2$ Hz, 1H), 1.92 – 1.81 (m, 2H), 1.75 – 1.67 (m, 1H), 1.58 (t, $J = 6.3$ Hz, 1H); ^{13}C NMR (151 MHz, CDCl_3) δ 166.21, 132.80, 130.71, 129.56, 128.25, 125.66, 68.54, 31.60, 28.37, 24.92, 18.90; IR (film) 2937, 1710, 1451, 1266, 1110, 916 cm^{-1} ; HRMS (ESI^+) calcd for $\text{C}_{13}\text{H}_{14}\text{O}_2$ $[\text{M}+\text{Na}]^+$ 225.0886, found 225.0892. (The physical data were in full accordance with the literature value in all respects: Shi, E. Shao, Y.; Chen, S.; Hu, H.; Liu, Z.; Zhang, J.; Wan, X. *Org. Lett.*, **2012**, *14*, 3382–3387.)

4-8d was prepared according to the literature procedure (Ladika, M.; Sunko, D. E. *J. Org. Chem.*, **1985**, *50*, 4544–4548.)

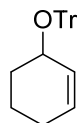
Tert-butyl cyclohex-2-en-1-yl carbonate (4-8j):



To a solution of 2-cyclohexen-1-ol (2.19 mL, 22.3 mmol, 1 eq) in 10 mL of methylene chloride was added Boc_2O (6.00 g, 27.5 mmol, 1.2 eq) and Bu_4NHSO_4 (20 mg, 0.38 mmol, 0.02 eq) at room temperature. The solution was cooled to 0 °C and NaOH (12.0 mL, 30% w/w) was added dropwise. The solution was then continuously stirred at room temperature. After 24 hours, the reaction was quenched with 30mL water and extracted with ether (3 x 50mL). The organic

layers were combined and washed with 1M HCl and brine. The solution was then dried with anhydrous MgSO_4 and concentrated *in vacuo*. The residue was then purified by flash column chromatography (9:1 hexane/ethyl acetate) to yield the Boc-protected alcohol as a colourless liquid. ^1H NMR (600 MHz, CDCl_3) δ 5.98 – 5.92 (m, 1H), 5.79 – 5.73 (m, 1H), 5.09 – 5.03 (m, 1H), 2.07 (dddd, $J = 13.7, 5.7, 3.8, 2.0$ Hz, 1H), 2.01 – 1.94 (m, 1H), 1.92 – 1.86 (m, 1H), 1.84 – 1.73 (m, 2H), 1.61 (qdd, $J = 5.8, 4.8, 2.2$ Hz, 1H), 1.49 (s, 9H) ppm; ^{13}C NMR (151 MHz, CDCl_3) δ 153.27, 132.81, 125.35, 81.68, 70.72, 28.21, 27.79, 24.80, 18.70 ppm; IR (film): 2980, 2937, 1731, 1368, 1272, 1248, 1155, 929, 869 cm^{-1} ; HRMS (ESI^+) calcd for $\text{C}_{11}\text{H}_{18}\text{O}_3$ $[\text{M}+\text{Na}]^+$: 221.1148, found 221.1156.

((cyclohex-2-en-1-yloxy)methanetriyl)tribenzene (4-8k):

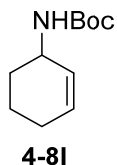


4-8k

To a solution of 2-cyclohexen-1-ol (0.50 g, 5.10 mmol, 1 eq) and trityl chloride (3.18 g, 11.4 mmol, 2 eq) in 20 mL of methylene chloride was added 1,8-diazabicyclo[5.4.0]undec-7-ene (2 mL, 13 mmol, 2.5 eq). After 72 hours, the solution was diluted with 40 mL of methylene chloride and washed with saturated NaHCO_3 (50 mL). The aqueous layer was extracted with methylene chloride (2 x 50 mL). The combined organic layers were dried with MgSO_4 and concentrated *in vacuo*. The residue was then purified by flash column chromatography (9:1 hexane/ethyl acetate) to afford the trityl-protected alcohol. ^1H NMR (600 MHz,

CDCl_3) δ 7.53 (ddd, $J = 4.4, 3.3, 1.9$ Hz, 6H), 7.31 – 7.27 (m, 6H), 7.25 – 7.21 (m, 3H), 5.62 (dd, $J = 10.2, 1.3$ Hz, 1H), 5.04 (dd, $J = 10.2, 2.8$ Hz, 1H), 4.06 (s, 1H), 1.98 (ddt, $J = 10.6, 5.8, 2.8$ Hz, 1H), 1.84 – 1.78 (m, 1H), 1.73 (ddd, $J = 14.4, 9.3, 4.4$ Hz, 1H), 1.40 – 1.32 (m, 3H) ppm; ^{13}C NMR (151 MHz, CDCl_3) δ 145.35, 129.96, 129.61, 129.01, 127.68, 126.85, 86.87, 67.82, 30.19, 25.03, 19.69 ppm; IR (film): 3031, 2931, 1596, 1490, 1448, 1394, 1316, 1275, 1218, 1151, 1048, 1021, 764, 746, 703 cm^{-1} ; HRMS (ESI^+) calcd for $\text{C}_{25}\text{H}_{24}\text{O}$ $[\text{M}+\text{Na}]^+$: 363.1719, found 363.1725. (The physical data were in full accordance with the literature value in all respects: Schwizer, D., Patton, J. T., Cutting, B., Smieško, M., Wagner, B., Kato, A., Weckerle, C., Binder, F. P. C., Rabbani, S., Schwaradt, O., Magnani, J. L. and Ernst, B. *Chem. Eur. J.*, **2012**, 18, 1342–1351.)

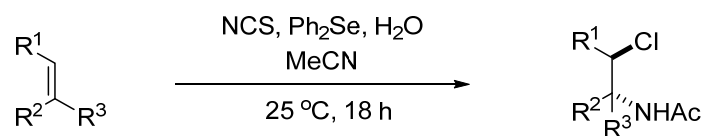
tert-butyl cyclohex-2-en-1-ylcarbamate (**4-8I**):



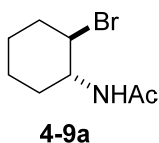
3-amino-1-cyclohexene (2.16 g, 22.3 mmol, 1 eq) was dissolved in 20 mL of methylene chloride was added Boc_2O (6.00 g, 27.5 mmol, 1.2 eq) and triethylamine (2.78 g, 27.5 mmol, 1.2 eq.) at room temperature. The solution was then continuously stirred at room temperature. After 1 hour, the reaction was quenched with water and extracted with methylene chloride. The organic layers were combined and washed with brine, dried with anhydrous MgSO_4 and concentrated *in vacuo*. The mixture was then purified by flash column

chromatography (19:1 hexane/ethyl acetate) to yield the Boc-protected amine as a colourless liquid. ^1H NMR (600 MHz, CDCl_3) δ 5.80 (ddd, $J = 9.5, 5.3, 3.6$ Hz, 1H), 5.60 (dd, $J = 10.0, 2.4$ Hz, 1H), 4.54 (d, $J = 18.8$ Hz, 1H), 4.21 – 4.06 (m, 1H), 2.00 – 1.95 (m, 2H), 1.90 – 1.85 (m, 1H), 1.66 (s, 1H), 1.63 (d, $J = 6.4$ Hz, 1H), 1.51 (s, 1H), 1.44 (d, $J = 3.2$ Hz, 9H) ppm; ^{13}C NMR (151 MHz, CDCl_3) δ 130.43, 128.09, 45.70, 33.52, 29.80, 28.40, 25.51, 24.76, 19.60 ppm; IR (film): 3332, 2931, 1688, 1498, 1365, 1240, 1166, 1020, 724 cm^{-1} . HRMS (ESI^+) calcd for $\text{C}_{11}\text{H}_{19}\text{NO}_2$ $[\text{M}+\text{Na}]^+$: 220.1308, found 220.1342.

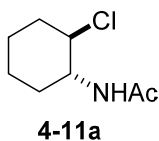
(B) General procedure for chloroamidation in acetonitrile.



To a solution of N-chlorosuccinimide (66.7 mg, 0.50 mmol) in dry acetonitrile (0.65 mL) at 25 °C in dark was added the olefin (0.25 mmol), diphenyl selenide (**4-10j**) (8.7 μL , 0.05 mmol), and water (5.4 μL , 0.30 mmol). After 18 hours, saturated Na_2SO_3 (0.75 mL) and NaHCO_3 (0.75 mL) were added to quench the reaction mixture and the aqueous layer was extracted with ethyl acetate (4 x 4 mL). The combined extracts were dried (MgSO_4), filtered, and *concentrated in vacuo*. The residue was purified by flash column chromatography to yield the corresponding chloroamides.

N-(2-bromocyclohexyl)acetamide (**4-9a**):

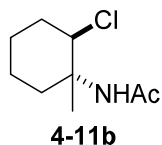
Synthesized according to the general procedure and purified by flash column chromatography (hexanes/ethyl acetate = 1:1) to afford a white solid (yield: 56 %). m.p.: 122-124 °C; ^1H NMR (600 MHz, CDCl_3) δ 5.53 (s, 1H), 3.99 – 3.90 (m, 1H), 3.86 (td, J = 10.7, 4.2 Hz, 1H), 2.41 – 2.35 (m, 1H), 2.24 – 2.18 (m, 1H), 2.00 (d, J = 4.3 Hz, 3H), 1.94 – 1.87 (m, 1H), 1.76 – 1.71 (m, 2H), 1.43 (ddd, J = 13.3, 9.2, 6.1 Hz, 1H), 1.32 – 1.23 (m, 2H) ppm; ^{13}C NMR (151 MHz, CDCl_3) δ 169.46, 55.29, 55.14, 37.07, 33.33, 26.47, 24.27, 23.49 ppm; IR (film): 3272, 2936, 2859, 1650, 1558, 1448, 1374, 1317, 1190, 691 cm^{-1} ; HRMS (ESI $^+$) calcd for $\text{C}_8\text{H}_{14}\text{BrNO}$ $[\text{M}+\text{Na}]^+$: 242.0151, found 242.0157. (The physical data were in full accordance with the literature value in all respects: Yeung, Y.; Gao, X.; Corey, E. *J. Am. Chem. Soc.*, **2006**, 128, 9644–9645)

N-(2-chlorocyclohexyl)acetamide (**4-11a**):

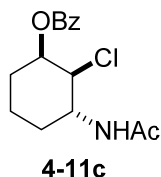
Synthesized according to the general procedure and purified by flash column chromatography (hexanes/ethyl acetate = 1:1) to afford a white solid (yield: 85 %). m.p.: 122-123 °C; ^1H NMR (600 MHz, CDCl_3) δ 5.56 (s, 1H), 3.86 (tdd, J = 10.8, 8.2, 4.2 Hz, 1H), 3.71 (td, J = 10.5, 4.2 Hz, 1H), 2.28 – 2.23 (m, 1H), 2.21 –

2.16 (m, 1H), 2.01 (s, 3H), 1.80 – 1.76 (m, 1H), 1.73 – 1.62 (m, 2H), 1.44 – 1.37 (m, 1H), 1.26 (dddd, $J = 13.1, 11.1, 5.4, 2.9$ Hz, 2H) ppm; ^{13}C NMR (151 MHz, CDCl_3) δ 169.69, 62.48, 55.07, 36.05, 32.77, 25.39, 24.14, 23.48 ppm; IR (film): 3262, 2935, 2860, 1638, 1562, 117, 736 cm^{-1} ; HRMS (ESI^+) calcd for $\text{C}_8\text{H}_{14}\text{ClNO}$ $[\text{M}+\text{Na}]^+$: 198.0656, found 198.0649. (The physical data were in full accordance with the literature value in all respects: Yeung, Y.; Gao, X.; Corey, E. *J. Am. Chem. Soc.*, **2006**, 128, 9644–9645)

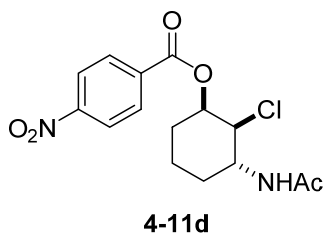
N-(2-chloro-1-methylcyclohexyl)acetamide (**4-11b**):



Synthesized according to the general procedure and purified by flash chromatography (hexanes/ethyl acetate = 1:1) to afford a white solid (yield: 65 %). m.p: 172-173 $^{\circ}\text{C}$; ^1H NMR (600 MHz, CDCl_3) δ 5.44 (s, 1H), 4.79 (dd, $J = 10.8, 4.3$ Hz, 1H), 2.08 (dddd, $J = 9.0, 7.8, 5.5, 0.9$ Hz, 3H), 1.95 – 1.94 (m, 3H), 1.78 – 1.68 (m, 3H), 1.61 – 1.54 (m, 1H), 1.42 (dd, $J = 6.0, 2.0$ Hz, 1H), 1.35 (s, 3H) ppm; ^{13}C NMR (151 MHz, CDCl_3) δ 169.73, 64.48, 57.98, 35.26, 32.71, 24.86, 24.61, 21.82, 19.27 ppm; IR (film): 3309, 2939, 2867, 1651, 1549, 1371, 760 cm^{-1} ; HRMS (ESI^+) calcd for $\text{C}_9\text{H}_{16}\text{ClNO}$ $[\text{M}+\text{Na}]^+$: 212.0813, found: 212.0817.

3-acetamido-2-chlorocyclohexyl benzoate (4-11c):

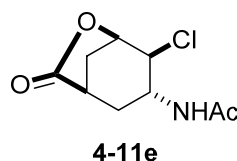
Synthesized according to the general procedure and purified by flash chromatography (hexanes/ethyl acetate = 1:1) to afford a white solid (yield: 76 %). m.p: 49–51 °C; ^1H NMR (600 MHz, CD_3CN) δ 8.06 (dd, J = 8.4, 1.2 Hz, 2H), 7.65 (d, J = 7.5 Hz, 1H), 7.55 – 7.52 (m, 2H), 6.52 (s, 1H), 5.57 – 5.52 (m, 1H), 4.23 (dd, J = 9.0, 6.4 Hz, 1H), 4.01 (d, J = 9.2 Hz, 1H), 2.06 – 2.00 (m, 2H), 1.88 (s, 3H), 1.78 – 1.71 (m, 2H), 1.67 – 1.62 (m, 1H), 1.47 – 1.42 (m, 1H) ppm; ^{13}C NMR (151 MHz, CD_3CN) δ 170.20, 166.23, 134.28, 131.15, 130.31, 129.65, 129.60, 76.96, 73.68, 64.15, 51.50, 23.12, 20.06 ppm; IR (film): 3281, 2942, 1720, 1653, 1271, 1113, 711 cm^{-1} ; HRMS (ESI^+) calcd for $\text{C}_{15}\text{H}_{18}\text{ClNO}_3$ $[\text{M}+\text{Na}]^+$: 318.0867, found: 318.0871.

3-acetamido-2-chloro-3-methylcyclohexyl 4-nitrobenzoate (4-11d):

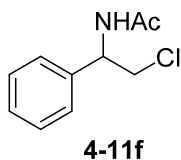
Synthesized according to the general procedure and purified by flash column chromatography (hexanes/ethyl acetate = 1:1) to afford a white solid (yield: 55 %). m.p: 136–138 °C; ^1H NMR (600 MHz, CDCl_3) δ 8.29 (dd, J = 8.7, 1.1 Hz,

2H), 8.24 – 8.20 (m, 2H), 5.36 (s, 1H), 5.23 – 5.16 (m, 2H), 2.70 (td, $J = 13.4, 4.1$ Hz, 1H), 2.27 – 2.21 (m, 1H), 1.99 (s, 3H), 1.86 (d, $J = 13.6$ Hz, 1H), 1.78 (d, $J = 13.6$ Hz, 1H), 1.69 – 1.61 (m, 2H), 1.56 (dd, $J = 13.5, 3.8$ Hz, 1H), 1.37 (s, 3H) ppm; ^{13}C NMR (151 MHz, CDCl_3) δ 170.05, 163.94, 150.63, 135.42, 130.90, 123.54, 75.13, 65.17, 58.72, 34.40, 31.37, 24.57, 20.58, 19.33 ppm; IR (film): 3303, 3078, 2947, 1725, 1655, 1528, 1275, 1103, 719 cm^{-1} ; HRMS (ESI^+) calcd for $\text{C}_{16}\text{H}_{19}\text{ClN}_2\text{O}_5$ $[\text{M}+\text{Na}]^+$: 377.0875, found: 377.0887.

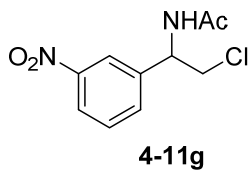
N-(4-chloro-7-oxo-6-oxabicyclo[3.2.1]octan-3-yl)acetamide (**4-11e**):



Synthesized according to the general procedure and purified by flash column chromatography (hexanes/ethyl acetate = 4:1) to afford a yellow oil (yield: 79 %). ^1H NMR (600 MHz, CDCl_3) δ 5.97 (s, 1H), 4.91 – 4.86 (m, 1H), 4.54 (t, $J = 7.3$ Hz, 1H), 4.24 – 4.20 (m, 1H), 2.66 (dd, $J = 7.5, 4.6$ Hz, 1H), 2.55 (d, $J = 12.5$ Hz, 1H), 2.37 (ddd, $J = 14.7, 6.5, 2.7$ Hz, 2H), 2.03 (ddd, $J = 14.9, 4.1, 2.2$ Hz, 1H), 1.96 (s, 3H) ppm; ^{13}C NMR (151 MHz, CDCl_3) δ 178.37, 169.08, 79.04, 54.95, 49.69, 35.59, 30.97, 30.01, 23.22 ppm; IR (film): 3287, 2925, 1781, 1657, 1529, 1150, 974 cm^{-1} ; HRMS (ESI^+) calcd for $\text{C}_9\text{H}_{12}\text{ClNO}_3$ $[\text{M}+\text{Na}]^+$: 240.0398, found: 240.0396.

N-(2-chloro-1-phenylethyl)acetamide (**4-11f**):

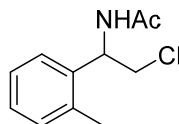
Synthesized according to the general procedure and purified by flash column chromatography (hexanes/ethyl acetate = 1:1) to afford a white solid (yield: 65 %). m.p: 99–100 °C; ^1H NMR (600 MHz, CDCl_3) δ 7.40 – 7.27 (m, 5H), 6.19 (s, 1H), 5.35 (dt, J = 7.8, 5.3 Hz, 1H), 3.91 – 3.82 (m, 2H), 2.08 – 2.04 (m, 3H) ppm; ^{13}C NMR (151 MHz, CDCl_3) δ 169.64, 138.37, 128.77, 128.12, 126.67, 53.55, 47.53, 23.28 ppm; IR (film): 3276, 3064, 2926, 1647, 1542, 1372, 1296, 725, 698 cm^{-1} ; HRMS (ESI^+) calcd for $\text{C}_{10}\text{H}_{12}\text{ClNO}$ $[\text{M}+\text{Na}]^+$: 220.0500, found: 220.0500.

N-(2-chloro-1-(3-nitrophenyl)ethyl)acetamide (**4-11g**):

Synthesized according to the general procedure and purified by flash column chromatography (hexanes/ethyl acetate = 1:1) to afford a white solid (yield: 89 %). m.p: 181–183 °C; ^1H NMR (600 MHz, CDCl_3) δ 8.21 – 8.15 (m, 2H), 7.66 (dd, J = 4.6, 3.9 Hz, 1H), 7.55 (t, J = 7.9 Hz, 1H), 6.51 (d, J = 7.3 Hz, 1H), 5.51 – 5.45 (m, 1H), 3.88 (ddd, J = 28.5, 11.6, 4.9 Hz, 2H), 2.12 – 2.09 (m, 3H) ppm. ^{13}C NMR (151 MHz, CDCl_3) δ 169.90, 148.44, 140.85, 133.17, 129.73, 123.07,

121.51, 52.90, 47.45, 23.18 ppm; IR (film): 3283, 1652, 1529, 1349, 906, 726 cm^{-1} ; HRMS (ESI^+) calcd for $\text{C}_{10}\text{H}_{11}\text{ClN}_2\text{O}_3$ $[\text{M}+\text{Na}]^+$: 265.0350, found: 265.0361.

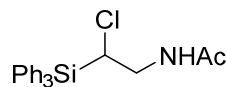
N-(2-chloro-1-(*o*-tolyl)ethyl)acetamide (**4-11h**):



4-11h

Synthesized according to the general procedure and purified by flash column chromatography (hexanes/ethyl acetate = 1:1) to afford a white solid (yield: 50 %). m.p: 120–121 °C; ^1H NMR (600 MHz, CDCl_3) δ 7.27 (s, 1H), 7.24 – 7.18 (m, 3H), 6.01 (s, 1H), 5.51 (d, J = 7.6 Hz, 1H), 3.80 (d, J = 6.1 Hz, 2H), 2.41 (s, 3H), 2.02 (s, 3H) ppm; ^{13}C NMR (151 MHz, CDCl_3) δ 169.46, 136.66, 136.24, 130.98, 128.09, 126.29, 125.36, 50.29, 46.18, 23.19, 19.31 ppm; IR (film): 3280, 3072, 1649, 1545, 1373, 1297, 763, 736 cm^{-1} ; HRMS (ESI^+) calcd for $\text{C}_{11}\text{H}_{14}\text{ClNO}$ $[\text{M}+\text{H}]^+$: 212.0837, found: 212.0844.

N-(2-chloro-2-(triphenylsilyl)ethyl)acetamide (**4-11i**):

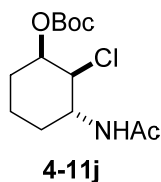


4-11i

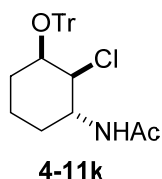
Synthesized according to the general procedure and purified by flash column chromatography (hexanes/ethyl acetate = 4:1) to afford a white solid (yield: 86 %). m.p: 152–153 °C; ^1H NMR (600 MHz, CDCl_3) δ 7.65 (dd, J = 8.1, 1.4 Hz, 6H), 7.46 (d, J = 7.4 Hz, 3H), 7.42 – 7.39 (m, 6H), 5.86 (s, 1H), 4.32 (dd, J =

10.5, 2.9 Hz, 1H), 4.17 (ddd, $J = 14.7, 6.8, 2.9$ Hz, 1H), 3.31 (ddd, $J = 14.8, 10.5, 4.5$ Hz, 1H), 1.89 (s, 3H) ppm; ^{13}C NMR (151 MHz, CDCl_3) δ 170.15, 136.15, 131.47, 130.27, 128.15, 47.96, 43.37, 23.12 ppm; IR (film): 3288, 3072, 1650, 1555, 1428, 1276, 1111, 750, 698 cm^{-1} ; HRMS (ESI^+) calcd for $\text{C}_{22}\text{H}_{22}\text{ClNOSi}$ $[\text{M}+\text{Na}]^+$: 402.1051, found: 402.1055.

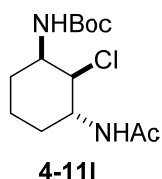
3-acetamido-2-chlorocyclohexyl tert-butyl carbonate (4-11j):



Synthesized according to the general procedure and purified by flash column chromatography (hexanes/ethyl acetate = 1:1) to afford a white solid (yield: 76 %). m.p: 155–156 $^{\circ}\text{C}$; ^1H NMR (600 MHz, CDCl_3) δ 5.47 (s, 1H), 5.14 – 5.05 (m, 1H), 4.23 – 4.09 (m, 2H), 2.21 – 2.15 (m, 1H), 2.01 (s, 3H), 1.78 (tdd, $J = 10.7, 7.5, 3.9$ Hz, 1H), 1.58 (ddd, $J = 17.9, 9.5, 6.2$ Hz, 3H), 1.52 – 1.47 (m, 9H), 1.45 – 1.39 (m, 1H) ppm; ^{13}C NMR (151 MHz, CDCl_3) δ 169.78, 152.93, 82.42, 74.08, 61.93, 51.34, 29.69, 28.71, 27.76, 23.54, 19.05 ppm; IR (film): 3284, 2943, 1744, 1657, 1549, 1371, 1281, 1157, 746 cm^{-1} ; HRMS (ESI^+) calcd for $\text{C}_{13}\text{H}_{22}\text{ClNO}_4$ $[\text{M}+\text{Na}]^+$: 314.1130, found: 314.1141.

N-(2-chloro-3-(trityloxy)cyclohexyl)acetamide (**4-11k**):

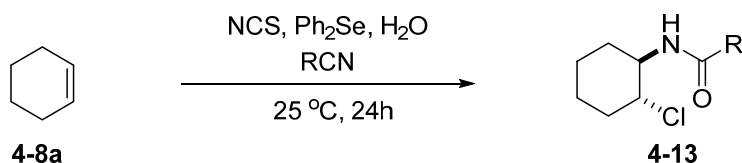
Synthesized according to the general procedure and purified by flash column chromatography (hexanes/ethyl acetate = 1:1) to afford a white solid (yield: 70 %). m.p: 208–210 °C; ^1H NMR (600 MHz, CDCl_3) δ 7.53 (dd, J = 8.3, 1.1 Hz, 6H), 7.29 (d, J = 7.8 Hz, 6H), 7.26 – 7.24 (m, 3H), 5.12 (d, J = 7.3 Hz, 1H), 4.16 – 4.11 (m, 1H), 3.70 – 3.63 (m, 1H), 3.30 (s, 1H), 2.08 – 2.02 (m, 1H), 1.86 (s, 3H), 1.71 – 1.65 (m, 1H), 1.46 – 1.40 (m, 1H), 1.26 (d, J = 3.2 Hz, 2H), 1.13 (dt, J = 12.4, 6.2 Hz, 1H) ppm; ^{13}C NMR (151 MHz, CDCl_3) δ 168.68, 144.61, 129.00, 127.75, 127.27, 87.36, 70.27, 62.74, 60.39, 51.13, 27.62, 23.40, 20.00 ppm; IR (film): 3303, 2924, 1644, 1538, 1076, 750, 699 cm^{-1} ; HRMS (ESI^+) calcd for $\text{C}_{27}\text{H}_{28}\text{ClNO}_2$ $[\text{M}+\text{Na}]^+$: 456.1701, found: 456.1708.

tert-butyl (3-acetamido-2-chlorocyclohexyl)carbamate (**4-11l**):

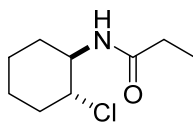
Synthesized according to the general procedure and purified by flash column chromatography (hexanes/ethyl acetate = 1:1) to afford a thin film (yield: 40%). ^1H NMR (600 MHz, CDCl_3) δ 5.91 (s, 1H), 4.90 (d, J = 8.5 Hz, 1H), 4.29 (d, J = 19.0 Hz, 2H), 3.95 (s, 1H), 2.08 (s, 1H), 2.01 (d, J = 0.9 Hz, 3H), 1.69 (d, J = 6.9

Hz, 4H), 1.44 (s, 9H), 1.28 – 1.24 (m, 1H) ppm; ^{13}C NMR (151 MHz, CDCl_3) δ 169.78, 155.08, 79.92, 62.65, 50.56, 48.36, 28.32, 26.96, 23.41, 19.75, 14.18 ppm; IR (film): 3312, 2933, 1692, 1656, 1532, 1366, 1248, 1165, 1049, 912, 732 cm^{-1} ; HRMS (ESI^+) calcd for $\text{C}_{13}\text{H}_{23}\text{ClN}_2\text{O}_3$ $[\text{M}+\text{Na}]^+$: 313.1289, found: 313.1298.

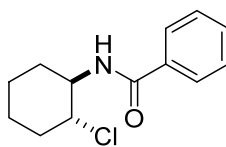
(C) General procedure for chloroamidation in various nitriles.



To a solution of *N*-chlorosuccinimide (66.7 mg, 0.50 mmol) and 15 equivalents of nitrile (total volume 0.65 mL) at 25 °C in the dark was added cyclohexene (0.25 mmol), diphenyl selenide (8.7 μL , 0.05 mmol), and water (5.4 μL , 0.30 mmol). After 24 hours, saturated Na_2SO_3 (0.75 mL) and NaHCO_3 (0.75 mL) were added. The organic layer was separated and the aqueous layer was extracted with ethyl acetate (4 x 4 mL). The combined organic extracts were dried (MgSO_4), filtered, and concentrated *in vacuo*. The residue was purified by flash column chromatography to yield the corresponding chloroamides.

N-(2-chlorocyclohexyl)propionamide (**4-13a**):**4-13a**

Synthesized according to the general procedure and purified by flash column chromatography (hexanes/ethyl acetate = 4:1) to afford a white solid (yield: 70 %). m.p: 118–119 °C; ^1H NMR (600 MHz, CDCl_3) δ 5.59 (s, 1H), 3.90 – 3.81 (m, 1H), 3.74 (dd, J = 10.6, 4.2 Hz, 1H), 2.23 (s, 4H), 1.79 – 1.67 (m, 3H), 1.40 (dt, J = 13.5, 3.4 Hz, 1H), 1.32 – 1.22 (m, 2H), 1.16 (t, J = 7.5 Hz, 3H) ppm; ^{13}C NMR (151 MHz, CDCl_3) δ 173.44, 62.57, 54.88, 36.05, 32.76, 29.86, 25.40, 24.16, 9.87 ppm; IR (film): 3289, 3080, 2929, 2858, 1646, 1546, 1449, 1376, 1272, 1214, 1137, 737 cm^{-1} ; HRMS (ESI^+) calcd for $\text{C}_9\text{H}_{16}\text{ClNO}$ $[\text{M}+\text{Na}]^+$: 212.0813, found: 212.0816.

N-(2-chlorocyclohexyl)benzamide (**4-13b**):**4-13b**

Synthesized according to the general procedure and purified by flash column chromatography (hexanes/ethyl acetate = 4:1) to afford a white solid (yield: 83 %). m.p: 140–141 °C; ^1H NMR (600 MHz, CDCl_3) δ 7.78 (dd, J = 8.2, 1.1 Hz, 2H), 7.50 (s, 1H), 7.44 (t, J = 7.5 Hz, 2H), 6.13 (s, 1H), 4.10 – 4.01 (m, 1H), 3.88

(d, $J = 4.1$ Hz, 1H), 2.39 – 2.26 (m, 2H), 1.88 – 1.72 (m, 3H), 1.48 (d, $J = 13.2$ Hz, 1H), 1.42 – 1.30 (m, 2H) ppm; ^{13}C NMR (151 MHz, CDCl_3) δ 167.24, 134.73, 131.49, 128.58, 126.92, 62.54, 55.67, 36.13, 32.74, 25.46, 24.19 ppm; IR (film): 3309, 2940, 2860, 1637, 1544, 1328, 694 cm^{-1} ; HRMS (ESI $^+$) calcd for $\text{C}_{13}\text{H}_{16}\text{ClNO}$ $[\text{M}+\text{Na}]^+$: 260.0813, found: 260.0815.

4.5 References

1. (a) Griffith, D. A.; Danishefsky, S. J., *J. Am. Chem. Soc.* **1991**, *113*, 5863;
(b) Driguez, H.; Vermes, J. P.; Lessard, J., *Can. J. Chem.* **1978**, *56*, 119;
(c) Orlek, B. S.; Stemp, G., *Tetrahedron Lett.* **1991**, *32*, 4045; (d) Barton, D. H. R.; Britten-Kelly, M. R.; Ferreira, D., *J. Chem. Soc., Perkin Trans. I* **1978**, 1090.
2. (a) Karur, S.; Kotti, S. R. S. S.; Xu, X.; Cannon, J. F.; Headley, A.; Li, G., *J. Am. Chem. Soc.* **2003**, *125*, 13340; (b) Li, G.; Wei, H.-X.; Kim, S. H., *Org. Lett.* **2000**, *2*, 2249; (c) Wei, H. X.; Kim, S. H.; Li, G., *Tetrahedron* **2001**, *57*, 3869; (d) Chen, D.; Timmons, C.; Chao, S.; Li, G., *Eur. J. Org. Chem.* **2004**, 3097; (e) Kotti, S. R. S. S.; Xu, X.; Wang, Y.; Headley, A. D.; Li, G., *Tetrahedron Lett.* **2004**, *45*, 7209; (f) Thakur, V. V.; Talluri, S. K.; Sudalai, A., *Org. Lett.* **2003**, *5*, 861; (g) Bach, T.; Schlummer, B.; Harms, K., *Chem. Commun. (Cambridge)* **2000**, 287; (h) Kirschning, A.; Abul, H. M.; Monenschein, H.; Rose, L.; Schoening, K.-U., *J. Org. Chem.* **1999**, *64*, 6522; (i) Bellucci, G.; Bianchini, R.; Chiappe, C., *J. Org. Chem.* **1991**, *56*, 3067; (j) Jung, S. H.; Kohn, H., *J. Am. Chem. Soc.* **1985**, *107*, 2931; (k) Wang, Z.-G.; Warren, J. D.; Dudkin, V. Y.; Zhang, X.; Iserloh, U.; Visser, M.; Eckhardt, M.; Seeberger, P. H.; Danishefsky, S. J., *Tetrahedron* **2006**, *62*, 4954; (l) Li, G.; Saibau, K. S. R. S.; Timmons, C., *Eur. J. Org. Chem.* **2007**, 2745; (m) Cai, Y.; Liu, X.; Jiang, J.; Chen, W.; Lin, L.; Feng, X., *J. Am. Chem. Soc.* **2011**, *133*, 5636; (n) Cai, Y.; Liu, X.;

- Li, J.; Chen, W.; Wang, W.; Lin, L.; Feng, X., *Chem. - Eur. J.* **2011**, *17*, 14916.
3. Yeung, Y.-Y.; Gao, X.; Corey, E. J., *J. Am. Chem. Soc.* **2006**, *128*, 9644.
4. Yadav, J. S.; Reddy, B. V. S.; Chary, D. N.; Chandrakanth, D., *Tetrahedron Lett.* **2009**, *50*, 1136.
5. (a) Denmark, S. E.; Beutner, G. L., *Angew. Chem., Int. Ed.* **2008**, *47*, 1560; (b) Denmark, S. E.; Collins, W. R., *Org. Lett.* **2007**, *9*, 3801; (c) Denmark, S. E.; Burk, M. T., *Proc. Natl. Acad. Sci. U. S. A.* **2010**, *107*, 20655; (d) Denmark, S. E.; Kalyani, D.; Collins, W. R., *J. Am. Chem. Soc.* **2010**, *132*, 15752; (e) Mellegaard, S. R.; Tunge, J. A., *J. Org. Chem.* **2004**, *69*, 8979; (f) Balkrishna, S. J.; Prasad, C. D.; Panini, P.; Detty, M. R.; Chopra, D.; Kumar, S., *J. Org. Chem.* **2012**, *77*, 9541; (g) Denmark, S. E.; Kornfilt, D. J. P.; Vogler, T., *J. Am. Chem. Soc.* **2011**, *133*, 15308; (h) Chu, Q.; Wang, Z.; Huang, Q.; Yan, C.; Zhu, S., *New J. Chem.* **2003**, *27*, 1522; (i) Zhou, L.; Chen, J.; Tan, C. K.; Yeung, Y.-Y., *J. Am. Chem. Soc.* **2011**, *133*, 9164; (j) Zhou, L.; Tan, C. K.; Jiang, X.; Chen, F.; Yeung, Y.-Y., *J. Am. Chem. Soc.* **2010**, *132*, 15474; (k) Tan, C. K.; Chen, F.; Yeung, Y.-Y., *Tetrahedron Lett.* **2011**, *52*, 4892; (l) Tan, C. K.; Le, C.; Yeung, Y.-Y., *Chem. Commun.* **2012**, *48*, 5793; (m) Tan, C. K.; Zhou, L.; Yeung, Y.-Y., *Org. Lett.* **2011**, *13*, 2738; (n) Chen, F.; Tan, C. K.; Yeung, Y.-Y., *J. Am. Chem. Soc.* **2013**, *135*, 1232; (o) Chen, J.; Zhou, L.; Tan, C. K.; Yeung, Y.-Y., *J. Org. Chem.* **2012**, *77*, 999; (p) Chen, J.; Zhou, L.; Yeung, Y.-Y., *Org. Biomol. Chem.* **2012**, *10*, 3808; (q) Cheng, Y. A.; Chen, T.; Tan, C.

- K.; Heng, J. J.; Yeung, Y.-Y., *J. Am. Chem. Soc.* **2012**, *134*, 16492; (r) Jiang, X.; Tan, C. K.; Zhou, L.; Yeung, Y.-Y., *Angew. Chem., Int. Ed.* **2012**, *51*, 7771.
6. (a) Brook, M. A.; Hadi, M. A.; Neuy, A., *J. Chem. Soc., Chem. Commun.* **1989**, 957; (b) Zhang, W.; Stone, J. A.; Brook, M. A.; McGibbon, G. A., *J. Am. Chem. Soc.* **1996**, *118*, 5764.
7. (a) Detty, M. R., *J. Org. Chem.* **1980**, *45*, 274; (b) Detty, M. R.; Friedman, A. E.; Oseroff, A. R., *J. Org. Chem.* **1994**, *59*, 8245.

Chapter 5

*Towards the Development of a New
Catalyst for Asymmetric Halocyclization*

5.1 Introduction

At the onset of this study, our group reported a series of enantioselective bromocyclization reactions, catalyzed by cinchona-derived aminothiobamates catalysts. Generally, all three major types of bromocyclization reactions – bromolactonization¹, bromoaminocyclization² (Chapter 2) and bromoetherification (Chapter 3), proceeded well, giving products with good yields and enantioselectivity. The catalyst acts via a dual activation mechanism whereby the bromine atom is activated through interaction with the Lewis basic sulfur atom and the nucleophile is activated *via* the interaction of the acidic proton of the substrate with the nitrogen atom on the quinuclidine.

Despite the good yields and enantioselectivity obtained in these cyclizations, there are two limitations of these catalysts. Firstly, catalysts made from the pseudo-enantiomeric pair of cinchona alkaloids do not always give the corresponding enantiomeric products with equally good enantioselectivity.^{2b} Secondly, the efficiency of the catalysts at low temperature conditions was poor. In some cases, 3–5 days at -78 °C were required for the reaction to be completed.²

To resolve these issues, we initiated a project towards the design and development of a new class of organocatalyst aimed at performing asymmetric halocyclization reactions. We set out two important criteria when searching for an initial catalyst. Firstly, both enantiomers of the catalyst must be inexpensive and

commercially available. Next, the catalyst must have readily modifiable handles so that its enantioselectivity can be tuned to accommodate different substrates.

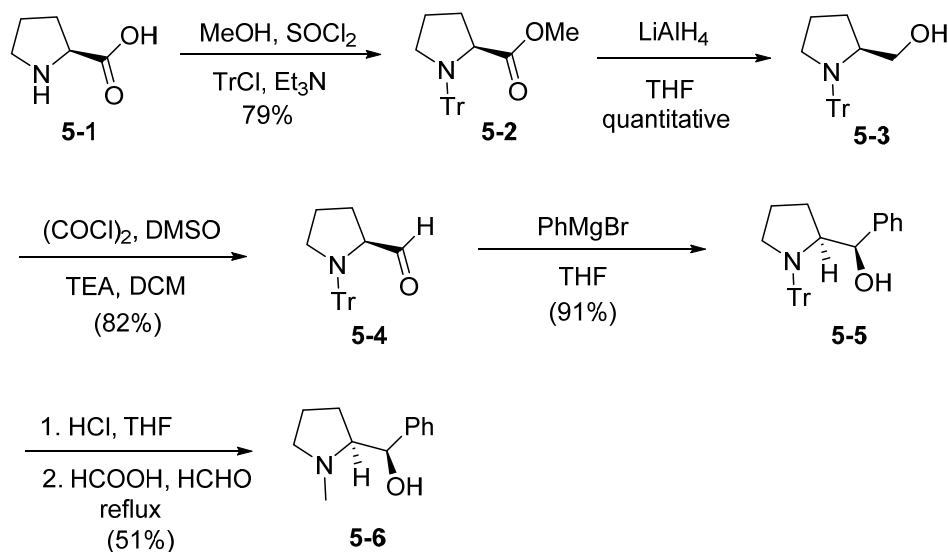
In the design of the new catalyst, we planned to mimick the amino-thiocarbamate catalyst by having a nitrogen atom acting as a Brønsted base as well as a Lewis basic functionality with improved reactivity. In Chapter 4, we have shown that selenium-containing compounds are excellent Lewis base catalysts for the activation of electrophilic halogen reagents. As such, we aim to develop a bifunctional catalyst by incorporating a Lewis basic selenium on a chiral amine scaffold. After much consideration, we chose (*L*)-proline to be our starting material as both the proline enantiomers are commercially available and inexpensive.

5.2 Results and Discussion

5.2.1 Synthesis of Catalysts and Preliminary Testing

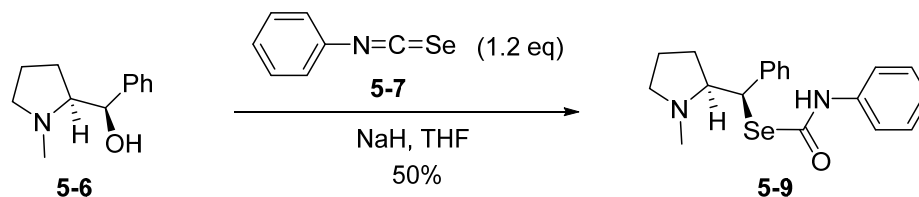
Using known procedures, (*L*)-proline **5-1** was first subjected thionyl chloride in methanol to form the proline methyl ester hydrochloride, and subsequently treated with triethylamine and trityl chloride to form the tritylated product **5-2** (Scheme 5.1). Subsequent reduction using lithium aluminium hydride followed by Swern oxidation furnished the aldehyde **5-4** in excellent yields. Treating the aldehyde **5-4** with phenylmagnesium bromide yielded the *N*-tritylated prolinol **5-5**

with excellent diastereoselectivity. The complete diastereoselectivity was achieved due to the bulkiness of the trityl group which blocks the approach of the Grignard reagent from the top face of the aldehyde **5-4**, resulting in only one product **5-5** being formed.³ Removal of the trityl moiety followed by the Eschweiler-Clarke methylation gave the prolinol **5-6** in good yields.



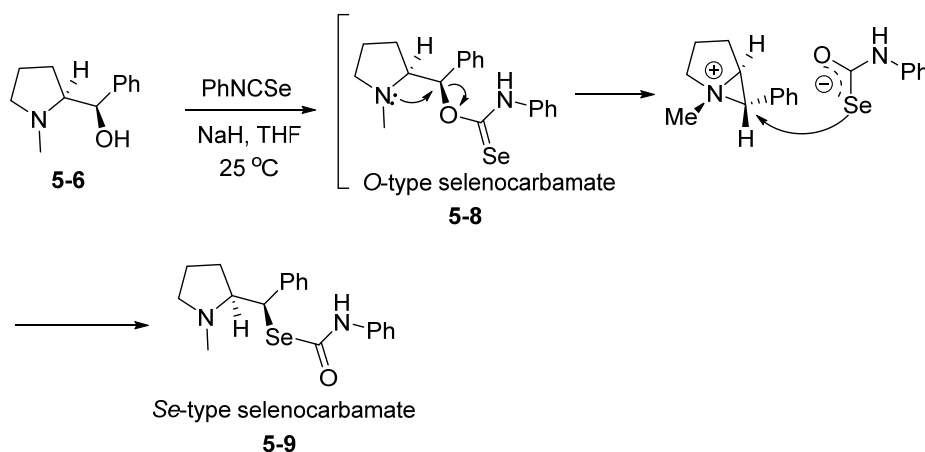
Scheme 5.1 Synthesis of prolinol **5-6**.

When the methylated prolinol **5-6** was treated with phenyl isoselenocyanate, a single product was isolated and subsequently identified to be the selenium-type amino-selenocarbamate catalyst **5-9** (Scheme 5.2).



Scheme 5.2 Synthesis of amino-selenocarbamate catalyst **5-9**.

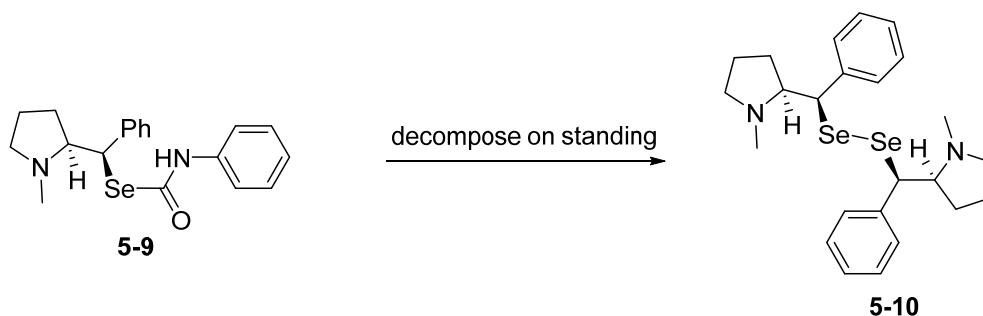
We believe that the product was obtained *via* a Newman-Kwart rearrangement whereby the *O*-type amino-selenocarbamate was first formed; this intermediate then underwent the rearrangement to form the *Se*-type catalyst. Conventionally, Newman-Kwart rearrangements are initiated under high temperature reaction conditions.⁴ However, the rearrangement of **5-8** to **5-9** proceeded under room temperature conditions and we believe this was due to the adjacent nitrogen atom providing anchimeric assistance (Scheme 5.3).⁵



Scheme 5.3 Proposed mechanism for the rearrangement of **5-8** to **5-9**.

Unfortunately, we could not test out the catalytic ability of this catalyst as it was highly unstable and decomposed after standing for 15 minutes. The

decomposed product was isolated and characterized to be the diselenide compound. The decomposition was probably due to the spontaneous hydrolysis of the selenocarbamate, and the resulting selenide was oxidized in the air to form the diselenide **5-10** (Scheme 5.4).



Scheme 5.4 Decomposition of **5-9** to form **5-10**.

In order to be sure that the instability is not just an isolated case, we synthesized five other analogues of the catalyst and investigated their stability (Figure 5.1). The bulkier and relatively more hydrophobic 1-naphthyl substituent was used to replace the phenyl group in one of the analogue **5-11**, while catalysts **5-12** to **5-14** possessed electron-rich and electron-deficient aryl groups that replaced the phenyl group on the selenocarbamate nitrogen. An allyl substituent was installed on the proline nitrogen of catalyst **5-15** to mimic the olefin moiety on the cinchona-derived thiocarbamate catalyst. Unfortunately, all of them seemed to be unstable and decomposed in a similar fashion to the corresponding diselenides.

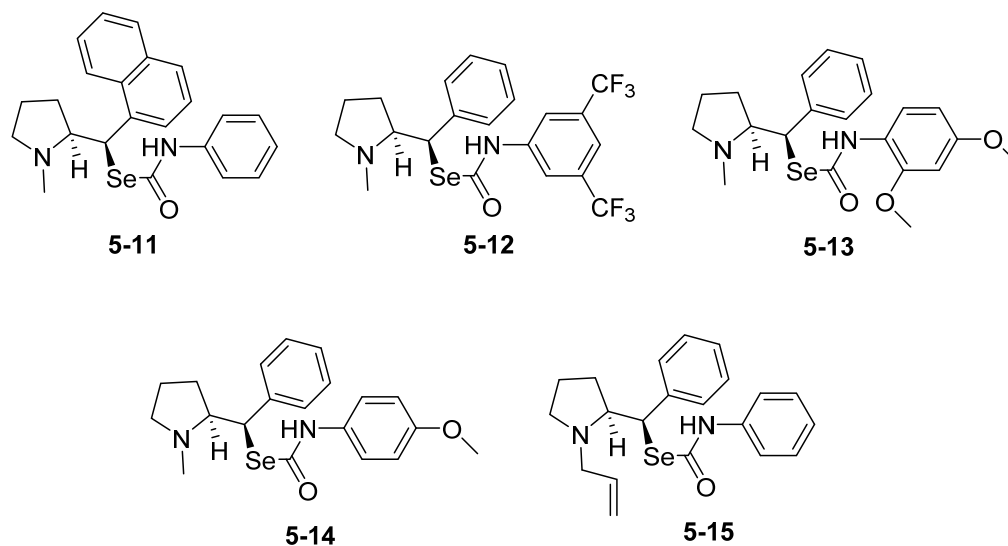
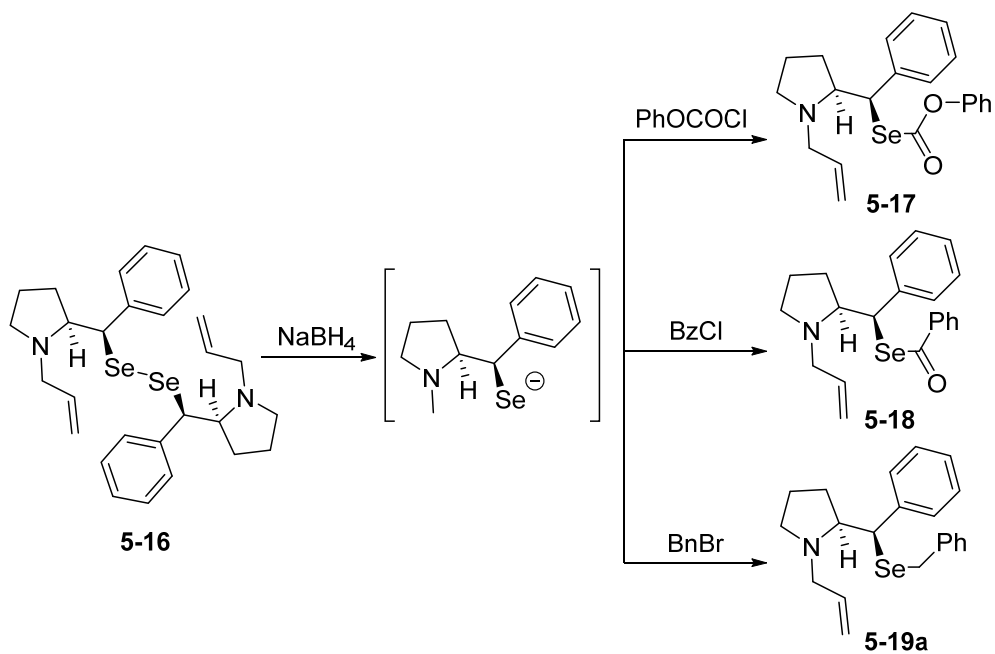


Figure 5.1 Other selenocarbamate catalysts synthesized to probe stability.

Undeterred, we thought that the diselenide products resulting from the decomposition of the selenocarbamates could be made useful by utilizing them to form other derivatives or even using them as a catalyst. Thus, the diselenide **5-16** was subsequently reduced and derivatized to the three other amino-selenium compounds (Scheme 5.5).



Scheme 5.5 Derivatization of diselenide **5-16**.

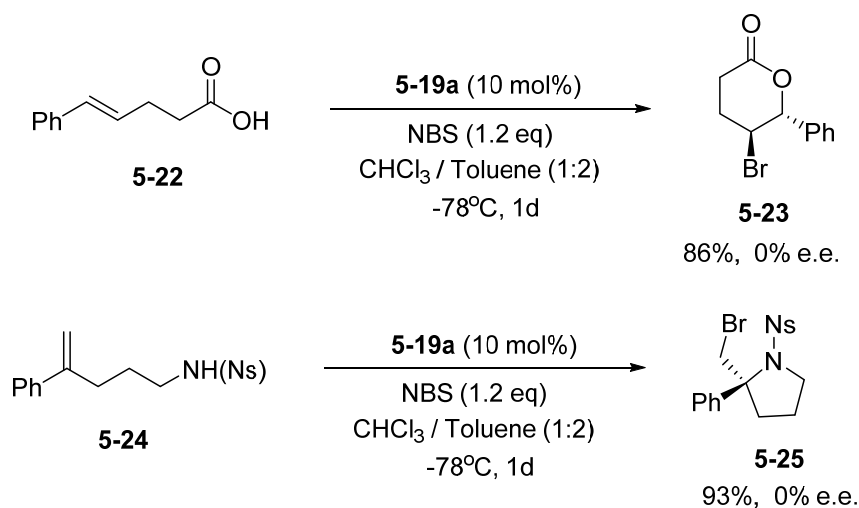
Diselenide **5-16** and its three derivatives **5-17** to **5-19** were tested for their catalytic activity using a standard model bromolactonization reaction (Table 5.1). It was observed that all the four catalysts were able to catalyze the halocyclization, with catalyst **5-17** giving a moderate yield of 57% while the rest gave almost quantitative yields. However, only the benzyl derivative **5-19** managed to achieve some enantioselectivity for the bromolactonization.

Table 5.1 Bromolactonization using different amino-selenium catalysts.

Entry ^a	Catalyst	Yield (%) ^b	ee (%)
1	5-16	96	0
2	5-17	57	0
3	5-18	90	0
4	5-19a	93	23

^a Reactions were carried out with **5-20** (0.1 mmol), NBS (0.12 mmol), catalyst (0.01 mmol) in CHCl₃/Toluene (1:2) (3 mL). ^b Isolated yield.

With these promising results, two other substrates that can undergo halocyclization were synthesized and subject to the cyclization conditions (Scheme 5.6).

**Scheme 5.6** Bromocyclizations of olefinic substrates **5-22** and **5-24** using **5-19a**.

It was observed that the catalyst was able to catalyze both cyclization reactions with good yields. However, the resulting products formed were racemic in both cases. Despite this, it was still worthy to note that the bromoaminocyclization of **5-24** proceeded at a much faster rate (93% yield achieved in 1 day) as compared to the same reaction that was catalyzed using the cinchonia-derived thiocarbamate catalysts (97% yield achieved in 3 days).

5.2.2 Reaction Conditions Optimization

With this, we began a series of screening reactions with the aim of optimizing the reaction conditions in the hope of obtaining better enantioselectivity (Table 5.2).

Table 5.2 Solvent optimization for the bromolactonization of **5-20**.

5-20 $\xrightarrow[\text{Solvent}]{\text{5-19a (10 mol\%)}, \text{NBS (1.2eq)}}$ **5-21**

Entry ^a	Halogen Source	Solvent	Yield (%) ^b	ee (%) ^b
1	NBS	CHCl ₃ /Toluene (1:2)	99	23
2	NBS	CHCl ₃ /Toluene (1:3)	97	19
3	NBS	CH ₂ Cl ₂	99	4
4	NBS	Toluene	<5	-
5	NBS	CHCl ₃ /Toluene (1:3)	98	22
6	NBS	CHCl ₃ /Toluene (1:5)	<5	-
7	NBS	C ₂ H ₄ Cl ₂ /Toluene	76	0
8	NBS	CHCl ₃ /Hexane (1:2)	94	6
9	NBS	Hexane	0	-

^a Reactions were carried out with **5-20** (0.1 mmol), NBS (0.12 mmol), catalyst (0.01 mmol) in solvent (3 mL). ^b Isolated yield.

It was observed that relatively non-polar solvents and non-polar solvent mixture such as toluene, chloroform/toluene (1:5) mixture and hexane can cause the yield to dramatically plunge (Table 5.2, entries 4, 6 and 9 respectively). The yields improved significantly when relatively polar solvent systems were used. As for the enantioselectivity of the reaction, the initial chloroform/toluene (1:2) composition remained the best solvent for the reaction, giving products with 23% ee.

5.2.3 Effect of Halogen Source

Following the solvent screening, the halogen source was also screened to determine the best halogen source for the reaction (Table 5.3).

Table 5.3 Halogen source screening for the bromolactonization of **5-20**.

$\text{Ph}-\text{CH}=\text{CH}-\text{CH}_2-\text{COOH}$ (5-20) $\xrightarrow[\text{Solvent}]{\text{5-19a (10 mol\%)}, \text{Halogen source (1.2eq)}}$ $\text{Ph}-\text{CH}(\text{O})-\text{CH}_2-\text{CH}_2-\text{CO}$ (lactone)

X = Br **5-21**
 = Cl **5-26**
 = I **5-27**

Entry ^a	Halogen Source	Solvent	Yield (%) ^b	ee (%) ^b
1	NBS	CHCl ₃ /Toluene (1:2)	97	23
2	DBH	CHCl ₃ /Toluene (1:2)	97	10
3	NBP	CHCl ₃ /Toluene (1:2)	98	5
4	NBA	CHCl ₃ /Toluene (1:2)	NR	-
5	TABCO	CHCl ₃ /Toluene (1:2)	94	12
6	NCS	CHCl ₃ /Toluene (1:2)	NR	-
7	NIS	CHCl ₃ /Toluene (1:2)	95	3

^a Reactions were carried out with **5-20** (0.1 mmol), halogen source (0.12 mmol), catalyst (0.01 mmol) in solvent (3 mL). ^b Isolated yield.

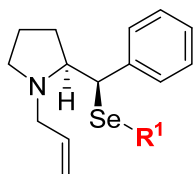
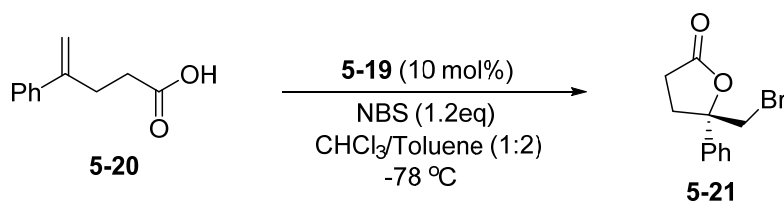
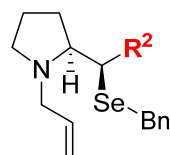
No reaction was observed for NBA and NCS (Table 5.3, entries 4 and 7), while 1,3-dibromo-5,5-dimethylhydantoin (DBH), NBP, TABCO and N-iodosuccinimide (NIS) (Table 5.3, entries 2, 3, 5 and 7) all gave near quantitative yields for the halocyclization albeit with diminished enantioselectivities when compared with NBS as the halogen source. Thus, NBS was selected to be the halogen source in the subsequent screening.

5.2.4 Catalyst Screening

After screening the solvent and the halogen source, analogues of this catalyst were synthesized and a brief structure-activity relationship study was carried out. The substituent on the selenium atom was first varied.

Both electron-rich and electron-deficient benzyl substituents caused the reaction yield to decrease, and the products obtained also have either lower or no ee (Table 5.4, entries 2–5). Interestingly, the less sterically hindered methyl substituted catalyst **5-19f** gave higher ee than benzyl substituted version **5-19a** (Table 5.4, entry 6) while it was observed that the ethyl substituted catalyst **5-19g** behaves similar to **5-19a** (Table 5.4 entry 7).

Next, the effect of the aryl substituent on the catalyst was investigated. Both the 1-naphthyl and 2-naphthyl substituted catalysts gave products with slightly reduced ee (Table 5.4, entry 8–9). Both the electron-deficient 4-fluorophenyl (catalyst **5-19j**) and electron-rich 4-methylphenyl group (catalyst **5-19k**) caused the ee also decreased to 18% ee (Table 5.4, entry 10–11). Sterically bulkier phenyl substituted catalysts also resulted in poorer enantioselectivities (Table 5.4, entries 12–13).

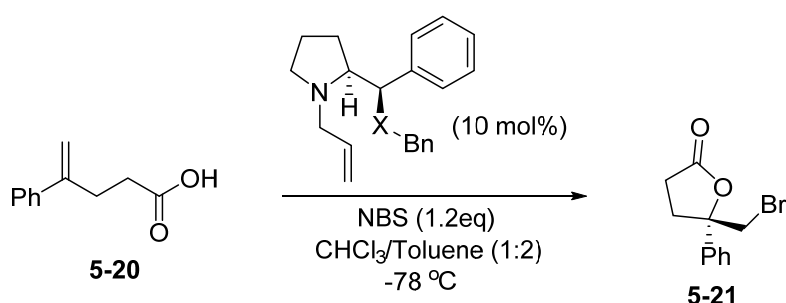
Table 5.4 Catalyst screening for the bromolactonization of **5-20**.**5-19a** R¹ = Bn**5-19b** R¹ = 4-MeO-C₆H₄CH₂**5-19c** R¹ = 4-F-C₆H₄CH₂**5-19d** R¹ = 4-*t*-Bu-C₆H₄CH₂**5-19e** R¹ = 2,5-(Me)₂-C₆H₃CH₂**5-19f** R¹ = Me**5-19g** R¹ = Et**5-19h** R² = 1-naphthyl**5-19i** R² = 2-naphthyl**5-19j** R² = 4-F-C₆H₄**5-19k** R² = 4-Me-C₆H₄**5-19l** R² = 4-*t*-Bu-C₆H₄**5-19m** R² = 2,4,6-(Me)₃-C₆H₂

Entry ^a	Catalyst	Yield (%) ^b	ee (%)
1	5-19a	97	23
2	5-19b	35	5
3	5-19c	56	0
4	5-19d	45	6
5	5-19e	63	11
6	5-19f	95	26
7	5-19g	90	23
8	5-19h	94	21
9	5-19i	98	20
10	5-19j	84	18
11	5-19k	92	18
12	5-19l	93	16
13	5-19m	93	10

^a Reactions were carried out with **5-20** (0.1 mmol), NBS (0.12 mmol), catalyst (0.01 mmol) in solvent (3 mL). Yields shown are isolated yields.

Following on, we investigated the importance of the selenium atom in catalyst **5-19a** by synthesizing the oxygen and sulfur analogues. Remarkably, both the oxygen and sulfur variants gave opposite and lower ee as compared to the selenium-containing catalyst. This highlights the importance of the selenium atom in the mode of action of the catalyst.

Table 5.5 Importance of the Lewis basic selenium atom in the catalyst.



Entry ^a	Catalyst	X	Yield (%) ^b	ee (%)
1	5-28	O	97	-10
2	5-29	S	96	-14
3	5-19a	Se	97	23

^a Reactions were carried out with **5-20** (0.1 mmol), NBS (0.12 mmol), catalyst (0.01 mmol) in solvent (3 mL). Yields shown are isolated yields.

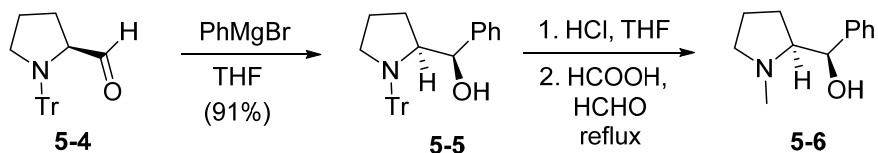
5.3 Summary

The results obtained from the above study built an excellent platform for a new catalyst to be developed. The improved rates of reaction from the use of these catalysts as compared to the cinchona-derived thiocarbamate catalysts highlight

the improved reactivity of these catalysts. The importance of the Lewis basic selenium atom in the catalyst was also emphasized through the use of the oxygen and sulfur analogues which gave products with opposite and lower ees. These observations serve as good preliminary results for the further development of an efficient and highly enantioselective amino-selenoether catalysts.

5.4 Experimental

(A) Synthesis of prolinol 5-6.

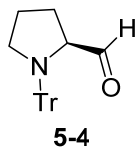


To a stirred solution of aldehyde **5-4** (5 mmol, 1.0 eq), synthesized using (*L*)-proline according to the literature procedure (J. Bejjani, F. Chemla, M. Audouin, *J. Org. Chem.* **2003**, 68, 9747–9752), in THF (5 mL) was added phenyl magnesium bromide (6 mL, 1M, 6 mmol, 1.2 eq) under argon at 0 °C. The reaction was allowed to warm up to room temperature and was stirred for an additional 12 hours. The reaction was quenched with saturated NH_4Cl solution and extracted with CH_2Cl_2 (3 X 10mL). The combined organic extracts were dried over MgSO_4 , filtered and concentrated *in vacuo*. The residue was purified by column chromatography (hexane/ethyl acetate 9:1) to give product **5-5**.

To a stirred solution of tritylated prolinol **5-5** (5 mmol, 1.0 eq) in THF (5 mL) was added 6M HCl (1mL). The reaction was stirred followed by TLC. After 3 hours of stirring, the reaction was diluted with water (5 mL) and washed with ether (3 X 5mL). The aqueous phase was made alkaline by the addition of NaOH and subsequently extracted with CH₂Cl₂ (3 X 10 mL). The combined organic extracts were dried over MgSO₄, filtered and concentrated *in vacuo* to give deprotected prolinol which was used without purification for the next step.

The deprotected prolinol (5mmol, 1.0 eq) was redissolved formic acid (3mL), added formaldehyde (1mL, 37% in water) and heated at 80 °C for 16 hours. The reaction was quenched with water and made basic using NaOH. The reaction mixture was extracted with CH₂Cl₂ (3 X 10mL). The combined organic extracts were dried over MgSO₄, filtered and concentrated *in vacuo*. The residue was purified by column chromatography (hexane/ethyl acetate 1:1) to give product **5-6**.

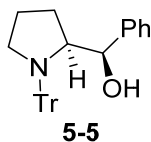
(S)-1-tritylpyrrolidine-2-carbaldehyde (**5-4**)



White solid, ¹H NMR (400 MHz, CDCl₃) δ 9.85 (d, *J* = 2.7 Hz, 1H), 7.58 – 7.53 (m, 6H), 7.30 – 7.23 (m, 7H), 7.21 – 7.15 (m, 3H), 3.81 – 3.72 (m, 1H), 3.28 (dt, *J* = 11.7, 7.2 Hz, 1H), 2.92 (ddd, *J* = 11.7, 7.6, 5.9 Hz, 1H), 1.59 (ddd, *J* = 12.5, 6.4, 3.6 Hz, 1H), 1.48 – 1.37 (m, 1H), 1.17 – 1.07 (m, 1H), 0.88 – 0.75 (m, 1H); ¹³C

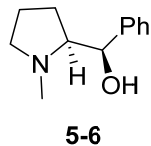
NMR (101 MHz, CDCl₃) δ 204.34, 144.41, 129.43, 127.74, 126.39, 77.32, 77.00, 76.92, 76.68, 68.46, 50.58, 27.98, 24.27; HRMS (ESI) calcd for C₂₄H₂₄NO m/z [M + H]⁺: 342.1852; found 342.1860.

(R)-phenyl((S)-1-tritylpyrrolidin-2-yl)methanol (5-5)



White solid, ¹H NMR (400 MHz, CDCl₃) δ 7.65 – 7.55 (m, 6H), 7.33 – 7.12 (m, 14H), 7.08 (d, *J* = 7.5 Hz, 2H), 5.10 (d, *J* = 3.2 Hz, 1H), 3.73 (td, *J* = 5.2, 2.6 Hz, 1H), 3.35 – 3.21 (m, 2H), 3.04 (ddd, *J* = 11.7, 7.9, 3.5 Hz, 1H), 1.41 (dt, *J* = 8.0, 4.2 Hz, 1H), 1.32 (dp, *J* = 11.7, 4.3 Hz, 1H), 0.80 (dt, *J* = 8.5, 4.5 Hz, 1H), 0.23 (dt, *J* = 11.2, 8.5 Hz, 1H); ¹³C NMR (101 MHz, CDCl₃) δ 144.59, 142.19, 129.91, 127.96, 127.57, 126.49, 126.35, 125.41, 78.15, 77.32, 77.00, 76.68, 75.54, 66.01, 53.32, 25.76, 24.74; HRMS (ESI) calcd for C₃₀H₃₀NO m/z [M + H]⁺: 420.2322; found: 420.2319.

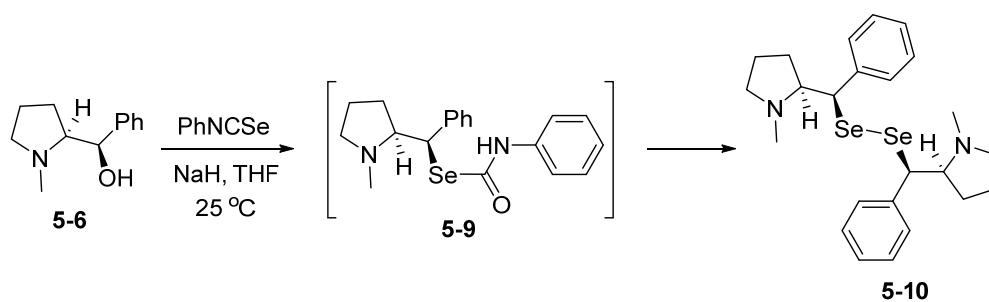
(R)-((S)-1-methylpyrrolidin-2-yl)(phenyl)methanol (5-6)



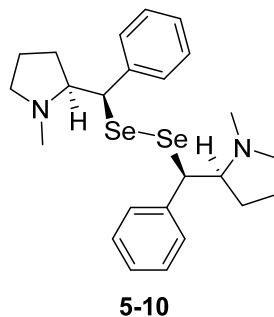
Colourless oil; ¹H NMR (600 MHz, CDCl₃) δ 7.39 – 7.30 (m, 4H), 7.25 – 7.21 (m, 1H), 4.89 (d, *J* = 2.9 Hz, 1H), 3.22 – 3.13 (m, 1H), 2.55 (td, *J* = 7.1, 6.4, 3.4 Hz, 1H), 2.49 (s, 3H), 2.37 (td, *J* = 9.4, 7.5 Hz, 1H), 1.78 – 1.58 (m, 3H), 1.34 – 1.23

(m, 1H); ^{13}C NMR (151 MHz, CDCl_3) δ 141.57, 128.09, 126.78, 125.45, 77.21, 77.00, 76.79, 71.11, 69.60, 57.52, 39.99, 23.82, 22.91; HRMS (ESI) calcd for $\text{C}_{12}\text{H}_{18}\text{NO}$ m/z $[\text{M} + \text{H}]^+$: 192.1383; found: 192.1385.

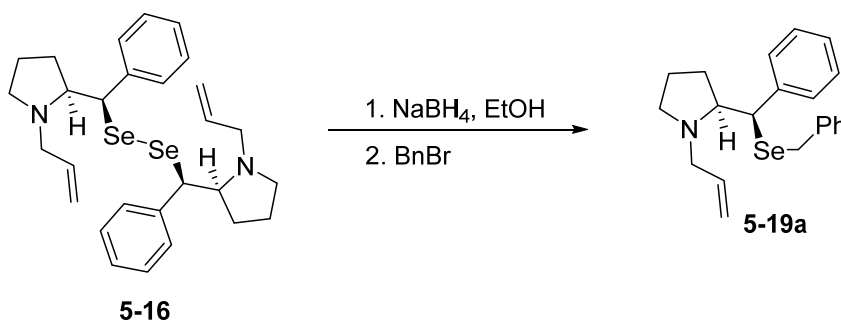
(B) Representative example for the synthesis of diselenide.



To a stirred solution of the prolinol **5-6** (5 mmol, 1 eq), phenylselenoisoocyanate (5 mmol, 1 eq) in THF (5 mL) was added NaH (6 mmol, 1.2 eq) at $25\text{ }^\circ\text{C}$. The resulting solution was allowed to stir for 16 hours. The reaction was quenched with water extracted with CH_2Cl_2 (3 X 10mL). The combined organic extracts were dried over MgSO_4 , filtered and concentrated *in vacuo*. The residue was purified by column chromatography (hexane/ethyl acetate 1:1) to give product **5-10**.

1,2-bis((R)-((S)-1-methylpyrrolidin-2-yl)(phenyl)methyl)diselane (5-10)

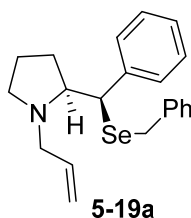
Colourless oil; ^1H NMR (600 MHz, CDCl_3) δ 7.30 – 7.16 (m, 5H), 4.08 (d, $J = 5.6$ Hz, 1H), 3.08 – 3.01 (m, 1H), 2.54 (q, $J = 7.3$ Hz, 1H), 2.19 (q, $J = 9.5$ Hz, 1H), 2.16 (s, 3H), 1.96 (dt, $J = 10.0, 7.3, 5.1$ Hz, 1H), 1.86 – 1.79 (m, 1H), 1.69 – 1.55 (m, 2H); ^{13}C NMR (151 MHz, CDCl_3) δ 141.51, 129.40, 127.99, 126.84, 77.21, 77.00, 76.79, 69.86, 57.63, 53.15, 41.75, 29.75, 22.47; HRMS (ESI) calcd for $\text{C}_{12}\text{H}_{18}\text{NO}$ m/z $[\text{M} + \text{H}]^+$: 509.0969 ; found: 509.0977.

(C) Representative example for the synthesis of amino selenoether catalyst.

To a stirred solution the diselenide **5-16** (5 mmol, 1 eq) in ethanol (5 mL) was added sodium borohydride (10 mmol, 2 eq). The reaction mixture was allowed to stir for 30 minutes before benzyl bromide (10 mmol, 2 eq) was added into the

reaction mixture. The reaction was left to stir for 12 hours. The reaction was quenched with water extracted with CH₂Cl₂ (3 X 10mL). The combined organic extracts were dried over MgSO₄, filtered and concentrated *in vacuo*. The residue was purified by column chromatography (hexane/ethyl acetate 1:1) to give product **5-19**.

(S)-1-allyl-2-((R)-(benzylselanyl)(phenyl)methyl)pyrrolidine (**5-19a**)



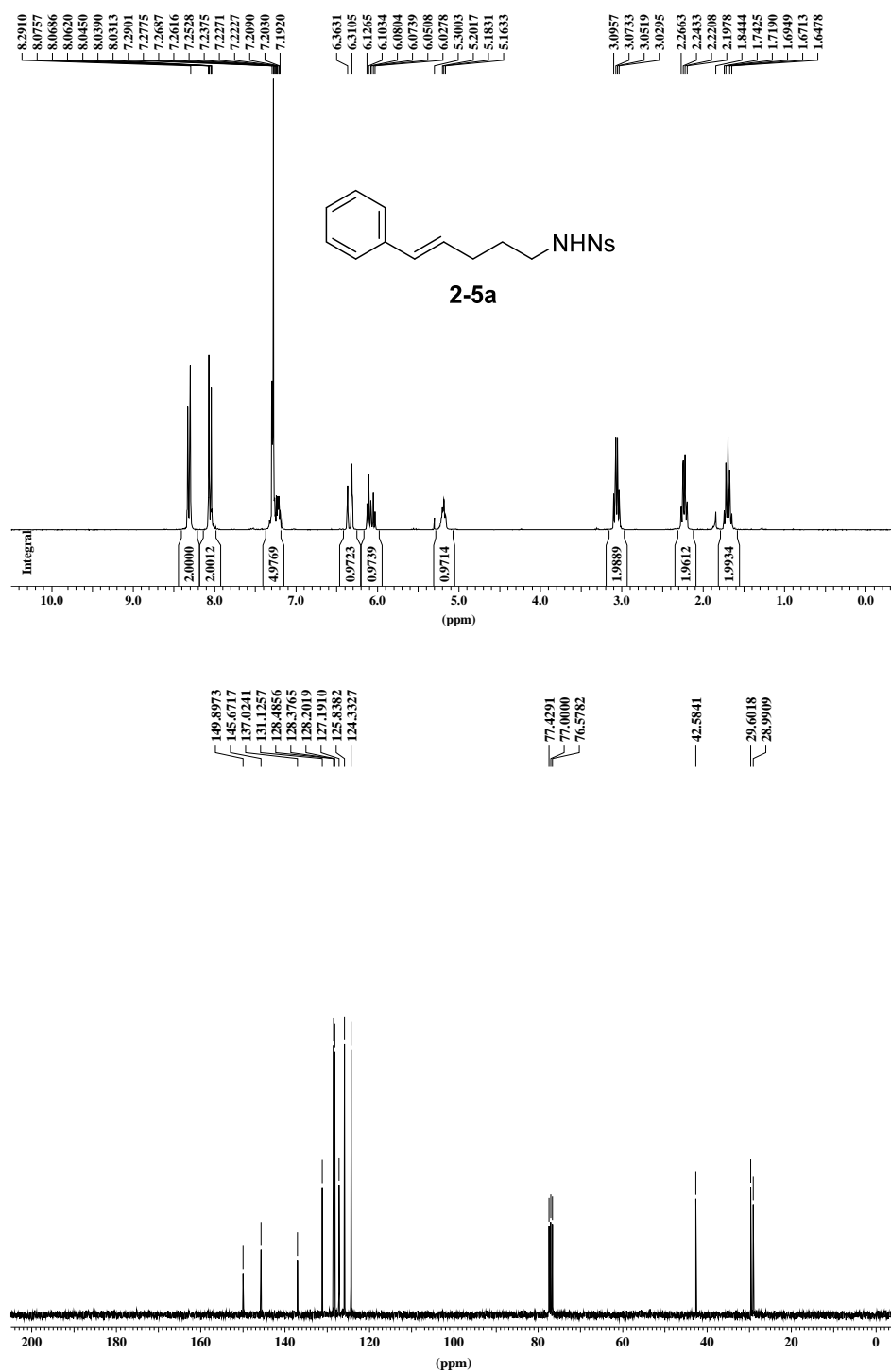
Colourless oil; ¹H NMR (600 MHz, Chloroform-*d*) δ 7.38 (s, 2H), 7.31 (s, 2H), 7.22 (d, *J* = 7.6 Hz, 3H), 7.13 (d, *J* = 1.3 Hz, 3H), 5.83 – 5.73 (m, 1H), 5.06 – 4.99 (m, 2H), 4.15 (d, *J* = 5.2 Hz, 1H), 3.54 (s, 1H), 3.47 (s, 1H), 3.21 – 3.12 (m, 1H), 3.07 (s, 1H), 2.79 – 2.68 (m, 2H), 2.24 (d, *J* = 8.0 Hz, 1H), 1.97 (d, *J* = 9.3 Hz, 1H), 1.81 – 1.54 (m, 4H); ¹³C NMR (151 MHz, CDCl₃) δ 141.28, 139.49, 135.75, 129.55, 128.98, 128.23, 128.20, 126.84, 126.40, 116.62, 77.21, 77.00, 76.79, 67.96, 57.32, 53.96, 49.71, 29.48, 26.93, 22.65; HRMS (ESI) calcd for C₂₁H₂₆NSe *m/z* [M + H]⁺: 372.1225 ; found: 372.1223.

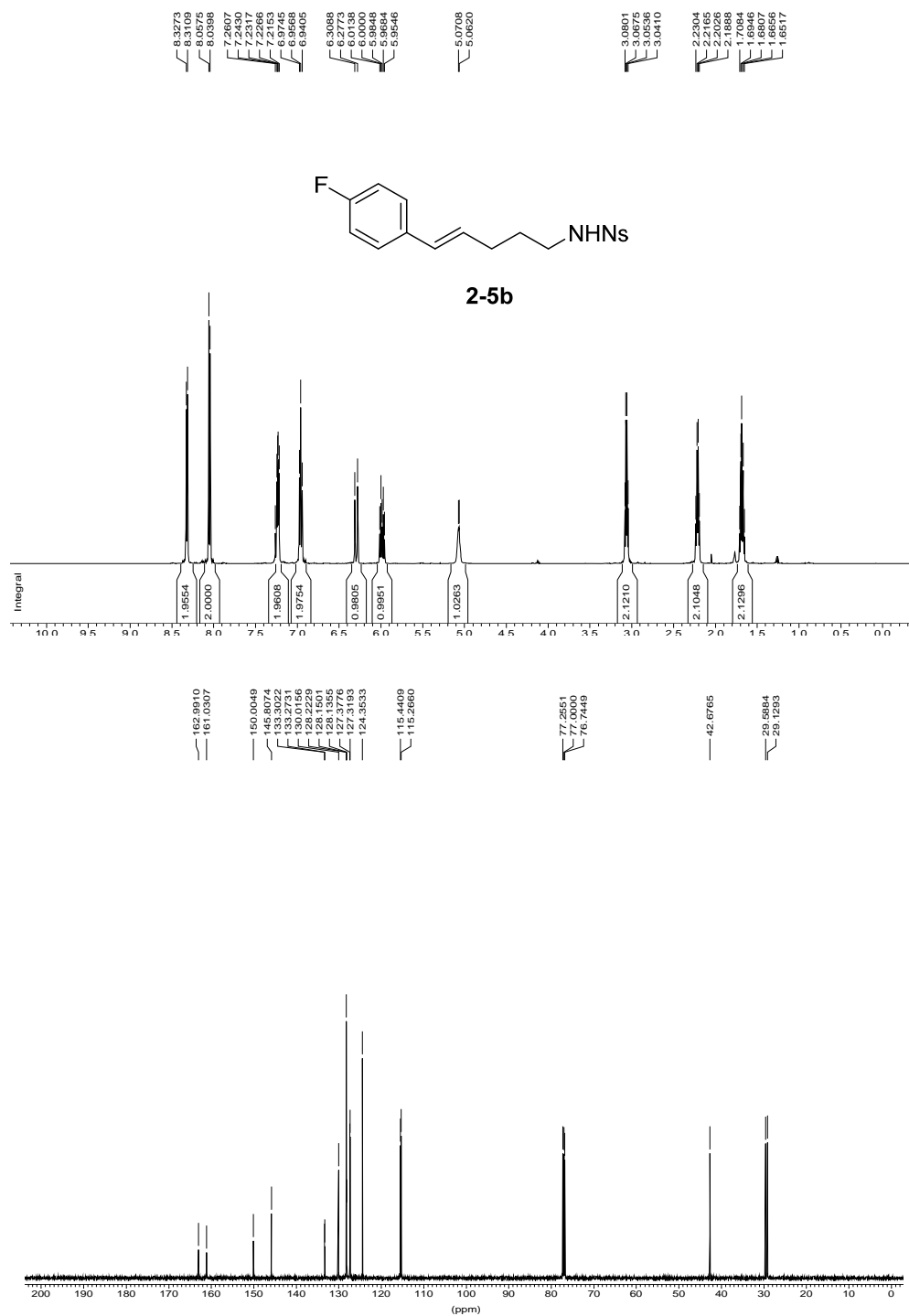
5.5 References

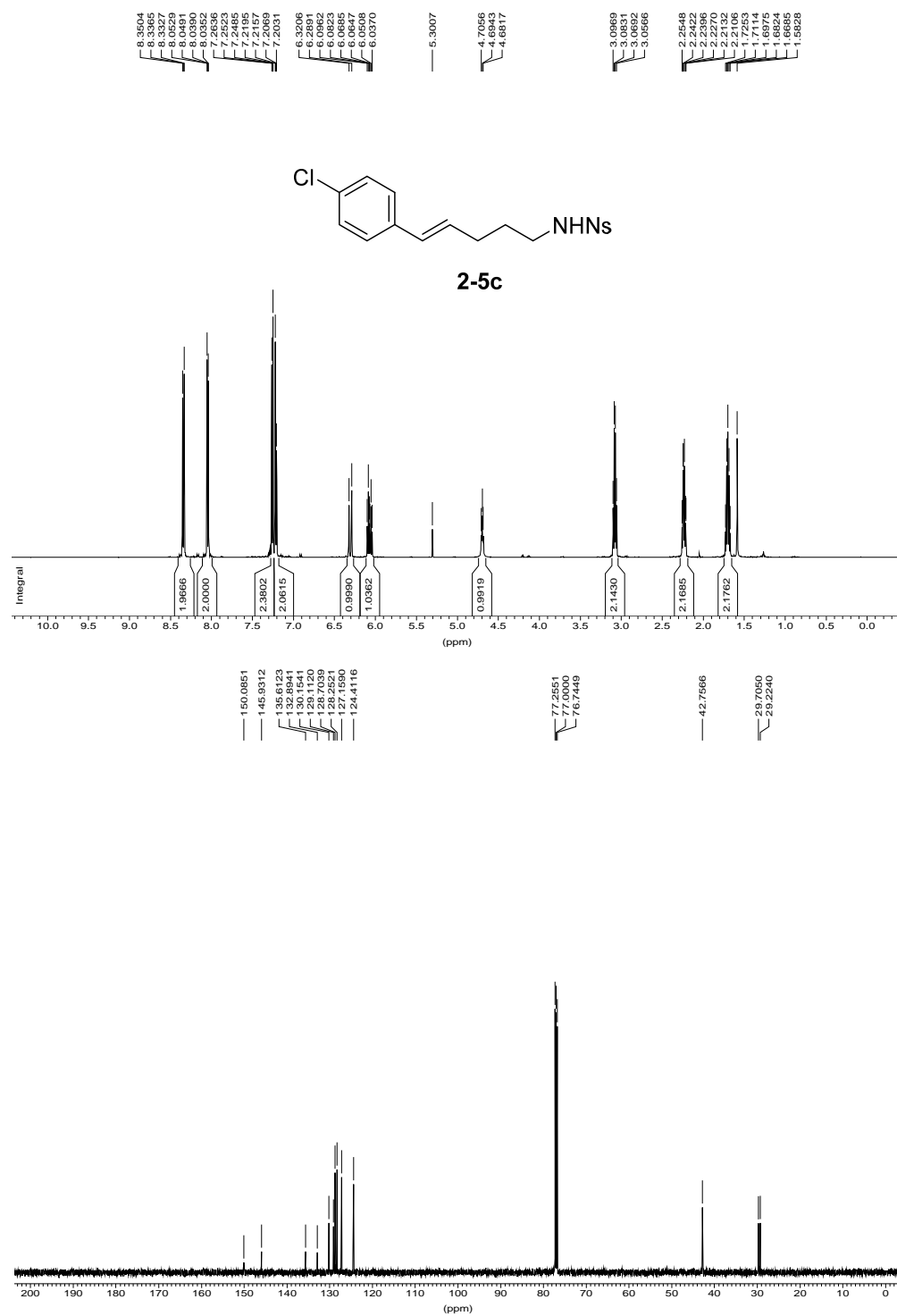
1. (a) Zhou, L.; Tan, C. K.; Jiang, X.; Chen, F.; Yeung, Y.-Y., *J. Am. Chem. Soc.* **2010**, *132*, 15474; (b) Tan, C. K.; Zhou, L.; Yeung, Y.-Y., *Org. Lett.* **2011**, *13*, 2738; (c) Tan, C. K.; Le, C.; Yeung, Y.-Y., *Chem. Commun.* **2012**, *48*, 5793.
2. (a) Zhou, L.; Chen, J.; Tan, C. K.; Yeung, Y.-Y., *J. Am. Chem. Soc.* **2011**, *133*, 9164; (b) Zhou, L.; Tay, D. W.; Chen, J.; Leung, G. Y. C.; Yeung, Y.-Y., *Chemical Communications* **2013**, *49*, 4412.
3. J. Bejjani; F. Chemla; M. Audouin, *J. Org. Chem.* **2003**, *68*, 9747.
4. Lloyd-Jones, G. C.; Moseley, J. D.; Renny, J. S., *Synthesis* **2008**, 661.
5. (a) Hackler, R. E.; Balko, T. W., *J. Org. Chem.* **1973**, *38*, 2106; (b) Alajarin, M.; Marin-Luna, M.; Ortin, M.-M.; Sanchez-Andrada, P.; Vidal, A., *Tetrahedron* **2009**, *65*, 2579.

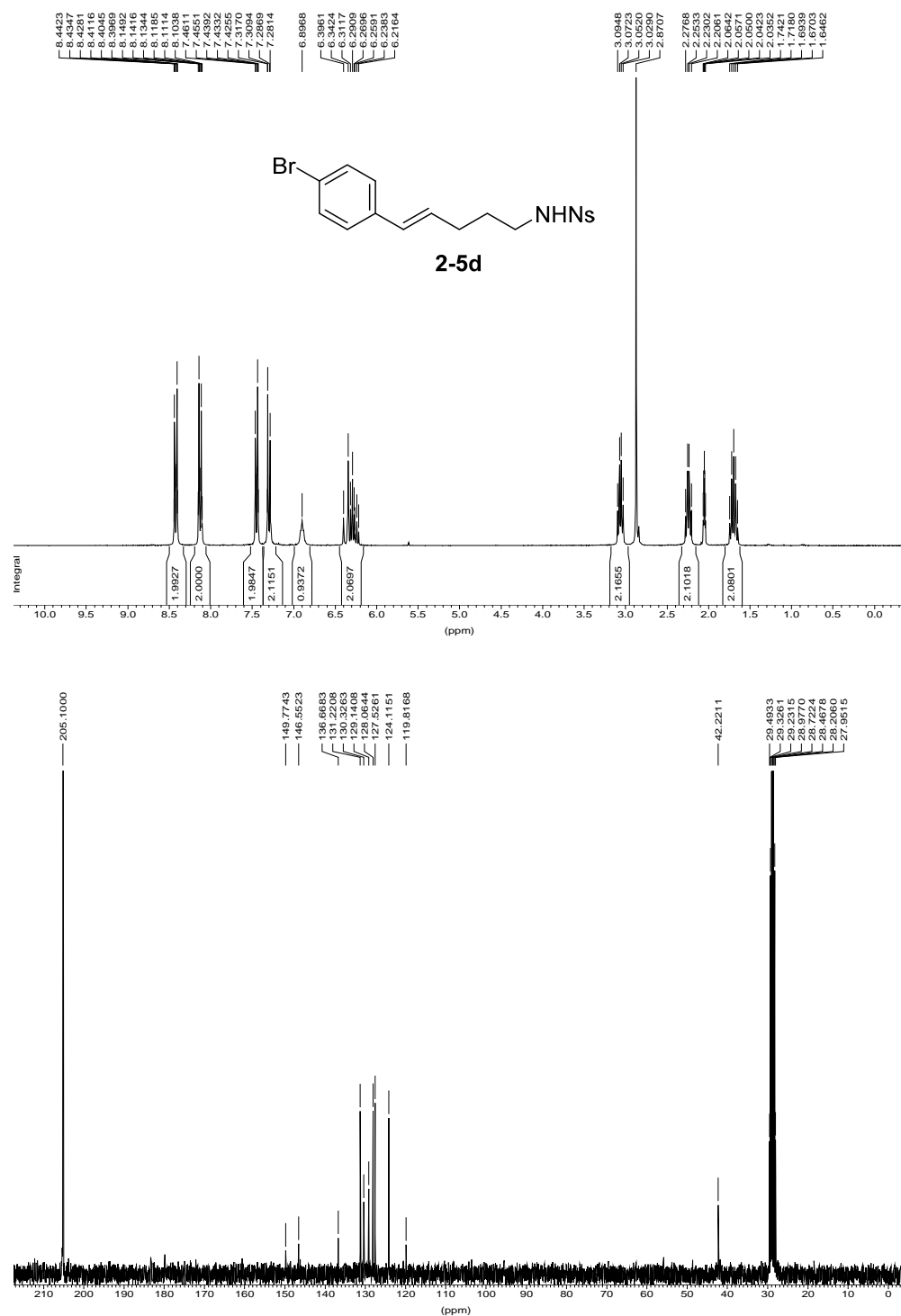
Appendix A

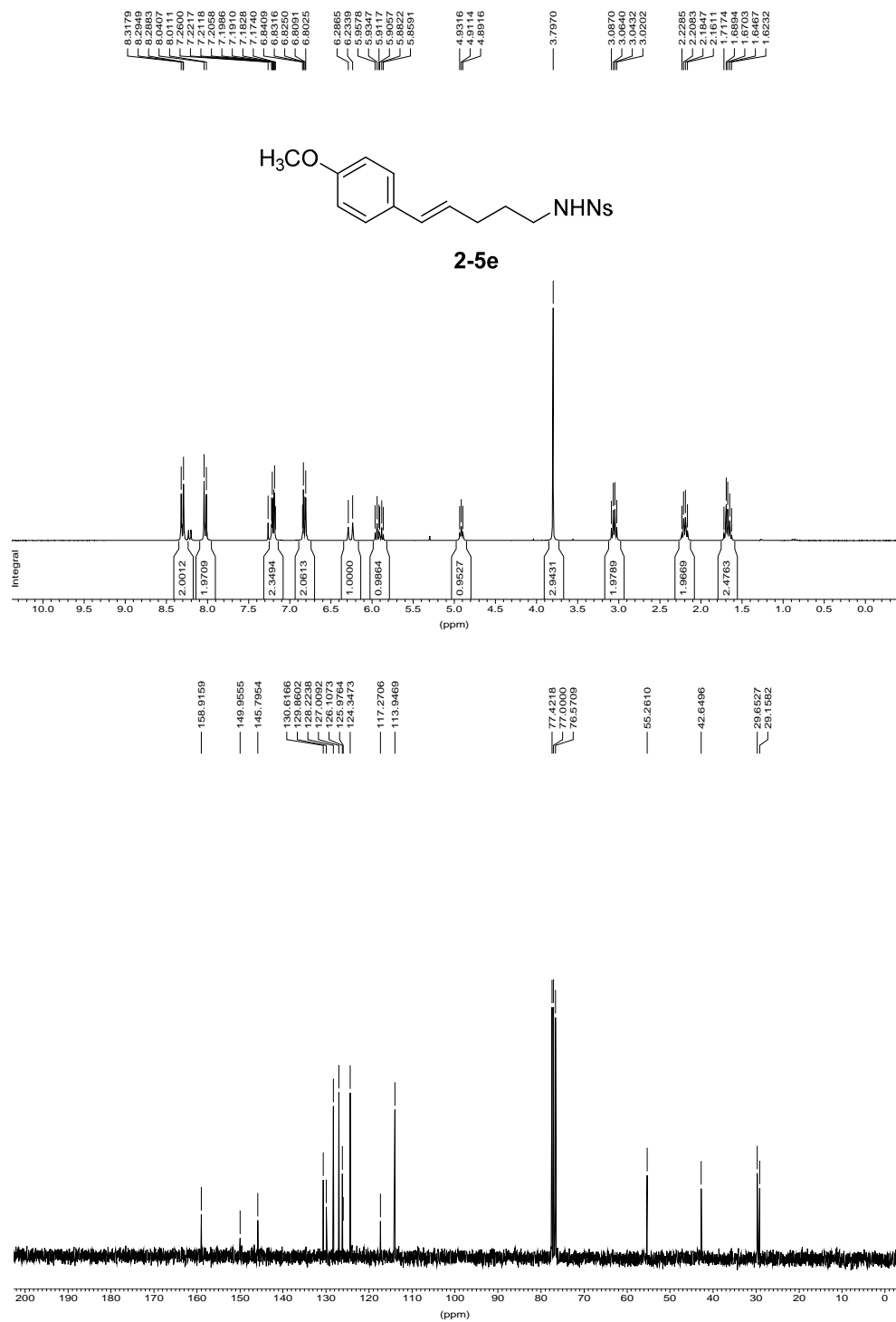
*NMR Spectra of Synthetic Intermediates
and Products of Chapter 2*

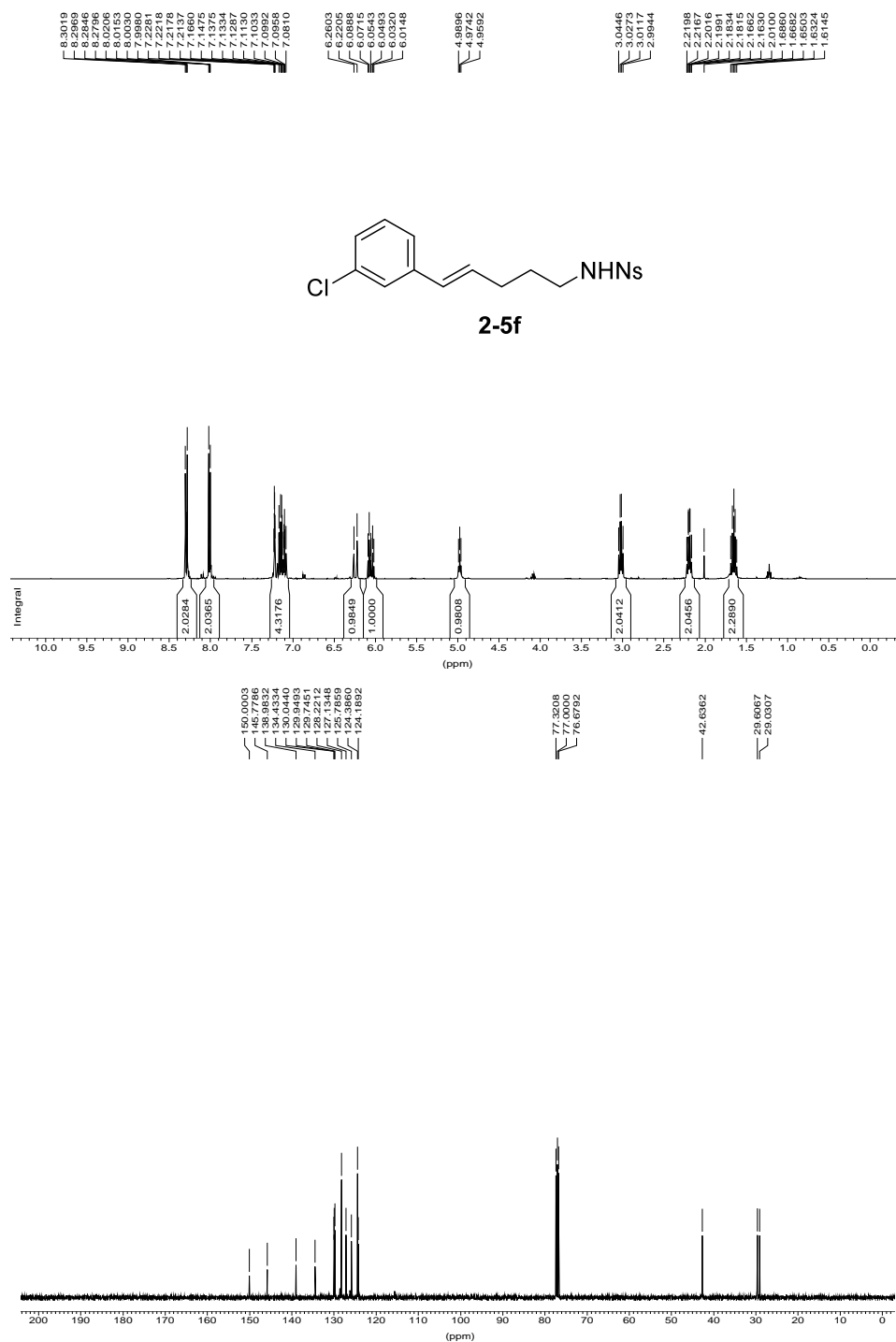


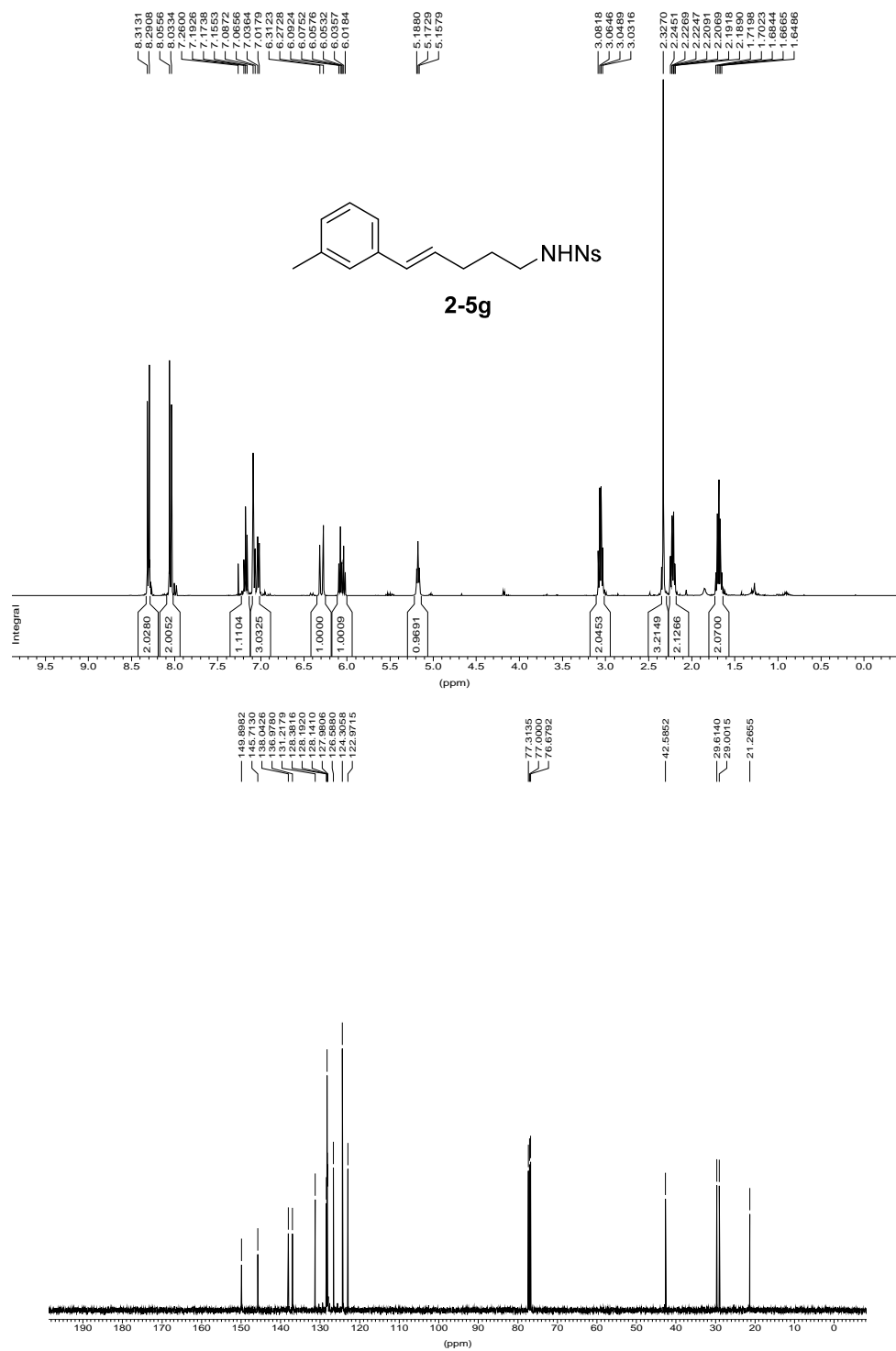


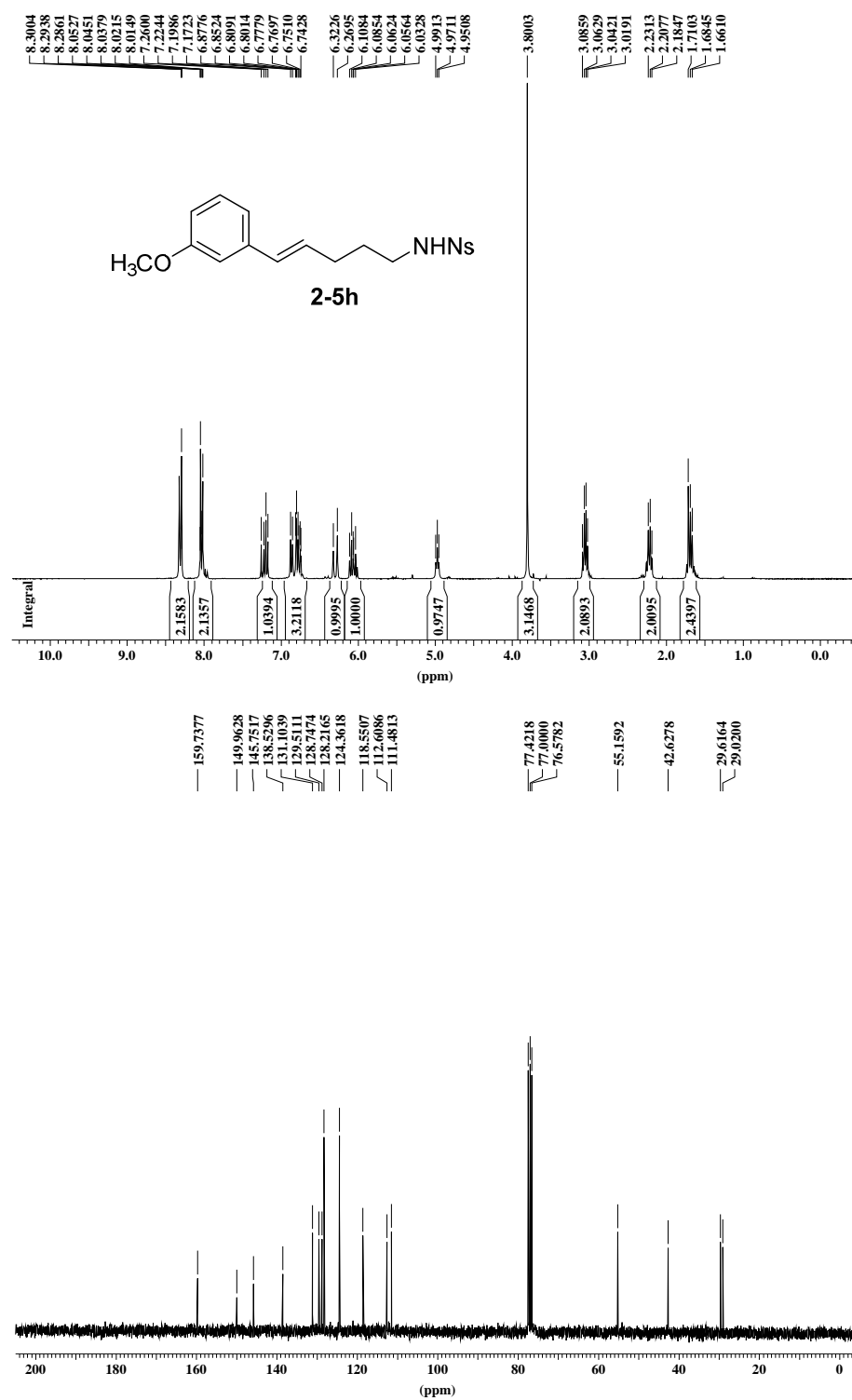


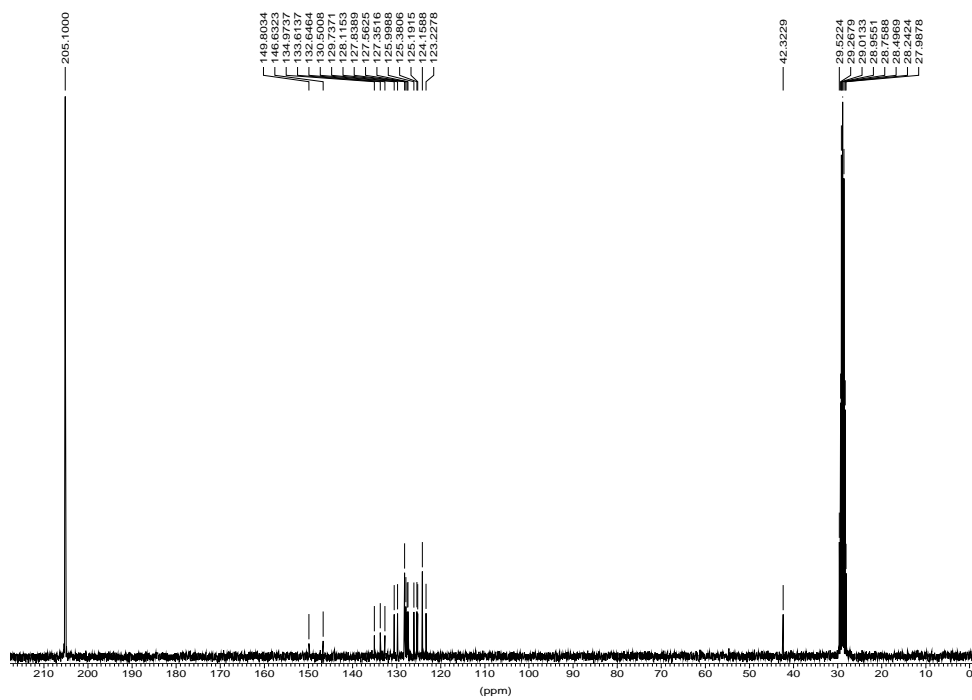
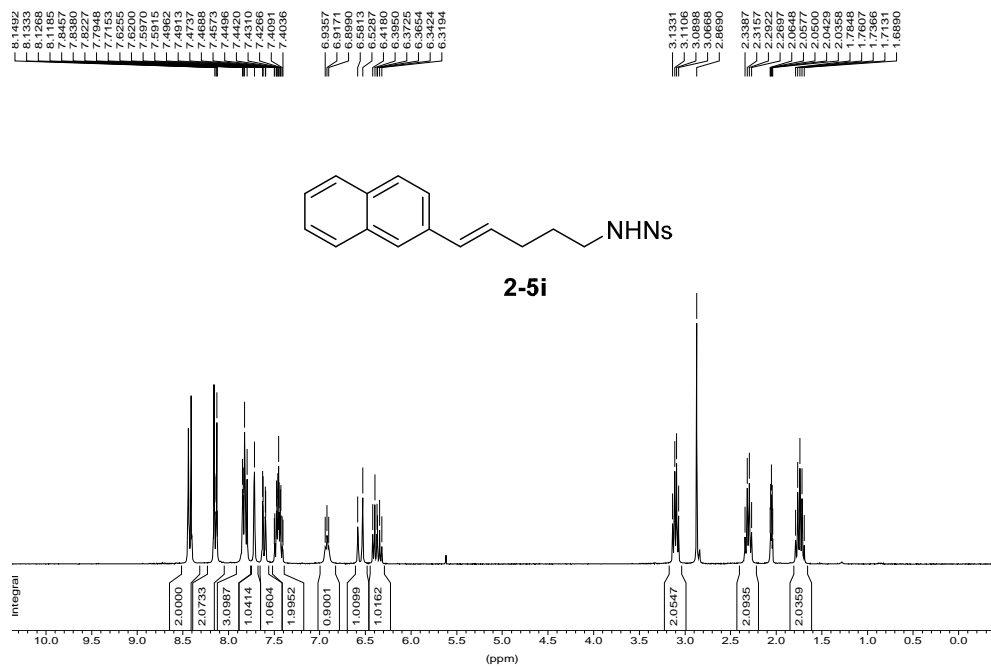


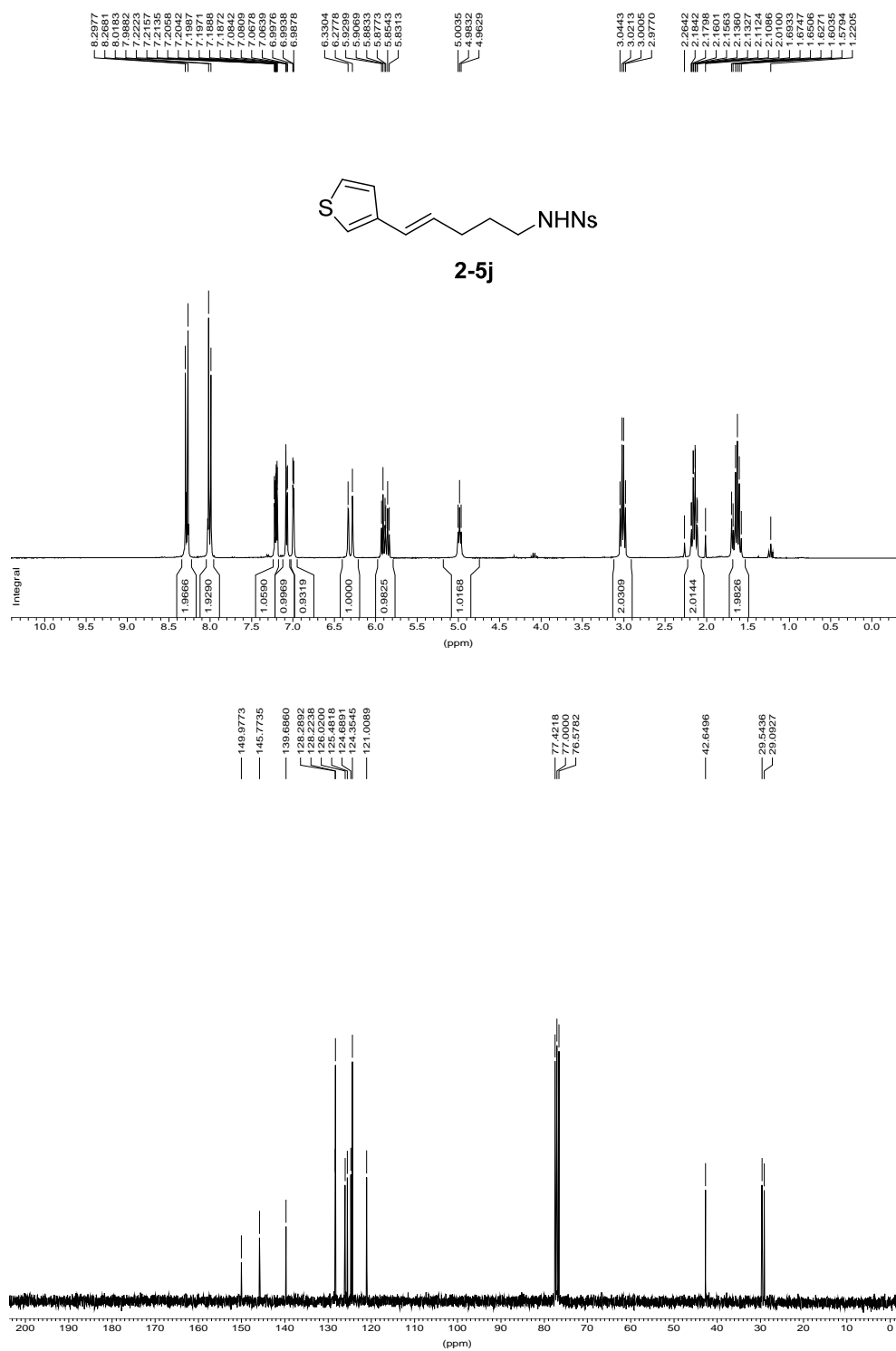


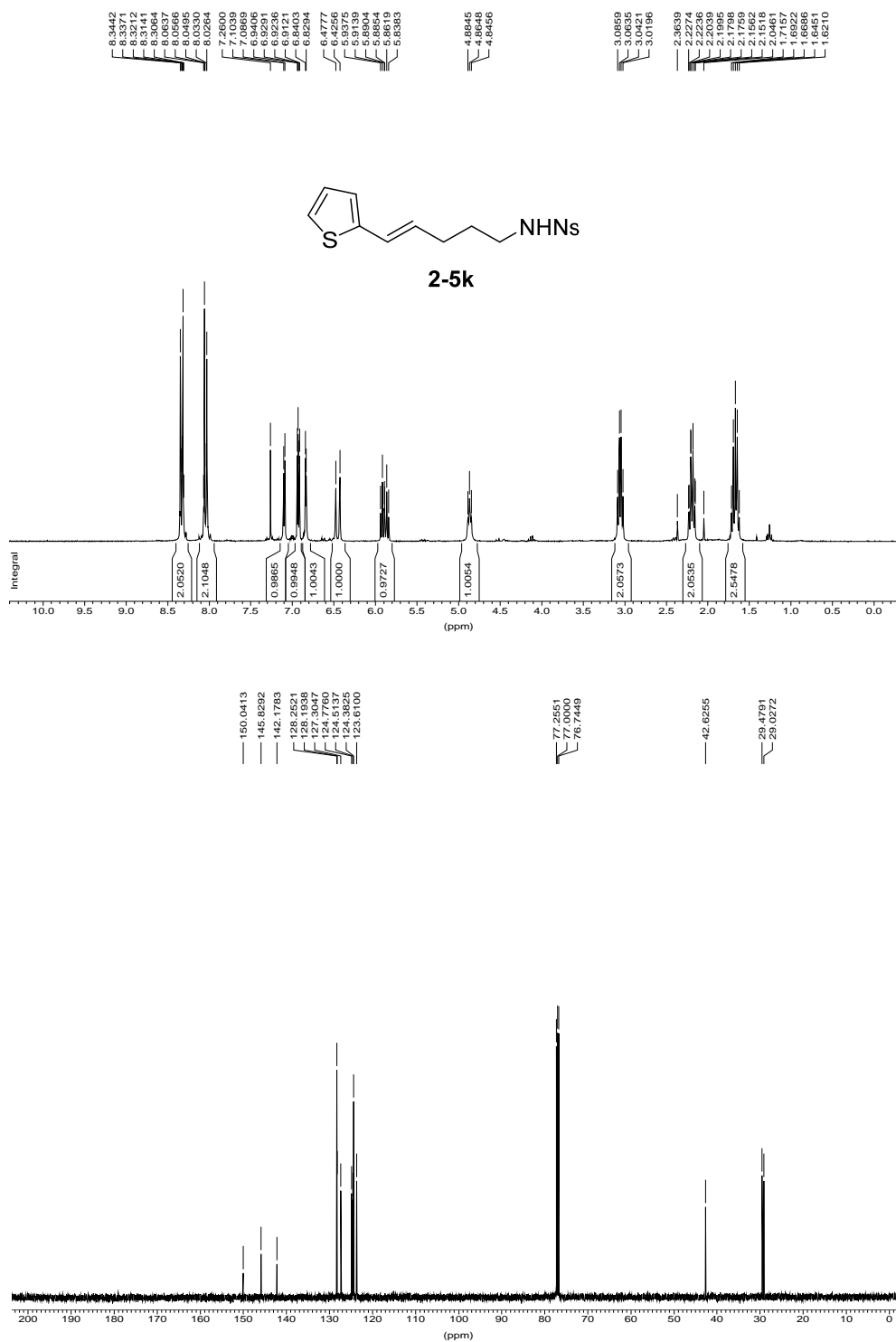


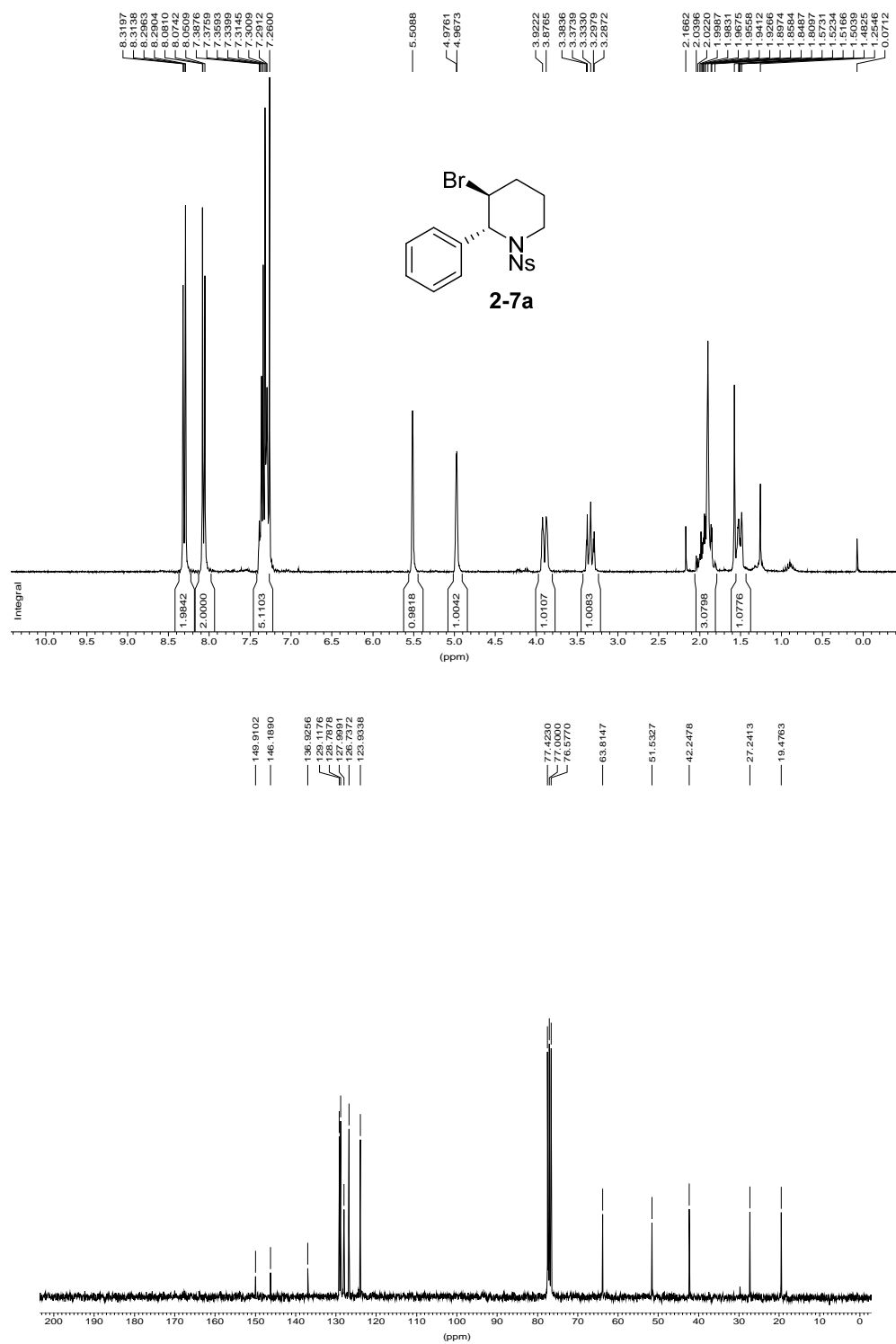


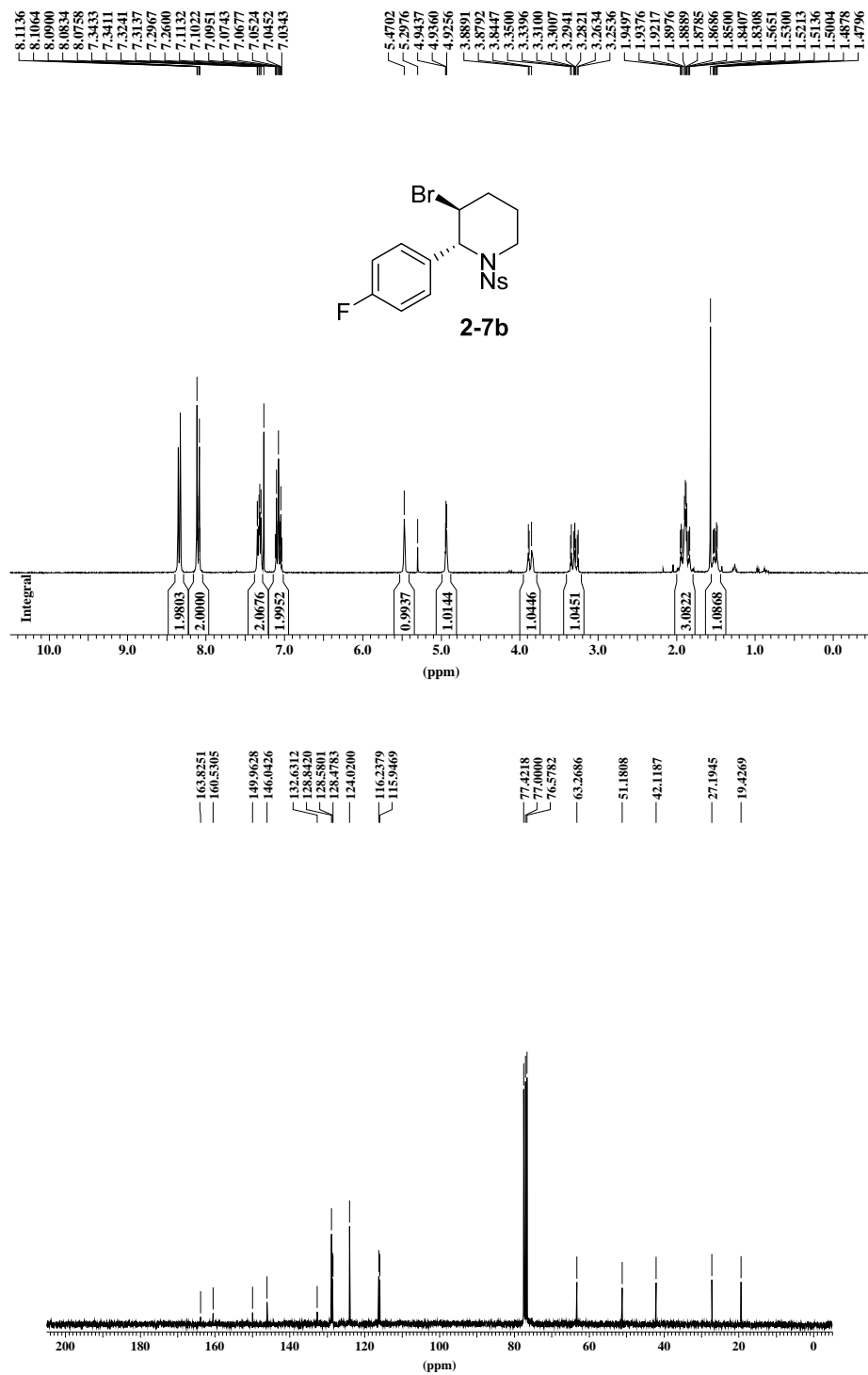


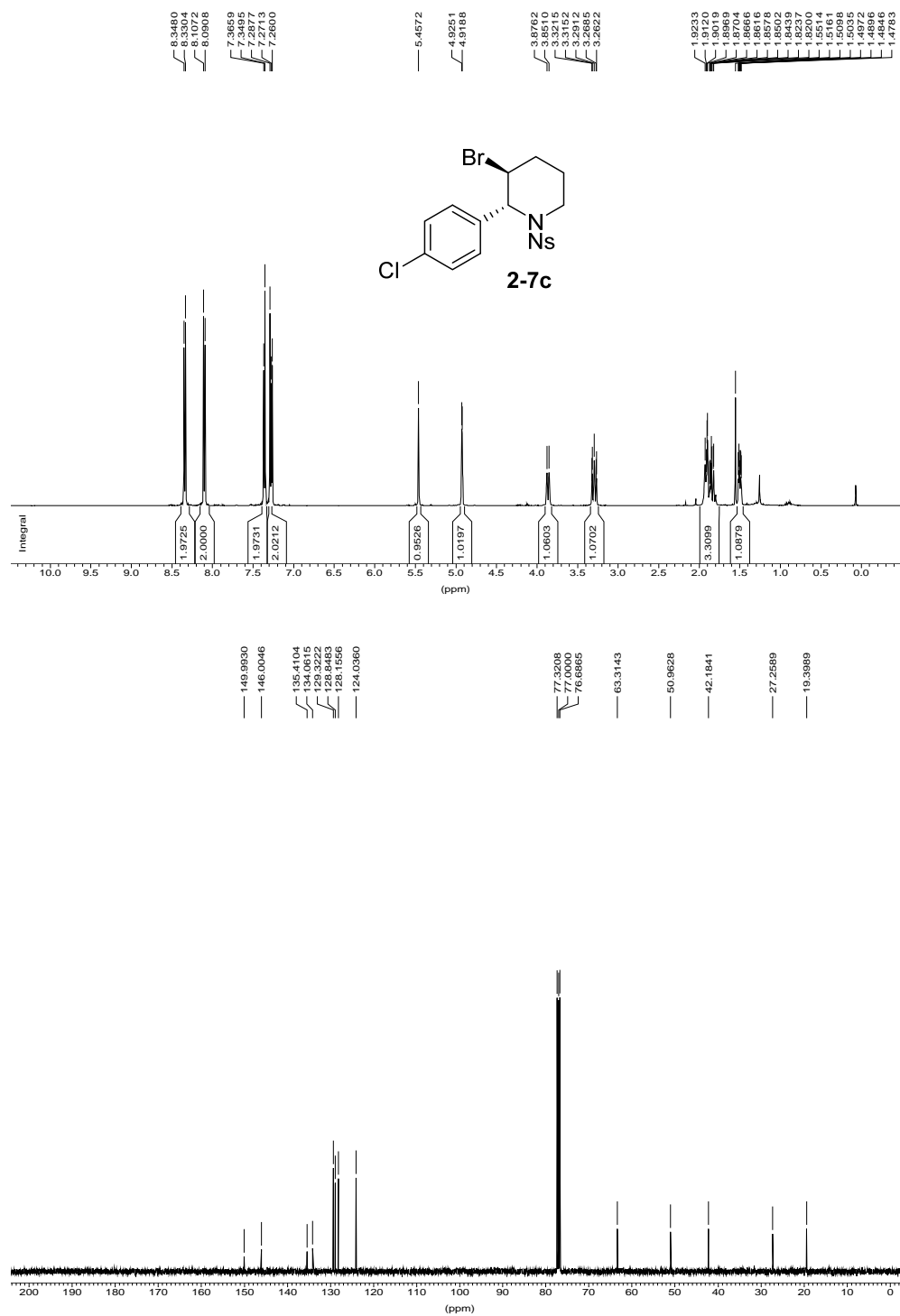


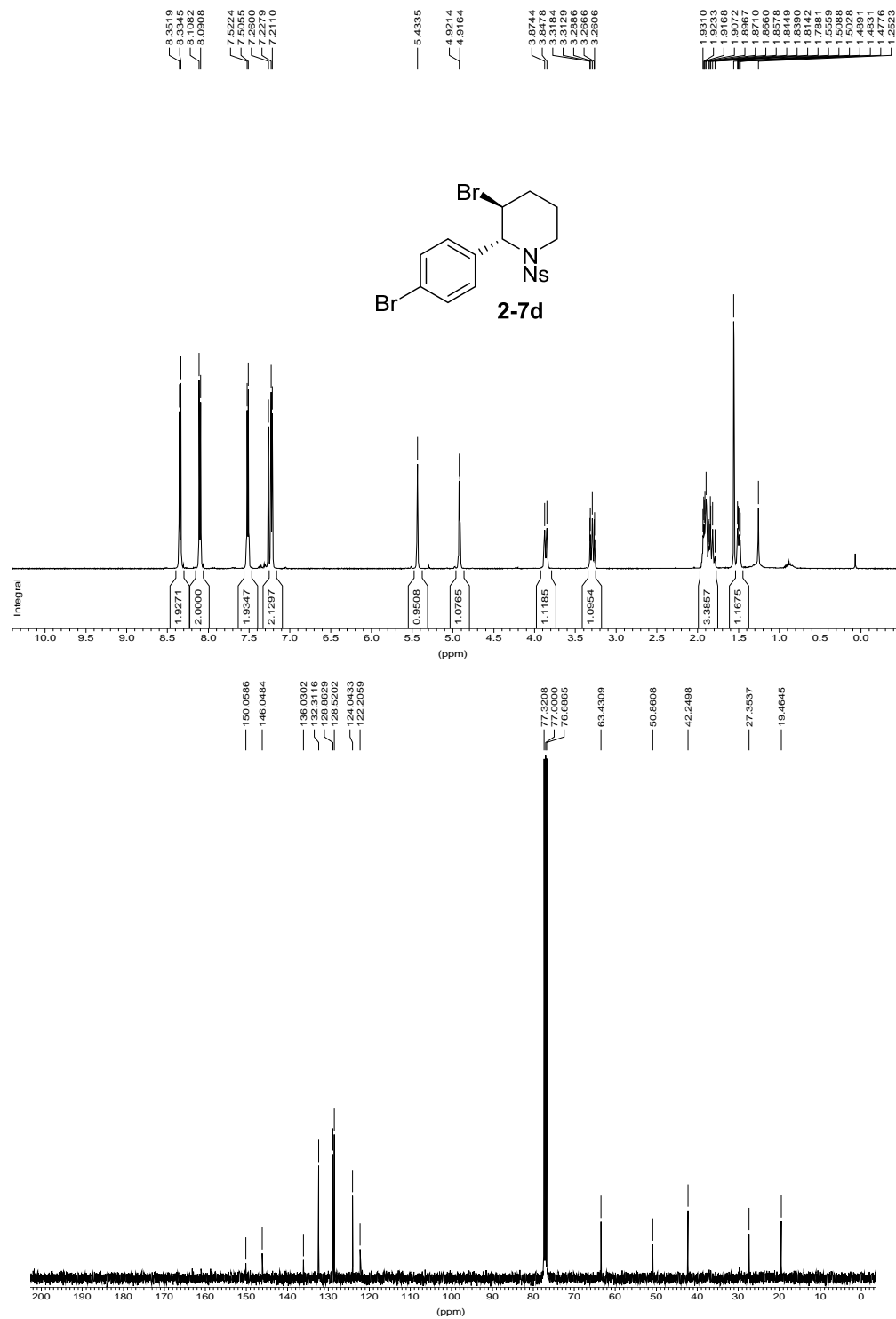


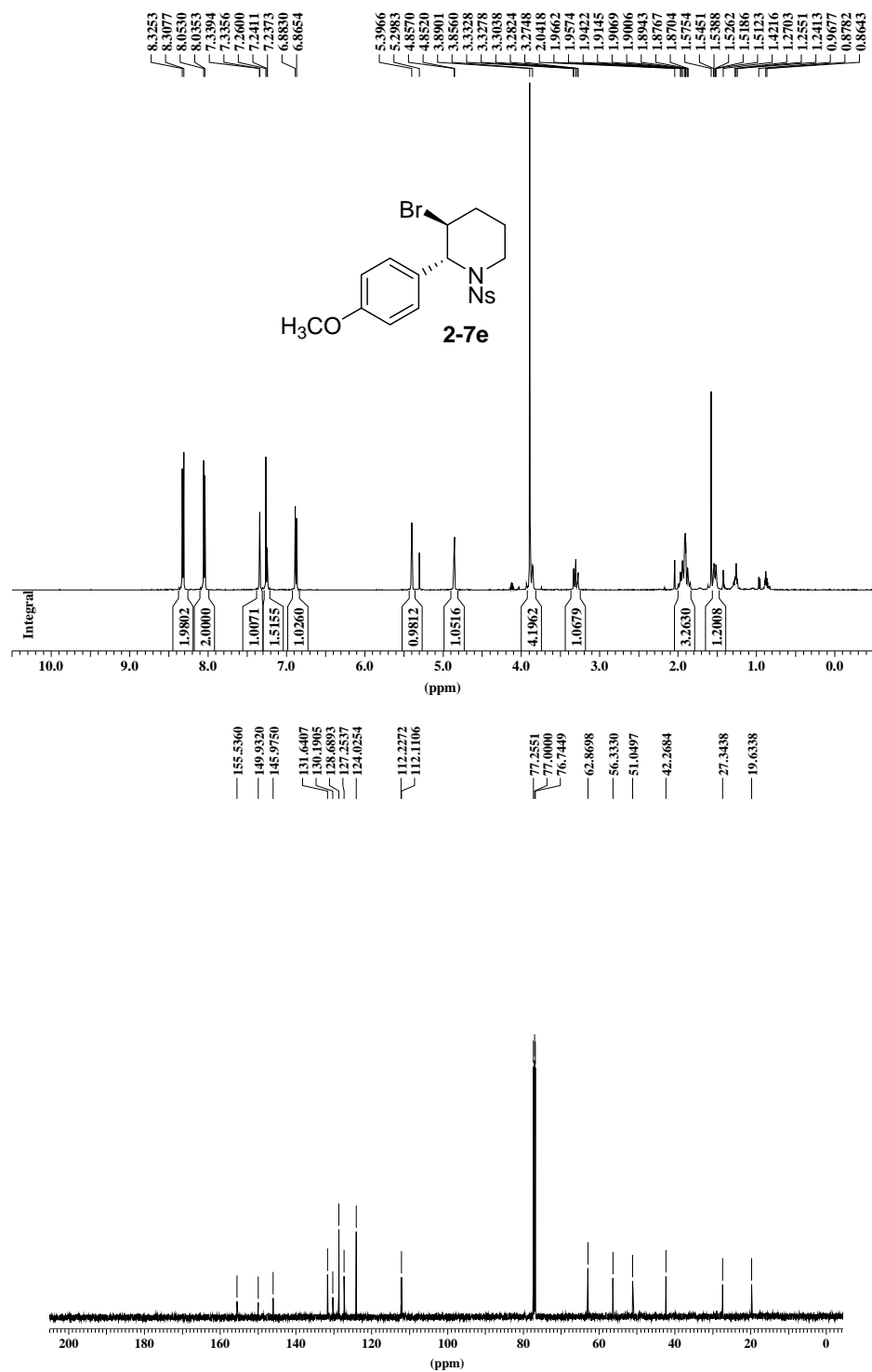


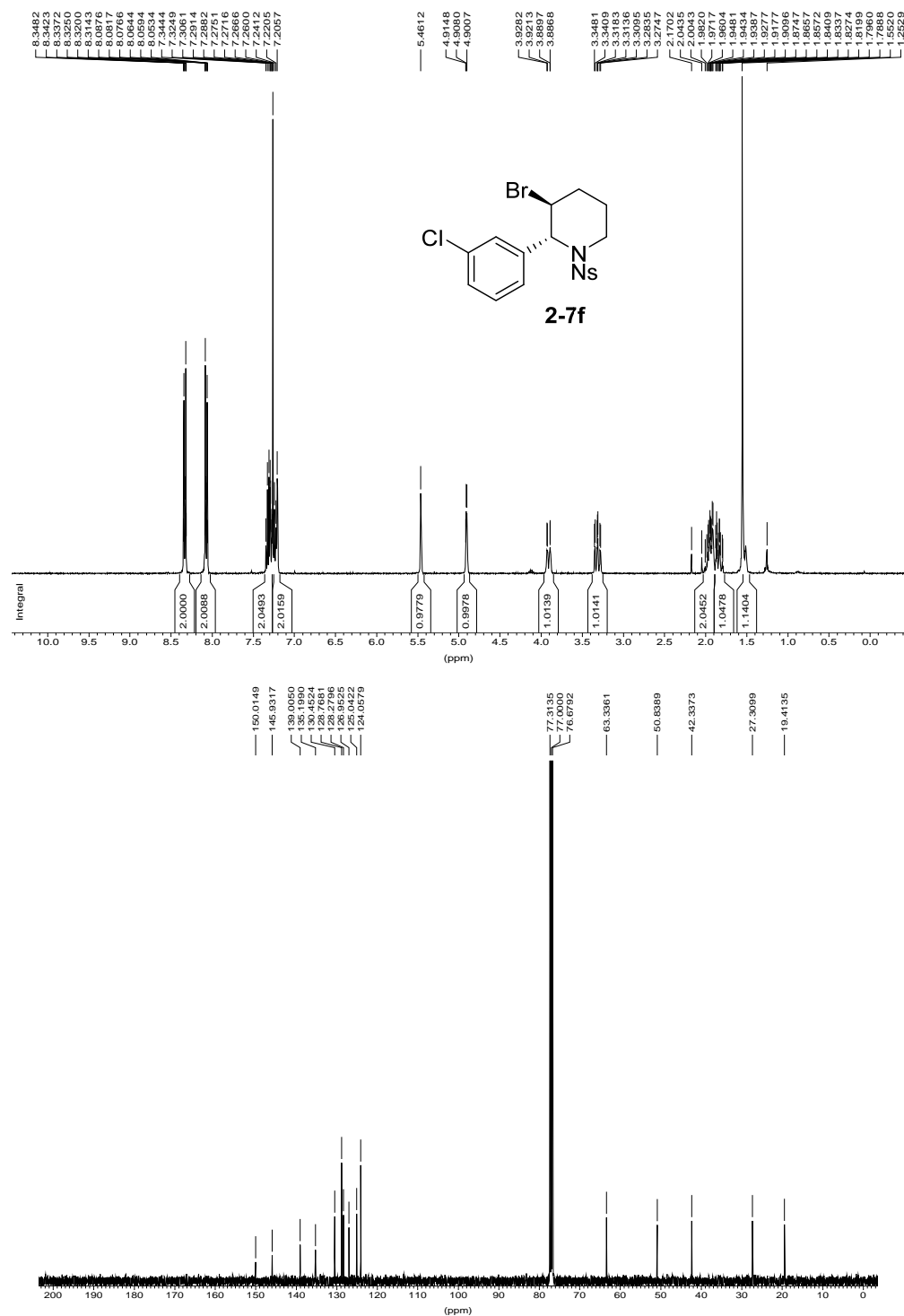


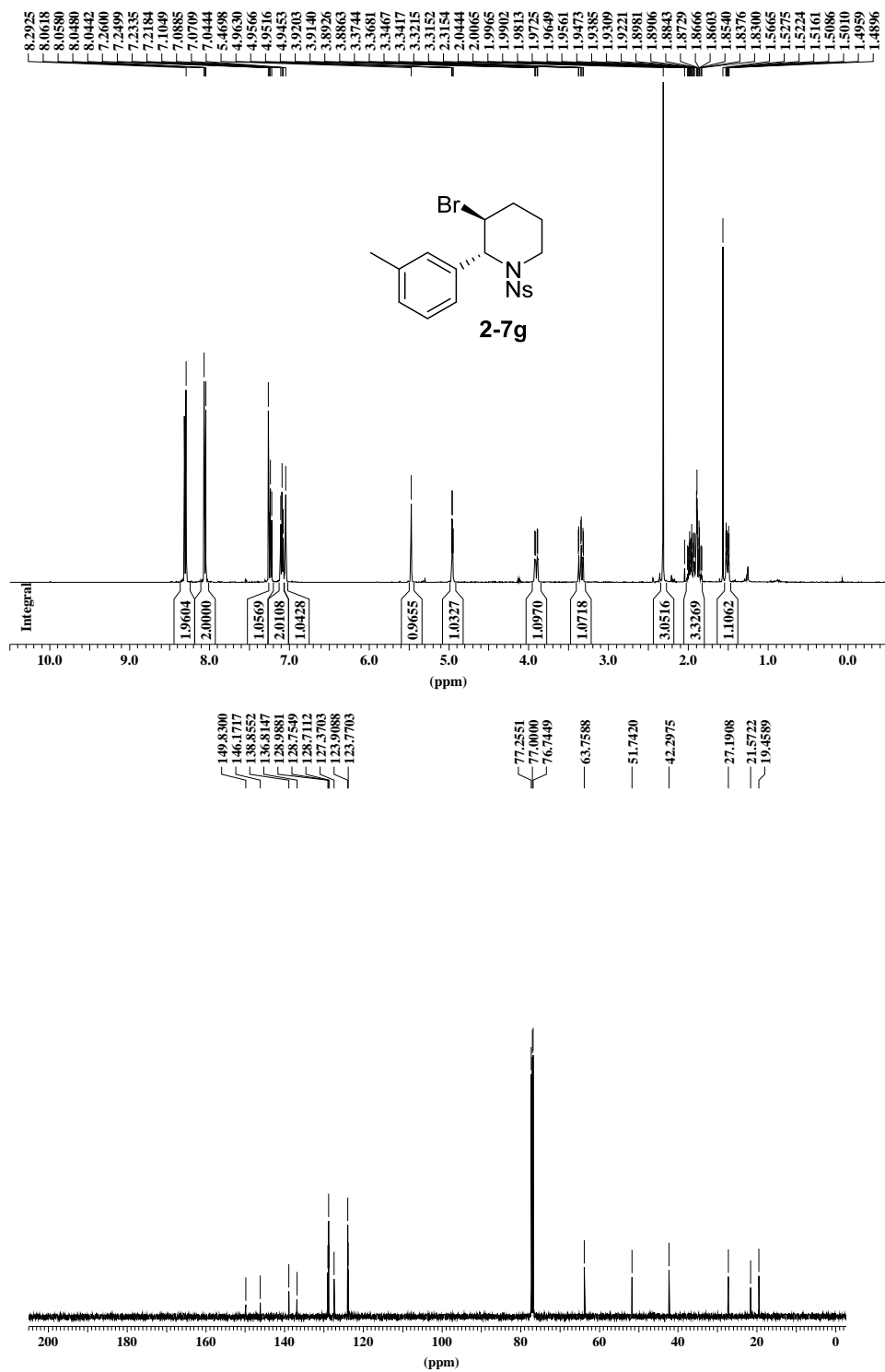


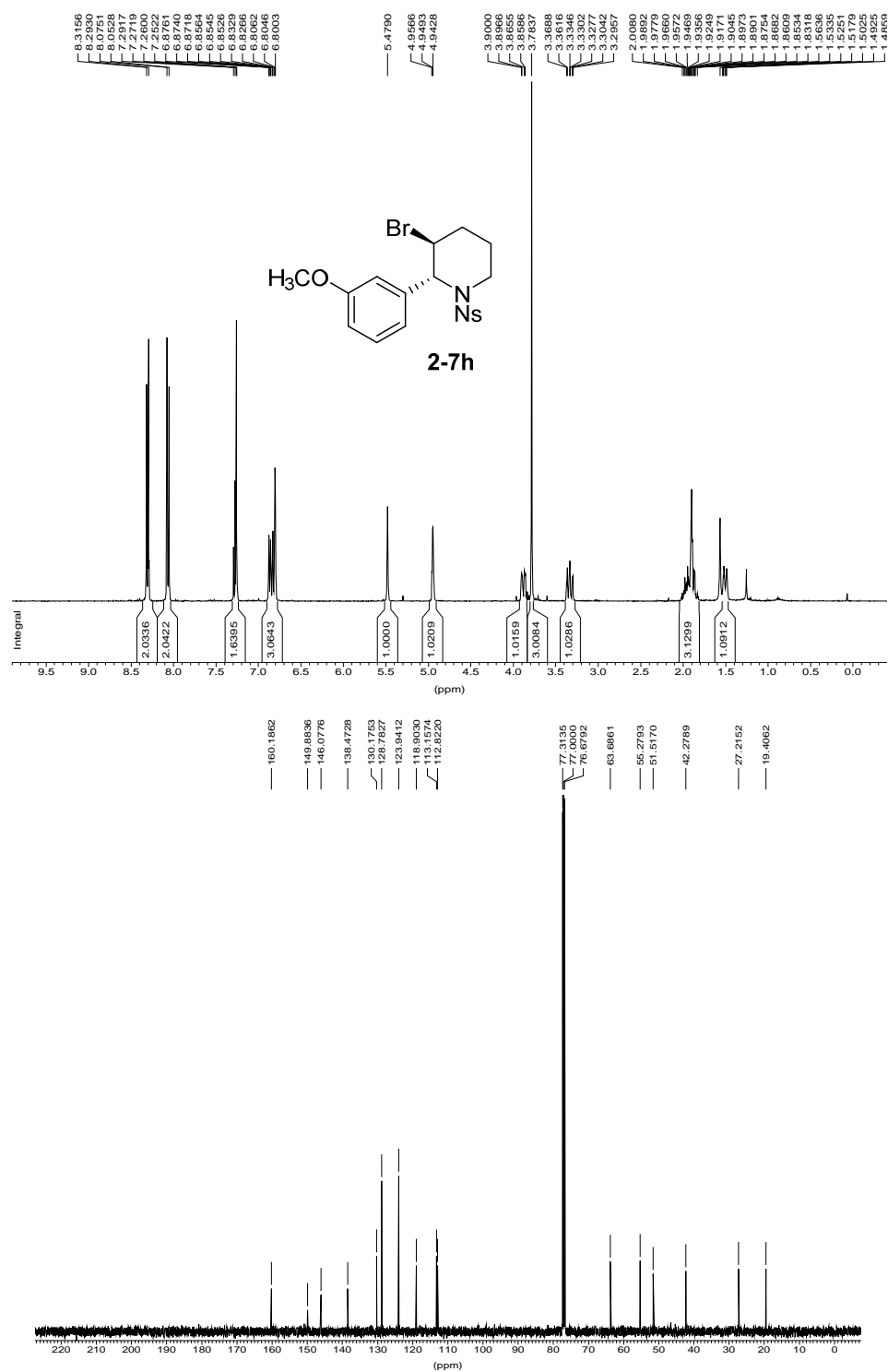


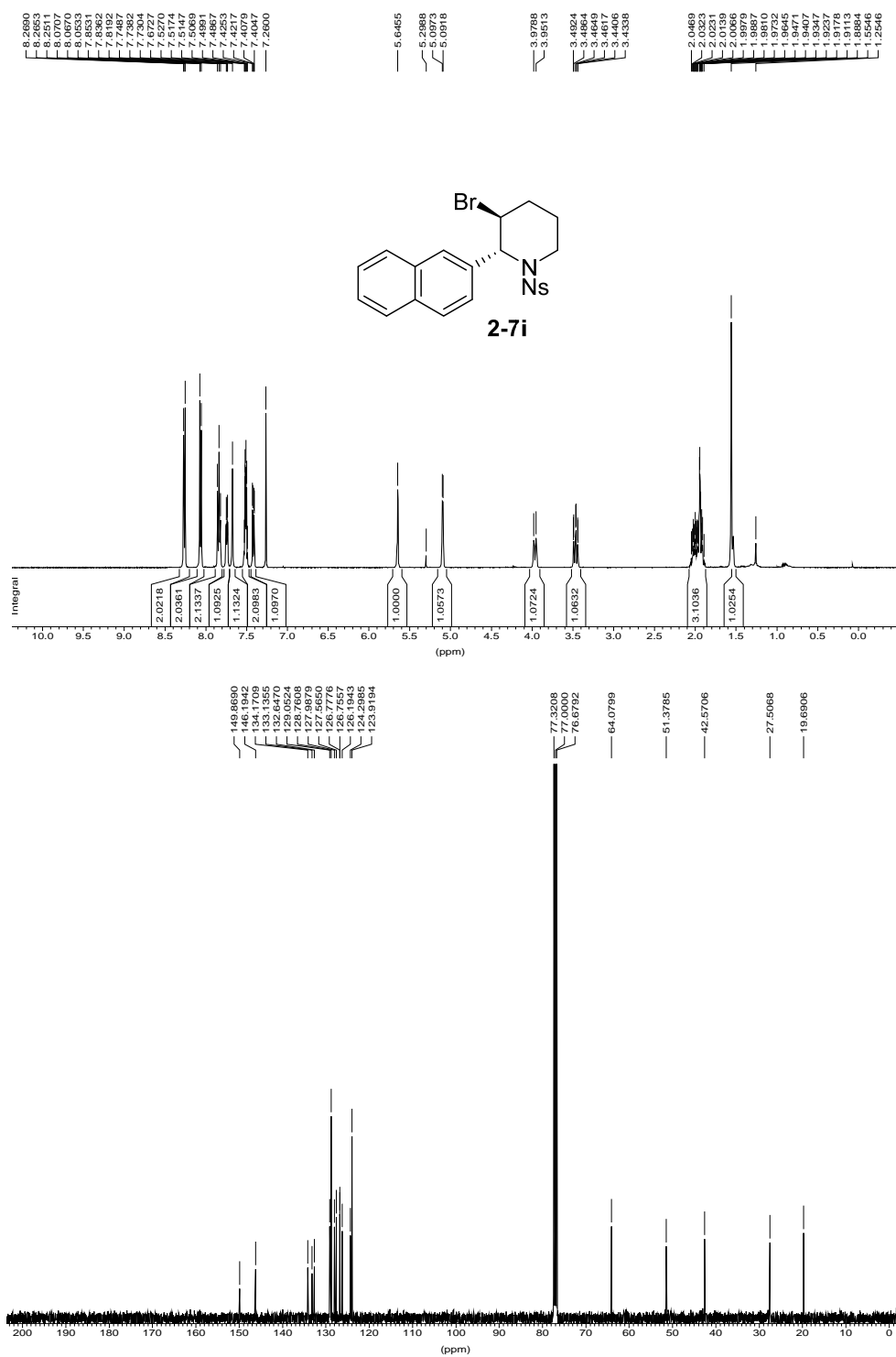


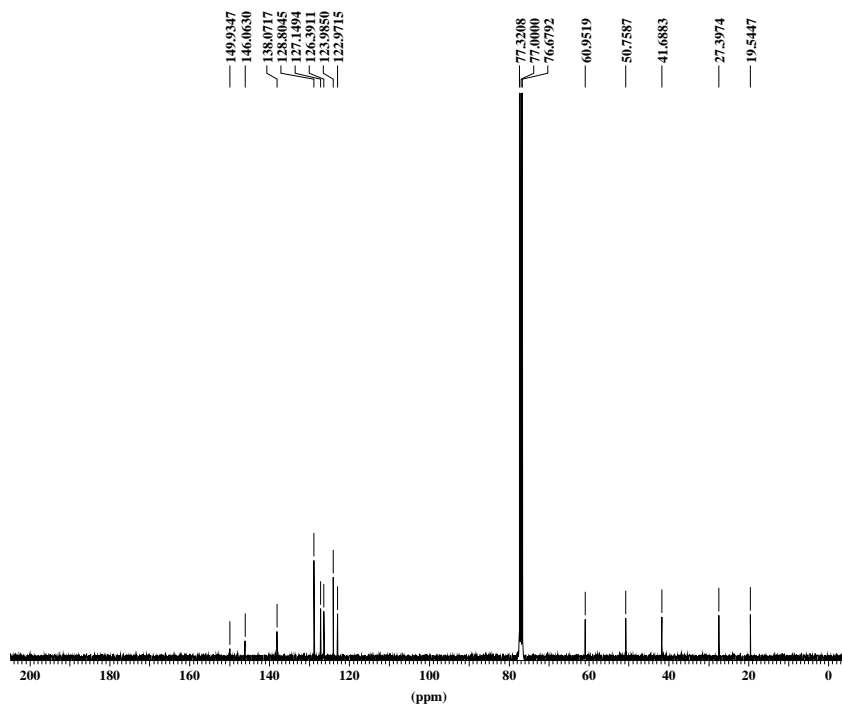
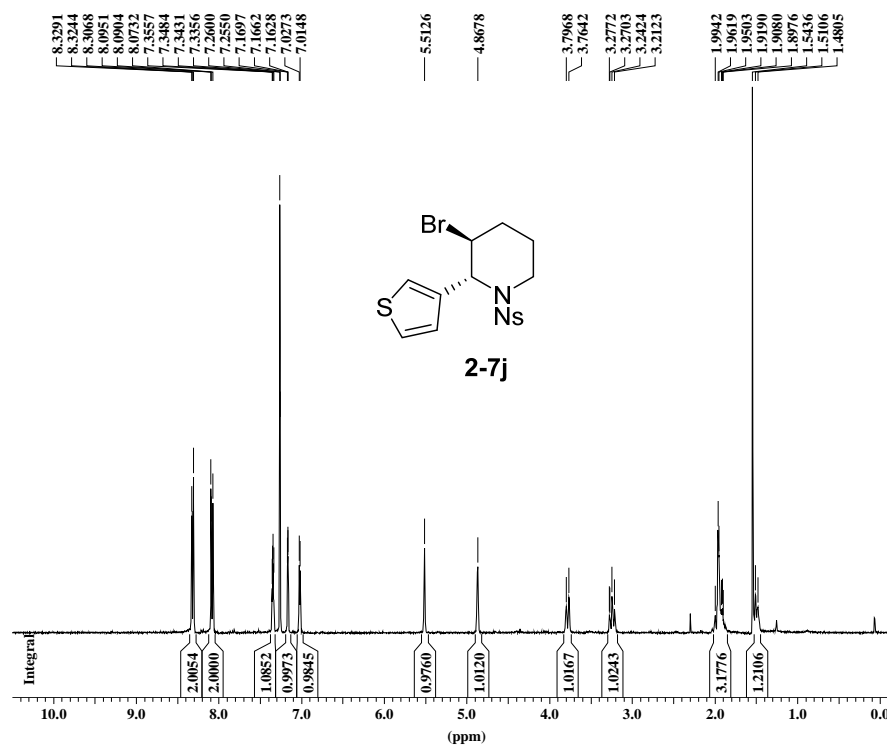


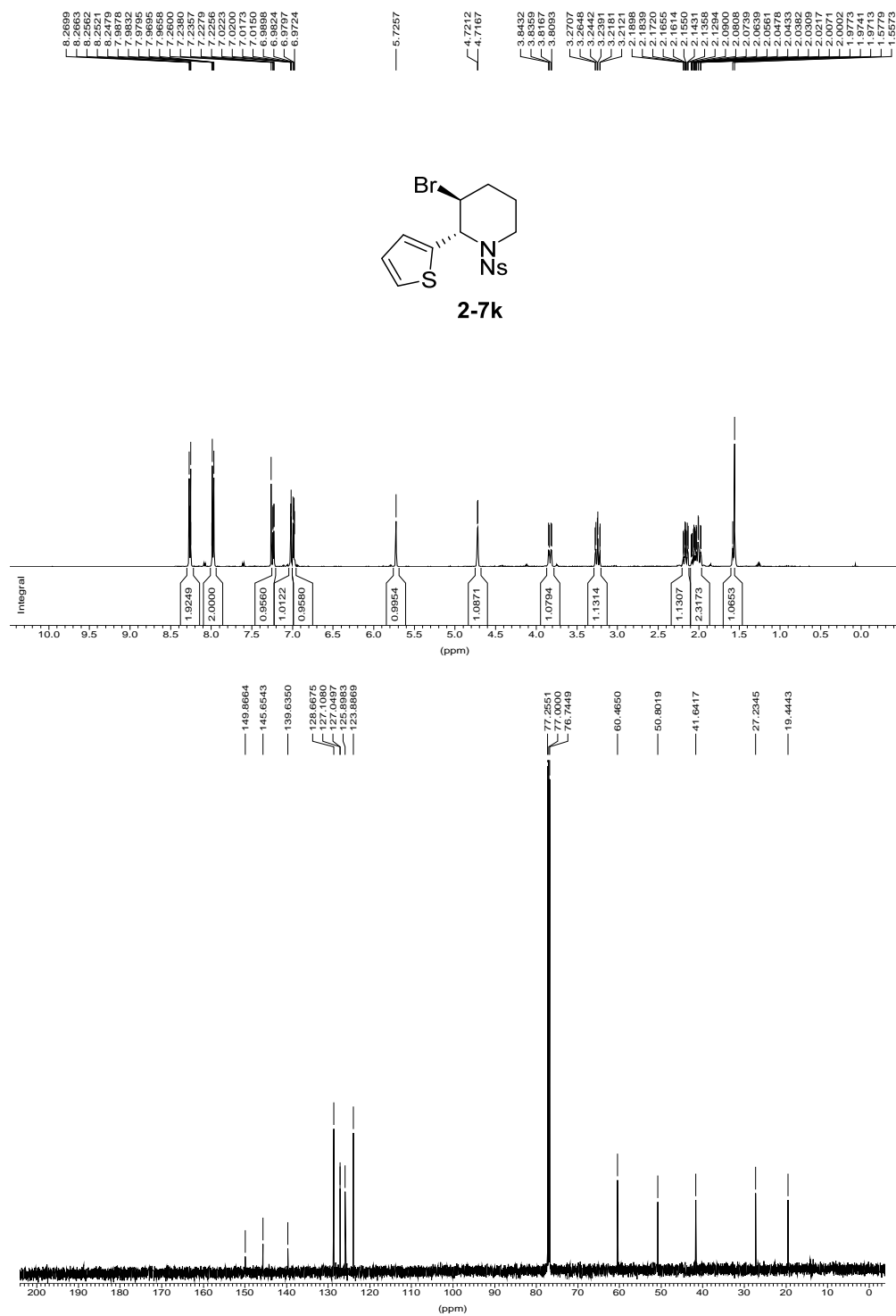


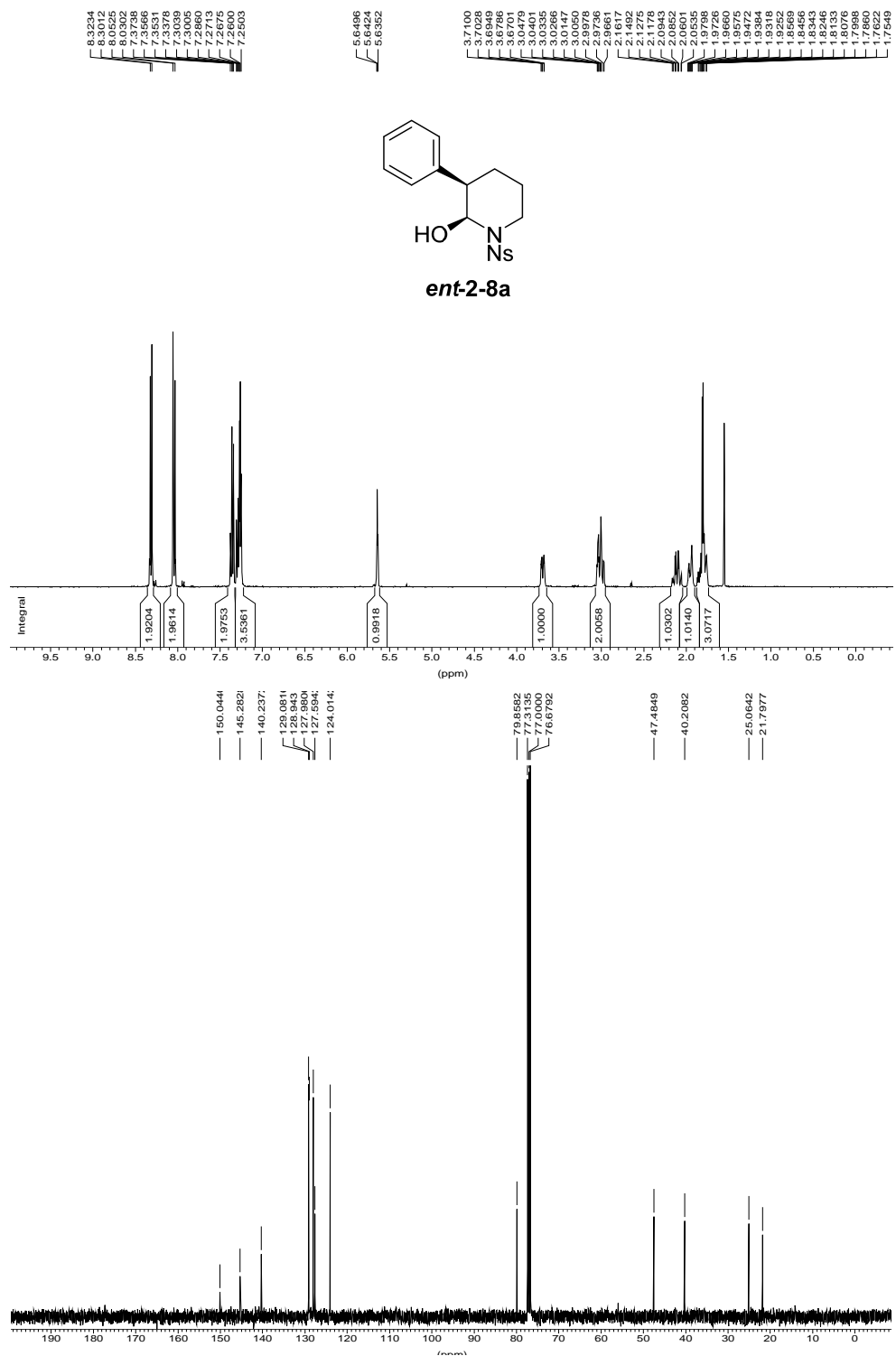


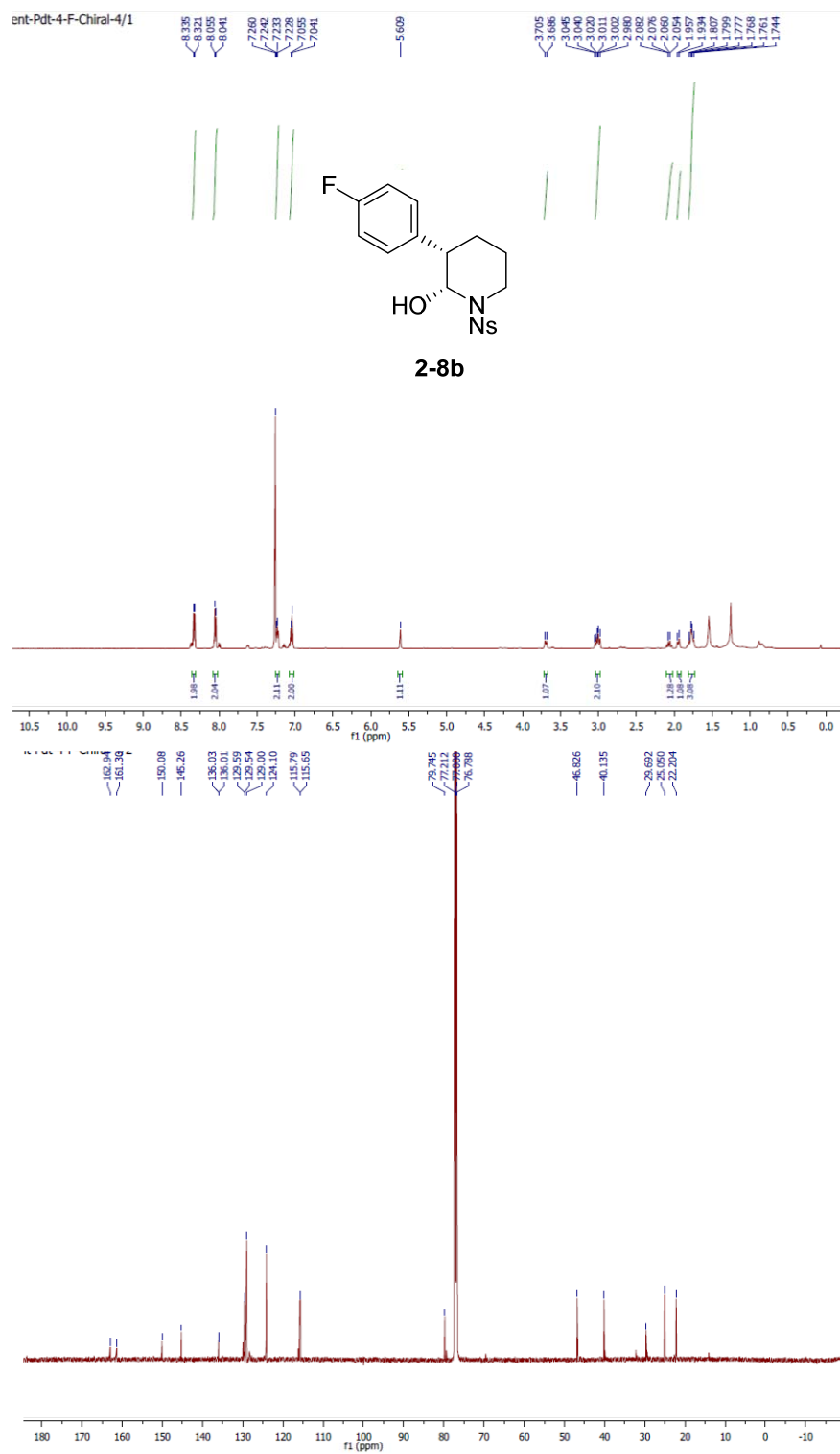


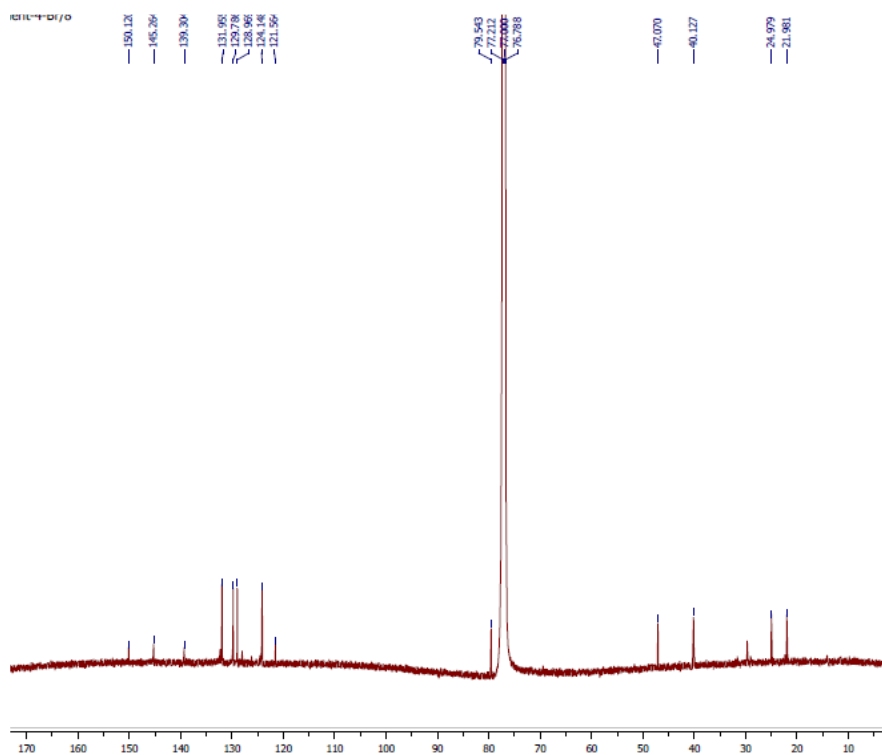
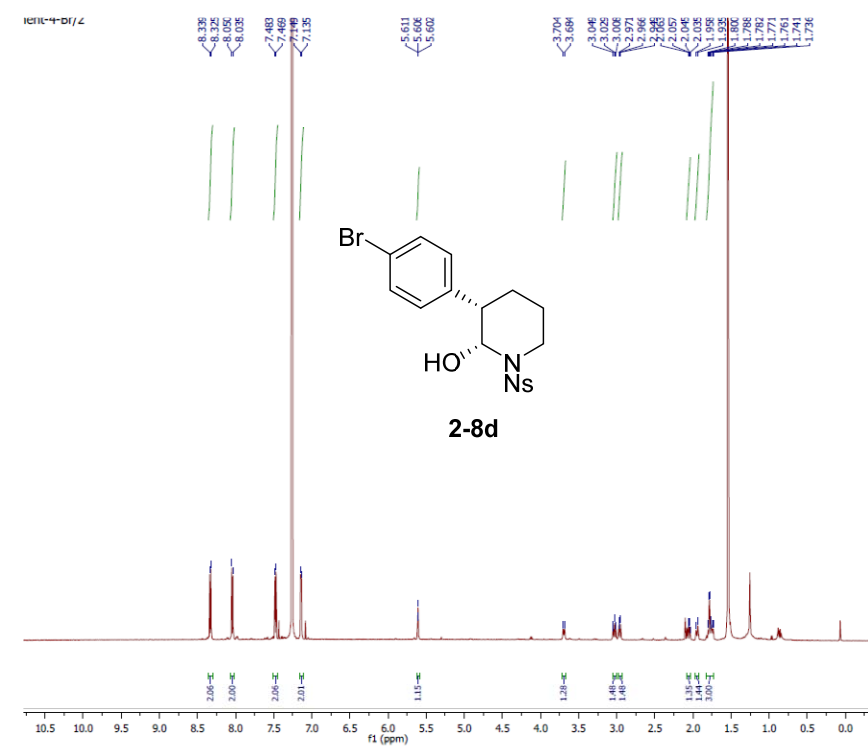


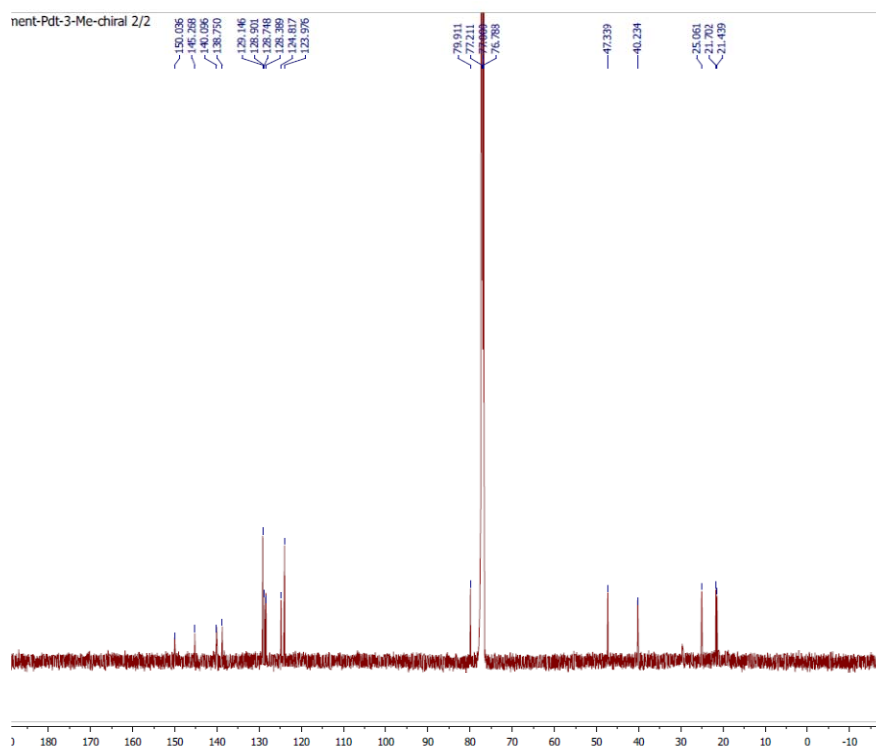
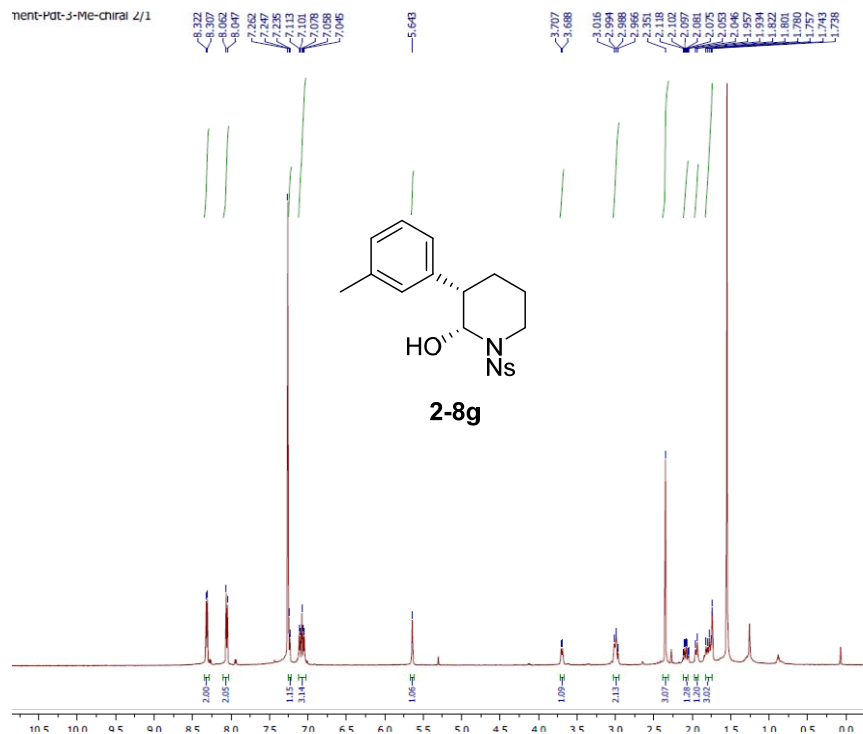


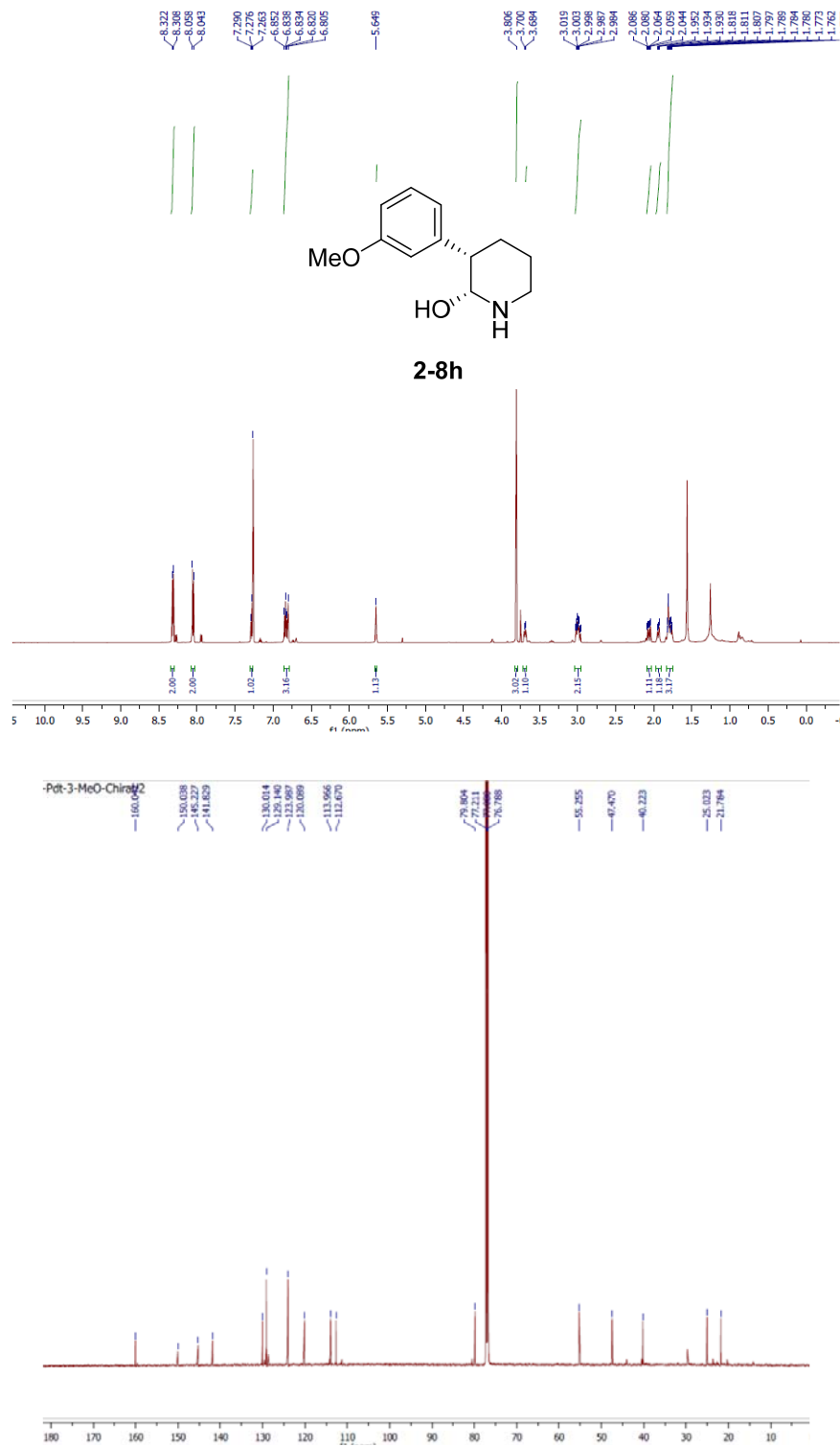


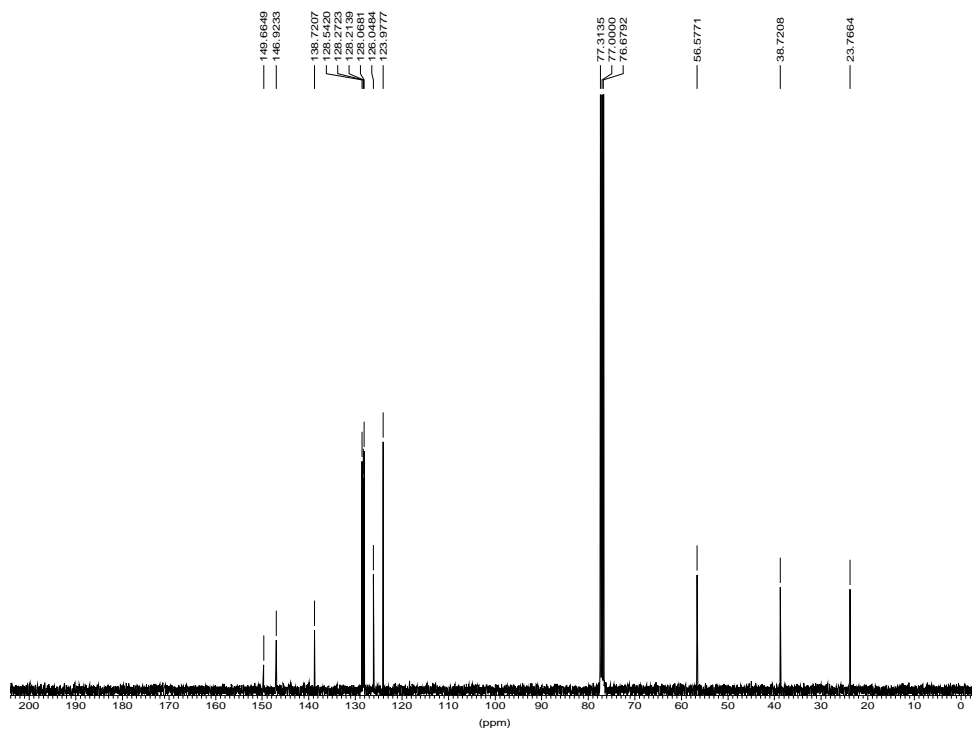
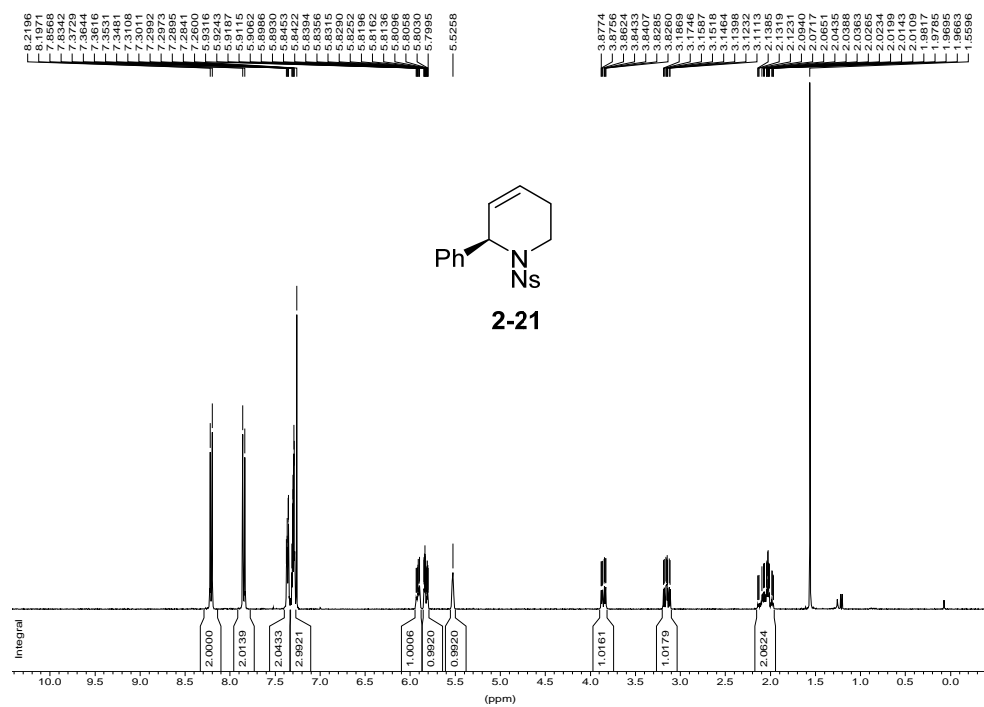


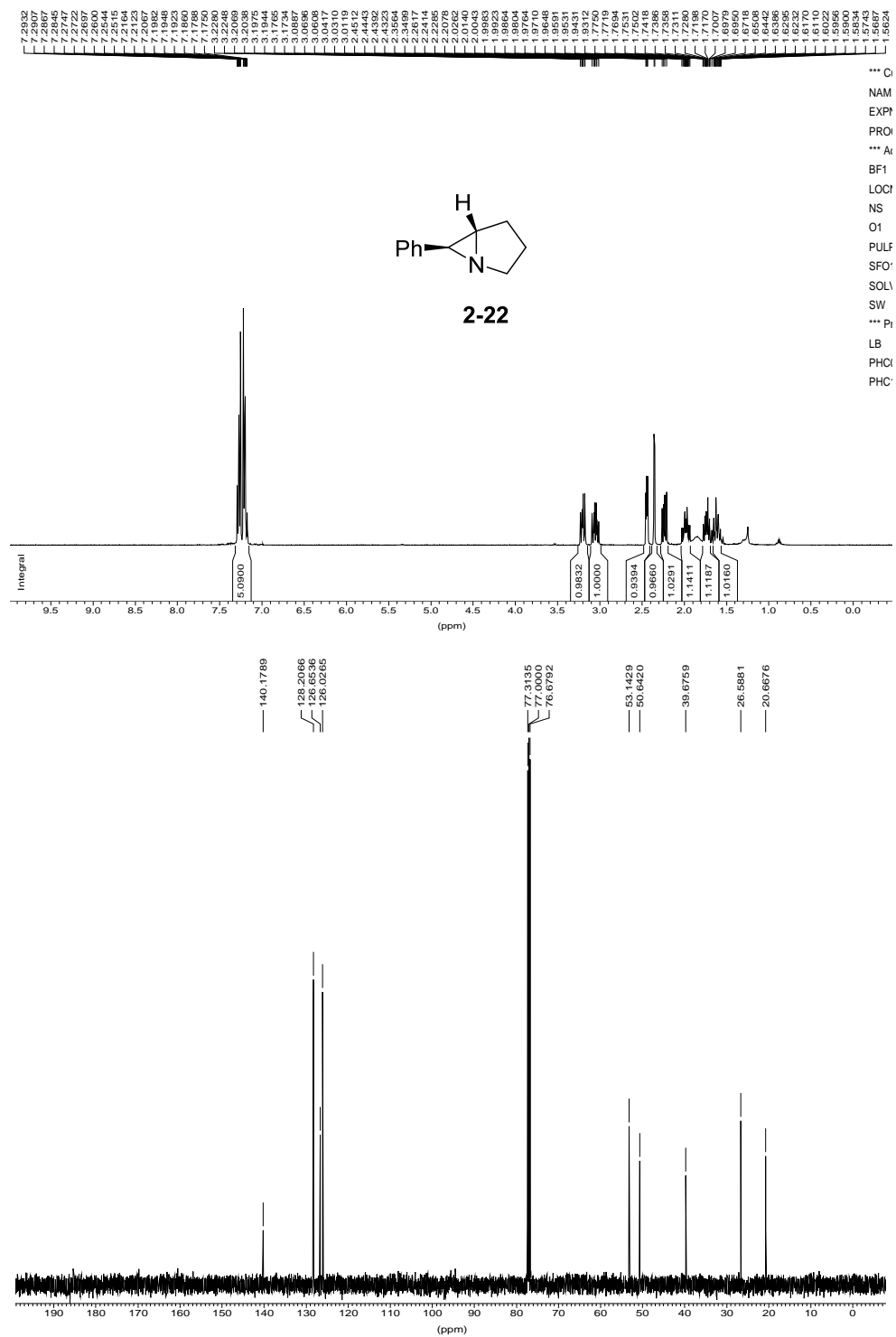


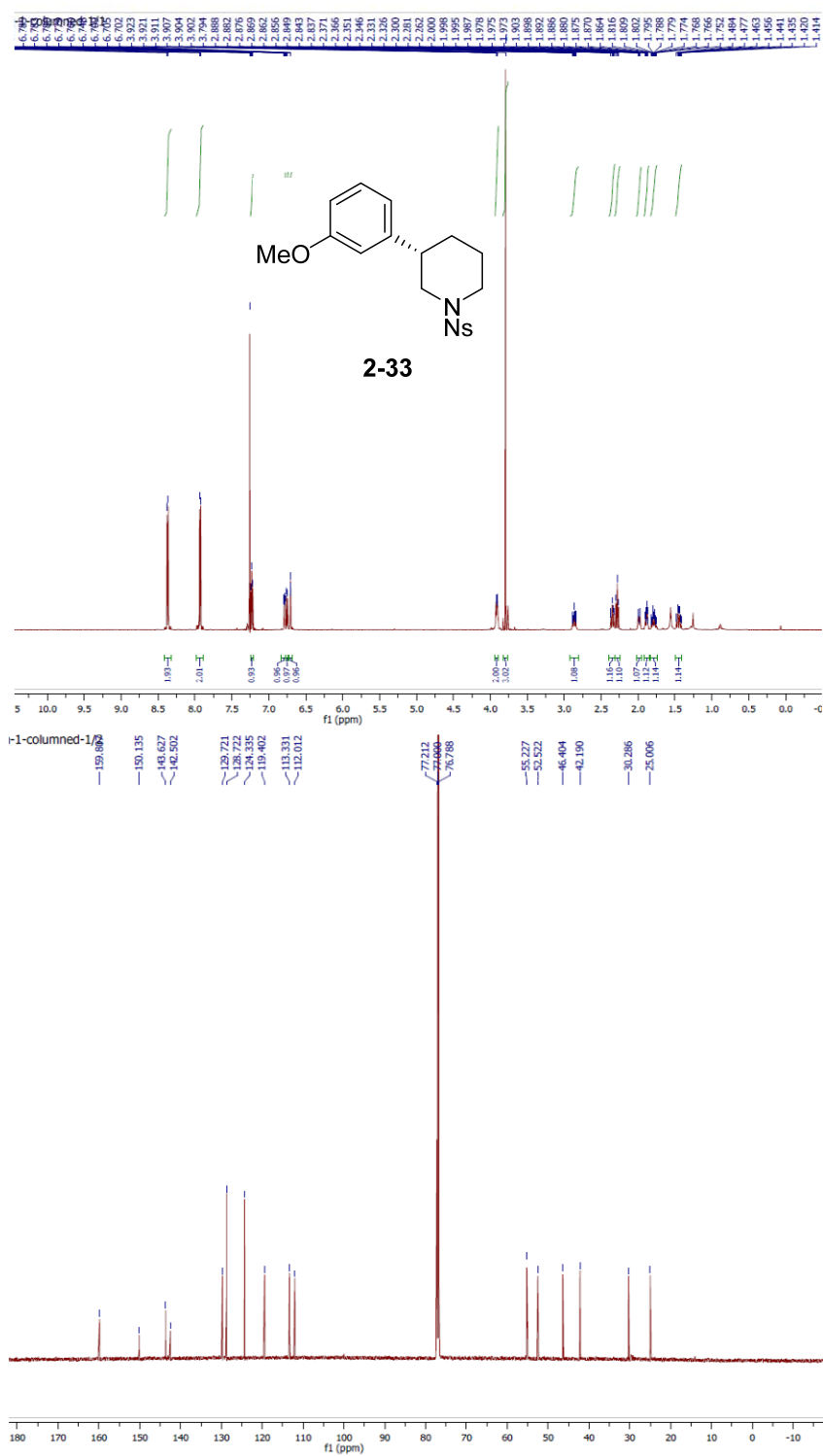




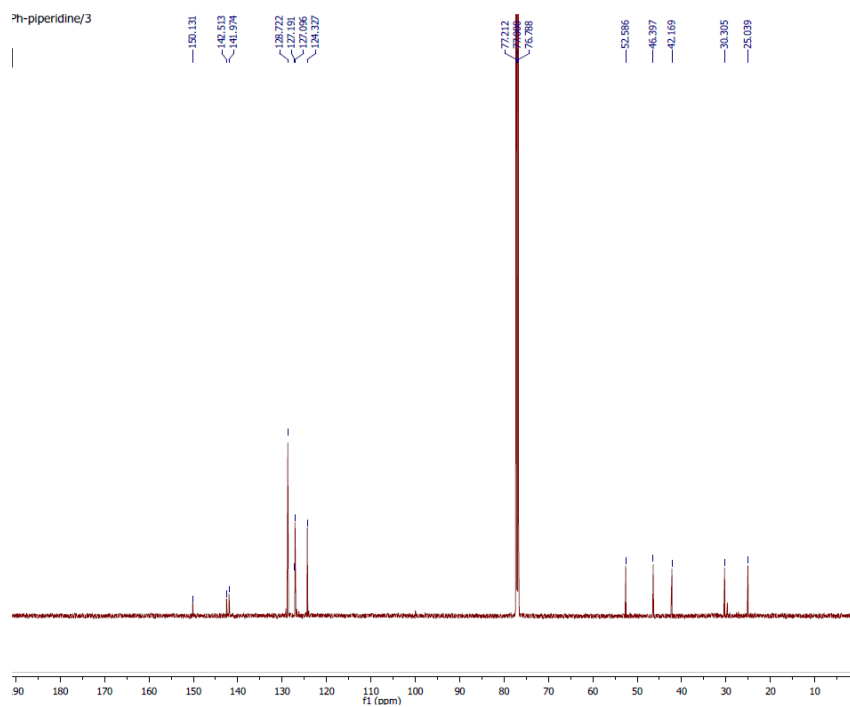
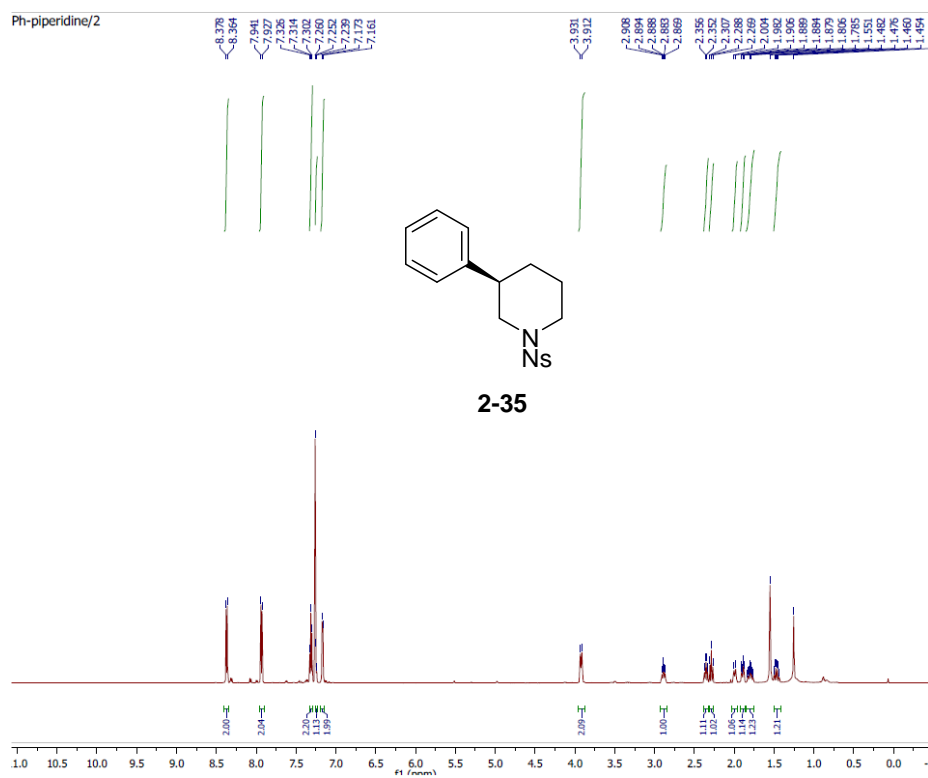


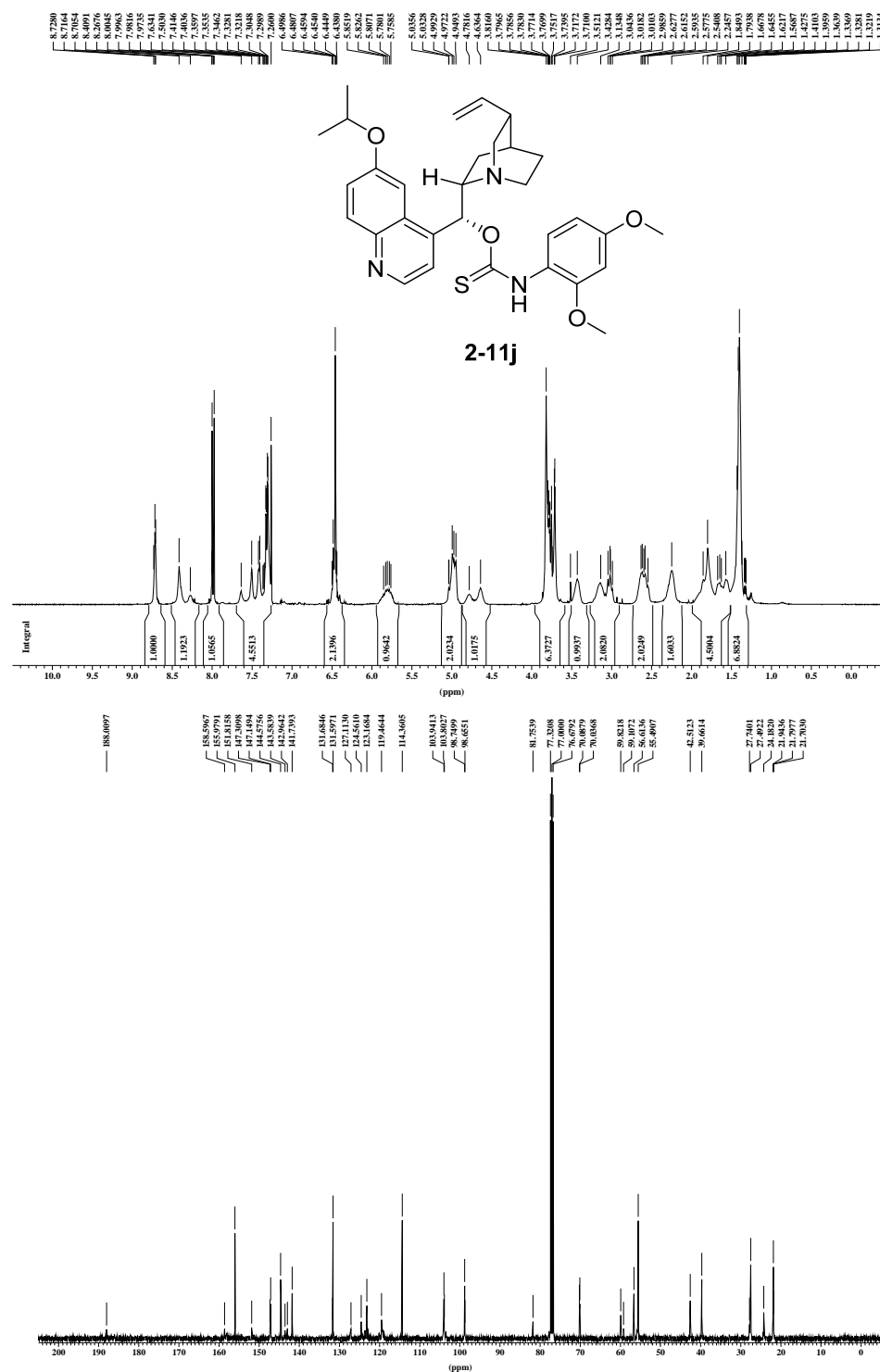


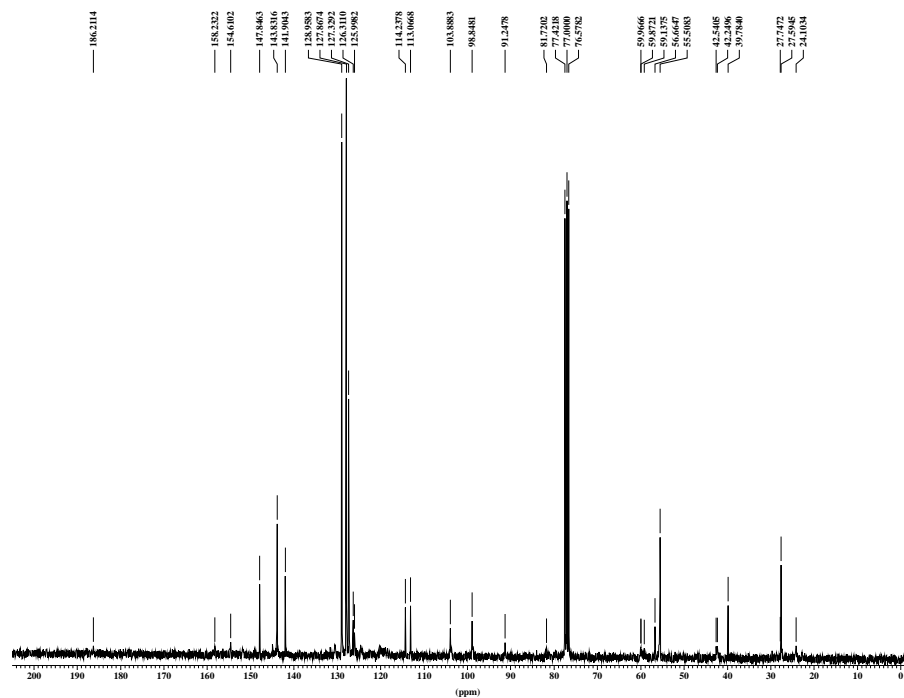
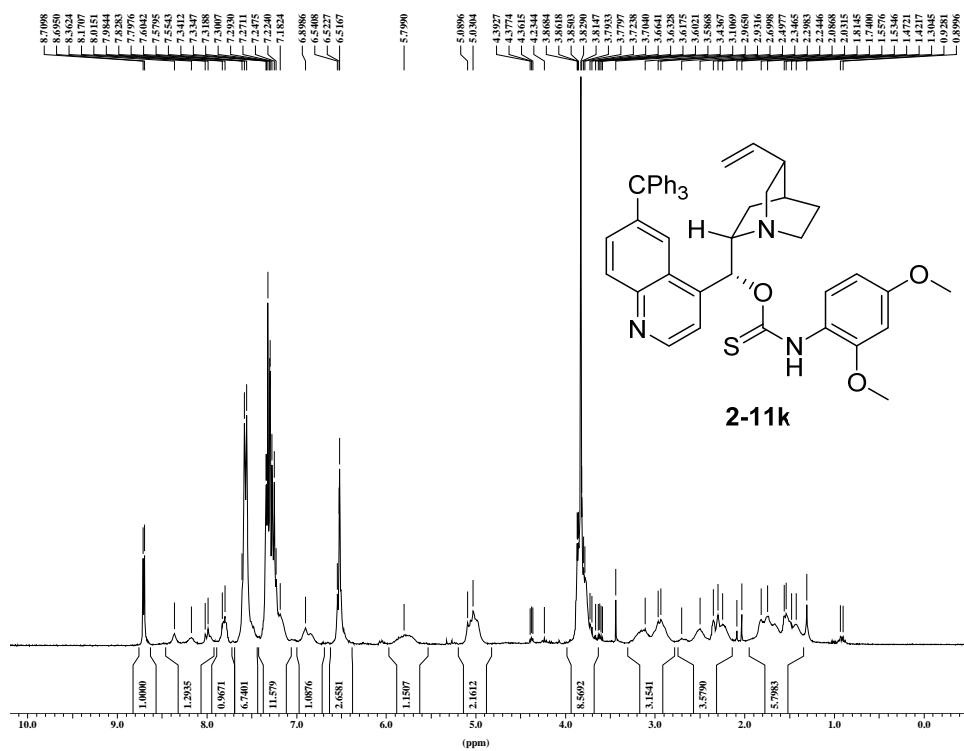


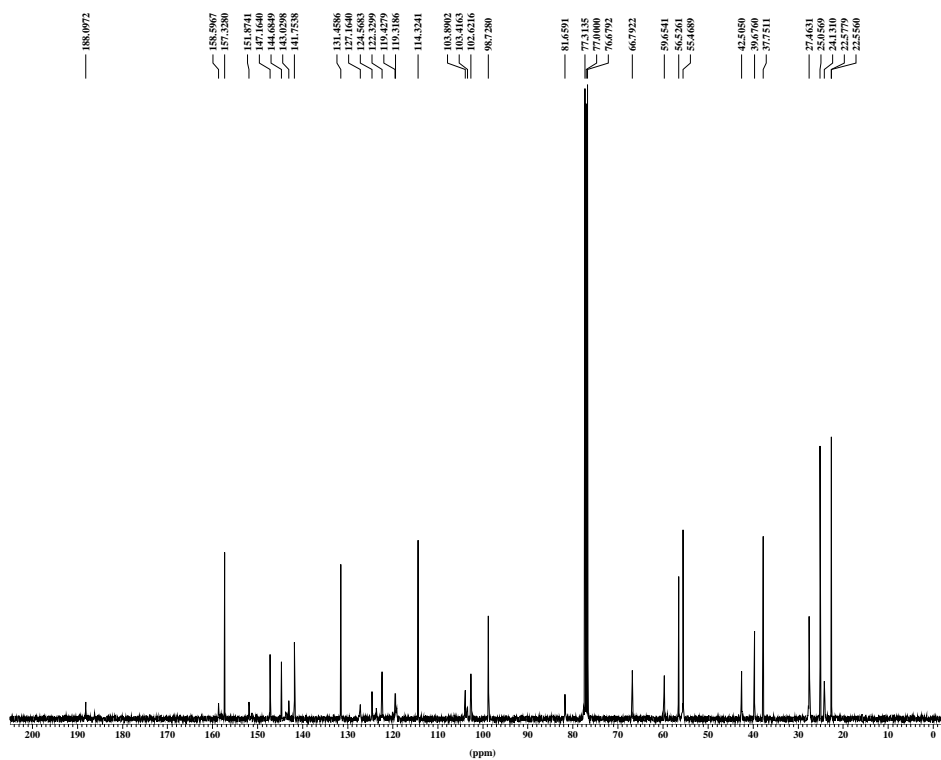
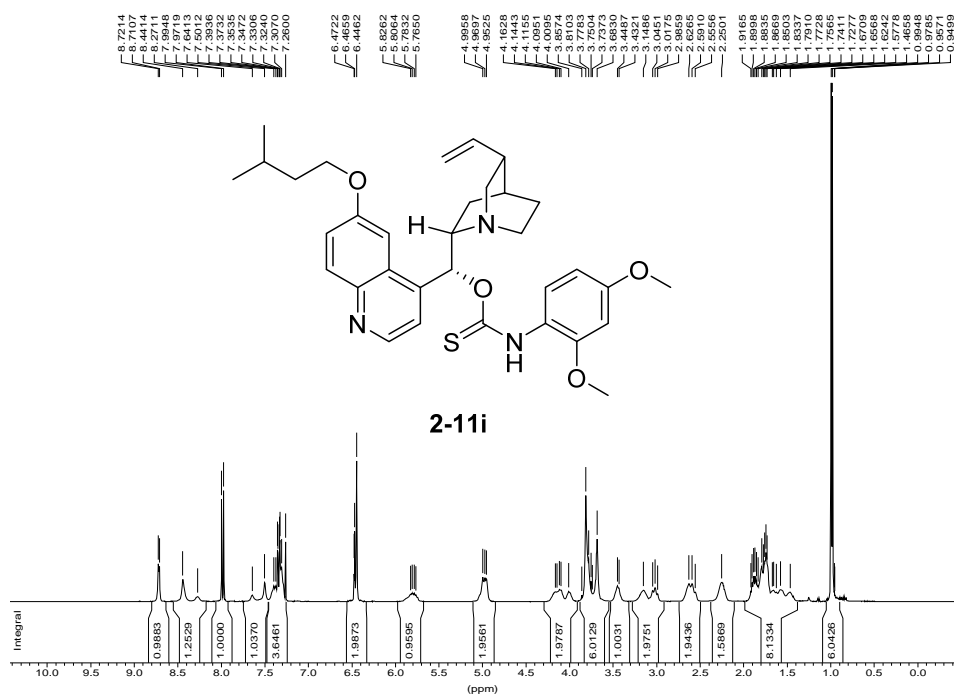


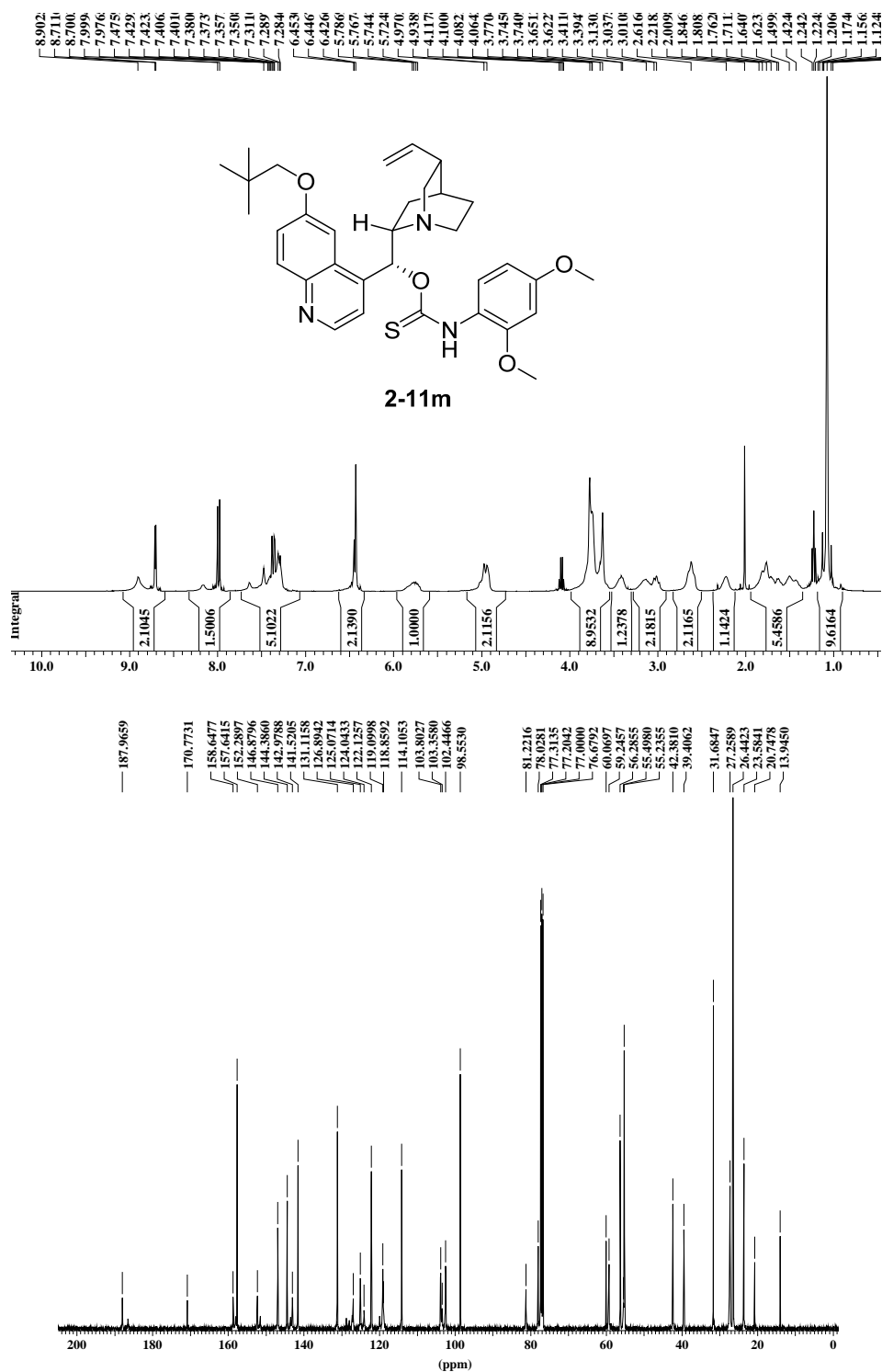


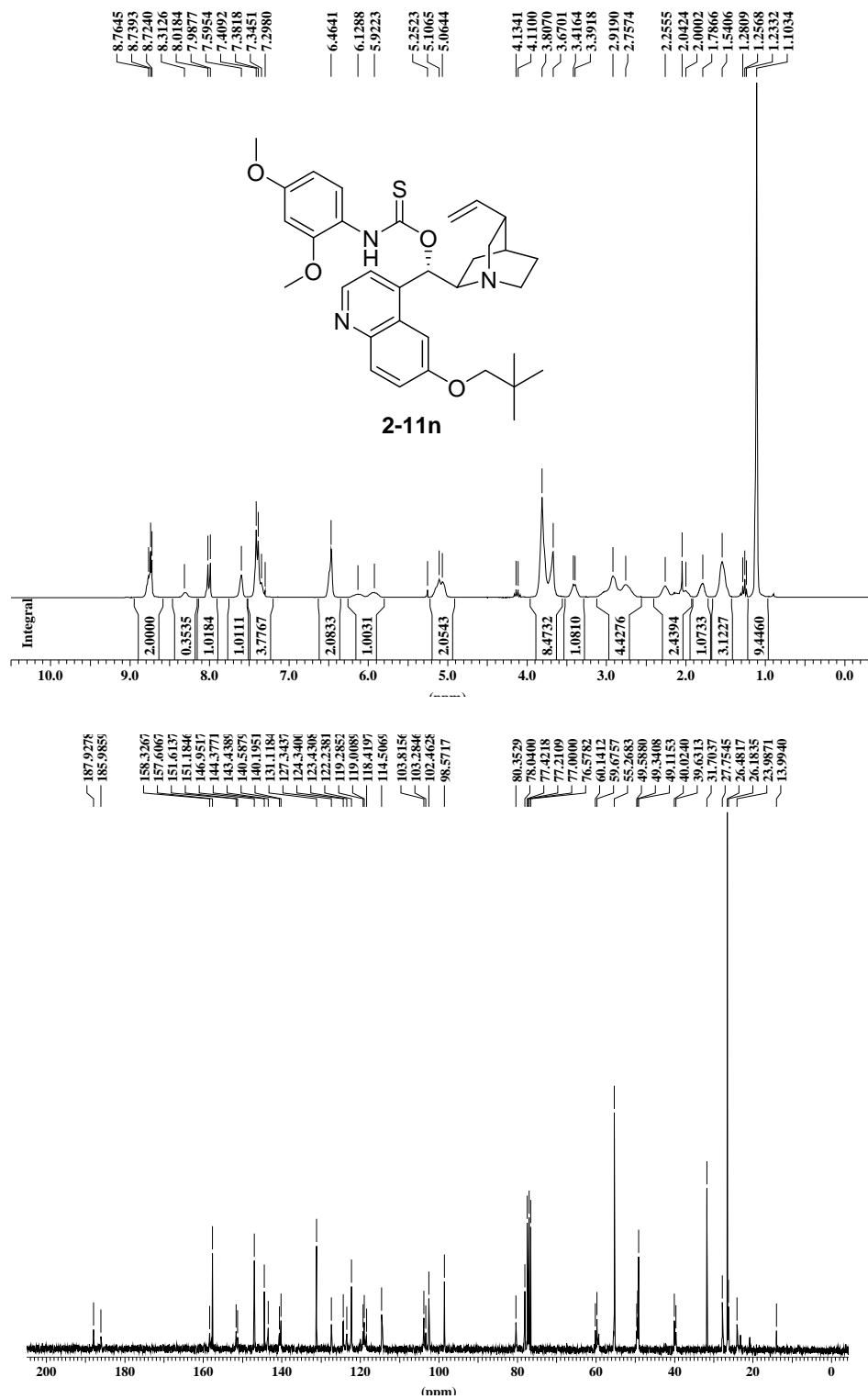






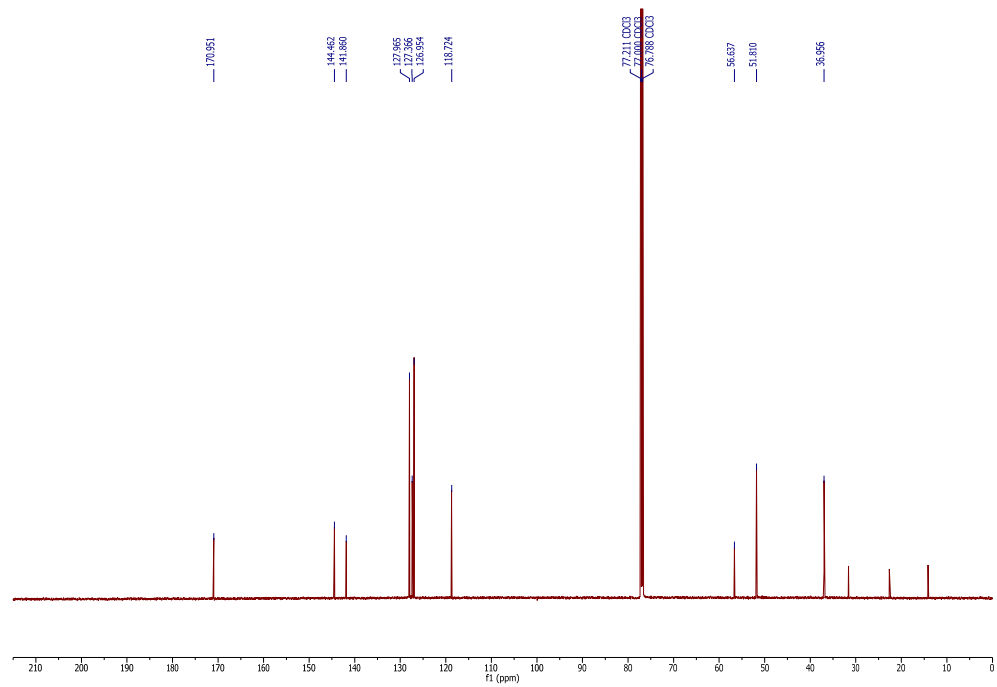
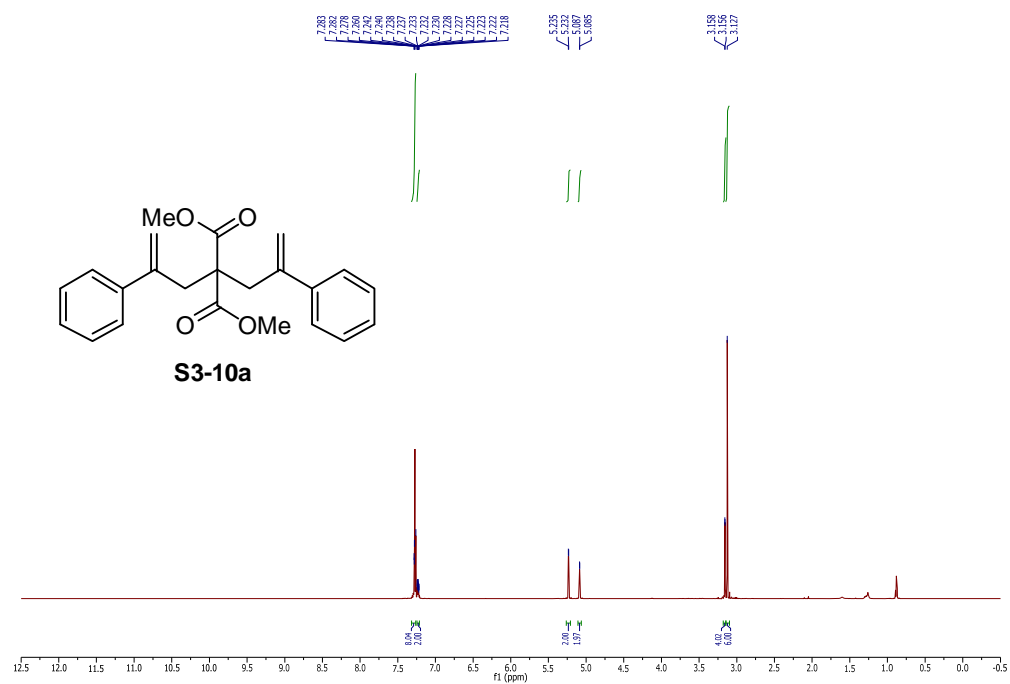


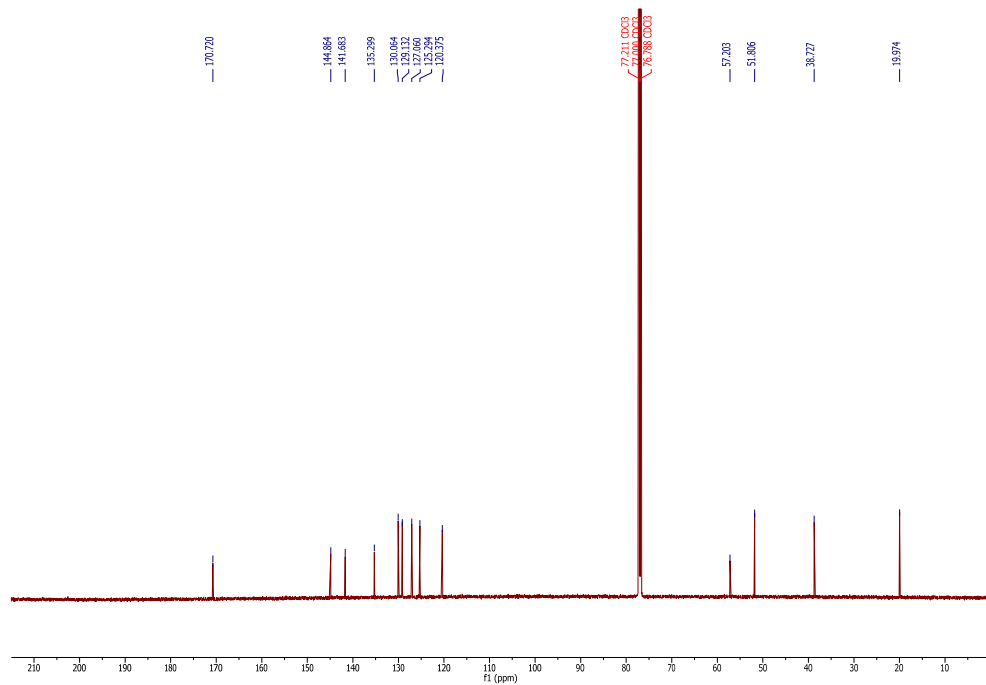
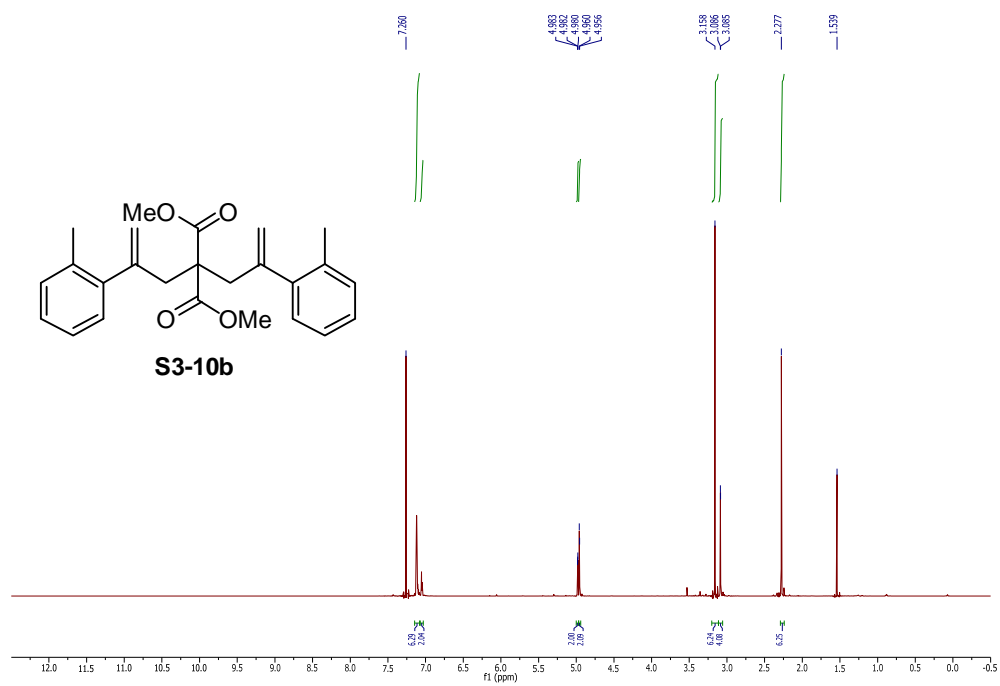


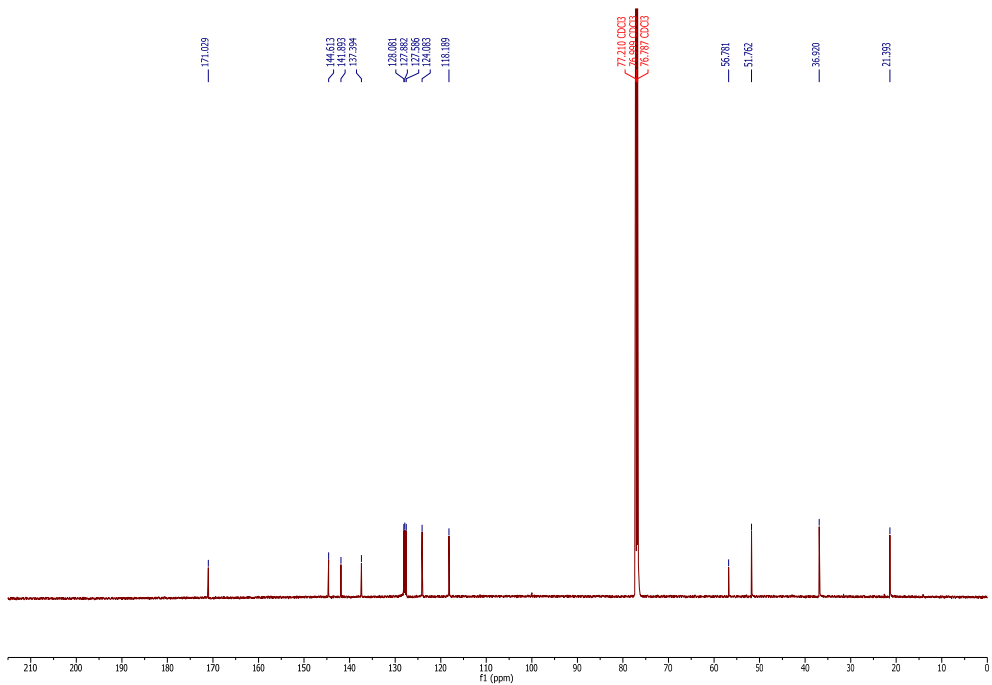
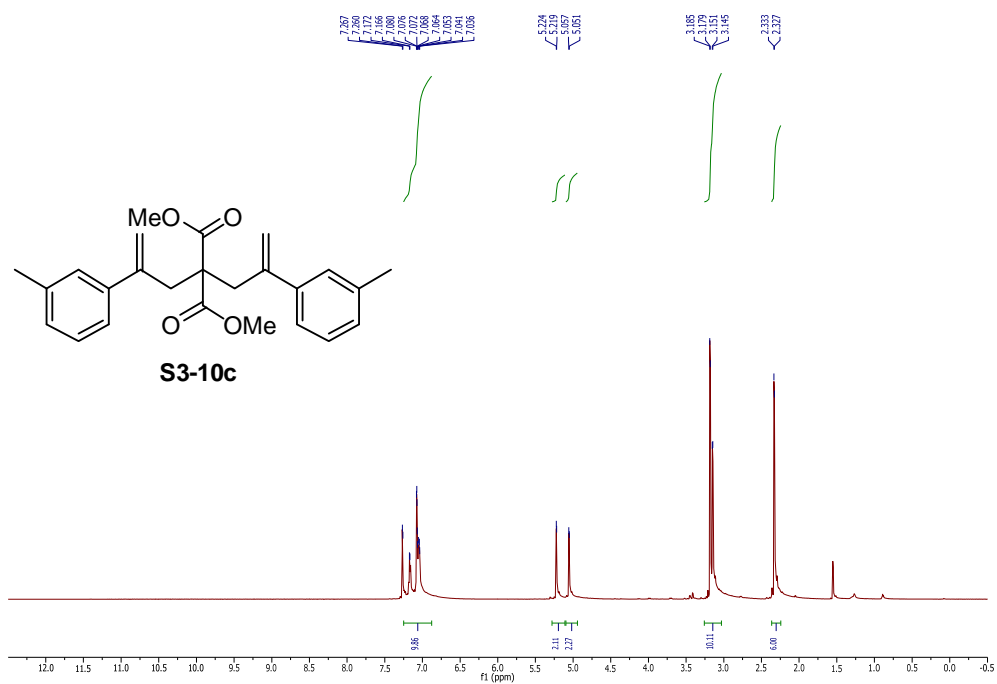


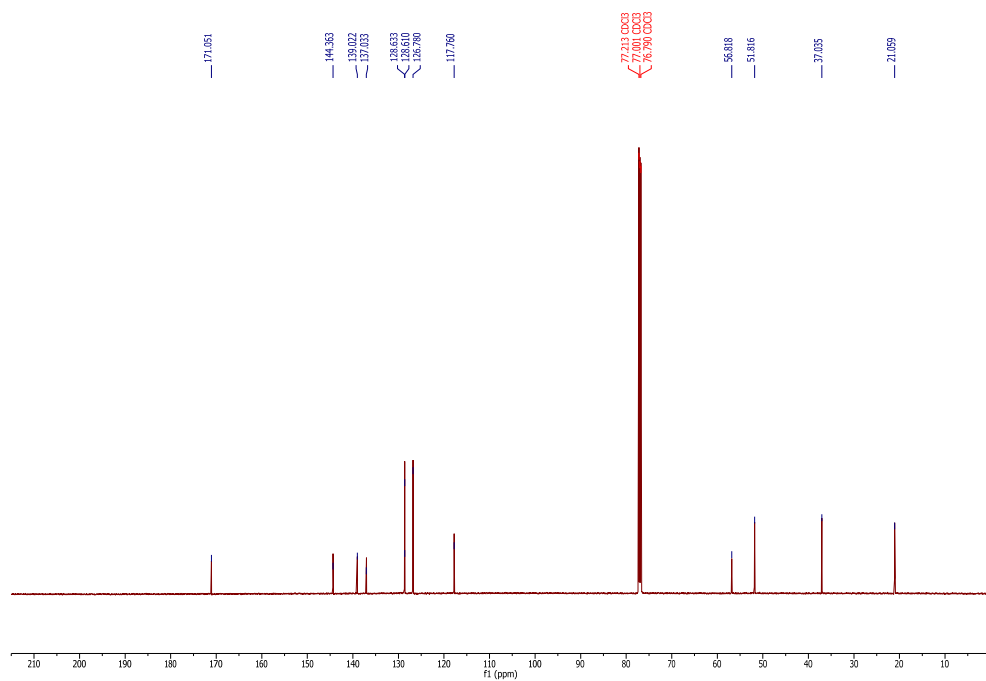
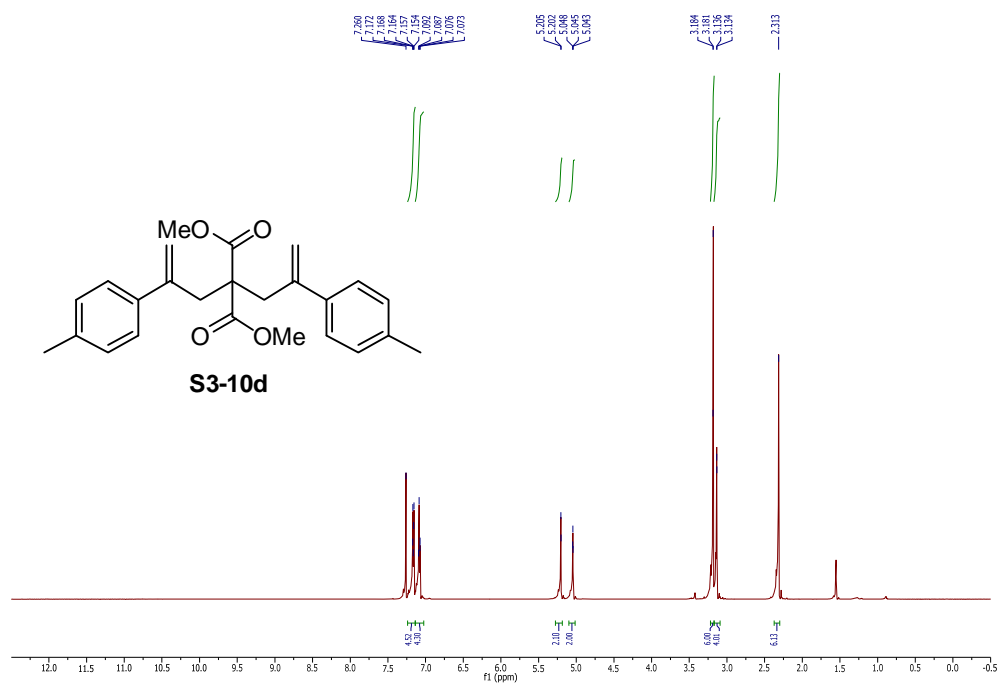
Appendix B

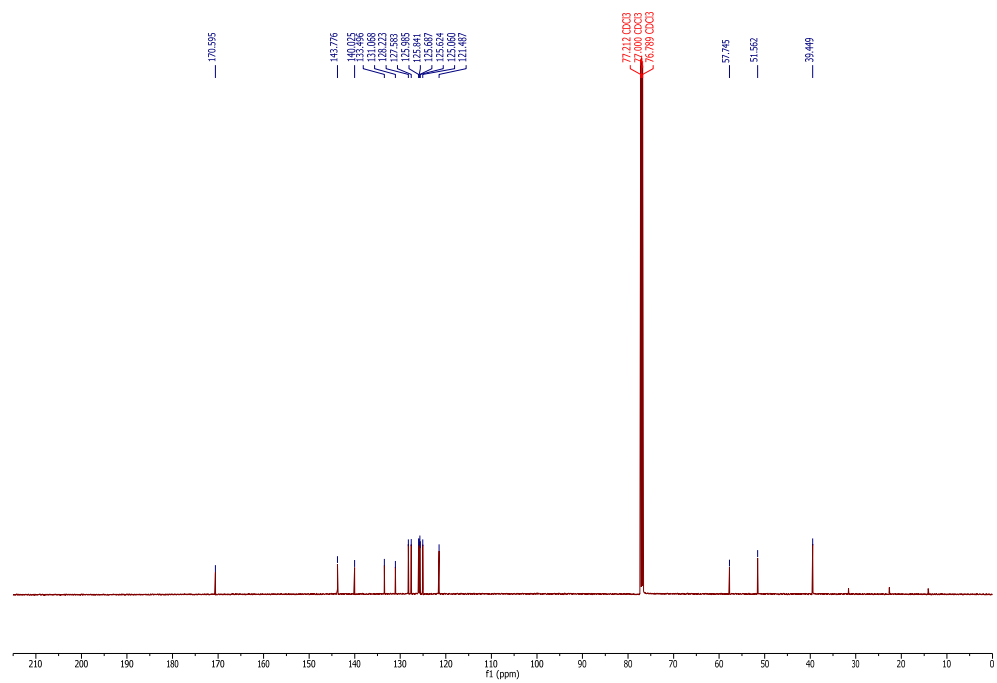
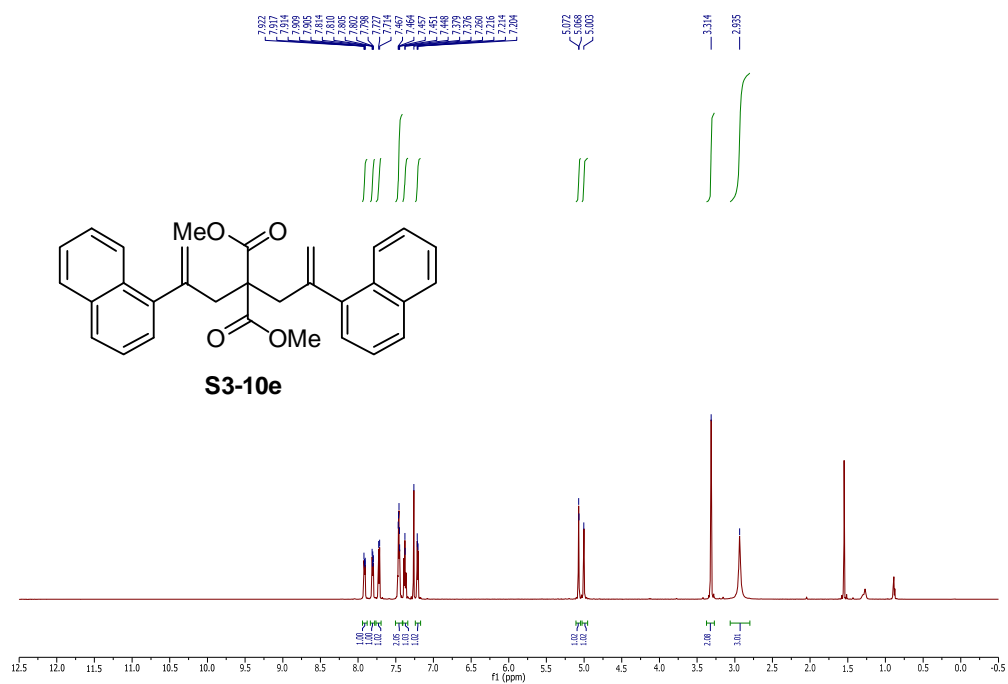
NMR Spectra of Synthetic Intermediates and Products of Chapter 3

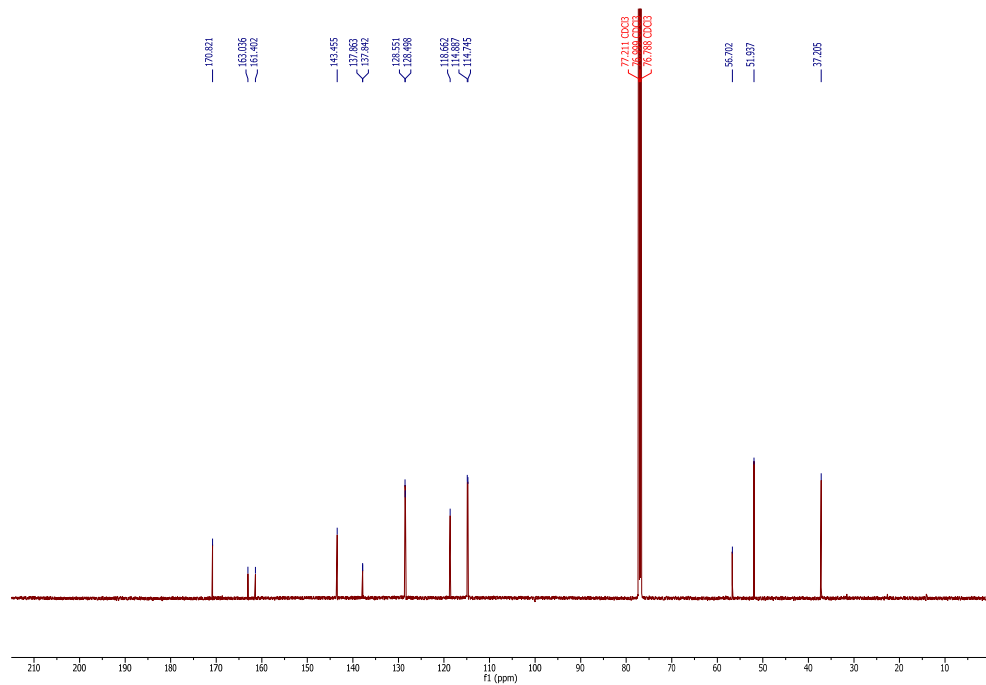
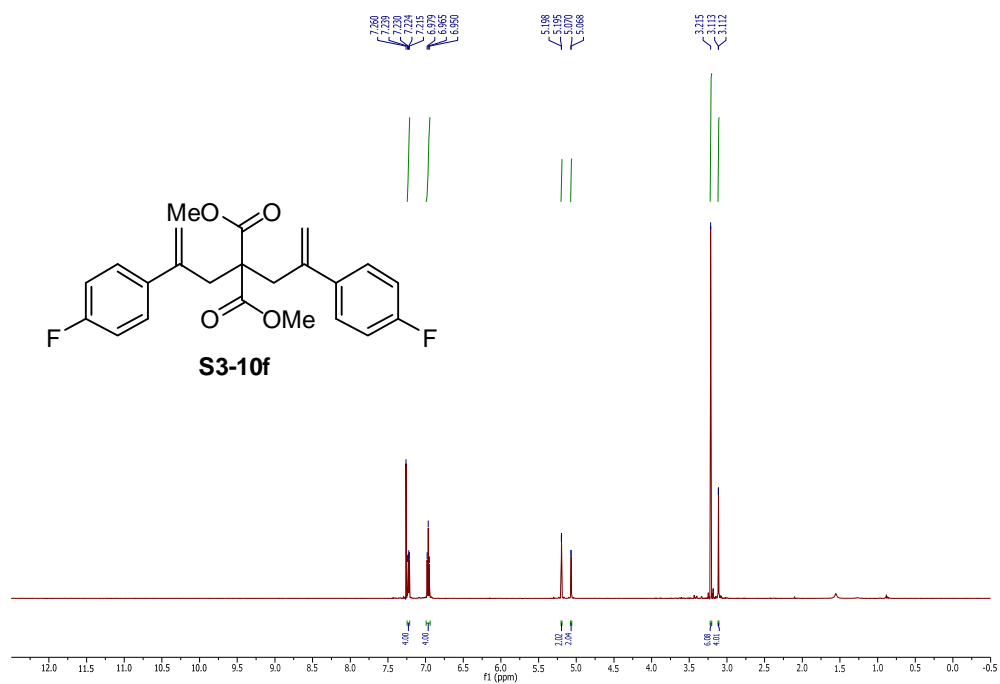


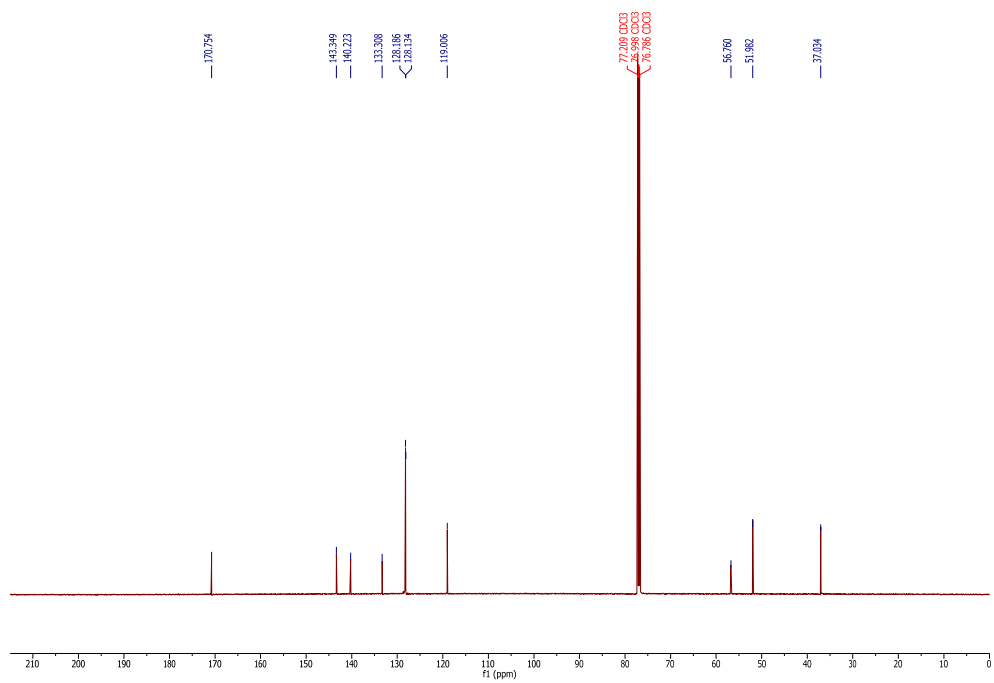
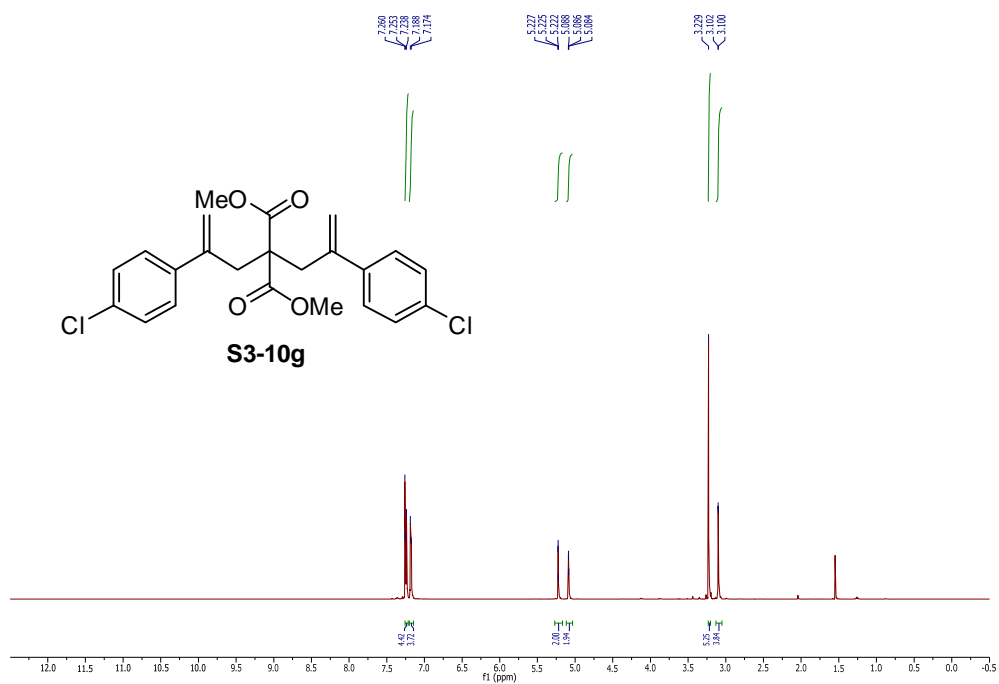


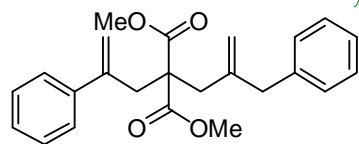




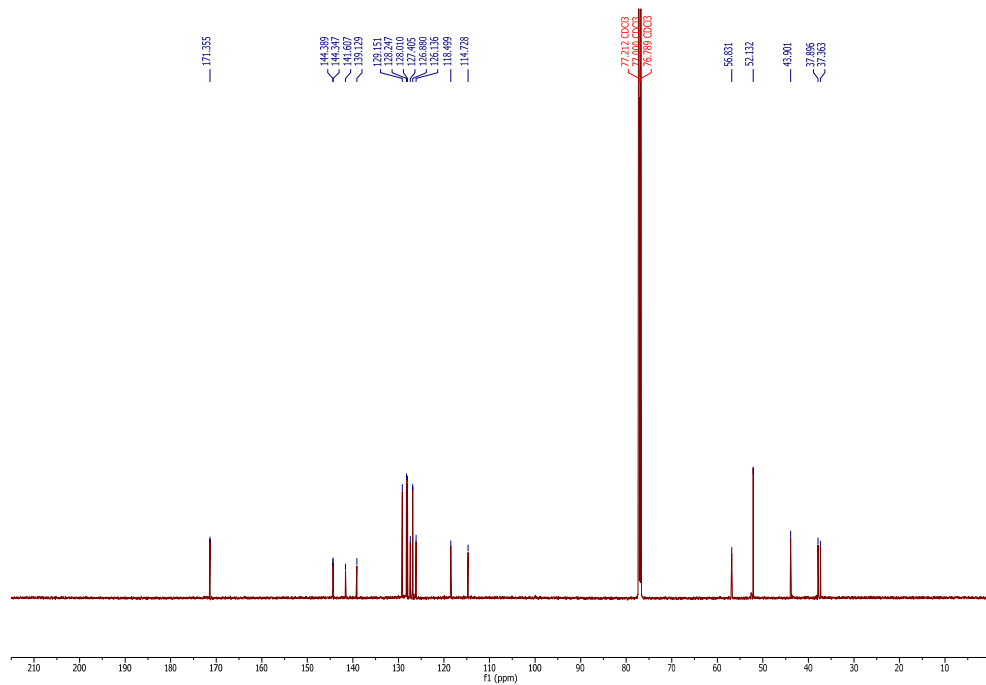


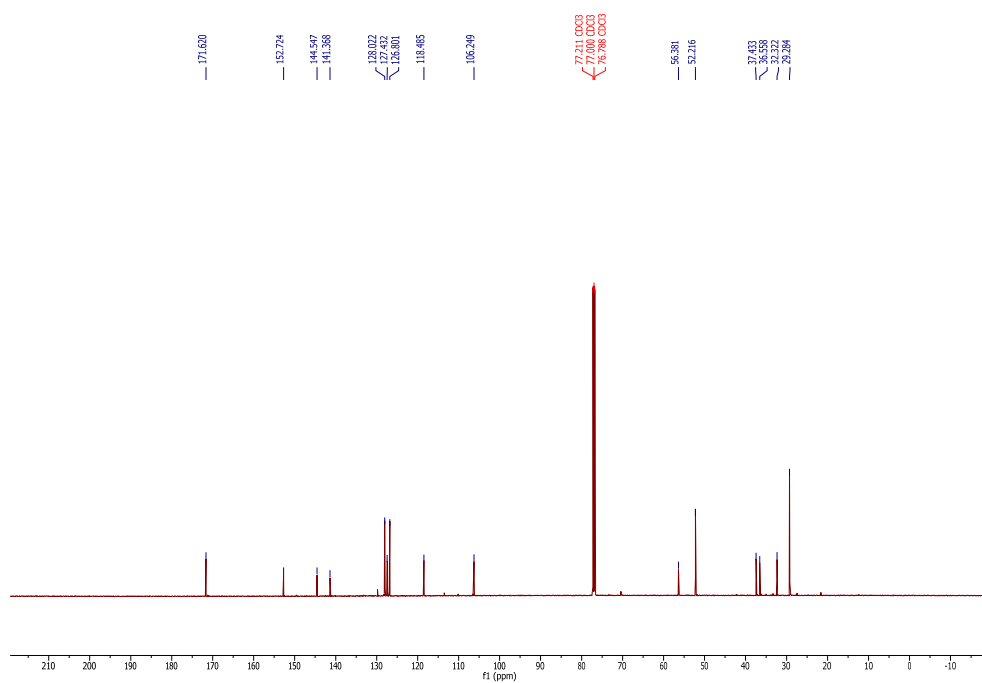
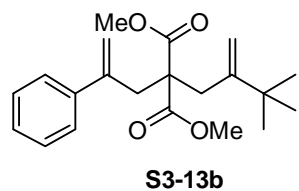


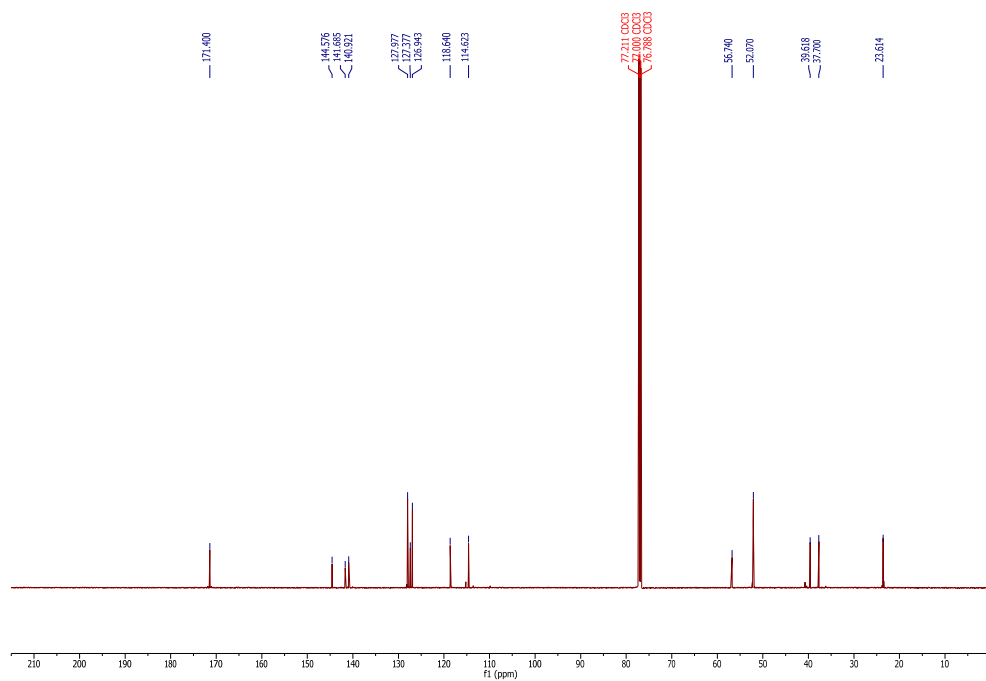
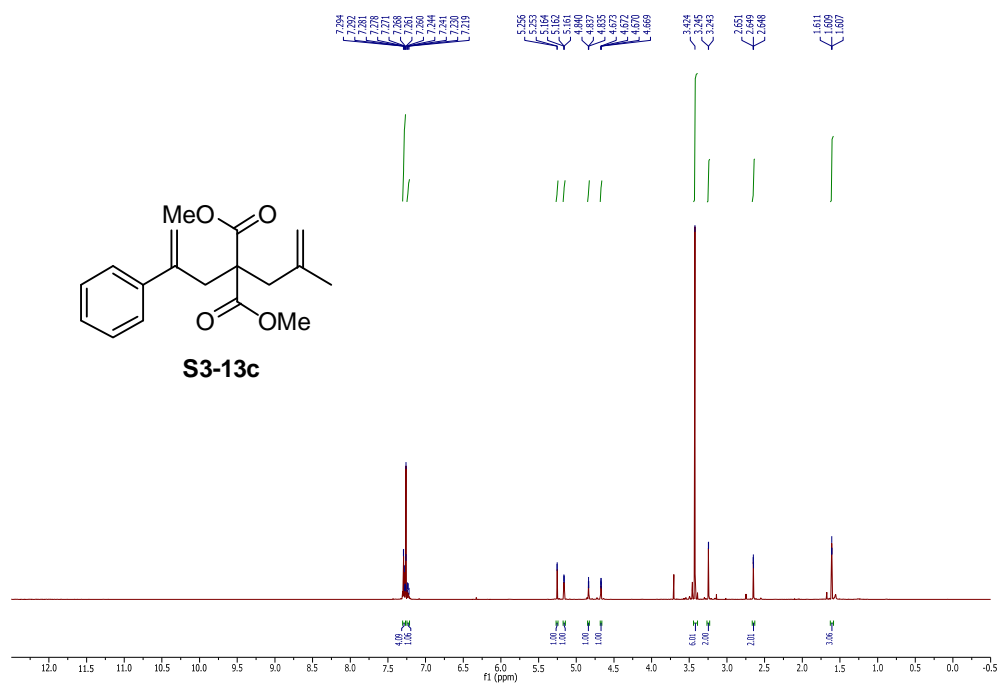


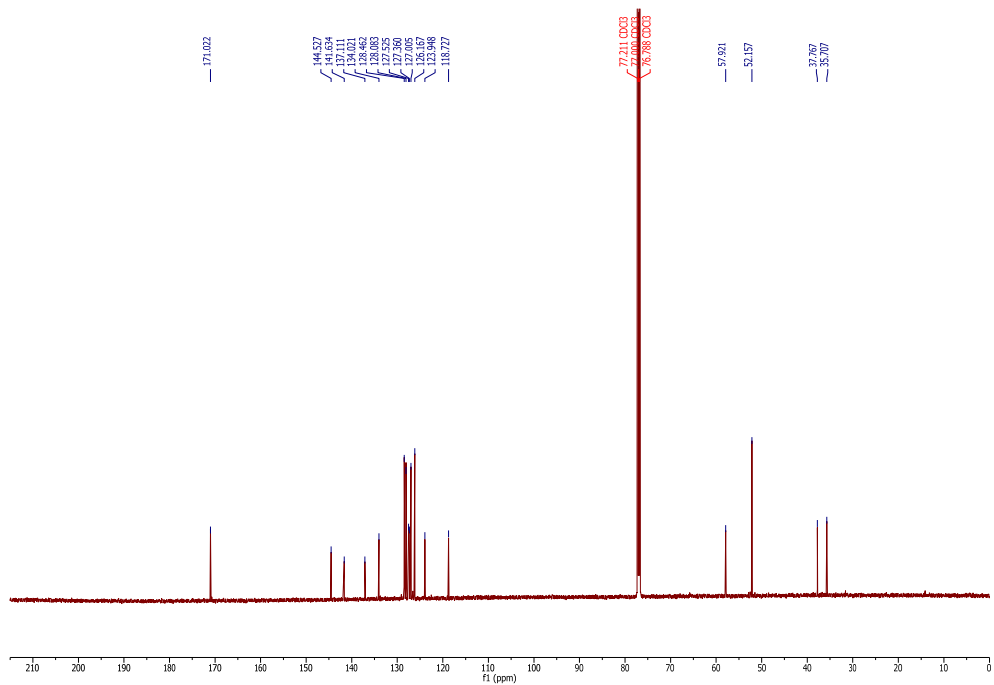
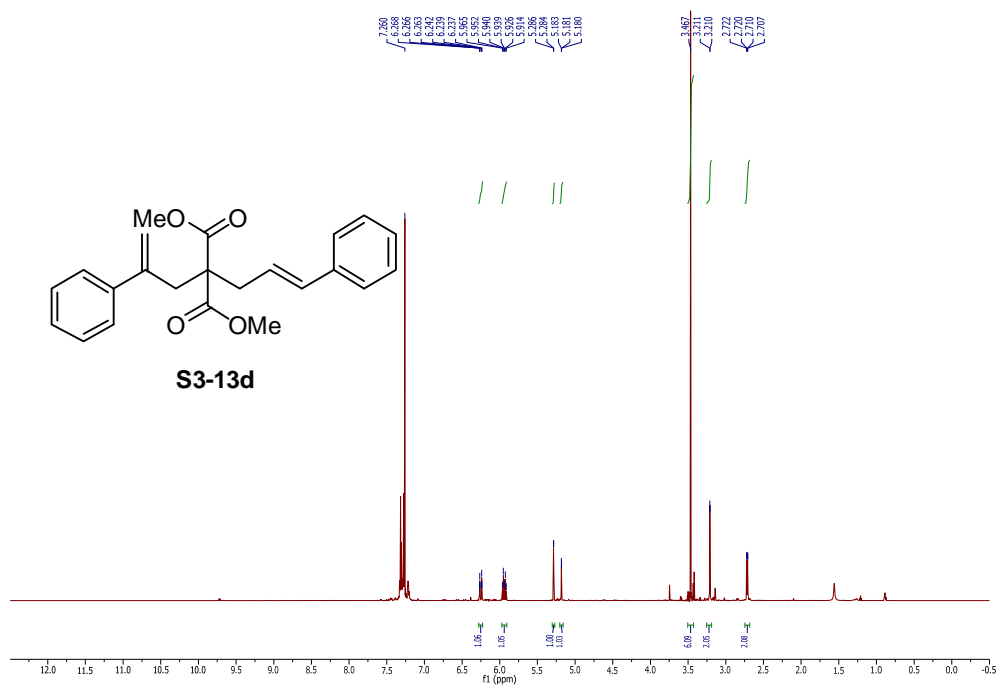


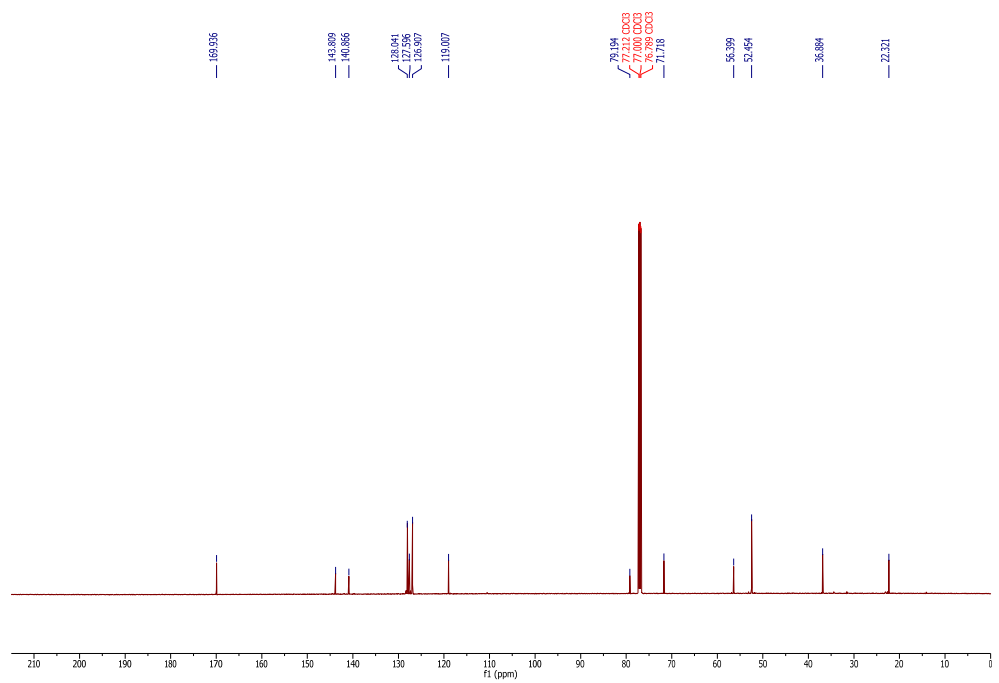
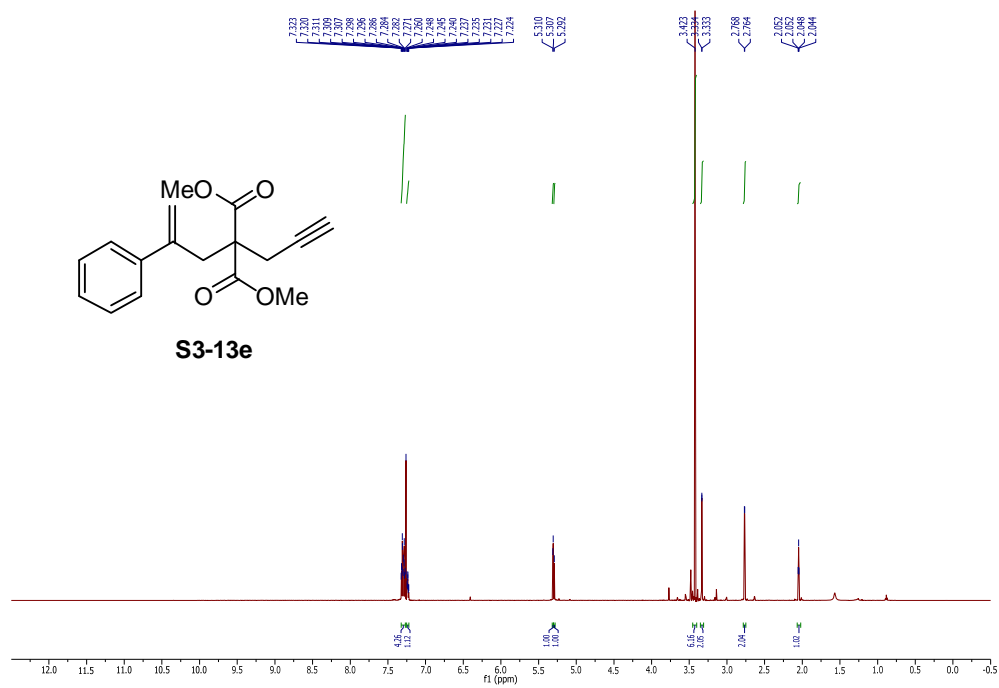
S3-13a

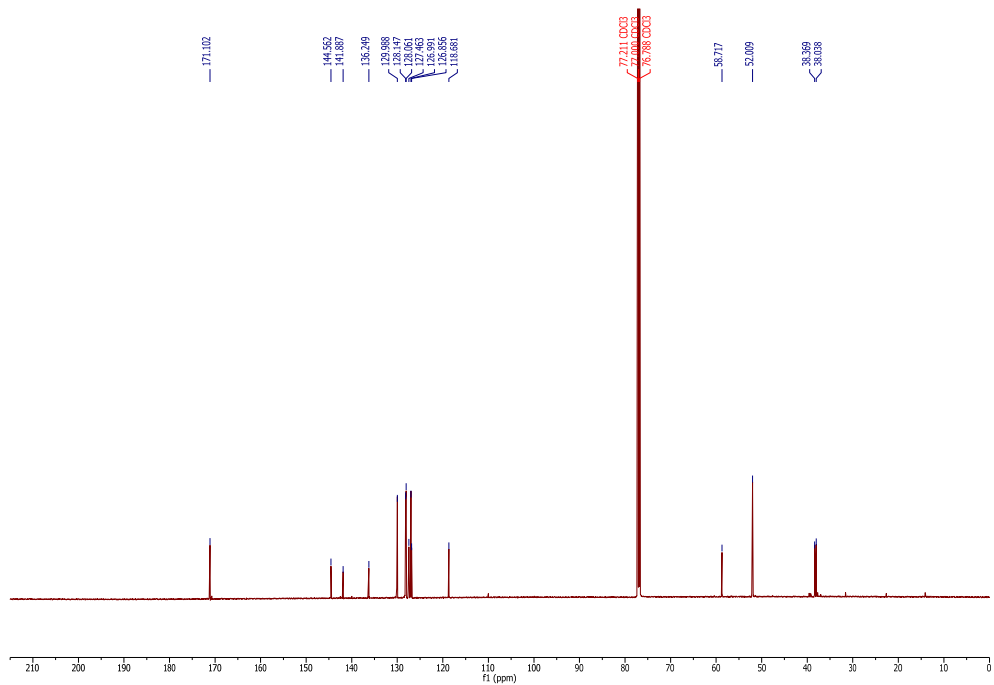
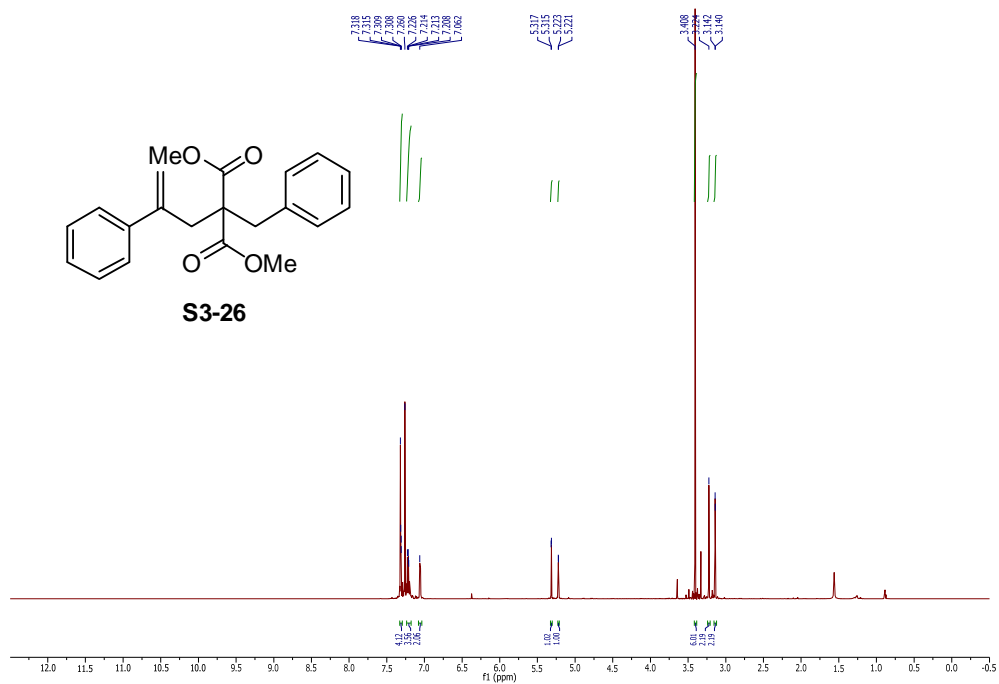


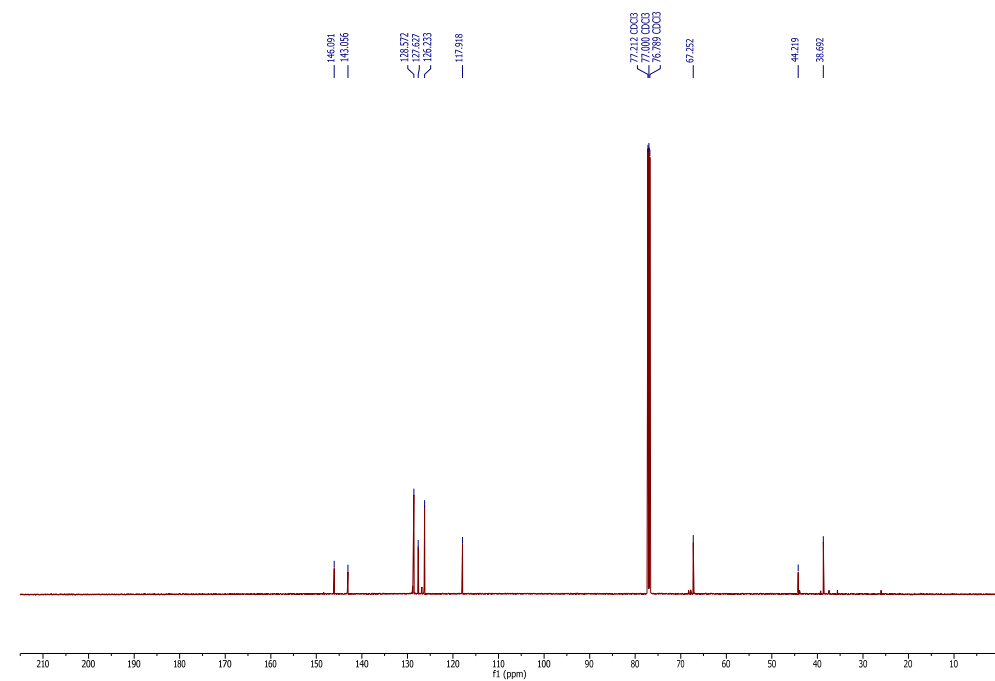


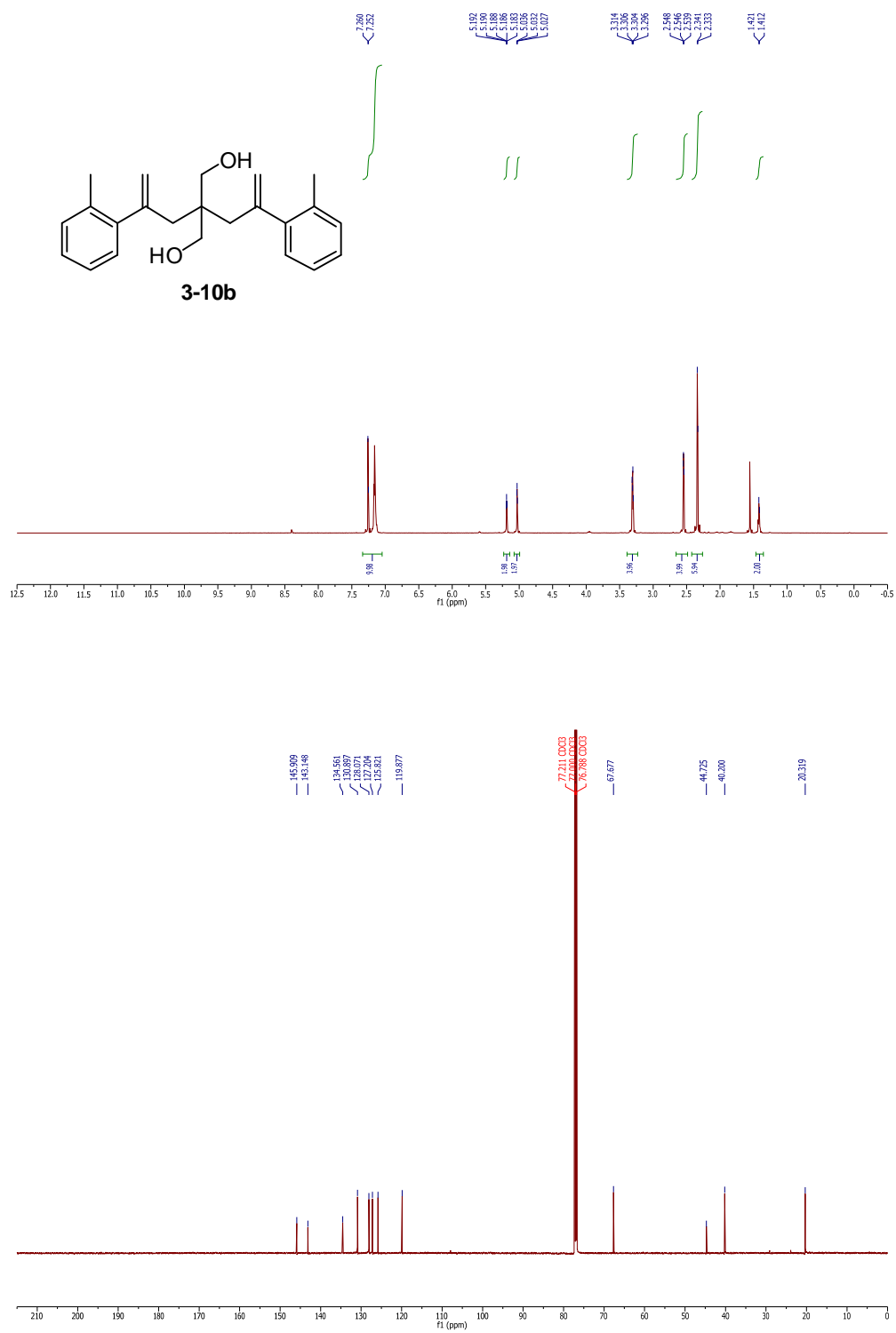


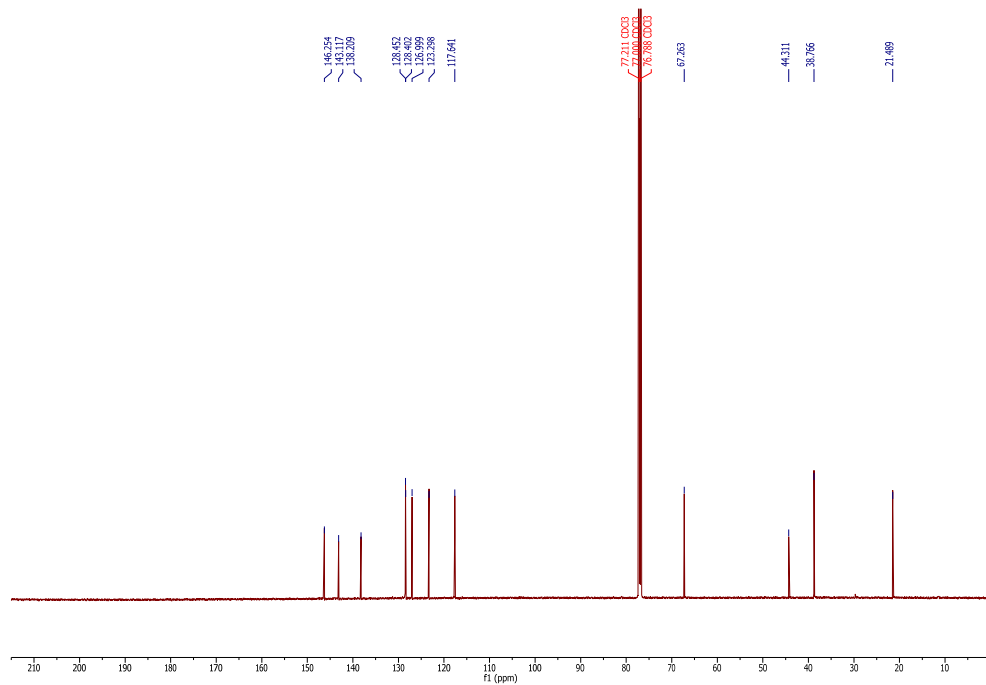
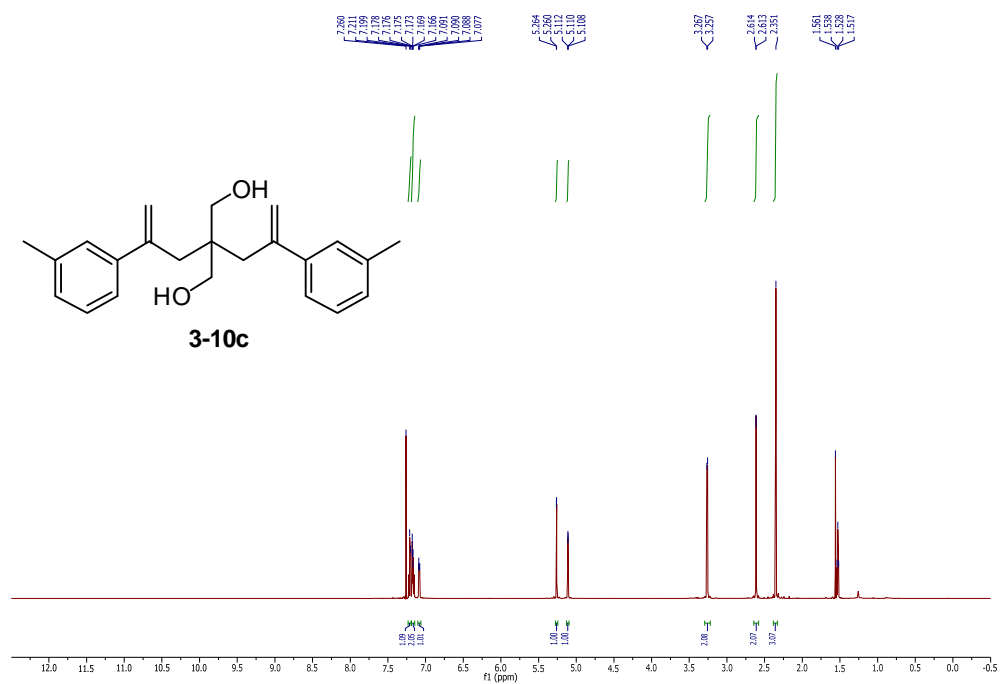


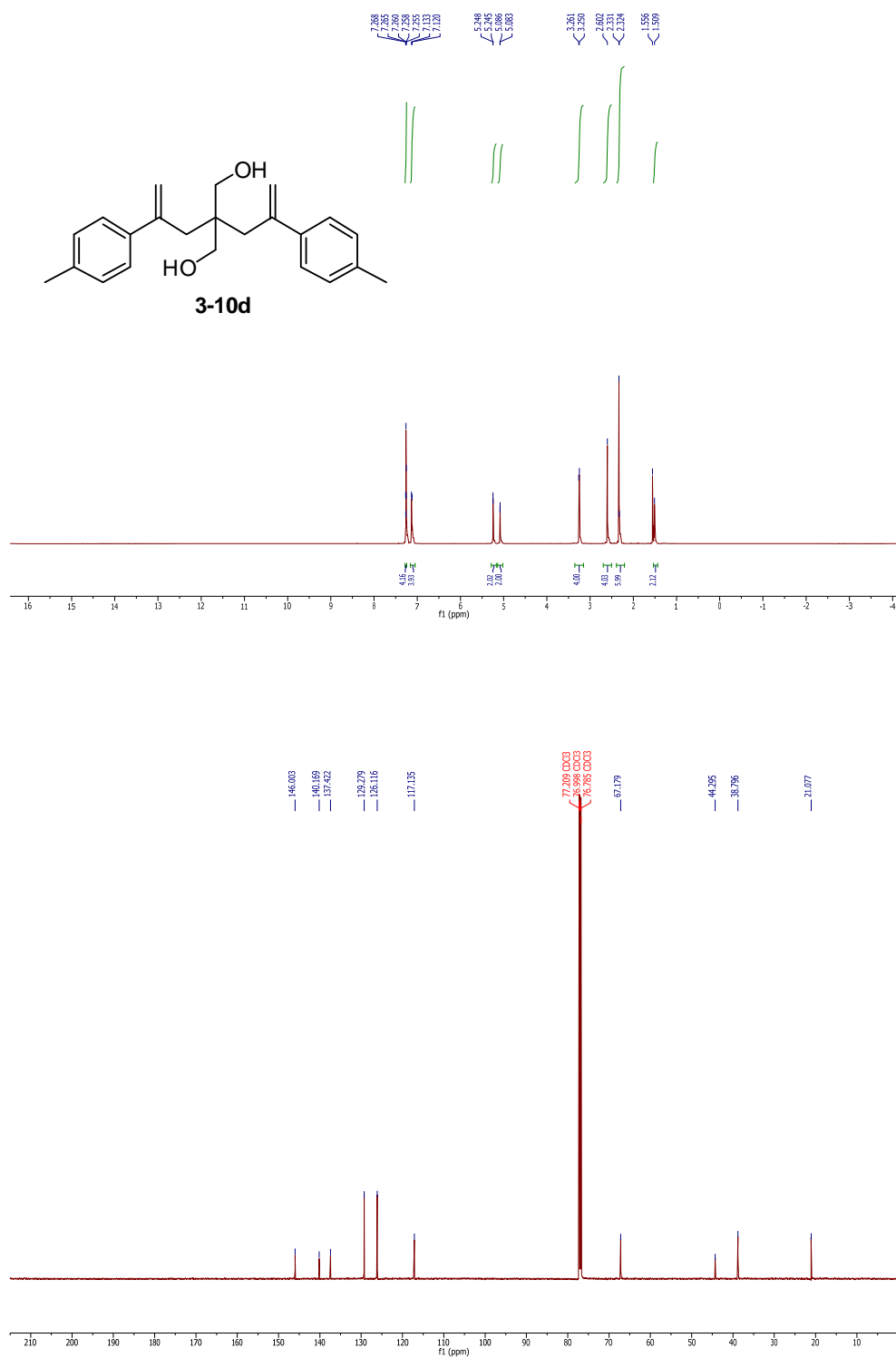


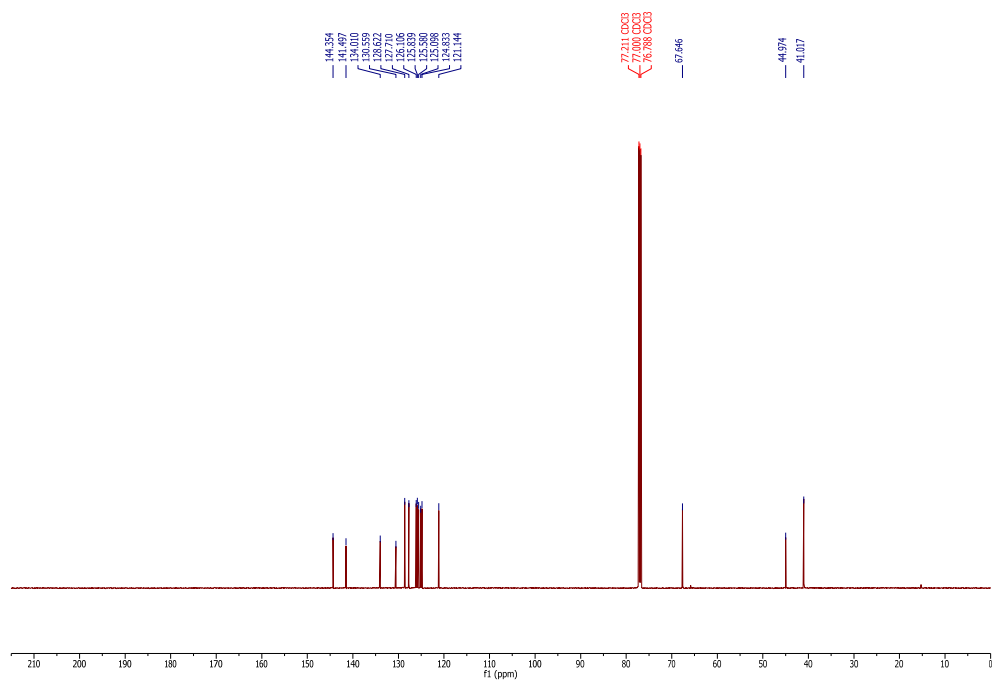
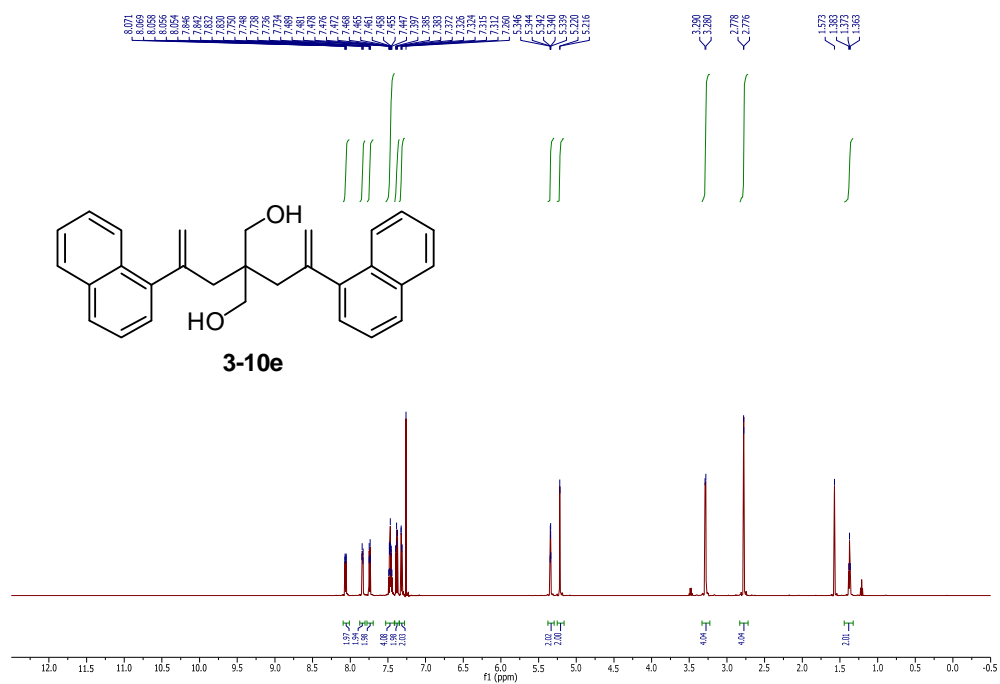


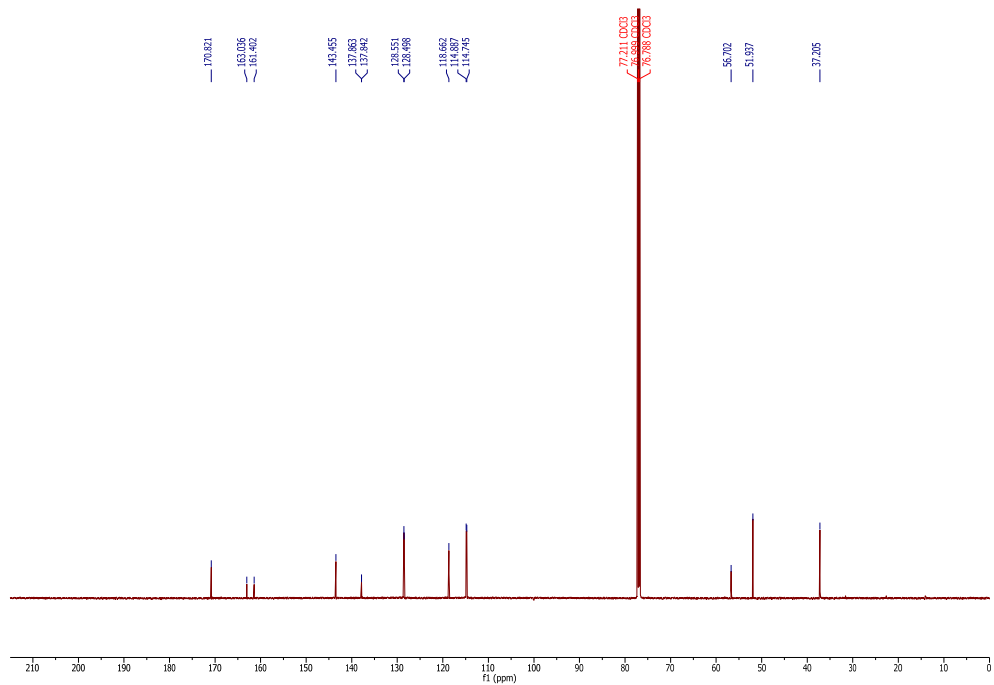
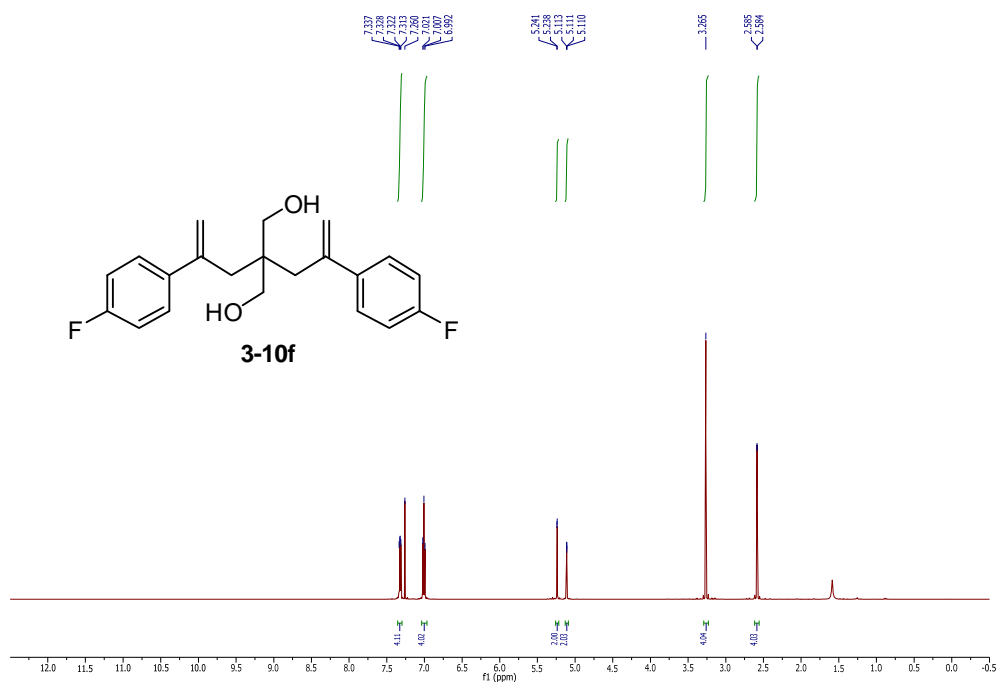


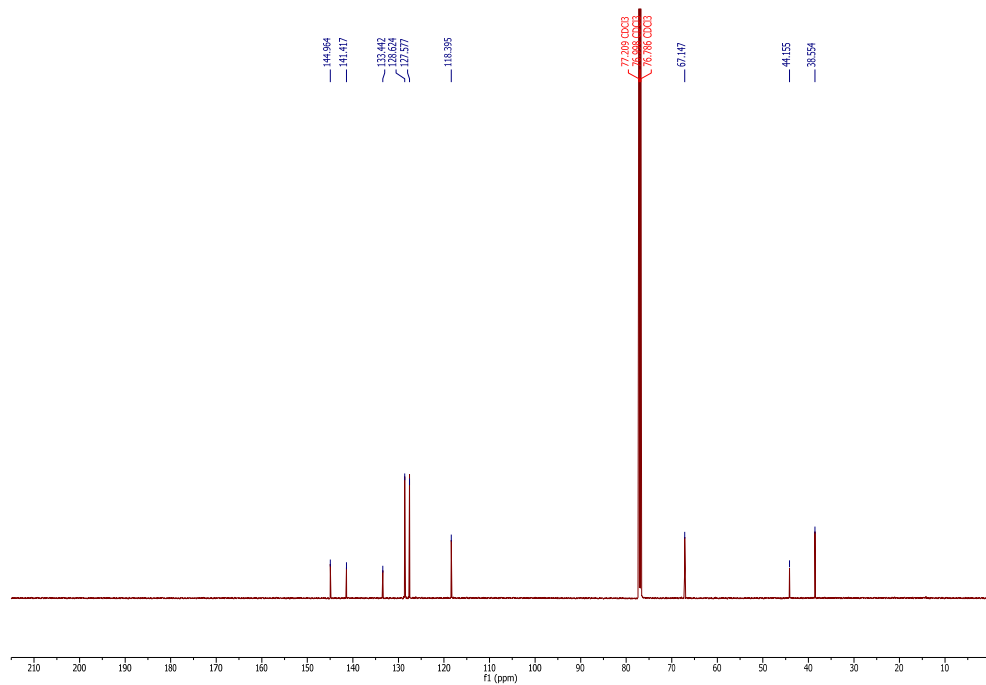
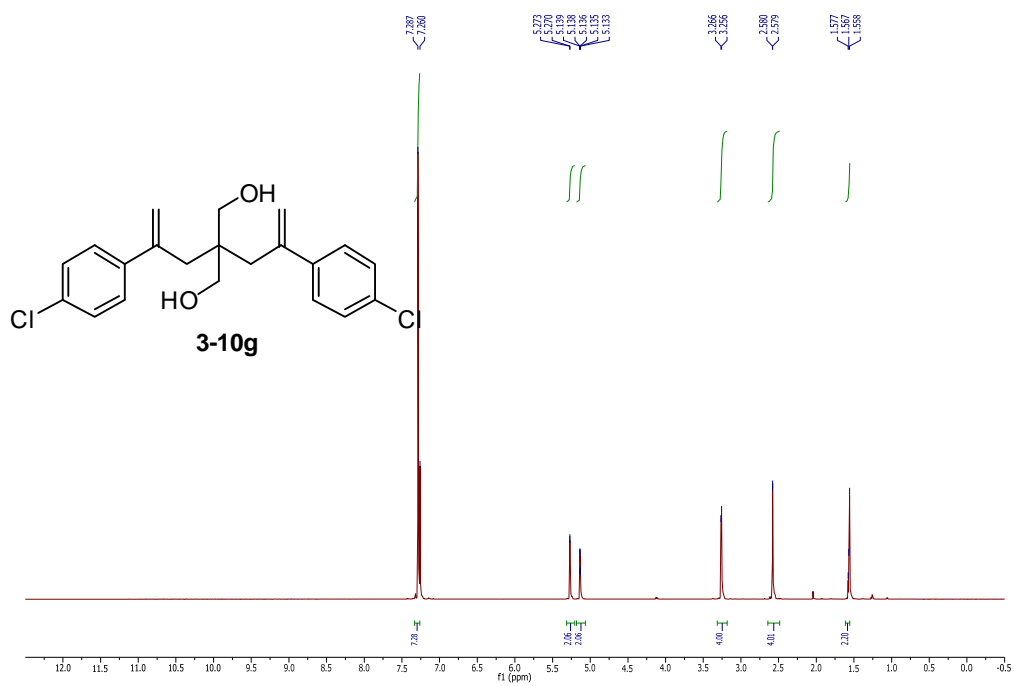


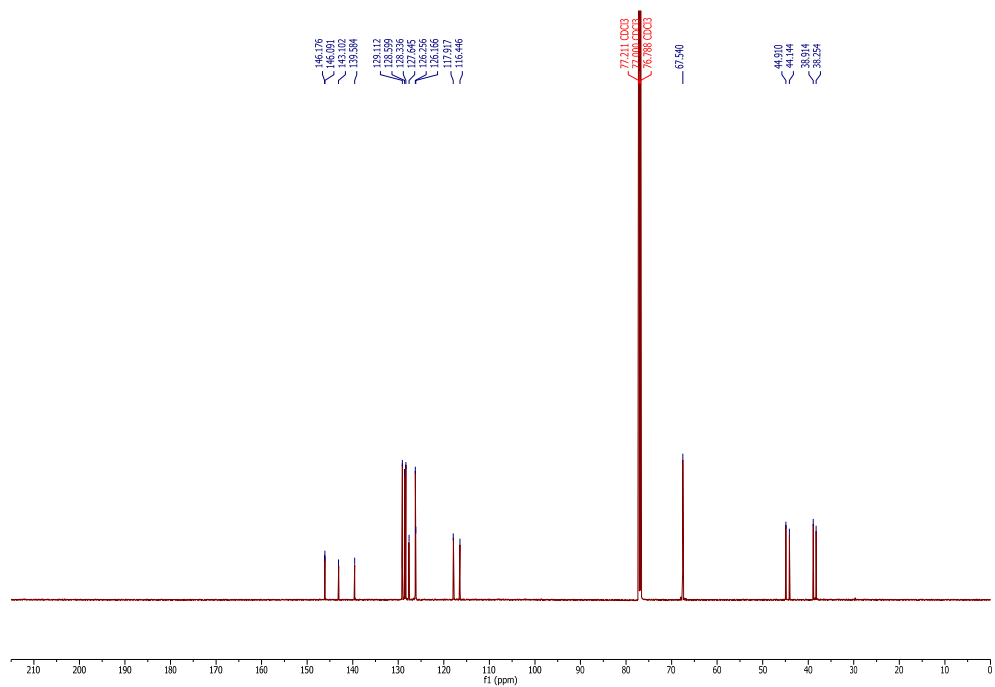
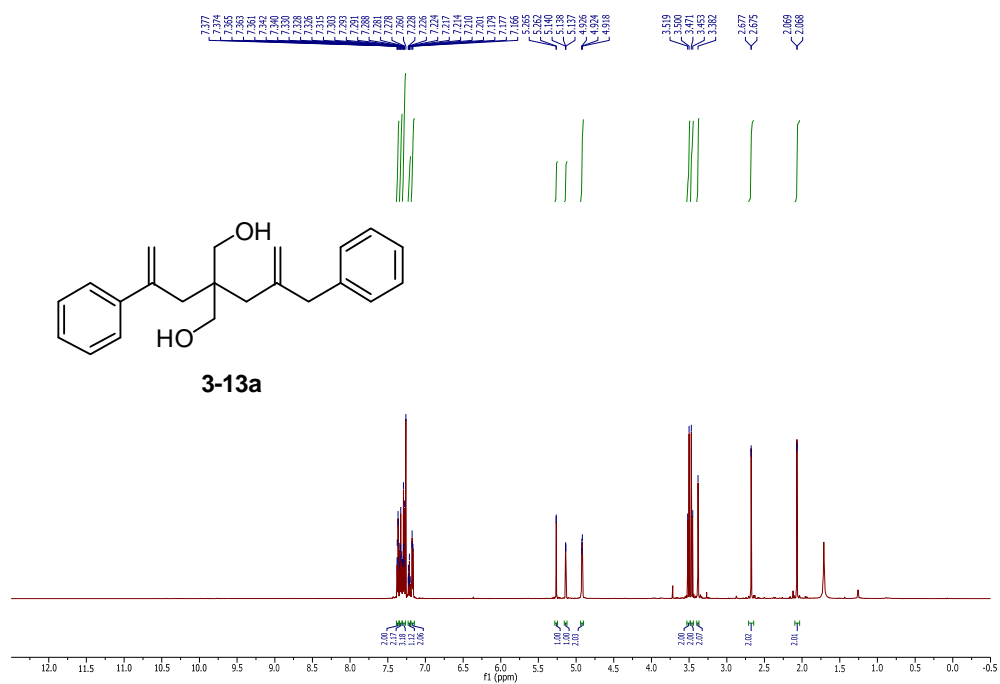


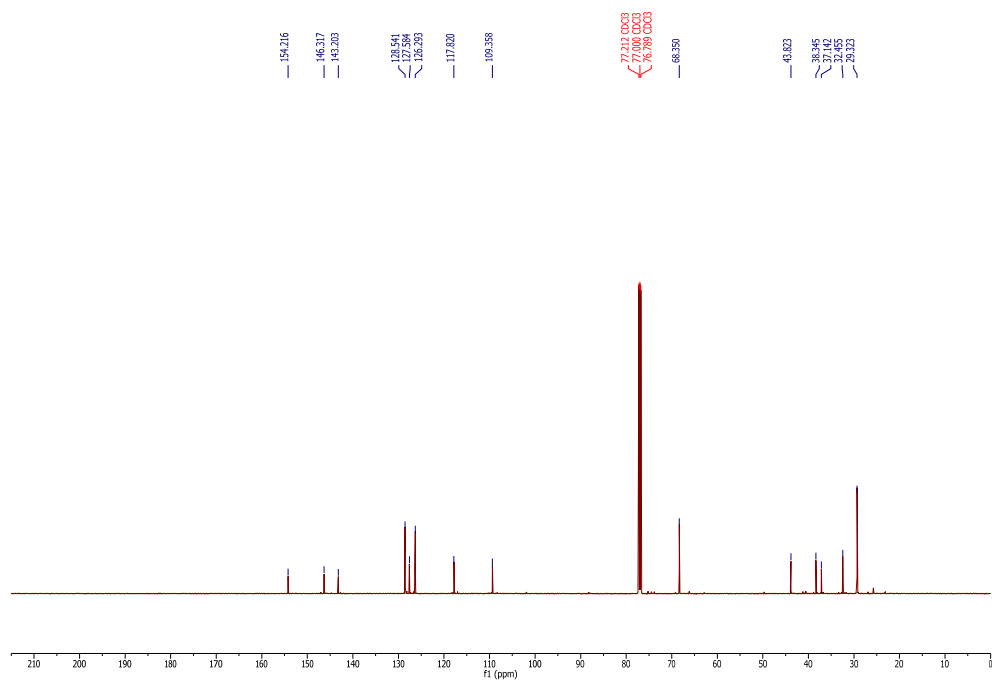
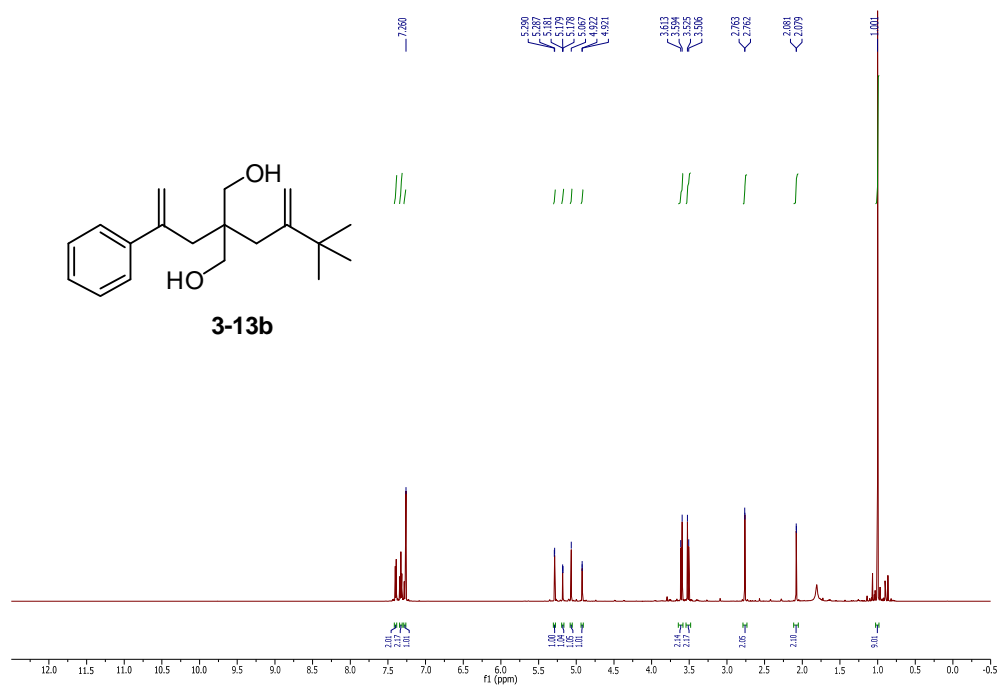


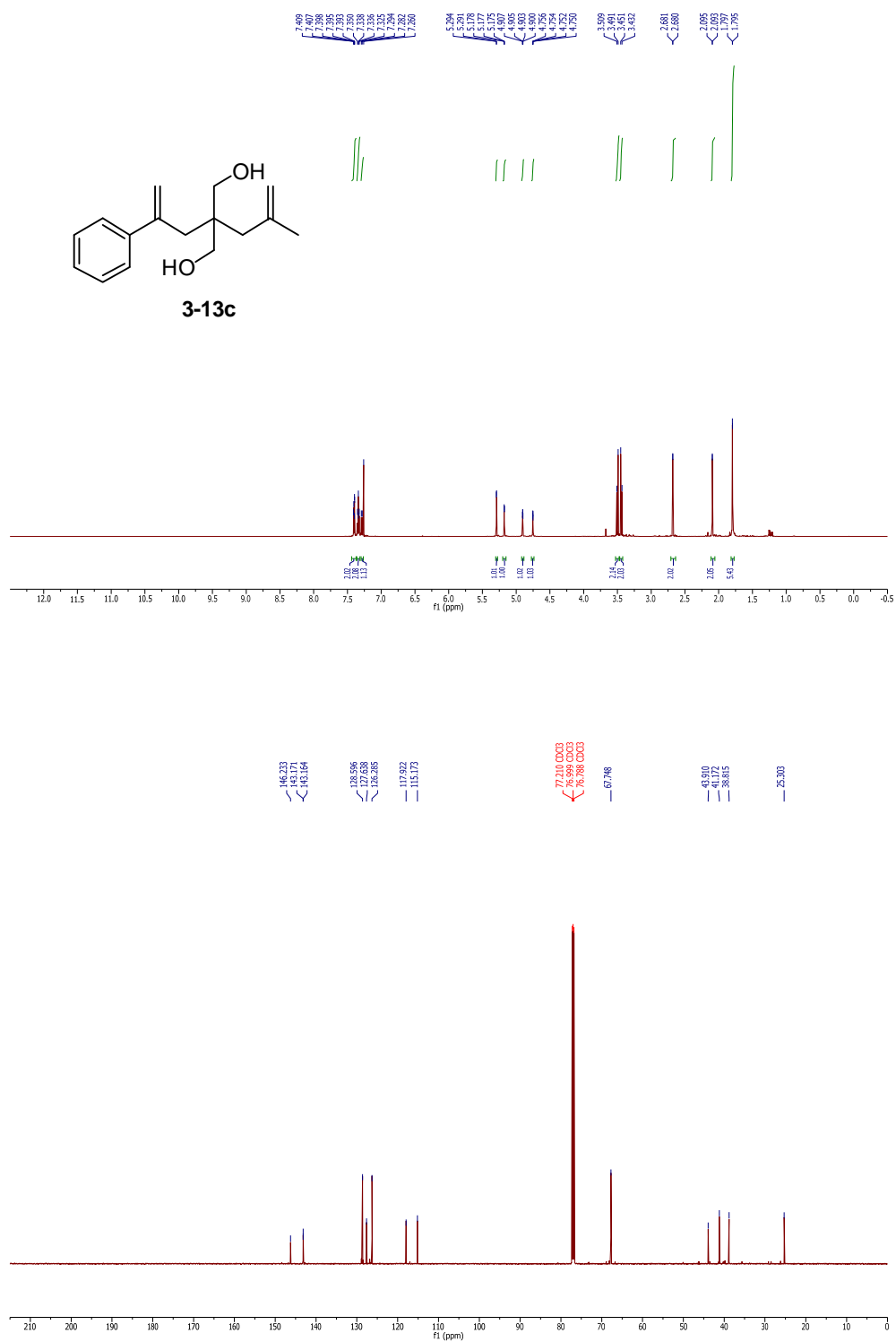


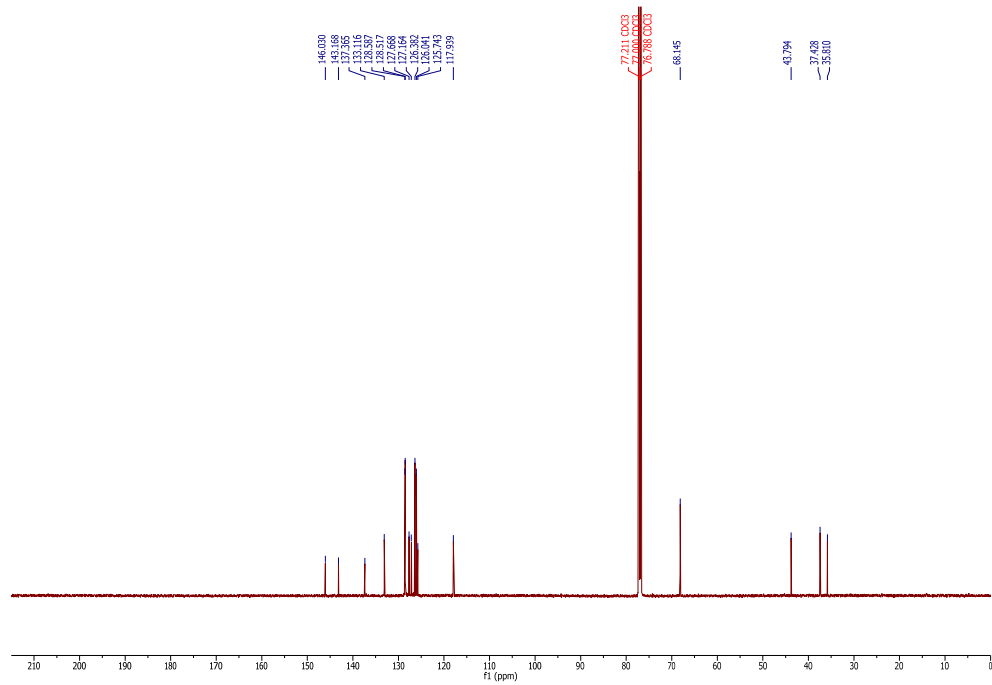
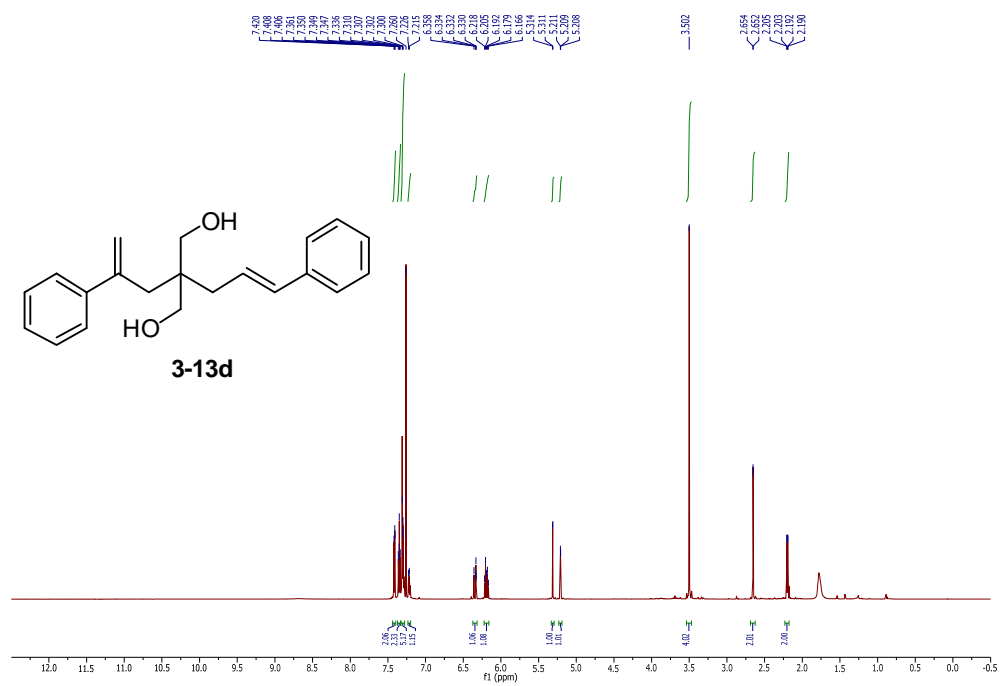


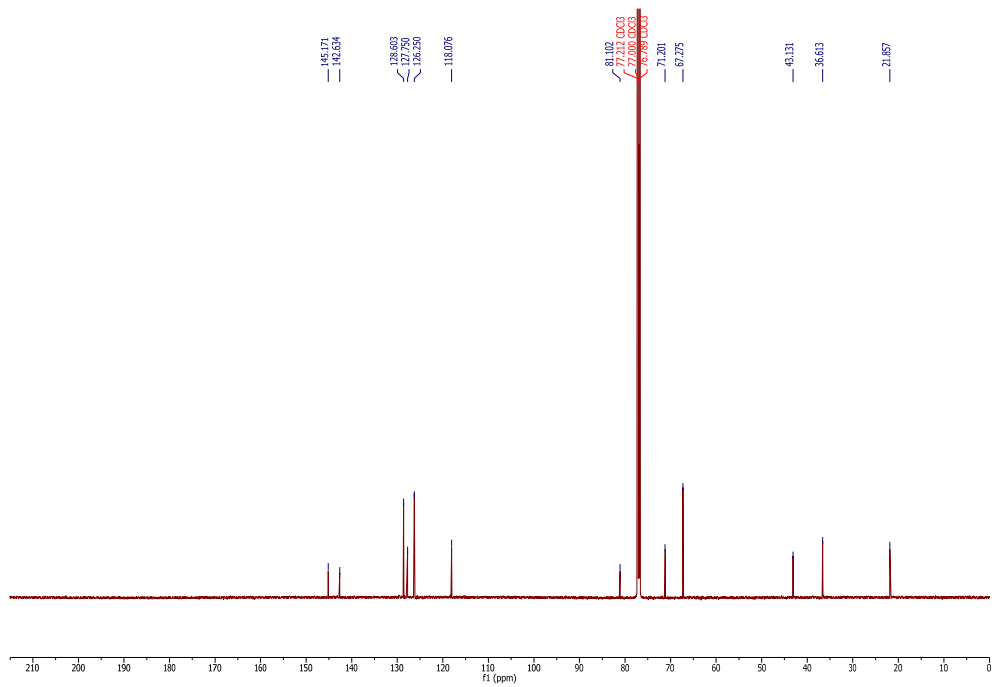
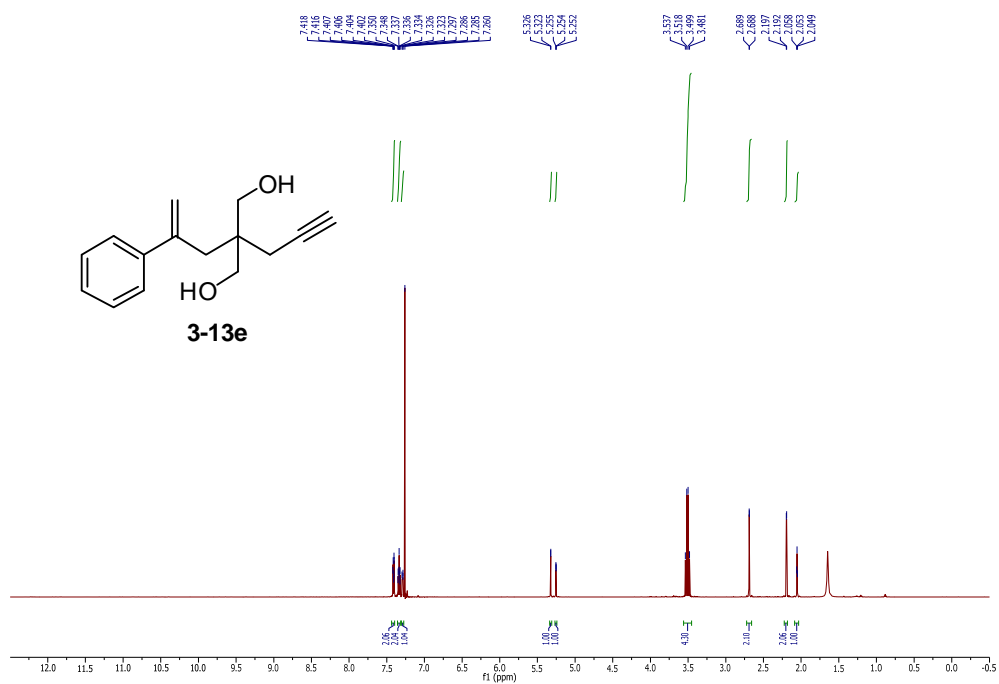


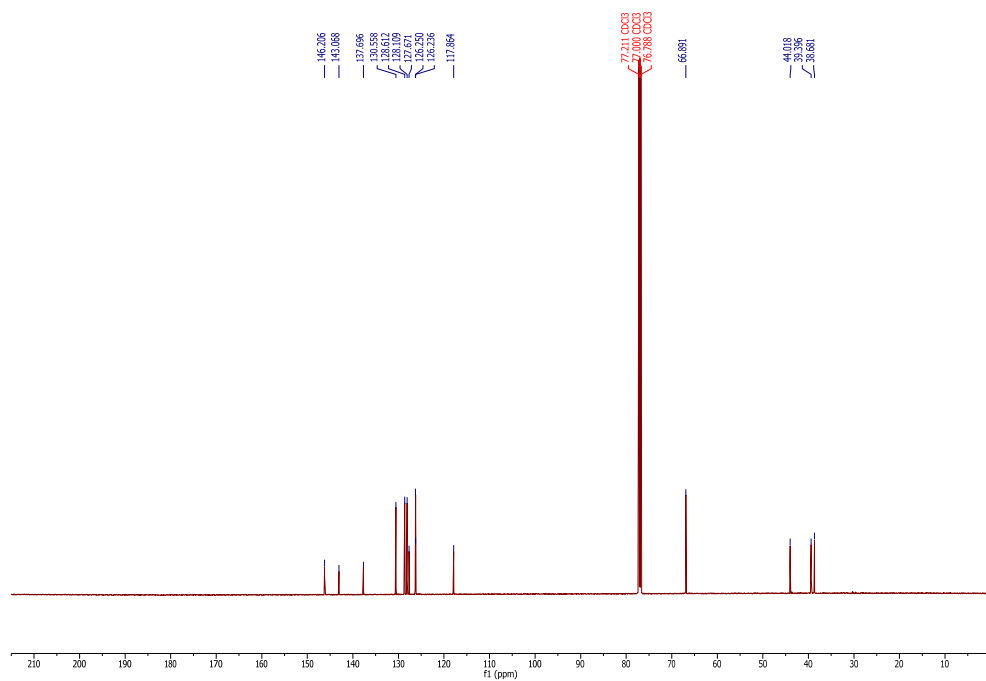
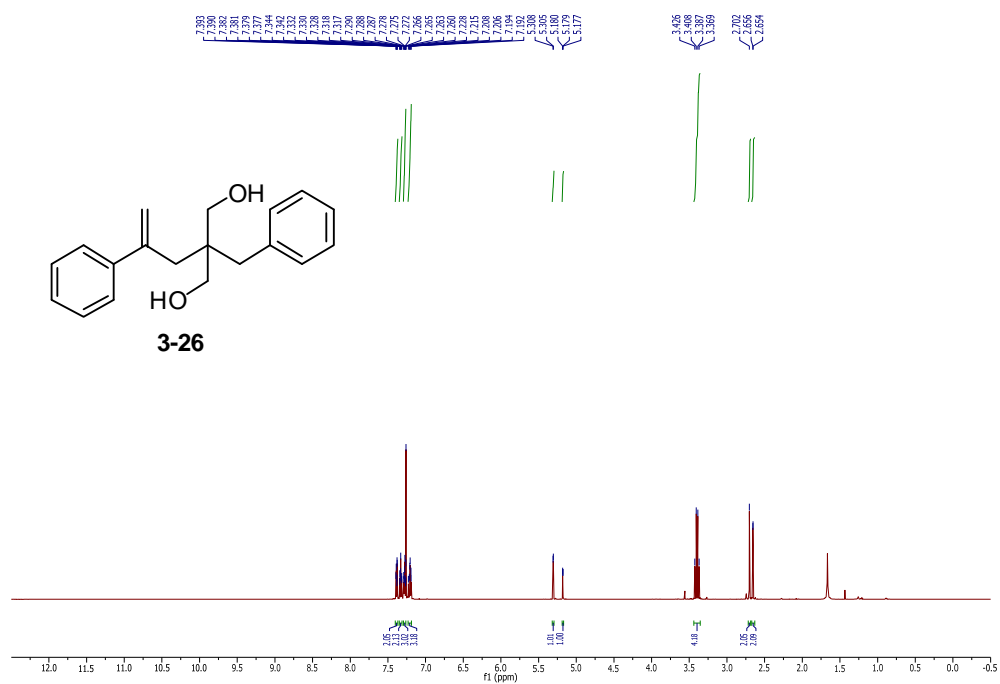


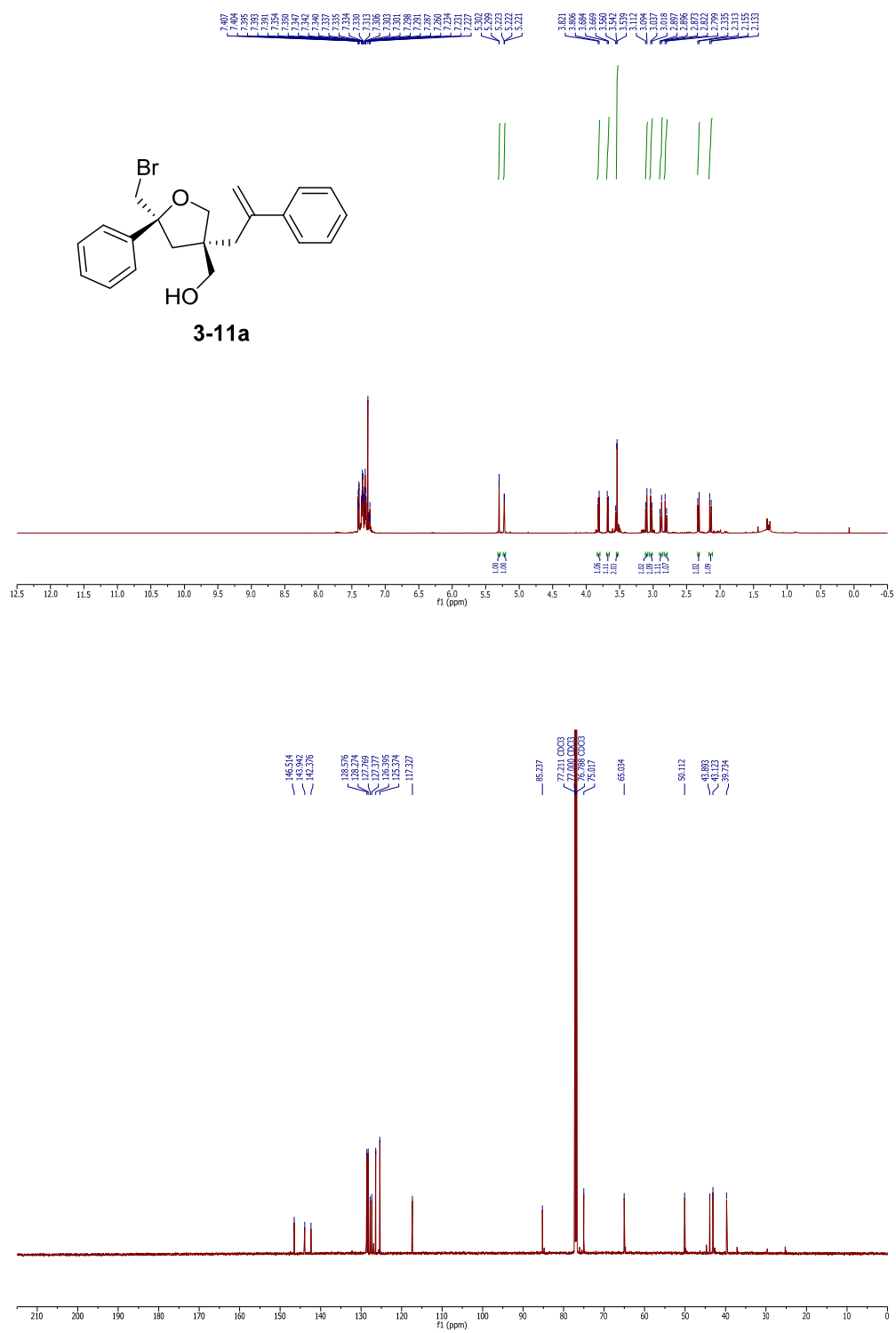


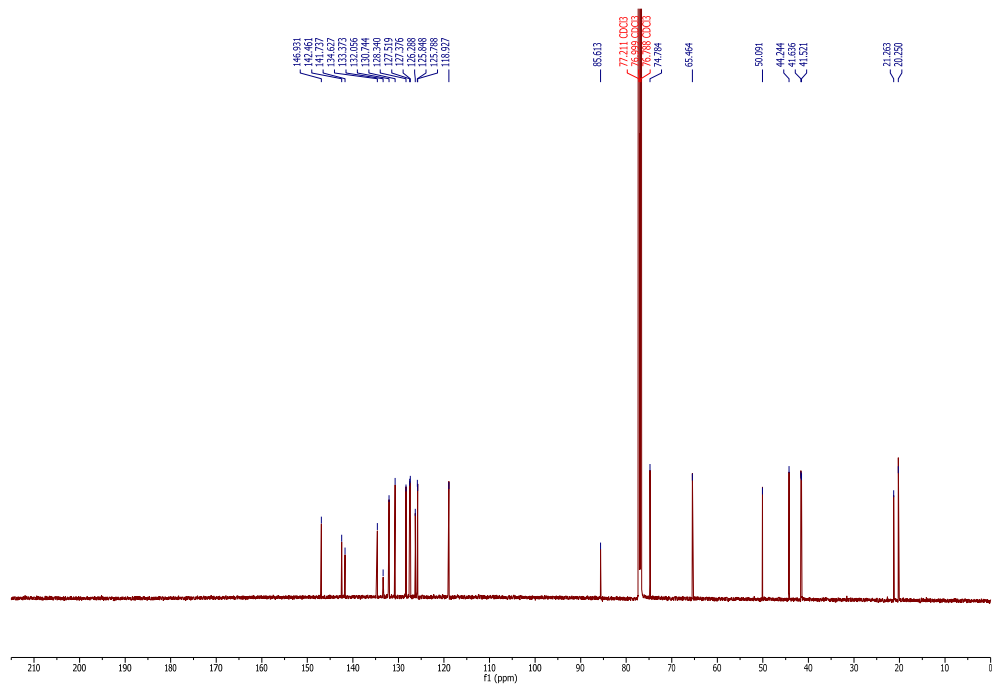


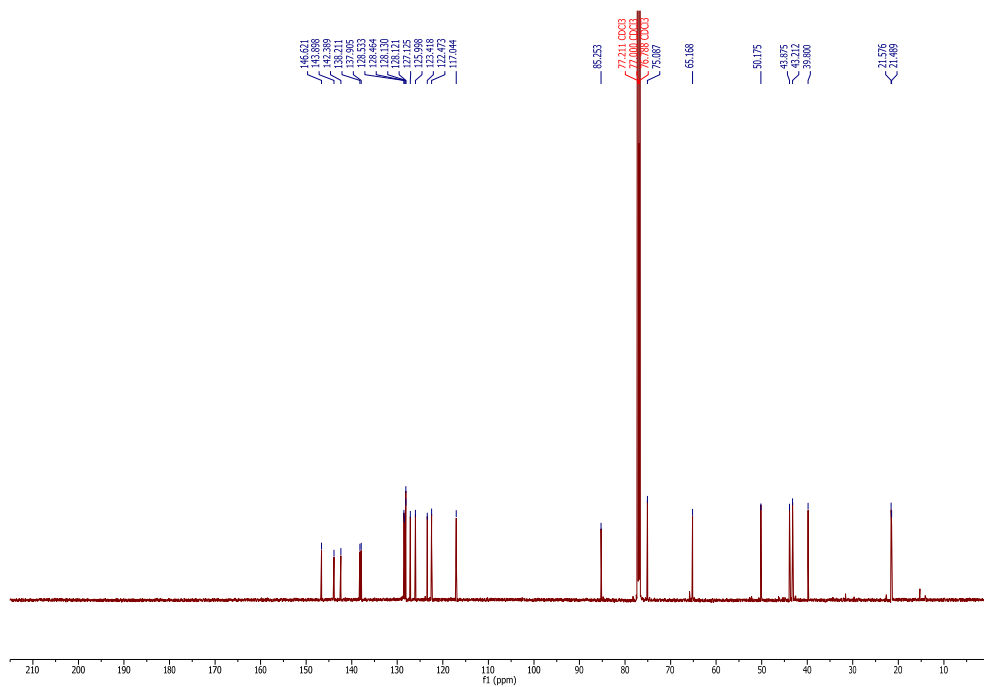


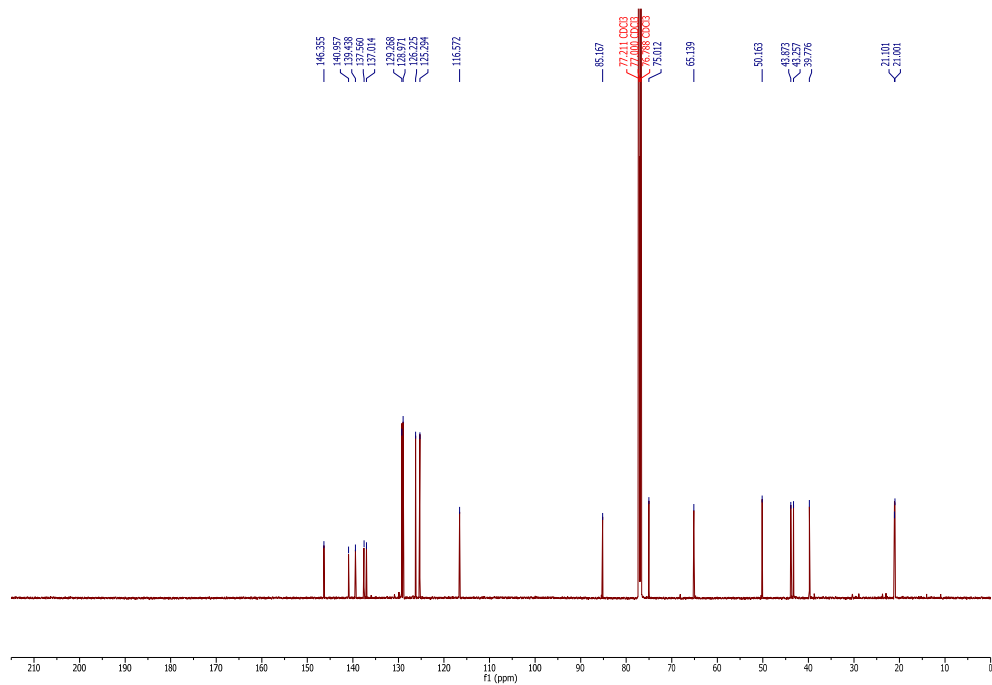
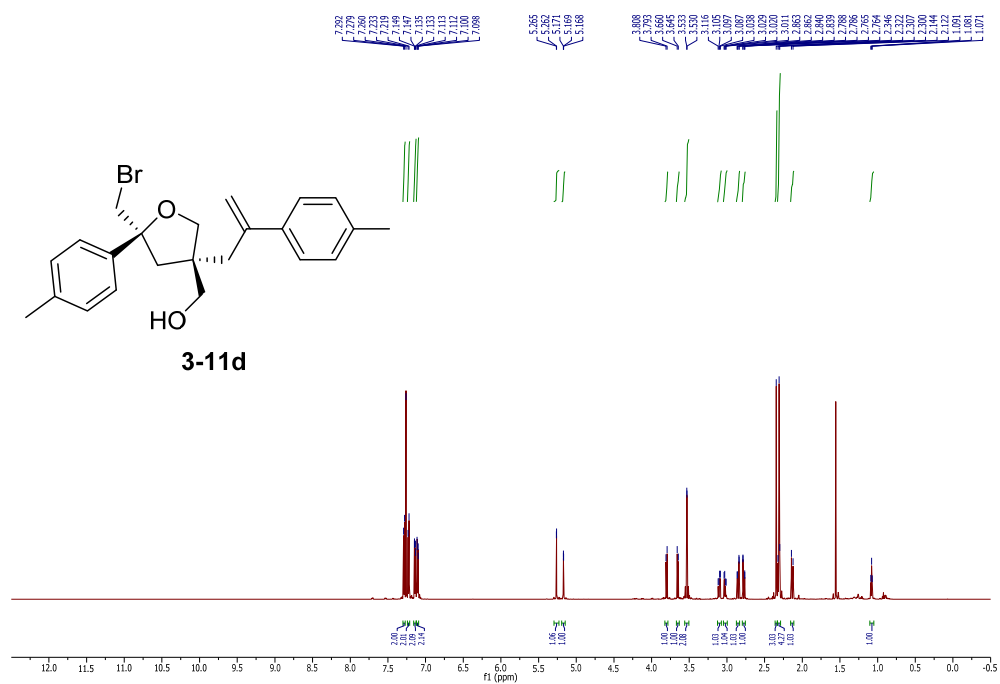


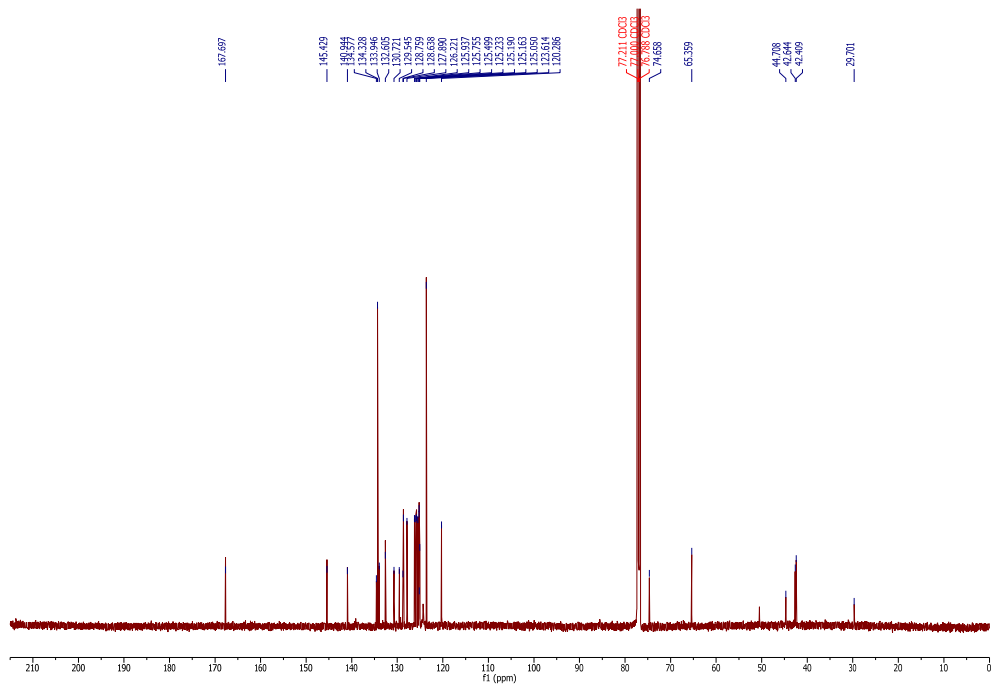


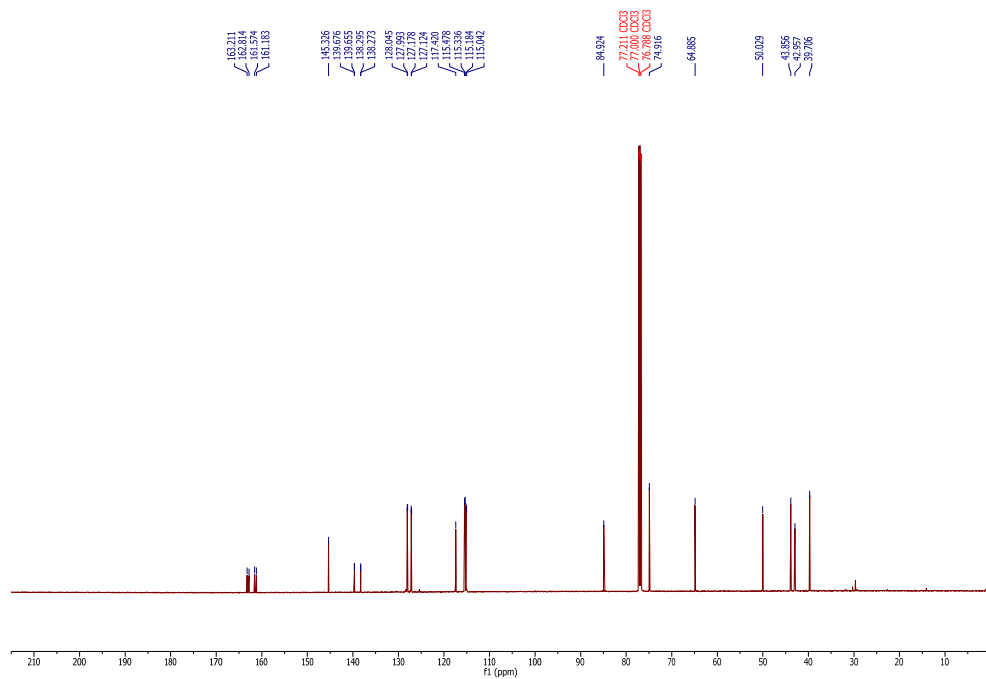
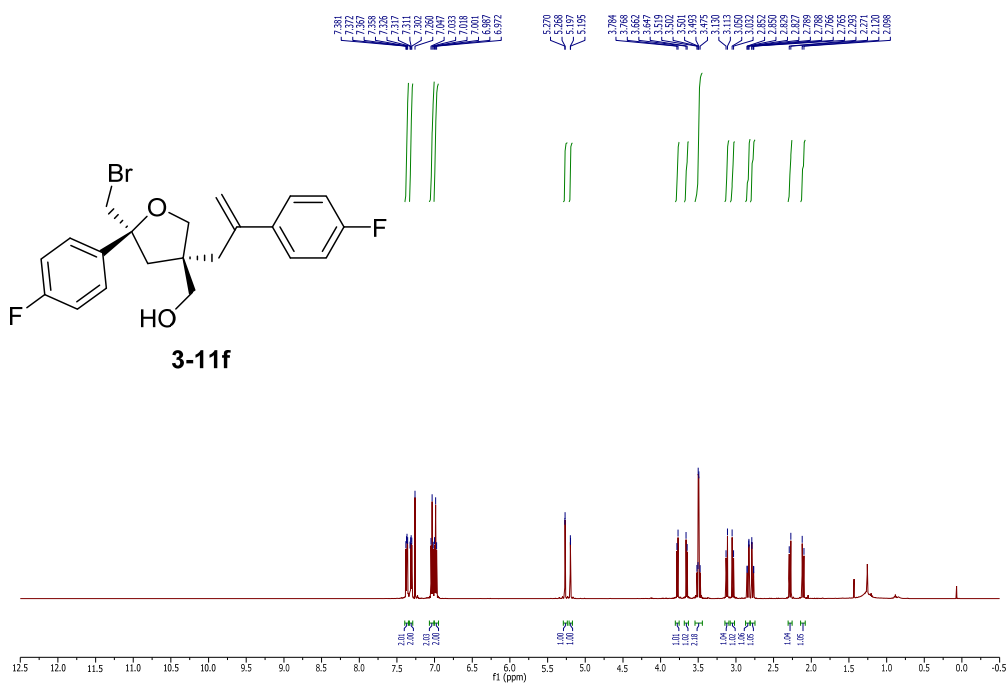


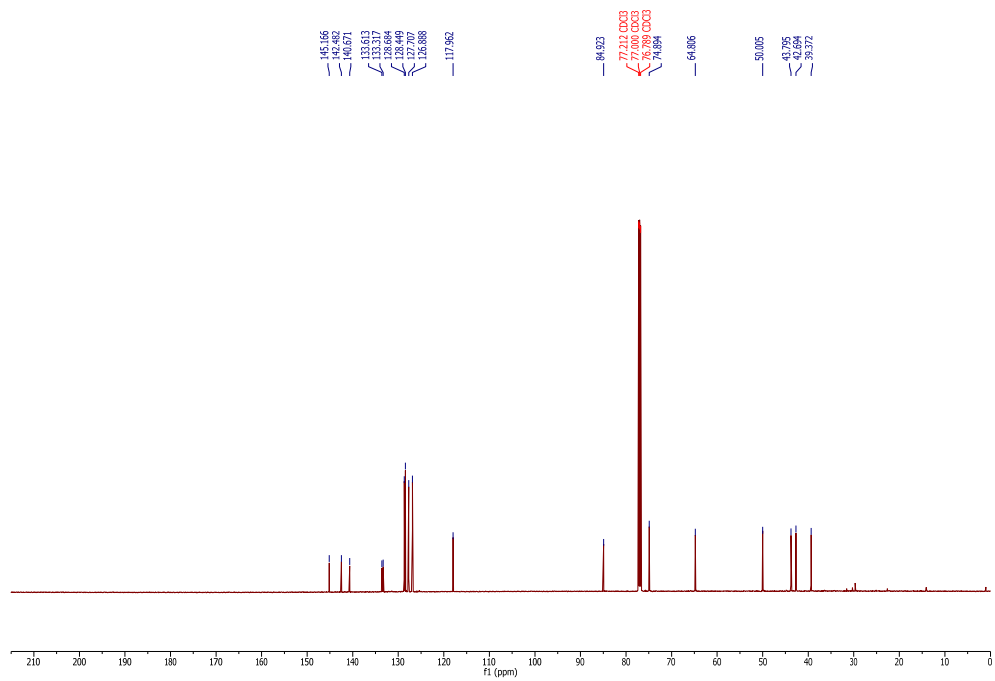
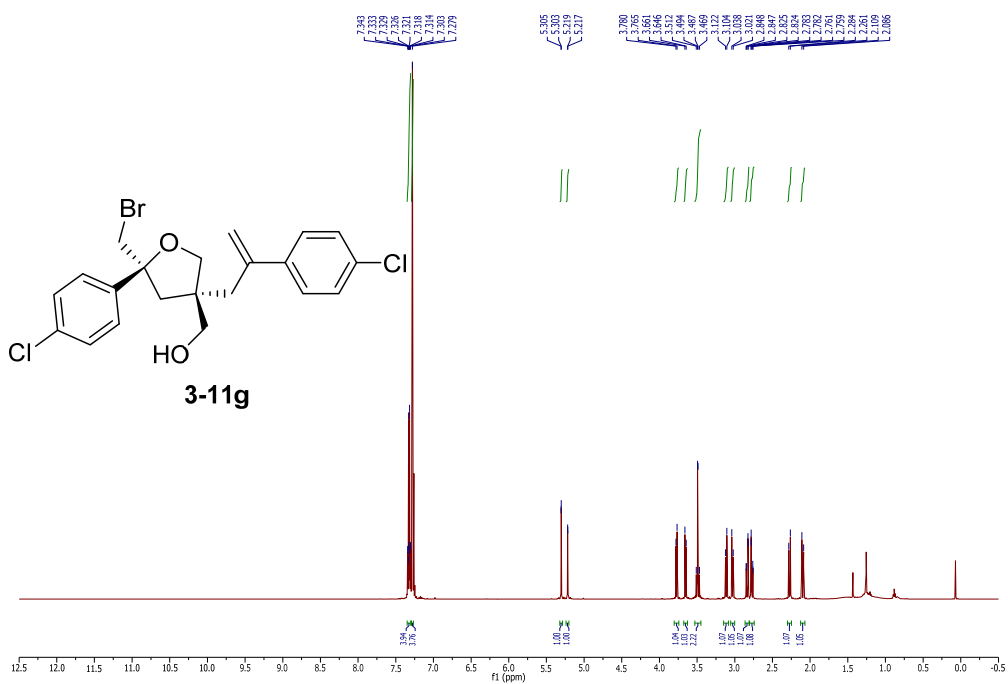


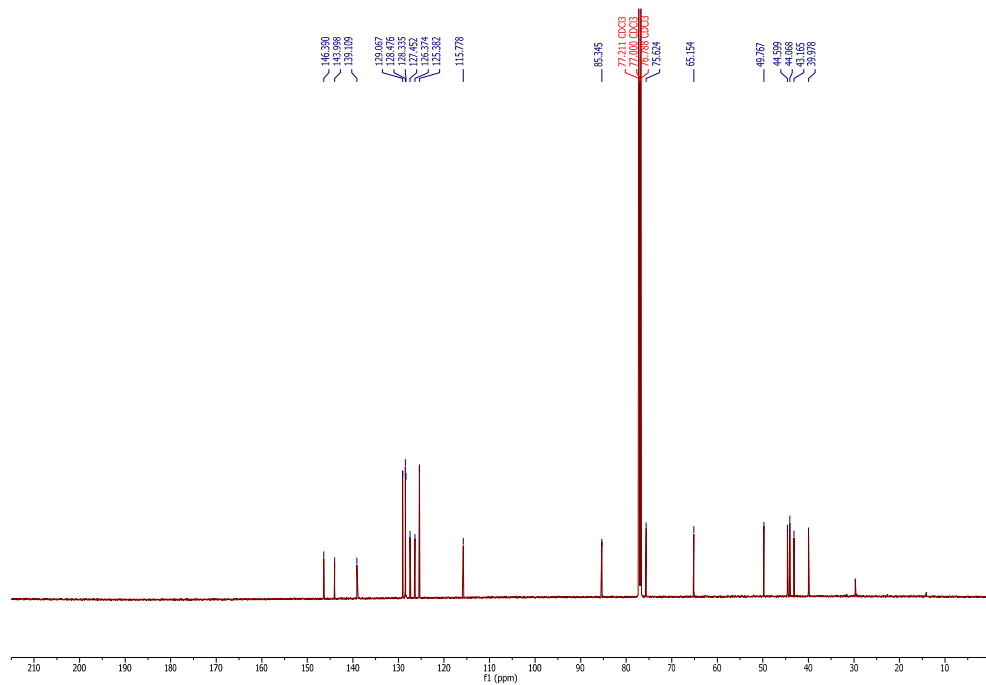


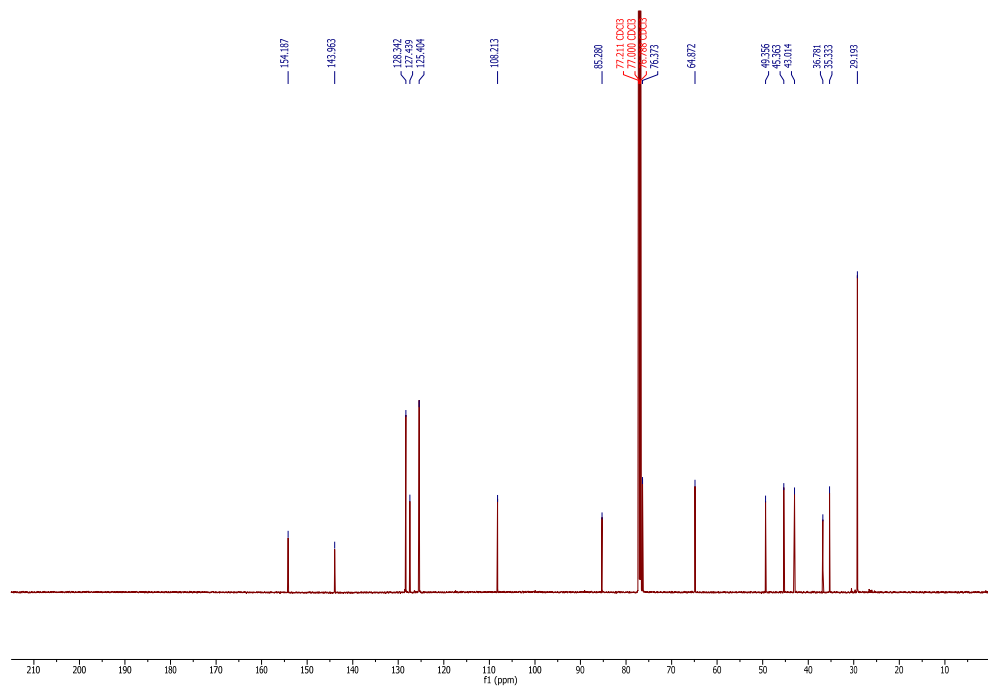
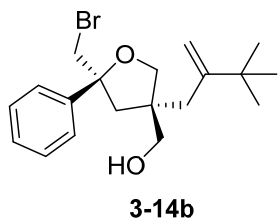


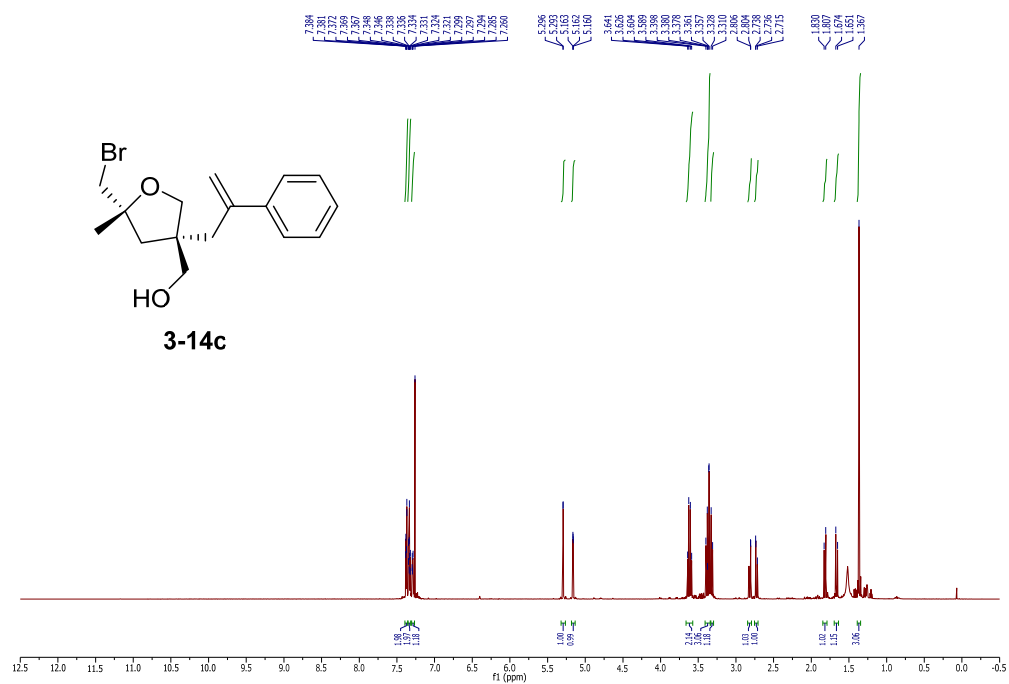


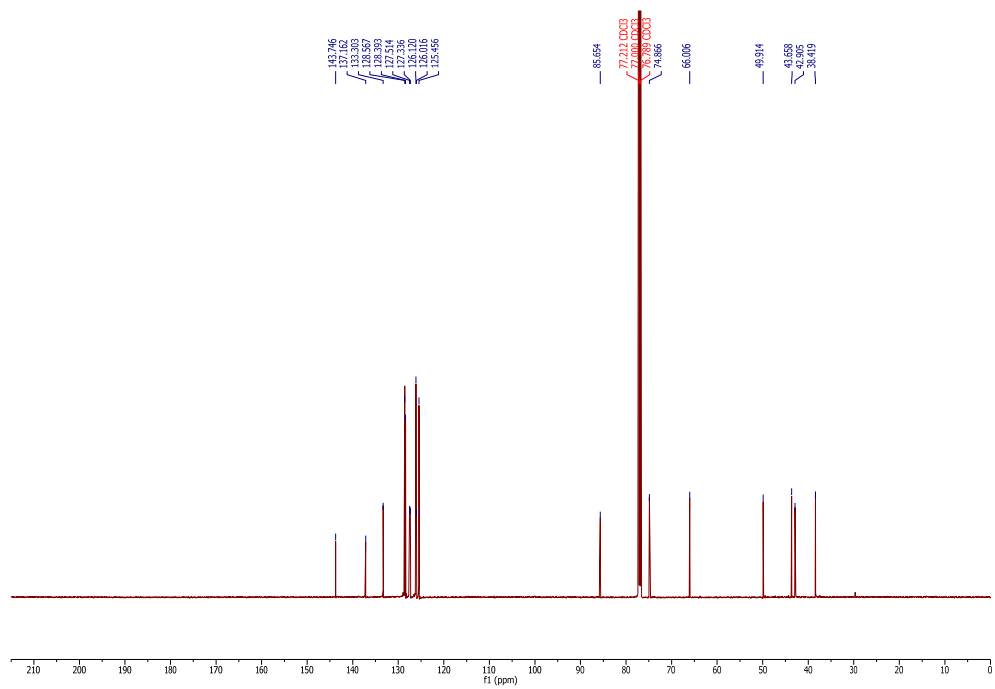
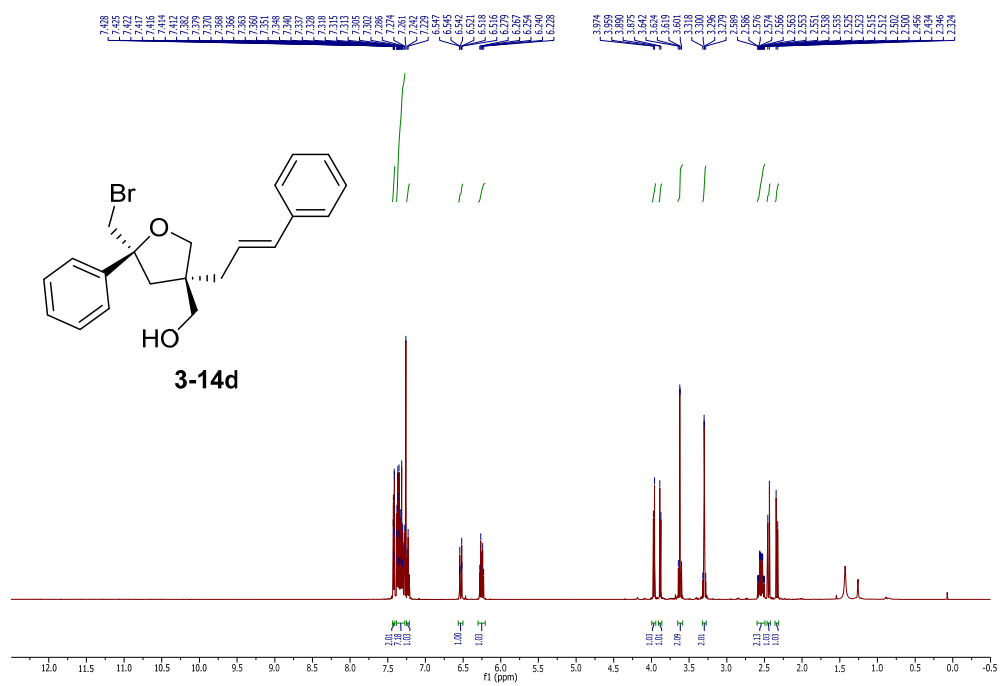


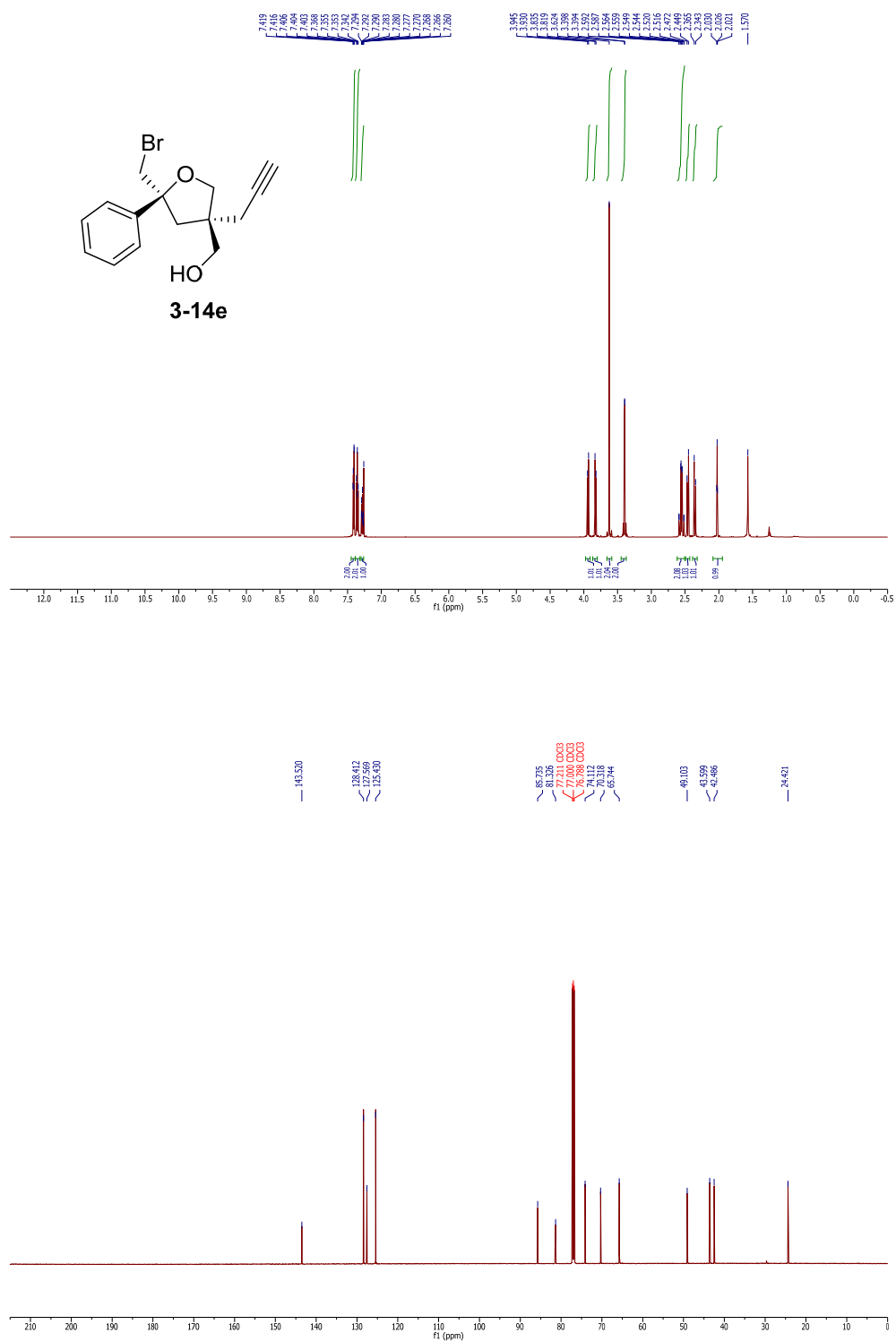


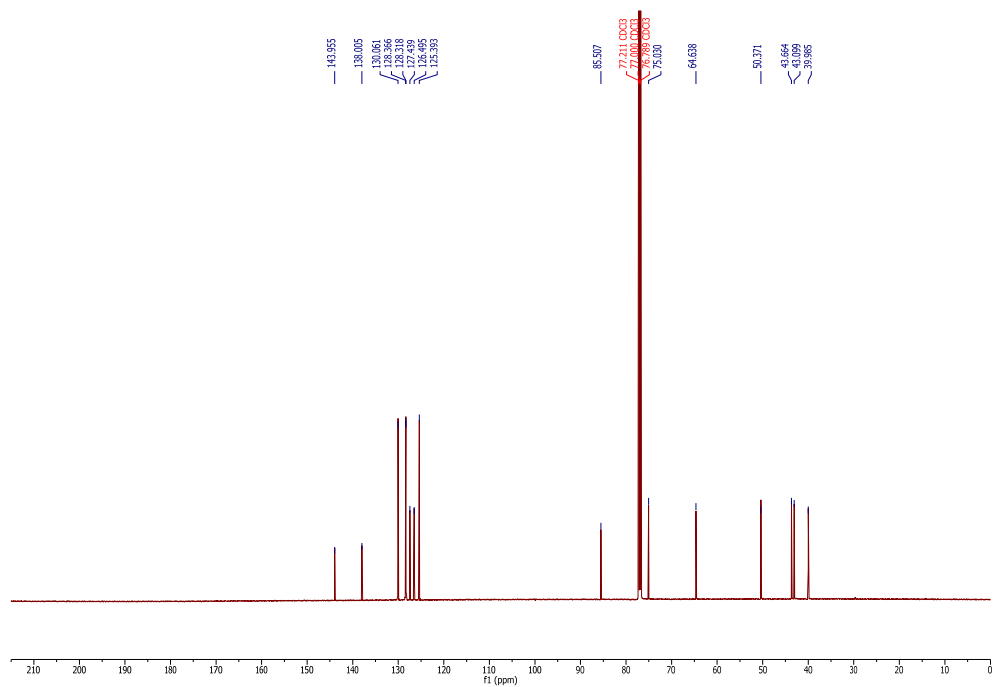
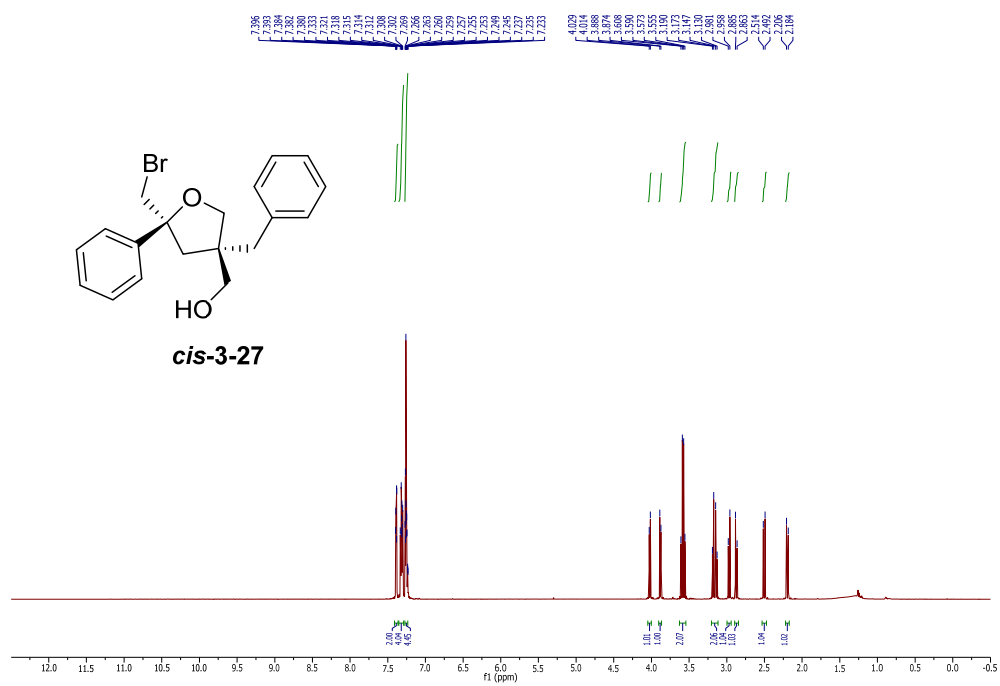


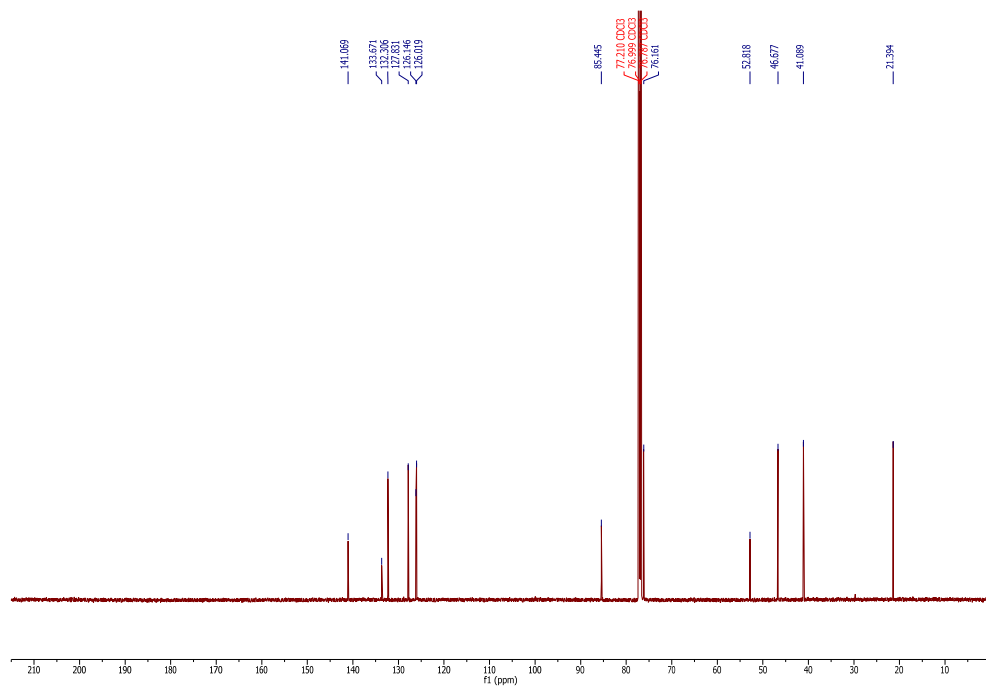


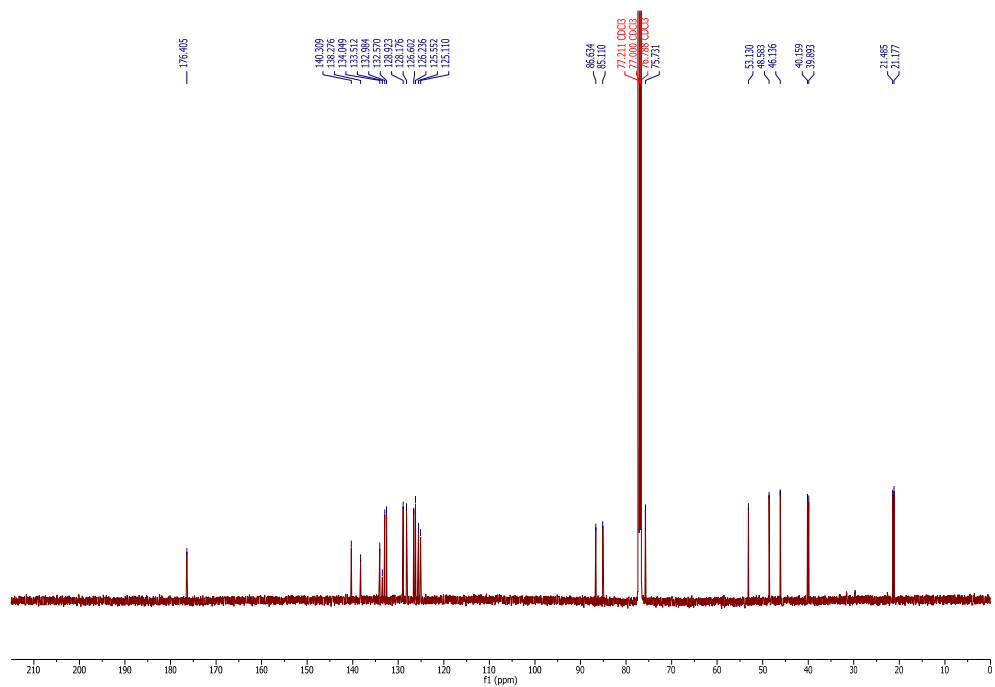


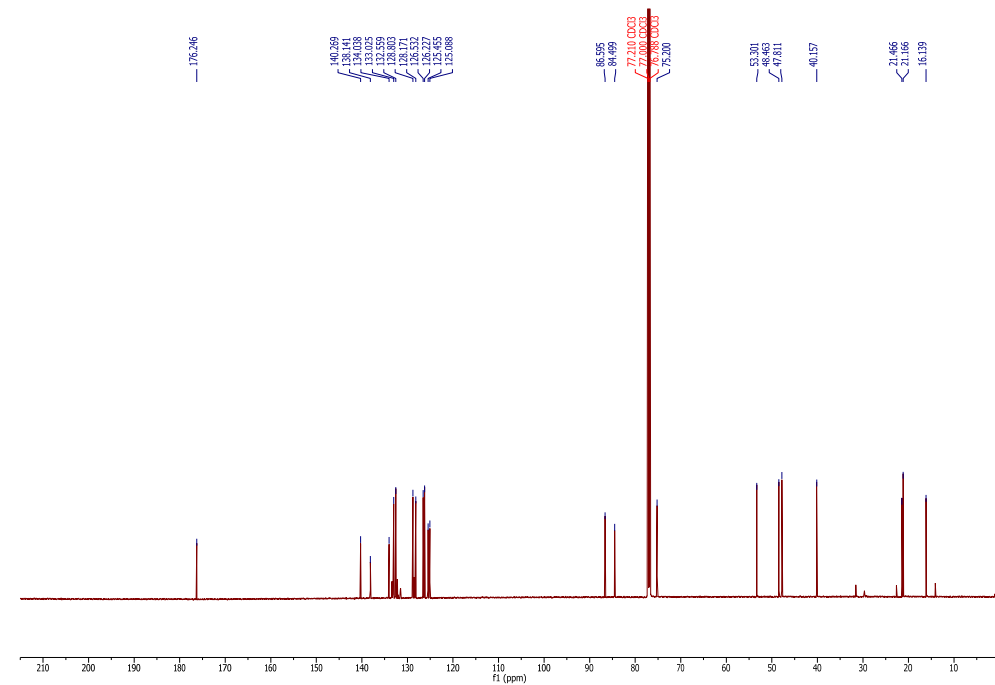


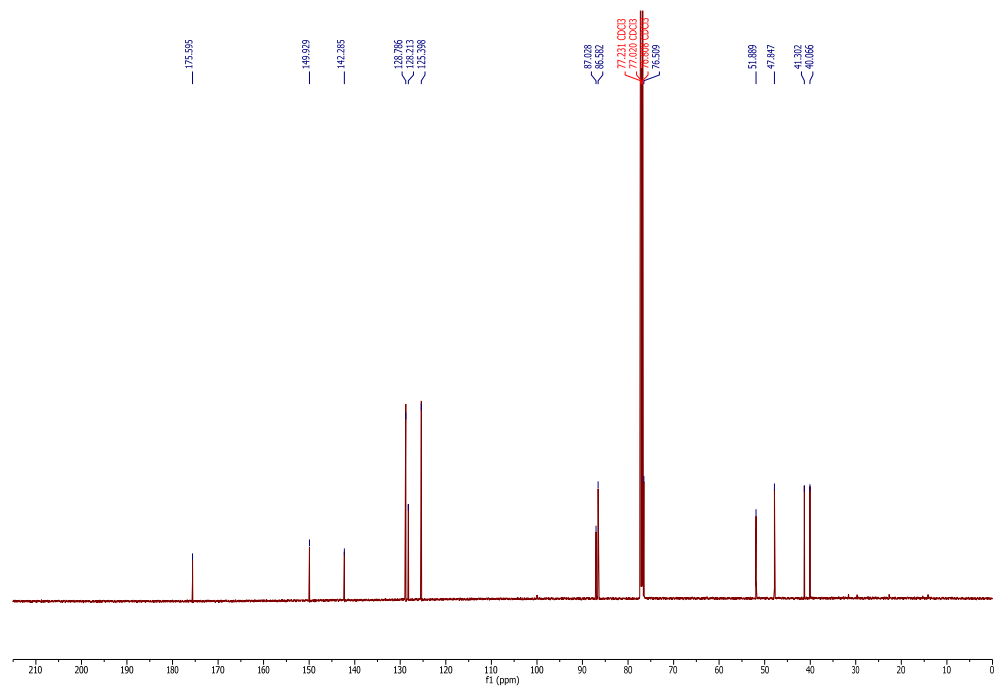
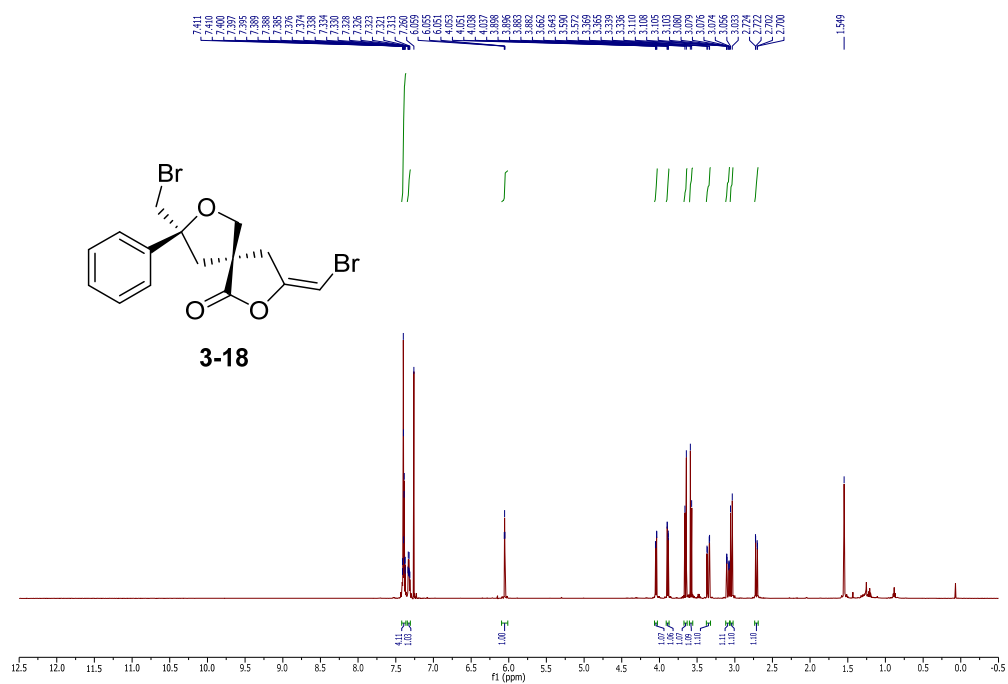




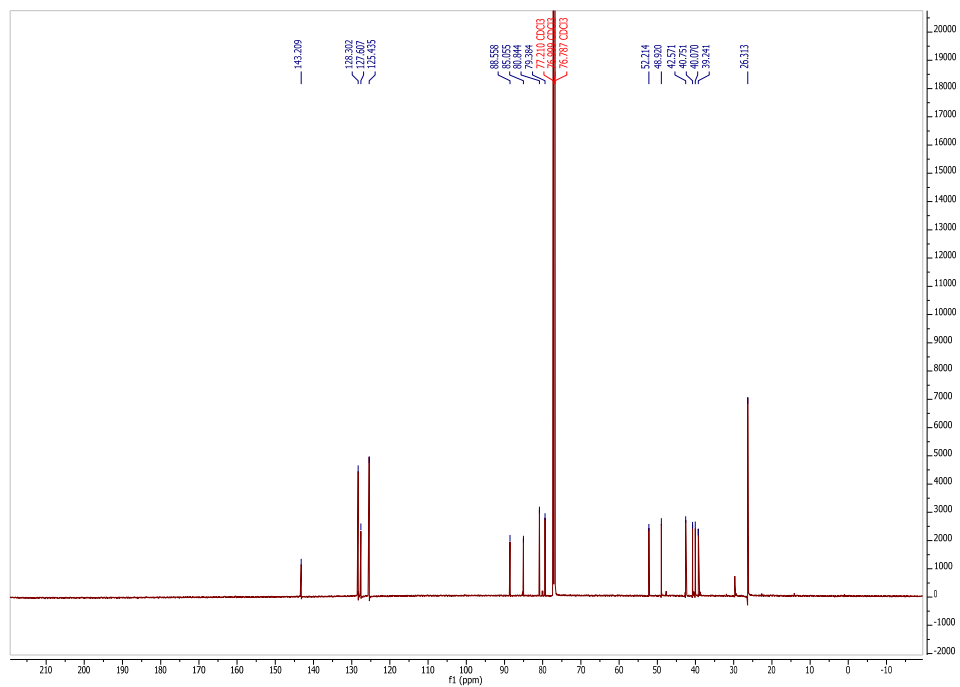
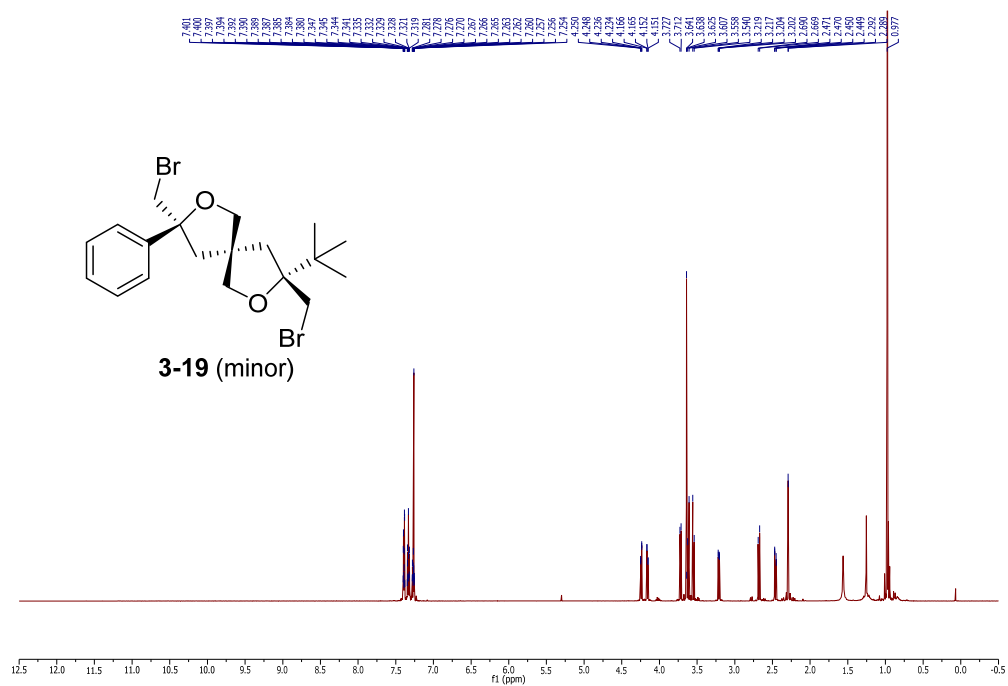


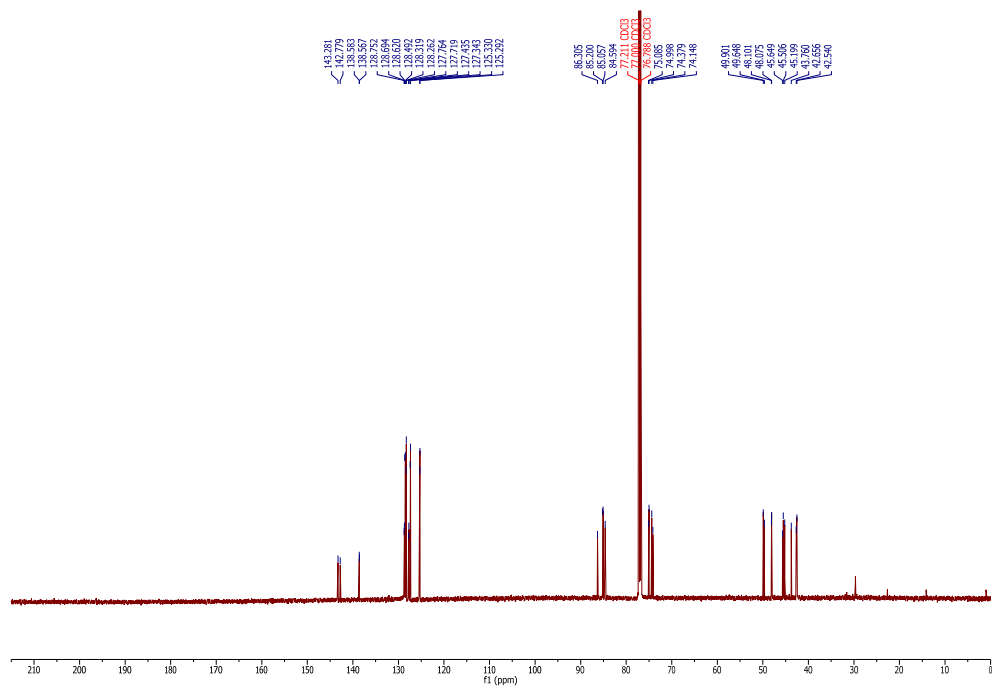


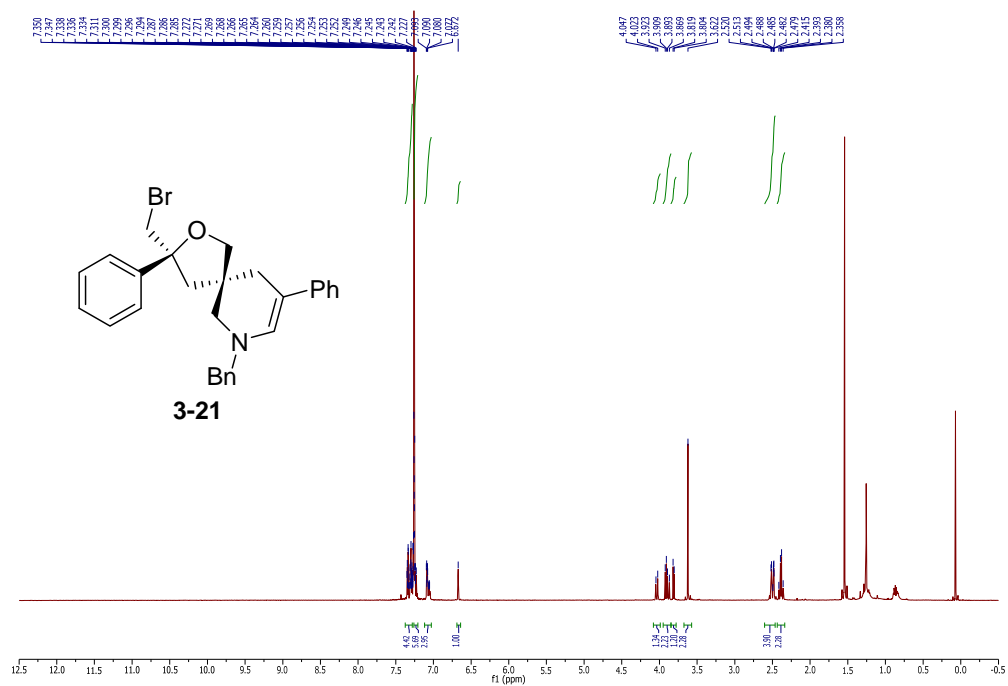


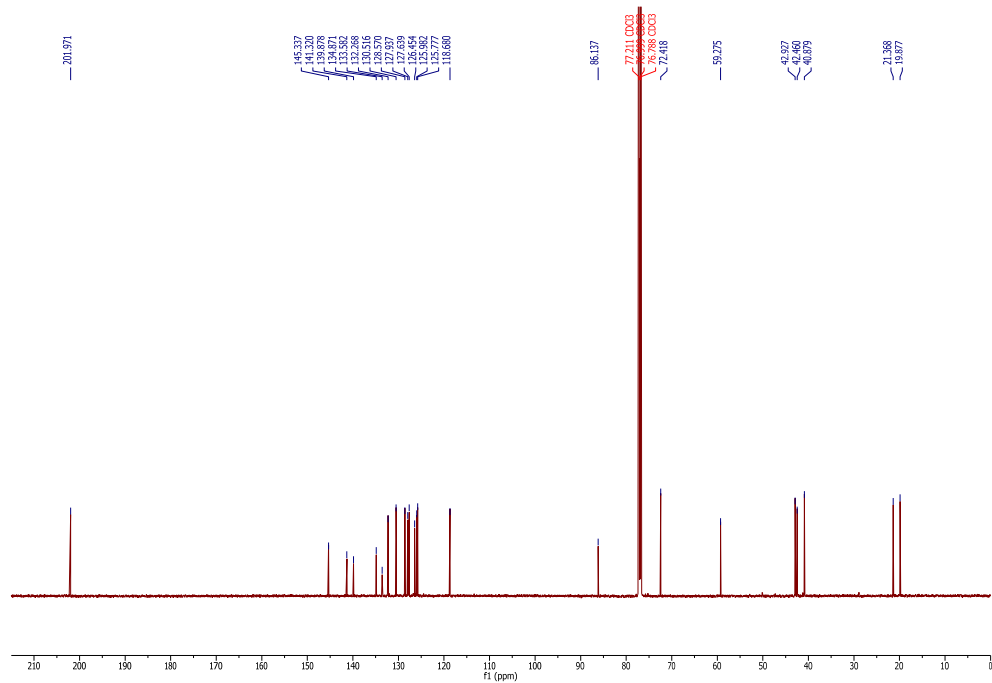
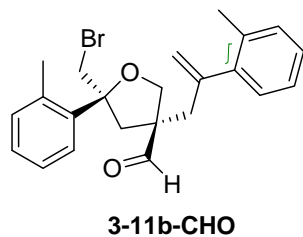


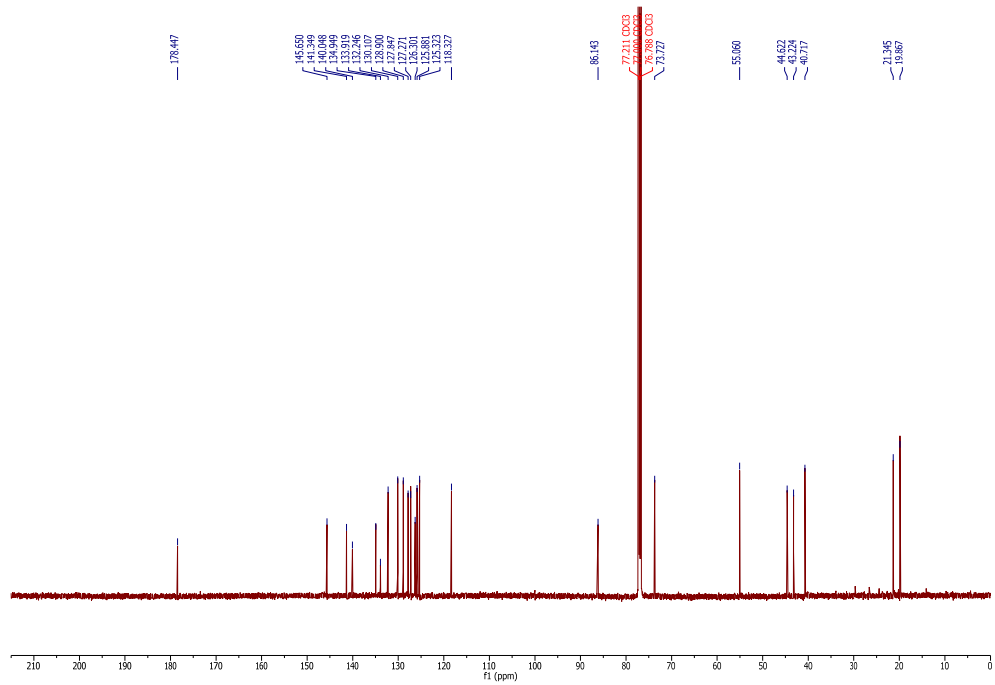
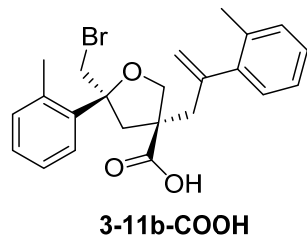


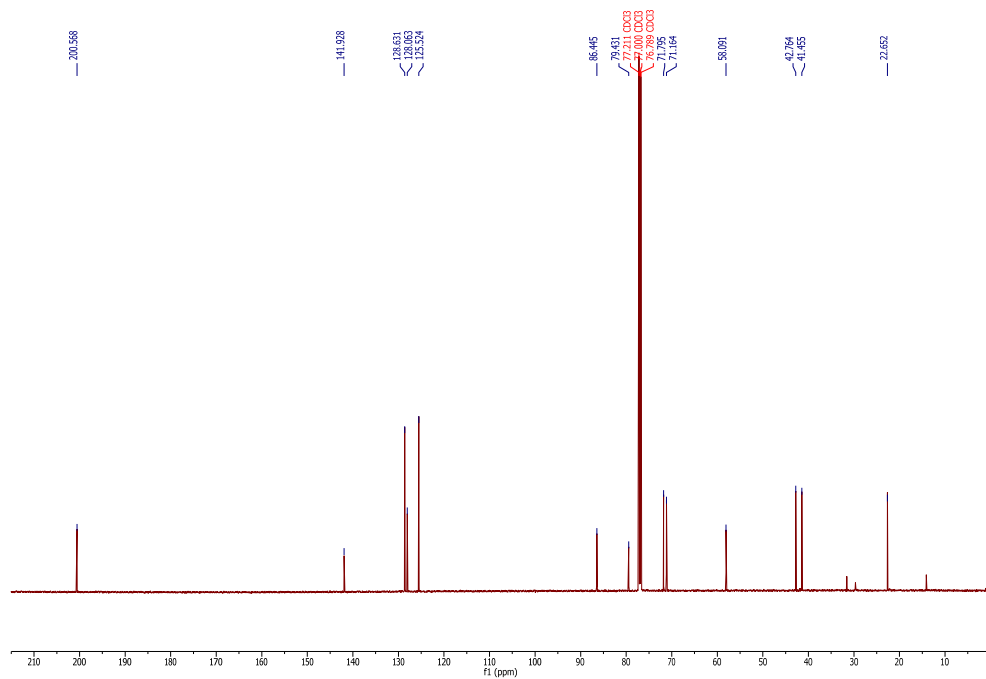
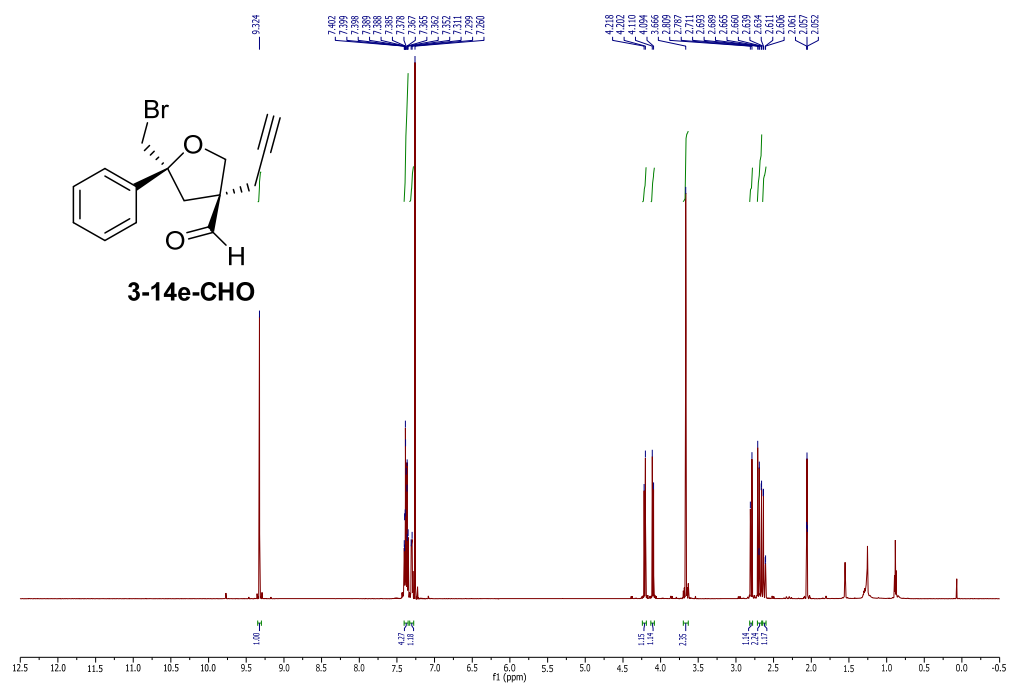




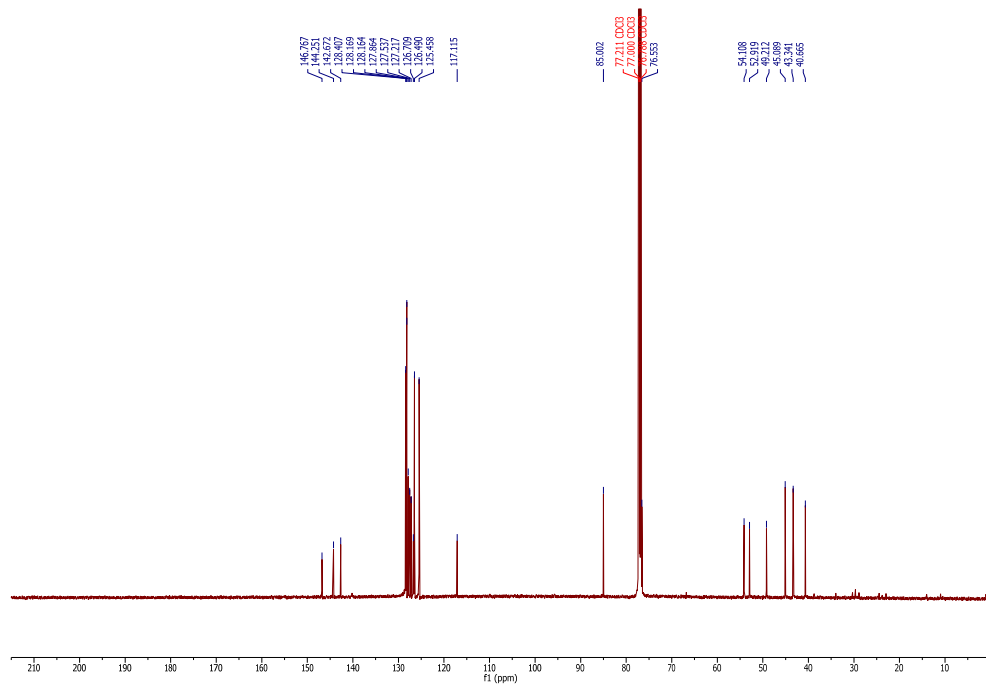
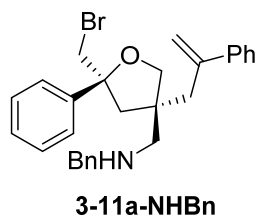


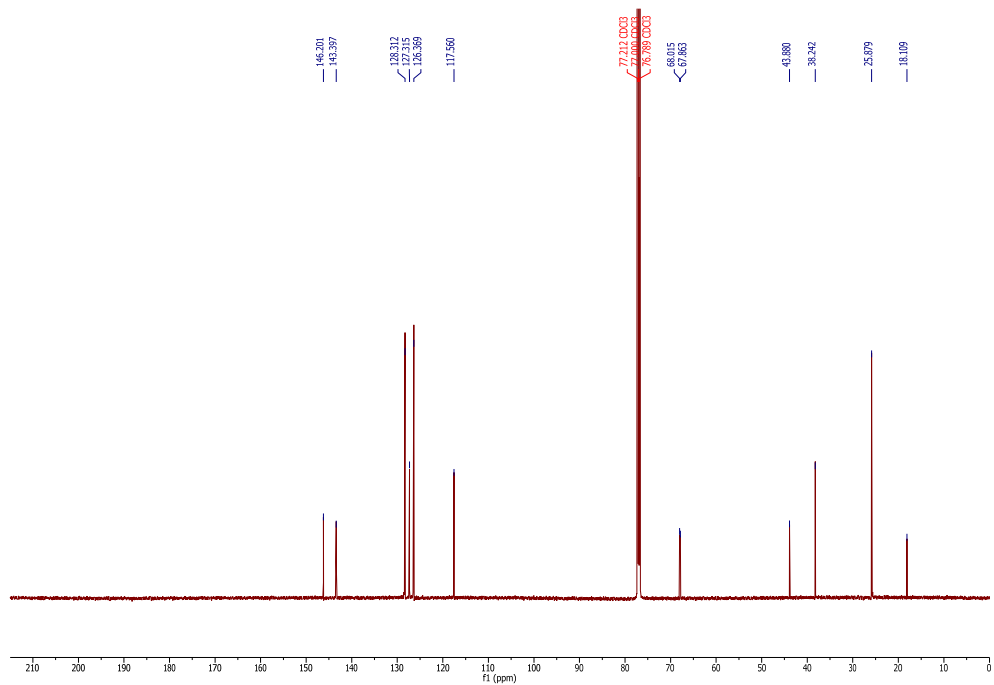
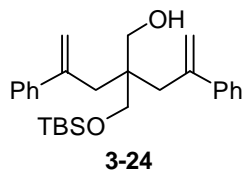






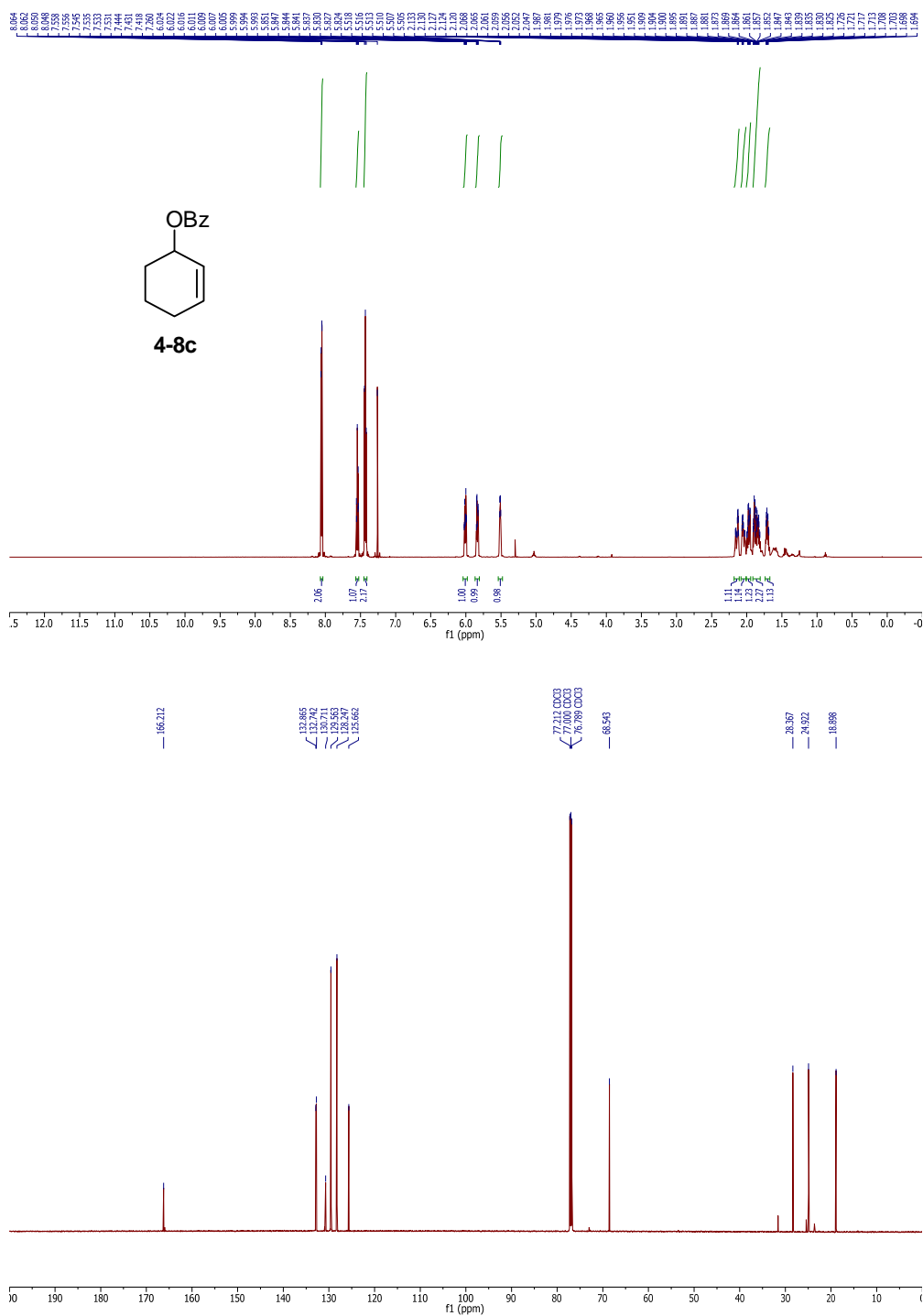


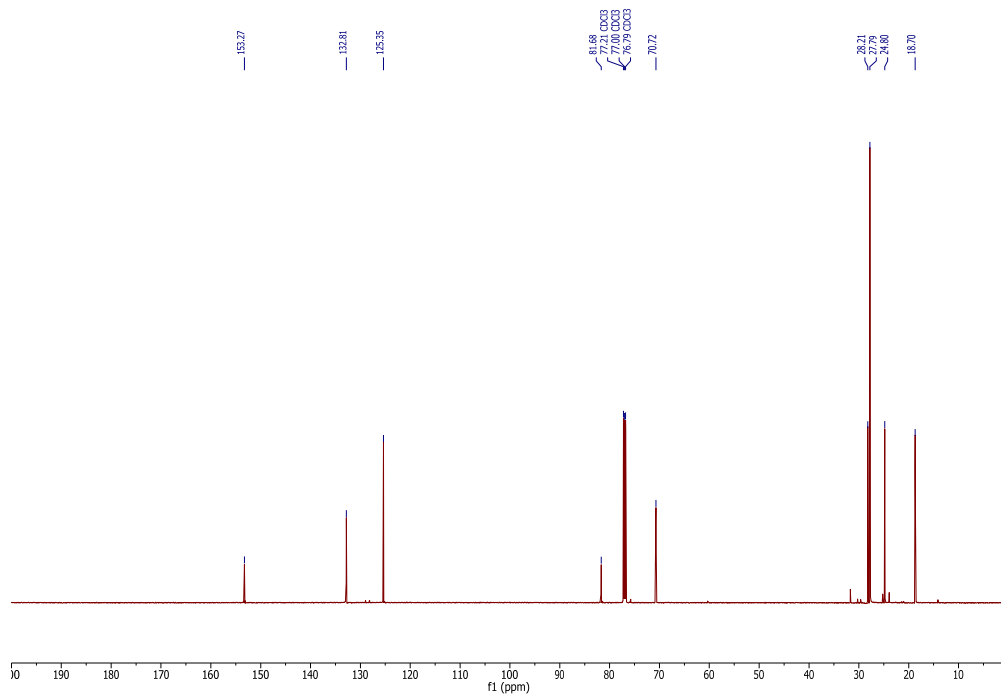
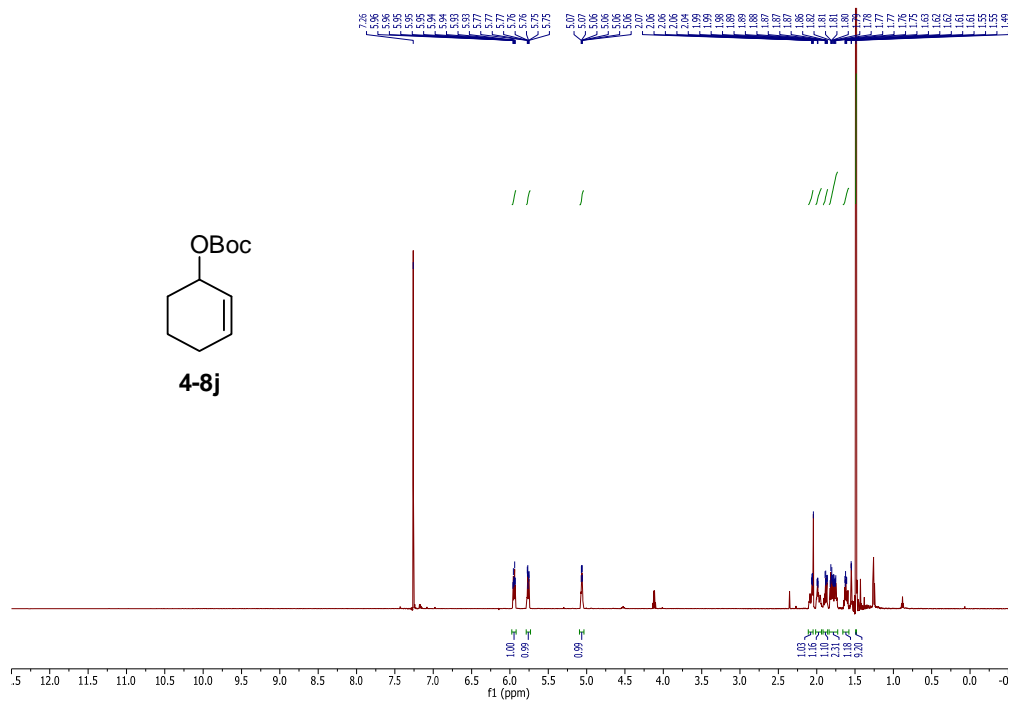


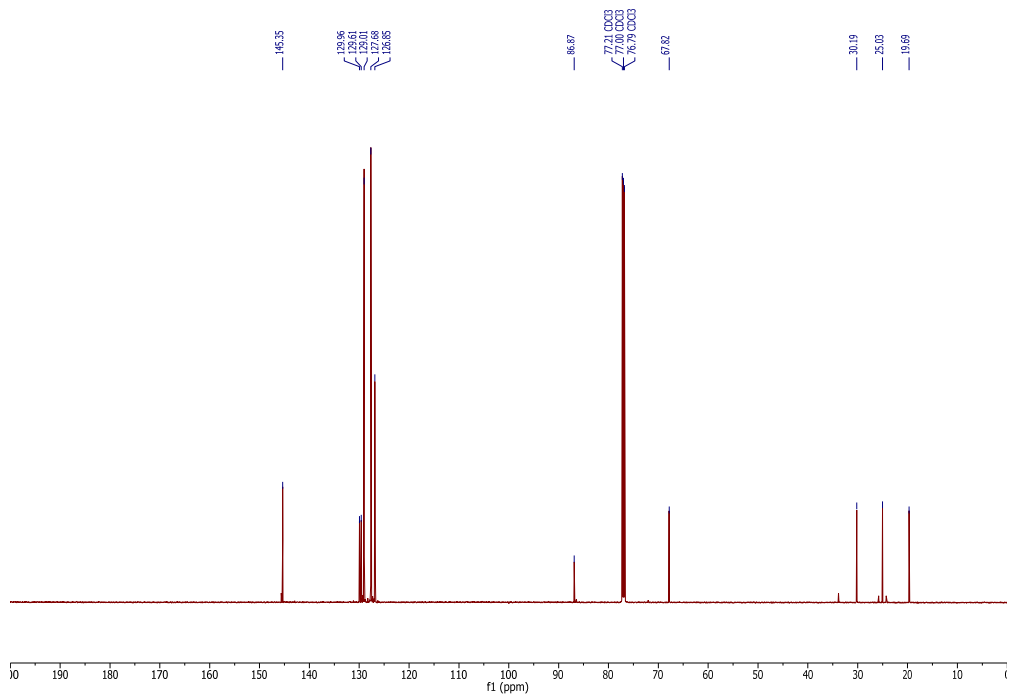
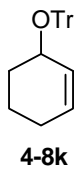


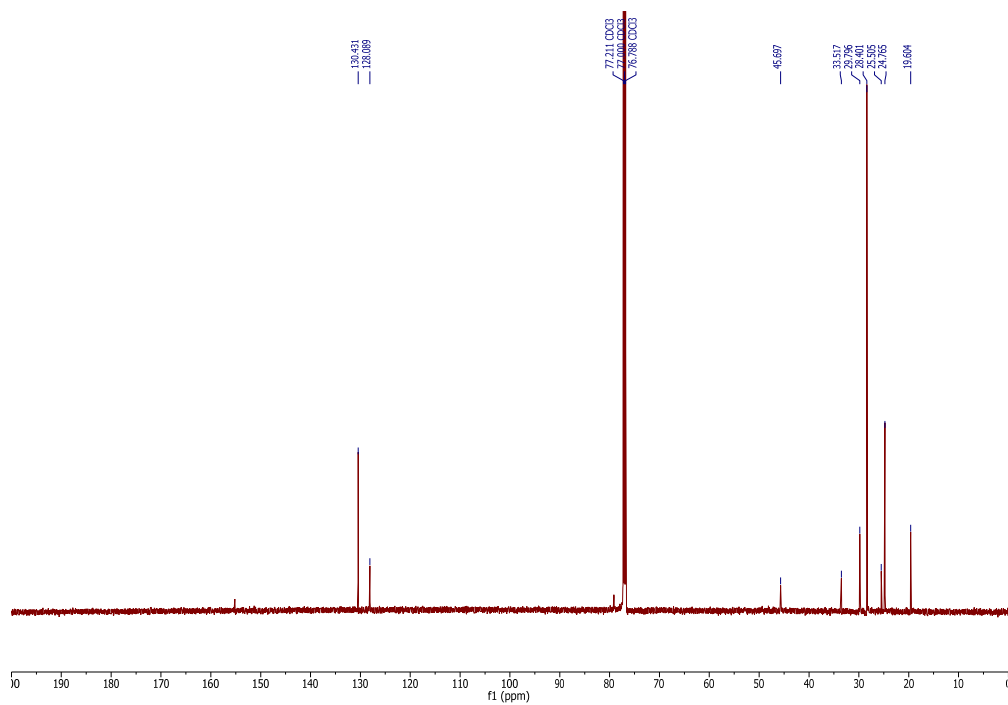
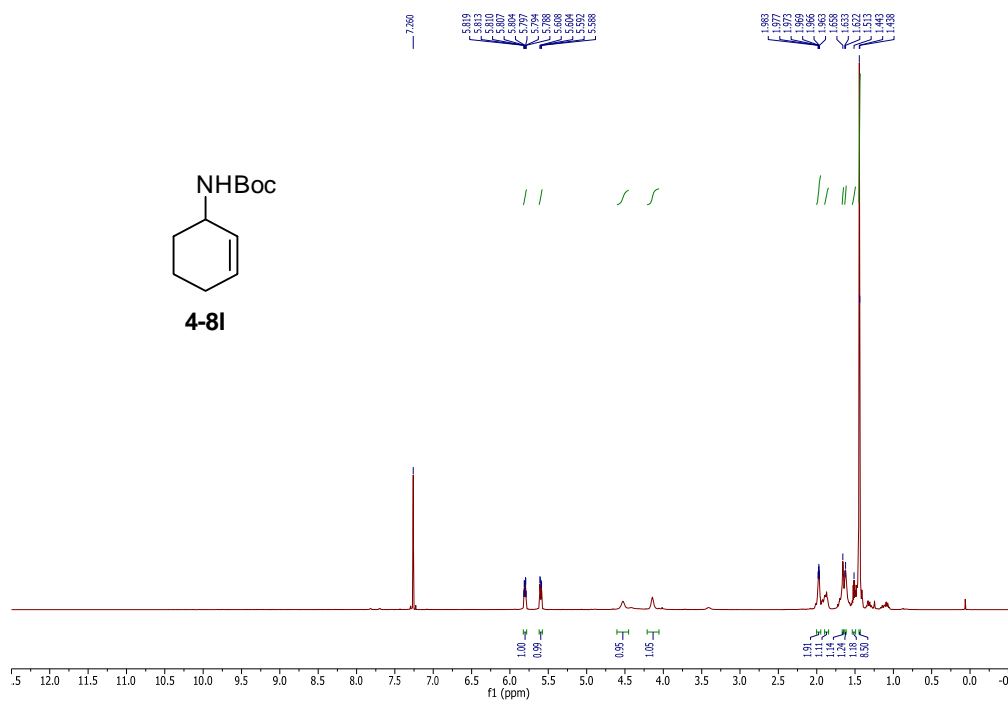
Appendix C

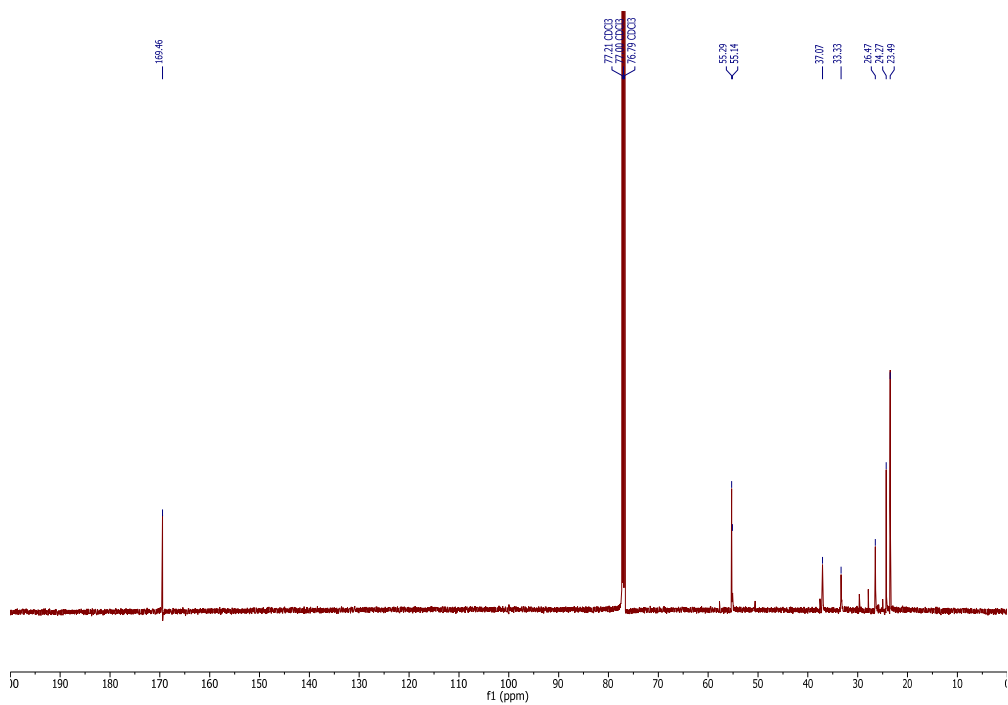
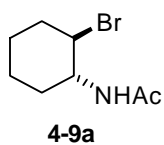
*NMR Spectra of Synthetic Intermediates
and Products of Chapter 4*

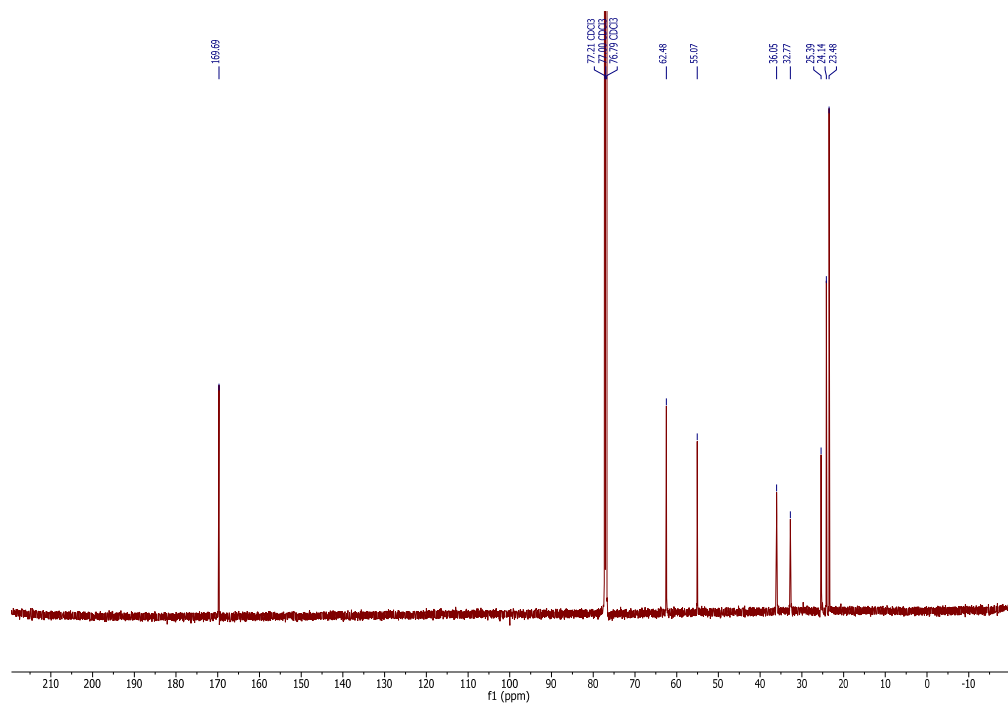
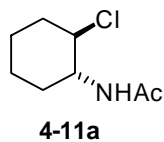


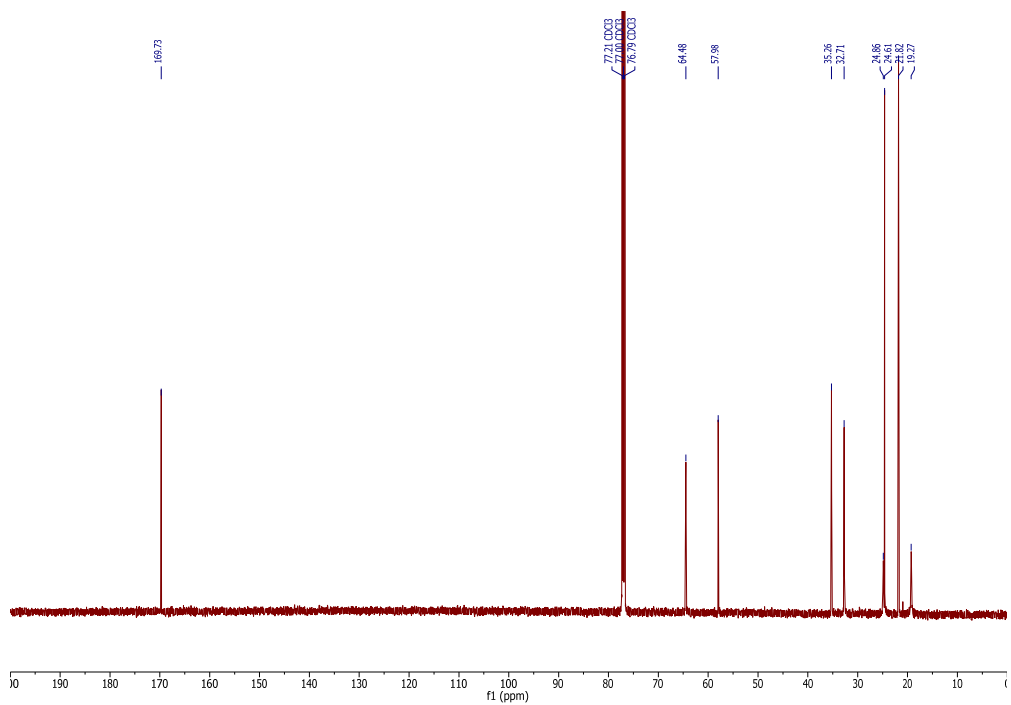
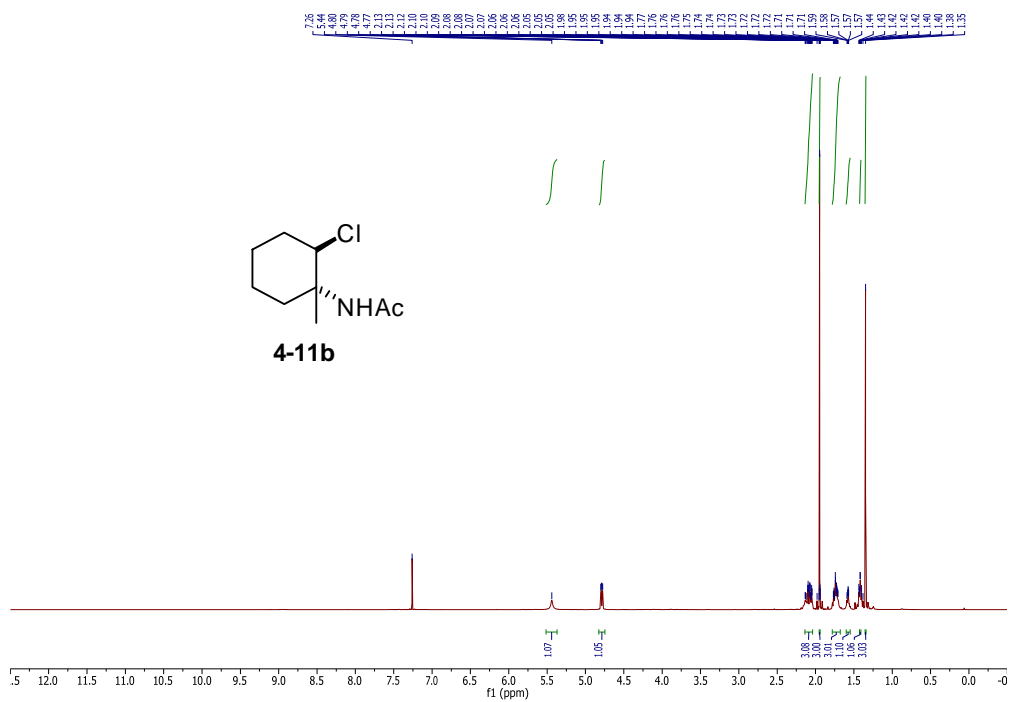


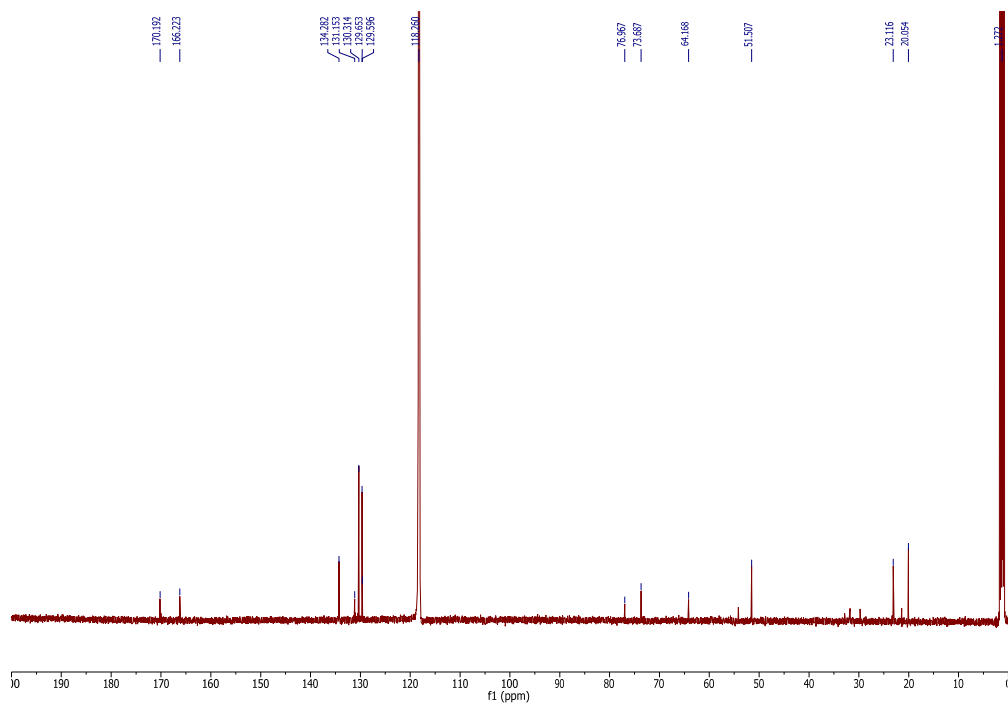


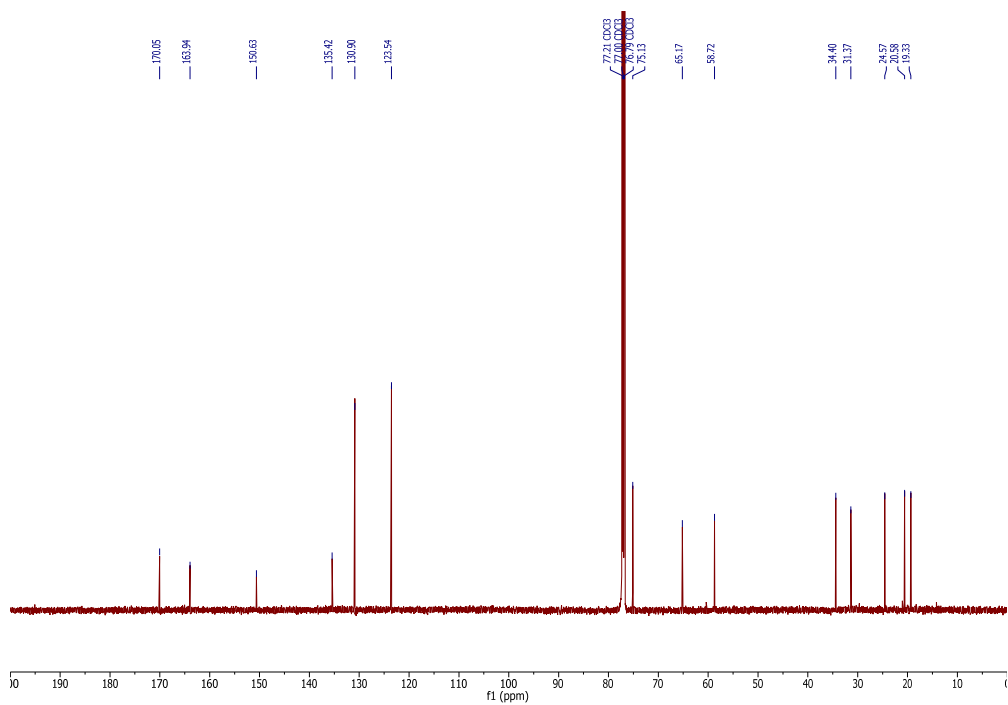
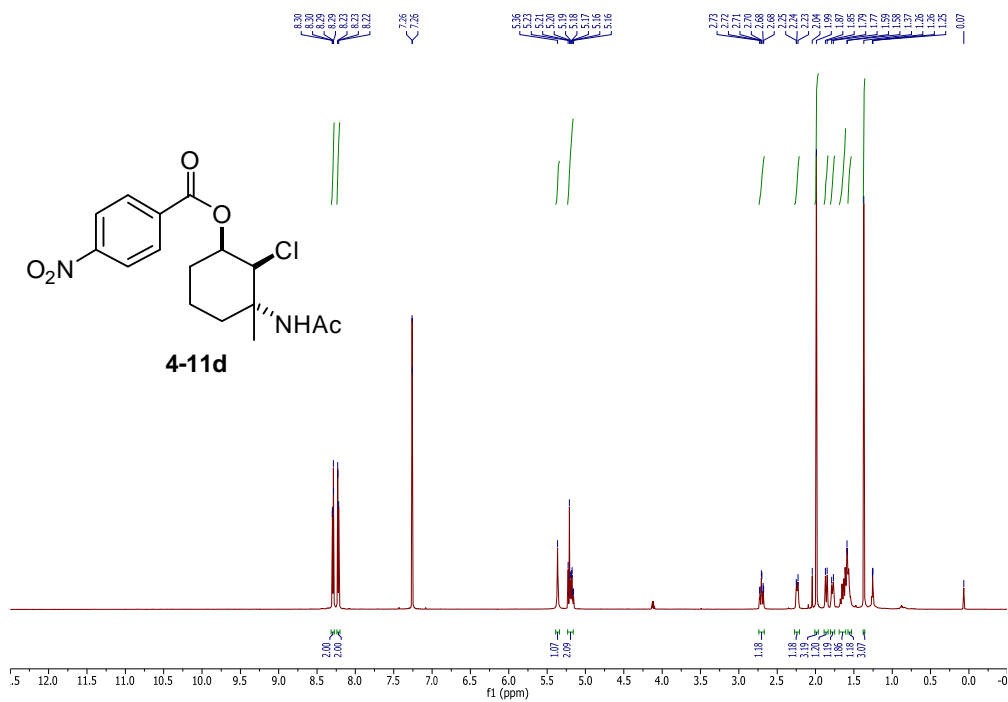


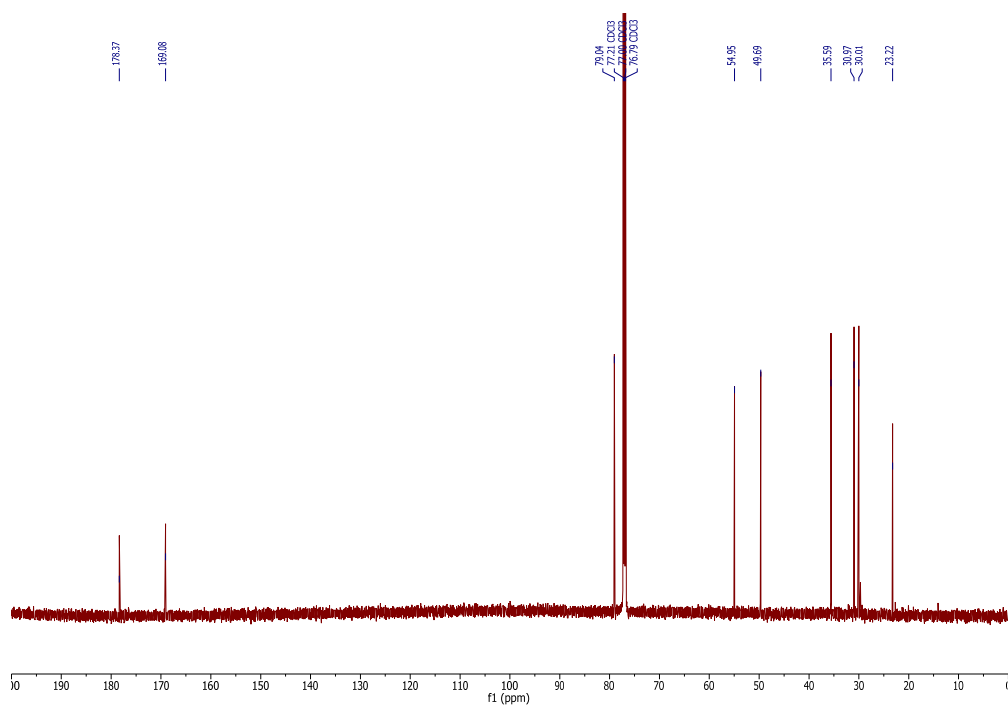
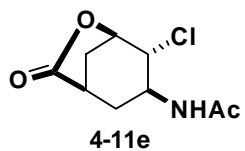


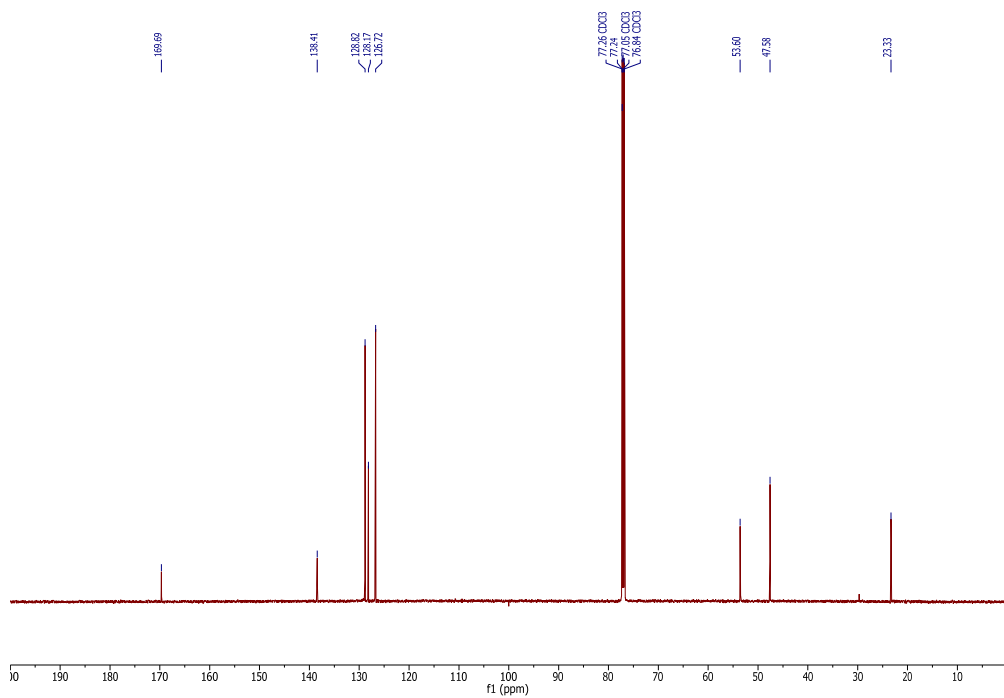
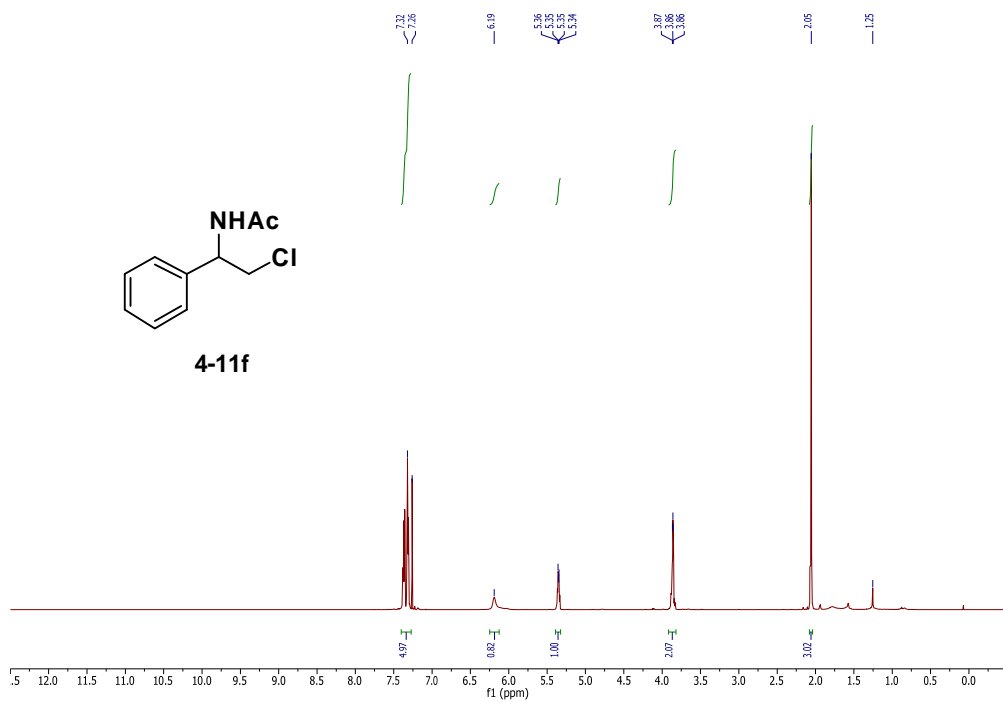


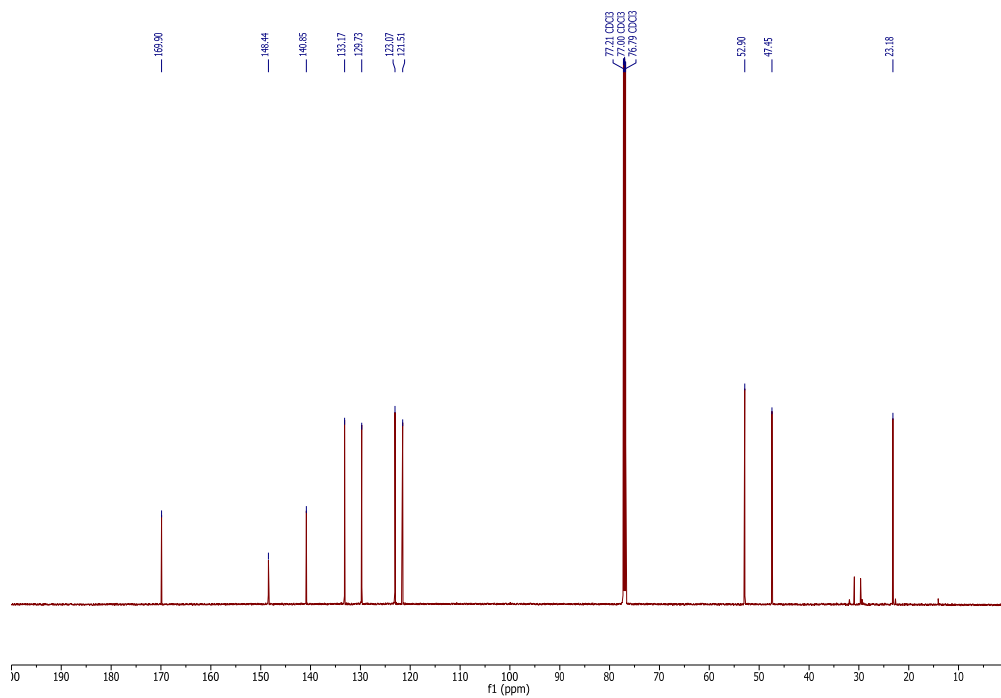
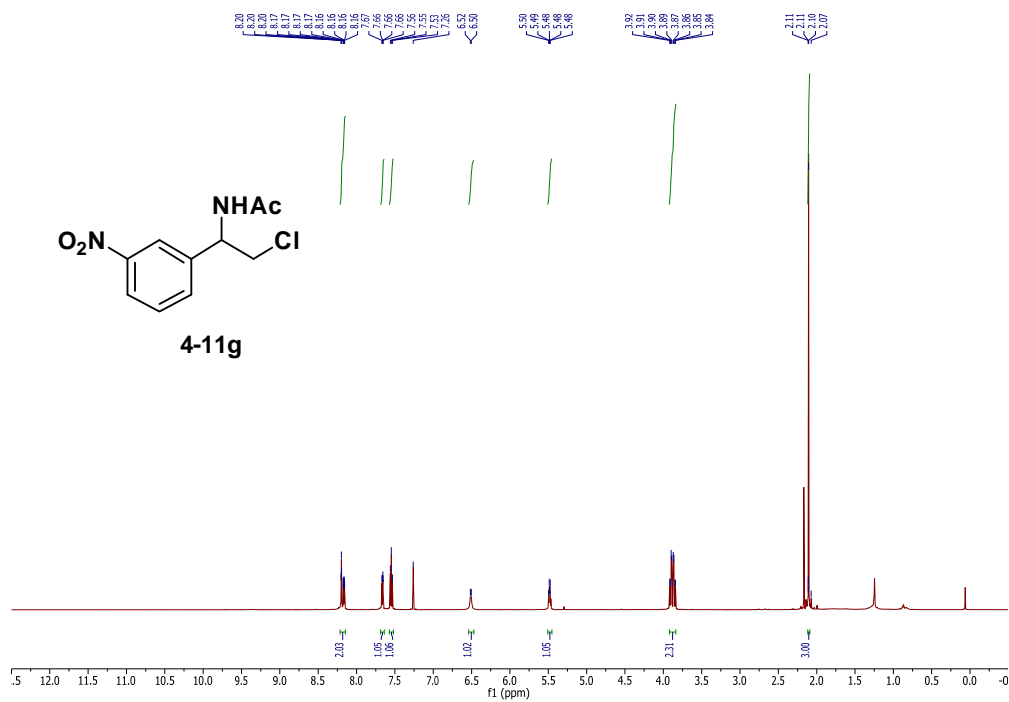


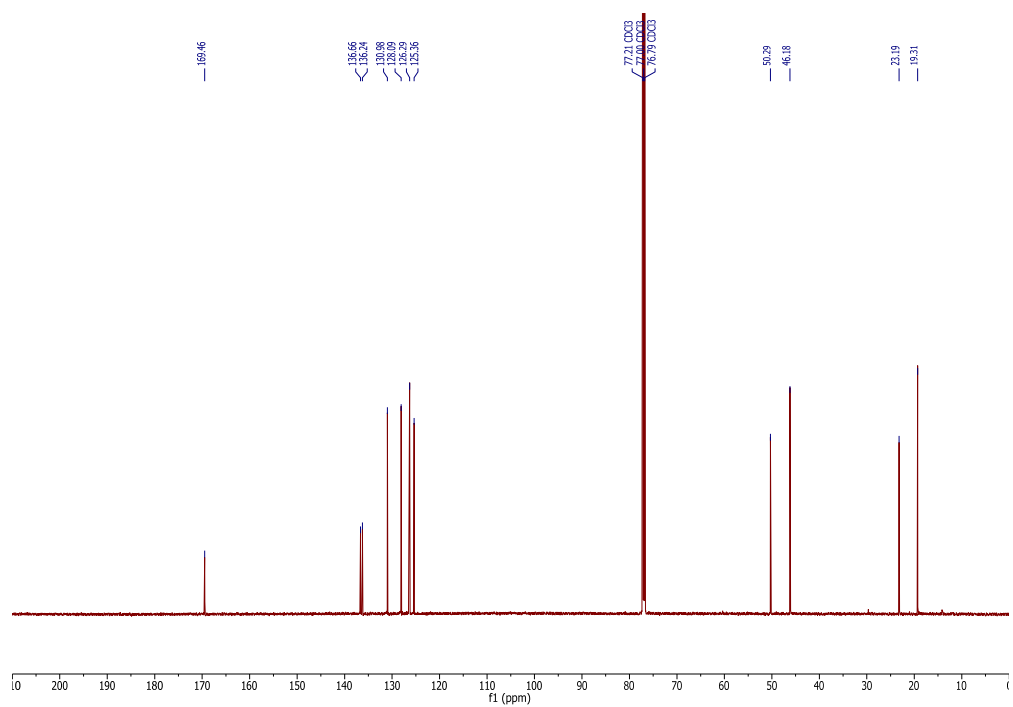
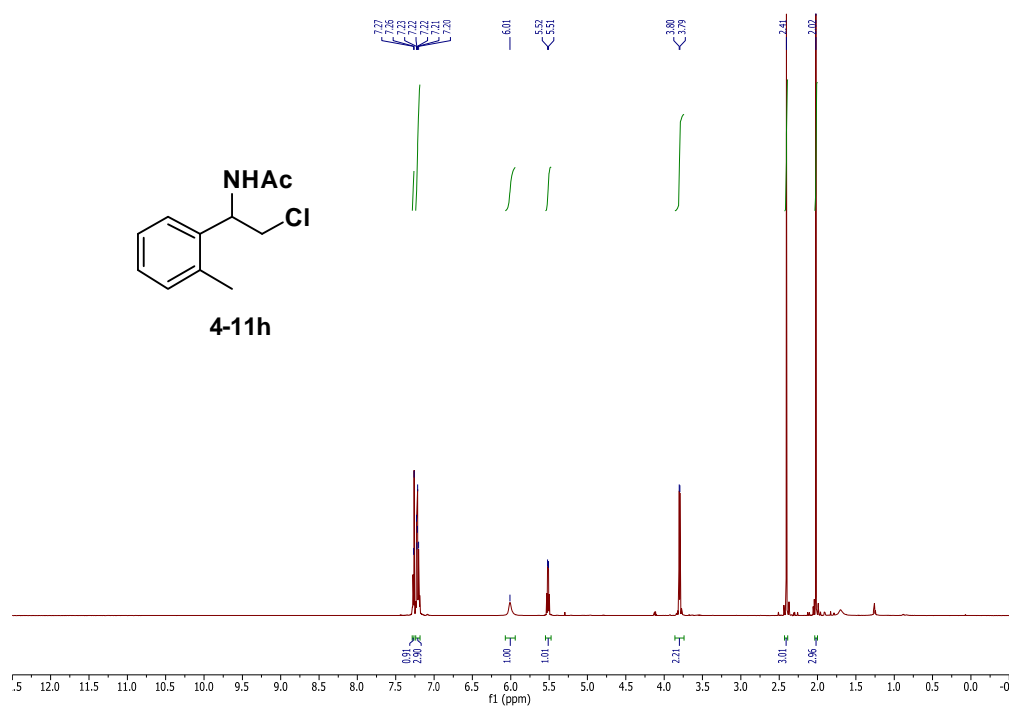


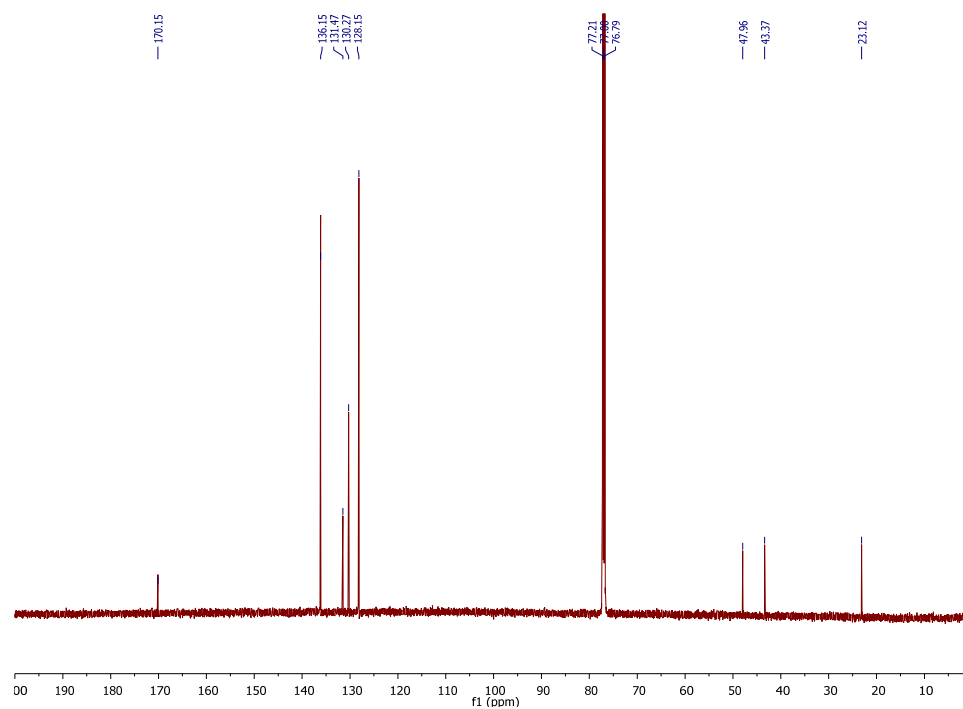
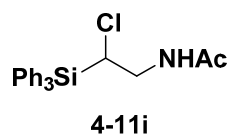


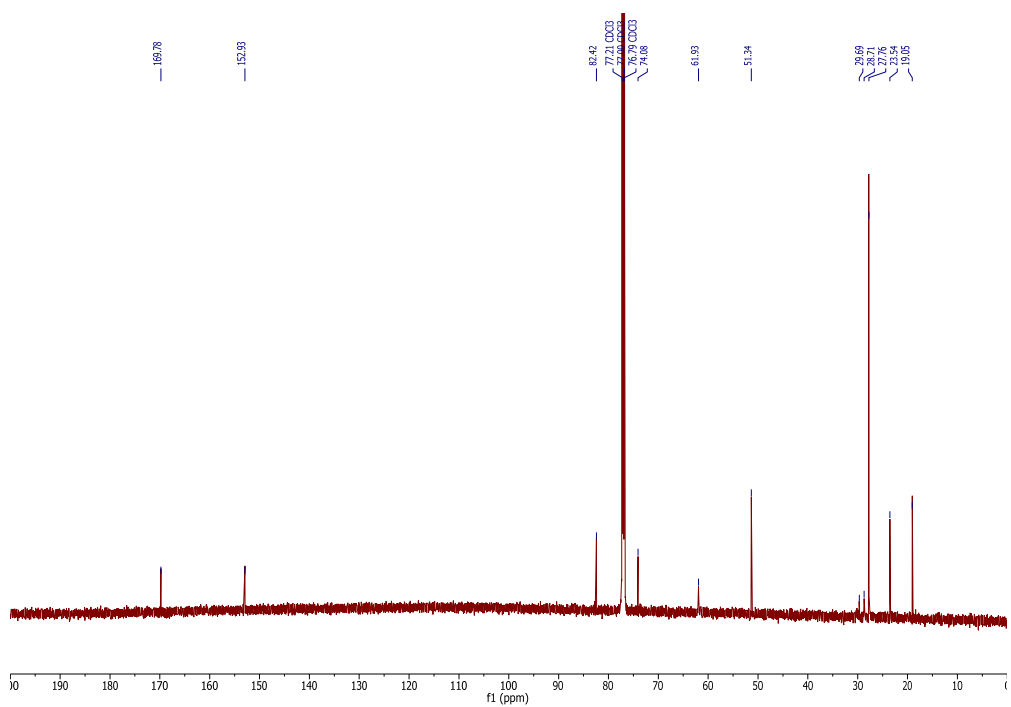
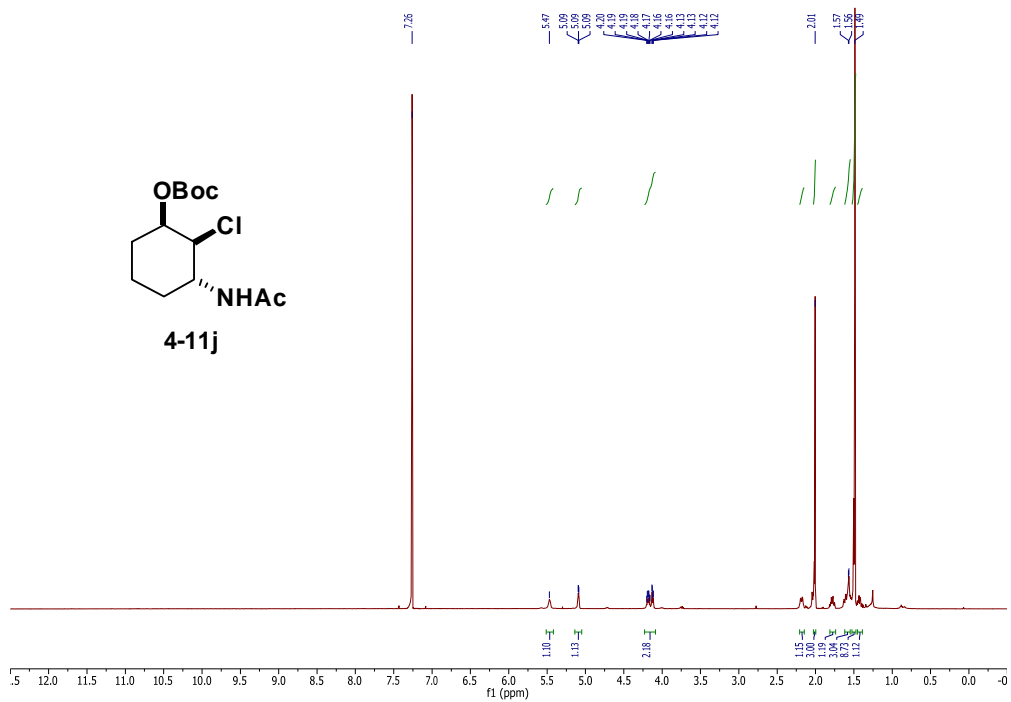


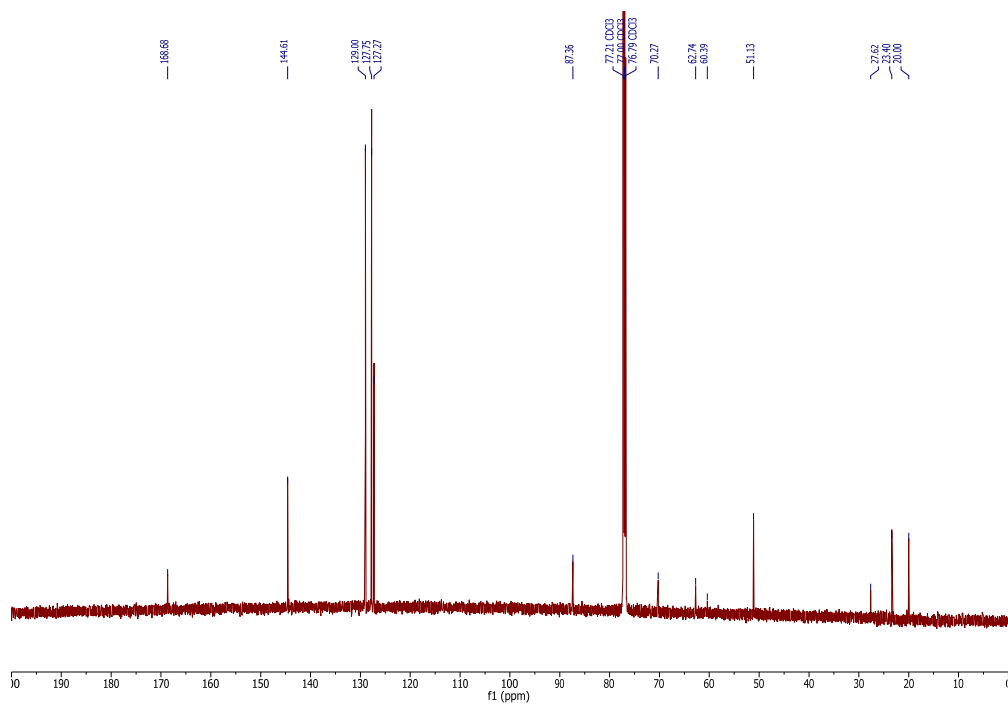
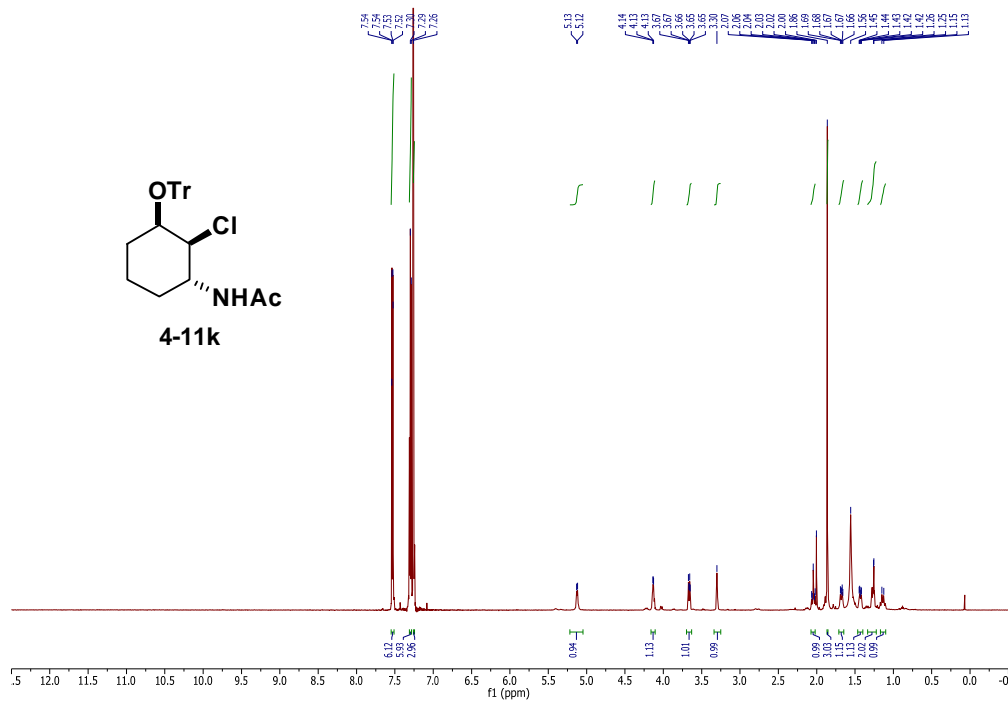


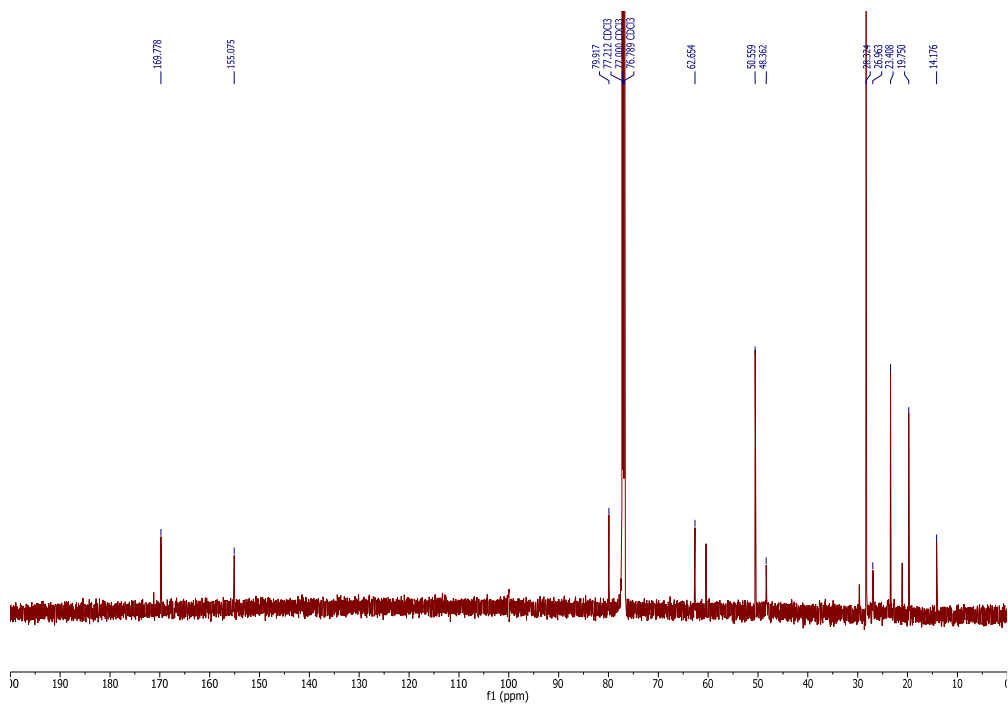
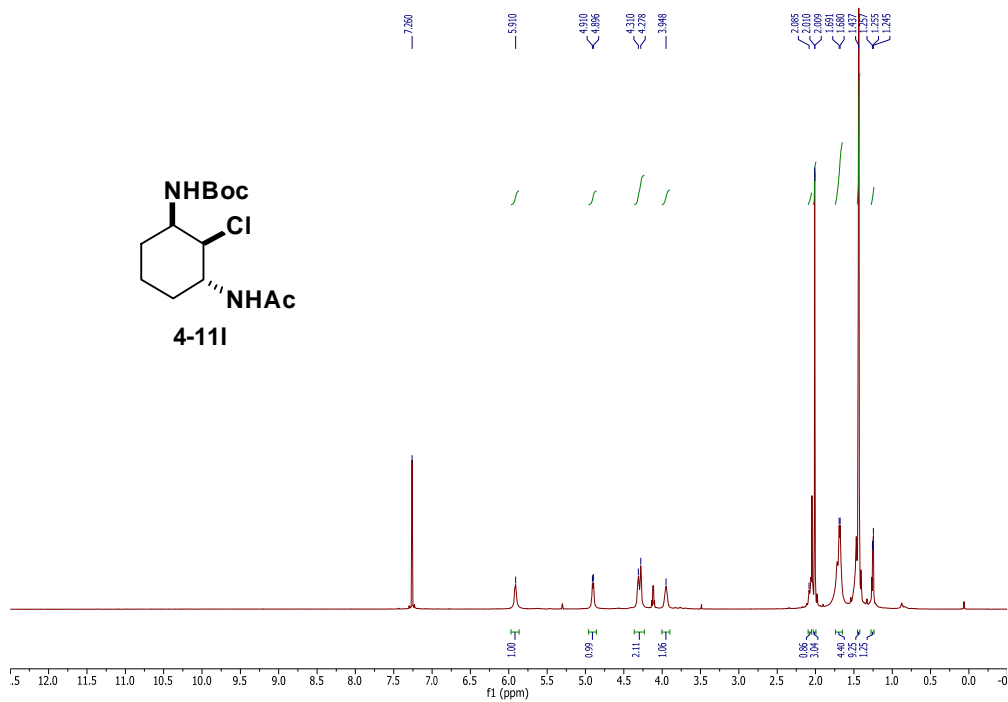


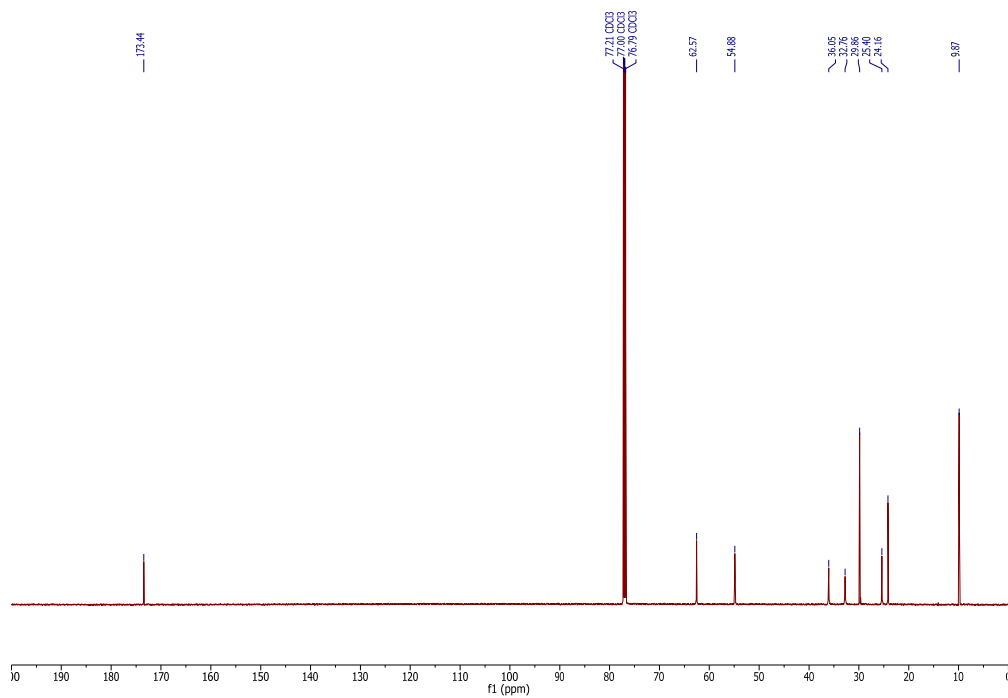
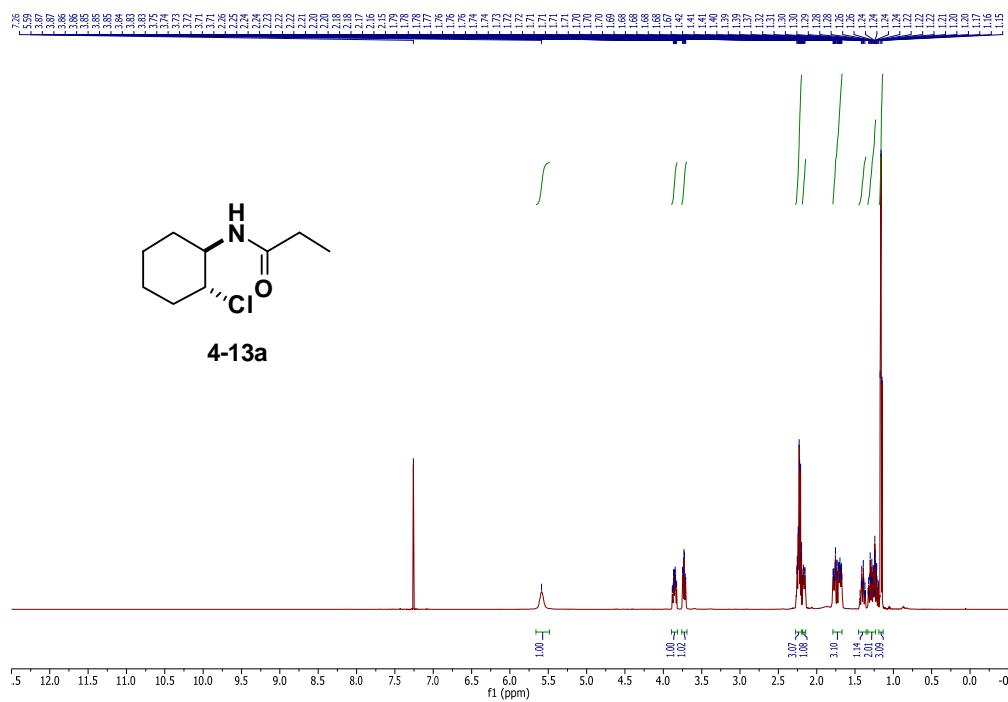


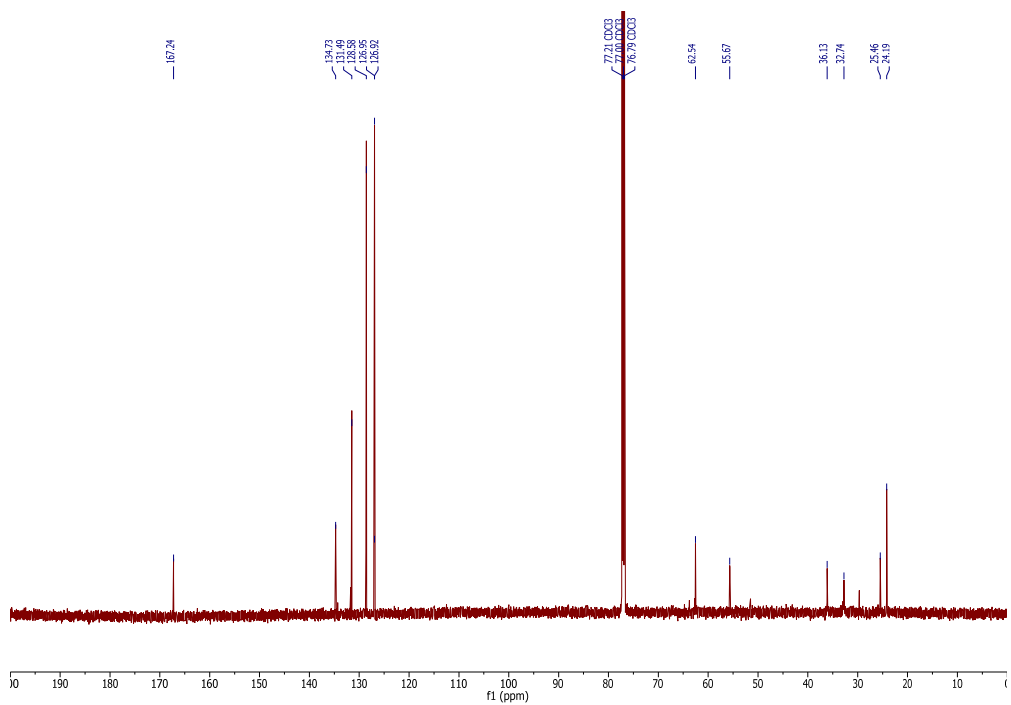
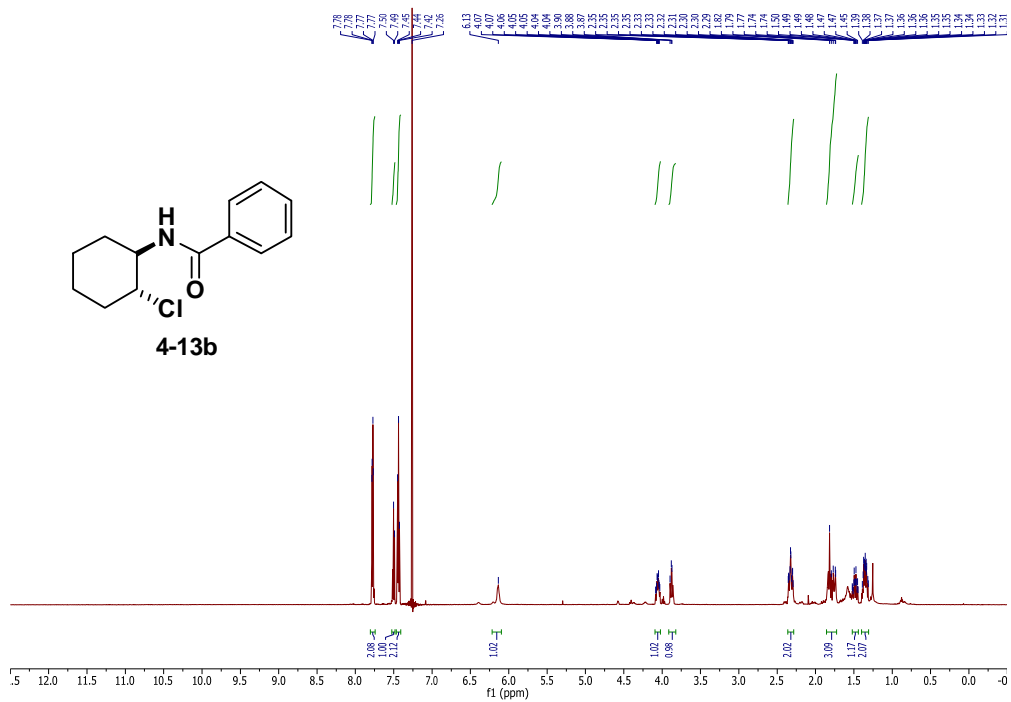












Appendix D

*NMR Spectra of Synthetic Intermediates
and Products of Chapter 5*

